

**LIFESTYLE TREATMENT IN THE REGRESSION OF NASH:
INSULIN RESISTANCE, LIPID SYNTHESIS, AND
METHODOLOGICAL INNOVATION**

A Dissertation

Presented to the Faculty of the Graduate School
University of Missouri, Columbia

In partial fulfillment
of the requirements for the Degree:
Doctor of Philosophy

By: JUSTINE M. MUCINSKI

Doctoral Candidate

Department of Nutrition and Exercise Physiology

University of Missouri, Columbia

Advisor: Elizabeth Parks, PhD

Co-Advisor: R. Scott Rector, PhD

July 2022

The undersigned, appointed by the dean of the Graduate School, have examined the dissertation entitled

LIFESTYLE TREATMENT IN THE REGRESSION OF NASH: INSULIN
RESISTANCE, LIPID SYNTHESIS, AND METHODOLOGICAL INNOVATION

presented by Justine M. Mucinski,

a candidate for the degree of Doctor of Philosophy,

and hereby certify that, in their opinion, it is worthy of acceptance.

Professor Elizabeth Parks

Associate Professor R. Scott Rector

Professor Kevin Fritsche

Professor Frank Booth

DEDICATION

This dissertation is dedicated to my family (Jackie, John, Josh, and Tori) and my beloved partner, Drew, who have all been a source of strength and encouragement to me. In particular, I must thank Drew for his support, constant unending love, and especially his humor that has kept me laughing in even the darkest times.

ACKNOWLEDGEMENTS

I express my deepest gratitude to Dr. Elizabeth Parks for serving as my graduate mentor and supporting me throughout my training. Dr. Parks was a consistent source of information and ideas, and I am incredibly thankful for the time and resources she committed to making me the scholar I am today. I am also grateful for my co-mentor, Dr. Scott Rector for being supportive of my projects, navigating me through coursework, and allowing me to train in his lab. I would have accomplished my academic goals without their support.

My gratitude extends to the other members in my dissertation committee, Drs. Kevin Fritsche and Frank Booth. Both have contributed significantly to my education as professors and through their excellent input into my independent research projects. Dr. Takhar Kasumov was also instrumental in my ceramide biology training, and I must acknowledge him for the hours he spent helping me analyze and interpret my data.

Next, I must recognize each of the lab members and fellow graduate students who have supported my academic journey. Kimberlee Bingham and Whitney Reist – my first colleagues and friends in a new lab and a new city, they made the transition into graduate school a time I will always cherish. Thank you to Mary Moore for your friendship and for your contributions to my training and the data collected and presented in this dissertation. To Nhan Lee for his leadership in Parks lab and Dr. Majid Syed-Abdul for his calm demeanor and help with any graduate student problems. To Jen Anderson – she has had a hand in organizing and collecting many of the outcomes reported in this

dissertation and it would not have been possible without her. Her bright presence in my life will be missed. To Talyia Fordham for her excellent organizational skills that helps Parks lab run so smoothly and for her contributions to data collection. To Dr. Amadeo Salvador for his perspectives on science, post-doc life, and career options. To all of the undergraduate students within Parks lab that I have had the pleasure of working with – they are one of the best parts of science (Ramiro, Brad, Steven, Jillian, Zereque, Alisha, Christian, Emma, Katelyn, and Jonas). In particular, I must thank Jonas McCaffrey for the help he provided in completing my dissertation project. Thank you to Dr. Rector's lab, in particular Grace Meers and Ryan Dashek for training me in techniques that were crucial to finishing my data collection. Finally, I would also like to acknowledge all of the professors who have supported me throughout my training and the NEP staff who are fundamental for the success of the department – science doesn't happen without you. I wish each of these excellent people the best in life and am indebted to every one of them.

I would also like to thank the participants (humans and animal) who have committed their time and effort to the studies included in this dissertation. Additionally, I must acknowledge the nursing staff who helped collect the clinical data and the vivarium staff who maintained animal housing. Thank you to the physicians who recruited patients and oversaw data collection. Finally, I would like to acknowledge the National Institute of Diabetes and Digestive and Kidney Diseases for financially contributing to these studies and to the MU graduate school for funding me through a dissertation year fellowship.

TABLE OF CONTENTS

ACKNOWLEDGEMENTS	ii
ABBREVIATIONS	vi
LIST OF TABLES	ix
LIST OF FIGURES	xi
ABSTRACT	xv
CHAPTER I – Introduction and literature review	1
SCIENTIFIC PREMISE: Review of background literature	2
SPECIFIC AIMS	24
FIGURES	28
REFERENCES	38
CHAPTER II – High-throughput LC-MS method to investigate postprandial lipemia: Considerations for future precision nutrition research ..	60
ABSTRACT	61
NEW & NOTEWORTHY	63
INTRODUCTION	64
METHODS	68
RESULTS	73
DISCUSSION	79
TABLES	88
FIGURES	95
SUPPLEMENTARY DATA	102
SUPPORTING INFORMATION	106
REFERENCES	107
CHAPTER III – Hepatic and mitochondrial ceramide kinetics	114
ABSTRACT	115
INTRODUCTION	117
METHODS	120
RESULTS	128
DISCUSSION	136
EXTENDED METHODOLOGY	152
TABLES	162
FIGURES	168
SUPPLEMENTARY DATA	182
SUPPORTING INFORMATION	197
REFERENCES	198
CHAPTER IV – Histological improvements from increased peripheral substrate disposal: Muscle glucose uptake spares the liver	208
ABSTRACT	209
INTRODUCTION	211
METHODS	214
RESULTS	225
DISCUSSION	243
EXTENDED METHODOLOGY	262
TABLES	269
FIGURES	276

SUPPLEMENTARY DATA	315
SUPPORTING INFORMATION.....	330
REFERENCES.....	331
CHAPTER V – Noninvasive fatty acid oxidation in NASH: The utility of labeled breath tests to monitor changes in liver health?	349
ABSTRACT	350
INTRODUCTION.....	352
METHODS	355
RESULTS.....	360
DISCUSSION.....	363
TABLES	371
FIGURES	373
SUPPLEMENTARY DATA	380
SUPPORTING INFORMATION.....	384
REFERENCES.....	385
APPENDIX A – NAFLD activity scoring system	393
APPENDIX B – Curriculum vita.....	394
VITA.....	409

ABBREVIATIONS

AASLD - American association for the study of liver disease
ACC - acetyl-CoA carboxylase
ACL - ATP citrate lyase
ALP - alkaline phosphatase
ALT - alanine aminotransferase
ANOVA - analysis of variance
ApoB48 - apolipoprotein B48
ApoB100 - apolipoprotein B100
AST - aspartate aminotransferase
ASAH – acid ceramidase
ATGL - Adipose triglyceride lipase
AUC - area under the curve
 β -ox - beta oxidation
BCA - Bicinchoninic acid assay
BMI - body mass index
BSA - bovine serum albumin
BSTFA +10% TMCS - bis(trimethylsilyl) trifluoroacetamide 10%
trimethylchlorosilane
BW - body weight
CD - control diet
CD36 - cluster of differentiation 36
CER - ceramide
CERS - ceramide synthase
CERT - ceramide transfer protein
CoA - coenzyme A
CO₂ - carbon dioxide
COVID-19 - Coronavirus disease
CPT1 - carnitine palmitoyltransferase 1
CRC - clinical research center
CV - coefficient of variation
D₂O - deuterated water
DAG - diacylglycerol
DEGS - dihydroceramide desaturase
DEXA - dual-energy X-ray absorptiometry
DGAT - diacylglycerol acyltransferase enzyme
dhCER - dihydroceramide
DNL - de novo lipogenesis
EASL - European Association for the Study of the Liver
ECG - electrocardiogram
EGP - endogenous glucose production
ER - endoplasmic reticulum
ELOV - elongases
ESI - electrospray ionization
ETC - electron transport chain
ETT - exercise tolerance test

FA - fatty acid
FADH₂ - flavin adenine dinucleotide
FAME - fatty acid methyl ester
FAS/FASN - fatty acid synthase
FAO - fatty acid oxidation
FCR - fractional clearance rate
FFA - free fatty acids
FK - fructose kinase
FOXO1 - forkhead box 1
FSR - fractional synthesis rate
F1P ALD - fructose 1-phosphatase aldolase
F1,6BPT - fructose 1,6 bisphosphatase
GC - gas chromatography
GC/MS - gas chromatography/mass spectrometry
GNG - gluconeogenesis
G6P - glucose 6 phosphatase
HbA1c - hemoglobin A1C/ glycosylated hemoglobin
HDL - high-density lipoprotein
HIIT - high intensity interval training
HF - high fat
HFD - high fat diet
HK – hexokinase
HR - heart rate
HSL - hormone sensitive lipase
HOMA-IR - homeostatic model assessment for insulin resistance
HPLC/MS/MS - high-performance liquid chromatography tandem mass spectrometry
H&E - hematoxylin and eosin
ISI - insulin sensitivity index
IHTG - intrahepatic triglycerides
IRB - institutional review board
k - pools / day
Kcal - kilocalories
kg - kilograms
KDHR - 3-ketodihydrosphingosine reductase
LDL- low-density lipoprotein
LF - low fat
LPL - lipoprotein lipase
MAFLD - metabolic associated fatty liver disease
MAG - monoacylglycerol
MF - moderate fat
MGL - monoglyceride lipase
MGAT - monoacylglycerol acyltransferase enzyme
MICT - moderate intensity continuous training
MIDA - mass isotopomer distribution analysis
mRNA - messenger ribonucleic acid

MRI - magnetic resonance imaging
MRS - magnetic resonance spectroscopy
MRM - multiple reaction monitoring
MS - mass spectrometry
MTP - microsomal triglyceride transfer protein
MTT - meal tolerance test
MU - University of Missouri
MUFA - monounsaturated fatty acids
m/z - mass to charge
NADH - nicotinamide adenine dinucleotide
NADPH - nicotinamide adenine dinucleotide phosphate.
NAFLD - nonalcoholic fatty liver disease
NAS - NAFLD activity score
NASH - nonalcoholic steatohepatitis
NDSR - nutrition data systems for research
NEFA - nonesterified fatty acids
NICE - National Institute for Health and Care Excellence
NIH - National Institutes of Health
OctOx - octanoate oxidation
OGTT - oral glucose tolerance test
PEPCK - phosphoenoyl pyruvate carboxykinase
PFK - phosphofructokinase
PK - pyruvate kinase
PUFA - polyunsaturated fatty acids
QUICKI - quantitative insulin-sensitivity check index
ROS - reactive oxygen species
SCD - stearoyl-CoA desaturase
SD - standard deviation
SEM - standard error
S_f - Svedberg floatation rate
SM - sphingomyelin
SMPD - acid sphingomyelinase
SPT - serine palmitoyl transferase
SREBP1c - sterol regulatory element binding protein 1c
TCA - tricarboxylic acid cycle
TC - total cholesterol
TG - triglyceride
TLC - thin layer chromatography
TNF- α - tumor necrosis factor α
TRL - triglyceride rich lipoprotein
T2D - type 2 diabetes
VLDL - very low-density lipoproteins
VO₂ - maximal oxygen consumption
%E - percent enrichment
%E - percent energy

LIST OF TABLES

Chapter II

Table 2.1. Composition of the test meals.....	89
Table 2.2. TRL-TG: Model fit, absolute entry rate (slope), and fractional entry rate (k) of label in singly- and doubly- labeled 54:3 and 52:2.....	90
Table 2.3. S _r >400 -TG: Model fit, absolute entry rate (slope), and fractional entry rate (k) of label in singly- and doubly- labeled 54:3 and 52:2.....	92
Table 2.4. Key factors to consider when designing studies for precision nutrition.....	94

Chapter III

Table 3.1. Macronutrient composition and ingredients for control and high fat diets.....	163
Table 3.2. Fatty acid composition of control and high fat diets.....	164
Table 3.3. Energy and water intake.....	165
Table 3.4. Inter- and intraassay precision for liver and mitochondrial CER.....	166
Table 3.5. Kinetics of liver and mitochondrial CER 16:0.....	167
Supplementary Table S3.1. Sex differences for serum biochemistries and hepatic TG content.....	183
Supplementary Table S3.2. Day of euthanasia body and organ weights.....	184
Supplementary Table S3.3. Liver free serine enrichment.....	185
Supplementary Table S3.4. Sex differences for hepatic protein expression of key enzymes related to CER synthesis, oxidative phosphorylation complexes, and mitochondrial citrate synthase activity.....	186
Supplementary Table S3.5. Correlation matrix for CERS protein content and liver CER and dhCER concentrations.....	187
Supplementary Table S3.6. Correlation matrix for CERS protein content and mitochondrial CER and dhCER concentrations.....	188
Supplementary Table S3.7. Correlation matrix for SPT, DEGS, SMPD, and ASAH protein content and liver CER and dhCER concentrations.....	189
Supplementary Table S3.8. Correlation matrix for SPT, DEGS, SMPD, and ASAH protein content and mitochondrial CER and dhCER concentrations.....	190

Chapter IV

Table 4.1. Criteria for inclusion and exclusion in Phase II.....	270
Table 4.2. Phase one subject characteristics.....	271
Table 4.3. Baseline phase two subject characteristics.....	272
Table 4.4. Blood lipids.....	273
Table 4.5. Hepatic and peripheral insulin sensitivity and insulin-stimulated substrate metabolism.....	274

Supplementary Table S4.1. Results of mixed model ANOVA for 18-h metabolite concentration data separated into three time periods (postprandial, night, and clamp).....	316
Supplementary Table S4.2. Baseline correlation analysis of ceramide and dihydroceramides with weight, fasting glucose, total cholesterol, LDL cholesterol, EGP, and R_d	317
Supplementary Table S4.3. Change correlation analysis of ceramide and dihydroceramides with weight, BMI, fat mass, AST, and ALT.....	318
Supplementary Table S4.4. Change correlation analysis of ceramide and dihydroceramides with NAS, NAS components, fibrosis, and total liver fat by MRI.....	319

Chapter V

Table 5.1. Subject characteristics.....	372
Supplementary Table S5.1. Baseline diabetic status and subject medications.....	381

LIST OF FIGURES

Chapter I

Figure 1.1. Integration of hepatic metabolic pathways.....	29
Figure 1.2. Reductions in liver fat with energy restriction.....	30
Figure 1.3. Reductions in liver fat with HIIT and MICT in adults with obesity....	31
Figure 1.4. Reductions in VLDL-TG DNL with diet.....	32
Figure 1.5. 16:0 CER (A), a product of de novo CER synthesis (B), and (C) acyl chain length specific to the CERS1-6	33
Figure 1.6. De novo CER synthesis with ¹³ C ₃ , ¹⁵ N L-serine.....	34
Figure 1.7. Serine-labeled serum, liver, and mitochondrial 16:0 CER	35
Figure 1.8. Schematic illustrating specific aims 1 and 2	36

Chapter II

Figure 2.1. Overall study design, protocol for meal tests, and molecular structures of the stable isotope and the TG 54:3 and 52:2 containing oleic acid moieties that were measured.....	96
Figure 2.2. TRL- and Sf>400-TG: Total TG concentrations following the meal tests.....	97
Figure 2.3. TRL-TG: Variability in concentrations across subjects.....	98
Figure 2.4. Sf>400-TG: Variability in concentrations across subjects	99
Figure 2.5. TRL-TG: Temporal patterns of 54:3 and 52:2 TG containing singly- and doubly-labeled oleate	100
Figure 2.6. Sf>400-TG: Temporal patterns of 54:3 and 52:2 TG containing singly- and doubly-labeled oleate	101
Supplementary Figure S2.1. TRL- and Sf>400-TG: Reproducibility of total TG between two HF test meals	103
Supplementary Figure S2.2. TRL-TG: Reproducibility of singly- and doubly-labeled 54:3 and 52:2 between two HF test meals.....	104
Supplementary Figure S2.3. Sf>400 – TG: Reproducibility of singly- and doubly- labeled 54:3 and 52:2 between two HF test meals.	105

Chapter III

Figure 3.1. Experimental design and labeled serine stable isotope	169
Figure 3.2. Anthropometrics and liver weight.....	170
Figure 3.3. Serum and liver biochemistries.....	171
Figure 3.4. Whole liver CER and dhCER concentrations.....	172
Figure 3.5. Molar percent of individual liver CER.....	173
Figure 3.6. Isolated mitochondrial CER and dhCER concentrations.....	174
Figure 3.7. Molar percent of individual mitochondrial CER	175
Figure 3.8. Relationship between total liver and mitochondrial CER	176
Figure 3.9. Percent enrichment of 16:0 CER across days	177
Figure 3.10. Fractional and absolute synthesis rate of 16:0 CER in liver and isolated mitochondria.....	178
Figure 3.11. Whole liver homogenate protein expression of key CER synthetic enzymes	179
Figure 3.12. Mitochondrial citrate synthase activity and hepatic protein expression of the oxidation phosphorylation complexes.....	180
Figure 3.13. Model demonstrating effects of HFD on hepatic CER synthesis	181
Supplementary Figure S3.1. Sex differences in liver CER and dhCER	191
Supplementary Figure S3.2. Sex differences in mitochondrial CER and dhCER	192
Supplementary Figure S3.3. Relationships between liver and mitochondrial CER.....	193
Supplementary Figure S3.4. Fractional and absolute liver and mitochondrial 16:0 CER turnover by sex	194
Supplementary Figure S3.5. Percent enrichment of free serine across days	195
Supplementary Figure S3.6. Metabolic conversion for the generation of a $^{13}\text{C}_2$ labeled serine	196

Chapter IV

Figure 4.1. Overall study design	277
Figure 4.2. Participant recruitment.....	278
Figure 4.3. Metabolic testing day study design (repeated at baseline and follow-up in all subjects).....	279
Figure 4.4. Changes in liver histology.....	280
Figure 4.5. Changes in anthropometrics.....	282
Figure 4.6. Relationships between changes in liver histology, weight, and fat mass.....	283
Figure 4.7. Changes in fasting blood biochemistries	285
Figure 4.8. 18-hour dynamics of plasma glucose	286
Figure 4.9. 18-hour dynamics of plasma insulin.....	288
Figure 4.10. 18-hour dynamics of plasma NEFA	290
Figure 4.11. 18-hour dynamics of plasma TG.....	292
Figure 4.12. Changes in energy intake and macronutrients	294
Figure 4.13. Fitness and physical activity	295
Figure 4.14. Changes in VO_2 peak with changes in body weight and NAS	296
Figure 4.15. Absolute glucose production and percent change	297
Figure 4.16. EGP suppression and absolute change in EGP suppression from basal to step one and basal to step two	298
Figure 4.17. Absolute glucose disposal and percent change.....	299
Figure 4.18. Baseline relationships between EGP and R_d with NAS component, lobular inflammation	300
Figure 4.19. Change in EGP and R_d with change in NAS and the components, lobular inflammation, and hepatocellular ballooning	301
Figure 4.20. Change in EGP and R_d with change in VO_2 peak and activity	302
Figure 4.21. Change in EGP and R_d with follow-up carbohydrate consumption	303
Figure 4.22. NEFA suppression during step one and step two of the clamp and change from baseline to follow-up.....	304
Figure 4.23. Proportion of fatty acid sources becoming labeled in TRL-TG over time.....	305
Figure 4.24. Absolute fatty acid sources used for VLDL-TG synthesis and correlations with fasting fractional DNL	306
Figure 4.25. Plasma ceramide (CER) concentrations.....	307
Figure 4.26. Plasma dihydroceramide (dhCER) concentrations	309
Figure 4.27. Relationships between change in total ceramides and dihydroceramides with anthropometrics	311
Figure 4.28. Ceramide 18:1/16:0 and liver fat.....	312
Figure 4.29. Reverse J shaped curve of EGP and NAS and hypothesized model	313

Chapter IV Continued

Supplementary Figure S4.1. Body weight changes over time.....	320
Supplementary Figure S4.2. Time period AUC for plasma (A) Glucose, (B) Insulin, (C) NEFA, and (D) TG.....	321
Supplementary Figure S4.3. Plasma NEFA sources from midnight to 8AM .	323
Supplementary Figure S4.4. Absolute TRL-TG concentrations across time .	325
Supplementary Figure S4.5. Relationships between change in 18-hour NEFA AUC and NAS, lobular inflammation, and EGP	326
Supplementary Figure S4.6. Relationships between change in EGP and R_d during different steps of the clamp and EGP with non-oxidative glucose disposal	327
Supplementary Figure S4.7. Relationships between change in fasting fractional DNL and steatosis, lobular inflammation, and glucose production	328
Supplementary Figure S4.8. Baseline relationships between total ceramides and dihydroceramides with weight, fasting glucose, and total cholesterol	329

Chapter V

Figure 5.1. Molecular structure of labeled octanoate and study design of noninvasive breath test.....	374
Figure 5.2. Time course of percent octanoate dose oxidized (OctOx) per minute and baseline correlations with markers of glucose metabolism.....	375
Figure 5.3. Average and individual changes in NAS, steatosis, fibrosis, and percent (%) octanoate dose oxidized (OctOx).....	376
Figure 5.4. Correlations between changes in octanoate oxidized (OctOx) and fasting glucose and fasting EGP.....	377
Figure 5.5. Correlations between changes in octanoate oxidized (OctOx) and markers of liver health – steatosis and ALT.....	378
Figure 5.6. Model of improved liver health with changes in FAO.....	379
Supplementary Figure S5.1. Schematic demonstrating delivery of oral $^{13}\text{C}_4$ octanoate to the liver through portal transport and oxidation.....	382
Supplementary Figure S5.2. Individual changes in NAS, steatosis, fibrosis, and total octanoate oxidized (OctOx)	383

ABSTRACT

This dissertation is focused on factors that increase risk for nonalcoholic fatty liver disease (NALFD) and the more advanced form nonalcoholic steatohepatitis (NASH). These factors include postprandial lipid handling (chapter II); ceramide (CER) turnover (chapter III), hepatic and mitochondrial CER content (chapter III); glucose turnover (chapter IV), de novo lipogenesis (chapter IV), and hepatic fatty acid oxidation (chapter V). With regard to postprandial lipemia, healthy men consumed an oral isotope ($^2\text{H}_{11}$ -oleate) in liquid meals of varying fat content and labeled triglycerides (TG) tracked into chylomicrons and triglyceride rich lipoproteins (TRL). This method may be applied to future studies of postprandial lipemia. Similar analytical methods (liquid chromatography mass spectrometry) were used to track the synthesis of CERs within hepatic tissues of mice consuming $^{13}\text{C}_3$ ^{15}N L-serine dissolved in their water and a high fat (60% energy, HFD) or a control (low fat, 20%E, CD) diet for two weeks. The mice fed a HFD exhibited greater absolute CER turnover in both whole liver tissue and isolated mitochondria. Furthermore, while total liver concentrations did not differ between diet groups, the HFD elicited greater mitochondrial CER content which was related to total liver CER only in these animals. Plasma CER concentrations were measured in subjects with advanced NASH before and after a nine-month lifestyle program (and a standard care group) and the change in 16:0 CER was negatively related to improvements in liver fat. Similarly, an increase in glucose production and disposal were related negatively to histologic improvements. Together, these data support a hepatic benefit of routing substrates - glucose

and lipotoxic lipids – away from the liver. In addition to testing changes in glucose metabolism, these subjects had significant reductions in lipogenesis but no changes in a non-invasive breath test ($^{13}\text{C}_4$ Octanoate) to quantify total hepatic fatty acid oxidation using expelled breath. Correlations between baseline and the change in octanoate oxidation, glucose turnover, and steatosis support the utility of this method to investigate physiological processes that improve hepatic lipid burden. Currently, no drug therapies exist for the treatment of NAFLD or NASH and the results from the current studies support future investigations in identifying key factors for the regression of advanced liver disease through methodological innovation and novel findings with combined intensive lifestyle treatment.

CHAPTER I – Introduction and literature review

SCIENTIFIC PREMISE: Review of background literature

Nonalcoholic fatty liver disease

In 1970, the first descriptions of a fatty liver occurring in patients with type 2 diabetes mellitus (T2D) was published (1). Ten years later, the disease was named nonalcoholic fatty liver disease (NAFLD) because the histopathological features were reminiscent of alcohol-associated liver disease but occurred in the absence of excess alcohol intake and often in individuals with obesity and T2D (2). Since the first descriptions of this disease, our understanding of the NAFLD spectrum of liver injury and the progression to more advanced forms, nonalcoholic steatohepatitis (NASH), fibrosis, and cirrhosis, has grown considerably. NAFLD and NASH are characterized by the presence of steatosis (liver fat $\geq 5\%$ of liver volume) while NASH also includes hepatocellular ballooning and lobular inflammation with or without fibrosis (3, 4). NAFLD is differentiated from other liver diseases by the absence of significant alcohol intake (≥ 14 or ≥ 21 drinks per week for women or men, respectively), hereditary disorders (e.g., Wilson's disease, lipodystrophy), use of steatogenic drugs (e.g., corticosteroids), or the presence of other conditions that may result in acute liver fat accrual (e.g., pregnancy, hepatitis C) (4). Recently, because NAFLD is characterized as a metabolic condition, new nomenclature was proposed – metabolic-associated fatty liver disease (MAFLD) (5-7), which puts more emphasis on the role of metabolic dysfunction in NAFLD. For the purposes of this dissertation, the commonly accepted nomenclature NAFLD will be used throughout the text.

NAFLD prevalence and staging

NAFLD is the leading cause of liver disease in the U.S., affecting approximately 25% of people globally (8, 9) with prevalence rates much higher (40-90%) in populations with associated clinical risk factors (e.g., obesity, metabolic syndrome, T2D) (9). Liver injury due to NAFLD is the most rapidly increasing indication for liver transplantation in the U.S. (10) and it is now well established that NAFLD is a multi-organ disease, affecting many extrahepatic tissues (11). Indeed, NAFLD is an independent risk factor for cardiovascular-related and all-cause mortality (8, 12, 13).

Development of NAFLD can occur in the presence or absence of obesity and occurs in four general stages (14). The first stage, hepatic steatosis, is characterized by intrahepatic lipid accumulation, mainly triacylglycerols (TG; intrahepatic triacylglycerols, IHTG), above 5% of the total liver volume (4, 15). When left untreated 20-30% of individuals with hepatic steatosis will progress to NASH which is characterized by the presence of hepatocellular ballooning and lobular inflammation (16). Individuals with NASH have higher rates of hepatocellular apoptosis and cellular stress which can promote scarring of the tissue – fibrosis, the third stage of NAFLD. Advanced fibrosis ($\geq 3/4$ fibrosis score) occurs in ~15% of individuals with NASH and on average, these individuals progress one stage of fibrosis approximately every seven years (17, 18). Permanent liver damage induced by fibrosis promotes the advancement to the fourth stage of the disease – cirrhosis and/or hepatocellular carcinoma. In

those individuals with advanced fibrosis, 22% will develop cirrhosis or decompensated liver disease within two to four years (19, 20).

Detection of NAFLD in the first two stages remains a crucial treatment goal to prevent irreversible liver damage. While an imprecise measure for diagnosis, elevated plasma liver enzymes, alanine aminotransferase (ALT) and aspartate aminotransferase (AST), are often the first indication of liver injury (14). Recent work from our lab demonstrated the addition of serum alkaline phosphatase (ALP) to a prediction model of liver fibrosis ($\geq 2/4$ fibrosis score) in patients with obesity and NAFLD (21). Beyond blood markers, imaging techniques (i.e., ultrasound, magnetic resonance spectroscopy/imaging- MRS/MRI, transient elastography) are also frequently used to detect liver fat and estimate the level of scarring. These imaging methods are useful for establishing IHTG content, but a liver biopsy is required to diagnose NASH via histology for grading of steatosis, lobular inflammation, and hepatocellular ballooning – the components of the NAFLD activity score (NAS, 0-8) (22). If the disease progresses to cirrhosis and associated complications, a liver transplant may be advised, however work is ongoing to understand the reversibility of these advanced stages (23, 24). Further research is needed to understand the mechanisms that contribute to NAFLD progression and identify biomarkers that can detect early stages of NAFLD.

NAFLD pathogenesis

Despite the growing prevalence, the mechanisms contributing to NAFLD development are not fully understood. For many years a “two-hit” theory was used to explain NAFLD pathogenesis with the first “hit” being hepatic steatosis and the second “hit” being another factor that predisposed the liver to NASH development (e.g., oxidative stress) (25). With the identification of more advanced mechanisms, a new theory suggests multiple parallel “hits” contribute to the pathogenesis of NAFLD (26). These “hits” include the interactions between genetic, environmental, hormonal, and dietary factors in addition to inter-organ cross talk (26-28). Overnutrition and inactivity (positive energy balance) may result in obesity and excess nutrient flux that overload hepatic metabolic pathways. This is exacerbated through the loss of tissue insulin sensitivity, a key factor contributing to the progression of NAFLD (29).

Multi-tissue insulin resistance

Loss of post-receptor insulin signaling at the adipose tissue disrupts insulin-mediated suppression of lipolysis which subsequently increases circulating concentrations of free fatty acids (FFA) (29, 30). At the periphery, elevated FFA can promote the development of skeletal muscle insulin resistance thus reducing glucose uptake (31). At the liver, FFA can be re-esterified to TG, made into other lipid species, or oxidized in the mitochondria (32-34). Ultimately, some lipid is exported from the liver in very low-density lipoproteins (VLDL), however, the sum of the hepatic lipid export and oxidation often does not exceed the influx of FFA into the liver, resulting in an accumulation of liver fat (35). At the same time,

hepatic insulin resistance results in a failure to suppress gluconeogenesis thereby contributing to elevations in endogenous glucose production (EGP) (29, 36). Elegant work has demonstrated a paradox known as selective hepatic insulin resistance in obesity and T2D where insulin fails to suppress EGP while simultaneously maintaining stimulation of key lipogenic regulatory control genes (36, 37). With regard to EGP, insulin should phosphorylate FoxO1 (forkhead box O1), a transcription factor for gluconeogenesis (GNG), at the liver which prevents the translocation to the nucleus (38). Ultimately this downregulates genes required for GNG (e.g., phosphoenolpyruvate carboxykinase, PEPCK and glucose-6-phosphatase, G6P). In a state of hepatic insulin resistance, the FoxO1 pathway becomes insulin-resistant and the expression of PEPCK and G6P remain high as does EGP. On the other hand, lipogenesis promotes the conversion of carbons, from predominantly carbohydrate sources, to fatty acids through de novo lipogenesis (DNL, **figure 1.1**) (36) although select amino acids may also induce lipogenesis (39). While dietary and circulating FFA are recognized as contributing to steatosis (32-34, 40-42), dietary carbohydrates have been shown to play a major role in the development of NAFLD (43-45).

Lipid synthesis

DNL is a metabolic pathway responsible for the conversion of carbohydrates to fatty acids occurring predominantly in the liver (36). Sterol regulatory element binding protein (SREBP-1c), a regulatory control gene of lipid synthesis, is activated in the presence of insulin (46). Once activated, SREBP-1c enhances

the transcription of genes involved in fatty acid biosynthesis (47, 48). As shown in **figure 1.1**, four key enzymes are involved in the lipogenic pathway; acetyl coenzyme-A carboxylase (ACC), fatty acid synthase (FASN), stearoyl-CoA desaturase (SCD), and a set of enzymes called elongases (ELOV). The primary product of lipogenesis is the saturated palmitic acid (16:0). Once formed, the fatty acids may then be elongated and desaturated by the ELOV and SCD-1 enzymes, respectively. They may also be used for energy production through beta-oxidation (β -ox) or esterified to form TG, phospholipids, and other bioactive lipid species like ceramides (CER). Both SREBP-1c and the enzymes within the DNL pathway are elevated in animal and cell culture models of NAFLD (49-55) and secretions as well as humans with NAFLD (49, 56, 57).

Lipid sources: DNL is uniquely elevated in NAFLD

In addition to hepatic DNL, two additional sources of fatty acids funnel into liver TG synthesis – dietary fatty acids and those that arise from adipose tissue lipolysis (58-60). Within the intestinal lumen, pancreatic lipases hydrolyze dietary lipids and the resulting FFA and monoglycerides (MAG) enter the enterocyte through a transporter (CD36) for synthesis of TG, phospholipids, and cholesterol esters at the endoplasmic reticulum (ER). The lipids may either be stored in the cytosol or added to chylomicrons through microsomal TG transfer protein (MTP) with ApoB48, transported to the Golgi, and then released into circulation from the basolateral side (61). The TG rich particle then deposits lipids into peripheral tissues through endothelial bound lipoprotein lipase (LPL) and chylomicron

remnants are eventually taken up by the liver. At adipose tissue, stored TG are hydrolyzed to FFA and glycerol through adipose TG lipase (ATGL), hormone sensitive lipase (HSL), and monoglyceride lipase (MGL) and can be re-esterified or released into circulation where they are taken up at the liver for TG synthesis. From hepatic DNL, fatty acyl-CoAs are formed, some are elongated and desaturated. Fatty acids from these three (dietary, adipose, and DNL) sources are then added to glycerol-3 phosphate, forming lysophosphatidate. A second acyl-CoA is added to form phosphatidate and then converted to a diglyceride (DAG). DAGs may also be formed directly from monoglycerides and can be added to a VLDL particle without receiving a third fatty acid (62). Alternatively, a third fatty acyl-CoA is added to DAG via diacylglycerol acyltransferase enzyme (DGAT) to form a TG molecule. In addition to DAG and TG, CERs are also formed from fatty-acyl CoA within the liver. As shown in **figure 1.1**, the newly-formed TG (DAG or CER) may then be shunted to hepatic storage or undergo VLDL assembly for secretion. The isoforms (1 and 2) of the DGAT enzyme are used to incorporate TG onto a pre-VLDL particle (in the presence of Apolipoprotein B-100 (apoB100) or into a lipid droplet for storage, respectively. MTP is responsible for transferring the bulk of TG (and other lipids like CERs (63)) to the endoplasmic reticulum for VLDL assembly and is required for the secretion of apoB100 from the liver (64). CERs are also transferred directly from the ER to the Golgi through CER transfer protein (CERT). Using stable isotopic labeling, our group previously demonstrated a strong correlation between labeled liver-TG and labeled VLDL-TG (arising from diet, adipose, or DNL) (60, 65)

supporting the utility of VLDL-TG in noninvasively measuring the incorporation of various sources of fatty acids into hepatic TG synthesis .

Previous work from the Parks lab studying individuals with NAFLD has demonstrated more than half of hepatic TG arises from circulating FFA (60%), around 15% from dietary fat, and greater than 25% originates from DNL (65). Our group (60, 65), and others (46, 66-68), have demonstrated VLDL-TG arising from DNL is uniquely elevated in individuals with high liver fat when compared to subjects with low liver fat. Considering these strong data, pharmacological therapies targeting enzymes within the DNL pathway have been developed and tested. In early clinical trials, these drugs have been shown to reduce DNL and IHTG in subjects with NAFLD and the metabolic syndrome (49, 69-73). Other drugs including glucose-lowering drugs, statins or other lipid-lowering medications, antioxidants, and bile agonists have also been targets to treat NAFLD (reviewed here: (74-79)), however, no pharmacological therapies are approved for the direct treatment of NAFLD. Instead, the current guidelines support general strategies like lifestyle modification promoting weight loss and the control and correction of associated risk factors (cardiovascular, hepatic, extra-hepatic etc.) for the treatment and prevention of the disease (74).

NAFLD treatment

General strategies

Four general strategies have been applied for the treatment and management of NAFLD, they include: 1 – indirect pharmacological treatments (e.g., glucose-lowering therapies, antioxidants), 2 – bariatric surgery, 3 – in select cases, liver transplantation, and 4 – in most cases, lifestyle modifications. While no specific agents are available for the treatment of NAFLD, many potential pharmacological therapies have been investigated over the last few decades (74-79). These therapies have specifically targeted insulin resistance and/or lipid metabolism¹, lipotoxicity and oxidative stress², inflammation and immune activation³, apoptosis and necrosis⁴, and fibrogenesis or collagen turnover⁵. Alternatively, data support bariatric surgery in reducing histological severity of steatosis, inflammation, ballooning, and fibrosis in many, but not all who undergo the surgery (80-84). In the most advanced cases of the disease, like NASH-cirrhosis, liver transplantation may be indicated (85). Finally, a large body of evidence supports lifestyle modification with an emphasis on gradual weight loss as an effective approach to manage NAFLD and NASH (14, 86-89). Indeed, these investigations have demonstrated improvements in plasma liver enzymes, liver fat content, degree of hepatic inflammation, and fibrosis in addition to the

¹ Glucose lowering: biguanides, PPAR γ agonists - thiazolidinediones, GLP-1 receptor agonists, SGLT-2 inhibitors

Lipid lowering: statins, ezetimibe, fibrates, omega – 3 PUFAs

Farnesoid X receptor agonists: obeticholic acid, tropifexor

DGAT2 inhibitors

Thyroid hormone receptor agonists

² Antioxidants: vitamin E

³ CCR2/5 inhibitor: Cenicriviroc

⁴ Pan-caspase inhibitor: Emricasan

⁵ Immunomodulator via LOXL2: simtuzumab

ASK-1 inhibitor: selonsertib

regression of many underlying factors associated with NAFLD risk like obesity, T2D, and hyperlipidemia (90). These lifestyle investigations are described in more detail below.

Energy restriction, exercise training, and combined lifestyle interventions

The current guidelines set forth by the American Association for the Study of Liver Diseases (AASLD), the European Association for the Study of the Liver (EASL), and the National Institute for Health and Care Excellence (NICE) recommend a 5-10% weight loss through energy restriction (500-1,000 kcal/day) and moderate intensity physical activity (14, 86, 87). Many dietary patterns have been tested in individuals with NAFLD (91). In particular, the Mediterranean diet is recommended by AASLD. Small clinical trials testing this diet in NAFLD subjects reported reductions in liver fat and improvements to metabolic profiles, regardless of weight loss (14, 86). Nevertheless, energy restriction lessens the burden on the liver by relieving it of chronic overnutrition and the associated nutrient toxicity that contributes to IHTG accumulation (92-95) and therefore *remains the key recommendation for the management of NAFLD*. In a study from the Parks lab including 10 men and women with NAFLD, weight loss through energy restriction (~550 kcal/day) over six months resulted in a significant reduction in liver fat content measured via MRS (**figure 1.2**, (59, 60)). Many other studies examining impacts of dietary restrictions on liver fat have used noninvasive imaging methods (92, 96-99) while very few studies have reported direct histological outcomes (100, 101). One pilot study examining the

effects of a low carbohydrate, ketogenic diet in five subjects with biopsy-proven NAFLD reported a reduction in steatosis, inflammation, and fibrosis after an average weight loss of 10.9% (101). While these data are promising, dietary modification is only one method to offset energy balance. Increasing energy expenditure through physical activity is another method that has been studied extensively in subjects with NAFLD.

Increased physical activity through both aerobic and resistance training, with (102-105) or without (106-113) weight loss has reduced hepatic fat content. Recently, high intensity interval training (HIIT) has gained popularity owing to its effectiveness in the treatment of NAFLD (112, 114, 115), through reductions in liver fat (116), the time effectiveness, and safety of the exercise modality (117, 118). Recent work from our group showed similar reductions in IHTG when adults with obesity underwent HIIT or moderate intensity continuous training (MICT), matched for energy expenditure (~400 kcal/session) (108). Subjects were randomized to complete four weeks of HIIT ($n = 8$) or MICT ($n = 8$) and liver fat, measured via MRS, was tightly matched between the training groups at baseline. After training, a $20.1 \pm 6.6\%$ and $37.0 \pm 12.4\%$ reduction in IHTG was reported in MICT and HIIT groups, respectively (**figure 1.3**). Overall, this study demonstrated the effectiveness of HIIT in reducing liver fat in subjects with obesity, independent of any significant reductions in body weight.

Lifestyle intervention programs in which both energy restriction and exercise are combined have demonstrated robust reductions in liver fat (90, 119-122) and a some studies have assessed histological changes (89, 90, 100, 119, 123-126). In lifestyle intervention studies with repeat liver biopsies, a weight loss of 5% reduced steatosis, 7-9% reduced inflammation and ballooning, while a 10% or greater weight loss exerted the greatest effect on fibrosis and resolved NASH in 90% of subjects (74, 89). While these are promising findings, studies with repeat liver biopsies examining the effect of lifestyle modifications, via energy restriction and exercise, on NASH regression are limited. Thus, *we will examine the impact of a lifestyle intervention – weight loss via energy restriction and exercise – on histological outcomes in individuals with NASH (Aim 1a, figure 1.8A)*. Beyond liver fat and histology, both energy restriction and exercise have been shown to modulate key factors that characterize NAFLD – e.g., insulin sensitivity and lipid synthesis. While the precise mechanisms by which energy restriction and exercise exert beneficial impacts on hepatic and peripheral outcomes is not well understood and is likely multifactorial. Further investigation is needed to understand the combined effects of a rigorous lifestyle intervention on said factors associated with NAFLD.

Lifestyle interventions on insulin sensitivity

It is well established that insulin sensitivity declines in NAFLD (97, 127-129). Development of insulin resistance has been implicated in contributing to the pathogenesis of NAFLD and progression to more advance forms of the disease,

like NASH (130, 131). Thus, treatments that improve insulin resistance may be effective therapies to manage NAFLD. Lifestyle interventions have been tested in NAFLD patients to understand their impact on glucose control and insulin sensitivity. Most of these studies report data from oral glucose tolerance tests (OGTT) and validated models like the homeostatic model assessment for insulin resistance (HOMA-IR) (132), while fewer treatment studies have utilized the gold standard, hyperinsulinemic-euglycemic clamp technique. In regards to dietary interventions, many studies have reported a reduction in EGP with an improved ability to suppress EGP (92, 96, 133-135) while some (96-98, 134), but not all (92, 94), demonstrated increased glucose rate of disposal (R_d) or overall insulin sensitivity (as reported by glucose infusion rates). These improvements in EGP and glucose disposal have been shown with (92, 96, 97, 133-135) and without (98) significant weight loss. Interventions specifically testing exercise training have reported improvements in R_d with little change in absolute EGP or EGP suppression (109, 110, 136-141). In general, these results are similar between aerobic and resistance training although one study in adolescent boys with obesity found resistance exercise improved R_d compared to sedentary controls while aerobic exercise did not (138). Some (109, 110, 138) but not all (136, 137) of the reported improvements in R_d with exercise are independent of significant weight loss. One study compared an exercise intervention with and without weight loss and observed similar improvements in R_d with no change in EGP in both groups (140). Conversely, a similar study found exercise with or without weight loss improved both glucose disposal and EGP suppression (141). Fewer

studies have examined the combined effects of diet and exercise programs on insulin sensitivity in NAFLD (94, 123, 140, 142, 143). In a population of biopsy-diagnosed NASH patients, a hypocaloric diet and daily aerobic exercise (40 minutes) reduced liver disease severity (as reported by NAS) by 50% on average and insulin sensitivity via the HOMA-IR improved significantly (35% reduction) (123). Another report found reduced IHTG and increased glucose infusion rate, suggesting improved glucose sensitivity, in subjects with T2D who underwent a two-week diet and exercise intervention (94). A one-year intensive lifestyle intervention (body weight reduction ~10% via 500 kcal/day deficit and moderate physical activity ≥ 175 minutes/week) in subjects with obesity demonstrated a reduction in liver fat with concomitant increase in R_d (142). In a similar study of subjects with T2D, six months of nutritional therapy (~500 kcal/day deficit) with encouragement to gradually increase moderate physical activity (40-60 minutes/week) reduced EGP by 46% while R_d significantly increased by 35% (143). In sum, these data support lifestyle interventions that include both energy restriction and exercise in improving both hepatic and peripheral insulin sensitivity in subjects with obesity and elevated liver fat.

Lifestyle interventions on hepatic lipogenesis

As described above, an interaction exists between insulin resistance and lipid synthesis in NAFLD. Recent work demonstrated hepatic lipogenesis was inversely related to hepatic and whole-body insulin sensitivity while hyperglycemia and hyperinsulinemia were positively related to DNL (97). These

results suggest hepatic DNL, a key contributor to hepatic fat content, is partially driven by factors associated with insulin resistance, namely elevated circulating glucose and insulin concentrations. Utilizing stable isotope methods described above, the Parks lab (59, 60) and others (97) have measured DNL in individuals with NAFLD, before and after weight loss through energy restriction. In the same subjects from **figure 1.2** who underwent energy restriction for weight loss, our group found VLDL-TG DNL was reduced 57% (**figure 1.4**). Another study found a 35% reduction in TG-rich lipoproteins (TRL)-TG DNL with the same amount of weight loss (97). Overall, newly-made lipids contribute significantly to IHTG and their synthesis is stimulated in hyperinsulinemic and hyperglycemic states. *In subjects with NASH, we will quantify the changes in peripheral and hepatic nutrient kinetics to understand the effects of a lifestyle intervention on insulin sensitivity, lipid metabolism, and the relationships with liver histology (Aim 1b, figure 1.8B).*

Liver fat accumulation contributes to hepatic lipotoxicity (144, 145) through the accumulation of bioactive lipid species (144, 146-148). For example, CERs and DAGs have received attention for their pro-inflammatory and pro-apoptotic effects in the liver (149-154) and other tissues (e.g., promoting insulin resistance) (155-158).

Ceramides: Structure and metabolism

CERs are sphingolipids which consist of a sphingoid base (sphingosine) *N*-linked to a variety of fatty acyl groups (**figure 1.5A**). Unlike DAGs, CERs are structural lipid molecules often found in membranes and are minor constituents of the cellular lipidome when compared to glycerolipids (62, 159). CERs may be synthesized through multiple pathways – the three most common are the de novo, recycling, and salvage pathways. De novo CER synthesis occurs in the endoplasmic reticulum (ER) with strong evidence to suggest the enzymes involved are located on the cytosolic leaflet (160). The pathway, shown in **figure 1.5B**, begins with the rate-limiting step catalyzed by serine palmitoyl transferase (SPT). Through condensation of serine and palmitoyl coenzyme-A (CoA), 3-keto-dihydrosphingosine is formed and then rapidly reduced to dihydrosphingosine (161). From here, dihydrosphingosine is *N*-acylated by one of six ceramide synthases (CerS1-6, specific to fatty acid, **figure 1.5C**) to form dihydroceramides (dhCERs) which are desaturated to form CERs. The enzymes within the CER biosynthetic pathway have also been located within the mitochondria, thus CERs may also be formed in other cellular organelles (162). The recycling pathway converts sphingomyelin to CER through sphingomyelinase and the salvage pathway reforms CER via a synthase from sphingosine (derived from more complex sphingolipids) (163).

Many early studies used thin layer chromatography and the diacylglycerol kinase assay to quantify CERs, however within the past 20 years, mass detection and quantitation of CER has been accomplished with mass spectrometry (MS) (164,

165). Most of the recent literature reporting CER content has employed liquid chromatography tandem MS (LC-MS/MS) multiple reaction monitoring (MRM) to quantify multiple CER species within a single run. These methods have been used to measure CERs within a context of insulin resistance, T2D, cardiovascular disease, and NAFLD (156, 166-169). While CER synthesis can occur in all organs, evidence from cell culture, animal models, and humans suggest the liver is a key site for CER production (63, 168, 170, 171). Data support de novo synthesis as contributing the greatest amount of CER to the total liver pool, thus this pathway is a target for development of new pharmacologic compounds to reduce CER synthesis in humans (150). Once formed in the ER, de novo CERs are transferred to the Golgi to serve as a substrate for more complex sphingolipids (172) or may be packed in very low-density lipoproteins (VLDL) and secreted into circulation (173-175). The amount of CER within the plasma compartment is predictive of metabolic disease risk including NAFLD/NASH (120, 148, 149, 155, 176-181).

Ceramides in NAFLD and lifestyle interventions

An increasing number of studies have highlighted the link between elevated plasma and liver CER concentrations and various measures of NAFLD/NASH and other metabolic and cardiovascular diseases (120, 148-150, 152, 153, 155, 176-195). In a recent report, serum CERs were measured in 104 humans across a spectrum of liver injury (healthy, NASH, and hepatitis B) (196). Total circulating CERs were highest in subjects with NASH (irrespective of hepatitis B status)

although limited data on specific CER species were available. In eight subjects undergoing bariatric surgery, total CER concentrations were compared between serum and liver tissue (197). The relative amount of CERs were similar in the serum and liver but overall made up a very small portion of the lipidome.

Unfortunately, this study did not report the content of individual CER species.

Specific CER species have been characterized as lipotoxic (16:0, 18:0) (149-153) while others appear protective (24:0) (191, 192) and ratios between these species (16:0/24:0 and 18:0/24:0) have recently been used to assess disease risk (195).

Dietary (194, 198-202) and exercise (202-206) interventions have been applied in human populations to determine the impact on plasma CER content and composition. In terms of dietary interventions, a subtrial of the PREDIMED studies showed a Mediterranean diet maintained CER concentrations over a year while participants with no dietary modifications increased plasma CER concentrations and risk of a cardiovascular event (198). Alternatively, in subjects with obesity, overfeeding saturated fatty acids for three to eight weeks resulted in elevated IHTG and plasma CER concentrations while overfeeding unsaturated fat or carbohydrates did not (194, 201). These findings were recently confirmed in healthy subjects during a short-term (two-week) study demonstrating a diet enriched with saturated fat (when compared to unsaturated fat) increased plasma CER and HOMA-IR (200). Interestingly, calorie restriction following saturated fat overfeeding reduced the adverse metabolic effects of the diet, including a

reduction of CER concentrations to the level of control subjects (201). Most (194, 198, 200-202), but not all (199, 202), studies support dietary modifications positively impacting plasma CERs through reductions in total CERs and specific lipotoxic species. No studies in humans have investigated CER concentrations directly in liver tissue in a setting of dietary modifications although many studies in rodent models have (149, 167, 207).

With regard to exercise interventions, most of the data available suggest an improvement in the CER plasma profile following training (i.e., less lipotoxic CER/reduced concentrations). In individuals with obesity, a 12-week high intensity training program reduced body weight and increased insulin sensitivity with a simultaneous reduction in total plasma CER. The change in CER was related to the change in insulin sensitivity – as CER went down, insulin sensitivity improved (204, 205). A collection of work has investigated CER within skeletal muscle. These studies reported an acute increase in skeletal muscle CER concentrations during or immediately following a bout of activity and a decrease in CER during recovery (203, 206). The reduction in muscle CER may be one mechanism that supports the insulin sensitizing effect of exercise on skeletal muscle (203, 206, 208-213). No studies have reported changes in liver CER content in a setting of exercise interventions.

Only one study has tested the impact of a diet and exercise intervention (two-month) in humans on plasma CER concentrations (214). Unexpectedly, the

lifestyle changes resulted in increased plasma CERs. One potential explanation for these results was the increase in physical activity. However, the intervention also resulted in no changes in weight, HOMA-IR, or lipid profiles, and therefore the results may also be explained by poor program efficacy. Strong evidence from patients who underwent gastric bypass surgery demonstrated significant reductions in plasma CER content that were related to the improvements in insulin sensitivity (185, 215, 216). Indeed, the addition of exercise following surgery resulted in even greater reductions in CER concentrations (216). Thus, *we aim to test the therapeutic effects of a nine-month lifestyle intervention on reducing plasma CER concentrations and improving the composition of the CER lipidome in subjects with NASH (Aim 1b, figure 1.8B).*

Ceramide kinetics

As already established, elevated plasma CER concentrations contribute to tissue dysfunction (149, 150, 176, 177, 182-187, 217) and are linked to NAFLD (150, 194). The kinetics of CER synthesis, which are not fully documented, may be more mechanistically related to cellular injury. New methods for isotopic labeling of CER synthesis have recently been published (164, 218). In cell culture and rodent models, kinetic studies using stable isotopes (168, 219-229) and non-naturally occurring odd-chain analogs (230, 231) are available, and in humans, CER synthesis in skeletal muscle has been measured via isotope labeling (232-234).

Much of the available literature measuring CER synthesis has focused on the incorporation of a tracer molecule into CER within cell culture lines (164). Studies have labeled CERs using polar molecules like serine (168, 223, 224, 226, 227), labeled fatty acids like palmitate (222, 223, 225, 228, 229), and, in rare cases, sphingolipids containing labeled fatty acids (228). Both labeled serine and palmitate can be incorporated into the backbone of the sphingolipid (**figure 1.5A-B**) through the SPT enzymatic reaction between palmitoyl-CoA and L-serine while palmitate can also be incorporated into the fatty acyl chain through CerS5 and CerS6 enzymes (**figure 1.5C**). Labeled serine and palmitate have been used in rodent models (219-221) while only one study has used labeled water (D₂O) to quantify CER kinetics in mice (219). In humans, a U-¹³C palmitate infusion has been used to determine the in vivo incorporation of plasma FFA into intramyocellular CER (232).

Our lab has recently labeled CER synthesis with a stable isotope of serine (¹³C₃,¹⁵N L-serine) in the serum, liver, and hepatic mitochondria of C57Bl/6 mice. **Figure 1.6** demonstrates the de novo synthesis pathway of CER using a ¹³C₃,¹⁵N L-serine molecule. The first and rate-limiting reaction, catalyzed by SPT, results in the loss of a CoA and a labeled CO₂ resulting in a mass shift of three for the labeled CER species on the MS (e.g., CER 16:0 unlabeled: 538 *m/z*, labeled: 541 *m/z*). **Figure 1.7** presents preliminary data in which serum, liver, and mitochondrial CER 16:0 was labeled with ¹³C₃,¹⁵N L-serine – dissolved in the drinking water. This results in an isotopic enrichment (%E) of the CER molecules

extracted from the respective biological specimens between 1-3%E. The same method will be used to quantify CER 16:0 kinetics in the current study. The ability to measure ceramide kinetics in vivo may support the investigation of potential therapeutic targets aimed at altering CER pathway biology. We will use stable isotopes to establish and optimize a method in mice to measure liver and mitochondrial CER synthesis (Aim 2a, **figure 1.8C**). Furthermore, we aim to test whether liver CER synthesis plays a role in mitochondrial CER content and measure how an acute, high fat diet alters the synthesis and composition of newly-made CERs (Aim 2b, **figure 1.8C**).

SPECIFIC AIMS

Aim 1a: Determine the therapeutic effect of a lifestyle intervention (energy restriction and exercise) on histology in individuals with biopsy-proven

NASH. Subjects with histologically-confirmed NASH enter a nine-month lifestyle intervention aimed at weight loss through energy restriction and HIIT. Subjects undergo liver biopsies before and after the intervention to grade for severity of disease. Changes in liver histology are compared to subjects receiving standard care. *We hypothesize the lifestyle intervention will reduce histological features of NASH including steatosis, hepatocellular ballooning, lobular inflammation, and fibrosis.*

Aim 1b: Using stable isotopes, quantify the changes in peripheral nutrient disposal and hepatic nutrient flux to understand the impact on insulin

sensitivity, plasma CERs, and the relationship with liver histology. The same subjects from aim 1a undergo extensive metabolic testing pre- and post-intervention to determine the rates of nutrient production and clearance (glucose and FFA) during fasting and insulin-stimulated conditions. Plasma CERs are measured to investigate the impact of a lifestyle intervention on species composition and content. *We hypothesize, when compared to standard care, active treatment will improve hepatic and peripheral glucose metabolism, lipid metabolism – FFA suppression and DNL, and plasma CER profiles. These findings will be related to the changes in liver histology.*

Aim 2a: Using an L-serine stable isotope, quantitate the synthesis of newly-made CER in liver and hepatic mitochondria in male and female mice. Control diet (20% protein, 70% carbohydrate, 10% fat) fed male and female C57Bl/6 consume $^{13}\text{C}_3$, ^{15}N L-serine, dissolved in the drinking water, to labeled newly-made liver and hepatic mitochondria CER. Labeled CER is measured using targeted high performance (HP)LC-MS/MS MRM analysis. *While this aim is designed for method development and optimization, we hypothesize the synthesis of liver CER will be related to mitochondrial CER content.*

Aim 2b: Determine if an acute, high fat diet alters the composition or synthesis of hepatic and mitochondrial CERs in male and female mice. The composition and turnover of liver and mitochondrial CER will be measured in male and female C57Bl/6 mice fed a high fat diet for two weeks (20% protein, 20% carbohydrate, 60% fat; sucrose content matched across aim 2a and 2b diets). *We hypothesize that an acute, high fat diet will shift the distribution of the CER profile to reflect the fatty acid composition of the diet and increase the synthesis of CER species when compared to control diet fed mice.*

Impact and innovation

This project 1- examines the effects of lifestyle intervention on histologic features in a population with NASH, 2- in the same subjects, quantifies nutrient flux and plasma CERs for direct comparisons with liver health changes, 3- optimizes a method to quantify the synthesis of newly-made liver and mitochondrial CERs, and 4- measures the impact of dietary fat on altering CER synthesis *in vivo*. The experiments described in this proposal are translational in nature, technically and conceptually innovative, and will produce results that will be applicable to multiple disciplines.

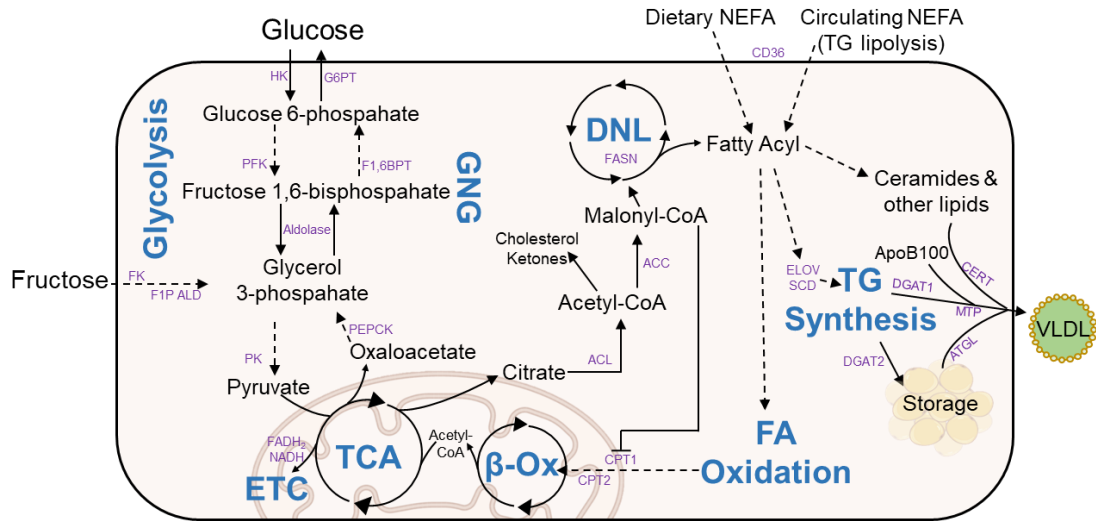
With specific regard to aim 1, the work proposed here translates the findings from multiple animal and human studies to an intervention in humans with direct measurements of liver histology before and after treatment. The results from our lifestyle intervention study will contribute to the development of future therapies to treat and prevent NASH. Additionally, it will advance our understanding of the role of liver energy partitioning in improving liver health and function. Together, these will support the therapeutic advancement of treatments for NASH and other metabolic diseases.

In aim 2, for the *first time*, *liver and mitochondrial CER turnover will be measured in vivo*. We will optimize a novel method to track CER synthesis and test these methods in an acute setting of overnutrition to determine the impact on CER turnover and composition. An overwhelming amount of evidence supports CERs in contributing to disease and the methods developed here will provide a better

understanding of CER flux in vivo. For future therapies aimed at modulating CER concentrations, the ability to measure and alter metabolic flux through the CER synthesis pathways represents the first step to achieve this goal. This proposal will advance the understanding of liver and mitochondrial CER synthesis and support the use of this method in future investigations, both clinical and preclinical, aimed at understanding the impact of CERs on metabolic diseases. In sum, this project is both highly impactful – through the translational nature of the experiments – and technically and conceptually innovative – through the development and use of methodology to measure newly-made CER.

FIGURES

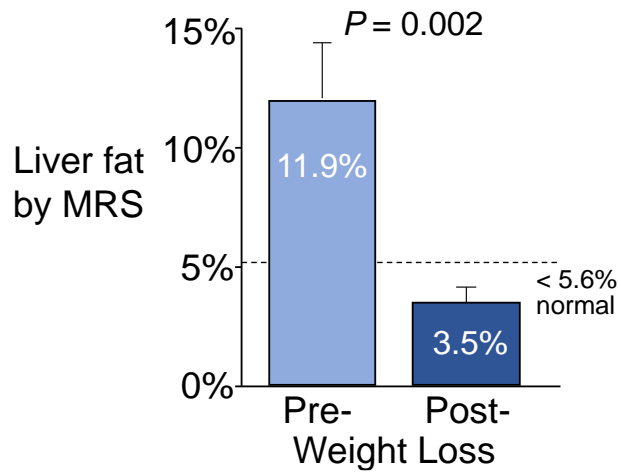
Figure 1.1. Integration of hepatic metabolic pathways



Abbreviations: ACC, acetyl-CoA carboxylase; ACL, ATP citrate lyase; ATGL, adipose triglyceride lipase; β -Ox, beta oxidation; CERT, ceramide transfer protein; CD36, cluster of differentiation 36 (fatty acid transporter); CoA, coenzyme A; DGAT1/2, diacylglycerol acyltransferase enzyme; DNL, de novo lipogenesis; ELOV, elongases; SCD, stearoyl CoA-desaturase; ETC, electron transport chain; FADH₂, flavin adenine dinucleotide; FASN, fatty acid synthase complex; FK, fructose kinase; F1P ALD, fructose 1-phosphatase aldolase; F1,6BPT, fructose 1,6 bisphosphatase; GNG, gluconeogenesis; G6PT, glucose 6 phosphatase; HK, hexokinase; MTP, microsomal TG transfer protein; NADH, nicotinamide adenine dinucleotide; NEFA, non-esterified fatty acids; PEPCK, phosphoenoyl pyruvate carboxykinase; PFK, phosphofruktokinase; PK, pyruvate kinase; TCA, tricarboxylic acid cycle; TG, triglyceride; VLDL, very low density lipoproteins.

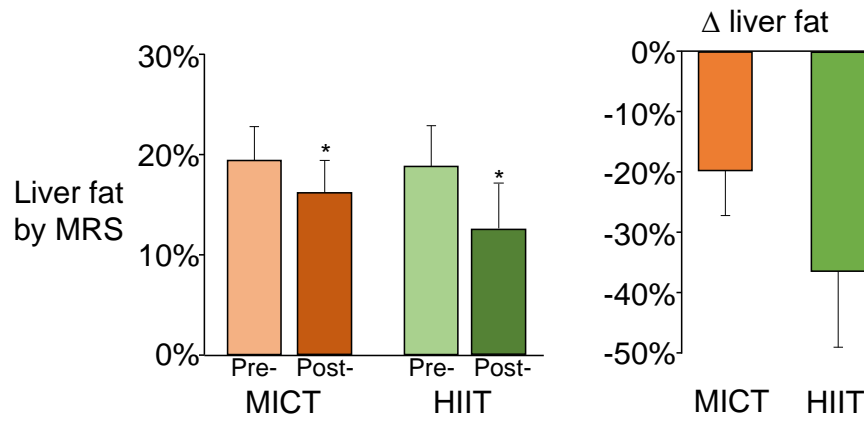
Not pictured: Glucose activation of carbohydrate response element binding protein (ChREBP) and insulin activation of sterol regulatory element-binding protein 1 (SREBP1c).

Figure 1.2. Reductions in liver fat with energy restriction



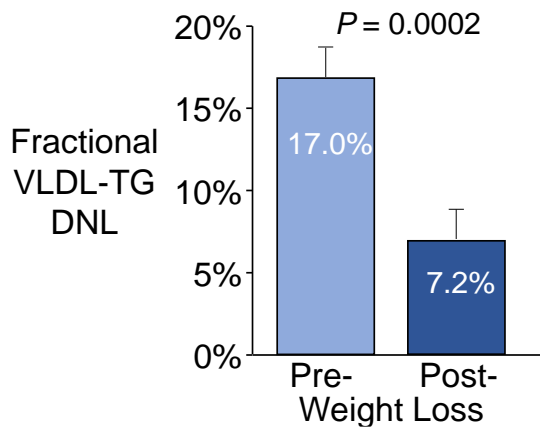
EJP unpublished data from (59, 60).

Figure 1.3. Reductions in liver fat with HIIT and MICT in adults with obesity



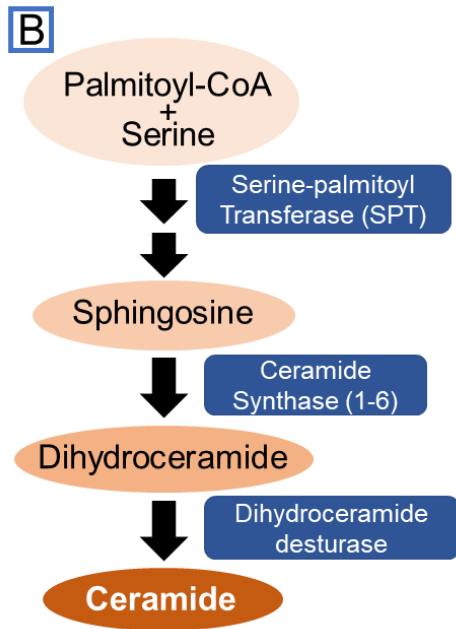
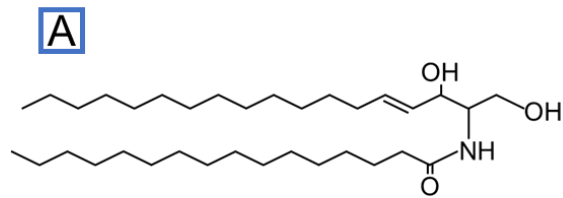
Data adapted from (108).
Data are mean \pm SEM. * $P < 0.05$

Figure 1.4. Reductions in VLDL-TG DNL with diet



EJP unpublished data from (59, 60).

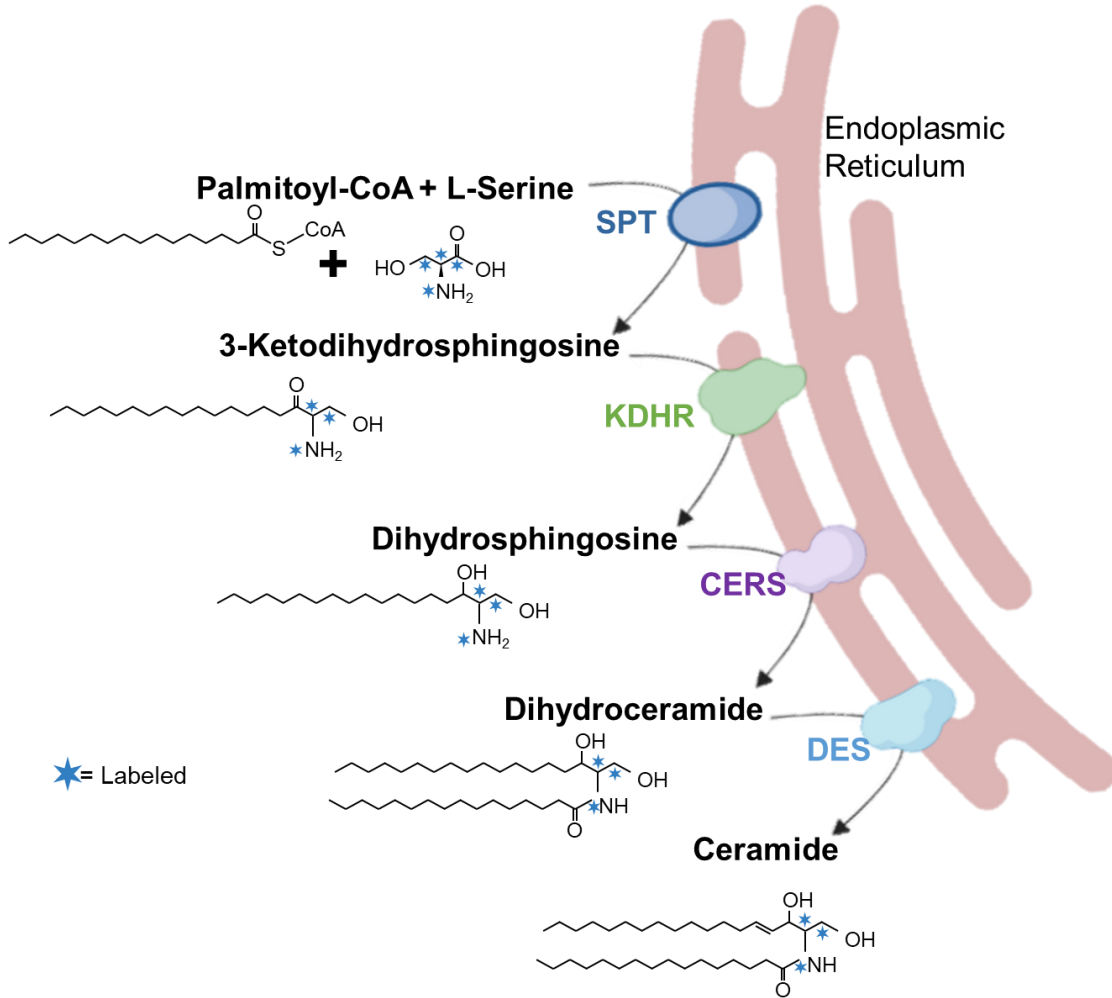
Figure 1.5. 16:0 CER (A), a product of de novo CER synthesis (B), and (C) acyl chain length specific to the CERS1-6



C

CERS	Acyl Chain
CERS1	C18:0
CERS2	C20:0-C26:0
CERS3	C22:0-C26:0
CERS4	C18:0, C20:0
CERS5	C16:0
CERS6	C14:0, C16:0

Figure 1.6. De novo CER synthesis with $^{13}\text{C}_3,^{15}\text{N}$ L-serine



Abbreviations: SPT, Serine-palmitoyl transferase; KDHR, 3-ketodihydrosphingosine reductase; CERS, ceramide synthase 1-6 – fatty acyl chain length listed in **figure 1.5C**; DES, dihydroceramide desaturase

Figure 1.7. Serine-labeled serum, liver, and mitochondrial 16:0 CER

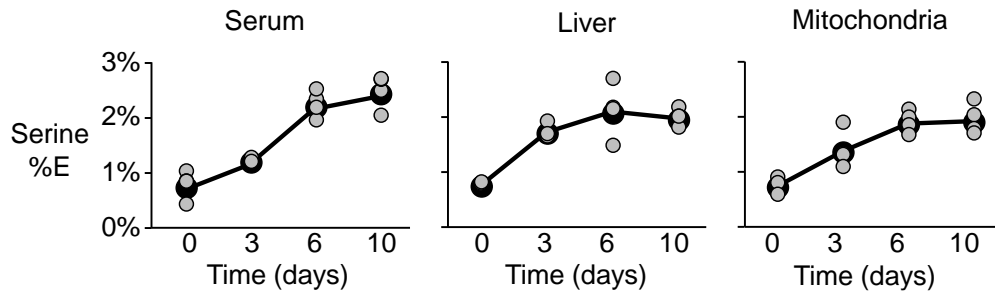
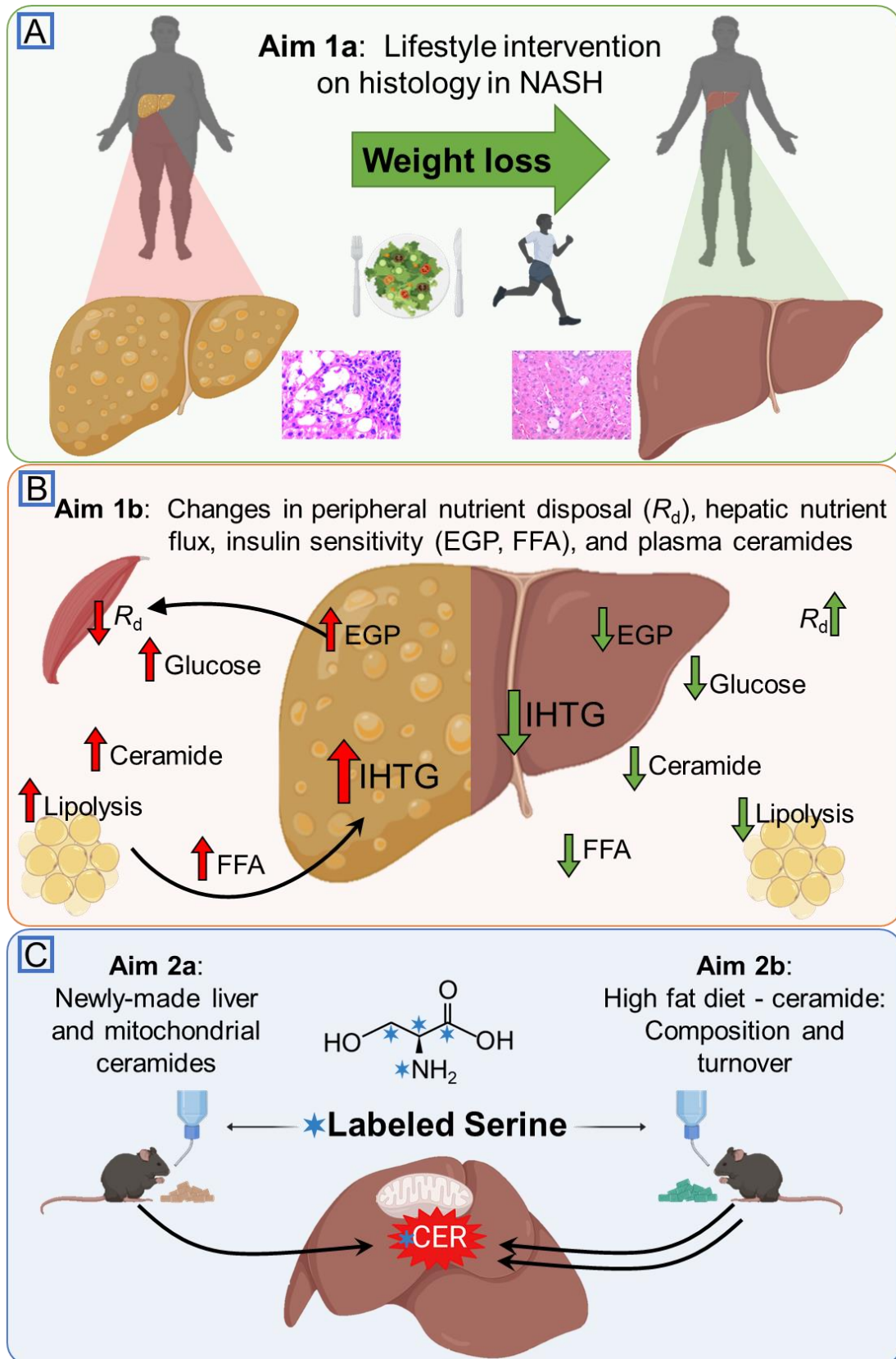


Figure 1.8. Schematic illustrating specific aims 1 and 2



Abbreviations: CER, ceramide; EGP, endogenous glucose production; FFA, free fatty acids; IHTG, intrahepatic triglyceride; NASH, nonalcoholic steatohepatitis
 R_d , rate of glucose disposal.

- A:** Aim 1a - Impacts of lifestyle intervention (weight loss via energy restriction and exercise) on histological outcomes in subjects with NASH.
- B:** Aim 1b - Changes in nutrient flux – hepatic and peripheral – on insulin sensitivity and plasma ceramides in relation to the histological changes observed from aim 1a.
- C:** Aim 2a - Tracing the synthesis of ceramides in mouse liver and mitochondria using a labeled L-serine stable isotope, and Aim 2b - assessing the impacts of an acute, high fat diet on the composition and turnover of ceramides.

REFERENCES

1. Beringer A, and Thaler H. Relationships between diabetes mellitus and fatty liver. *Deutsche Medizinische Wochenschrift* 95, 836-838, (1970), PMID:5439535.
2. Ludwig J, Viggiano TR, McGill DB, and Oh BJ. Nonalcoholic steatohepatitis: Mayo Clinic experiences with a hitherto unnamed disease. *Mayo Clinic Proceedings* 55, 434-438, (1980), PMID:7382552.
3. Kleiner DE, Brunt EM, Van Natta M, Behling C, Contos MJ, Cummings OW, Ferrell LD, Liu Y-C, Torbenson MS, Unalp-Arida A, Yeh M, McCullough AJ, Sanyal AJ, and Network NSCR. Design and validation of a histological scoring system for nonalcoholic fatty liver disease. *Hepatology* 41, 1313-1321, (2005), PMID:15915461.
4. (UK) NGC. *Non-alcoholic fatty liver disease: Assessment and management*. London: National Institute for Health and Care Excellence (UK): 2016.
5. Tilg H, and Effenberger M. From NAFLD to MAFLD: when pathophysiology succeeds. *Nature Reviews Gastroenterology & Hepatology* 17, 387-388, (2020), PMID:32461575.
6. Eslam M, Newsome PN, Sarin SK, Anstee QM, Targher G, Romero-Gomez M, Zelber-Sagi S, Wai-Sun Wong V, Dufour J-F, Schattenberg JM, Kawaguchi T, Arrese M, Valenti L, Shiha G, Tiribelli C, Yki-Järvinen H, Fan J-G, Grønbaek H, Yilmaz Y, Cortez-Pinto H, Oliveira CP, Bedossa P, Adams LA, Zheng M-H, Fouad Y, Chan W-K, Mendez-Sanchez N, Ahn SH, Castera L, Bugianesi E, Ratziu V, and George J. A new definition for metabolic dysfunction-associated fatty liver disease: An international expert consensus statement. *Journal of Hepatology* 73, 202-209, (2020), PMID:32278004.
7. Mantovani A. MAFLD vs NAFLD: Where are we? *Digestive and Liver Disease* 53, 1368-1372, (2021), PMID:34108096.
8. Younossi Z, Anstee QM, Marietti M, Hardy T, Henry L, Eslam M, George J, and Bugianesi E. Global burden of NAFLD and NASH: trends, predictions, risk factors and prevention. *Nature Reviews Gastroenterology & Hepatology* 15, 11-20, (2017), PMID:28930295.
9. Dufour J-F, Scherer R, Balp M-M, McKenna SJ, Janssens N, Lopez P, and Pedrosa M. The global epidemiology of nonalcoholic steatohepatitis (NASH) and associated risk factors—A targeted literature review. *Endocrine and Metabolic Science* 3, 100089, (2021).
10. Younossi ZM, Stepanova M, Ong J, Trimble G, AlQahtani S, Younossi I, Ahmed A, Racila A, and Henry L. Nonalcoholic steatohepatitis is the most rapidly increasing indication for liver transplantation in the United States. *Clinical Gastroenterology and Hepatology* 19, 580-589.e585, (2021), PMID:32531342.
11. Byrne CD, and Targher G. NAFLD: A multisystem disease. *Journal of Hepatology* 62, S47-S64, (2015), PMID:25920090.

12. Lonardo A, Nascimbeni F, Mantovani A, and Targher G. Hypertension, diabetes, atherosclerosis and NASH: Cause or consequence? *Journal of Hepatology* 68, 335-352, (2018), PMID:29122390.
13. Byrne CD, and Targher G. NAFLD: a multisystem disease. *Journal of Hepatology* 62, S47-64, (2015), PMID:25920090.
14. Chalasani N, Younossi Z, Lavine JE, Diehl AM, Brunt EM, Cusi K, Charlton M, and Sanyal AJ. The diagnosis and management of non-alcoholic fatty liver disease: practice Guideline by the American Association for the Study of Liver Diseases, American College of Gastroenterology, and the American Gastroenterological Association. *Hepatology* 55, 2005-2023, (2012), PMID:22488764.
15. Kleiner DE, Brunt EM, Van Natta M, Behling C, Contos MJ, Cummings OW, Ferrell LD, Liu YC, Torbenson MS, Unalp-Arida A, Yeh M, McCullough AJ, and Sanyal AJ. Design and validation of a histological scoring system for nonalcoholic fatty liver disease. *Hepatology* 41, 1313-1321, (2005), PMID:15915461.
16. Anstee QM, Targher G, and Day CP. Progression of NAFLD to diabetes mellitus, cardiovascular disease or cirrhosis. *Nature Reviews: Gastroenterology & Hepatology* 10, 330-344, (2013), PMID:23507799.
17. Younossi ZM, Marchesini G, Pinto-Cortez H, and Petta S. Epidemiology of nonalcoholic fatty liver disease and nonalcoholic steatohepatitis: Implications for liver transplantation. *Transplantation* 103, 22-27, (2019), PMID:30335697.
18. Singh S, Allen AM, Wang Z, Prokop LJ, Murad MH, and Loomba R. Fibrosis progression in nonalcoholic fatty liver vs nonalcoholic steatohepatitis: a systematic review and meta-analysis of paired-biopsy studies. *Clinical Gastroenterology and Hepatology* 13, 643-654 e641-649; quiz e639-640, (2015), PMID:24768810.
19. Sanyal AJ, Harrison SA, Ratziu V, Abdelmalek MF, Diehl AM, Caldwell S, Shiffman ML, Aguilar Schall R, Jia C, McColgan B, Djedjos CS, McHutchison JG, Subramanian GM, Myers RP, Younossi Z, Muir AJ, Afdhal NH, Bosch J, and Goodman Z. The natural history of advanced fibrosis due to nonalcoholic steatohepatitis: Data from the Simtuzumab trials. *Hepatology* 70, 1913-1927, (2019), PMID:30993748.
20. Loomba R, and Adams LA. The 20% rule of NASH progression: The natural history of advanced fibrosis and cirrhosis caused by NASH. *Hepatology* 70, 1885-1888, (2019), PMID:31520407.
21. Ali AH, Petroski GF, Diaz-Arias AA, Al Juboori A, Wheeler AA, Ganga RR, Pitt JB, Spencer NM, Hammoud GM, Rector RS, Parks EJ, and Ibdah JA. A model incorporating serum alkaline phosphatase for prediction of liver fibrosis in adults with obesity and nonalcoholic fatty liver disease. *Journal of Clinical Medicine* 10, (2021), PMID:34362095.
22. Brunt EM, Janney CG, Bisceglie AM, Neuschwander-Tetri BA, and Bacon BR. Nonalcoholic steatohepatitis: a proposal for grading and staging the histological lesions. *The American Journal of Gastroenterology* 94, 2467-2474, (1999), PMID:10484010.

23. Glass LM, Dickson RC, Anderson JC, Suriawinata AA, Putra J, Berk BS, and Toor A. Total body weight loss of $\geq 10\%$ is associated with improved hepatic fibrosis in patients with nonalcoholic steatohepatitis. *Digestive Diseases and Sciences* 60, 1024-1030, (2015), PMID:25354830.
24. Caldwell SH, and Argo CK. Reversing advanced hepatic fibrosis in NASH: Clearly possible, but widely at hand? *Digestive Diseases and Sciences* 60, 810-812, (2015), PMID:25618312.
25. Day CP, and James OFW. Steatohepatitis: A tale of two "hits"? *Gastroenterology* 114, 842-845, (1998), PMID:9547102.
26. Tilg H, and Moschen AR. Evolution of inflammation in nonalcoholic fatty liver disease: the multiple parallel hits hypothesis. *Hepatology* 52, 1836-1846, (2010), PMID:21038418.
27. Makkonen J, Pietiläinen KH, Rissanen A, Kaprio J, and Yki-Järvinen H. Genetic factors contribute to variation in serum alanine aminotransferase activity independent of obesity and alcohol: a study in monozygotic and dizygotic twins. *Journal of Hepatology* 50, 1035-1042, (2009), PMID:19303161.
28. Romeo S, Kozlitina J, Xing C, Pertsemlidis A, Cox D, Pennacchio LA, Boerwinkle E, Cohen JC, and Hobbs HH. Genetic variation in PNPLA3 confers susceptibility to nonalcoholic fatty liver disease. *Nature Genetics* 40, 1461-1465, (2008), PMID:18820647.
29. Utzschneider KM, and Kahn SE. The role of insulin resistance in nonalcoholic fatty liver disease. *The Journal of Clinical Endocrinology & Metabolism* 91, 4753-4761, (2006), PMID:16968800.
30. Lomonaco R, Ortiz-Lopez C, Orsak B, Webb A, Hardies J, Darland C, Finch J, Gastaldelli A, Harrison S, Tio F, and Cusi K. Effect of adipose tissue insulin resistance on metabolic parameters and liver histology in obese patients with nonalcoholic fatty liver disease. *Hepatology* 55, 1389-1397, (2012), PMID:22183689.
31. Sylow L, Tokarz VL, Richter EA, and Klip A. The many actions of insulin in skeletal muscle, the paramount tissue determining glycemia. *Cell Metabolism* 33, 758-780, (2021), PMID: 33826918.
32. Sanyal AJ, Campbell-Sargent C, Mirshahi F, Rizzo WB, Contos MJ, Sterling RK, Luketic VA, Shiffman ML, and Clore JN. Nonalcoholic steatohepatitis: association of insulin resistance and mitochondrial abnormalities. *Gastroenterology* 120, 1183-1192, (2001), PMID:11266382.
33. Fabbrini E, Mohammed BS, Magkos F, Korenblat KM, Patterson BW, and Klein S. Alterations in adipose tissue and hepatic lipid kinetics in obese men and women with nonalcoholic fatty liver disease. *Gastroenterology* 134, 424-431, (2008), PMID:18242210.
34. Iozzo P, Turpeinen AK, Takala T, Oikonen V, Bergman Jr, Grönroos T, Ferrannini E, Nuutila P, and Knuuti J. Defective liver disposal of free fatty acids in patients with impaired glucose tolerance. *The Journal of Clinical Endocrinology & Metabolism* 89, 3496-3502, (2004), PMID:15240637.

35. Malhi H, and Gores G. Molecular mechanisms of lipotoxicity in nonalcoholic fatty liver disease. *Seminars in Liver Disease* 28, 360-369, (2008), PMID:18956292.
36. Brown MS, and Goldstein JL. Selective versus total insulin resistance: a pathogenic paradox. *Cell Metabolism* 7, 95-96, (2008), PMID:18249166.
37. Shimomura I, Matsuda M, Hammer RE, Bashmakov Y, Brown MS, and Goldstein JL. Decreased IRS-2 and increased SREBP-1c lead to mixed insulin resistance and sensitivity in livers of lipodystrophic and ob/ob mice. *Molecular Cell* 6, 77-86, (2000), PMID:10949029.
38. Matsumoto M, Han S, Kitamura T, and Accili D. Dual role of transcription factor FoxO1 in controlling hepatic insulin sensitivity and lipid metabolism. *Journal of Clinical Investigation* 116, 2464-2472, (2006), PMID:16906224.
39. Charidemou E, Ashmore T, Li X, McNally BD, West JA, Liggi S, Harvey M, Orford E, and Griffin JL. A randomized 3-way crossover study indicates that high-protein feeding induces de novo lipogenesis in healthy humans. *JCI Insight* 4, (2019), PMID:31145699.
40. Parks E, Yki-Järvinen H, and Hawkins M. Out of the frying pan: dietary saturated fat influences nonalcoholic fatty liver disease. *Journal of Clinical Investigation* 127, 454-456, (2017), PMID:28112684.
41. Rosqvist F, Iggman D, Kullberg J, Cedernaes J, Johansson HE, Larsson A, Johansson L, Ahlstrom H, Arner P, Dahlman I, and Riserus U. Overfeeding polyunsaturated and saturated fat causes distinct effects on liver and visceral fat accumulation in humans. *Diabetes* 63, 2356-2368, (2014), PMID:24550191.
42. Velázquez KT, Enos RT, Bader JE, Sougiannis AT, Carson MS, Chatzistamou I, Carson JA, Nagarkatti PS, Nagarkatti M, and Murphy EA. Prolonged high-fat-diet feeding promotes non-alcoholic fatty liver disease and alters gut microbiota in mice. *World Journal of Hepatology* 11, 619-637, (2019), PMID:31528245.
43. Basaranoglu M, Basaranoglu G, and Bugianesi E. Carbohydrate intake and nonalcoholic fatty liver disease: fructose as a weapon of mass destruction. *Hepatobiliary Surgery and Nutrition* 4, 109-116, (2015), PMID:26005677.
44. Lim JS, Mietus-Snyder M, Valente A, Schwarz JM, and Lustig RH. The role of fructose in the pathogenesis of NAFLD and the metabolic syndrome. *Nature Reviews Gastroenterology & Hepatology* 7, 251-264, (2010), PMID:20368739.
45. Todoric J, Di Caro G, Reibe S, Henstridge DC, Green CR, Vrbancic A, Ceteci F, Conche C, McNulty R, Shalpour S, Taniguchi K, Meikle PJ, Watrous JD, Moranchel R, Najhawan M, Jain M, Liu X, Kisseleva T, Diaz-Meco MT, Moscat J, Knight R, Greten FR, Lau LF, Metallo CM, Febbraio MA, and Karin M. Fructose stimulated de novo lipogenesis is promoted by inflammation. *Nature Metabolism* 2, 1034-1045, (2020), PMID:32839596.
46. Ferré P, and Fouchelle F. Hepatic steatosis: a role for de novo lipogenesis and the transcription factor SREBP-1c. *Diabetes, Obesity and Metabolism* 12, 83-92, (2010), PMID:21029304.

47. Horton JD, Goldstein JL, and Brown MS. SREBPs: activators of the complete program of cholesterol and fatty acid synthesis in the liver. *Journal of Clinical Investigation* 109, 1125-1131, (2002), PMID:11994399.
48. Brown MS, and Goldstein JL. The SREBP pathway: regulation of cholesterol metabolism by proteolysis of a membrane-bound transcription factor. *Cell* 89, 331-340, (1997), PMID:9150132.
49. Kim C-W, Addy C, Kusunoki J, Anderson NN, Deja S, Fu X, Burgess SC, Li C, Ruddy M, Chakravarthy M, Previs S, Milstein S, Fitzgerald K, Kelley DE, and Horton JD. Acetyl CoA Carboxylase Inhibition Reduces Hepatic Steatosis but Elevates Plasma Triglycerides in Mice and Humans: A Bedside to Bench Investigation. *Cell Metabolism* 26, 394-406.e396, (2017), PMID:28768177.
50. Savage DB, Choi CS, Samuel VT, Liu ZX, Zhang D, Wang A, Zhang XM, Cline GW, Yu XX, Geisler JG, Bhanot S, Monia BP, and Shulman GI. Reversal of diet-induced hepatic steatosis and hepatic insulin resistance by antisense oligonucleotide inhibitors of acetyl-CoA carboxylases 1 and 2. *Journal of Clinical Investigation* 116, 817-824, (2006), PMID:16485039.
51. Jiang G, Li Z, Liu F, Ellsworth K, Dallas-Yang Q, Wu M, Ronan J, Esau C, Murphy C, Szalkowski D, Bergeron R, Doebber T, and Zhang BB. Prevention of obesity in mice by antisense oligonucleotide inhibitors of stearoyl-CoA desaturase-1. *Journal of Clinical Investigation* 115, 1030-1038, (2005), PMID:15761499.
52. Mao J, DeMayo FJ, Li H, Abu-Elheiga L, Gu Z, Shaikenov TE, Kordari P, Chirala SS, Heird WC, and Wakil SJ. Liver-specific deletion of acetyl-CoA carboxylase 1 reduces hepatic triglyceride accumulation without affecting glucose homeostasis. *Proceedings of the National Academy of Sciences of the United States of America* 103, 8552-8557, (2006), PMID:16717184.
53. Matsuzaka T, and Shimano H. Insulin-dependent and -independent regulation of sterol regulatory element-binding protein-1c. *Journal of Diabetes Investigation* 4, 411-412, (2013), PMID:24843688.
54. Dif N, Euthine V, Gonnet E, Laville M, Vidal H, and Lefai E. Insulin activates human sterol-regulatory-element-binding protein-1c (SREBP-1c) promoter through SRE motifs. *Biochemical Journal* 400, 179-188, (2006), PMID:16831124.
55. Wu M, Singh SB, Wang J, Chung CC, Salituro G, Karanam BV, Lee SH, Powles M, Ellsworth KP, Lassman ME, Miller C, Myers RW, Tota MR, Zhang BB, and Li C. Antidiabetic and antisteatotic effects of the selective fatty acid synthase (FAS) inhibitor platensimycin in mouse models of diabetes. *Proceedings of the National Academy of Sciences of the United States of America* 108, 5378-5383, (2011), PMID:21389266.
56. Pettinelli P, Del Pozo T, Araya J, Rodrigo R, Araya AV, Smok G, Csendes A, Gutierrez L, Rojas J, Korn O, Maluenda F, Diaz JC, Rencoret G, Braghetto I, Castillo J, Poniachik J, and Videla LA. Enhancement in liver SREBP-1c/PPAR-alpha ratio and steatosis in obese patients: correlations with insulin resistance and n-3 long-chain polyunsaturated fatty acid

- depletion. *Biochimica et Biophysica Acta* 1792, 1080-1086, (2009), PMID:19733654.
57. Kohjima M, Enjoji M, Higuchi N, Kato M, Kotoh K, Yoshimoto T, Fujino T, Yada M, Yada R, Harada N, Takayanagi R, and Nakamuta M. Re-evaluation of fatty acid metabolism-related gene expression in nonalcoholic fatty liver disease. *International Journal of Molecular Medicine* 20, 351-358, (2007), PMID:17671740.
 58. Barrows BR, and Parks EJ. Contributions of different fatty acid sources to very low-density lipoprotein-triacylglycerol in the fasted and fed states. *Journal of Clinical Endocrinology and Metabolism* 91, 1446-1452, (2006), PMID:16449340.
 59. Jacome-Sosa MM, and Parks EJ. Fatty acid sources and their fluxes as they contribute to plasma triglyceride concentrations and fatty liver in humans. *Current Opinion in Lipidology* 25, 213-220, (2014), PMID:24785962.
 60. Lambert JE, Ramos-Roman MA, Browning JD, and Parks EJ. Increased de novo lipogenesis is a distinct characteristic of individuals with nonalcoholic fatty liver disease. *Gastroenterology* 146, 726-735, (2014), PMID:24316260.
 61. Xiao C, and Lewis GF. Regulation of chylomicron production in humans. *Biochimica et Biophysica Acta* 1821, 736-746, (2012), PMID:22001638.
 62. Mucinski JM, Manrique-Acevedo C, Kasumov T, Garrett TJ, Gaballah A, and Parks EJ. Relationships between very low-density lipoproteins-ceramides, -diacylglycerols, and -triacylglycerols in insulin-resistant men. *Lipids* 55, 387-393, (2020), PMID:32415687.
 63. Iqbal J, Walsh MT, Hammad SM, Cuchel M, Tarugi P, Hegele RA, Davidson NO, Rader DJ, Klein RL, and Hussain MM. Microsomal triglyceride transfer protein transfers and determines plasma concentrations of ceramide and sphingomyelin but not glycosylceramide. *Journal of Biological Chemistry* 290, 25863-25875, (2015), PMID:26350457.
 64. Raabe M, Veniant MM, Sullivan MA, Zlot CH, Bjorkegren J, Nielsen LB, Wong JS, Hamilton RL, and Young SG. Analysis of the role of microsomal triglyceride transfer protein in the liver of tissue-specific knockout mice. *Journal of Clinical Investigation* 103, 1287-1298, (1999), PMID:10225972.
 65. Donnelly KL, Smith CI, Schwarzenberg SJ, Jessurun J, Boldt MD, and Parks EJ. Sources of fatty acids stored in liver and secreted via lipoproteins in patients with nonalcoholic fatty liver disease. *Journal of Clinical Investigation* 115, 1343-1351, (2005), PMID:15864352.
 66. Schwarz JM, Linfoot P, Dare D, and Aghajanian K. Hepatic de novo lipogenesis in normoinsulinemic and hyperinsulinemic subjects consuming high-fat, low-carbohydrate and low-fat, high-carbohydrate isoenergetic diets. *American Journal of Clinical Nutrition* 77, 43-50, (2003), PMID:12499321.

67. Softic S, Cohen DE, and Kahn CR. Role of dietary fructose and hepatic de novo lipogenesis in fatty liver disease. *Digestive Diseases and Sciences* 61, 1282-1293, (2016), PMID:26856717.
68. Diraison F, Moulin P, and Beylot M. Contribution of hepatic de novo lipogenesis and reesterification of plasma non esterified fatty acids to plasma triglyceride synthesis during non-alcoholic fatty liver disease. *Diabetes & Metabolism Journal* 29, 478-485, (2003), PMID:14631324.
69. Syed-Abdul MM, Parks EJ, Gaballah AH, Bingham K, Hammoud GM, Kemble G, Buckley D, McCulloch W, and Manrique CM. First-in-class fatty acid synthase inhibitor TVB-2640 reduces hepatic de novo lipogenesis in males with metabolic abnormalities. *Hepatology*, (2019), PMID:31630414.
70. Francque S, Szabo G, Abdelmalek MF, Byrne CD, Cusi K, Dufour JF, Roden M, Sacks F, and Tacke F. Nonalcoholic steatohepatitis: the role of peroxisome proliferator-activated receptors. *Nature Reviews Gastroenterology & Hepatology* 18, 24-39, (2021), PMID:33093663.
71. Loomba R, Kayali Z, Nouredin M, Ruane P, Lawitz EJ, Bennett M, Wang L, Harting E, Tarrant JM, McColgan BJ, Chung C, Ray AS, Subramanian GM, Myers RP, Middleton MS, Lai M, Charlton M, and Harrison SA. GS-0976 Reduces hepatic steatosis and fibrosis markers in patients with nonalcoholic fatty liver disease. *Gastroenterology* 155, 1463-1473 e1466, (2018), PMID:30059671.
72. Lawitz EJ, Coste A, Poordad F, Alkhoury N, Loo N, McColgan BJ, Tarrant JM, Nguyen T, Han L, Chung C, Ray AS, McHutchison JG, Subramanian GM, Myers RP, Middleton MS, Sirlin C, Loomba R, Nyangau E, Fitch M, Li K, and Hellerstein M. Acetyl-CoA carboxylase inhibitor GS-0976 for 12 weeks reduces hepatic de novo lipogenesis and steatosis in patients with nonalcoholic steatohepatitis. *Clinical Gastroenterology and Hepatology* 16, 1983-1991 e1983, (2018), PMID:29705265.
73. Stiede K, Miao W, Blanchette HS, Beysen C, Harriman G, Harwood HJ, Jr., Kelley H, Kapeller R, Schmalbach T, and Westlin WF. Acetyl-coenzyme A carboxylase inhibition reduces de novo lipogenesis in overweight male subjects: A randomized, double-blind, crossover study. *Hepatology* 66, 324-334, (2017), PMID:28470676.
74. Mantovani A, and Dalbeni A. Treatments for NAFLD: State of art. *International Journal of Molecular Sciences* 22, (2021), PMID:33652942.
75. Mantovani A, Byrne CD, Scorletti E, Mantzoros CS, and Targher G. Efficacy and safety of anti-hyperglycaemic drugs in patients with non-alcoholic fatty liver disease with or without diabetes: An updated systematic review of randomized controlled trials. *Diabetes & Metabolism Journal* 46, 427-441, (2020), PMID:31923578.
76. Sanyal AJ, Chalasani N, Kowdley KV, McCullough A, Diehl AM, Bass NM, Neuschwander-Tetri BA, Lavine JE, Tonascia J, Unalp A, Van Natta M, Clark J, Brunt EM, Kleiner DE, Hoofnagle JH, Robuck PR, and Nash CRN. Pioglitazone, vitamin E, or placebo for nonalcoholic steatohepatitis. *New England Journal of Medicine* 362, 1675-1685, (2010), PMID:20427778.

77. Mantovani A, Petracca G, Beatrice G, Csermely A, Lonardo A, and Targher G. Glucagon-like peptide-1 receptor agonists for treatment of nonalcoholic fatty liver disease and nonalcoholic steatohepatitis: An updated meta-analysis of randomized controlled trials. *Metabolites* 11, (2021), PMID:33513761.
78. Mantovani A, Petracca G, Csermely A, Beatrice G, and Targher G. Sodium-glucose cotransporter-2 inhibitors for treatment of nonalcoholic fatty liver disease: A meta-analysis of randomized controlled trials. *Metabolites* 11, (2020), PMID:33396949.
79. Musso G, Cassader M, Paschetta E, and Gambino R. Thiazolidinediones and advanced liver fibrosis in nonalcoholic steatohepatitis: A meta-analysis. *JAMA Internal Medicine* 177, 633-640, (2017), PMID:28241279.
80. Laursen TL, Hagemann CA, Wei C, Kazankov K, Thomsen KL, Knop FK, and Gronbaek H. Bariatric surgery in patients with non-alcoholic fatty liver disease - from pathophysiology to clinical effects. *World Journal of Hepatology* 11, 138-149, (2019), PMID:30820265.
81. Lee Y, Doumouras AG, Yu J, Brar K, Banfield L, Gmora S, Anvari M, and Hong D. Complete resolution of nonalcoholic fatty liver disease after bariatric surgery: A systematic review and meta-analysis. *Clinical Gastroenterology and Hepatology* 17, 1040-1060 e1011, (2019), PMID:30326299.
82. Lassailly G, Caiazzo R, Buob D, Pigeyre M, Verkindt H, Labreuche J, Raverdy V, Leteurtre E, Dharancy S, Louvet A, Romon M, Duhamel A, Pattou F, and Mathurin P. Bariatric surgery reduces features of nonalcoholic steatohepatitis in morbidly obese patients. *Gastroenterology* 149, 379-388; quiz e315-376, (2015), PMID:25917783.
83. Caiazzo R, Lassailly G, Leteurtre E, Baud G, Verkindt H, Raverdy V, Buob D, Pigeyre M, Mathurin P, and Pattou F. Roux-en-Y gastric bypass versus adjustable gastric banding to reduce nonalcoholic fatty liver disease: a 5-year controlled longitudinal study. *Annals of Surgery* 260, 893-898; discussion 898-899, (2014), PMID:25379859.
84. Klein S, Mittendorfer B, Eagon JC, Patterson B, Grant L, Feirt N, Seki E, Brenner D, Korenblat K, and McCrea J. Gastric bypass surgery improves metabolic and hepatic abnormalities associated with nonalcoholic fatty liver disease. *Gastroenterology* 130, 1564-1572, (2006), PMID:16697719.
85. Pais R, Barritt ASt, Calmus Y, Scatton O, Runge T, Lebray P, Poynard T, Ratzu V, and Conti F. NAFLD and liver transplantation: Current burden and expected challenges. *Journal of Hepatology* 65, 1245-1257, (2016), PMID:27486010.
86. European Association for the Study of the L, European Association for the Study of D, and European Association for the Study of O. EASL-EASD-EASO Clinical Practice Guidelines for the management of non-alcoholic fatty liver disease. *Journal of Hepatology* 64, 1388-1402, (2016), PMID:27062661.

87. Glen J, Floros L, Day C, Pryke R, and Guideline Development G. Non-alcoholic fatty liver disease (NAFLD): summary of NICE guidance. *British Medical Journal* 354, i4428, (2016), PMID:27605111.
88. Petroni ML, Brodosi L, Bugianesi E, and Marchesini G. Management of non-alcoholic fatty liver disease. *British Medical Journal* 372, m4747, (2021), PMID:33461969.
89. Romero-Gomez M, Zelber-Sagi S, and Trenell M. Treatment of NAFLD with diet, physical activity and exercise. *Journal of Hepatology* 67, 829-846, (2017), PMID:28545937.
90. Vilar-Gomez E, Martinez-Perez Y, Calzadilla-Bertot L, Torres-Gonzalez A, Gra-Oramas B, Gonzalez-Fabian L, Friedman SL, Diago M, and Romero-Gomez M. Weight loss through lifestyle modification significantly reduces features of nonalcoholic steatohepatitis. *Gastroenterology* 149, 367-378.e365, (2015), PMID:25865049.
91. Moore MP, Cunningham RP, Dashek RJ, Mucinski JM, and Rector RS. A fad too far? Dietary strategies for the prevention and treatment of NAFLD. *Obesity (Silver Spring)*, (2020), PMID:32893456.
92. Petersen KF, Dufour S, Befroy D, Lehrke M, Hendler RE, and Shulman GI. Reversal of nonalcoholic hepatic steatosis, hepatic insulin resistance, and hyperglycemia by moderate weight reduction in patients with type 2 diabetes. *Diabetes* 54, 603-608, (2005), PMID:15734833.
93. Westerbacka J, Lammi K, Häkkinen A-M, Rissanen A, Salminen I, Aro A, and Yki-Järvinen H. Dietary fat content modifies liver fat in overweight nondiabetic subjects. *The Journal of Clinical Endocrinology & Metabolism* 90, 2804-2809, (2005), PMID:15741262.
94. Tamura Y, Tanaka Y, Sato F, Choi JB, Watada H, Niwa M, Kinoshita J, Ooka A, Kumashiro N, Igarashi Y, Kyogoku S, Maehara T, Kawasumi M, Hirose T, and Kawamori R. Effects of diet and exercise on muscle and liver intracellular lipid contents and insulin sensitivity in type 2 diabetic patients. *The Journal of Clinical Endocrinology & Metabolism* 90, 3191-3196, (2005), PMID:15769987.
95. Tamura S, and Shimomura I. Contribution of adipose tissue and de novo lipogenesis to nonalcoholic fatty liver disease. *The Journal of Clinical Investigation* 115, 1139-1142, (2005), PMID:15864343.
96. Yoshino M, Kayser BD, Yoshino J, Stein RI, Reeds D, Eagon JC, Eckhouse SR, Watrous JD, Jain M, Knight R, Schechtman K, Patterson BW, and Klein S. Effects of diet versus gastric bypass on metabolic function in diabetes. *The New England Journal of Medicine* 383, 721-732, (2020), PMID:32813948.
97. Smith GI, Shankaran M, Yoshino M, Schweitzer GG, Chondronikola M, Beals JW, Okunade AL, Patterson BW, Nyangau E, Field T, Sirlin CB, Talukdar S, Hellerstein MK, and Klein S. Insulin resistance drives hepatic de novo lipogenesis in nonalcoholic fatty liver disease. *Journal of Clinical Investigation* 130, 1453-1460, (2020), PMID:31805015.
98. Ryan MC, Itsiopoulos C, Thodis T, Ward G, Trost N, Hofferberth S, O'Dea K, Desmond PV, Johnson NA, and Wilson AM. The Mediterranean diet

- improves hepatic steatosis and insulin sensitivity in individuals with non-alcoholic fatty liver disease. *Journal of Hepatology* 59, 138-143, (2013), PMID:23485520.
99. Larson-Meyer DE, Newcomer BR, Heilbronn LK, Volaufova J, Smith SR, Alfonso AJ, Lefevre M, Rood JC, Williamson DA, Ravussin E, and Pennington CT. Effect of 6-month calorie restriction and exercise on serum and liver lipids and markers of liver function. *Obesity (Silver Spring)* 16, 1355-1362, (2008), PMID:18421281.
 100. Huang MA, Greenon JK, Chao C, Anderson L, Peterman D, Jacobson J, Emick D, Lok AS, and Conjeevaram HS. One-year intense nutritional counseling results in histological improvement in patients with non-alcoholic steatohepatitis: a pilot study. *The American Journal of Gastroenterology* 100, 1072-1081, (2005), PMID:15842581.
 101. Tendler D, Lin S, Yancy WS, Jr., Mavropoulos J, Sylvestre P, Rockey DC, and Westman EC. The effect of a low-carbohydrate, ketogenic diet on nonalcoholic fatty liver disease: a pilot study. *Digestive Diseases and Sciences* 52, 589-593, (2007), PMID:17219068.
 102. Zhang HJ, He J, Pan LL, Ma ZM, Han CK, Chen CS, Chen Z, Han HW, Chen S, Sun Q, Zhang JF, Li ZB, Yang SY, Li XJ, and Li XY. Effects of moderate and vigorous exercise on nonalcoholic fatty liver disease: A randomized clinical trial. *Journal of the American Medical Association Internal Medicine* 176, 1074-1082, (2016), PMID:27379904.
 103. Orzi LA, Gariani K, Oldani G, Delaune V, Morel P, and Toso C. Exercise-based interventions for nonalcoholic fatty liver disease: A meta-analysis and meta-regression. *Clinical Gastroenterology and Hepatology* 14, 1398-1411, (2016), PMID:27155553.
 104. Keating SE, Hackett DA, Parker HM, O'Connor HT, Gerofi JA, Sainsbury A, Baker MK, Chuter VH, Caterson ID, George J, and Johnson NA. Effect of aerobic exercise training dose on liver fat and visceral adiposity. *Journal of Hepatology* 63, 174-182, (2015), PMID:25863524.
 105. Kantartzis K, Thamer C, Peter A, Machann J, Schick F, Schraml C, Konigsrainer A, Konigsrainer I, Krober S, Niess A, Fritsche A, Haring HU, and Stefan N. High cardiorespiratory fitness is an independent predictor of the reduction in liver fat during a lifestyle intervention in non-alcoholic fatty liver disease. *Gut* 58, 1281-1288, (2009), PMID:19074179.
 106. Hallsworth K, Fattakhova G, Hollingsworth KG, Thoma C, Moore S, Taylor R, Day CP, and Trenell MI. Resistance exercise reduces liver fat and its mediators in non-alcoholic fatty liver disease independent of weight loss. *Gut* 60, 1278-1283, (2011), PMID:21708823.
 107. Sullivan S, Kirk EP, Mittendorfer B, Patterson BW, and Klein S. Randomized trial of exercise effect on intrahepatic triglyceride content and lipid kinetics in nonalcoholic fatty liver disease. *Hepatology* 55, 1738-1745, (2012), PMID:22213436.
 108. Winn NC, Liu Y, Rector RS, Parks EJ, Ibdah JA, and Kanaley JA. Energy-matched moderate and high intensity exercise training improves nonalcoholic fatty liver disease risk independent of changes in body mass

- or abdominal adiposity — A randomized trial. *Metabolism: Clinical and Experimental* 78, 128-140, (2018), PMID:28941598.
109. Sargeant JA, Bawden S, Aithal GP, Simpson EJ, Macdonald IA, Turner MC, Cegielski J, Smith K, Dorling JL, Gowland PA, Nimmo MA, and King JA. Effects of sprint interval training on ectopic lipids and tissue-specific insulin sensitivity in men with non-alcoholic fatty liver disease. *European Journal of Applied Physiology* 118, 817-828, (2018), PMID:29411128.
 110. Brouwers B, Schrauwen-Hinderling VB, Jelenik T, Gemmink A, Sparks LM, Havekes B, Bruls Y, Dahlmans D, Roden M, Hesselink MKC, and Schrauwen P. Exercise training reduces intrahepatic lipid content in people with and people without nonalcoholic fatty liver. *American Journal of Physiology: Endocrinology and Metabolism* 314, E165-E173, (2018), PMID:29118014.
 111. Johnson NA, and George J. Fitness versus fatness: moving beyond weight loss in nonalcoholic fatty liver disease. *Hepatology* 52, 370-381, (2010), PMID:20578153.
 112. van der Heijden GJ, Wang ZJ, Chu ZD, Sauer PJ, Haymond MW, Rodriguez LM, and Sunehag AL. A 12-week aerobic exercise program reduces hepatic fat accumulation and insulin resistance in obese, Hispanic adolescents. *Obesity (Silver Spring)* 18, 384-390, (2010), PMID:19696755.
 113. Keating SE, Hackett DA, George J, and Johnson NA. Exercise and non-alcoholic fatty liver disease: A systematic review and meta-analysis. *Journal of Hepatology* 57, 157-166, (2012).
 114. Trovato GM, Catalano D, Martines GF, Pirri C, and Trovato FM. Western dietary pattern and sedentary life: independent effects of diet and physical exercise intensity on NAFLD. *American Journal of Gastroenterology* 108, 1932-1933, (2013), PMID:24300872.
 115. Kistler KD, Brunt EM, Clark JM, Diehl AM, Sallis JF, Schwimmer JB, and Group NCR. Physical activity recommendations, exercise intensity, and histological severity of nonalcoholic fatty liver disease. *American Journal of Gastroenterology* 106, 460-468; quiz 469, (2011), PMID:21206486.
 116. Sabag A, Barr L, Armour M, Armstrong A, Baker CJ, Twigg SM, Chang D, Hackett DA, Keating SE, George J, and Johnson NA. The effect of high-intensity interval training versus moderate-intensity continuous training on liver fat: a systematic review and meta-analysis. *Journal of Clinical Endocrinology and Metabolism*, (2021), PMID:34724062.
 117. Rognmo O, Moholdt T, Bakken H, Hole T, Molstad P, Myhr NE, Grimsmo J, and Wisloff U. Cardiovascular risk of high- versus moderate-intensity aerobic exercise in coronary heart disease patients. *Circulation* 126, 1436-1440, (2012), PMID:22879367.
 118. Rognmo O, Hetland E, Helgerud J, Hoff J, and Slordahl SA. High intensity aerobic interval exercise is superior to moderate intensity exercise for increasing aerobic capacity in patients with coronary artery disease. *The European Journal of Cardiovascular Prevention & Rehabilitation* 11, 216-222, (2004), PMID:15179103.

119. Promrat K, Kleiner DE, Niemeier HM, Jackvony E, Kearns M, Wands JR, Fava JL, and Wing RR. Randomized controlled trial testing the effects of weight loss on nonalcoholic steatohepatitis. *Hepatology* 51, 121-129, (2010), PMID:19827166.
120. Promrat K, Longato L, Wands JR, and de la Monte SM. Weight loss amelioration of non-alcoholic steatohepatitis linked to shifts in hepatic ceramide expression and serum ceramide levels. *Hepatology Research* 41, 754-762, (2011), PMID:21794038.
121. Wong VW, Chan RS, Wong GL, Cheung BH, Chu WC, Yeung DK, Chim AM, Lai JW, Li LS, Sea MM, Chan FK, Sung JJ, Woo J, and Chan HL. Community-based lifestyle modification programme for non-alcoholic fatty liver disease: a randomized controlled trial. *Journal of Hepatology* 59, 536-542, (2013), PMID:23623998.
122. Lazo M, Solga SF, Horska A, Bonekamp S, Diehl AM, Brancati FL, Wagenknecht LE, Pi-Sunyer FX, Kahn SE, Clark JM, and Fatty Liver Subgroup of the Look ARG. Effect of a 12-month intensive lifestyle intervention on hepatic steatosis in adults with type 2 diabetes. *Diabetes Care* 33, 2156-2163, (2010), PMID:20664019.
123. Vilar Gomez E, Rodriguez De Miranda A, Gra Oramas B, Arus Soler E, Llanio Navarro R, Calzadilla Bertot L, Yasells Garcia A, and Del Rosario Abreu Vazquez M. Clinical trial: a nutritional supplement Viusid, in combination with diet and exercise, in patients with nonalcoholic fatty liver disease. *Alimentary Pharmacology and Therapeutics* 30, 999-1009, (2009), PMID:19691668.
124. Eckard C, Cole R, Lockwood J, Torres DM, Williams CD, Shaw JC, and Harrison SA. Prospective histopathologic evaluation of lifestyle modification in nonalcoholic fatty liver disease: a randomized trial. *Therapeutic Advances in Gastroenterology* 6, 249-259, (2013), PMID:23814606.
125. Nobili V, Manco M, Devito R, Di Ciommo V, Comparcola D, Sartorelli MR, Piemonte F, Marcellini M, and Angulo P. Lifestyle intervention and antioxidant therapy in children with nonalcoholic fatty liver disease: a randomized, controlled trial. *Hepatology* 48, 119-128, (2008), PMID:18537181.
126. Ueno T, Sugawara H, Sujaku K, Hashimoto O, Tsuji R, Tamaki S, Torimura T, Inuzuka S, Sata M, and Tanikawa K. Therapeutic effects of restricted diet and exercise in obese patients with fatty liver. *Journal of Hepatology* 27, 103-107, (1997), PMID:9252081.
127. Marchesini G, Brizi M, Morselli-Labate AM, Bianchi G, Bugianesi E, McCullough AJ, Forlani G, and Melchionda N. Association of nonalcoholic fatty liver disease with insulin resistance. *The American Journal of Medicine* 107, 450-455, (1999), PMID:10569299.
128. Kitade H, Chen G, Ni Y, and Ota T. Nonalcoholic fatty liver disease and insulin resistance: New insights and potential new treatments. *Nutrients* 9, (2017), PMID:28420094.
129. Croci I, Byrne NM, Choquette S, Hills AP, Chachay VS, Clouston AD, O'Moore-Sullivan TM, Macdonald GA, Prins JB, and Hickman IJ. Whole-

- body substrate metabolism is associated with disease severity in patients with non-alcoholic fatty liver disease. *Gut* 62, 1625-1633, (2013), PMID:23077135.
130. Khan RS, Bril F, Cusi K, and Newsome PN. Modulation of insulin resistance in nonalcoholic fatty liver disease. *Hepatology* 70, 711-724, (2019), PMID:30556145.
 131. Angulo P, Kleiner DE, Dam-Larsen S, Adams LA, Bjornsson ES, Charatcharoenwitthaya P, Mills PR, Keach JC, Lafferty HD, Stahler A, Haflidadottir S, and Bendtsen F. Liver fibrosis, but no other histologic features, is associated with long-term outcomes of patients with nonalcoholic fatty liver disease. *Gastroenterology* 149, 389-397 e310, (2015), PMID:25935633.
 132. Matthews DR, Hosker JP, Rudenski AS, Naylor BA, Treacher DF, and Turner RC. Homeostasis model assessment: insulin resistance and beta-cell function from fasting plasma glucose and insulin concentrations in man. *Diabetologia* 28, 412-419, (1985), PMID:3899825.
 133. Kirk E, Reeds DN, Finck BN, Mayurranjan SM, Patterson BW, and Klein S. Dietary fat and carbohydrates differentially alter insulin sensitivity during caloric restriction. *Gastroenterology* 136, 1552-1560, (2009), PMID:19208352.
 134. Viljanen AP, Iozzo P, Borra R, Kankaanpaa M, Karmi A, Lautamaki R, Jarvisalo M, Parkkola R, Ronnema T, Guiducci L, Lehtimaki T, Raitakari OT, Mari A, and Nuutila P. Effect of weight loss on liver free fatty acid uptake and hepatic insulin resistance. *Journal of Clinical Endocrinology and Metabolism* 94, 50-55, (2009), PMID:18957499.
 135. Lim EL, Hollingsworth KG, Aribisala BS, Chen MJ, Mathers JC, and Taylor R. Reversal of type 2 diabetes: normalisation of beta cell function in association with decreased pancreas and liver triacylglycerol. *Diabetologia* 54, 2506-2514, (2011), PMID:21656330.
 136. Bacchi E, Negri C, Targher G, Faccioli N, Lanza M, Zoppini G, Zanolin E, Schena F, Bonora E, and Moghetti P. Both resistance training and aerobic training reduce hepatic fat content in type 2 diabetic subjects with nonalcoholic fatty liver disease (the RAED2 randomized trial). *Hepatology* 58, 1287-1295, (2013), PMID:23504926.
 137. Cuthbertson DJ, Shojaee-Moradie F, Sprung VS, Jones H, Pugh CJ, Richardson P, Kemp GJ, Barrett M, Jackson NC, Thomas EL, Bell JD, and Umpleby AM. Dissociation between exercise-induced reduction in liver fat and changes in hepatic and peripheral glucose homeostasis in obese patients with non-alcoholic fatty liver disease. *Clinical Science (London, England: 1979)* 130, 93-104, (2016), PMID:26424731.
 138. Lee S, Bacha F, Hannon T, Kuk JL, Boesch C, and Arslanian S. Effects of aerobic versus resistance exercise without caloric restriction on abdominal fat, intrahepatic lipid, and insulin sensitivity in obese adolescent boys: a randomized, controlled trial. *Diabetes* 61, 2787-2795, (2012), PMID:22751691.

139. Shojaee-Moradie F, Baynes KC, Pentecost C, Bell JD, Thomas EL, Jackson NC, Stolinski M, Whyte M, Lovell D, Bowes SB, Gibney J, Jones RH, and Umpleby AM. Exercise training reduces fatty acid availability and improves the insulin sensitivity of glucose metabolism. *Diabetologia* 50, 404-413, (2007), PMID:17149589.
140. Haus JM, Solomon TP, Marchetti CM, Edmison JM, Gonzalez F, and Kirwan JP. Free fatty acid-induced hepatic insulin resistance is attenuated following lifestyle intervention in obese individuals with impaired glucose tolerance. *The Journal of Clinical Endocrinology and Metabolism* 95, 323-327, (2010), PMID:19906790.
141. Coker RH, Williams RH, Yeo SE, Kortebein PM, Bodenner DL, Kern PA, and Evans WJ. The impact of exercise training compared to caloric restriction on hepatic and peripheral insulin resistance in obesity. *The Journal of Clinical Endocrinology & Metabolism* 94, 4258-4266, (2009), PMID:19808853.
142. Albu JB, Heilbronn LK, Kelley DE, Smith SR, Azuma K, Berk ES, Pi-Sunyer FX, Ravussin E, and Look AARG. Metabolic changes following a 1-year diet and exercise intervention in patients with type 2 diabetes. *Diabetes* 59, 627-633, (2010), PMID:20028945.
143. Kelley DE, Kuller LH, McKolanis TM, Harper P, Mancino J, and Kalhan S. Effects of moderate weight loss and orlistat on insulin resistance, regional adiposity, and fatty acids in type 2 diabetes. *Diabetes Care* 27, 33-40, (2004), PMID:14693963.
144. Unger RH. Lipotoxicity in the pathogenesis of obesity-dependent NIDDM: Genetic and clinical implications. *Diabetes* 44, 863-870, (1995), PMID:7621989.
145. Rada P, González-Rodríguez Á, García-Monzón C, and Valverde ÁM. Understanding lipotoxicity in NAFLD pathogenesis: is CD36 a key driver? *Cell Death & Disease* 11, 802, (2020), PMID:32978374.
146. Summers S. Ceramides in insulin resistance and lipotoxicity. *Progress in Lipid Research* 45, 42-72, (2006), PMID:16445986.
147. Trauner M, Arrese M, and Wagner M. Fatty liver and lipotoxicity. *Biochimica et Biophysica Acta (BBA) - Molecular and Cell Biology of Lipids* 1801, 299-310, (2010), PMID:19857603.
148. Alkhouri N, Dixon LJ, and Feldstein AE. Lipotoxicity in nonalcoholic fatty liver disease: not all lipids are created equal. *Expert Review of Gastroenterology & Hepatology* 3, 445-451, (2009), PMID:19673631.
149. Kasumov T, Li L, Li M, Gulshan K, Kirwan JP, Liu X, Previs S, Willard B, Smith JD, and McCullough A. Ceramide as a mediator of non-alcoholic fatty liver disease and associated atherosclerosis. *PloS One* 10, e0126910, (2015), PMID:25993337.
150. Luukkonen PK, Zhou Y, Sädevirta S, Leivonen M, Arola J, Orešič M, Hyötyläinen T, and Yki-Järvinen H. Hepatic ceramides dissociate steatosis and insulin resistance in patients with non-alcoholic fatty liver disease. *Journal of Hepatology* 64, 1167-1175, (2016), PMID:26780287

151. Raichur S, Wang S, Chan P, Li Y, Ching J, Chaurasia B, Dogra S, Öhman M, Takeda K, Sugii S, Pewzner-Jung Y, Futerman A, and Summers S. CerS2 haploinsufficiency inhibits β -oxidation and confers susceptibility to diet-induced steatohepatitis and insulin resistance. *Cell Metabolism* 20, 687-695, (2014), PMID:25295789.
152. Kurek K, Piotrowska DM, Wiesiolek-Kurek P, Lukaszuk B, Chabowski A, Gorski J, and Zendzian-Piotrowska M. Inhibition of ceramide de novo synthesis reduces liver lipid accumulation in rats with nonalcoholic fatty liver disease. *Liver International* 34, 1074-1083, (2014), PMID:24106929.
153. Xia JY, Holland WL, Kusminski CM, Sun K, Sharma AX, Pearson MJ, Sifuentes AJ, McDonald JG, Gordillo R, and Scherer PE. Targeted induction of ceramide degradation leads to improved systemic metabolism and reduced hepatic steatosis. *Cell Metabolism* 22, 266-278, (2015), PMID:26190650.
154. Perry RJ, Samuel VT, Petersen KF, and Shulman GI. The role of hepatic lipids in hepatic insulin resistance and type 2 diabetes. *Nature* 510, 84-91, (2014), PMID:24899308.
155. Chaurasia B, and Summers SA. Ceramides – Lipotoxic inducers of metabolic disorders. *Trends in Endocrinology and Metabolism* 26, 538-550, (2015), PMID:26412155.
156. Chaurasia B, and Summers SA. Ceramides in Metabolism: Key Lipotoxic Players. *Annual Review of Physiology* 83, null, (2021), PMID:33158378.
157. Li Y, Talbot CL, and Chaurasia B. Ceramides in adipose tissue. *Frontiers in Endocrinology* 11, (2020), PMID:32636806.
158. Kovilakath A, Jamil M, and Cowart LA. Sphingolipids in the heart: From cradle to grave. *Frontiers in Endocrinology* 11, (2020), PMID:33042014.
159. Summers SA. Editorial: The role of ceramides in diabetes and cardiovascular disease. *Frontiers in Endocrinology* 12, (2021), PMID:33776946.
160. Gault C, Obeid L, and Hannun Y. An overview of sphingolipid metabolism: From synthesis to breakdown. *Advances in Experimental Medicine and Biology* 688, 1-23, (2010), PMID:20919643.
161. Merrill AH. De Novo Sphingolipid Biosynthesis: A Necessary, but Dangerous, Pathway*. *The Journal of Biological Chemistry* 277, (2002), PMID:12011104.
162. Bionda C, Portoukalian J, Schmitt D, Rodriguez-Lafrasse C, and Ardail D. Subcellular compartmentalization of ceramide metabolism: MAM (mitochondria-associated membrane) and/or mitochondria? *Biochemical Journal* 382, 527-533, (2004), PMID:15144238.
163. Pagadala M, Kasumov T, McCullough AJ, Zein NN, and Kirwan JP. Role of ceramides in nonalcoholic fatty liver disease. *Trends in Endocrinology and Metabolism* 23, 365-371, (2012), PMID:22609053.
164. Snider JM, Luberto C, and Hannun YA. Approaches for probing and evaluating mammalian sphingolipid metabolism. *Analytical Biochemistry* 575, 70-86, (2019), PMID:30917945.

165. Perry DK, and Hannun YA. The use of diglyceride kinase for quantifying ceramide. *Trends in Biochemical Sciences* 24, 226-227, (1999), PMID:10366848.
166. Chavez JA, and Summers SA. A ceramide-centric view of insulin resistance. *Cell Metabolism* 15, 585-594, (2012), PMID:22560211.
167. Holland WL, Brozinick JT, Wang LP, Hawkins ED, Sargent KM, Liu Y, Narra K, Hoehn KL, Knotts TA, Siesky A, Nelson DH, Karathanasis SK, Fontenot GK, Birnbaum MJ, and Summers SA. Inhibition of ceramide synthesis ameliorates glucocorticoid-, saturated-fat-, and obesity-induced insulin resistance. *Cell Metabolism* 5, 167-179, (2007), PMID:17339025.
168. Chaurasia B, Tippetts TS, Monibas RM, Liu J, Li Y, Wang L, Wilkerson JL, Sweeney CR, Pereira RF, Sumida DH, Maschek JA, Cox JE, Kaddai V, Lancaster GI, Siddique MM, Poss A, Pearson M, Satapati S, Zhou H, McLaren DG, Previs SF, Chen Y, Qian Y, Petrov A, Wu M, Shen X, Yao J, Nunes CN, Howard AD, Wang L, Erion MD, Rutter J, Holland WL, Kelley DE, and Summers SA. Targeting a ceramide double bond improves insulin resistance and hepatic steatosis. *Science* 365, 386-392, (2019), PMID:31273070.
169. Erion DM, and Shulman GI. Diacylglycerol-mediated insulin resistance. *Nature Medicine* 16, 400-402, (2010), PMID:20376053.
170. Holland WL, and Summers SA. Sphingolipids, insulin resistance, and metabolic disease: New insights from in vivo manipulation of sphingolipid metabolism. *Endocrine Reviews* 29, 381-402, (2008), PMID:18451260.
171. Novgorodov SA, Wu BX, Gudz TI, Bielawski J, Ovchinnikova TV, Hannun YA, and Obeid LM. Novel pathway of ceramide production in mitochondria: thioesterase and neutral ceramidase produce ceramide from sphingosine and acyl-CoA. *Journal of Biological Chemistry* 286, 25352-25362, (2011), PMID:21613224.
172. Insausti-Urkiola N, Solsona-Vilarrasa E, Garcia-Ruiz C, and Fernandez-Checa JC. Sphingomyelinases and Liver Diseases. *Biomolecules* 10, (2020), PMID:33143193.
173. Boon J, Hoy AJ, Stark R, Brown RD, Meex RC, Henstridge DC, Schenk S, Meikle PJ, Horowitz JF, Kingwell BA, Bruce CR, and Watt MJ. Ceramides contained in LDL are elevated in type 2 diabetes and promote inflammation and skeletal muscle insulin resistance. *Diabetes* 62, 401-410, (2013), PMID:23139352.
174. Lightle S, Tosheva R, Lee A, Queen-Baker J, Boyanovsky B, Shedlofsky S, and Nikolova-Karakashian M. Elevation of ceramide in serum lipoproteins during acute phase response in humans and mice: role of serine-palmitoyl transferase. *Archives of Biochemistry and Biophysics* 419, 120-128, (2003), PMID:14592455.
175. Wiesner P, Leidl K, Boettcher A, Schmitz G, and Liebisch G. Lipid profiling of FPLC-separated lipoprotein fractions by electrospray ionization tandem mass spectrometry. *Journal of Lipid Research* 50, 574-585, (2009), PMID:18832345.

176. Summers SA. Could ceramides become the new cholesterol? *Cell Metabolism* 27, 276-280, (2018), PMID:29307517.
177. Meeusen J, Donato L, Bryant S, Baudhuin L, Berger P, and Jaffe A. Plasma ceramides. *Arteriosclerosis, Thrombosis, and Vascular Biology* 38, 1933-1939, (2018), PMID:29903731.
178. Hilvo M, Salonurmi T, Havulinna AS, Kauhanen D, Pedersen ER, Tell GS, Meyer K, Teeriniemi AM, Laatikainen T, Jousilahti P, Savolainen MJ, Nygard O, Salomaa V, and Laaksonen R. Ceramide stearic to palmitic acid ratio predicts incident diabetes. *Diabetologia* 61, 1424-1434, (2018), PMID:29546476.
179. Neeland IJ, Singh S, McGuire DK, Vega GL, Roddy T, Reilly DF, Castro-Perez J, Kozlitina J, and Scherer PE. Relation of plasma ceramides to visceral adiposity, insulin resistance and the development of type 2 diabetes mellitus: the Dallas Heart Study. *Diabetologia*, (2018).
180. Wasilewska N, Bobrus-Chociej A, Harasim-Symbor E, Tarasów E, Wojtkowska M, Chabowski A, and Lebensztejn DM. Increased serum concentration of ceramides in obese children with nonalcoholic fatty liver disease. *Lipids in Health and Disease* 17, 216, (2018), PMID:30208901.
181. Simon J, Ouro A, Ala-Ibanibo L, Presa N, Delgado TC, and Martínez-Chantar ML. Sphingolipids in non-alcoholic fatty liver disease and hepatocellular carcinoma: Ceramide turnover. *International Journal of Molecular Sciences* 21, (2019), PMID:31861664.
182. Tarasov K, Ekroos K, Suoniemi M, Kauhanen D, Sylvanne T, Hurme R, Gouni-Berthold I, Berthold H, Kleber M, Laaksonen R, and Marz W. Molecular lipids identify cardiovascular risk and are efficiently lowered by simvastatin and PCSK9 deficiency. *Journal of Clinical Endocrinology and Metabolism* 99, E45-E52, (2014), PMID:24243630.
183. Laaksonen R, Ekroos K, Sysi-Aho M, Hilvo M, Vihervaara T, Kauhanen D, Suoniemi M, Hurme R, Marz W, Scharnagl H, Stojakovic T, Vlachopoulou E, Lokki ML, Nieminen MS, Klingenberg R, Matter CM, Hornemann T, Juni P, Rodondi N, Raber L, Windecker S, Gencer B, Pedersen ER, Tell GS, Nygard O, Mach F, Sinisalo J, and Luscher TF. Plasma ceramides predict cardiovascular death in patients with stable coronary artery disease and acute coronary syndromes beyond LDL-cholesterol. *European Heart Journal* 37, 1967-1976, (2016), PMID:27125947.
184. Samad F, Hester KD, Yang G, Hannun YA, and Bielawski J. Altered adipose and plasma sphingolipid metabolism in obesity A potential mechanism for cardiovascular and metabolic risk. *Diabetes* 55, 2579-2587, (2006), PMID:16936207.
185. Heneghan HM, Huang H, Kashyap SR, Gornik HL, McCullough AJ, Schauer PR, Brethauer SA, Kirwan JP, and Kasumov T. Reduced cardiovascular risk after bariatric surgery is linked to plasma ceramides, apolipoprotein-B100, and ApoB100/A1 ratio. *Surgery for Obesity and Related Diseases* 9, 100-107, (2013), PMID:22264909.
186. Anroedh S, Hilvo M, Akkerhuis KM, Kauhanen D, Koistinen K, Oemrawsingh R, Serruys P, van Geuns RJ, Boersma E, Laaksonen R, and

- Kardys I. Plasma concentrations of molecular lipid species predict long-term clinical outcome in coronary artery disease patients. *Journal of Lipid Research* 59, 1729-1737, (2018), PMID:29858423.
187. Havulinna A, Sysi-Aho M, Hilvo M, Kauhanen D, Hurme R, Ekroos K, Salomaa V, and Laaksonen R. Circulating ceramides predict cardiovascular outcomes in the population-based FINRISK 2002 cohort. *Arteriosclerosis, Thrombosis, and Vascular Biology* 36, 2424-2430, (2016), PMID:27765765.
 188. Poss AM, Maschek JA, Cox JE, Chaurasia B, Holland WL, Summers S, and Playdon MC. Using plasma ceramide to predict premature familial coronary artery disease. *FASEB*, (2019).
 189. de Carvalho LP, Tan SH, Ow GS, Tang Z, Ching J, Kovalik JP, Poh SC, Chin CT, Richards AM, Martinez EC, Troughton RW, Fong AY, Yan BP, Seneviratna A, Sorokin V, Summers SA, Kuznetsov VA, and Chan MY. Plasma ceramides as prognostic biomarkers and their arterial and myocardial tissue correlates in acute myocardial infarction. *JACC: Basic to Translational Science* 3, 163-175, (2018), PMID:30062203.
 190. Petrocelli JJ, McKenzie AI, Mahmassani ZS, Reidy PT, Stoddard GJ, Poss AM, Holland WL, Summers SA, and Drummond MJ. Ceramide biomarkers predictive of cardiovascular disease risk increase in healthy older adults after bed rest. *The Journals of Gerontology: Series A* 75, 1663-1670, (2020), PMID:32215553.
 191. Nwabuo CC, Duncan M, Xanthakis V, Peterson LR, Mitchell GF, McManus D, Cheng S, and Vasani RS. Association of circulating ceramides with cardiac structure and function in the community: The Framingham Heart Study. *Journal of the American Heart Association* 8, e013050, (2019), PMID:31549564.
 192. Peterson LR, Xanthakis V, Duncan MS, Gross S, Friedrich N, Völzke H, Felix SB, Jiang H, Sidhu R, Nauck M, Jiang X, Ory DS, Dörr M, Vasani RS, and Schaffer JE. Ceramide remodeling and risk of cardiovascular events and mortality. *Journal of the American Heart Association* 7, (2018), PMID:29728014.
 193. Lemaitre RN, Yu C, Hoofnagle A, Hari N, Jensen PN, Fretts AM, Umans JG, Howard BV, Sitlani CM, Siscovick DS, King IB, Sotoodehnia N, and McKnight B. Circulating Sphingolipids, Insulin, HOMA-IR, and HOMA-B: The Strong Heart Family Study. *Diabetes* 67, 1663-1672, (2018), PMID:29588286.
 194. Luukkonen PK, Sädevirta S, Zhou Y, Kayser B, Ali A, Ahonen L, Lallukka S, Pelloux V, Gaggini M, Jian C, Hakkarainen A, Lundbom N, Gylling H, Salonen A, Orešič M, Hyötyläinen T, Orho-Melander M, Rissanen A, Gastaldelli A, Clément K, Hodson L, and Yki-Järvinen H. Saturated fat is more metabolically harmful for the human liver than unsaturated fat or simple sugars. *Diabetes Care* 41, 1732-1739, (2018), PMID:29844096.
 195. Tippetts TS, Holland WL, and Summers SA. The ceramide ratio: a predictor of cardiometabolic risk. *Journal of Lipid Research* 59, 1549-1550, (2018), PMID:29987126.

196. Yang RX, Pan Q, Liu XL, Zhou D, Xin FZ, Zhao ZH, Zhang RN, Zeng J, Qiao L, Hu CX, Xu GW, and Fan JG. Therapeutic effect and autophagy regulation of myriocin in nonalcoholic steatohepatitis. *Lipids in Health and Disease* 18, 179, (2019), PMID:31639005.
197. Kotronen A, Seppänen-Laakso T, Westerbacka J, Kiviluoto T, Arola J, Ruskeepää A-L, Yki-Järvinen H, and Oresic M. Comparison of lipid and fatty acid composition of the liver, subcutaneous and intra-abdominal adipose tissue, and serum. *Obesity (Silver Spring, Md)* 18, 937-944, (2010), PMID:19798063.
198. Wang DD, Toledo E, Hruby A, Rosner BA, Willett WC, Sun Q, Razquin C, Zheng Y, Ruiz-Canela M, Guasch-Ferre M, Corella D, Gomez-Gracia E, Fiol M, Estruch R, Ros E, Lapetra J, Fito M, Aros F, Serra-Majem L, Lee CH, Clish CB, Liang L, Salas-Salvado J, Martinez-Gonzalez MA, and Hu FB. Plasma ceramides, Mediterranean diet, and incident cardiovascular disease in the PREDIMED trial (Prevencion con dieta Mediterranea). *Circulation* 135, 2028-2040, (2017), PMID:28280233.
199. Mathews AT, Famodu OA, Olfert MD, Murray PJ, Cuff CF, Downes MT, Haughey NJ, Colby SE, Chantler PD, Olfert IM, and McFadden JW. Efficacy of nutritional interventions to lower circulating ceramides in young adults: FRUVEDomic pilot study. *Physiological Reports* 5, e13329, (2017), PMID:28694327.
200. Tuccinardi D, Di Mauro A, Lattanzi G, Rossini G, Monte L, Beato I, Spiezia C, Bravo M, Watanabe M, Soare A, Kyanvash S, Armirotti A, Bertozzi SM, Gastaldelli A, Pedone C, Khazrai YM, Pozzilli P, and Manfrini S. An extra virgin olive oil-enriched chocolate spread positively modulates insulin-resistance markers compared with a palm oil-enriched one in healthy young adults: A double-blind, cross-over, randomised controlled trial. *Diabetes/Metabolism Research and Reviews*, e3492, (2021), PMID:34435429.
201. Rosqvist F, Kullberg J, Stahlman M, Cedernaes J, Heurling K, Johansson HE, Iggman D, Wilking H, Larsson A, Eriksson O, Johansson L, Straniero S, Rudling M, Antoni G, Lubberink M, Orho-Melander M, Boren J, Ahlstrom H, and Riserus U. Overeating saturated fat promotes fatty liver and ceramides compared with polyunsaturated fat: A randomized trial. *Journal of Clinical Endocrinology and Metabolism* 104, 6207-6219, (2019), PMID:31369090.
202. Dube JJ, Amati F, Toledo FG, Stefanovic-Racic M, Rossi A, Coen P, and Goodpaster BH. Effects of weight loss and exercise on insulin resistance, and intramyocellular triacylglycerol, diacylglycerol and ceramide. *Diabetologia* 54, 1147-1156, (2011), PMID:21327867.
203. Bergman BC, Brozinick JT, Strauss A, Bacon S, Kerege A, Bui HH, Sanders P, Siddall P, Wei T, Thomas MK, Kuo MS, and Perreault L. Muscle sphingolipids during rest and exercise: a C18:0 signature for insulin resistance in humans. *Diabetologia* 59, 785-798, (2016), PMID:26739815.
204. Kasumov T, Solomon TPJ, Hwang C, Huang H, Haus JM, Zhang R, and Kirwan JP. Improved insulin sensitivity after exercise training is linked to

- reduced plasma C14:0 ceramide in obesity and type 2 diabetes *Obesity* 23, 1414-1421, (2015), PMID:25966363.
205. Kasumov T, Huang H, Chung Y-M, Zhang R, McCullough AJ, and Kirwan JP. Quantification of ceramide species in biological samples by liquid chromatography electrospray ionization tandem mass spectrometry. *Analytical Biochemistry* 401, 154-161, (2010), PMID:20178771.
 206. Dube JJ, Amati F, Stefanovic-Racic M, Toledo FG, Sauers SE, and Goodpaster BH. Exercise-induced alterations in intramyocellular lipids and insulin resistance: the athlete's paradox revisited. *American Journal of Physiology: Endocrinology and Metabolism* 294, E882-888, (2008), PMID:18319352.
 207. Chocian G, Chabowski A, Zendzian-Piotrowska M, Harasim E, Lukaszuk B, and Gorski J. High fat diet induces ceramide and sphingomyelin formation in rat's liver nuclei. *Molecular and Cellular Biochemistry* 340, 125-131, (2010), PMID:20174962.
 208. Straczkowski M, Kowalska I, Nikolajuk A, Dzienis-Straczkowska S, Kinalska I, Baranowski M, Zendzian-Piotrowska M, Brzezinska Z, and Gorski J. Relationship between insulin sensitivity and sphingomyelin signaling pathway in human skeletal muscle. *Diabetes* 53, 1215-1221, (2004), PMID:15111489.
 209. Adams JM, Pratipanawatr T, Berria R, Wang E, DeFronzo RA, Sullards MC, and Mandarino LJ. Ceramide content is increased in skeletal muscle from obese insulin-resistant humans. *Diabetes* 53, 25-31, (2004), PMID:14693694.
 210. Reidy PT, Mahmassani ZS, McKenzie AI, Petrocelli JJ, Summers SA, and Drummond MJ. Influence of exercise training on skeletal muscle insulin resistance in aging: Spotlight on muscle ceramides. *International Journal of Molecular Sciences* 21, (2020), PMID:32098447.
 211. Perreault L, Newsom SA, Strauss A, Kerege A, Kahn DE, Harrison KA, Snell-Bergeon JK, Nemkov T, D'Alessandro A, Jackman MR, MacLean PS, and Bergman BC. Intracellular localization of diacylglycerols and sphingolipids influences insulin sensitivity and mitochondrial function in human skeletal muscle. *JCI Insight* 3, (2018), PMID:29415895.
 212. Helge JW, Tobin L, Drachmann T, Hellgren LI, Dela F, and Galbo H. Muscle ceramide content is similar after 3 weeks' consumption of fat or carbohydrate diet in a crossover design in patients with type 2 diabetes. *European Journal of Applied Physiology* 112, 911-918, (2012), PMID:21695523.
 213. Straczkowski M, Kowalska I, Baranowski M, Nikolajuk A, Otziomek E, Zabielski P, Adamska A, Blachnio A, Gorski J, and Gorska M. Increased skeletal muscle ceramide level in men at risk of developing type 2 diabetes. *Diabetologia* 50, 2366-2373, (2007), PMID:17724577.
 214. Mietus-Snyder M, Narayanan N, Krauss RM, Laine-Graves K, McCann JC, Shigenaga MK, McHugh TH, Ames BN, and Suh JH. Randomized nutrient bar supplementation improves exercise-associated changes in plasma

- metabolome in adolescents and adult family members at cardiometabolic risk. *PLoS One* 15, e0240437, (2020), PMID:33079935.
215. Huang H, Kasumov T, Gatmaitan P, Heneghan HM, Kashyap SR, Schauer PR, Brethauer SA, Kirwan JP, and Kirwan JP. Gastric bypass surgery reduces plasma ceramide subspecies and improves insulin sensitivity in severely obese patients. *Obesity* 19, (2011), PMID:21546935.
 216. Coen PM, Menshikova EV, Distefano G, Zheng D, Tanner CJ, Standley RA, Helbling NL, Dubis GS, Ritov VB, Xie H, Desimone ME, Smith SR, Stefanovic-Racic M, Toledo FG, Houmard JA, and Goodpaster BH. Exercise and weight loss improve muscle mitochondrial respiration, lipid partitioning, and insulin sensitivity after gastric bypass surgery. *Diabetes* 64, 3737-3750, (2015), PMID:26293505.
 217. Obanda DN, Yu Y, Wang ZQ, and Cefalu WT. Modulation of sphingolipid metabolism with calorie restriction enhances insulin action in skeletal muscle. *The Journal of Nutritional Biochemistry* 26, 687-695, (2015), PMID:25771159.
 218. Ecker J, and Liebisch G. Application of stable isotopes to investigate the metabolism of fatty acids, glycerophospholipid and sphingolipid species. *Progress in Lipid Research* 54, 14-31, (2014), PMID:24462586.
 219. Chen Y, Berejnaia O, Liu J, Wang S-P, Daurio NA, Yin W, Mayoral R, Petrov A, Kasumov T, Zhang G-F, Previs SF, Kelley DE, and McLaren DG. Quantifying ceramide kinetics in vivo using stable isotope tracers and LC-MS/MS. *American Journal of Physiology-Endocrinology and Metabolism* 315, E416-E424, (2018), PMID:29509438.
 220. Zabielski P, Daniluk J, Hady HR, Markowski AR, Imierska M, Górski J, and Błachnio-Zabielska AU. The effect of high-fat diet and inhibition of ceramide production on insulin action in liver. *Journal of Cellular Physiology*, (2018), PMID:30067865.
 221. Zabielski P, Błachnio-Zabielska AU, Wójcik B, Chabowski A, and Górski J. Effect of plasma free fatty acid supply on the rate of ceramide synthesis in different muscle types in the rat. *PLoS One* 12, e0187136, (2017), PMID:29095868.
 222. Noto D, Di Gaudio F, Altieri IG, Cefalu AB, Indelicato S, Fayer F, Spina R, Scrimali C, Giammanco A, Mattina A, Indelicato S, Greco M, Bongiorno D, and Aversa M. Automated untargeted stable isotope assisted lipidomics of liver cells on high glucose shows alteration of sphingolipid kinetics. *Biochim Biophys Acta Mol Cell Biol Lipids* 1865, 158656, (2020), PMID:32045699.
 223. Wigger D, Gulbins E, Kleuser B, and Schumacher F. Monitoring the sphingolipid de novo synthesis by stable-isotope labeling and liquid chromatography-mass spectrometry. *Frontiers in Cell and Developmental Biology* 7, 210, (2019), PMID:31632963.
 224. Skotland T, Ekroos K, Kavaliauskiene S, Bergan J, Kauhanen D, Lintonen T, and Sandvig K. Determining the turnover of glycosphingolipid species by stable-isotope tracer lipidomics. *Journal of Molecular Biology* 428, 4856-4866, (2016), PMID:27363608.

225. Haynes CA, Allegood JC, Wang EW, Kelly SL, Sullards MC, and Merrill AH, Jr. Factors to consider in using [U-C]palmitate for analysis of sphingolipid biosynthesis by tandem mass spectrometry. *Journal of Lipid Research* 52, 1583-1594, (2011), PMID:21586681.
226. Berdyshev EV, Gorshkova I, Skobeleva A, Bittman R, Lu X, Dudek SM, Mirzapoiazova T, Garcia JG, and Natarajan V. FTY720 inhibits ceramide synthases and up-regulates dihydrosphingosine 1-phosphate formation in human lung endothelial cells. *Journal of Biological Chemistry* 284, 5467-5477, (2009), PMID:19119142.
227. Berdyshev EV, Gorshkova IA, Usatyuk P, Zhao Y, Saatian B, Hubbard W, and Natarajan V. De novo biosynthesis of dihydrosphingosine-1-phosphate by sphingosine kinase 1 in mammalian cells. *Cellular Signalling* 18, 1779-1792, (2006), PMID:16529909.
228. Tserng KY, and Griffin RL. Ceramide metabolite, not intact ceramide molecule, may be responsible for cellular toxicity. *Biochemical Journal* 380, 715-722, (2004), PMID:14998372.
229. Tserng KY, and Griffin R. Studies of lipid turnover in cells with stable isotope and gas chromatograph-mass spectrometry. *Analytical Biochemistry* 325, 344-353, (2004), PMID:14751270.
230. Snider JM, Snider AJ, Obeid LM, Luberto C, and Hannun YA. Probing de novo sphingolipid metabolism in mammalian cells utilizing mass spectrometry. *Journal of Lipid Research* 59, 1046-1057, (2018), PMID:29610123.
231. Martinez-Montanes F, and Schneiter R. Following the flux of long-chain bases through the sphingolipid pathway in vivo using mass spectrometry. *Journal of Lipid Research* 57, 906-915, (2016), PMID:26977056.
232. Blachnio-Zabielska AU, Persson X-MT, Koutsari C, Zabielski P, and Jensen MD. A liquid chromatography/tandem mass spectrometry method for measuring the in vivo incorporation of plasma free fatty acids into intramyocellular ceramides in humans. *Rapid Communications in Mass Spectrometry* 26, 1134-1140, (2012), PMID:22467464.
233. Chung JO, Koutsari C, Blachnio-Zabielska AU, Hames KC, and Jensen MD. Intramyocellular ceramides: Subcellular concentrations and fractional de novo synthesis in postabsorptive humans. *Diabetes* 66, 2082-2091, (2017), PMID:28483801.
234. Chung JO, Koutsari C, Blachnio-Zablieska AU, Hames KC, and Jensen MD. Effects of meal ingestion on intramyocellular ceramide concentrations and fractional de novo synthesis in humans. *American Journal of Physiology-Endocrinology and Metabolism* 314, E105-E114, (2018), PMID:28970356

CHAPTER II – High-throughput LC-MS method to investigate postprandial lipemia: Considerations for future precision nutrition research

ABSTRACT

Elevated postprandial lipemia is an independent risk factor for cardiovascular disease, yet methods to quantitate post-meal handling of dietary lipids in humans are limited. This study tested a new method to track dietary lipid appearance using a stable isotope tracer ($^2\text{H}_{11}$ -oleate) in liquid meals containing three levels of fat (low-LF, 15 g; moderate-MF, 30 g; high-HF, 60 g). Meals were fed to 12 healthy men (mean \pm SD, age 31.3 ± 9.2 y, BMI 24.5 ± 1.9 kg/m 2) during four randomized study visits; the HF meal was administered twice for reproducibility. Blood was collected over eight hours postprandially, TG-rich lipoproteins (TRL) and particles with a Svedberg flotation rate >400 ($S_f > 400$, $n = 8$) were isolated by ultracentrifugation, and labeling of two TG species (54:3 and 52:2) quantified by LC-MS. Total plasma TRL-TG concentrations were three-fold greater than $S_f > 400$ -TG. Both $S_f > 400$ - and TRL-TG 54:3 were present at higher concentrations than 52:2 and singly-labeled TG concentrations were higher than doubly-labeled. Further, TG 54:3 and the singly-labeled molecules demonstrated higher plasma absolute entry rates differing significantly across fat levels within a single TG species ($P < 0.01$). Calculation of fractional entry showed no significant differences in label handling supporting the utility of either TG species for appearance rate calculations. These data demonstrate the utility of labeling research meals with stable isotopes to investigate human postprandial lipemia while simultaneously highlighting the importance of examining individual responses. Meal type and timing, control of pre-study activities, and effects of sex on outcomes should match the research goals. The method, optimized here,

will be beneficial to conduct basic science research in precision nutrition and clinical drug development.

NEW & NOTEWORTHY

A novel method to test human intestinal lipid handling using stable isotope labeling is presented and, for the first time, plasma appearance and lipid turnover was quantified in 12 healthy men following meals with varying amounts of fat. The method can be applied to studies in precision nutrition characterizing individual response to support basic science research or drug development. This report discusses key questions for consideration in precision nutrition that were highlighted by the data

INTRODUCTION

Elevated postprandial lipemia is an independent risk factor for the development of cardiovascular disease and related metabolic conditions (i.e., metabolic syndrome, NAFLD, type 2 diabetes) (1-4). As a result, numerous studies have focused on investigating chylomicron production and turnover in plasma to understand its contribution to hyperlipidemia (5). Seminal work by Grundy et al measured postprandial chylomicron fractional clearance rates (FCRs) in healthy and hyperlipidemic men who underwent an enteral infusion of a high-fat lipid emulsion (6). Chylomicron FCRs were calculated based on the assumption that the rates of appearance of TG in chylomicron particles in plasma were equivalent to the duodenal lipid infusion rates, and by extension, the results were based on the assumption that enterocyte lipid handling was similar between normolipidemic and hyperlipidemic individuals. However, methods utilizing direct intestinal tissue sampling during bariatric and other surgeries, followed by gene expression studies, have supported greater expression of genes related to chylomicron assembly and secretion in individuals who were obese and insulin-resistant (7, 8). More recent in vivo methods quantifying postprandial chylomicron apolipoprotein B48 (apoB48) production have utilized protocols of continuous feeding of small meals every 30 minutes to one hour (h), over 8-15h in duration, with simultaneous IV infusion of the stable isotope $^2\text{H}_3$ -leucine (5, 9-11). Such oral feeding regimens result in steady-state production of chylomicron particles that are smaller than intestinal particles produced when fat is fed in a bolus (i.e. similar to regular intake of meals containing fat). Nonetheless, isotopic

apoB48 labeling has been an important innovation revealing elevations in particle production rates, as well as delayed clearance of postprandial chylomicrons, in individuals who are insulin resistant (5, 9). These apoB48 data suggest that insulin resistance may also be associated with altered enterocyte lipid handling (less lipid storage) and highlight the need for better methods to measure intestinal lipid processing in vivo in humans. Recently, a comprehensive report highlighted the high variability between healthy subjects with regard to their postprandial lipemic responses to a standardized meal (12). Similar subject variability has been reported in clinical trials investigating weight loss through dietary interventions where wide ranges of weight change were observed from 25 kg body weight lost up to 5 kg body weight gained (13-15). These observations have prompted a recent shift in the focus of nutritional research to place greater emphasis on understanding variations in individual response (16) driven by both genetic and environmental factors (e.g., gut microbiome, glycemic profile, sleep status, activity level, meal timing) (12, 17, 18). Future postprandial studies focusing on lipid metabolism require methods to quantify the entry of dietary fat into the blood. Such quantitation would be also clinically relevant because a number of important research investigations currently utilize specialized diets to bring about weight loss and treat seizure disorders (19) or Alzheimer's disease (20), study drugs in development to target intestinal lipid handling (21-27), and aim to understand the effects of varying the timing of food intake (28, 29).

To track the postprandial presence of meal lipid in blood, we (30-34) and others (35, 36) have added stable isotopes of fat to meals that were of moderate fat content. These studies have shown that between eating occasions, fat from a previous meal is stored in the enterocyte and is mobilized to support chylomicron synthesis during the next meal - i.e., fat from dinner is stored overnight and released at the onset of breakfast the next morning, and can continue to be secreted for as long as 16h after original consumption (30, 32, 37). Although it is known that monounsaturated fatty acids are highly absorbable (98-99%) (38), the duration of time to full absorption can be surprisingly long. These effects can confound measurements of meal-lipid absorption and likely underscore the observation of multiple peaks of postprandial lipemia in plasma after a standardized meal (39). Further, the quantity of lipid stored in the enterocyte can vary between individuals based on the meals consumed and metabolic health status of the subject(s), thus contributing to interindividual variations observed in feeding studies (7, 8). Here, we tested a strategy for quantifying plasma chylomicron appearance in vivo by labeling meal fat with $^2\text{H}_{11}$ -oleate and investigating the effects of meals with varying fat contents (low, LF; medium, MF; and high, HF). We compared two different TG species (54:3 and 52:2) becoming labeled within the 1) TG-rich lipoprotein (TRL) fraction and 2) lipoprotein particles with a Svedberg flotation rate (S_f) of >400 , isolated using additional ultracentrifugation steps (40). These effects were investigated to allow future research to employ the most practical method that best quantifies the intestinal lipid entry into circulation, while optimizing protocol efficiency for larger studies in

precision nutrition (16). Active areas of research that may benefit from this methodology include the influence of intestinal hormones on lipid transport and insulin sensitivity (e.g., GIP, GLP) (21, 22, 27), discovery of an axis of gut-brain communication that may impact bile acids, endocannabinoids, and satiety (41), and the potential for drug development in the field of obesity and NAFLD (21, 23-27).

METHODS

Protocol

The project's research protocol was approved by the University of Texas Southwestern Medical Center (UTSW IRB#: STU 102011001) and the study was conducted according to the principles expressed in the Declaration of Helsinki. This was a four-period, crossover study and given the level of early development of this technology (phase I use of synthesized $^2\text{H}_{11}$ -oleate), only healthy male participants were recruited. Inclusion criteria included male sex, age 18-40y and healthy, based on medical history completed at a screening visit, physical examination, vital signs, biochemical tests, creatinine clearance >80 mL/min, and no use of nicotine containing products. Each participant agreed to refrain from consuming alcohol for the duration of the study. Exclusion criteria included a history of metabolic illness or disease, clinically-significant abnormalities, excessive alcohol or caffeine use, recent surgical procedures, or allergies to the ingredients in the meal tests.

Study design

As shown in **figure 2.1A**, each of the four study visits consisted of a 24h, inpatient stay at the Clinical Translational Research Center (CTRC) at UTSW Medical Center. At 6:00 PM the subject was fed a low-fat dinner of their preference, chosen ahead of time from a standard list of menu items (e.g., baked chicken, salad, pita chips, jello). This same low-fat meal was fed the night before each of the four meal tests and averaged $1,067 \pm 112$ kcal, 23.4 % of energy

(%E) from protein, 57.9 %E carbohydrate, and 18.7 %E fat and provided approximately 40% of each subjects' daily energy needs (**table 2.1**). The participants slept overnight in the unit and the next morning arose at 6:00 AM to wash up, after this, an IV line was placed in an antecubital vein for blood drawing. Indirect calorimetry was performed in the fasted state using the hooded mode and a metabolic cart (VMax Encore, Viasys Healthcare, San Diego, CA) and energy expenditure, fat, and glucose oxidation were calculated using the standard equations of Jequier (42). At 8:00 AM, the participant received one of three liquid test meals. Blood samples were collected at -10 and -5 min., and at 0.5h, 1h, 1h 20 min., 1h 40 min., 2h, 2.5h, 3h, 4h, 6h, and 8h after the meal (**figure 2.1A**). Whole blood was collected into chilled EDTA tubes and the samples centrifuged at 4°C. Plasma was transferred to an Eppendorf tube containing 0.5 mg of paraoxon to prevent in vitro lipolysis (43). An aliquot was immediately processed for lipoprotein isolation and other aliquots were stored at -80°C until further analysis. At noon, indirect calorimetry was again performed to measure fed-state substrate oxidation. Body composition was measured by DEXA (Hologic Discovery W, QDR series; Bedford, MA).

Meal tests

Each participant completed four meal tests on four occasions, separated by a washout period of two weeks (**figure 2.1A**). The tests were as follows: LF (15g total fat in the meal), MF (30g), and HF (60g), with the HF test being administered twice in sequential order to assess reproducibility. The LF, MF, and

HF tests were administered in a randomized order and **table 2.1** presents the composition of the meals. The stable isotope, $^2\text{H}_{11}$ -oleate (**figure 2.1B**), was added to the liquid meals with the goal to achieve a consistent ~17% enrichment of total meal oleic acid. An Ensure Plus® shake (350 kcal, 10 mg cholesterol, 13 g protein, 49 g carbohydrate, 11 g fat) was used as the base ingredient and differing quantities of heavy cream, corn oil, and canola oil were added to maintain a consistent fatty acid composition of 14.4% saturated, 50.5% monounsaturated, and 35.0% polyunsaturated fatty acids. The three primary fatty acids in the shake (palmitate, linoleate, and oleate) made up 7.8%, 24.0%, and 44.6% of the total fatty acids, respectively. The label and other fats were warmed briefly to achieve melting, and all ingredients were blended on high speed for eight minutes to achieve a homogenous solution. The meal was presented to the participants within five minutes of preparation and the participant was instructed to complete meal consumption within 15 minutes. At the end of the meal the participant drank a four oz glass of water that had been used to rinse the container holding the liquid meal.

Laboratory analysis

Immediately following the completion of the daily testing protocol, aliquots of the plasma underwent ultracentrifugation ($1.3 \times 10^8 \text{ g}$ at 15°C) in a Beckman 50.3 rotor to isolate TRL as described previously (44). For eight participants, large lipoproteins containing mainly chylomicrons and some very large VLDL were isolated with a Svedberg flotation rate (S_f) of >400 (40). Because isolation of

S_r>400 fraction is associated with greater time and effort (two additional days of dialysis followed by two separate ultracentrifugation spins), the isolation was completed in eight subjects only. Concentrations of TG in plasma, TRL, and S_r>400 aliquots were quantified by enzymatic assay (Wako #994-02891, CV 11.2%, Mountain View, CA). Other aliquots from the TRL and S_r>400 fractions were used for liquid chromatography – multiple reaction monitoring (LC-MRM) analysis of intact, individual TG, as described in detail previously (45). Briefly, 40 µl of sample (TRL or S_r>400 fractions) was diluted with 180 µl of phosphate buffer solution and 20 µl of internal standard then underwent protein precipitation (350 µl of 3:1 pentanol:methanol). Following centrifugation, 10 µl of the supernatant was diluted (90 µl of 3:1 pentanol:methanol) and then 1 µl was injected into a Sciex 5000 triple quadrupole mass spectrometer (SCIEX, Framingham, MA, USA) coupled with a Waters Acquity UPLC system (Waters, Milford, MA, USA) for LC-MRM analysis. An Acquity UPLC BEH C18 column (2.1 x 100mm, 1.7µm, Waters, MA, USA, Part # 186002350) was used for chromatographic separation of the analytes.

Calculations and statistical analysis

Given that the ²H₁₁-oleate label was added to the meals, 54:3 and 52:2 were chosen as representative TG species to track the entry of dietary label into the plasma compartment. **Figure 2.1C** shows the molecular structure of these two TG species, triolein (54:3) and palmitate-diolein (52:2, which contains 18:1/16:0/18:1). Concentrations obtained during the postprandial period between

one and three hours were used for production rate calculations because after this time, recycling of the label would likely occur through the liver resulting in plasma lipoproteins containing TG made from two different precursor pools (the intestine and the liver) (30, 46-48). Plasma fractional entry rates of dietary fat (denoted k) were calculated as follows:

$$k = \text{slope}/(\text{concentration at 3h} - \text{concentration at 1h}) \quad (\text{equation 2.1})$$

The slope of the increase in concentrations of labeled 54:3 and 52:2 in TRL between 1h and 3h after meal consumption was divided by the absolute concentration rise between 1h and 3h (45). Calculations were performed using Microsoft Excel 2013 and statistics performed using StatView®, 5.0.1 software (2008) and R, 3.5.1 (2018) (49). One-way, repeated measures ANOVAs were completed using the ezANOVA function (ez package) in R when comparing absolute entry rates and k across fat levels. Post-hoc pairwise t -tests with Bonferroni adjustments were completed when significance (alpha level < 0.05) was achieved. Paired, two-tailed t -tests were used when comparing means of independent observations. Data are presented as mean \pm SD for static variables (body weights, age) and as mean \pm SEM for values measured over time.

RESULTS

All participants ($n = 12$) were healthy men with the mean (\pm SD) ages of 31.3 ± 9.2 y, BMI of 24.5 ± 1.9 kg/m², and body weights of 75.6 ± 6.6 kg. Weight was stable during the two months of subject participation – remaining within 2-3% of baseline body weight. All subjects had normal fasting concentrations of plasma glucose (81 ± 8 mg/dL), TG (82 ± 35 mg/dL), and total cholesterol (162 ± 27 mg/dL). No differences were observed between fasting and fed levels of substrate oxidation for any of the tests (data not shown). Reproducibility of the HF tests revealed that no differences were detected in absolute area-under-the-curve (AUC) of TG concentrations for either TRL or S_f>400 lipoproteins (**supplementary fig. 2.1A & 2.1B**, bar graphs). Therefore, for further analysis of the effect of the quantity of meal fat on the study outcomes, data from the HF test completed on a date closest to the dates of the LF and MF tests were used for subsequent analysis. The mean concentrations of total TRL-TG and S_f>400-TG for the three meal tests are presented in **figure 2.2**. The LF meal (15 g of fat) is represented by the light blue line, the MF meal (30 g) by the darker blue line, and the HF meal (60 g) by the black line. For all fat levels, the TG concentrations in either TRL or S_f>400 lipoproteins peaked at approximately three hours following meal consumption. Although the ANOVA across meals demonstrated an increase in TRL-TG AUC (**figure 2.2A**, bar graph), no significant post-hoc differences in AUC of the TRL-TG concentrations were observed between meal types. A high variability between subject responses was observed as shown in **figures 2.3 and 2.4** (discussed below). Interestingly, when examining the mean

data for the LF and MF meals (**figure 2.2A**), the nadirs in average TRL-TG concentrations occurring at hour eight were lower than the fasting levels. For large chylomicron particles ($S_f > 400$, **figure 2.2B**, bar graph), a significant difference in AUC was observed between LF and MF ($P < 0.01$) and between LF and HF ($P < 0.01$). The AUCs for $S_f > 400$ -TG concentrations of the MF and HF meals were similar.

Individual responses

Unique patterns in TRL-TG and $S_f > 400$ -TG concentrations were observed for each subject, and upon close inspection of **figures 2.3** and **2.4**, it is clear no one subject exhibited a TG pattern that mirrored the mean pattern of the group. The stars on **figures 2.3A** and **2.3B** highlight the distinct patterns observed for a single subject (#9) both in the dramatic peak in total TRL-TG concentrations observed following the MF meal (**figure 2.3B**) and the sawtooth pattern of label appearance (**figure 2.3A**), suggesting either intermittent gastric emptying following the LF meal, or a pulsatile rate of production or clearance of chylomicrons. Similar variability was observed in the $S_f > 400$ -TG (**figure 2.4A**); for example, following the LF meal, one subject (#7) had an AUC that was two times that of the next greatest subject (**figure 2.4A**, bar graph) and a different individual (#11) had a substantially larger peak in $S_f > 400$ -TG than any other subject following the HF meal (**figure 2.4C**). These data highlight the importance of analyzing both the mean of the group and individual subject data, and the

significant impact differences in lipid clearance can have four to eight hours after a meal.

Singly- and doubly-labeled TG

Two representative TRL- and $S_{f>400}$ -TG species (54:3 and 52:2, **figure 2.1C**) were analyzed by LC-MRM to track the dietary label into the plasma compartment. The concentrations of doubly-labeled and singly-labeled species of both TRL- and $S_{f>400}$ -TG 54:3 and 52:2 are presented in **figures 2.5** and **2.6**, respectively. A number of independent observations based on these data underscore the internal validity of the method. First, as shown in all graphs in **figure 2.5**, TRL-TG 52:2 (grey line) was found in smaller concentrations than TRL-TG 54:3 (black line). This reflects the meal fatty acid composition which averaged 44.6% oleic acid and 7.8% palmitic acid; thus, a large amount of oleate was available to support 54:3 synthesis and only a small amount of palmitate was available to support 52:2 synthesis. Second, the doubly-labeled (i.e., two labeled fatty acid moieties incorporated into the molecule) TRL-TG species (**figure 2.5F-H**, note y-axis) were three-times lower in concentration than the singly-labeled species (**figure 2.5A-C**, compare y-axis). This results from the fact that at any given enterocyte label precursor enrichment, the probability of making a doubly-labeled species is lower than the probability of making a singly-labeled molecule. Third, with regard to the $S_{f>400}$ fraction (**figure 2.6**), similar to past studies (30), the concentration of total $S_{f>400}$ -TG observed here was less than 1/3 that of the total TG in the TRL fraction (**figure 2.5**) highlighting the

contribution of remnant lipoproteins to TRL. Lastly, similar to TRL-TG, across all levels of meal fat, the concentration of $S_{f>400}$ TG 54:3 (**figure 2.6**, black lines) was two-fold greater than 52:2 (**figure 2.6**, grey lines) and doubly-labeled species (**figure 2.6F-H**) were three-times lower in concentration than the singly-labeled species (**figure 2.6A-C**). With regard to the two HF meals, similar observations in both the quantity of 54:3 versus 52:2 and concentration of doubly-labeled versus singly labeled TRL- and $S_{f>400}$ -TG are shown in **supplementary figures 2.2** and **2.3**. These data support a high level of reproducibility between HF test meals in these subjects.

Fractional entry rates

We used the slope of the early rise in labeled TRL-TG entering the plasma to estimate early production of 54:3 and 52:2 both doubly- and singly-labeled across meal fat level (a single example of this was introduced in a previous preliminary report (43)). The linear rises between one to three hours in TRL-TG label concentrations were plotted and a linear regression model generated. Given the accuracy of the model fits ($r^2=0.95 - 0.98$, **table 2.2**), the absolute turnover rates were calculated. The slopes of the early rise in TRL-TG label entering the plasma represents the actions of intestinal lipid secretion and clearance. At early timepoints, before insulin would have had its effect to increase clearance (56), this slope predominantly represents the intestinal secretion rate. As expected, given the higher concentration of 54:3, the absolute entry rates (in $\mu\text{mol/L/h}$) were larger than 52:2 (**table 2.2**, horizontal

comparisons). Similarly, doubly-labeled molecules were found in lower concentrations than the singly-labeled molecules (**figures 2.5 & 2.6**) and this resulted in higher observed absolute entry rates ($\mu\text{mol/L/h}$) for the TG species containing one labeled oleic acid. Further, within a TG species, absolute entry rate was significantly different across fat levels, increasing as quantity of fat increased (**table 2.2**, vertical comparisons). The fractional entry rate (k , the proportion of the pool that is becoming labeled in units of pools/h) of the meal lipid in TRL was then calculated by dividing the slope ($\mu\text{mol/L/h}$) by the change in TRL concentration ($\mu\text{mol/L}$) over time (one to three hours) for both doubly- and singly-labeled TRL-TG 54:3 and 52:2 (see equation 2.1).

We would not expect any differences in the entry rates (pools/hr) of TG molecules based on species (54:3 and 52:2) or number of labels integrated into a TG molecule as this would suggest an inconsistency in the export of the labeled molecules into the plasma (i.e., discrimination in intestinal handling of label). Indeed, no differences in k were observed between singly-labeled or doubly-labeled 52:2 and 54:3 at each level of fat. Further, no significant differences were found when k was compared across fat levels within a specific TG molecule. This means either TRL-TG species (52:2 or 54:3) may be used for the calculations of production rate. The same analysis was completed for the $S_r > 400$ fraction and similar observations were noted (**table 2.3**). First, absolute entry rates are higher in 54:3 when compared to 52:2 and in singly-labeled TG when compared to doubly-labeled (horizontal comparison within the same level of fat).

Second, for singly- and doubly-labeled 52:2, a similar significant trend in increasing absolute entry rates were found across meal fat levels (vertical comparison within a TG species with the same number of labels). For singly-labeled 54:3, entry rates were significantly different as meal fat increased and trended towards significance for doubly-labeled 54:3. Third, fractional entry rate (k) was not different between TG species, number or labels, or amount of fat.

DISCUSSION

This is the first study to utilize meal-lipid labeling in vivo to quantify newly-made, intact TG in lipoproteins using LC-MRM. Further, the present method was tested during postprandial meal tests with differing fat contents and used a stable isotope tracer, homogenized into test meals, to unequivocally identify meal fat present in plasma chylomicrons (50). In the area of nutritional research, a recent recommendation (51) has been made highlighting the concept that to investigate the physiologic impact of any food component, it should be tested using various “doses” of the component – similar to pharmacological investigations of drugs in development. Thus, the present project investigated labeling of dietary fat across test meals containing low, medium, and high fat contents to determine how increasing meal fat altered post-meal lipid handling in healthy men.

The quantity of fat fed in the meal tests

The seminal work of Dubois and colleagues was crucial to understanding how the greater the quantity of fat fed in meals, the more TG are found in plasma chylomicrons and TRL particles (46, 48). In this well-designed study, without the addition of an isotope to the test meals, the data could not be used to distinguish between endogenous and dietary lipid contributions to postprandial lipemia. By comparing meals of increasing fat content, from 0-50 g/meal, Dubois demonstrated that 15 g of dietary fat may be the lower threshold needed to stimulate lipid absorption in healthy humans (46). Data from the LF meal in the current study, which also provided 15 g of fat, exhibited an irregular pattern of

rise in blood lipids (**figure 2.2A**) suggesting that gastric emptying was intermittent. Indeed, data from one subject's TRL-TG concentrations (denoted by a star on **figure 2.3A**) demonstrated a sawtooth pattern following the LF meal. These data raise the question of how the effects of gastric emptying, slower or faster based on the fat content and meal type, impact the observed appearance of blood lipid. The AUC of the MF and HF meals (**figure 2.2**, bar graphs) were similar suggesting a certain threshold of fat fed in a liquid bolus may decrease gastric emptying, which would slow absorption, and promote a more efficient clearance of TG from the blood. Whether this holds true for solid meals requires further investigation. These observations demonstrate the importance of feeding enough fat to accurately measure label absorption in studies such as this. Further, the small rise in concentrations of the labeled 54:3 and 52:2 after LF feeding (**figures 2.5 & 2.6**) made it more challenging to model the slopes of their appearances, resulting in less accuracy in the calculated entry rates of the labeled TG species, and their doubly- and singly-labeled forms (**tables 2.2 & 2.3**). The $S_{r>400}$ lipoprotein responses to the MF (30 g) meal observed here were similar to the chylomicron-TG responses observed with the 31 g fat challenge of Dubois et al (46, 48). These data suggest that future postprandial lipemia research should include at least 30 g of fat in the test meals. One goal of this study was to optimize this methodology for future, high-throughput investigations of postprandial metabolism and disease risk which can be utilized to develop targeted nutrition therapies for diverse populations. Presented next is

a discussion of how these findings can inform future precision nutrition research. These concepts are also presented in **table 2.4**.

Meal type and timing

The current study utilized a liquid meal, which is advocated to reduce significant confounding results of delayed gastric emptying (34, 52). On the other hand, the use of solid meals offers greater generalizability as most humans consume meals in solid form. Whether in liquid or solid form, mixed meals containing carbohydrate, fat, and protein provide a more physiological measurement compared to single nutrient challenge tests (an oral glucose tolerance test (12)). With regard to the length of data collection, feeding a solid meal may require longer postprandial sampling. Furthermore, feeding two meals in succession may be necessary to fully characterize the postprandial response (32). Historically, data have been collected out to eight hours post-meal (53) keeping in mind that late events in the postprandial phase will be strongly influenced by lipid clearance from plasma. Similar to Dubois' observations of late (seven hours) postprandial TRL-TG concentrations falling below the fasting values after a moderate 31 g fat challenge (46, 48), the nadir in TRL-TG concentrations in the present study occurred eight hours after the LF and MF meal tests were consumed (**figure 2.2A**). This observation is thought to be due to a delayed upregulation of lipoprotein lipase by insulin following a meal containing carbohydrate (54-56). Another key question that requires considerable thought when designing nutritional studies is the timing of the meal – whether the meal

should be fed early in the morning (i.e., breakfast) or later in the day (lunch or dinner). This, along with the fasting status of the subject, will impact the appearance of label in the blood and the metabolic fates of the macronutrients consumed. For example, multiple reports have demonstrated nocturnal feeding can contribute to metabolic dyshomeostasis (57-63), which may be a target of future research utilizing the present method. The importance of distribution of macronutrients consumed across the day is also highlighted by these data. It is likely that a standardized lunch following a HF breakfast will result in greater lipemia because, 1) lipid from the breakfast has not cleared from the blood yet (**figure 2.2**) and 2) the second meal effect will cause intestinally-stored fat from breakfast to be released upon consumption of lunch (30, 32). In the present study, to reduce the effect of an intestinal cold (unlabeled) pool, the evening meal fed the night before the meal test was low in fat (19% of energy, or ~22 g of fat). Nonetheless, some of this lipid may have remained in the intestine overnight. With the development of the present technique, it is now possible to test a hypothesis suggested by our earlier studies (30), that prestored-TG are more likely to be packaged into larger chylomicrons compared to smaller chylomicrons. If true, this would provide a physiologic benefit since larger chylomicrons are more easily lipolyzed by lipoprotein lipase (64). It is also possible that larger chylomicrons may be supported by greater basolateral uptake of plasma free fatty acids (65). Lastly, because chylomicrons of all sizes are made in the postprandial period (66), small and large TRL carrying the dietary lipid label (within the first one-two hours of meal ingestion) represent intestinally-produced

lipoproteins, even if hepatically-derived VLDL and IDL are present in the TRL fraction at the same time.

Pre-study activities

Similar to previous reports (12, 67), wide variations in individual responses were observed in the current cohort of healthy men (**figures 2.3 & 2.4**). Presenting individual data in studies also highlights that fact that no single subjects' postprandial-TG pattern is identical to the mean presented in most past publications. However, this raises the important question of how the individual data will aid to inform researchers and policy makers in developing nutritional recommendations for varying populations across the lifespan. Past research in large populations (e.g., using GWAS) has uncovered important physiologic concepts by analyzing outliers. Since blood TG concentrations are highly sensitive to many factors, these were controlled for in the present study (e.g., alcohol consumption, time of day, exercise) (68). Future investigations should consider the outcomes they wish to study when deciding which pre-study activities should be tightly controlled, if any. If the research goals are to investigate the meal composition's effect on absorption (e.g., gastric emptying, lipid clearance, specific components of the meal) then it would be prudent to control pre-study activities as described by our group previously (68). It is equally beneficial to study individuals in their natural environment. Thus, if natural variability within a population is the primary outcome, pre-study activities should remain uncontrolled and consistent with each subjects' daily habits.

Effects of sex and reproducibility of response

Future research will include the test of sex as a biological variable on the study outcomes because factors of daily living will impact postprandial lipemia differently in men and women. For example, men are more susceptible to fructose-induced hypertriglyceridemia than women (69, 70). With regard to reproducibility, individual responses can also be compared within the same subject. Here, a HF test was administered twice to each subject and high reproducibility of this meal test was observed (**supplementary figures 2.1-2.3**), perhaps due to control of pre-study actions. This was in line with a recent publication presenting a machine-learning model that predicted an individual's response to a food intake (12). Berry et al reported high variations between subjects, but individual responses to the same meal were similar and therefore predictable. This is a key finding especially because studies in precision nutrition aim to predict an individual's response to various meal components in an effort to improve individualized dietary recommendations (12). While high reproducibility of the HF meal was observed in the current study, we cannot extend this observation to the low and moderate fat meal tests. Future work should test reproducibility of low and moderate fat meals in a similar manner.

Limitations and potential applications of the method

This study had a number of limitations important to consider. First, given the newly-synthesized isotope used here, only men were included as participants.

Compared to women, past data suggest that men are more susceptible to elevations in postprandial lipemia as dietary fat increases (71) - thus, studies in women are warranted to determine if a sex effect exists in intestinal lipid handling. Second, the total energy in the meals increased as more fat was added from the LF to HF tests, and thus ratios of energy from fat and carbohydrate in the meals varied – factors shown to influence postprandial lipemia (46, 48, 68, 72). The present study was designed to determine the effect of increasing levels of fat and therefore both fat and carbohydrate would have to be increased to keep their ratio constant and this would have increased the total energy in the meal tests in a non-physiologic manner. Third, only two TG species were measured and for dietary lipid entry and turnover rates, data from hours one-three were used. Beyond modeling the rise of blood lipid, data from these time points were used because late in the postprandial period (after four hours), recycling of label through the liver, followed by re-secretion of label in newly-made VLDL particles would make calculations of entry rate and turnover of the lipid pools inaccurate (46, 48). On the other hand, the utility of this method demonstrates that it can be used in studies of larger sample size while analyzing lower amounts of plasma (51). The present study labeled meals with $^2\text{H}_{11}$ -oleate, while our past studies have utilized dietary per-deuterated tripalmitin (31, 73, 74). It is quite likely that similar methods can be employed when palmitate is used to label the test meal, although this fatty acid may be less absorbable (38). The two TG species analyzed in this report, triolein and palmitate-diolein, were appropriate targets for current analysis considering the stable isotope of oleate

was used. If future projects utilize a different label (e.g., $^{13}\text{C}_4$ palmitate), the TG species analyzed should of course, be chosen accordingly. With regard to applications, this method may aid in facilitating research across a number of scientific fields. For instance, similar studies could be conducted in individuals who are lean, overweight, and obese to test whether insulin-resistant individuals increase their absorption of meal lipid resulting in greater production of chylomicron particles in the immediate postprandial phase.

Summary and conclusions

The National Institutes of Health (NIH) recently developed a strategic plan for precision nutrition research that cites four goals aimed at answering key questions surrounding the role of diet in health and disease (16). This strategic plan calls for high-throughput, large-scale clinical trials in which advanced methodology is utilized to better characterize dietary habits and the impact on health. The method described here can easily be scaled-up to meet the goals set forth by the NIH and applied in conjunction with other 'omics and bioinformatic methods (75) to understand the impact of the gut microbiome, exercise, circadian rhythms, meal timing, glycemic profile, macronutrient composition, or varying types of fats on human intestinal lipid secretion. Further, interest has grown in the area of intestinal signaling events that may influence post-meal satiety (endocannabinoids, bile acids) and future pharmacological studies may investigate the impact of drugs that alter lipid absorption from the intestine (21, 23-26).

In conclusion, the use of meal-fat labeling, followed by LC-MRM analysis, holds substantial promise as a technique to investigate chylomicron appearance and handling in humans. The method will enable future studies of basic enterocyte biology to discover how lipid handling varies across physiological states and identify factors that can be manipulated to lower postprandial hyperlipidemia and reduce risk of cardiovascular and metabolic diseases, including NAFLD and type 2 diabetes. Precision nutrition studies will be designed with large sample sizes, generalizability, and simplicity of study design to understand how an individual's dietary pattern influences their health throughout the lifespan.

TABLES

Table 2.1. Composition of the test meals

Prior evening meal composition ¹			
Energy (kcal)	1067 ± 112		
Protein (%E)	23.4		
Carbohydrate (%E)	57.9		
Fat (%E)	18.7		
<u>Test meals contents</u>	Low fat	Moderate fat	High fat
Ingredients			
Ensure (fl. oz)	8.0	8.0	8.0
Dextrose (g)	14.0	14.0	14.0
Heavy cream (g)	0.0	9.0	22.0
Corn oil (g)	0.0	6.0	16.0
Canola oil (g)	2.0	7.0	21.0
Labeled oleate (g)	1.7	2.7	5.3
Composition			
Energy (kcal)	439	577	859
Cholesterol (mg)	10.0	20.5	35.7
Protein (g)	13.0	13.2	13.4
Carbohydrate (g)	63.0	63.2	63.6
Fat (g)	14.7	30.0	61.4
Fatty acid content			
16:0 (g)	1.0	2.6	5.5
18:2, n-6 (g)	3.6	7.7	15.7
18:1, n-9 (g) ²	8.2	13.3	25.7
Meal enrichment of 18:1	17.2%	16.9%	17.1%

¹ Data are mean ± SD, *n* = 12 participants. The same low-fat meal was fed the evening before all meal tests and provided 40% of the subject's estimated total daily energy needs (%E, energy as a percentage of total daily energy needs).

² The sum of the unlabeled 18:1 in the various meal ingredients.

Table 2.2. TRL-TG: Model fit, absolute entry rate (slope), and fractional entry rate (k) of label in singly- and doubly- labeled 54:3 and 52:2

Meal fat quantity	Units	Singly-labeled 54:3	Doubly-labeled 54:3	Singly-labeled 52:2	Doubly-labeled 52:2
Low Fat	r^2	0.95±0.06	0.96±0.06	0.95±0.03	0.95±0.05
	Absolute entry rate (µmol/L/h)	42.1±23.0 †‡	13.0±6.4 †‡	18.7±10.3 †	1.5±0.8 †
	k (pools/h)	1.1±0.3	1.2±0.4	0.9±0.3	1.2±0.4
Moderate Fat	r^2	0.96±0.03	0.97±0.03	0.98±0.02	0.96±0.03
	Absolute entry rate (µmol/L/h)	39.9±13.7 †‡	12.1±3.9 ‡	25.6±8.4 #	2.4±0.7
	k (pools/h)	1.1±0.3	1.1±0.2	1.0±0.2	1.1±0.3
High Fat	r^2	0.97±0.03	0.98±0.03	0.95±0.07	0.98±0.03
	Absolute entry rate (µmol/L/h)	68.6±33.7 ‡	21.9±12.8 ‡	40.0±17.0	4.4±3.0
	k (pools/h)	1.1±0.3	1.2±0.3	1.1±0.3	1.2±0.3
	P – value*	0.002	0.008	<0.001	0.001

Data are mean ± SD, $n = 12$.

Absolute entry rate (µmol/L/h)

Horizontal comparison

‡ Significantly different ($P < 0.001$) absolute entry rate (µmol/L/h), when 54:3 is compared to the 52:2 TG species with the same number of labels by t -test – e.g., horizontally across the table, LF singly-labeled 54:3 compared to LF singly-labeled 52:2.

Vertical comparison

* P -value for repeated measures ANOVA comparison of absolute entry rate (µmol/L/h) between LF, MF, and HF, data within a single column of TRL-TG species.

† Post-hoc analysis (pairwise t -test with Bonferroni adjustment), significantly different ($P < 0.05$) absolute entry rate (µmol/L/h), when compared to HF entry rate – e.g., vertically down the column, LF singly-labeled 54:3 compared to HF singly-labeled 54:3.

Absolute entry rate for the MF singly-labeled 52:2 compared to HF singly-labeled 52:2

($P = 0.078$, t -test with Bonferroni adjustment post-hoc test).

k (fractional entry rate) = slope of the early rise of labeled TG/absolute change in TRL-TG concentration 1h to 3h ($\mu\text{mol/L}$).

No significant differences in k were detected by ANOVA across (vertical comparison) fat levels within specific TG species, singly- or doubly- labeled, or by *t*-tests (horizontal comparison) between singly-labeled TG 54:3 and 52:2 or doubly-labeled TG 54:3 and 52:2 in LF, MF, or HF.

Table 2.3. S_r>400 -TG: Model fit, absolute entry rate (slope), and fractional entry rate (k) of label in singly- and doubly- labeled 54:3 and 52:2

Meal fat quantity	Units	Singly-labeled 54:3	Doubly-labeled 54:3	Singly-labeled 52:2	Doubly-labeled 52:2
Low Fat	r^2	0.94±0.05	0.95±0.05	0.94±0.07	0.95±0.05
	Absolute entry rate (µmol/L/h)	19.3±14.7 ‡	5.5±4.2 ‡	6.1±5.4	0.6±0.4
	k (pools/h)	0.9±0.4	1.0±0.4	1.0±0.5	1.0±0.4
Moderate Fat	r^2	0.96±0.03	0.97±0.03	0.97±0.03	0.97±0.02
	Absolute entry rate (µmol/L/h)	19.1±11.1 ‡	4.9±2.8 ‡	10.2±5.7	1.0±0.6
	k (pools/h)	0.8±0.5	1.0±0.5	0.9±0.4	1.0±0.4
High Fat	r^2	0.96±0.03	0.96±0.03	0.96±0.03	0.97±0.03
	Absolute entry rate (µmol/L/h)	42.5±40.8 ‡	11.9±12.4 ‡	24.6±24.1	2.6±2.7
	k (pools/h)	1.1±0.4	1.0±0.3	1.2±0.4	1.1±0.4
	<i>P</i> – value*	0.040	0.065	0.022	0.033

Data are mean ± SD, $n = 8$.

Absolute entry rate (µmol/L/h)

Horizontal comparison

‡ Significantly different ($P < 0.05$) absolute entry rate (µmol/L/h), when 54:3 is compared to the 52:2 TG species with the same number of labels by *t*-test – e.g., horizontally across the table, LF singly-labeled 54:3 compared to LF singly-labeled 52:2.

Vertical comparison

* *P*-value for repeated measures ANOVA comparison of absolute entry rate (µmol/L/h) between LF, MF, and HF, data within a single column of S_r>400-TG species.

Post-hoc analysis (pairwise *t*-test with Bonferroni adjustment), indicated no significant differences in absolute entry rates (µmol/L/h) when compared to HF entry rate.

k (fractional entry rate) = slope of the early rise of labeled TG/absolute change in S_r>400-TG concentration 1h to 3h (µmol/L).

No significant differences in k were detected by ANOVA across (vertical comparison) fat levels within specific TG species, singly- or doubly- labeled, or by

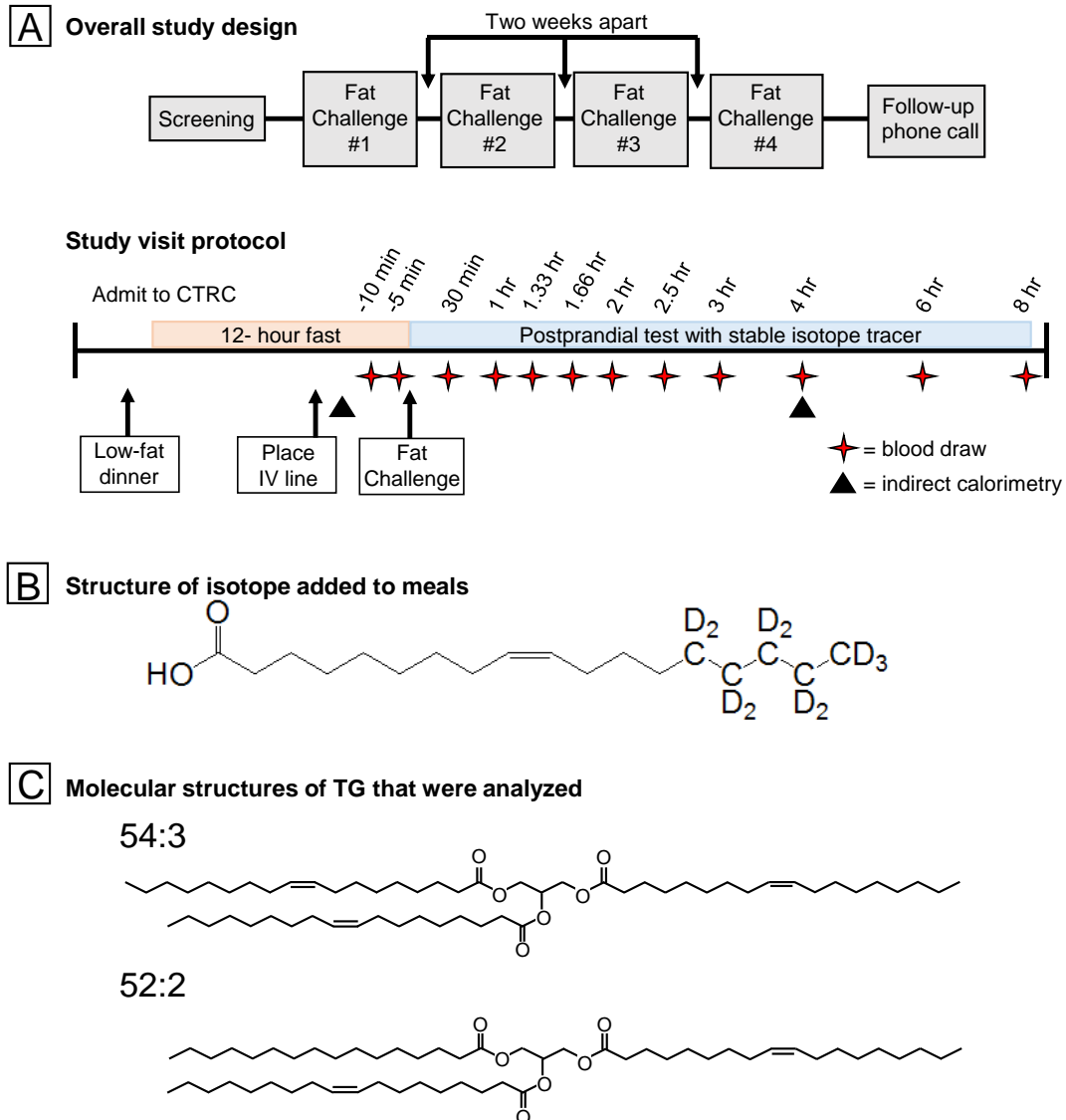
t -tests (horizontal comparison) between singly-labeled TG 54:3 and 52:2 or doubly-labeled TG 54:3 and 52:2 in LF, MF, or HF.

Table 2.4. Key factors to consider when designing studies for precision nutrition

<p>1) Type and timing of the study meal?</p> <ul style="list-style-type: none">- Solid versus liquid meals?- Length of postprandial sample collection?- Fasting status of the subjects?- Previous meal timing and composition (second meal effect)?- Distribution of macronutrients across the day?- Nocturnal effects of feeding on postprandial lipid metabolism? <p>2) Controlling pre-study activities?</p> <ul style="list-style-type: none">- If yes, the outcomes should be focused on biology and metabolism.- If no, the goals should be focused on behavior and generalizability.- Individual responses <p>3) Effects of sex on metabolism?</p> <ul style="list-style-type: none">- Factors, such as fructose (5, 61), affect postprandial lipemia in men and women differently.- Which factors should be controlled for when including men and women?- How do these factors impact the sexes differently?
--

FIGURES

Figure 2.1. Overall study design, protocol for meal tests, and molecular structures of the stable isotope and the TG 54:3 and 52:2 containing oleic acid moieties that were measured.

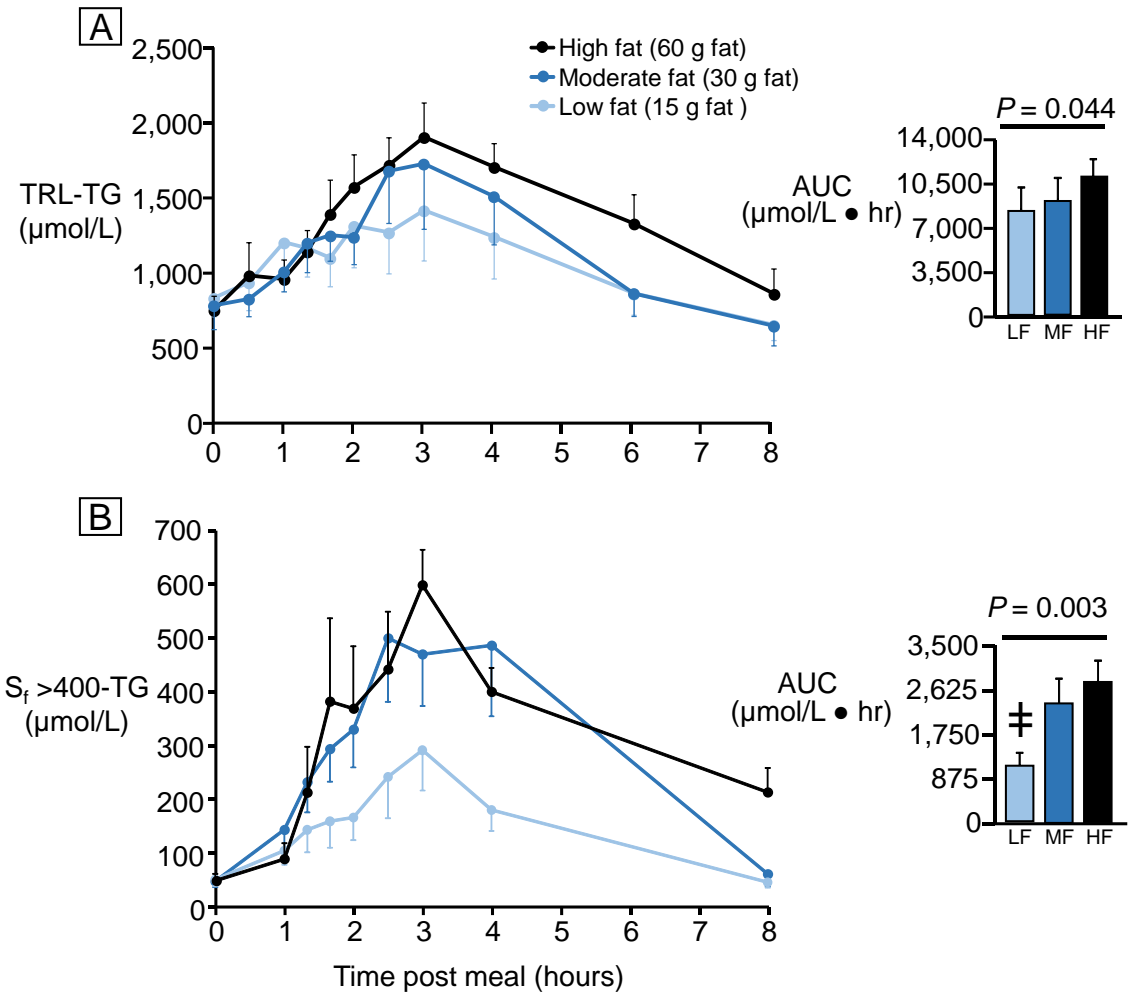


2.1A: The four fat challenges containing $^2\text{H}_{11}$ -oleate were low fat (LF, 15 g), moderate fat (MF, 30 g), and two high fat (HF, 60 g) tests to evaluate reproducibility. The two HF test meals were given in succession and the results of one of the HF meals was chosen for comparison with LF and MF as described in the methods section.

2.1B: The structure of $^2\text{H}_{11}$ -oleate.

2.1C: Note that after feeding $^2\text{H}_{11}$ -oleate, circulating TG species will contain labeled oleic acid in either one (singly) or two (doubly) positions on these TG molecules.

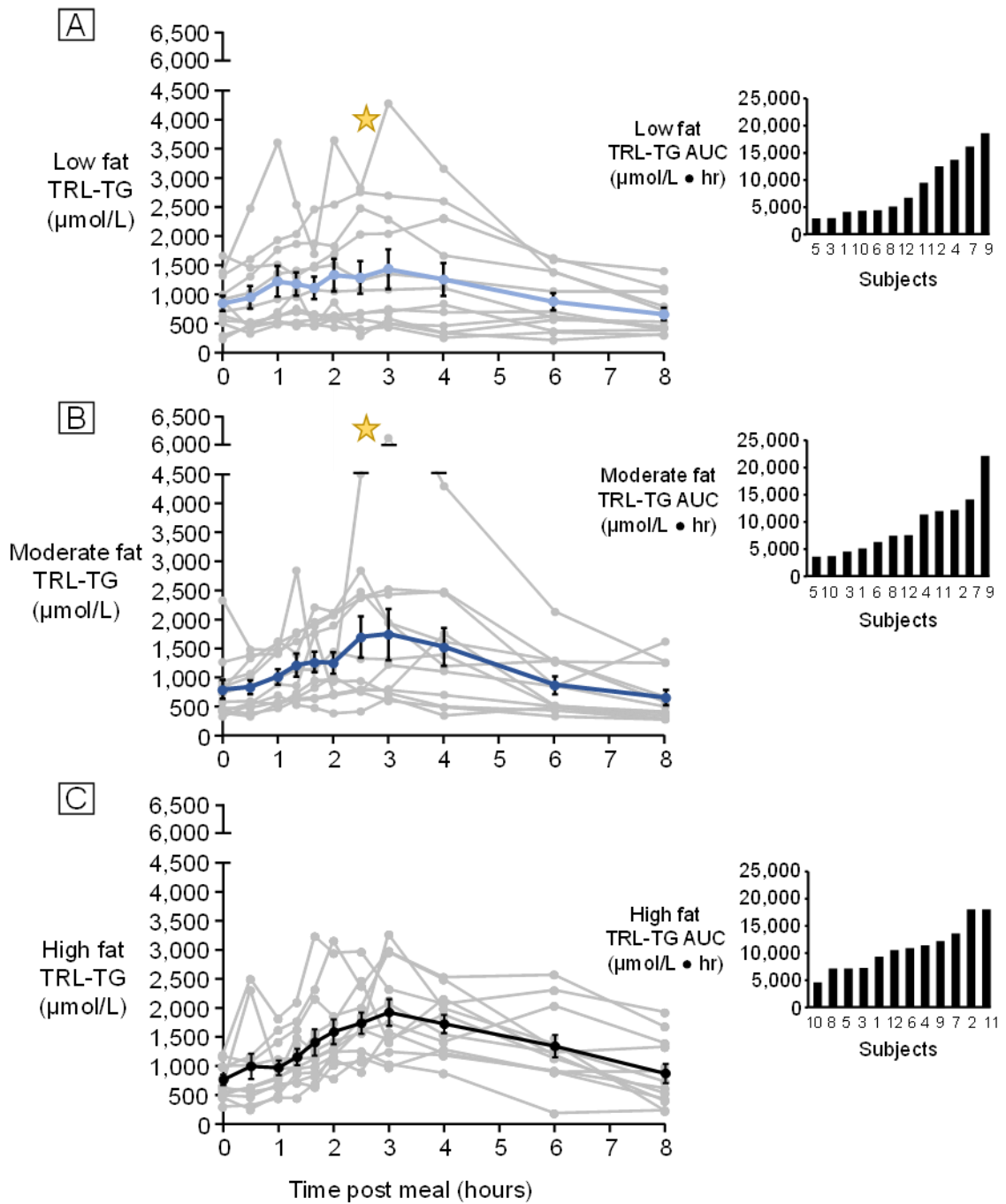
Figure 2.2. TRL- and S_f>400-TG: Total TG concentrations following the meal tests



Data are mean ± SEM, $n = 12$ for TRL-TG and $n = 8$ for S_f>400 lipoprotein-TG. Main effect of meal fat level was compared for AUC of TRL-TG and S_f>400 lipoprotein-TG using ANOVA and post-hoc analysis (pairwise t -test with Bonferroni adjustment).

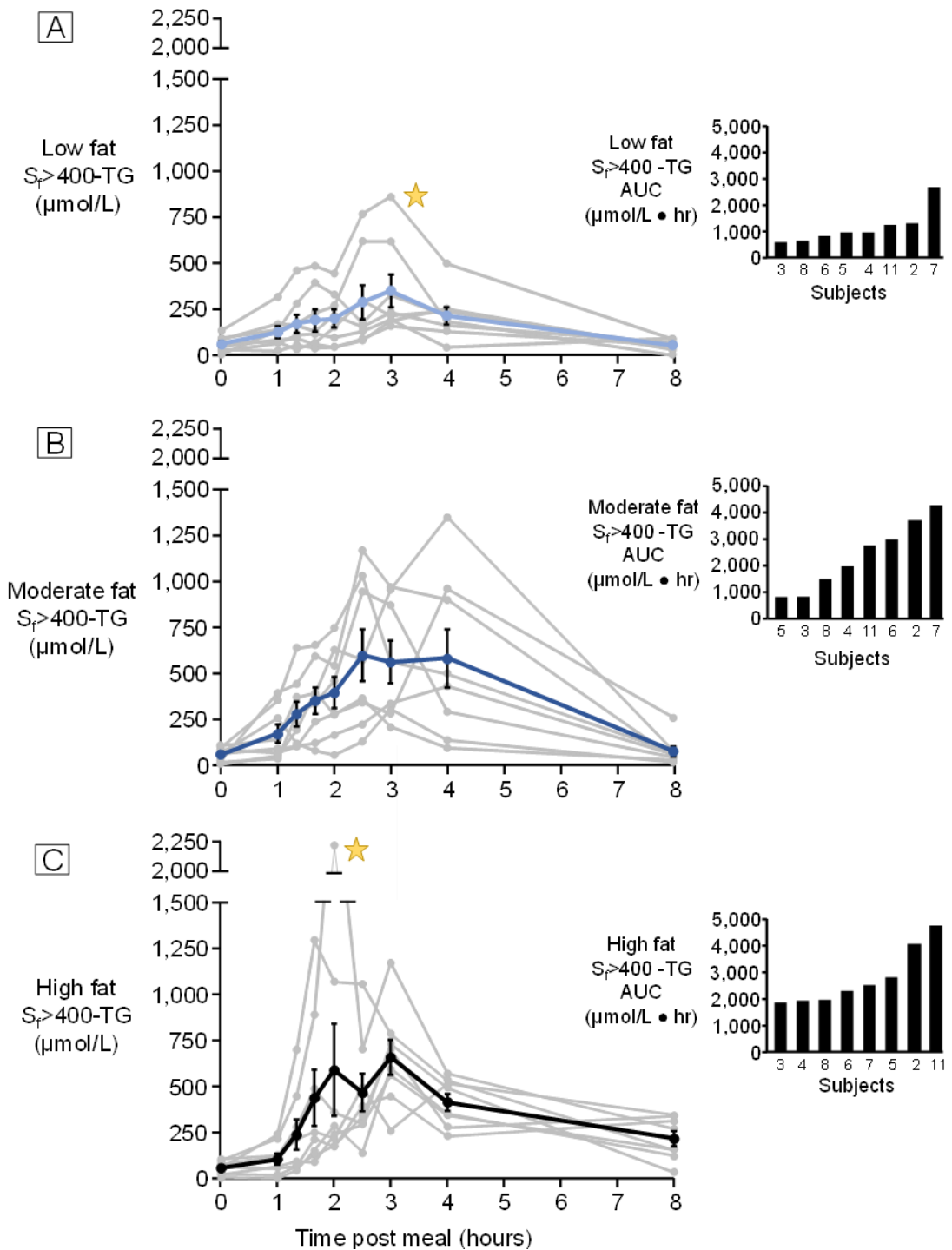
‡ post-hoc testing indicated significant ($P < 0.01$) differences between the LF and the MF and HF meals.

Figure 2.3. TRL-TG: Variability in concentrations across subjects



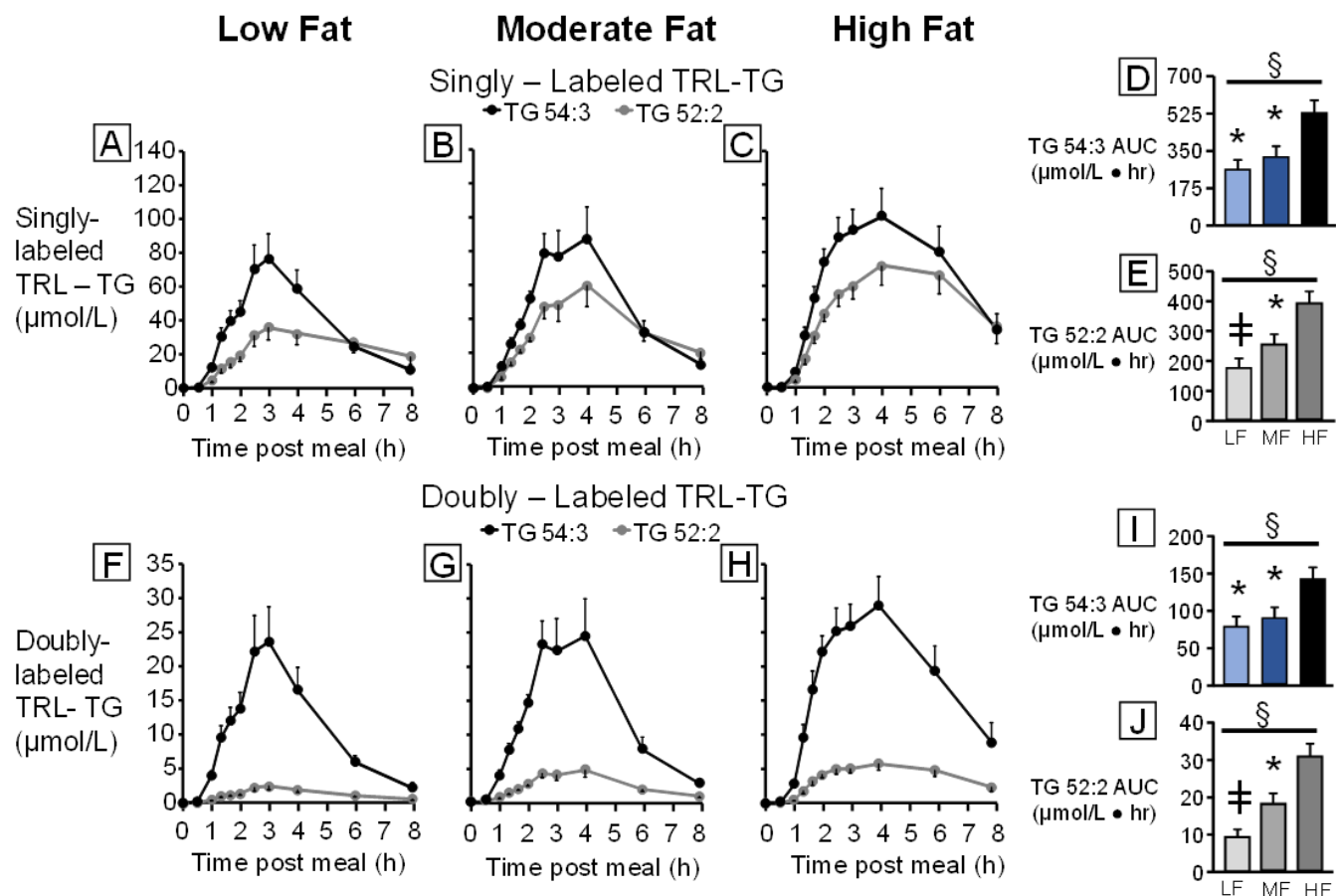
Grey lines are individual subject data with the mean \pm SEM plotted in black on top, $n = 12$. Stars are indicative of outliers in the group and are discussed in the text in detail. Bar graphs show individual subject AUC.

Figure 2.4. Sf>400-TG: Variability in concentrations across subjects



Grey lines are individual subject data with the mean \pm SEM plotted in black on top, $n = 8$. Stars are indicative of outliers in the group and are discussed in the text in detail. Bar graphs show individual subject AUC.

Figure 2.5. TRL-TG: Temporal patterns of 54:3 and 52:2 TG containing singly- and doubly-labeled oleate



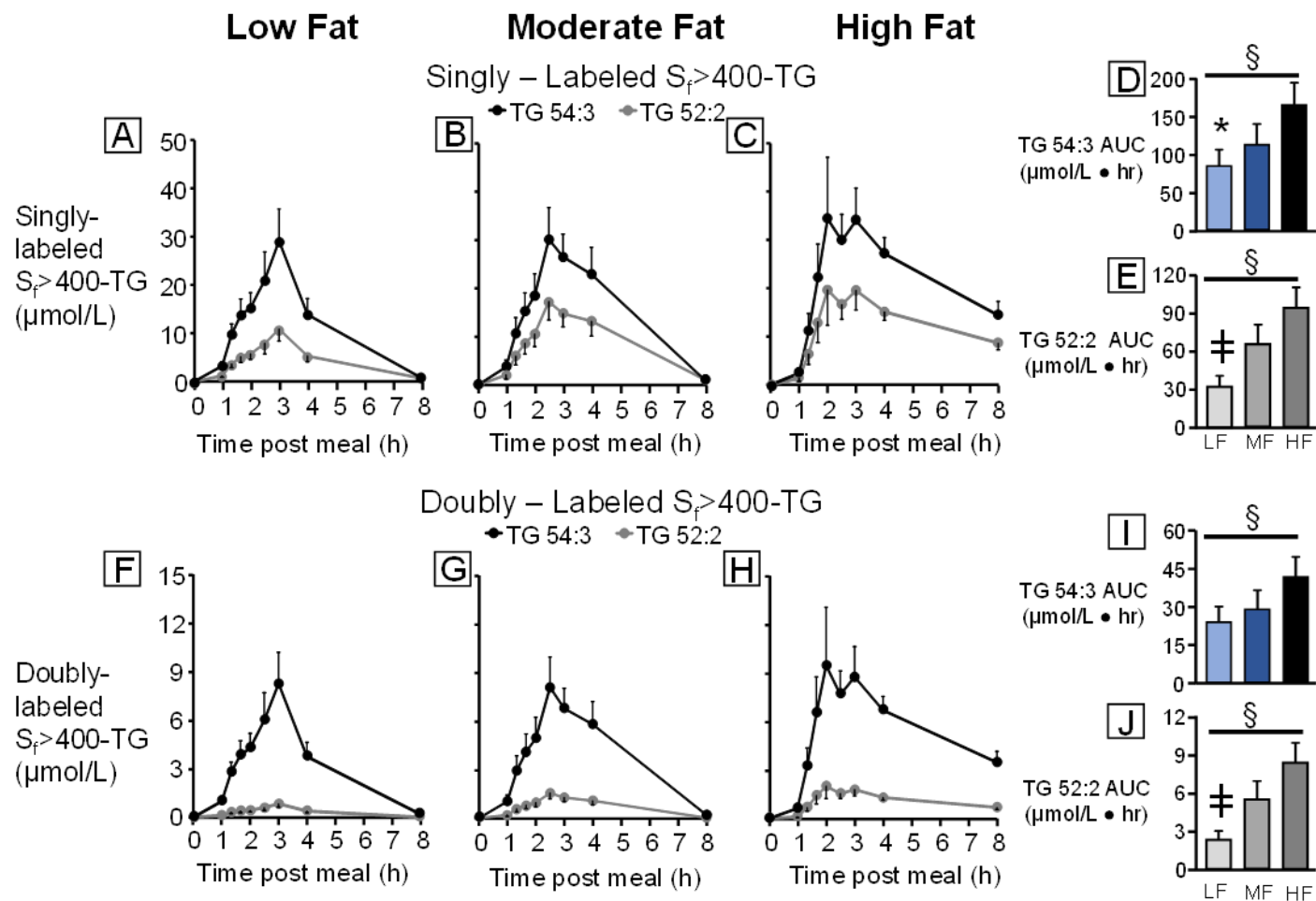
Data are mean \pm SEM, $n = 12$. Note the differing magnitudes on the ordinate of the singly- (**figure 2.5A-C**) versus doubly-labeled (**figure 2.5F-H**) graphs.

§ Significant main effect ($P < 0.00001$) of meal fat level on AUC of labeled TRL-TG using ANOVA and post-hoc analysis (pairwise t -test with Bonferroni adjustment).

‡ Significantly ($P < 0.05$) different than MF and HF meals.

* Significantly ($P < 0.001$) different than HF meal.

Figure 2.6. $S_{f>400}$ -TG: Temporal patterns of 54:3 and 52:2 TG containing singly- and doubly-labeled oleate



Data are mean \pm SEM, $n = 8$ for $S_{f>400}$ lipoproteins.

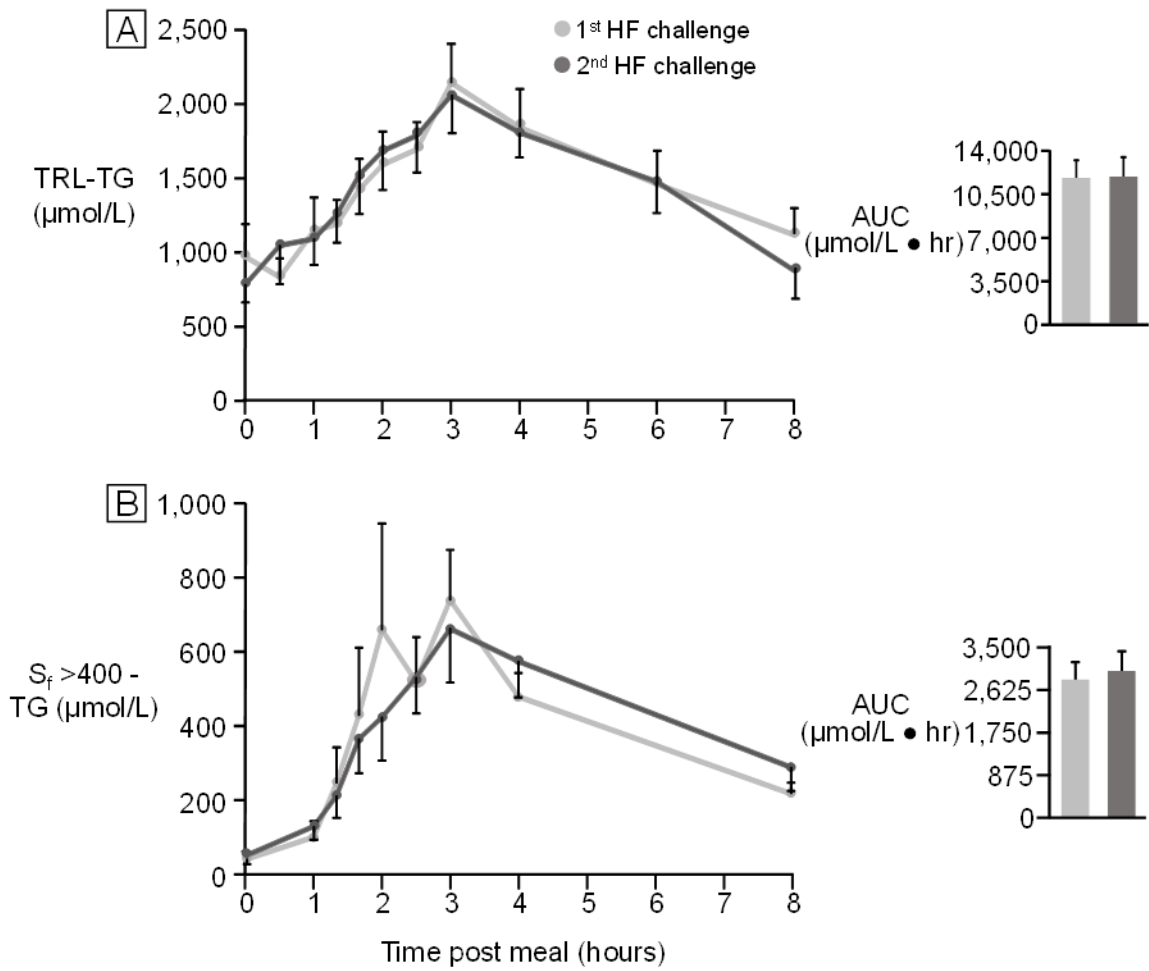
§ Significant main effect ($P < 0.05$) of meal fat level on AUC of labeled $S_{f>400}$ -TG using ANOVA and post-hoc analysis (pairwise t -test with Bonferroni adjustment).

† Significantly ($P < 0.05$) different that MF and HF meals.

* Significantly ($P < 0.05$) different than HF meal.

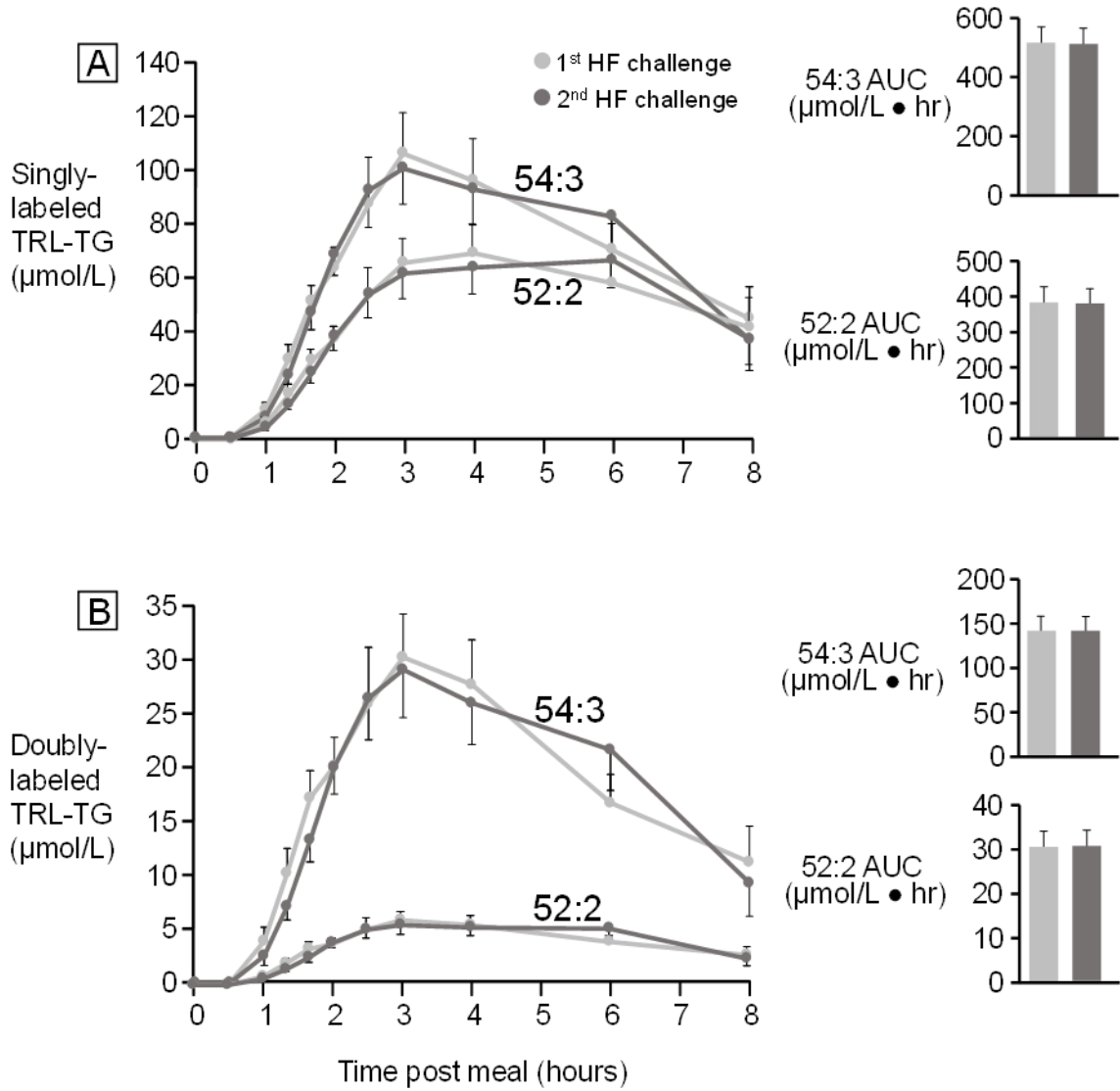
SUPPLEMENTARY DATA

Supplementary Figure S2.1. TRL- and $S_f > 400$ -TG: Reproducibility of total TG between two HF test meals



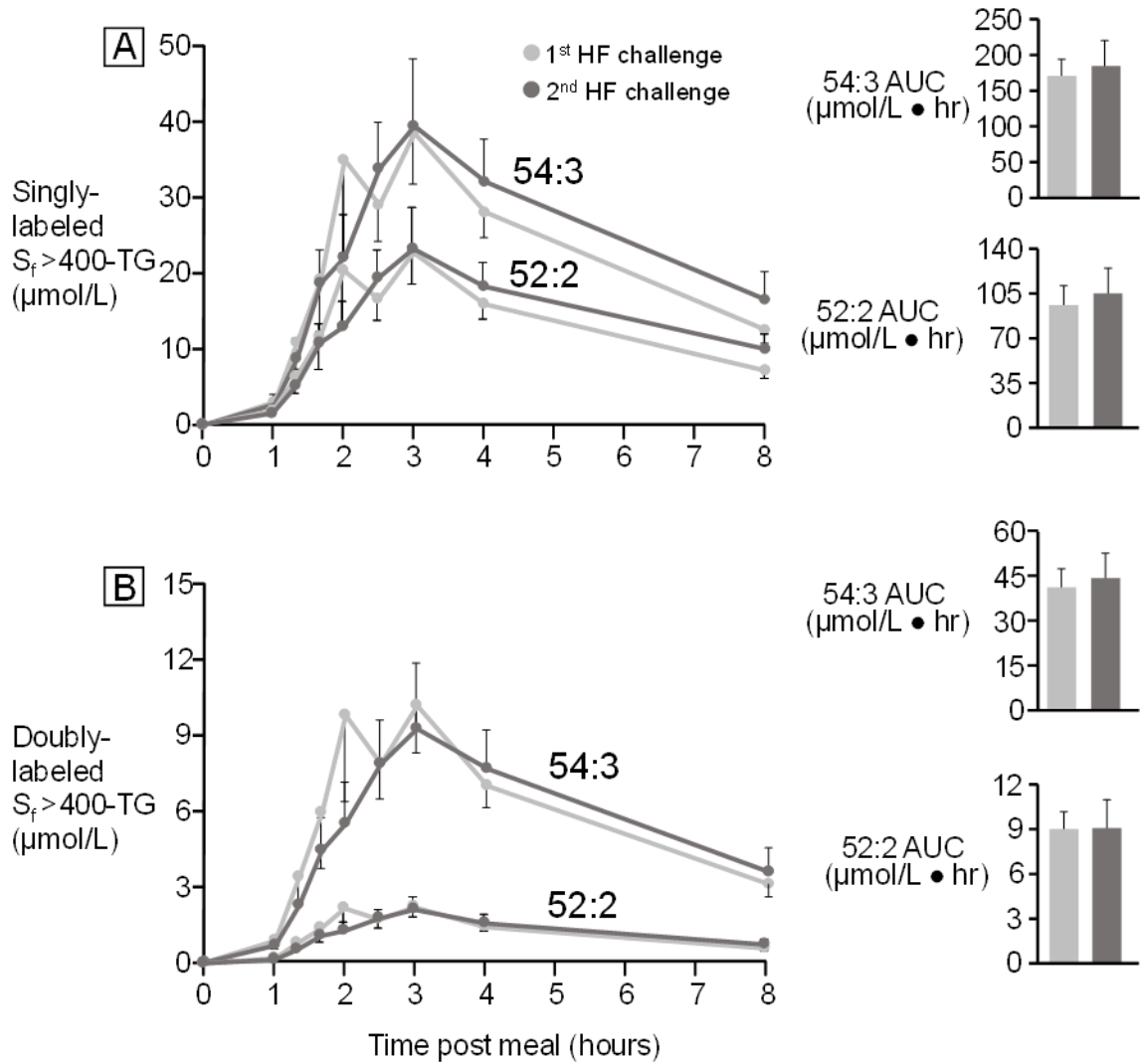
Data are mean \pm SEM, $n = 12$ for TRL and $n = 8$ for $S_f > 400$ lipoproteins. The two HF test meals were given in succession and randomized amongst LF and MF.

Supplementary Figure S2.2. TRL-TG: Reproducibility of singly- and doubly-labeled 54:3 and 52:2 between two HF test meals



Data are mean \pm SEM, $n = 12$.

Supplementary Figure S2.3. $S_f > 400$ – TG: Reproducibility of singly- and doubly- labeled 54:3 and 52:2 between two HF test meals.



Data are mean \pm SEM, $n = 8$.

SUPPORTING INFORMATION

High throughput LC-MS method to investigate postprandial lipemia: Considerations for future precision nutrition research

Justine M. Mucinski¹, Jennifer E. Vena², Maria A. Ramos-Roman³, Michael E. Lassman⁴, Magdalene Szuszkiewicz-Garcia⁵, David G. McLaren⁴, Stephen F. Previs⁴, Sudha S. Shankar⁴, Elizabeth J. Parks^{1,6,*}

¹ Department of Nutrition and Exercise Physiology, University of Missouri, Columbia, MO 65211

² Alberta's Tomorrow Project, CancerControl Alberta, Alberta Health Services, Calgary Alberta, T2T 5C7, Canada

³ Department of Internal Medicine, Division of Endocrinology, University of Texas Southwestern Medical Center, Dallas, TX, USA

⁴ MRL, Merck & Co., Inc., Kenilworth, NJ, USA

⁵ Methodist Mansfield Medical Center, Mansfield, TX, USA

⁶ Department of Medicine, Division of Gastroenterology and Hepatology, University of Missouri School of Medicine, Columbia, MO 65201

*CORRESPONDING AUTHOR:

Elizabeth J. Parks, PhD

Email: parksej@missouri.edu

AUTHOR CONTRIBUTION: JEV, MEL, and EJP generated the data; DGM, SFP, and SSS, provided technical input on the study design and methods; MARR and MSG were overseeing physicians; JMM analyzed and wrote the first draft; All authors contributed to data interpretation and to editing the manuscript.

AUTHOR DISCLOSURES: MEL, DGM, and SFP are employees of Merck Sharp & Dohme Corp., a subsidiary of Merck & Co., Inc., Kenilworth, NJ, USA. SSS is a former employee of Merck Sharp & Dohme Corp., a subsidiary of Merck & Co., Inc., Kenilworth, NJ, USA and currently an employee of AstraZeneca in the United States.

FULL CITATION:

Mucinski JM, Vena JE, Ramos-Roman MA, Lassman ME, Szuszkiewicz-Garcia M, McLaren DG, Previs SF, Shankar SS, Parks EJ. High-throughput LC-MS method to investigate postprandial lipemia: considerations for future precision nutrition research. *Am J Physiol Endocrinol Metab.* 2021 Apr 1;320(4):E702-E715. doi: 10.1152/ajpendo.00526.2020. Epub 2021 Feb 1. PMID: 33522396.

REFERENCES

1. Zilversmit DB. Atherogenesis: a postprandial phenomenon. *Circulation* 60, 473-485, (1979), PMID:222498.
2. Karpe F. Postprandial lipoprotein metabolism and atherosclerosis. *Journal of Internal Medicine* 246, 341-355, (1999), PMID:10583705.
3. Ginsberg HN, and Illingworth DR. Postprandial dyslipidemia: an atherogenic disorder common in patients with diabetes mellitus. *American Journal of Cardiology* 88, 9h-15h, (2001), PMID:11576520.
4. Kolovou GD, Mikhailidis DP, Kovar J, Lairon D, Nordestgaard BG, Ooi TC, Perez-Martinez P, Bilianou H, Anagnostopoulou K, and Panotopoulos G. Assessment and clinical relevance of non-fasting and postprandial triglycerides: an expert panel statement. *Current Vascular Pharmacology* 9, 258-270, (2011), PMID:21314632.
5. Duez H, Lamarche B, Uffelman KD, Valero R, Cohn JS, and Lewis GF. Hyperinsulinemia is associated with increased production rate of intestinal apolipoprotein B-48-containing lipoproteins in humans. *Arteriosclerosis, Thrombosis, and Vascular Biology* 26, 1357-1363, (2006), PMID:16614317.
6. Grundy SM, and Mok HY. Chylomicron clearance in normal and hyperlipidemic man. *Metabolism: Clinical and Experimental* 25, 1225-1239, (1976), PMID:185486.
7. Drouin-Chartier JP, Tremblay AJ, Lemelin V, Lamarche B, and Couture P. Differential associations between plasma concentrations of insulin and glucose and intestinal expression of key genes involved in chylomicron metabolism. *American Journal of Physiology: Gastrointestinal and Liver Physiology* 315, G177-g184, (2018), PMID:29698057.
8. Couture P, Tremblay AJ, Kelly I, Lemelin V, Droit A, and Lamarche B. Key intestinal genes involved in lipoprotein metabolism are downregulated in dyslipidemic men with insulin resistance. *Journal of Lipid Research* 55, 128-137, (2014), PMID:24142110.
9. Hogue JC, Lamarche B, Tremblay AJ, Bergeron J, Gagne C, and Couture P. Evidence of increased secretion of apolipoprotein B-48-containing lipoproteins in subjects with type 2 diabetes. *Journal of Lipid Research* 48, 1336-1342, (2007), PMID:17337758.
10. Phillips ML, Pullinger C, Kroes I, Kroes J, Hardman DA, Chen G, Curtiss LK, Gutierrez MM, Kane JP, and Schumaker VN. A single copy of apolipoprotein B-48 is present on the human chylomicron remnant. *Journal of Lipid Research* 38, 1170-1177, (1997), PMID:9215545.
11. Zheng C, Ikewaki K, Walsh BW, and Sacks FM. Metabolism of apoB lipoproteins of intestinal and hepatic origin during constant feeding of small amounts of fat. *Journal of Lipid Research* 47, 1771-1779, (2006), PMID:16685082.
12. Berry SE, Valdes AM, Drew DA, Asnicar F, Mazidi M, Wolf J, Capdevila J, Hadjigeorgiou G, Davies R, Al Khatib H, Bonnett C, Ganesh S, Bakker E, Hart D, Mangino M, Merino J, Linenberg I, Wyatt P, Ordovas JM, Gardner CD, Delahanty LM, Chan AT, Segata N, Franks PW, and Spector TD.

- Human postprandial responses to food and potential for precision nutrition. *Nature Medicine* 26, 964-973, (2020), PMID:32528151.
13. Gardner CD, Kiazand A, Alhassan S, Kim S, Stafford RS, Balise RR, Kraemer HC, and King AC. Comparison of the Atkins, Zone, Ornish, and LEARN diets for change in weight and related risk factors among overweight premenopausal women: the A TO Z Weight Loss Study: a randomized trial. *Journal of the American Medical Association* 297, 969-977, (2007), PMID:17341711.
 14. Sacks FM, Bray GA, Carey VJ, Smith SR, Ryan DH, Anton SD, McManus K, Champagne CM, Bishop LM, Laranjo N, Leboff MS, Rood JC, de Jonge L, Greenway FL, Loria CM, Obarzanek E, and Williamson DA. Comparison of weight-loss diets with different compositions of fat, protein, and carbohydrates. *New England Journal of Medicine* 360, 859-873, (2009), PMID:19246357.
 15. Shai I, Schwarzfuchs D, Henkin Y, Shahar DR, Witkow S, Greenberg I, Golan R, Fraser D, Bolotin A, Vardi H, Tangi-Rozental O, Zuk-Ramot R, Sarusi B, Brickner D, Schwartz Z, Sheiner E, Marko R, Katorza E, Thiery J, Fiedler GM, Blüher M, Stumvoll M, and Stampfer MJ. Weight loss with a low-carbohydrate, Mediterranean, or low-fat diet. *New England Journal of Medicine* 359, 229-241, (2008), PMID:18635428.
 16. Rodgers GP, and Collins FS. Precision Nutrition—the Answer to “What to Eat to Stay Healthy”. *Journal of the American Medical Association* 324, 735-736, (2020), PMID:32766768.
 17. Corbin KD, Krajmalnik-Brown R, Carnero EA, Bock C, Emerson R, Rittmann BE, Marcus AK, Davis T, Dirks B, Ilhan ZE, Champagne C, and Smith SR. Integrative and quantitative bioenergetics: Design of a study to assess the impact of the gut microbiome on host energy balance. *Contemporary Clinical Trials Communications* 19, 100646, (2020), PMID:32875141.
 18. Mills S, Lane JA, Smith GJ, Grimaldi KA, Ross RP, and Stanton C. Precision Nutrition and the Microbiome Part II: Potential Opportunities and Pathways to Commercialisation. *Nutrients* 11, (2019), PMID:31252674.
 19. deCampo DM, and Kossoff EH. Ketogenic dietary therapies for epilepsy and beyond. *Current Opinion in Clinical Nutrition and Metabolic Care* 22, 264-268, (2019), PMID:31033577.
 20. Lilamand M, Porte B, Cognat E, Hugon J, Mouton-Liger F, and Paquet C. Are ketogenic diets promising for Alzheimer's disease? A translational review. *Alzheimer's Research & Therapy* 12, 42, (2020), PMID:32290868.
 21. Xiao C, Dash S, Morgantini C, Adeli K, and Lewis GF. Gut peptides are novel regulators of intestinal lipoprotein secretion: Experimental and pharmacological manipulation of lipoprotein metabolism. *Diabetes* 64, 2310-2318, (2015), PMID:26106188.
 22. Adeli K, and Lewis GF. Intestinal lipoprotein overproduction in insulin-resistant states. *Current Opinion in Lipidology* 19, 221-228, (2008), PMID:18460911.
 23. Gao X, Zhang Q, Meng D, Isaac G, Zhao R, Fillmore TL, Chu RK, Zhou J, Tang K, Hu Z, Moore RJ, Smith RD, Katze MG, and Metz TO. A reversed-

- phase capillary ultra-performance liquid chromatography–mass spectrometry (UPLC-MS) method for comprehensive top-down/bottom-up lipid profiling. *Analytical and Bioanalytical Chemistry* 402, 2923-2933, (2012), PMID:22354571.
24. Xiao C, Dash S, Morgantini C, and Lewis GF. New and emerging regulators of intestinal lipoprotein secretion. *Atherosclerosis* 233, 608-615, (2014), PMID:24534456.
 25. Xiao C, Dash S, Morgantini C, Patterson BW, and Lewis GF. Sitagliptin, a DPP-4 inhibitor, acutely inhibits intestinal lipoprotein particle secretion in healthy humans. *Diabetes* 63, 2394-2401, (2014), PMID:24584549.
 26. Bandsma RH, and Lewis GF. Newly appreciated therapeutic effect of GLP-1 receptor agonists: reduction in postprandial lipemia. *Atherosclerosis* 212, 40-41, (2010), PMID:20638063.
 27. Liu J, McLaren DG, Chen D, Kan Y, Stout SJ, Shen X, Murphy BA, Forrest G, Karanam B, Sonatore L, He S, Roddy TP, and Pinto S. Potential mechanism of enhanced postprandial glucagon-like peptide-1 release following treatment with a diacylglycerol acyltransferase 1 inhibitor. *Pharmacology Research & Perspectives* 3, e00193, (2015), PMID:27022467.
 28. Varady KA. Meal frequency and timing: impact on metabolic disease risk. *Current Opinion in Endocrinology, Diabetes, and Obesity* 23, 379-383, (2016), PMID:27455514.
 29. de Cabo R, and Mattson MP. Effects of intermittent fasting on health, aging, and disease. *New England Journal of Medicine* 381, 2541-2551, (2019), PMID:31881139.
 30. Timlin MT, Barrows BR, and Parks EJ. Increased dietary substrate delivery alters hepatic fatty acid recycling in healthy men. *Diabetes* 54, 2694-2701, (2005), PMID:16123359.
 31. Barrows BR, Timlin MT, and Parks EJ. Spillover of dietary fatty acids and use of serum nonesterified fatty acids for the synthesis of VLDL-triacylglycerol under two different feeding regimens. *Diabetes* 54, 2668-2673, (2005), PMID:16123356.
 32. Chavez-Jauregui RN, Mattes RD, and Parks EJ. Dynamics of fat absorption and effect of sham feeding on postprandial lipemia. *Gastroenterology* 139, 1538-1548, (2010), PMID:20493191.
 33. Lambert JE, Ramos-Roman MA, Browning JD, and Parks EJ. Increased de novo lipogenesis is a distinct characteristic of individuals with nonalcoholic fatty liver disease. *Gastroenterology* 146, 726-735, (2014), PMID:24316260.
 34. Lambert JE, and Parks EJ. Getting the label in: practical research strategies for tracing dietary fat. *International Journal of Obesity Supplements* 2, S43-50, (2012), PMID:27152153.
 35. Hodson L, Bickerton AS, McQuaid SE, Roberts R, Karpe F, Frayn KN, and Fielding BA. The contribution of splanchnic fat to VLDL triglyceride is greater in insulin-resistant than insulin-sensitive men and women: studies in the postprandial state. *Diabetes* 56, 2433-2441, (2007), PMID:17601988.

36. McQuaid SE, Hodson L, Neville MJ, Dennis AL, Cheeseman J, Humphreys SM, Ruge T, Gilbert M, Fielding BA, Frayn KN, and Karpe F. Downregulation of adipose tissue fatty acid trafficking in obesity: a driver for ectopic fat deposition? *Diabetes* 60, 47-55, (2011), PMID:20943748.
37. Robertson MD, Parkes M, Warren BF, Ferguson DJ, Jackson KG, Jewell DP, and Frayn KN. Mobilisation of enterocyte fat stores by oral glucose in humans. *Gut* 52, 834-839, (2003), PMID:12740339.
38. Gabert L, Vors C, Louche-Pélissier C, Sauvinet V, Lambert-Porcheron S, Draï J, Laville M, Désage M, and Michalski MC. ¹³C tracer recovery in human stools after digestion of a fat-rich meal labelled with [1,1,1-¹³C₃]tripalmitin and [1,1,1-¹³C₃]triolein. *Rapid Communications in Mass Spectrometry* 25, 2697-2703, (2011), PMID:21913246.
39. Cohn JS, McNamara JR, Krasinski SD, Russell RM, and Schaefer EJ. Role of triglyceride-rich lipoproteins from the liver and intestine in the etiology of postprandial peaks in plasma triglyceride concentration. *Metabolism: Clinical and Experimental* 38, 484-490, (1989), PMID:2725288.
40. Parks EJ, Skokan LE, Timlin MT, and Dingfelder CS. Dietary sugars stimulate fatty acid synthesis in adults. *Journal of Nutrition* 138, 1039-1046, (2008), PMID:18492831.
41. Ahmad TR, and Haeusler RA. Bile acids in glucose metabolism and insulin signalling - mechanisms and research needs. *Nature Reviews: Endocrinology* 15, 701-712, (2019), PMID:31616073.
42. Jequier E, Acheson K, and Schutz Y. Assessment of Energy Expenditure and Fuel Utilization in Man. *Annual Review of Nutrition* 7, 187-208, (1987), PMID:3300732.
43. Zambon A, Hashimoto SI, and Brunzell JD. Analysis of techniques to obtain plasma for measurement of levels of free fatty acids. *Journal of Lipid Research* 34, 1021-1028, (1993), PMID:8354949.
44. Parks EJ, Krauss RM, Christiansen MP, Neese RA, and Hellerstein MK. Effects of a low-fat, high-carbohydrate diet on VLDL-triglyceride assembly, production, and clearance. *Journal of Clinical Investigation* 104, 1087-1096, (1999), PMID:10525047.
45. Li X, Parks EJ, McLaren DG, Lambert JE, Cardasis HL, Chappell DL, McAvoy T, Salituro G, Alon A, Dennie J, Chakravarthy M, Shankar SS, Laterza OF, and Lassman ME. An LC-MRM method for measuring intestinal triglyceride assembly using an oral stable isotope-labeled fat challenge. *Bioanalysis* 8, 1265-1277, (2016), PMID:27225968.
46. Dubois C, Beaumier G, Juhel C, Armand M, Portugal H, Pauli AM, Borel P, Latge C, and Lairon D. Effects of graded amounts (0-50 g) of dietary fat on postprandial lipemia and lipoproteins in normolipidemic adults. *American Journal of Clinical Nutrition* 67, 31-38, (1998), PMID:9440372.
47. Timlin MT, and Parks EJ. Temporal pattern of de novo lipogenesis in the postprandial state in healthy men. *American Journal of Clinical Nutrition* 81, 35-42, (2005), PMID:15640457.
48. Dubois C, Armand M, Azais-Brasco V, Portugal H, Pauli AM, Bernard PM, Latge C, Lafont H, Borel P, and Lairon D. Effects of moderate amounts of

- emulsified dietary fat on postprandial lipemia and lipoproteins in normolipidemic adults. *American Journal of Clinical Nutrition* 60, 374-382, (1994), PMID:8074068.
49. Team RC. R: A language and environment for statistical computing. Vienna, Austria: R Foundation for Statistical Computing, 2018.
 50. Lambert JE, and Parks EJ. Postprandial metabolism of meal triglyceride in humans. *Biochimica et Biophysica Acta* 1821, 721-726, (2012), PMID:22281699.
 51. Adams SH, Anthony JC, Carvajal R, Chae L, Khoo CSH, Latulippe ME, Matusheski NV, McClung HL, Rozga M, Schmid CH, Wopereis S, and Yan W. Perspective: Guiding principles for the implementation of personalized nutrition approaches that benefit health and function. *Advances in Nutrition* 11, 25-34, (2020), PMID:31504115.
 52. Dias CB, Zhu X, Thompson AK, Singh H, and Garg ML. Effect of the food form and structure on lipid digestion and postprandial lipaemic response. *Food & Function* 10, 112-124, (2019), PMID:30566166.
 53. Schneeman BO, Kotite L, Todd KM, and Havel RJ. Relationships between the responses of triglyceride-rich lipoproteins in blood plasma containing apolipoproteins B-48 and B-100 to a fat-containing meal in normolipidemic humans. *Proceedings of the National Academy of Sciences of the United States of America* 90, 2069-2073, (1993), PMID:8446630.
 54. Cryer A. Tissue lipoprotein lipase activity and its action in lipoprotein metabolism. *International Journal of Biochemistry* 13, 525-541, (1981), PMID:7016622.
 55. Pokrajac N, and Lossow WJ. The effect of tube feeding of glucose or corn oil on adipose tissue lipoprotein lipase activity and uptake of ¹⁴C-labeled palmitic acid of chyle triglycerides in vitro. *Biochimica et Biophysica Acta* 137, 291-295, (1967), PMID:4963805.
 56. Sadur CN, and Eckel RH. Insulin stimulation of adipose tissue lipoprotein lipase. Use of the euglycemic clamp technique. *Journal of Clinical Investigation* 69, 1119-1125, (1982), PMID:7040473.
 57. Holmbäck U, Forslund A, Forslund J, Hambraeus L, Lennernäs M, Lowden A, Stridsberg M, and Akerstedt T. Metabolic responses to nocturnal eating in men are affected by sources of dietary energy. *Journal of Nutrition* 132, 1892-1899, (2002), PMID:12097665.
 58. Sopowski MJ, Hampton SM, Ribeiro DC, Morgan L, and Arendt J. Postprandial triacylglycerol responses in simulated night and day shift: gender differences. *Journal of Biological Rhythms* 16, 272-276, (2001), PMID:11407787.
 59. Gill S, and Panda S. A smartphone app reveals erratic diurnal eating patterns in humans that can be modulated for health benefits. *Cell Metabolism* 22, 789-798, (2015), PMID:26411343.
 60. Imai S, Kajiyama S, Hashimoto Y, Yamane C, Miyawaki T, Ozasa N, Tanaka M, and Fukui M. Divided consumption of late-night-dinner improves glycemic excursions in patients with type 2 diabetes: A randomized cross-over clinical

- trial. *Diabetes Research and Clinical Practice* 129, 206-212, (2017), PMID:28549298.
61. Carlson O, Martin B, Stote KS, Golden E, Maudsley S, Najjar SS, Ferrucci L, Ingram DK, Longo DL, Rumpler WV, Baer DJ, Egan J, and Mattson MP. Impact of reduced meal frequency without caloric restriction on glucose regulation in healthy, normal-weight middle-aged men and women. *Metabolism: Clinical and Experimental* 56, 1729-1734, (2007), PMID:17998028.
 62. Sutton EF, Beyl R, Early KS, Cefalu WT, Ravussin E, and Peterson CM. Early time-restricted feeding improves linsulin sensitivity, blood pressure, and oxidative stress even without weight loss in men with prediabetes. *Cell Metabolism* 27, 1212-1221.e1213, (2018), PMID:29754952.
 63. Stote KS, Baer DJ, Spears K, Paul DR, Harris GK, Rumpler WV, Strycula P, Najjar SS, Ferrucci L, Ingram DK, Longo DL, and Mattson MP. A controlled trial of reduced meal frequency without caloric restriction in healthy, normal-weight, middle-aged adults. *American Journal of Clinical Nutrition* 85, 981-988, (2007), PMID:17413096.
 64. Cortner JA, Coates PM, Le NA, Cryer DR, Ragni MC, Faulkner A, and Langer T. Kinetics of chylomicron remnant clearance in normal and in hyperlipoproteinemic subjects. *Journal of Lipid Research* 28, 195-206, (1987), PMID:3572247.
 65. Storch J, Zhou YX, and Lagakos WS. Metabolism of apical versus basolateral sn-2-monoacylglycerol and fatty acids in rodent small intestine. *Journal of Lipid Research* 49, 1762-1769, (2008), PMID:18421071.
 66. Bjornson E, Packard CJ, Adiels M, Andersson L, Matikainen N, Soderlund S, Kahri J, Sihlbom C, Thorsell A, Zhou H, Taskinen MR, and Boren J. Investigation of human apoB48 metabolism using a new, integrated non-steady-state model of apoB48 and apoB100 kinetics. *Journal of Internal Medicine* 285, 562-577, (2019), PMID:30779243.
 67. Gardner CD, Trepanowski JF, Del Gobbo LC, Hauser ME, Rigdon J, Ioannidis JPA, Desai M, and King AC. Effect of low-fat vs low-carbohydrate diet on 12-month weight loss in overweight adults and the association with genotype pattern or insulin secretion: The DIETFITS randomized clinical trial. *Journal of the American Medical Association* 319, 667-679, (2018), PMID:29466592.
 68. Parks EJ. Recent findings in the study of postprandial lipemia. *Current Atherosclerosis Reports* 3, 462-470, (2001), PMID:11602066.
 69. Bantle JP, Raatz SK, Thomas W, and Georgopoulos A. Effects of dietary fructose on plasma lipids in healthy subjects. *American Journal of Clinical Nutrition* 72, 1128-1134, (2000), PMID:11063439.
 70. Stanhope KL, Schwarz JM, Keim NL, Griffen SC, Bremer AA, Graham JL, Hatcher B, Cox CL, Dyachenko A, Zhang W, McGahan JP, Seibert A, Krauss RM, Chiu S, Schaefer EJ, Ai M, Otokozawa S, Nakajima K, Nakano T, Beyesen C, Hellerstein MK, Berglund L, and Havel PJ. Consuming fructose-sweetened, not glucose-sweetened, beverages increases visceral adiposity and lipids and decreases insulin sensitivity in overweight/obese

- humans. *Journal of Clinical Investigation* 119, 1322-1334, (2009), PMID:19381015.
71. Sciarrillo CM, Koemel NA, Tomko PM, Bode KB, and Emerson SR. Postprandial lipemic responses to various sources of saturated and monounsaturated fat in adults. *Nutrients* 11, (2019), PMID:31100881.
 72. van Amelsvoort JM, van Stratum P, Kraal JH, Lussenburg RN, and Houtsmuller UM. Effects of varying the carbohydrate:fat ratio in a hot lunch on postprandial variables in male volunteers. *British Journal of Nutrition* 61, 267-283, (1989), PMID:2650734.
 73. Donnelly KL, Smith CI, Schwarzenberg SJ, Jessurun J, Boldt MD, and Parks EJ. Sources of fatty acids stored in liver and secreted via lipoproteins in patients with nonalcoholic fatty liver disease. *Journal of Clinical Investigation* 115, 1343-1351, (2005), PMID:15864352.
 74. Barrows BR, and Parks EJ. Contributions of different fatty acid sources to very low-density lipoprotein-triacylglycerol in the fasted and fed states. *Journal of Clinical Endocrinology and Metabolism* 91, 1446-1452, (2006), PMID:16449340.
 75. Karimpour M, Surowiec I, Wu J, Gouveia-Figueira S, Pinto R, Trygg J, Zivkovic AM, and Nording ML. Postprandial metabolomics: A pilot mass spectrometry and NMR study of the human plasma metabolome in response to a challenge meal. *Analytica Chimica Acta* 908, 121-131, (2016), PMID:26826694.

CHAPTER III – Hepatic and mitochondrial ceramide kinetics

ABSTRACT

Ceramides (CERs) are key intermediate sphingolipids implicated in contributing to mitochondrial dysfunction and the development of multiple metabolic conditions. Despite the growing implication of CERs role in disease risk, kinetic methods to measure CER turnover are lacking, particularly using in vivo models. We demonstrate the utility of an orally-delivered stable isotope, $^{13}\text{C}_3$, ^{15}N L-serine dissolved in the drinking water, to quantify CER 18:1/16:0 synthesis in 10 week old male and female C57Bl/6 mice. Animals consumed either a control or high fat diet (CD, HFD; $n = 24/\text{diet}$) for exactly two weeks and the serine-labeled water for 0-12 days (0, 1, 2, 4, 7, and 12; $n = \text{four}/\text{day}/\text{diet}$) to generate labeling curves. Hepatic and mitochondrial CERs and dihydroceramides (dhCERs) were quantified using liquid chromatography tandem mass spectrometry. Within hepatic and mitochondrial pools, HFD induced greater saturated CER concentrations ($P < 0.05$) and absolute turnover of 16:0 CER (liver: 28% and mitochondria: 159%). Total hepatic CER content did not differ between the two groups while total mitochondrial CERs increased with HFD feeding (60%, $P < 0.001$). Fractional synthesis of 16:0 mirrored these observations; HFD elicited a 2.5- fold increase in 16:0 CER turnover only in mitochondria while diet groups were not different with respect to fractional liver 16:0 turnover. Our findings demonstrate an acute HFD alters 16:0 CER turnover and content of mitochondrial CERs which may be an early event in the progression of hepatic mitochondrial dysfunction. Future studies should complete basic functional mitochondrial measurements in conjunction with this novel method to

characterize the relationship between early increases in mitochondrial CER with progressive losses in function.

INTRODUCTION

Ceramides (CERs) are a central hub of sphingolipid metabolism, often leading to the production of more advanced lipid molecules (e.g., sphingomyelin). The main biosynthetic pathway (de novo synthesis) occurs primarily in the endoplasmic reticulum (ER) (1, 2) and begins with the condensation of L-serine and, most often, a 16-carbon fatty acid (16:0, palmitate) by serine palmitoyl transferase (SPT). Other key enzymes within CER biosynthesis include CER synthase, which has six distinct isoforms (CERS1-6), and dihydroceramide desaturase (DEGS). While SPT has restricted ability to use acyl-chains of varying lengths (3), the addition of a second fatty acyl is completed through the CERS enzymes, each of which have specificity for different fatty acids (FA). For example, CERS1 catalyzes the addition of 18:0 (4), while CERS2 uses very long-chain FA (preferentially 20:0 and longer (5)) and CERS6 is specific to 14:0 and 16:0 (6). Finally, DEGS desaturates the Δ 4-5 carbon bond (trans) in the backbone thereby converting dihydroCER (dhCER) to CER. Other pathways also contribute to the formation of CERs, for example the salvage and sphingomyelinase pathways. The salvage pathway recycles sphingosine through re-acylation to CER by CERS (7), whereas acid sphingomyelinase (SMPD) catalyzes the conversion of sphingomyelin (SM) to CER (8). Both SPT and CERS are also present within mitochondrial membranes (9, 10) and an increase in mitochondrial CERs are implicated in contributing to organelle dysfunction (11-21) which is characteristic of multiple metabolic diseases (22).

Mitochondrial CERs contribute to increased cellular ROS (11-14) and apoptosis (11, 15) and decreased mitochondrial respiration and tissue function (12, 16-19). Additionally, a large body of evidence supports elevated plasma and tissue CERs in contributing to metabolic dysfunction (12, 23-35) and cardiovascular risk (34-43), with specific species (e.g., 16:0, 18:0) conferring greater cardiometabolic risk than others (e.g., 24:1). Despite an overwhelming amount of evidence implicating CERs in disease risk, minimal work has quantified the kinetics of de novo CER synthesis. Turnover of CER may be more mechanistically related to CER toxicity (compared to absolute concentrations) and this knowledge may be useful in the development of therapies to lower concentrations and thus reduced disease burden.

With advances in mass spectrometry (MS) sensitivity, new methods for isotopic labeling of CER synthesis have recently been published (44, 45). In cell culture and rodent models, kinetic studies using stable isotopes (19, 46-56) and non-naturally occurring odd-chain analogs (57, 58) are available, and in humans, CER synthesis in skeletal muscle has been measured via isotope labeling (59-61). Isotopically-labeled serine and palmitate can be incorporated into the backbone of the sphingolipid through the SPT enzymatic reaction, while palmitate can also be incorporated into the fatty acyl chain through CERS5 and CERS6. Labeled palmitate has been used in rat models (47, 48) for tissue CER kinetics, while only one study has used labeled water (D₂O) or serine to quantify plasma CER kinetics in mice (46). Only two studies, to our knowledge, have

comprehensively measured CER concentrations within hepatic mitochondria (9, 62) and no one has measured mitochondrial CER synthetic rates or compared the organelle content or synthesis to whole liver tissue content or synthesis.

The aim of the current study was to utilize the stable isotope $^{13}\text{C}_3$, ^{15}N L-serine, delivered orally, to quantify the production of whole liver and isolated hepatic mitochondrial CERs in C57Bl/6 mice fed a control (CD; low-fat) or high fat diet (HFD). We hypothesized the HFD would induce elevated tissue and organelle CER concentrations which would be associated with elevated turnover rates. Our results support the use of serine in quantifying 16:0 CER synthetic flux in hepatic tissue and mitochondria and may be adapted for use in other tissues/organelles, CER species, and experimental models.

METHODS

Study design

Following acclimatization, 10-week old male ($n = 24$) and female ($n = 24$) C57Bl/6 mice received either a CD (Research Diets Inc., D12450J) or HFD (Research Diets Inc., D12492). The animals remained on the assigned diet for exactly two weeks. Body composition was measured via echoMRI (4 in 1-1100 analyzer) before the start of the diet and the day before euthanasia. The animals received a stable isotope of serine ($^{13}\text{C}_3,^{15}\text{N}$ L-serine, Cambridge Isotope Laboratories, Andover MA) to label the backbone of de novo CERs. The isotope was delivered by intraperitoneal bolus (20 mg/kg BW) on day 0 and in the drinking water (0.90 mg/mL) until the day of euthanasia. To obtain CER kinetics, four mice/group (two males, two females) were euthanized on days -1 (unlabeled), 1, 2, 4, 7, and 12 after administration of the tracer as shown in **figure 3.1**. CERs and dhCERs were isolated from liver tissue and hepatic mitochondria and analyzed by high performance liquid chromatography – tandem mass spectrometry (HPLC-MS/MS) with multiple reaction monitoring (MRM).

Animal groups and diet

The mice were split into two groups based on diet. The formulated CD contained 20% kilocalories (kcal) protein, 10% kcal fat, and 70% kcal carbohydrate (7% kcal sucrose). The HFD contained 20% kcal protein, 60% kcal fat, and 20% kcal carbohydrate (7% sucrose). **Table 3.1** shows the macronutrient distribution and

ingredient list for each diet and **table 3.2** presents the fatty acid composition in units of gram/100 grams of diet.

Animal care and terminal procedures

Animals were obtained from Jackson Laboratories and housed two per cage with a light cycle from 0700 to 1900h in constant room temperature of 21-22°C. Food and water intake and body weight were recorded weekly. Body composition (fat and lean mass) was measured before starting the diet and the day prior to euthanasia. Energy intake was calculated by taking the difference in grams of food provided and grams of food remaining on the weighing day and multiplying the total amount food consumed by the energy content of the diet (CD: 3.83 kcal/g and HFD: 5.22 kcal/g, **table 3.1**). This was then divided by the number of days between food weighing to give kcal/day (**table 3.3**). Prior to each study day (-1 to 12, **figure 3.1**), food was removed from cages at 0500 and mice euthanized at 1000 (5-h fast, 2h dark & 3h light phase). The animals had free access to serine-labeled (or unlabeled for -1 day mice) water during this fast. Mice were anesthetized (sodium pentobarbital, 100 mg/kg) as described previously (63) and euthanized through cardiac exsanguination and removal. Blood was obtained through intra-aortic puncture and the liver was harvested immediately. From each mouse, serum samples were divided into aliquots for quantification of metabolites (glucose, insulin, TG, and free fatty acids). Livers were quickly excised, weighed, and aliquots were 1) placed in an ice-cold isolation buffer for mitochondrial isolation and 2) flash frozen in liquid nitrogen to

be stored at -80°C for later processing. All animals included in this study were cared for in accordance with NIH guidelines and the protocol approved in advance by the University of Missouri IACUC.

Mitochondrial isolation

Hepatic mitochondria were isolated as previously described (64). Once excised and weighed, approximately 333 ± 58 mg of liver tissue was minced and gently homogenized using a smooth surface probe in mitochondrial isolation buffer A (220 mM Mannitol, 70 mM sucrose, 10 mM tris-base, 1 mM EDTA; pH 7.4) (64). The sample was then centrifuged at 1,500 g for 10 minutes at 4°C. The pellet was discarded, and the supernatant underwent three centrifugations (6,000-8,000 g) where the resultant pellet was retained and resuspended (in buffer A or A with 0.1% bovine serum albumin) with gentle glass-on-glass homogenizations. The final pellet was homogenized with 400 μ L of phosphate buffered saline (~1:1 starting wt/vol), and the sample was stored at -80°C and used for protein determination via BCA assay (# 23225, ThermoFisher Scientific), CER extraction, and citrate synthase activity assays.

CER concentrations and enrichment

CERs were extracted from liver homogenate and isolated hepatic mitochondria. Briefly, ~50 mg (52.2 ± 0.4 mg) of frozen liver tissue was weighed and homogenized in buffer B (1,000 μ L, sucrose 250 mM, KCl 25 mM, tris-base 50 mM, and EDTA 0.5 mM). Following protein determination, CERs were extracted

from 200 μ L of the liver homogenate (equivalent to 1.2 ± 0.1 mg of protein or ~ 10 mg starting tissue). The homogenate was spiked with 50 μ L of C18:1/17:0 (50 ng) and then extracted according to the protocol of Bligh & Dyer (65). The organic phase was removed and dried under nitrogen gas. An azeotropic agent (methylene chloride) was used to remove any additional water and samples were stored in -80°C until LC/MS analysis. For mitochondrial CERs, 200 μ L of the mitochondrial extract (equating to 1.5 ± 0.2 mg of protein or ~ 150 mg starting tissue) was extracted as described for liver tissue. Both liver and mitochondria samples were analyzed using the same LC/MS method (66). CERs were quantified using HPLC-MS/MS electrospray ionization (ESI) in positive ion scanning mode. Standards and samples were dissolved in 100 μ L of 0.1% formic acid solution in methanol-water (85:15) and then injected into a Waters HPLC device (2690 Separation Module, Milford, MA) and separated through an Vydac[®] 200MS[™] C8 column (2.1 x 100 mm, 5 μ m, P.J.Cobert Associates, St. Louis, MO). CERs were analyzed using MRM scanning each molecular ion with the combination of mass to charge ratio (m/z) 264 daughter ion across all species. Chromatograms were analyzed using Xcalibur[™] (Thermo Scientific[™] 3.0.63). Individual unlabeled CER species and the labeled 16:0 CER MRM transitions are listed in extended methodology (**table EM3.2**). To label the backbone of 16:0 CER, each animal received an intraperitoneal bolus of $^{13}\text{C}_3,^{15}\text{N}$ L-serine (20 mg/kg) and the drinking water was enriched with 0.90 mg/mL of the same stable isotope (**figure 3.1**). Percent enrichment (%E) was calculated as the area under the peak for the labeled isotopomer (M3 16:0 CER) divided by the

sum of the area under the peaks for total label and unlabeled isotopomers (M0, M1, and M3 16:0 CER). To assess the accuracy of using the area ratios, we used exponential curves to model hypothetically-mixed labeled and unlabeled CER pools. Using the generated equations, we found excellent agreement between the enrichments observed and those generated using the model, therefore we used the calculated %E to generate labeling curves across time. The average of four mice per group represented a single data point within the labeling curves (unlabeled: -1 days and labeled: 1, 2, 4, 7, and 12 days). Fractional synthetic rates of de novo 16:0 CER (pools/day or k) were calculated by fitting single exponential curve (equation: $y = A_{\infty} \times [1 - e^{-kt}]$) to the enrichment curves (67). Absolute synthetic rates were calculated as the product of k and the absolute pool size.

Assay precision

Intra- and inter-assay reproducibility was determined by multiple analyses of a pooled liver or mitochondria sample. To measure intraassay variability, one sample was analyzed five times and for interassay variability, pooled liver and mitochondria samples were extracted on five separate occasions over a two week period.

Precursor enrichment (free hepatic serine)

Enrichment of the precursor pool (free L-serine) was analyzed as previously described (68). In brief, 500 μ L of liver homogenate (equivalent to ~25 mg liver

tissue) was eluted using an ion exchange column (50WX8-400, hydrogen form) with formic acid. Bonded amino acids were released using ammonium hydroxide and the eluate was dried under nitrogen. An azeotrope agent was added to the sample and dried under nitrogen to remove any remaining water. Samples were derivatized using 100 μ L bis(trimethylsilyl) trifluoroacetamide 10% trimethylchlorosilane (BSTFA + 10% TMCS) and then analyzed by GC/MS as described previously (68). The enrichment of L-serine was determined using electron impact ionization (70 eV) and selected ion monitoring (m/z : 204-207, see extended methodology section).

Western blots and citrate synthase activity

To assess if differences in CER content and turnover were driven by changes in protein content, key proteins involved in CER synthesis were measured via western blot in whole liver homogenate. Details of western blot methods can be found in the extended methodology section. Briefly, liver tissue (50.4 ± 1.4 mg) was homogenized in protein lysis buffer (1:10 wt/vol) and following centrifugation (4°C, 25 minutes, 1,500 g), the supernatant was used to determine protein content by BCA protein assay (# 23225, ThermoFisher Scientific). Samples (20 μ g) were loaded into gels and, following electrophoresis, transferred to polyvinylidene difluoride transfer membrane. Primary antibodies were diluted 1:1,000 and secondary antibodies 1:5,000. Blots were analyzed via densitometric analysis (Image Laboratory Beta 3, Bio-Rad Laboratories, Hercules, CA). Total protein was assessed with amido black (0.1%) to control for differences in protein

loading and transfer as previously described (69). The proteins quantified included dihydroceramide desaturase (DEGS1), ceramide synthases (CERS1, 2, 6), acid sphingomyelinase (SMPD1), acid ceramidase (ASAH1), and the oxidative phosphorylation complexes (I-V). Mitochondrial citrate synthase activity, a well-established surrogate of mitochondrial content, was measured as previously described (69) and expanded upon in extended methodology.

Serum and liver assays

Liver TG content was quantified by enzymatic assay using TG (#T2449, Sigma) and free glycerol reagent (#F6428, Sigma) following Folch lipid extraction.

Serum glucose (#997-03001, Wako), triglycerides (same reagents listed for liver TG), and free fatty acids (#999-34691; #995-34791; #994-02891; #990-02991, Wako) were quantified using commercially available enzymatic reagents. Serum insulin concentrations were determined using a commercially available ELISA (EZRMI-13K, Millipore Sigma).

Statistical analysis and calculations

Calculations were performed using Microsoft Excel (2016, Redmond, WA) and statistical analysis using R (version 4.1.3) and R studio (Boston, MA). Weight and body composition were compared across time with a two-way between factors analysis of variance (ANOVA, time x diet). The R packages ez and rstatix were used for ANOVA testing. Unpaired, two-tailed *t*-tests were used to compare static outcomes between diets. Supplemental analysis of sex differences were analyzed by a two-way factorial ANOVA (diet x sex). Significant interactions ($P <$

0.05) were followed-up by a post-hoc comparison with a Bonferroni correction. Pearson's R was used to quantify linear relationships between continuous variables. Data varying across time were reported as mean \pm standard error (SEM) while static variables were reported as a mean \pm standard deviation (SD). Significance was set at $P < 0.05$, and $P < 0.10$ reported as a trend. The homeostatic model assessment for insulin resistance (HOMA-IR) was calculated using glucose (mmol/L) and insulin concentrations (μ IU/mL) divided by the constant 22.5 (70, 71).

RESULTS

Animal Characteristics

Body weight was similar in all animals at the start of the diet (**figure 3.2**) with males weighing ~23-25% more than females (**supplementary table 3.1**). The two-week HFD induced significantly greater increases in total body mass than CD (**figure 3.2**). Animals consuming the HFD had increased percent fat mass and reduced percent lean mass after two weeks of feeding (**figure 3.2B**).

Animals consuming the CD had minimal changes in either lean or fat mass.

Liver weight was similar between groups (**figure 3.2C**).

While all animals had similar total daily food intake (in grams) throughout the two-week diet, the total energy intake was significantly higher (**table 3.3**) in the HFD animals due to the higher diet energy density when compared to CD (**table 3.1**; 3.4 vs 5.2 kcal/g). As expected, both total quantity and energy intake of macronutrients were different across groups, due to the differences in diet composition. Neither length of serine supplementation nor diet impacted daily water or food intake in either group, thus labeled serine intake was similar between groups (**table 3.3**).

Animals consuming HFD had elevated serum glucose while serum insulin was similar between diets and HOMA-IR also did not differ (**figure 3.3A-C**). Serum NEFA concentrations were higher in mice consuming the HFD. While serum TG was lower with HFD-feeding, hepatic TG content was elevated. With regard to

sex, female mice had lower serum glucose, insulin and TG, similar NEFA, and elevated liver TG concentrations compared to male mice ($P < 0.01$ – main effect of sex, **supplementary table S3.1**).

Liver and mitochondrial CER and dhCER content

Using a sophisticated MRM analytical technique, we are able to distinguish between CERs and dhCERs with the same fatty acyl chain (e.g., CER 16:0 and dhCER 16:0) due to the combined analysis of parent to daughter ion transition (a result of collision induced ionization within the second MS chamber, see **figure EM3.1**) and retention times which differ for CERs and dhCERs (see **table EM3.2**). Based on the area ratio of the sample to internal standard and the standard curves, absolute concentrations were calculated in units of nmol/gram tissue. Surprisingly, total liver CER concentrations were not impacted by diet (**figure 3.4A**) but were higher in female animals ($P = 0.042$, **supplementary figure S3.1**). Individual hepatic CER species are shown in **figure 3.4C**.

Following the two-week diet, HFD-fed animals had significantly higher liver 16:0 (30%), 18:0 (100%), and 20:0 (115%) saturated CER species than animals fed a CD. The major species contributing to the total hepatic CER pool (**figure 3.5**) were 22:0, 24:0, and 24:1 which together, encompassed $98.04 \pm 0.45\%$ and $96.58 \pm 0.60\%$ of the total CERs in CD and HFD animals, respectively. In addition to the elevated absolute concentrations of 16:0, 18:0, and 20:0 liver CERs, the molar percent of the total hepatic CER pool made up by each of these species was elevated in HFD animals while the percentage of 24:0 was reduced

(**figure 3.5C**, inset table). Total liver dhCER concentrations tended to be lower in HFD animals (31%, **figure 3.4B**), which was driven by lower dhCER 24:0 (32%; **figure 3.4D**).

Total mitochondrial CERs and dhCERs were elevated in HFD animals (**figure 3.6A-B**), with significant increases in 16:0 (CER: 46%; dhCER: 50%), 18:0 (CER: 128%; dhCER: 156%), 20:0 (CER: 255%), 22:0 (CER: 68%), and 24:0 (CER: 116%; dhCER: 158%) species. Further, females had higher total mitochondrial CERs and dhCERs than male mice (**supplementary figure S3.2**). Similar to total liver CERs, the species 22:0, 24:1, and 24:0 were in highest concentration within mitochondria (**figure 3.6C**) and thus, were proportionally the largest CER contributors to the total mitochondrial pool (**figure 3.7**), regardless of diet (CD: $96.55 \pm 1.15\%$ and HFD: $93.59 \pm 1.56\%$ of the total pool). Despite different absolute concentrations, the proportion of the total mitochondrial pool made up by 16:0 and 22:0 CER was not different between HFD and CD animals. The saturated CER species 18:0, 20:0, and 24:0 made up a greater portion of the total mitochondrial pool in animals consuming a HFD while the percentage of 14:0, 18:1, and 24:1 were lower in the same animals (**figure 3.7C**, inset table).

The relationship between total liver and hepatic mitochondrial CER has never been examined. Per gram of liver tissue, HFD-fed animals had a greater proportion of total liver CER within the mitochondrial pool than CD-fed animals ($46 \pm 12\%$ versus $30 \pm 11\%$, respectively; $P < 0.0001$). When all animals were

analyzed together, a significant positive relationship was found between the two pools ($r = 0.328$, $P = 0.023$) however, this relationship was driven solely by the HFD animals (**figure 3.8**). Whereas this observation was consistent with the individual species in greatest concentrations (20:0, 22:0, and 24:0), individual analysis revealed CER 16:0 and 18:0 hepatic and mitochondrial concentrations were positively related in both HFD and CD animals (**supplementary figure S3.3**).

Our analysis of the inter- and intraassay variability demonstrated high precision levels both between sample extractions and within the analytical method (**table 3.4**). Specifically, we observed interassay coefficient of variations (CV) between 0.5-5.4% for both hepatic CER pools (liver and isolated mitochondria) and 0.6-7.8% CV for the intraassay precision. These values agree with previous reports using the same analytical methods (66).

CER 16:0 turnover

A portion of newly-made CER within liver and hepatic mitochondria were labeled with $^{13}\text{C}_3$, ^{15}N L-serine and the percent enrichment of these labeled CER across days are presented in **figure 3.9**. CD animals are shown in white, HFD animals in green, and the mean of all animals within a labeling day and diet shown in black. Animals fed a HFD tended to reach plateau enrichments earlier (~2 to 4 days of labeling) than CD animals (between 4 and 7 days). As expected, enrichment across labeling days significantly increased ($P < 0.0001$), with

enrichments of day 12 animals being significantly higher than the unlabeled mice (day 0).

We generated exponential models using hypothetical mixtures of unlabeled and labeled CER 16:0 pools to test whether our enrichment data calculated using the area ratio of the labeled CER (M3/all) was similar to the expected distribution. Upon testing the LC/MS-generated area ratios of CER (triply-labeled and the ratios of triply-: singly-labeled) against the exponential models, we found excellent reproducibility between the results (%E from day 12 animals - calculated: $1.9 \pm 0.1\%$; model: $2.0 \pm 0.1\%$). Despite a lack of labeled CER standard curve, good agreement between the observed and modeled enrichments supports our use of the enrichment data generated from the area ratios to calculate turnover rates. Exponential growth curves were fit to the enrichment data (**figure 3.9**) and fractional turnover rates (k, pools per day) were generated (**figure 3.10**). We also generated the predicted asymptote of each curve, the amount of de novo 16:0 CER, and the half-life of the molecule (**table 3.5**).

Fractional whole liver CER 16:0 synthesis in pools per day was similar between diet groups while isolated mitochondrial 16:0 fractional synthesis was 43% greater in HFD animals (**figure 3.10C**). When comparing mitochondrial to liver 16:0 synthesis in pools per day (k), CD animals had 36% lower while HFD animals had 44% higher mitochondrial fractional synthesis than hepatic fractional

synthesis (**figure 3.10 A versus C**). Absolute synthesis rates in nmol/g tissue/day were calculated using the total 16:0 pool size and HFD animals demonstrated higher synthetic rates than CD in both liver (28%) and mitochondrial (159%) pools (**figure 3.10B and D**). In line with these observations, the half-life for liver 16:0 CER was similar between diets while mitochondrial half-life was almost double in CD when compared to HFD mitochondrial 16:0 CER (**table 3.5**). Further, the 16:0 CER made de novo that was labeled was significantly greater in HFD mitochondria than CD. Despite an extended labeling period, a large portion of the CER pool remained unlabeled due to intrahepatic stores and use of unlabeled serine during synthesis. Sex differences are shown in **supplementary figure S3.4**. Fractional liver synthesis was higher in CD males than females (29%, white bars, **S3.4A**) but lower in HFD males than females (-14%, green bars). Reflecting total pool size, female HFD-fed mice had the greatest absolute 16:0 synthesis (**S3.4B**). Mitochondrial fractional synthesis was similar between males and females within a diet (**S3.4C**) while HFD animals, regardless of sex, had greater absolute 16:0 mitochondrial synthesis (**S3.4D**).

Free serine enrichment was measured in total liver homogenate and is shown in **supplementary table S3.3 and figure S3.5**. Enrichments reached 1.0-1.5% in hepatic tissues on day 12 of labeling and were significantly different across labeling days. Plateau enrichment was achieved within two days of labeling and the increase %E observed after day 7 is likely recycling of serine from muscle

protein breakdown. Male and female mice did not differ in serine enrichments (data not shown).

Hepatic protein and mitochondrial content

Liver protein expression of CERS1, responsible for CER 18:0 synthesis, was similar between the diet groups. CERS2 (CER 20:0+) was significantly decreased (-22%) and CERS6 (CER 14:0 and 16:0) tended to be lower (-21%) in HFD animals (**figure 3.11A**). Other key enzymes within the CER synthetic pathway, either did not differ between groups (SPT, **figure 3.11B**) or was similarly lower in HFD animals (DEGS -20%, **figure 3.11B**). Protein content of acid sphingomyelinase, a key step in the sphingomyelinase CER synthetic pathway, was lower in HFD animals (-19%, **figure 3.11C**). Acid ceramidase, an enzyme within the CER salvage pathway that converts CER to sphingosine, was not different between groups (+6%, **figure 3.11C**). Markers of mitochondrial content, citrate synthase activity and mitochondrial electron transport chain complexes I-III and V, were lowered by the HFD (**figure 3.12**). Sex differences for each of these proteins are presented in **supplementary table S3.4** which demonstrates female animals had greater CERS2, CERS6, and SPT while male mice had greater CERS1 content.

Across all animals, CERS1 was negatively related to CER and dhCER 18:0 concentrations in both total liver and hepatic mitochondria (**supplementary tables S3.5-3.6**). CERS2 was negatively related to very long chain liver and

mitochondrial CER (e.g., 20:0, 22:0) only in HFD animals. Conversely, CERS6 was positively related to CER and dhCER 16:0 in both diets and pools.

Correlation matrixes were generated between SPT, DEGS, SMPD, and ASAH and CER and dhCER content. While SPT protein content did not differ between diet groups, we observed varying relationships with specific mitochondrial CERs (**supplementary table S3.8**). In HFD animals, mitochondrial CERs with fatty acyl chains between 14:0-18:0 were positively related to SPT content, while longer chain mitochondrial CERs (20:0 and 22:0) correlated negatively. This may suggest longer chain CERs are inhibitory to the SPT enzyme. This was also consistent for liver CER 18:0 and 20:0 in HFD animals (**supplementary table S3.7**). HFD animals had lower DEGS1 content which was negatively related to mitochondrial CER 20:0 and 22:0. Finally, SMPD content was also lower with HFD and negatively related to mitochondrial 22:0 and 24:1 and both liver and mitochondrial 20:0. Results from these studies are combined in the model presented in **figure 3.13**.

DISCUSSION

For the first time, an orally-delivered stable isotope of L-serine was used to quantify total liver and hepatic mitochondrial CER 16:0 synthesis in mice fed a CD or HFD. Animals consuming a HFD exhibited faster absolute synthesis rates in both liver tissue and isolated mitochondria, which was mirrored by an elevation in the saturated liver CERs as well as total and saturated mitochondrial CERs. With the expanding literature supporting CERs in contributing to metabolic diseases like type 2 diabetes, NAFLD, and cardiovascular disease (29, 30, 33, 34, 72-74), deeper knowledge of in vivo CER biology is needed. Methods to track CER synthesis would facilitate the development of therapies for reducing lipotoxicity of CERs, potentially through total content reduction, targeting synthesis of individual species, or increasing the degradation of the sphingolipid. While cell culture techniques are established (49-56), the translation to whole body models presents technical and analytical challenges for tracking CER synthesis.

Methodology: Selection of tracer, method of delivery, and analytical challenges

Studies measuring CER kinetics have used palmitate (e.g., U-¹³C, d₃) (55, 59-61, 75), D₂O (46), or L-serine (e.g., U-¹³C, d₃, ¹³C₃, ¹⁵N) (19, 46, 53, 54) isotopes to quantify synthesis, however most of these measurements were completed using cell culture models.

Recently, Chen and colleagues were the first to use D₂O to quantify plasma CER flux in mice (46). While the utility of D₂O supports the use for measurements of hepatic and plasma CER kinetics, multiple analytical challenges limit the use of this isotope for CER kinetic studies. One benefit of LC/MS is the ability to examine whole molecules without requiring derivatization. The incorporation of deuterium into a whole molecule like CER produces complicated labeling patterns (i.e., the potential for M1, M2, M3 isotopomers, and so on) that prove difficult to deconvolute. One must consider all of the potential locations and metabolic processes that may result in the incorporation of a deuterium into a newly-made CER molecule. To name a few, 1 - NADPH may add a ²H during the second and fourth steps in CER biosynthesis (76), 2 - de novo lipogenesis will result in the incorporation of deuterium into palmitate which can then enter CER synthesis and be added to serine, forming the sphingosine backbone, or the fatty acyl chain (77), and 3 - D₂O may also be incorporated into serine during serine-glycine transfer (78). Additionally, no study has completed the basic cell culture experiments to identify the maximum number of deuterium labels any individual CER may gain through metabolism and synthesis (i.e., 'polymerization factor' or 'n'). Together these complications are driven by the ubiquitous use of deuterium in many metabolic processes. This knowledge however can be used to estimate the number of monomers (²H) that may be incorporated in the polymer (CER in this case) (79, 80). Assuming the consistent incorporation of the equilibrated ²H into newly-made FA, according to the methods of Lee et al (79, 80), Chen and Colleagues estimated HFD-fed animals had lower

contributions of deuterium-labeled palmitate formed by hepatic lipogenesis that fed into de novo CER synthesis (when compared to a standard carbohydrate-based diet). Overall, oral D₂O deserves further testing and optimization for the quantification of CER biosynthesis and future studies should build upon the elegant method described by Chen et al to expand to tissue CER turnover.

The only data available in humans is a collection of publications from Jensen and colleagues who optimized a method to measure skeletal muscle CER synthesis using an infusion of ¹³C palmitate (59-61). Labeled palmitate, as an alternative tracer option, reduces the analytical challenges associated with D₂O, although the method of delivery - via infusion or orally in the food - adds an additional technical hurdle. With regard to feeding labeled palmitate to track hepatic lipid handling, our group has used d₃₁ tripalmitin, incorporated into the animal's food, to measure the liver TG arising from dietary sources (81). Using similar techniques, feeding a labeled palmitate FA could be adapted to track CER synthesis within the liver although it is likely this method would result in substantial label loss before reaching the liver where it could be used for CER synthesis – both to peripheral tissues and in the stool (82). Beyond the oral use of palmitate, which has not been evaluated for quantification of CER synthesis, infusing the isotope has demonstrated labeling of skeletal muscle CER in humans (59-61) and mice (48) as well as labeling of liver CERs in mice (47, 83). However, similar methods are challenging in rodent models due to the invasive nature of infusions over long periods of time (six+ hours) and the difficulty

associated with repeated blood and tissue samples in the same animal.

Regardless, infusing palmitate to measure hepatic CER synthesis is an attractive method that should be tested and optimized further. Using a palmitate FA – either dietary or infusion, mass isotopomer distribution analysis (MIDA) could be applied to calculate the intracellular precursor enrichment for 16:0 CER synthesis as a direct result of the potential for two labeled palmitates being incorporated into the CER molecule (55).

Unlike, D₂O and palmitate, L-serine can be incorporated at only one location within any CER molecule and only during the first and rate-limiting step of de novo CER synthesis (via SPT). Theoretically, this would simplify the labeling distribution, however due to systemic metabolism of serine (84) and depending on the positional labeling within the molecule (e.g., d₃ or ¹³C₃, ¹⁵N L serine), CER may become labeled with singly-, doubly-, and triply-labeled serine. Because serine is a common source for one-carbon units within the liver, the degradation and resynthesis (**supplementary figure S3.6**) may result in a shift of the labeling pattern within the molecule. However, this is greatly dependent upon the stable isotope used. For example, Gregory et al elegantly demonstrated d₃ serine infusion (2,3,3-²H₃) in a single male human resulted in the formation of ²H₁, ²H₃, and ²H₂ serine within apolipoprotein B100 (descending enrichments in the same order). The interconversion of serine and tetrahydrofolate to glycine and 5,10 methylenetetrahydrofolate produced the singly- and doubly-labeled serine within that subject. With regard to the current experiment, ¹³C₃, ¹⁵N L-serine may

undergo cytosolic or mitochondrial metabolism including serine-glycine cycling. However, due to the positional isotope labeling of $^{13}\text{C}_3$, ^{15}N , serine-glycine cycling would not result in a shift of CER labeling. In other words, the ^{13}C that is cleaved when serine is converted to glycine is the same that is lost during the first step in CER synthesis. Hence, our labeling pattern within CER would not be affected by this metabolic occurrence although, at the same time, we are unable to distinguish if the labeled serine used in CER synthesis had undergone serine-glycine interconversion. Alternatively, serine enters hepatic metabolism through pyruvate and, from here, has many fates. It is possible for singly- and doubly-labeled serine to be reformed following TCA cycling and gluconeogenic contributions to serine synthesis (an example is shown in **supplementary figure S3.6**). Indeed, we observed an increase in singly-labeled CER across labeling days (data not shown) and were able to test our enrichment data against hypothetically-derived exponential models which when applied to our data, were in agreement with our enrichment observations. In addition to the global metabolic use of serine, a second challenge is serine's rapid turnover rate that exceeds the rate of CER turnover. This can be observed in our free hepatic serine enrichment data that are lower than the CER 16:0 enrichments. Multiple explanations for this finding are possible. 1 – The serine enrichments reported here represent the fully-labeled molecule. As discussed above, it is likely hepatic metabolism of serine to generate a singly- or doubly-labeled serine (i.e., TCA and gluconeogenic activity) is partially responsible for the lower enrichments observed. In conjunction with fasting conditions and the rapid rate of serine

turnover, increased M1 or M2 serine would lower the observed enrichment of $^{13}\text{C}_3$, ^{15}N L-serine. 2 – Reduced water intake during the five hour fast prior to euthanasia may have resulted in rapid reductions in free serine enrichment that take much longer to translate to CERs. 3 – Muscle protein breakdown during the fast may have increased the pool of unlabeled or labeled serine (single or double) which could have diluted the fully-labeled pool in the liver. Based on these observations, free serine may not be the best precursor pool for measuring CER synthesis. Chen et al proposed the use of dhCERs as an appropriate precursor pool although our method was unable to detect any labeled 16:0 dhCERs due to low abundance. This is in opposition to previous findings (46) where CER enrichments were only 5-10% of the dhCER enrichments following a bolus dose of ^{13}C ^{15}N serine which suggested a slow conversion of dhCERs to CERs. These conflicting results require further investigation and emphasize the importance of identifying an appropriate precursor pool that can be reliably quantified.

In sum, as more data are generated implicating CERs in many metabolic conditions, methods to measure turnover are becoming increasingly crucial to better understand CER biology. The choice of stable isotope and the method of delivery deserve consideration when designing in vivo flux studies, particularly for analysis of whole molecules like CERs. The method presented here represents the first in depth investigation into total hepatic and liver mitochondrial turnover

using an oral serine isotope. In addition to development of the turnover method, we also tested the effects of a two-week HFD on CER content.

Interaction between total hepatic CERs and isolated mitochondrial CERs

For the first time, the amount of CERs within whole liver homogenate was compared to the hepatic mitochondrial pool. Both pools had increased saturated CERs with HFD feeding yet only mitochondria demonstrated significantly elevated total CER concentration with the HFD. A growing collection of work has demonstrated increased mitochondrial CERs contribute to the induction of apoptosis (20, 21, 85, 86). Mechanistically, CERs support the formation of large channels within the outer mitochondrial membrane (15, 87-90), increasing the permeability to small proteins like cytochrome c (15). However much of this work was completed in cell culture lines and using very short chain CER analogs to increase concentrations from exogenous sources (e.g., CER 2:0-6:0). While the current study did not characterize mitochondrial function beyond content, which was reduced in HFD animals, chronic elevations in energy intake result in deleterious metabolic derangements like nonalcoholic fatty liver disease and insulin resistance (91-94) and mitochondrial dysfunction may precede these developments (95). Altogether, increased mitochondrial CER concentrations may be an early event in the development of mitochondrial dysfunction and associated metabolic diseases. Our findings extend this hypothesis through the strong positive relationship between total hepatic and mitochondrial CERs only in HFD animals. This relationship supports an acute dietary effect on the storage or synthesis of hepatic CERs with preference for the mitochondrial pool. Simply

put, even with similar total hepatic content, two weeks of a 60% fat diet elicited elevations in mitochondrial CERs. Surprisingly, this relationship was driven by very long chain CER species. In other words, CER 16:0 and 18:0, which have been implicated in inducing mitochondrial apoptosis (20, 21), accumulated within mitochondrial and hepatic tissue linearly in both animal groups. The groups diverged with respect to CER 20:0, 22:0, and 24:0 – with higher total mitochondrial content being related to higher liver content in HFD animals only. The mechanism of increased CER only within mitochondria of HFD animals remains unclear and raises multiple questions regarding hepatic CER handling.

- 1- Are all mitochondrial CERs made locally, or can they be transported from other organelles (e.g., ER)?
- 2 – the opposite of #1 is also of interest: Are mitochondrial CERs trafficked away from mitochondria for storage or secretion? Might this be a protective mechanism for the organelle?
- 3 – Are hepatic CERs secreted to a greater extent with HFD, thus eliciting similar whole liver concentrations regardless of dietary composition or is it rather a matter of where the CER are located within hepatic tissues?
- 4 – What drives the differences in accumulation of specific CERs within mitochondrial and total hepatic tissues?

Answers to these key questions will be important in understanding early developments of CER-related mitochondrial dysfunction.

Key genes within the CER synthetic pathway were measured and demonstrated a unique negative feedback pattern of regulation shown graphically in **figure 3.13**. The rate limiting step in CER biosynthesis, SPT, was unaffected by the

HFD. We expect this is partially due to a protective mechanism for this enzyme, as CERs are necessary for survival (96), however another possibility is the length of the diet was not sufficient to produce noticeable hepatic SPT changes. Correlation analysis revealed some CERs were positively related to SPT content while others correlated negatively. Thus, differential regulation of the enzyme may be occurring in a setting of high fat feeding with specific CERs potentially inhibiting the enzyme (97). Previous reports found eight weeks of the same HFD elicited an increase in hepatic SPT protein content (47, 83) and mRNA (98). Thus, a longer dietary intervention may have greater impacts on the SPT enzyme. Similar to SPT, hepatic CERS1 was also unchanged by the two-week HFD while in contrast, both CERS2 and CERS6 were reduced in the same animals. Previous studies report varying results regarding gene expression or protein content of these CERS. With regard to gene expression, hepatic mRNA of CERS1 and 2 were elevated following an eight-week HFD in rats (98) while the same length diet in C57Bl/6 mice resulted in no changes to CERS2 or 6 mRNA (99). A 12-week HFD in mice resulted in decreased mRNA of the CERS2 and 6 (12) whereas 18 weeks of a HFD (but not six or 12 weeks) yielded increased mRNA of CERS1 and CERS6 (100). As for protein content, the same study (100) reported reduced CERS2 after six weeks of HFD and increased CERS6 after 18 weeks of HFD. It is clear the regulation of gene expression and protein content of the CERS enzymes is complicated. Our results support a feedback inhibition model of excess CER content early in nutrient excess. While CERS1 was unchanged between diets, CER and dhCER 18:0, the main products

of this enzyme, were negatively related the hepatic protein content of this synthase, suggesting excess CER 18:0 may inhibit this enzyme. Similarly, CERS2, which was reduced in HFD animals as has been previously reported with longer dietary interventions (100), may have been inhibited by the CER products 20:0, 22:0 and 24:1. CERS6 did tend to be reduced with the HFD but correlated positively with the content of CER and dhCER 16:0. We hypothesize that this enzyme may be susceptible for feedback regulation through other CER species as we report strong negative correlations with hepatic and mitochondrial 20:0 and 22:0. The next step within CER biosynthesis, DEGS1, was lower with the HFD feeding, and has been the target of recent research for lowering CER concentrations and improving hepatic steatosis and insulin resistance (19, 101). Finally, to monitor if changes in the other CER pathways were impacted through high fat feeding, we measured both acid sphingomyelinase and acid ceramidase, the former of which was lowered by HFD. This was in opposition to an eight-week HFD feeding study which reported increased mRNA and protein content of both SMPD and ASAH in rat liver (98). In sum, our results support early increases in hepatic and mitochondrial CERs may be interacting with the protein content of key biosynthetic enzymes in CER synthesis. Regardless of lower protein expression, we observed comparable changes between 16:0 CER content and turnover rates in hepatic and mitochondrial pools.

Turnover of hepatic and mitochondrial CER

We could detect the continuous incorporation of $^{13}\text{C}_3$, ^{15}N L-serine into the backbone of 16:0 liver and mitochondrial CERs. The enrichments rose

throughout the 12-day labeling period and reached steady state in both groups around day 4. The mice received an intraperitoneal bolus of the isotope on day 1 and then consumed the label in the drinking water until euthanasia. Thus, this labeling technique is analogous to a primed continuous infusion promoting the rapid attainment of steady state enrichments. Using the generated labeling curves, an exponential model was fit to the data and produced fractional synthetic rates. We report minimal differences in fractional liver 16:0 CER although absolute synthesis was 22% greater in HFD, due to higher liver 16:0 concentrations. Chen and colleagues (46) reported a 5-10 fold difference of plasma 16:0 CER within the same animal strain fed similar diets (HFD contained only 45% fat whereas the current study had a 60% fat diet). However, the previous study fed the diet for 12 weeks and measured synthesis in plasma whereas the current animals consumed the diet for only two weeks and hepatic synthetic rates were measured. Strong data from humans (102) and animals (19, 102) support the liver as the primary source of plasma CER (60-80%). Knowing this, plasma CER synthesis may reflect total hepatic CER synthesis. Compared to Chen et al, we observed similar but slightly lower fractional turnover rates in CD animals (~0.5 versus ~0.6 pools/day) whereas our HFD elicited much lower fractional hepatic turnover (~0.5) than previously reported (~1.1 pools/day). We believe these differences are due to the length of the dietary intervention (two versus 12 weeks). Although plasma 16:0 CER turnover may not reflect the hepatic pool, our results from CD animals encourage future studies to compare the two pools to determine their relationship. While a plasma measure of CER

turnover would eliminate the need for invasive tissue biopsies, it remains unclear how various hepatic pools of CER, particularly mitochondria may differ from plasma turnover.

In opposition to liver, synthesis of mitochondrial CER 16:0 was strikingly different between the diet groups, with HFD animals having 2.5-fold greater synthetic rates than the CD animals. In comparing these two related pools, we were surprised to find such vast differences in the turnover rate of the same CER species. Mitochondrial 16:0 CER accounted for 17-18% of the total liver pool in both groups, thus it is evident that the other hepatic CER pools (e.g., ER, cellular membranes) must be turning over at different rates (some much slower) in HFD diet animals. The same logic must then be applied to CD animals who demonstrated 36% greater total liver fractional synthesis when compared to mitochondria. In other words, with greater total hepatic turnover than mitochondria specific turnover, the other hepatic pools must have had greater synthetic rates with CD. A potential explanation for this finding is an inhibitory feedback response to greater total hepatic CER content in response to excess energy from the HFD which agrees with our observed decreases in protein content of multiple CER biosynthetic enzymes described above. This raises the question whether mitochondria also exhibit a similar early feedback inhibitory mechanism with HFD feeding that was not detected in the current investigation. Finally, dhCER concentrations deserve some mention as an intermediate lipid within the CER synthetic pathway. It remains unclear whether dhCERs

themselves are signaling molecules (101) or 'innocent' intermediates to sphingolipid synthesis thereby conferring minimal lipotoxic risk (19). Our data support dhCERs as markers of the rate of CER synthesis, as has been previously proposed (19). Specifically, total liver and mitochondrial dhCER 16:0 content mirrored our observed changes in 16:0 turnover; both hepatic dhCER 16:0 concentrations and fractional synthesis were unchanged between diet groups whereas the HFD animals exhibited significantly higher mitochondrial 16:0 dhCERs as well as 16:0 fractional turnover. Taken together, our basic kinetic studies demonstrate the regulation of hepatic CER pools are independent from whole tissue handling but may impact turnover rates in other pools and should be the focus of deeper investigation going forward.

Strengths, limitations, and future directions

The current study has many strengths that deserve mention. 1- this is the first investigation to present a method of oral-delivery of L-serine to quantify tissue and organelle CER synthesis. Oral delivery is simple, increases the throughput of the method, and may be translated to other models. With the elimination of an infusion, oral serine may allow for better understanding of CER synthesis in free living situations. The use of L-serine is especially convenient as it can be applied to measure the synthesis of all CER species and theoretically can be applied to measure dhCERs as well. However, a key limitation of the current method is the reproducibility of the isotope labeling with the LC/MS fragmentation scheme. It is likely with the current method, CERs in very small quantities along with dhCERs

may be unreliably detected and will require more sensitive techniques to minimize the background noise. Aggregating this analytical hurdle is the cost associated with labeled serine and the quantity required to achieve a detectable peak. Nevertheless, as we gain more knowledge regarding CERs implicated in disease progression, this method can be adapted and optimized for other CER species. 2- Unlike other precursors, L-serine is incorporated at only one location in the product molecule and the likelihood of recycling a serine-derived label into other parts of the molecule (i.e., palmitate) is expected to be low. Therefore, the use of this isotope allows for direct labeling of the CER backbone and subsequent incorporation into CER biosynthesis rather than indirect through the synthesis of palmitate with a deuterium label. 3- With the isolation of hepatic mitochondria, we were able to gain a greater understanding of the hepatic handling of CERs. Additionally, the inclusion of a HFD animal group allowed us to test how our method worked in a setting of perturbed metabolism and significantly contributed to our discovery of early hepatic partitioning of CERs that may be important in the development of mitochondrial dysfunction.

Above we outlined the technical and analytical considerations of this and other kinetic methods for CER synthesis. In addition to these considerations, our results are also limited in other ways. 1- As this was a method development project aimed at establishing turnover protocols, we did not measure mitochondrial function (e.g., respiration rates, apoptosis, ROS production). Future studies should combine these basic assessments with the current labeling

paradigm to ascertain if early alterations in CER synthesis are related to early in vivo mitochondrial dysfunction. 2- We did not measure serum CER concentrations or 16:0 synthetic rates. The background noise associated with serum extractions significantly limited the accuracy and reproducibility of the data. Thus, we are unable to determine how circulating CERs were related to hepatic and mitochondrial content. Future studies should allocate larger quantities for measurement of circulating serum CERs and turnover. 3- The concentrations reported here are above many previous reports (although not all (12)) which may be a result of greater sensitivity of the current protocol or could be a result of poorly-matched internal standards. Specifically, the very long chain CERs were found in high concentrations, greater than what was expected, which may be a result of the CER 18:1/17:0 internal standard which may unreliably inflate the area ratios of very long chain CERs based on the analytical detection of the various species. Currently the lack of a very long chain internal standard limits the quantification precision of these CER species and stable isotope internal standards may offer greater assay precision if they do not interfere with the labeling pattern within the biological samples. It is of note that the current method was optimized for the quantification of 16:0 CER and we are highly-confident in the results for this species which match other publications (19, 62, 66).

Conclusion

Strong genetic and pharmacologic evidence supports CERs directly contributing to many metabolic diseases thereby extending the sphingolipids role from simply

a biomarker to a functional driver in disease pathogenesis and progression. With our constantly evolving knowledge of CERs, methods for tracking CER synthesis will be essential for drug development in this area. Here we present evidence of an LC/MS method combined with a L-serine stable isotope to track the synthesis of hepatic and mitochondrial CERs. We are the first to report the robust increase in the turnover and content of CERs within mitochondria of HFD-fed animals. Future studies should assess whether early increases in mitochondrial CERs are implicated in the pathogenesis of related conditions like nonalcoholic fatty liver disease, which is characterized by mitochondrial dysfunction.

EXTENDED METHODOLOGY

Ceramide – Extraction and LC/MS

Liver and mitochondrial (200 μ L) samples and internal standard (CER 18:1/17:0, 50 ng) were extracted with chloroform and methanol according to Bligh and Dyer (65). The bottom (organic) layer was removed and dried and the remaining water layer re-extracted with an additional two mL of chloroform, and the organic layers collapsed then dried under nitrogen gas. An azeotropic agent (methylene chloride) was used to remove any remaining water. Samples were dissolved in 100 μ L of 0.1% formic acid solution in methanol-water (85:15) then were injected (5 μ L) into a Waters HPLC device (2690 Separation Module, Milford, MA) and separated through an Vydac® 200MS™ C8 column (2.1 x 100 mm, 5 μ m, P.J.Cobert Associates, St. Louis, MO). Details of the LC methodology are shown in **table EM3.1**. A Thermo Scientific TSQ (Triple-Stage Quadrupole) Quantiva mass spectrometer was used for ceramide identification and **table EM3.2** presents the transitions and retention times for all CERs and dhCERs monitored. **Figure EM3.1** demonstrates an example of the collision induced ionization for CER 18:1/16:0 (CER containing a palmitate on the fatty acyl chain, catalyzed by CERS5 or 6) using this method. The daughter ion includes the backbone of the CER or dhCER molecule, thus the transition would include the unlabeled or labeled (M3) serine molecule. An important note for the monitored transitions is the process of CER synthesis results in a loss of a single labeled ^{13}C within the original labeled serine (see **figure 1.6**).

Serine – Extraction and GC/MS

Serine was extracted from 500 μL (~25 mg starting tissue) of whole liver homogenate (homogenized as described for CER extraction in buffer B: 1,000 μL , sucrose 250 mM, KCl 25 mM, tris-base 50 mM, and EDTA 0.5mM). Formic acid (# AC270480010, Acros Organics, Waltham, MA) was added to the homogenate (forming a six percent formic acid solution) and the mixture diluted with two volumes of water (~1.1 mL) then run over an ion exchange column (# L13922.30, Alfa Aesar, Dowex 50WX8 resin, 200-400 hydrogen form) as described previously (68). The column was washed with water (six mL) and then the serine was eluted with 4N ammonium hydroxide (two mL; # AC423305000 Acros Organics, Waltham, MA). The eluent was dried and derivatized with 100 μL of bis(trimethylsilyl) trifluoroacetamide + 10% trimethylchlorosilane (BSTFA + 10% TMCS; # 15209, Supelco, Bellefonte, PA) at 80°C for two hours. The TMS serine derivatives were injected (one μL) into a 6890N gas chromatography coupled to a 5975 mass spectrophotometry detector (Agilent Technologies, Palo Alto, CA) using a DB-17MS capillary column (30 m length, inner diameter 0.25 mm, and 0.25 μm film, Part# 122-4732, Agilent J&W GC Columns, ChromTech, Inc., Apple Valley, MN) and helium as a carrier gas. Details of the serine GC/MS method are shown in **table EM3.3**. The free serine enrichment was determined using electron impact ionization (70 eV) and selected ion monitoring (m/z 204-207). The unlabeled and labeled serine derivatives (tri-trimethylsilyl) are shown in **figure EM3.2** with the GC/MS ion fragmentation.

Liver TG content

Liver tissue (29.9 ± 0.9 mg) was combined with one mL of a chloroform:methanol (2:1, vol:vol) mixture and homogenized at 20hz for two minutes and then an additional two minutes following ten minutes on ice. The samples were gently homogenized overnight on a slowly spinning wheel. The next day one mL of four mM magnesium chloride was added to each sample and the samples were centrifuged for one hour at 1000 g at 4°C. The bottom (organic) phase was removed (500 μ L) and dried overnight. The dried lipids were reconstituted with a tert-butanol (#471712 Sigma, St. Louis, MO) Triton-x114 (#X114, Sigma, St. Louis, MO) mix (3:2). Using reverse pipetting, three μ L of standards (#F7793, Sigma, St. Louis, MO) and samples were loaded into a 96 well plate and the reaction buffer (300 μ L; TG reagent #T2449 and free glycerol reagent #F6428, Sigma, St. Louis, MO) was added and the plate incubated at 37°C for 40 minutes. After the incubation, the plate was shaken for ~five minutes (or until the blank became clear) and read at 540 nm to quantify absorbance. The final value was reported in milligram TG per gram of liver tissue and the percent of total liver TG was calculated as the gram TG per gram of liver tissue.

Western blotting

Sample processing: Liver tissue (50.4 ± 1.4 mg) was weighed and homogenized in protein lysis buffer (ten μ L:one mg tissue, see below) at 20hz for two minutes and then an additional two minutes following ten minutes on ice. Samples were then centrifuged at 4°C and 1,500 g for 25 minutes and the supernatant removed. Protein content was measured via BCA assay (#23225, Thermo

Fisher Scientific, Rockford, IL). Using the protein concentration, the volume of sample needed to reach three μg protein/ μL was calculated and combined 1:1 with Laemmli 2X buffer (see below). The samples were heated within a water bath (100°C) for five minutes, immediately removed, vortexed, and frozen in -80°C for storage.

Sample run and analysis: Thawed samples (20 μg) were loaded into 4-20% gels (#5671085, Bio-Rad, Hercules, CA) in 1X tris-glycine sulfate-polyacrylamide (SDS) buffer (#1610772, Bio-Rad, Hercules, CA) and electrophoresed at 100 volts (V) for 10 minutes and then 200V for 40 minutes. Blots were transferred to a polyvinylidene difluoride transfer membrane (#88518; Thermo Fisher Scientific, Rockford, Ill., USA) and blocked with five percent milk in tris-buffered saline (TBS, #BP1525, Fisher Scientific, Fair Lawn, NJ) + tween 20 buffer (TBST, #B7337-500, Fisher Scientific, Fair Lawn, NJ) for one hour at room temperature. Primary antibodies (1:1,000) were then added to the membranes and left overnight in a cold room on a rocker. Membranes were washed with TBST and then secondary antibodies (1:5,000) were added and left to incubate at room temperature for one hour. Membranes were washed again with TBST, then TBS, and analyzed via densitometric analysis using ChemiDoc™ MP Imaging System (Image Laboratory Beta 3, Bio-Rad Laboratories, Hercules, CA). Each sample was adjusted to the average intensity of all samples on the membrane and total protein was quantified with 0.1% amido black (#100563, MP Biomedicals, Solon, OH) solution (500 ml distilled water, 400 ml methanol, 100 ml acetic acid, and one g Amido black). The staining controls for the differences in protein loading

and gel-membrane transfer. The total protein staining for each lane, quantified by laser densitometry was used to correct for any differences in protein loading or transfer of all band densities (69).

Protein lysis buffer: Stock solution (44.2 ml) containing 50 mM HEPES (#BP310-1, Fisher Scientific, Fair Lawn, NJ), 12 mM sodium pyrophosphate (#7772-88-5, Aldrich Chemicals, Milwaukee, WI), 100 mM sodium fluoride (#S6776, Sigma, St. Louis, MO), and 10 mM EDTA (#BP120-500, Fisher Scientific, Fair Lawn, NJ) was mixed with 400 μ L of each phosphatase inhibitors (#P0044 and P52726, St. Louis, MO) and five mL of 10% Triton (100X-Triton, #7-X198, JT Baker Chemicals, Phillipsburg, NJ). A protease inhibitor tablet (#1187358001, Roche Diagnostics, Indianapolis, IN) was added to this solution.

Laemmli buffer: β -mercaptoethanol (BME, #BP176, Fisher Scientific, Fair Lawn, NJ) was mixed with 2X Laemmli (#1610737, Bio-Rad, Hercules, CA) in a 1:20 ratio.

Primary and secondary antibodies: Primary antibodies used are as follows: SREBP-1 (Santa Cruz #13551, anti-mouse monoclonal IgG₁; 1:1,000 dilution), serine palmitoyl transferase (SPTLC1; Santa Cruz #374143, anti-mouse monoclonal IgG₁; 1:1,000 dilution), dihydroceramide desaturase (DES1/FADS7; Santa Cruz #134338, anti-mouse monoclonal IgM; 1:1,000 dilution), ceramide synthase 1 (CERS1/LASS1; Sigma Aldrich SAB2104843, anti-rabbit polyclonal; 1:1,000 dilution), ceramide synthase 2 (CERS2/LASS2; Santa Cruz #390745, anti-mouse monoclonal IgG₁; 1:1,000 dilution), ceramide synthase 6

(CERS6/LASS6; Santa Cruz #100554, anti-mouse monoclonal IgG_{2a}; 1:1,000 dilution), acid sphingomyelinase (SMPD1; Bio-Rad #AHP3001, anti-rabbit polyclonal IgG; 1:1,000 dilution), and acid ceramidase (ASAH1; Sigma-Aldrich #ABN468, anti-rabbit polyclonal; 1:1,000 dilution). The oxidative phosphorylation complexes I-V were also quantified by western blot (Total OxPhos cocktail; AbCam #ab110413, anti-mouse; 1:1,000 dilution). Secondary antibodies used include HRP-linked anti-mouse (#7076S, Cell Signaling, Danvers, MA) and anti-rabbit (#7074S, Cell Signaling, Danvers, MA) IgG at 1:5,000 dilution.

Citrate synthase activity

Isolated mitochondria used for CER analysis were diluted to reach a 1:30 dilution and freeze fractured (three times) in liquid nitrogen. The samples (ten μL , in triplicate) were loaded into a 96 well plate, six samples at a time along with a blank (water) and then the reaction buffer (see below) was added (170 μL). The samples and reaction buffer were incubated at 37°C for two minutes and then three mM acetyl-CoA (30 μL) was added immediately. The activity was monitored using a BioTek spectrophotometer (Synergy H1, New Castle, DE) at 405 nm over seven minutes, producing activity curves. The fit of the curves were examined ($r^2 = 0.98-1.00$), activity triplicates were averaged, the value divided by 73.82, multiplied by 1000 and divided by the quantity of protein loaded to produce nmol citrate produced /minute / μg protein.

Reaction buffer: 10.5 mL of 100 mM tris stock (#BP152, Fisher Scientific, Fair Lawn, NJ) was mixed with one and a half mL of one mM DTNB in tris stock

(#D8310, Sigma, St. Louis, MO) and 750 μ L of ten mM oxaloacetate in tris stock (#04126, Sigma, St. Louis, MO).

Power calculation

A power analysis (**extended methodology table EM4.4**) demonstrated two to four mice would be required to detect dietary and sex differences in liver CER 16:0 concentrations. With a current sample size of 24 animals per group (12/sex), we have 90% power to detect differences in these outcomes at between CD and HFD or male and female mice.

Extended Methodology Tables and Figures

Table EM3.1. Details of CER LC/MS methodology

Mobile phases	A) Water + 0.2% formic acid B) Acetonitrile/2-propanol (50/50) + 0.2% formic acid
Flow	0.3 mL/min
Gradient	0-1 minutes: 65% B 1-4 minutes: 65%B to 100%B 4-16 minutes: 100%B 16-16.1 minutes: 100%B to 65%B 16.1-22 minutes: 65%B

Table EM3.2. Transitions and retention time for all species analyzed

Ceramide	Transition (<i>m/z</i>)	Retention time (minutes)
18:1/17:0	552.6 → 264	4.42
18:1/14:0	510.5 → 264	4.10
18:1/16:0	538.5 → 264	4.32
18:1/18:0	566.4 → 264	4.50
18:1/18:1	564.4 → 264	4.35
18:1/20:0	594.4 → 264	4.69
18:1/22:0	622.6 → 264	4.84
18:1/24:0	650.6 → 264	4.98
18:1/24:1	648.6 → 264	4.81
Labeled Ceramide	Transition (<i>m/z</i>)	Retention time (minutes)
18:1/16:0- M1	539.5 → 265	4.32
18:1/16:0- M3	541.5 → 267	4.32
Dihydroceramide	Transition (<i>m/z</i>)	Retention time (minutes)
18:0/16:0	540.6 → 266	4.40
18:0/18:0	568.4 → 266	4.57
18:0/24:0	652.6 → 266	4.98
18:0/24:1	650.6 → 266	4.88

Table EM3.3. Details of GC/MS serine methodology

Injection volume	1 μ L
Injector temperature ($^{\circ}$ C)	240 $^{\circ}$ C
Transfer line temperature ($^{\circ}$ C)	310 $^{\circ}$ C
Split Ratio	1:30
Oven	0-2 minutes: 80 $^{\circ}$ C 2-19.5 minutes: 80 $^{\circ}$ C to 220 $^{\circ}$ C (8 $^{\circ}$ C/min) 19.5-21.5 minutes: 220 $^{\circ}$ C to 310 $^{\circ}$ C (45 $^{\circ}$ C/min) 21.5-27.5: 310 $^{\circ}$ C

Table EM3.4. Power calculation based on previous studies and pilot data

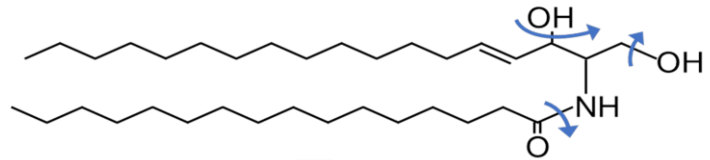
Two group comparisons	Control diet	High fat diet	Pooled SD	Power	Alpha	n/group
Liver total [CER] ¹	2.75	10.25	3.3	90%	0.05	4
	Male	Female				
Liver [16:0 CER] ³	2.3	3.2	0.3	90%	0.05	2

¹ Data from ref. (103), 3-day control and high fat diet fed C57Bl/6; Units: μ g/mg protein

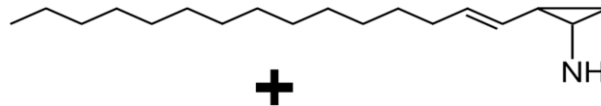
² Data from Mucinski-pilot data, Control diet; Units: nmol/g tissue

Figure EM3.1. Collision induced induced ionization of CER 18:1/16:0

Parent Molecule
(C₃₄O₃NH₆₇)
Ceramide 18:1/16:0
m/z = 538



Daughter Ion (C₁₈NH₃₄)
m/z = 264



Fragmented Ion (C₁₆O₃H₃₃)
m/z = 273

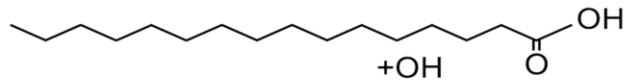
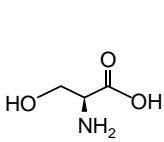
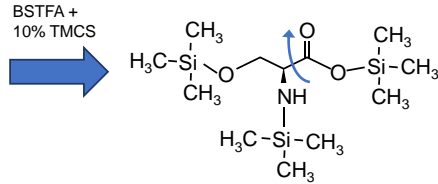


Figure EM3.2. Unlabeled and labeled serine derivatives (tri-trimethylsilyl)

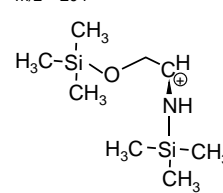
L-Serine
MW = 105



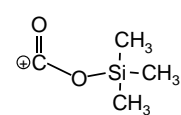
GC/MS Ion Fragmentation
MW = 321



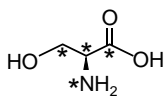
Daughter ion
(C₈NO₃Si₂H₂₂)
m/z = 204



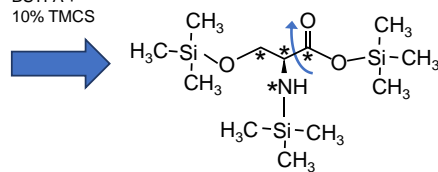
Fragmented ion
(C₄O₂SiH₉)
MW = 117



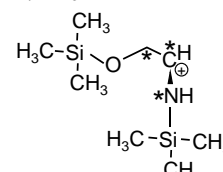
¹³C₃, ¹⁵N L-Serine
MW = 109



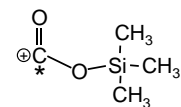
GC/MS Ion Fragmentation
MW = 325



Daughter ion
(¹³C₂¹⁵NC₆OSi₂H₂₂)
m/z = 207



Fragmented ion
(¹³C₃O₂SiH₉)
MW = 118



TABLES

Table 3.1. Macronutrient composition and ingredients for control and high fat diets

Macronutrient	Control Diet		High Fat Diet	
	<i>% total grams</i>	<i>% total kcal</i>	<i>% total grams</i>	<i>% total kcal</i>
<i>Protein</i>	19%	20%	26%	20%
<i>Carbohydrate</i>	67%	70%	26%	20%
<i>Fat</i>	4%	10%	35%	60%
Ingredient	<i>gram</i>	<i>kcal</i>	<i>gram</i>	<i>kcal</i>
<i>Casein</i>	200	800	200	800
<i>L-Cystine</i>	3	12	3	12
<i>Corn Starch</i>	506.2	2,024.8	0	0
<i>Lodex 10¹</i>	125	500	125	500
<i>Sucrose</i>	72.8	291.2	72.8	291.2
<i>Solka Floc²</i>	50	0	50	0
<i>Soybean Oil</i>	25	225	25	225
<i>Lard</i>	20	180	245	2,205
<i>Mineral Mix³</i>	50	0	50	0
<i>Vitamin Mix⁴</i>	1	4	1	4
<i>Choline Bitartrate</i>	2	0	2	0
<i>Yellow Dye #5</i>	0.04	0.00	0.00	0.00
<i>Blue Dye #1</i>	0.01	0.00	0.05	0.00
Total	1,055.05	4,037.00	773.85	4,037.00
<i>Kcal/gram</i>		3.38		5.22

Data adapted from researchdiets.com (CD: # D12450J and HFD: # D12492)

¹ Maltodextrin, ² Cellulose, ³ S10026, ⁴ V10001

Table 3.2. Fatty acid composition of control and high fat diets

Fat source	Control Diet g/100g	High Fat Diet g/100g
<i>Soybean oil</i>	2.37	3.23
<i>Lard</i>	1.90	31.66

Fatty acid	g/100g (%TFA)	g/100g (%TFA)
<i>Capric (10:0)</i>	<0.01 (0.04%)	0.03 (0.09%)
<i>Lauric (12:0)</i>	<0.01 (0.04%)	0.03 (0.09%)
<i>Myristic (14:0)</i>	0.03 (0.73%)	0.48 (1.38%)
<i>Palmitic (16:0)</i>	0.74 (17.52%)	8.57 (24.76%)
<i>Palmitoleic (16:1)</i>	0.06 (1.53%)	1.05 (3.03%)
<i>Stearic (18:0)</i>	0.35 (8.26%)	4.40 (12.71%)
<i>Oleic (18:1)</i>	1.38 (32.53%)	14.65 (42.29%)
<i>Linoleic (18:2)</i>	1.45 (34.20%)	4.74 (13.69%)
<i>Linolenic (18:3)</i>	0.19 (4.42%)	0.37 (1.07%)
<i>Arachidic (20:0)</i>	0.01 (0.26%)	0.07 (0.21%)
<i>Gondoic (20:1)</i>	0.01 (0.31%)	0.22 (0.64%)
<i>Behenic (22:0)</i>	0.01 (0.17%)	0.01 (0.03%)

Data are presented as grams of the fat source or fatty acid per 100 g of the respective diet (g/ 100 g) and percent of total fatty acids (%TFA).

Table 3.3. Energy and water intake

	Control Diet	High Fat Diet	P - value
<i>Food intake (g/day)</i>	2.38 ± 0.29	2.49 ± 0.23	0.156
<i>Carbohydrates</i>	1.60 ± 0.22	0.65 ± 0.08	< 0.0001
<i>Protein</i>	0.45 ± 0.06	0.65 ± 0.08	< 0.0001
<i>Fat</i>	0.10 ± 0.01	0.87 ± 0.11	< 0.0001
<i>Energy intake (kcal/day)</i>	9.35 ± 0.68	13.00 ± 1.21	< 0.0001
<i>Carbohydrates</i>	6.56 ± 0.56	2.61 ± 0.32	< 0.0001
<i>Protein</i>	1.87 ± 0.16	2.61 ± 0.32	< 0.0001
<i>Fat</i>	0.94 ± 0.08	7.82 ± 0.95	< 0.0001
<i>Water intake (mL/day)</i>	4.4 ± 0.6	4.3 ± 0.6	0.875
<i>Labeled serine intake¹</i>	3.9 ± 0.6	3.9 ± 0.6	0.875

Data are presented as mean ± SD; *n* = 24 per group; *P*-value represents one-tailed, unpaired *t*-test.

¹ mg/day; Calculated as the product of the water serine concentration (0.9 mg/mL) and average daily water intake.

Table 3.4. Inter- and intraassay precision for liver and mitochondrial CER

Liver ceramide	Interassay	Intraassay
<i>18:1/14:0</i>	0.8%	1.0%
<i>18:1/16:0</i>	3.5%	4.4%
<i>18:1/18:0</i>	0.5%	0.6%
<i>18:1/18:1</i>	4.5%	3.6%
<i>18:1/20:0</i>	3.7%	4.3%
<i>18:1/22:0</i>	0.5%	1.4%
<i>18:1/24:0</i>	2.1%	3.6%
<i>18:1/24:1</i>	2.3%	4.4%
Mitochondrial ceramide	Interassay	Intraassay
<i>18:1/14:0</i>	1.7%	1.6%
<i>18:1/16:0</i>	5.0%	2.9%
<i>18:1/18:0</i>	2.1%	4.3%
<i>18:1/18:1</i>	5.4%	3.7%
<i>18:1/20:0</i>	3.6%	5.8%
<i>18:1/22:0</i>	2.6%	5.9%
<i>18:1/24:0</i>	4.4%	7.8%
<i>18:1/24:1</i>	3.6%	4.3%

Data are presented as the coefficient of variation (CV) of the same pooled sample analyzed five times (inter-) and a pooled sample extracted five times on different days across two weeks (intra-).

Table 3.5. Kinetics of liver and mitochondrial CER 16:0

Liver ceramide	Control diet	High fat diet
Predicted asymptote	2.7%	2.4%
16:0 CER made de novo ¹	0.07 ± 0.02	0.08 ± 0.03
FSR (pools/d) ²	0.47	0.47
ASR (nmol/g tissue/day) ²	1.33	1.71
T1/2 (pools/ day)	1.5	1.5
Mitochondrial ceramide	Control diet	High fat diet
Predicted asymptote	2.5%	3.0%
16:0 CER made de novo ¹	0.03 ± 0.01	0.06 ± 0.02***
FSR (pools/d) ²	0.35	0.62
ASR (nmol/g tissue/day) ²	0.47	1.21
T1/2 (pools/ day)	2.0	1.1

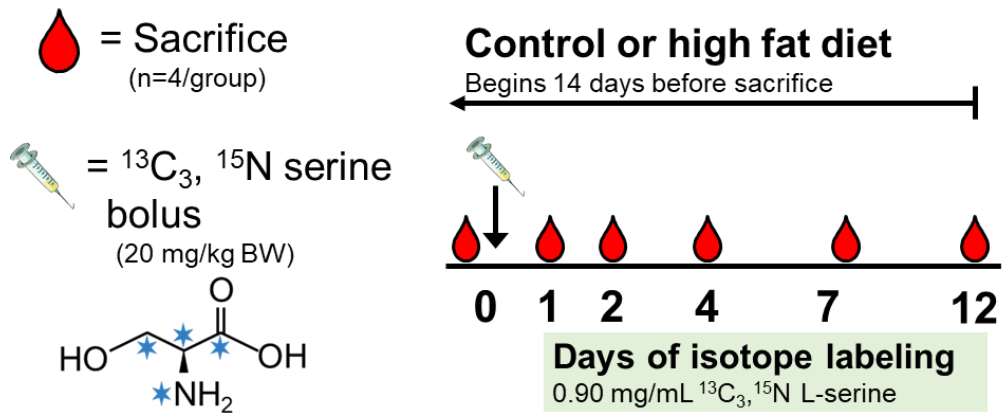
¹ $\mu\text{mol/g}$ tissue containing the serine label. It is important to note that not all newly-made 16:0 CER become labeled. Steady state contribution of the liver or mitochondrial CERs (days 4-12) were multiplied by the respective pool size.


² FSR, fractional synthesis rate and ASR, absolute synthesis rates are also shown in **figure 3.10**.


*** $P < 0.001$ compared to CD

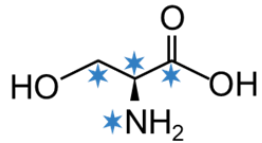
FIGURES

Figure 3.1. Experimental design and labeled serine stable isotope



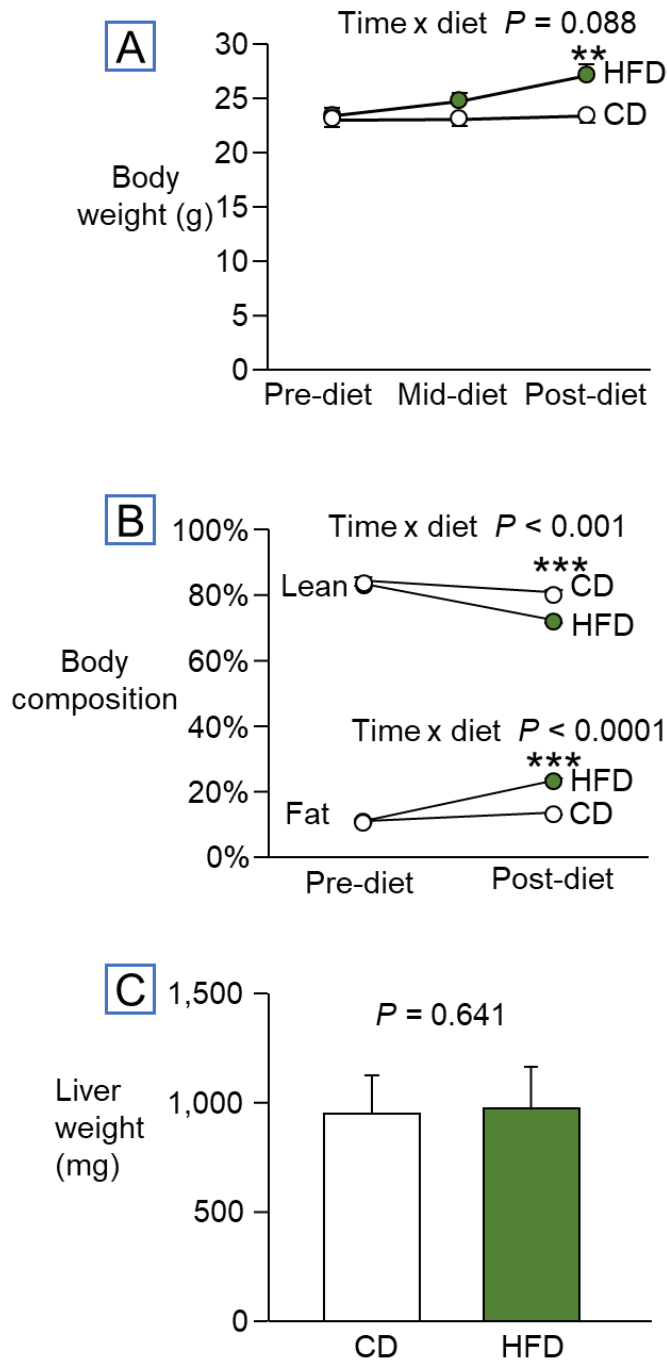
 = Sacrifice
(n=4/group)

 = $^{13}\text{C}_3, ^{15}\text{N}$ serine
bolus
(20 mg/kg BW)



Blue stars on the serine molecule indicate a ^{13}C or ^{15}N isotope.

Figure 3.2. Anthropometrics and liver weight



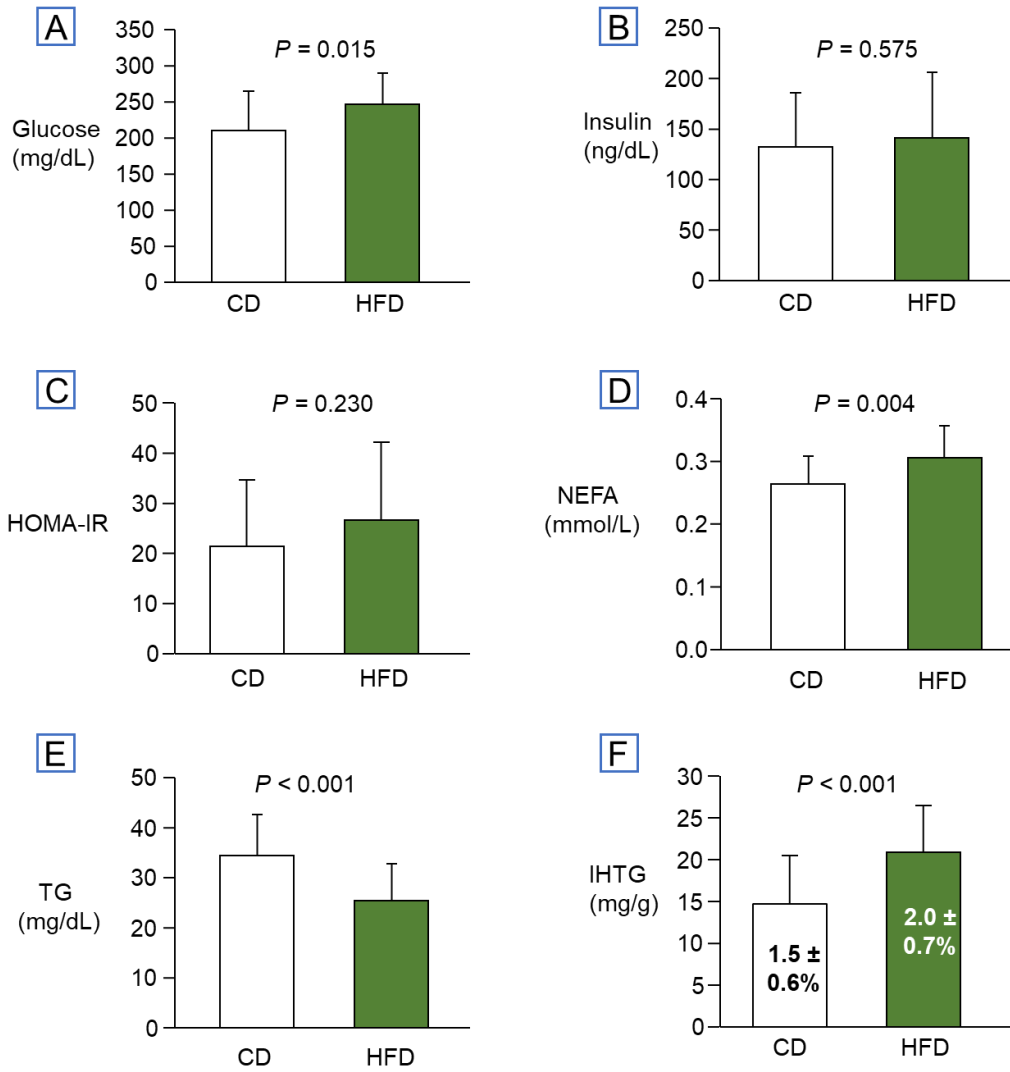
Data are presented as mean \pm SEM (**A-B**) and mean \pm SD (**C**); $n = 48$ (CD = 24; HFD = 24). ** $P < 0.01$; *** $P < 0.001$.

A: Changes in total body weight across the diet. Three-way between factors ANOVA (time x diet).

B: Changes in percent lean and fat mass across the pre- and post-diet. Two-way between factors ANOVA (time x diet).

C: Total liver weight; Unpaired, two-tailed t -test.

Figure 3.3. Serum and liver biochemistries



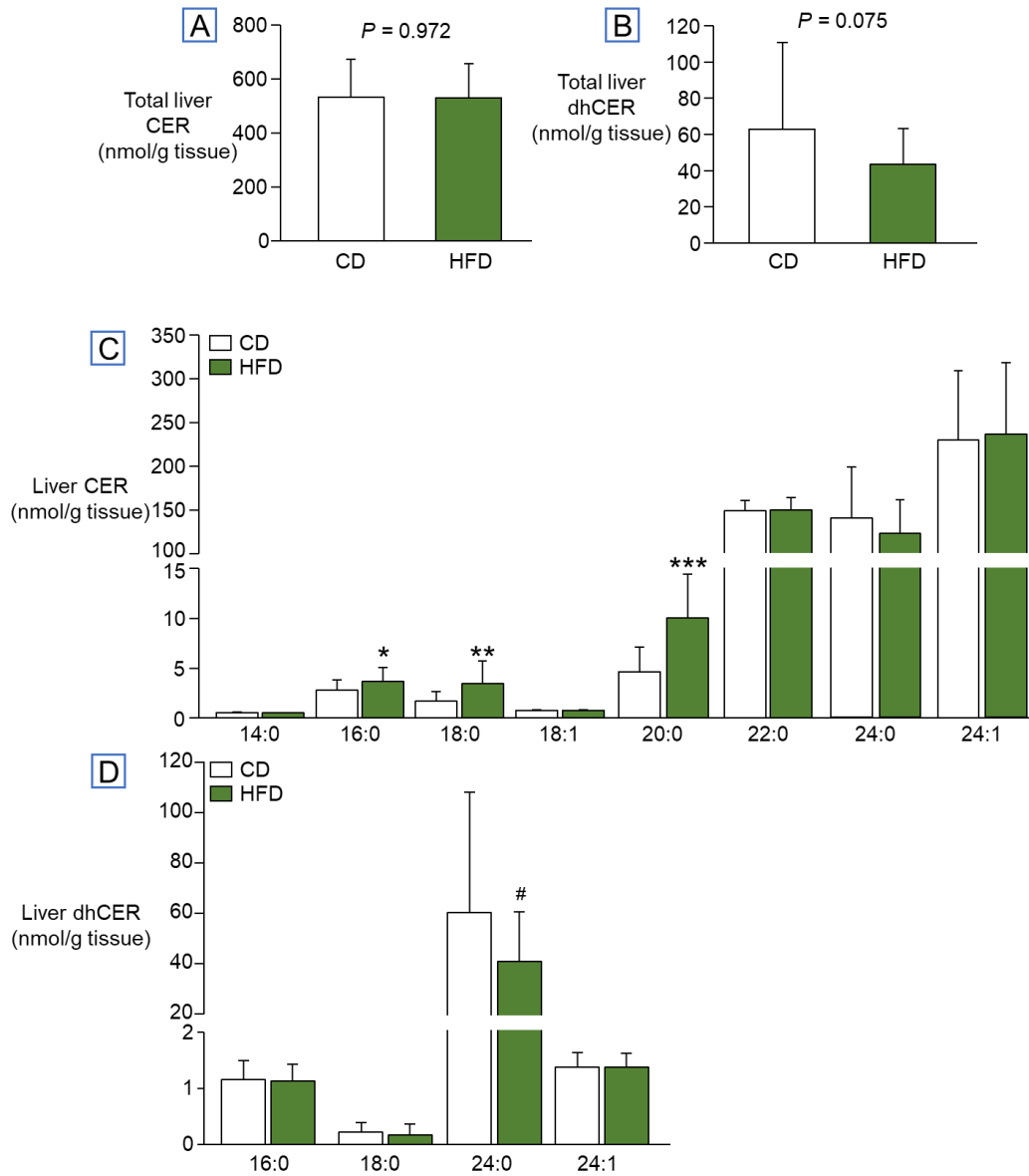
Data are mean ± SD; unpaired, two-tailed *t*-tests.

A-C: Serum (**A**) glucose ($n = 47$, 1 HFD missing) and (**B**) insulin ($n = 45$, 2 HFD and 1 CD missing) and (**C**) the homeostatic model assessment for insulin resistance (HOMA-IR, $n = 45$, 2 HFD and 1 CD missing) which was calculated at the product of glucose (mmol/L) and insulin (μ U/mL) divided by the constant 22.5 (70, 71).

D: Serum NEFA concentrations ($n = 47$, 1 HFD missing).

E-F: Serum (**E**, $n = 47$, 1 HFD missing) and intrahepatic (**F**, $n = 47$, 1 HFD missing) TG (IHTG) concentrations. Percentages within the IHTG bars represent the mean ± SD of the percent of liver fat present in each group.

Figure 3.4. Whole liver CER and dhCER concentrations

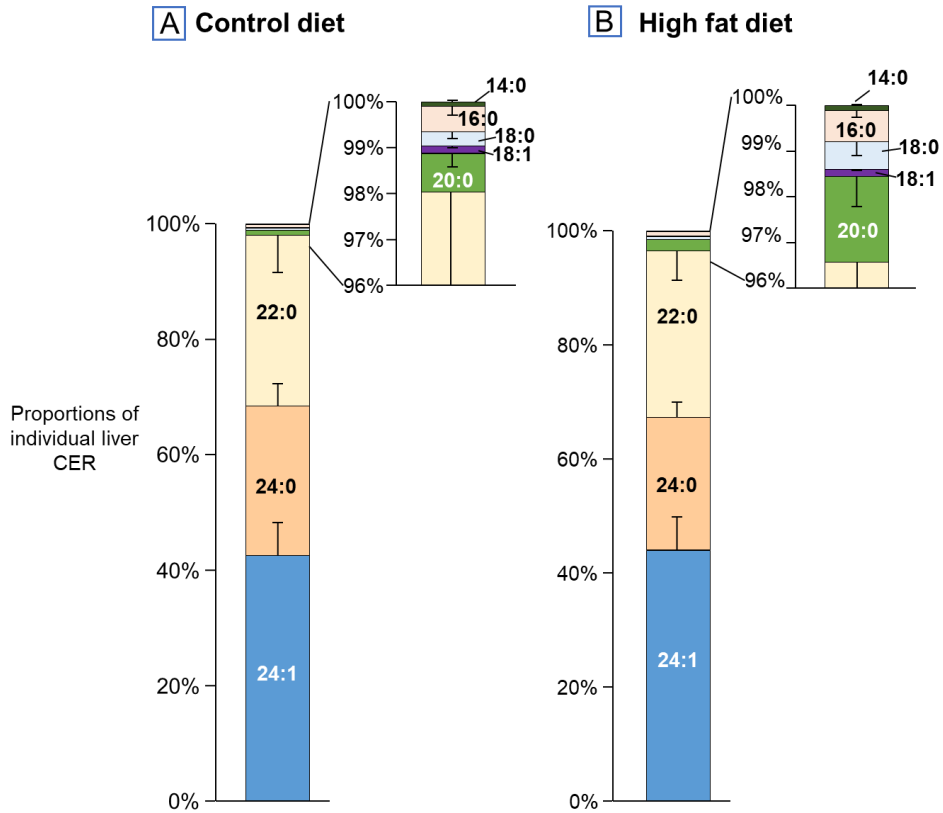


Data are presented as mean \pm SD; $n = 24/\text{diet}$; unpaired, two-tailed t -tests. CD (white bars) versus HFD (green bars) within total or individual species: # $P < 0.10$, * $P < 0.05$, ** $P < 0.01$, *** $P < 0.001$. All CER presented contain an 18:1 backbone whereas dhCER contain an 18:0 backbone.

A-B: Total liver (A) CER or (B) dhCER.

C-D: Individual liver (C) CER and (D) dhCER species.

Figure 3.5. Molar percent of individual liver CER



C

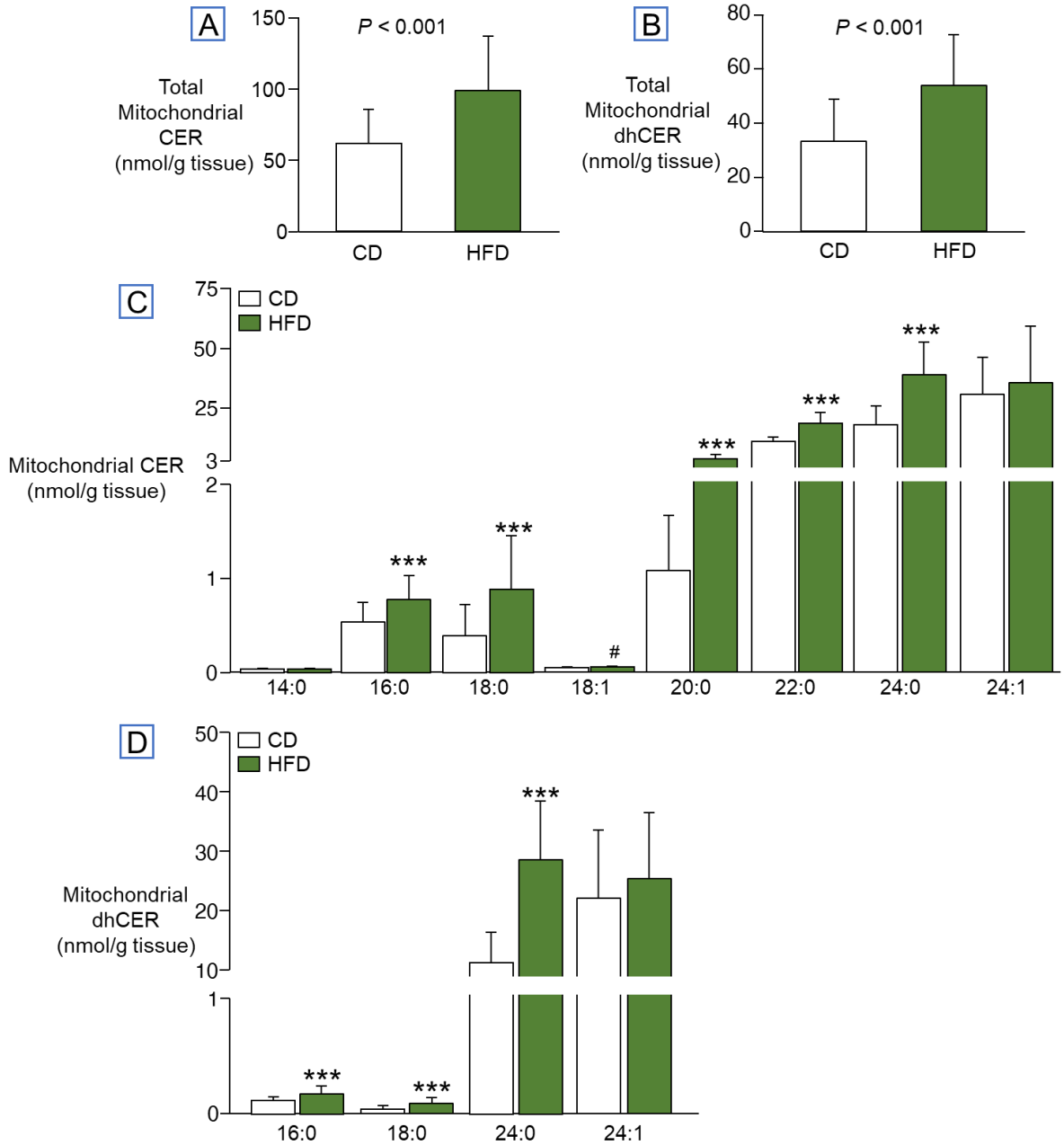
Molar percent of total liver CER			
CER species	Control diet	High fat diet	<i>P</i> value
14:0	0.10 ± 0.03%	0.10 ± 0.02%	0.365
16:0	0.55 ± 0.19%	0.68 ± 0.17%	0.015
18:0	0.32 ± 0.15%	0.61 ± 0.31%	< 0.001
18:1	0.15 ± 0.04%	0.15 ± 0.03%	0.589
20:0	0.84 ± 0.30%	1.87 ± 0.67%	< 0.0001
22:0	29.67 ± 6.55%	29.49 ± 5.28%	0.916
24:0	25.87 ± 3.81%	23.21 ± 2.67%	0.007
24:1	42.50 ± 5.63%	43.90 ± 5.73%	0.399

Data are presented as mean molar percent ± SD; *n* = 24/diet; unpaired, two-tailed *t*-tests. All CER presented contain an 18:1 backbone.

A-B: Proportions of individual hepatic CER making up the total pool in animals consuming a **(A)** control or **(B)** high fat diet.

C: Comparison of the molar percentages of each individual liver CER species between the animal groups.

Figure 3.6. Isolated mitochondrial CER and dhCER concentrations

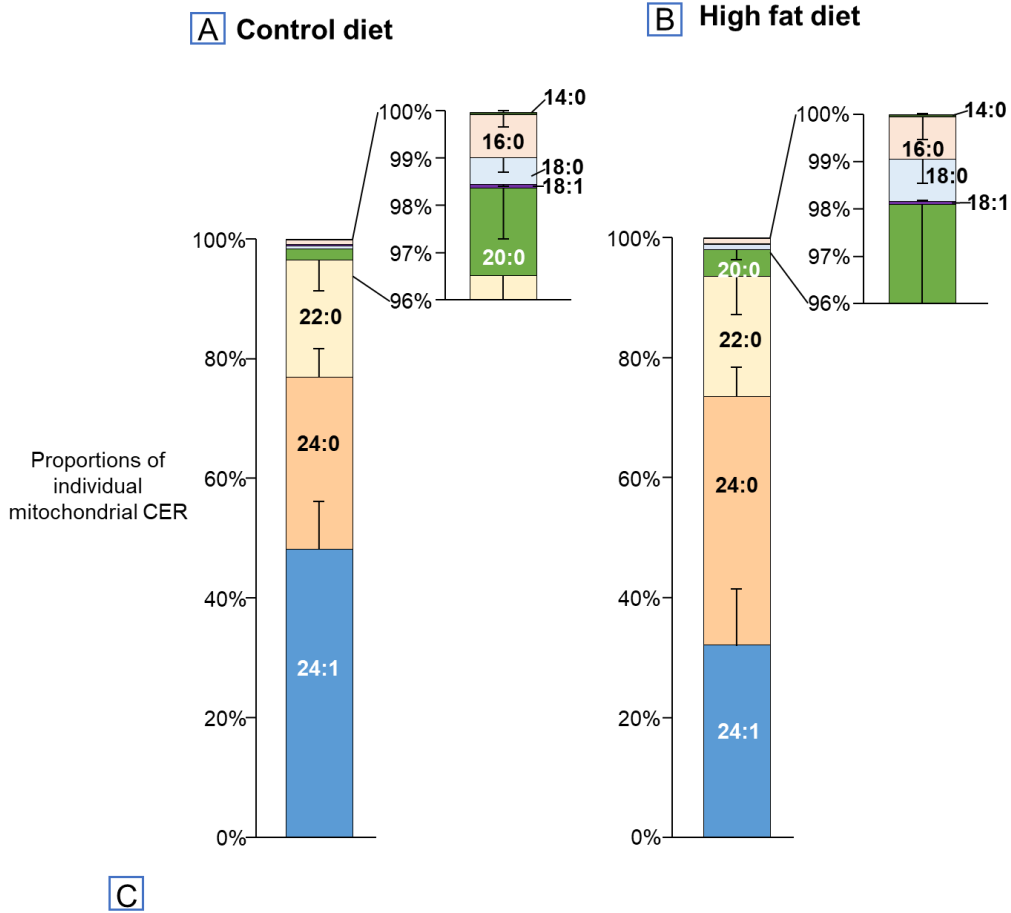


Data are presented as mean \pm SD; $n = 24/\text{diet}$; unpaired, two-tailed t -tests. CD (white bars) versus HFD (green bars) within total or individual species: # $P < 0.10$, * $P < 0.05$, ** $P < 0.01$, *** $P < 0.001$. All CER presented contain an 18:1 backbone whereas dhCER contain an 18:0 backbone.

A-B: Total mitochondrial (A) CER or (B) dhCER.

C-D: Individual mitochondrial (C) CER and (D) dhCER species.

Figure 3.7. Molar percent of individual mitochondrial CER



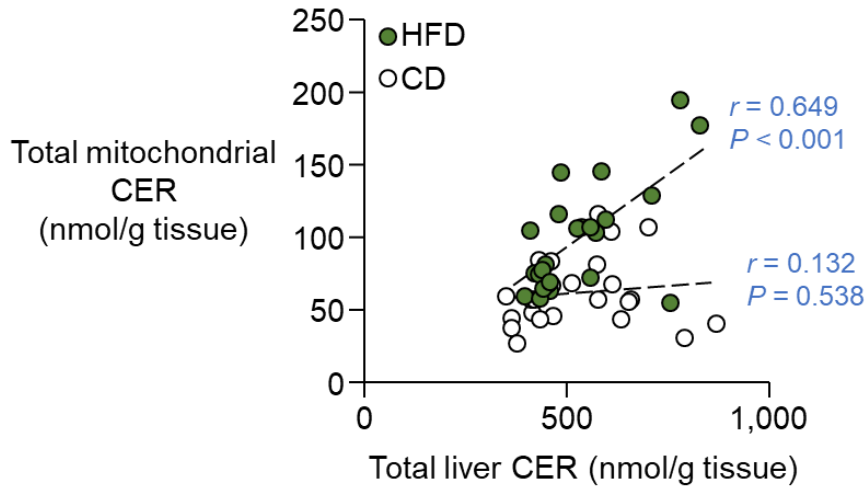
Molar percent of mitochondrial CER			
CER species	Control diet	High fat diet	<i>P</i> value
14:0	0.06 ± 0.02%	0.04 ± 0.02%	< 0.0001
16:0	0.89 ± 0.25%	0.90 ± 0.49%	0.955
18:0	0.56 ± 0.32%	0.90 ± 0.51%	0.008
18:1	0.09 ± 0.03%	0.06 ± 0.02%	< 0.001
20:0	1.84 ± 1.08%	4.50 ± 1.82%	< 0.0001
22:0	19.60 ± 5.29%	20.09 ± 6.43%	0.774
24:0	28.90 ± 4.62%	41.39 ± 4.90%	< 0.0001
24:1	48.04 ± 7.99%	32.11 ± 9.47%	< 0.0001

Data are presented as mean molar percent ± SD; *n* = 24/diet; unpaired, two-tailed *t*-tests. All CER presented contain an 18:1 backbone.

A-B: Proportions of individual hepatic mitochondria CER making up the total pool in animals consuming a (A) control or (B) high fat diet.

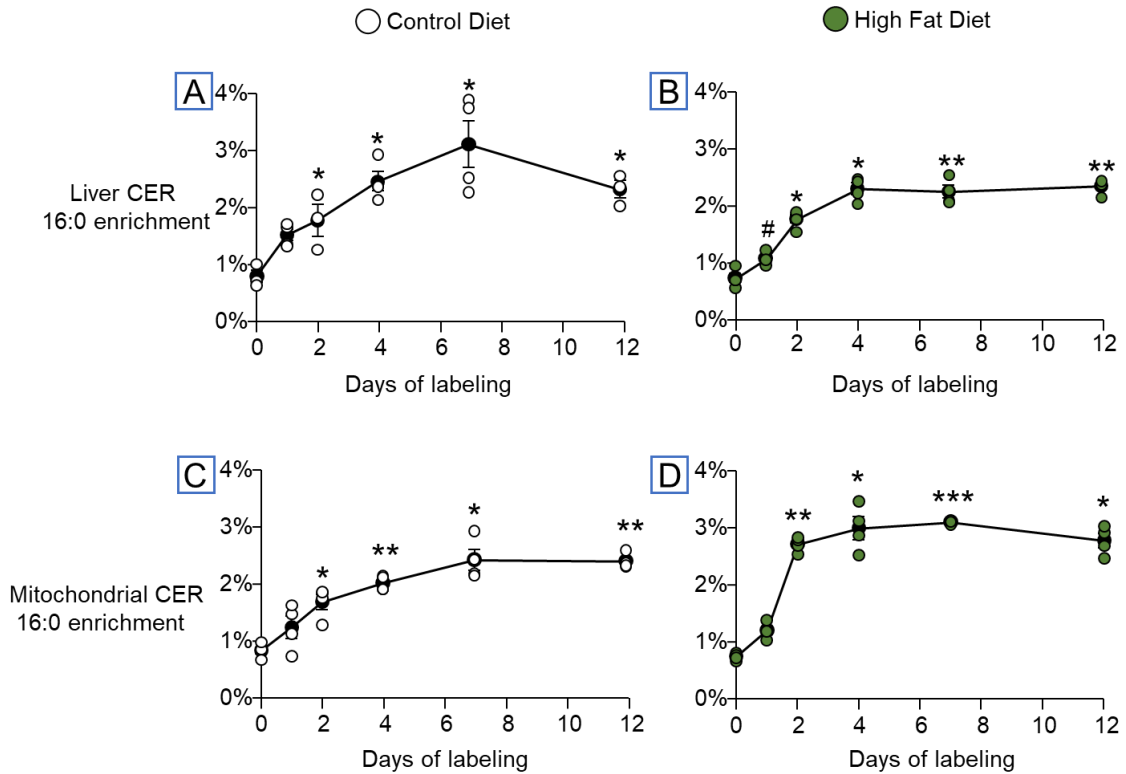
C: Comparison of the molar percentages of each individual mitochondrial CER species between the animal groups.

Figure 3.8. Relationship between total liver and mitochondrial CER



Relationship between total liver and hepatic mitochondrial CER (Pearson correlation). Animals fed a CD ($n = 24$) are shown in white and HFD in green ($n = 24$).

Figure 3.9. Percent enrichment of 16:0 CER across days

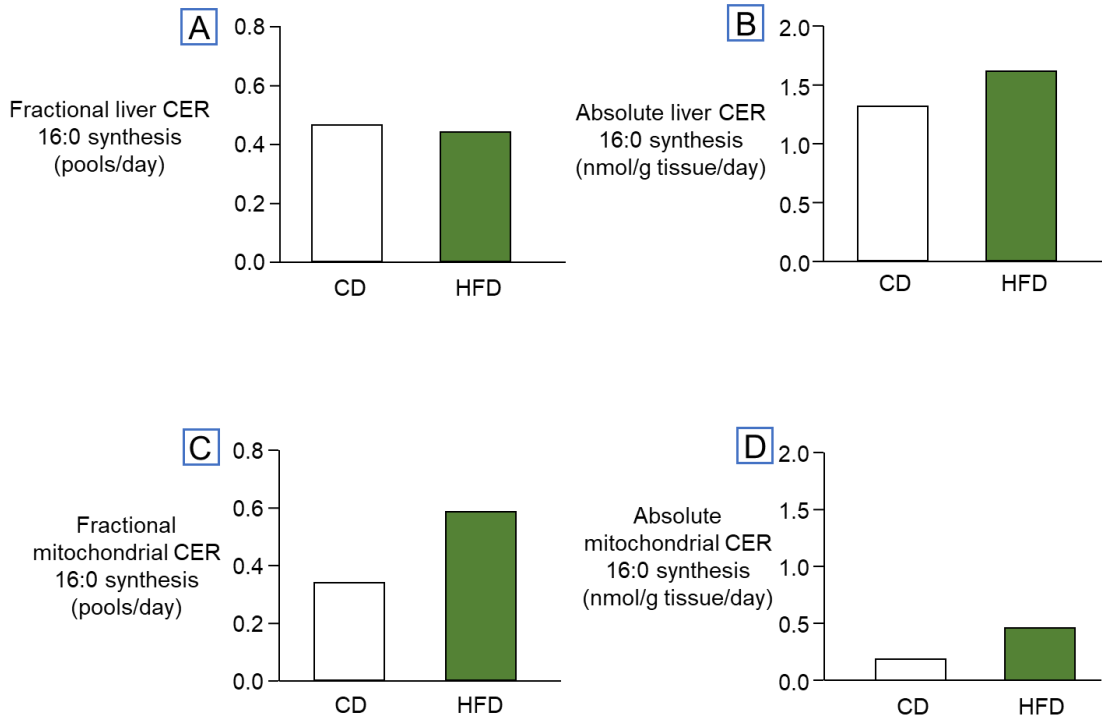


Data are presented as mean \pm SEM in black and individual animals are presented in white for CD and green for HFD ($n = 2-4/\text{timepoint}$). ANOVA for differences across labeling days (all $P < 0.0001$) and post-hoc t -test with Bonferroni adjustments # $P < 0.10$, * $P < 0.05$, ** $P < 0.01$, *** $P < 0.001$ versus unlabeled (day 0).

A-B: Liver CER 16:0 percent enrichment across labeling days (0, 1, 2, 4, 7, 12) for (A) CD and (B) HFD.

C-D: Mitochondrial CER 16:0 percent enrichment across labeling days (0, 1, 2, 4, 7, 12) for (C) CD and (D) HFD.

Figure 3.10. Fractional and absolute synthesis rate of 16:0 CER in liver and isolated mitochondria

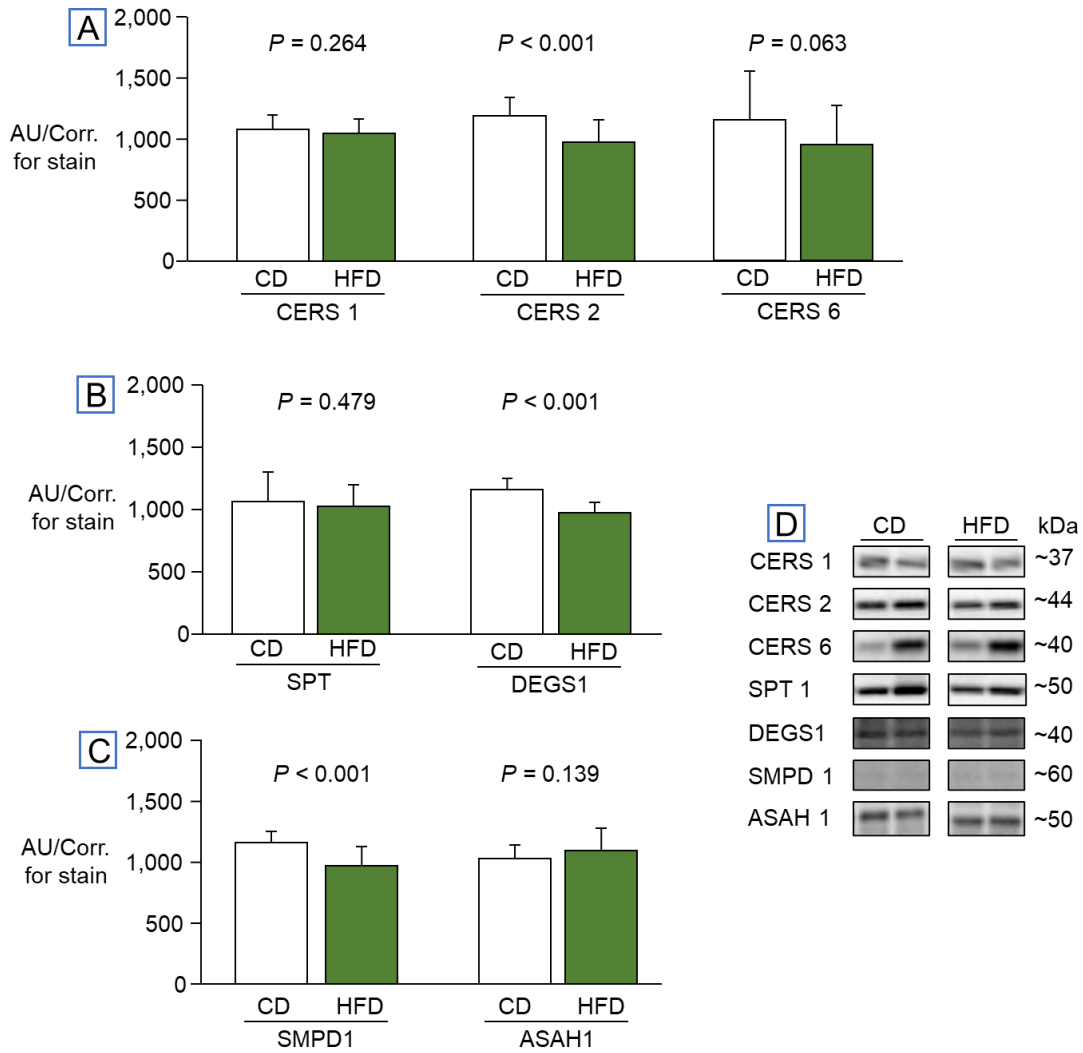


Data are calculated as fractional (pools/day) and absolute (nmol/g tissue/day) turnover. Enrichment data were fitted to a single exponential curve to produce fractional turnover and plateau %E. Fractional turnover was multiplied by the total pool of 16:0 CER to calculate absolute synthesis. Due to the nature of the experiment and the average of animals within a day used to create a single curve (black lines in **figure 3.9**), a single turnover rate was calculated within a diet and thus no statistical analysis was performed.

A-B: Liver 16:0 CER (**A**) fractional and (**B**) absolute synthesis rates.

C-D: Mitochondrial 16:0 CER (**C**) fractional and (**D**) absolute synthesis rates.

Figure 3.11. Whole liver homogenate protein expression of key CER synthetic enzymes



Data are mean \pm SD; unpaired, two-tailed *t*-tests. Animal fed a CD are shown in white bars and HFD in green bars.

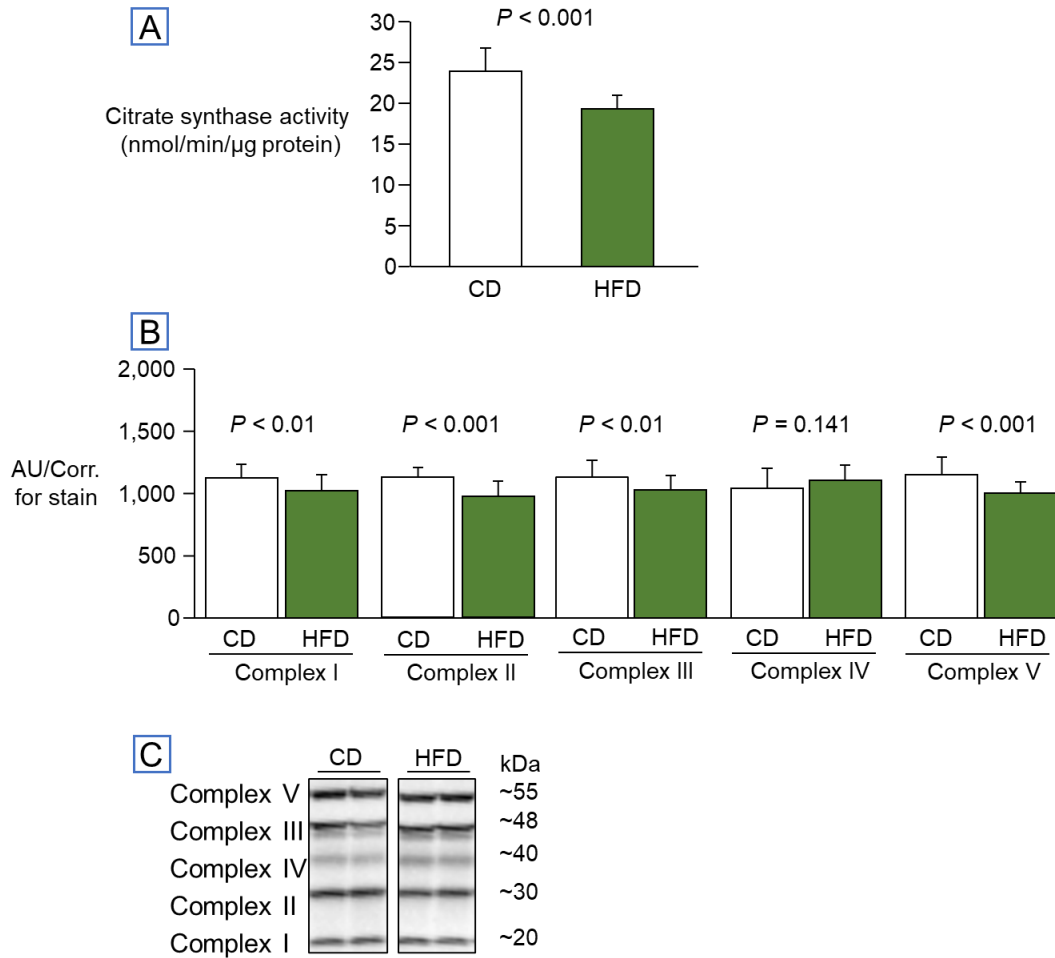
A: Total liver protein content of CER synthases 1,2, and 6 ($n = 24/\text{diet}$).

B: Total liver protein content of serine palmitoyl transferase (SPT 1, $n = 24/\text{diet}$) and dihydroceramide desaturase (DEGS1, $n = 24/\text{diet}$).

C: Total liver protein content of acid sphingomyelinase (SMPD 1, $n = 24/\text{diet}$) and acid ceramidase (ASAH 1, $n = 23/\text{HFD}$ and $24/\text{CD}$).

D: Representative blots for the target proteins for each diet.

Figure 3.12. Mitochondrial citrate synthase activity and hepatic protein expression of the oxidation phosphorylation complexes



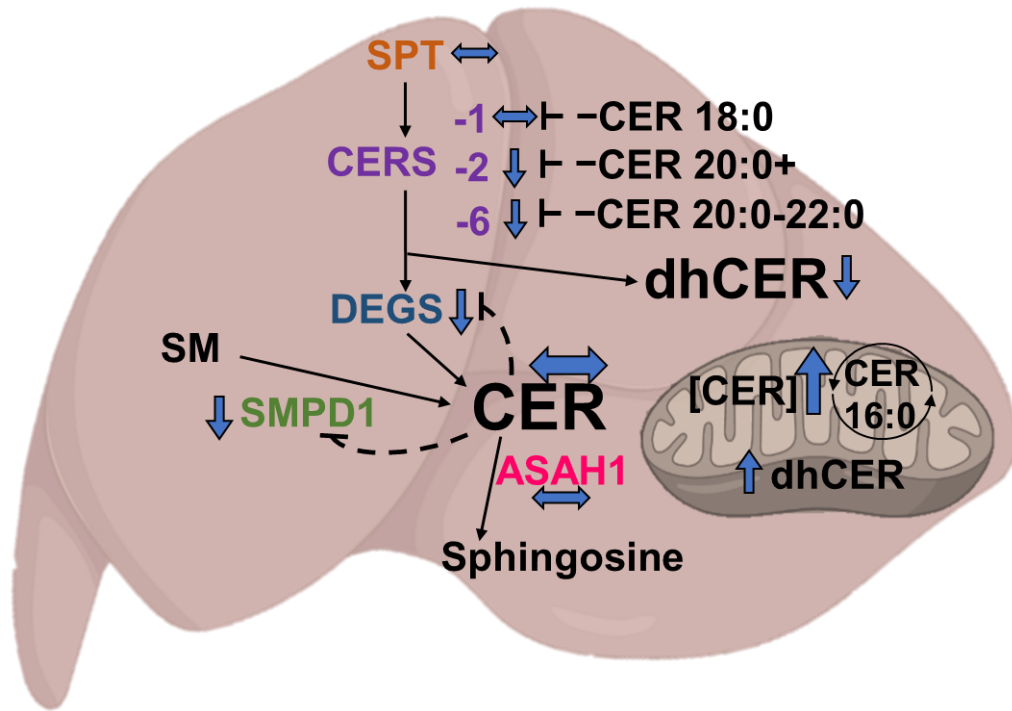
Data are mean \pm SD; unpaired, two-tailed *t*-tests. Animal fed a CD are shown in white bars and HFD in green bars.

A: Whole liver homogenate citrate synthase activity ($n = 24/\text{diet}$).

B: Total liver protein content of the oxidative phosphorylation complexes ($n = 24/\text{diet}$).

C: Representative blots for the target proteins for each diet.

Figure 3.13. Model demonstrating effects of HFD on hepatic CER synthesis



Blue arrows indicate an effect of the HFD and the dotted lines signify the hypothesized feedback inhibition of elevated CER concentrations.

SUPPLEMENTARY DATA

Supplementary Table S3.1. Sex differences for serum biochemistries and hepatic TG content

	Control Diet		High Fat Diet	
	Male	Female	Male	Female
Body weight (g) ^{*,#}	26.3 ± 2.5	20.5 ± 0.8	28.1 ± 1.5	23.0 ± 2.1
Lean mass (%)	83 ± 3	78 ± 3	72 ± 3	73 ± 5
Fat mass (%) [*]	12 ± 3	15 ± 3	24 ± 3	22 ± 5
Serum glucose (mg/dL) ^{*,#}	236 ± 60	185 ± 33	273 ± 40	217 ± 24
Serum Insulin (ng/dL) [#]	170 ± 53	101 ± 30	195 ± 46	92 ± 31
HOMA-IR [#]	31 ± 14	13 ± 4	39 ± 12	14 ± 5
Serum NEFA (mmol/L) [*]	0.27 ± 0.04	0.26 ± 0.05	0.31 ± 0.05	0.30 ± 0.06
Serum TG (mg/dL) ^{*,#, ‡}	41 ± 6	28 ± 4	27 ± 8	24 ± 6
Hepatic TG (mg/g) ^{*,#}	11 ± 3	18 ± 6	20 ± 6	22 ± 6

Data are presented as mean ± SD and are post-diet measurements ($n = 12/\text{diet}/\text{sex}$).

* Main effect of diet ($P < 0.01$)

Main effect of sex ($P < 0.001$)

‡ Interaction effect ($P < 0.05$)

Supplementary Table S3.2. Day of euthanasia body and organ weights

	Control Diet	High Fat Diet
<i>Total body weight (g)**</i>	23.0 ± 3.6	26.8 ± 4.7
<i>Liver (mg)</i>	946.9 ± 175.9	971.7 ± 190.7
<i>Heart (mg)</i>	107.7 ± 16.8	113.1 ± 14.9
<i>Kidneys (mg)*</i>	236.7 ± 38.8	267.1 ± 48.8
<i>Epididymal fat (mg)***</i>	433.8 ± 140.0	899.2 ± 357.8
<i>Inguinal fat (mg)***</i>	110.5 ± 34.4	196.7 ± 88.8
<i>Gastrocnemius (mg)</i>	181.9 ± 30.2	190.9 ± 31.0
<i>Heart:body weight (mg/g)**</i>	4.7 ± 0.4	4.3 ± 0.5

Data are presented as mean ± SD; (*n* = 24/diet).

Two-tailed, unpaired *t*-test; # *P* < 0.10, * *P* < 0.05, ** *P* < 0.01, *** *P* < 0.001

Supplementary Table S3.3. Liver free serine enrichment

Days on isotope	High Fat Diet		Control Diet	
	Male	Female	Male	Female
<i>Unlabeled (zero days)</i>	0.03 ± 0.00%	0.03 ± 0.00%	0.03 ± 0.00%	0.03 ± 0.00%
<i>One day</i>	0.52 ± 0.09%	0.58 ± 0.07%	0.68 ± 0.01%	0.66 ± 0.03%
<i>Two days</i>	1.21 ± 0.25%	0.98 ± 0.20%	0.98 ± 0.00%	0.96 ± 0.02%
<i>Four days</i>	1.04 ± 0.08%	0.88 ± 0.08%	0.88 ± 0.04%	1.00 ± 0.16%
<i>Seven days</i>	0.96 ± 0.02%	1.17 ± 0.20%	1.01 ± 0.14%	1.31 ± 0.39%
<i>Twelve days</i>	1.18 ± 0.28%	1.21 ± 0.13%	1.35 ± 0.13%	1.43 ± 0.07%

Data are presented as mean ± SD.

Taken from the average of two animals within a sex per day.

Supplementary Table S3.4. Sex differences for hepatic protein expression of key enzymes related to CER synthesis, oxidative phosphorylation complexes, and mitochondrial citrate synthase activity

	Control Diet		High Fat Diet	
	Male	Female	Male	Female
CER synthase 1 [#] ,	1,143 ± 102	1,019 ± 94	1,105 ± 129	981 ± 69
CER synthase 2 ^{*,#}	1,098 ± 128	1,273 ± 114	908 ± 181	1,037 ± 166
CER synthase 6 ^{*,#}	807 ± 155	1,500 ± 230	659 ± 102	1,249 ± 122
SPT [#]	978 ± 134	1,156 ± 283	908 ± 132	1,141 ± 129
dhCER desaturase [*]	1,142 ± 86	1,169 ± 95	937 ± 102	995 ± 56
Acid sphingomyelinase [*]	1,181 ± 75	1,138 ± 103	936 ± 180	1,009 ± 133
Acid ceramidase	1,006 ± 129	1,040 ± 92	1,047 ± 213	1,136 ± 146
SREBP 1	2,094 ± 265	2,111 ± 303	1,978 ± 477	2,303 ± 262
Complex I [*]	1,135 ± 96	1,113 ± 131	1,019 ± 126	1,028 ± 139
Complex II ^{*,#}	1,130 ± 76	1,174 ± 80	947 ± 139	1,050 ± 80
Complex III [*]	1,153 ± 113	1,099 ± 154	1,024 ± 142	1,022 ± 95
Complex IV	1,031 ± 134	1,050 ± 179	1,102 ± 121	1,099 ± 130
Complex V [*]	1,137 ± 153	1,167 ± 142	977 ± 98	1,031 ± 71
Citrate synthase ¹	22.4 ± 2.9	25.4 ± 1.9	19.6 ± 1.5	19.0 ± 1.9

Data are presented as arbitrary units, corrected for stain ± SD unless otherwise stated; ($n = 12/\text{diet}/\text{sex}$).

¹ nmol/ minute/ μg protein

* Main effect of diet ($P < 0.01$)

Main effect of sex ($P < 0.01$)

‡ Interaction effect ($P < 0.05$)

Supplementary Table S3.5. Correlation matrix for CERS protein content and liver CER and dhCER concentrations

Liver CER	Control Diet						High Fat Diet					
	CERS1		CERS2		CERS6		CERS1		CERS2		CERS6	
	<i>r</i>	<i>P</i>	<i>r</i>	<i>P</i>	<i>r</i>	<i>P</i>	<i>r</i>	<i>P</i>	<i>r</i>	<i>P</i>	<i>r</i>	<i>P</i>
Total	-0.226	0.288	0.171	0.424	0.269	0.203	-0.237	0.264	-0.244	0.251	0.175	0.413
14:0	-0.488	0.015	0.259	0.222	0.380	0.067	-0.288	0.172	-0.188	0.379	0.153	0.476
16:0	-0.612	0.001	0.286	0.175	0.684	0.000	-0.387	0.062	0.087	0.686	0.538	0.007
18:1	0.057	0.790	0.004	0.986	-0.119	0.578	-0.197	0.357	-0.257	0.226	-0.024	0.911
18:0	-0.597	0.002	0.375	0.071	0.826	0.000	-0.478	0.018	-0.002	0.993	0.665	0.000
20:0	-0.438	0.032	0.089	0.678	0.244	0.250	0.071	0.743	-0.446	0.029	-0.512	0.011
22:0	0.149	0.488	-0.055	0.798	-0.256	0.227	0.068	0.752	-0.453	0.026	-0.451	0.027
24:1	-0.266	0.208	0.206	0.335	0.407	0.049	-0.210	0.326	-0.161	0.452	0.252	0.235
24:0	-0.174	0.417	0.129	0.548	0.113	0.600	-0.314	0.135	-0.234	0.271	0.195	0.360
Liver dhCER	CERS1		CERS2		CERS6		CERS1		CERS2		CERS6	
	<i>r</i>	<i>P</i>	<i>r</i>	<i>P</i>	<i>r</i>	<i>P</i>	<i>r</i>	<i>P</i>	<i>r</i>	<i>P</i>	<i>r</i>	<i>P</i>
Total	-0.010	0.962	0.130	0.544	0.159	0.458	-0.333	0.112	0.014	0.947	0.458	0.024
16:0	-0.644	0.001	0.241	0.257	0.345	0.098	-0.302	0.151	0.452	0.027	0.444	0.030
18:0	-0.767	0.000	0.244	0.251	0.575	0.003	-0.446	0.029	0.347	0.097	0.648	0.001
24:1	-0.379	0.067	0.289	0.171	0.336	0.109	-0.273	0.197	0.173	0.419	0.519	0.009
24:0	-0.001	0.996	0.127	0.555	0.153	0.475	-0.325	0.121	0.002	0.993	0.445	0.029

n = 24/diet; Pearson's correlation was used to assess linear relationships between continuous variables. Significant (*P* < 0.05) relationships are highlighted by a dark grey cell and trending significant (*P* < 0.10) relationships are highlighted by a light grey cell.

Supplementary Table S3.6. Correlation matrix for CERS protein content and mitochondrial CER and dhCER concentrations

Mito CER	Control Diet						High Fat Diet					
	CERS1		CERS2		CERS6		CERS1		CERS2		CERS6	
	<i>r</i>	<i>P</i>	<i>r</i>	<i>P</i>	<i>r</i>	<i>P</i>	<i>r</i>	<i>P</i>	<i>r</i>	<i>P</i>	<i>r</i>	<i>P</i>
Total	-0.317	0.131	0.223	0.296	0.551	0.005	-0.342	0.102	-0.421	0.041	0.089	0.679
14:0	-0.461	0.023	-0.461	0.021	0.742	0.000	-0.483	0.017	0.361	0.083	0.777	0.000
16:0	-0.519	0.009	-0.519	0.073	0.875	0.000	-0.455	0.026	0.342	0.102	0.750	0.000
18:1	-0.359	0.085	-0.359	0.092	0.544	0.006	-0.430	0.036	0.407	0.049	0.701	0.000
18:0	-0.408	0.048	-0.408	0.081	0.709	0.000	-0.574	0.003	0.069	0.748	0.795	0.000
20:0	-0.050	0.817	-0.050	0.757	0.263	0.215	0.263	0.215	-0.515	0.010	-0.743	0.000
22:0	-0.128	0.551	-0.128	0.592	0.205	0.336	0.364	0.080	-0.438	0.032	-0.735	0.000
24:1	-0.331	0.114	-0.331	0.236	0.609	0.002	-0.424	0.039	-0.400	0.053	0.121	0.572
24:0	-0.244	0.251	-0.244	0.568	0.352	0.091	-0.342	0.101	-0.293	0.164	0.310	0.140
Mito dhCER	CERS1		CERS2		CERS6		CERS1		CERS2		CERS6	
	<i>r</i>	<i>P</i>	<i>r</i>	<i>P</i>	<i>r</i>	<i>P</i>	<i>r</i>	<i>P</i>	<i>r</i>	<i>P</i>	<i>r</i>	<i>P</i>
Total	-0.491	0.015	0.281	0.183	0.599	0.002	-0.311	0.139	0.159	0.458	0.609	0.002
16:0	-0.576	0.003	0.509	0.011	0.816	0.000	-0.344	0.100	0.361	0.083	0.567	0.004
18:0	-0.430	0.036	0.335	0.109	0.662	0.000	-0.490	0.015	0.273	0.197	0.854	0.000
24:1	-0.436	0.033	0.401	0.052	0.756	0.000	-0.480	0.018	0.083	0.698	0.603	0.002
24:0	-0.487	0.016	0.276	0.192	0.590	0.002	-0.307	0.144	0.156	0.466	0.604	0.002

n = 24/diet; Pearson's correlation was used to assess linear relationships between continuous variables. Significant (*P* < 0.05) relationships are highlighted by a dark grey cell and trending significant (*P* < 0.10) relationships are highlighted by a light grey cell.

Supplementary Table S3.7. Correlation matrix for SPT, DEGS, SMPD, and ASAH protein content and liver CER and dhCER concentrations

Liver CER	Control Diet								High Fat Diet							
	SPT		DEGS		SMPD		ASAH		SPT		DEGS		SMPD		ASAH	
	<i>r</i>	<i>P</i>	<i>r</i>	<i>P</i>	<i>r</i>	<i>P</i>	<i>r</i>	<i>P</i>	<i>r</i>	<i>P</i>	<i>r</i>	<i>P</i>	<i>r</i>	<i>P</i>	<i>r</i>	<i>P</i>
Total	0.164	0.445	0.167	0.434	-0.014	0.948	-0.086	0.690	0.067	0.757	0.079	0.712	-0.066	0.761	-0.049	0.824
14:0	0.471	0.020	-0.188	0.379	-0.553	0.005	-0.255	0.228	0.182	0.394	0.075	0.726	-0.089	0.679	0.105	0.635
16:0	0.399	0.053	0.078	0.718	-0.368	0.077	0.052	0.810	0.315	0.134	0.170	0.428	-0.066	0.760	0.098	0.655
18:1	-0.086	0.691	-0.197	0.357	-0.268	0.206	-0.303	0.151	0.081	0.705	-0.038	0.859	-0.122	0.569	0.071	0.746
18:0	0.168	0.434	-0.027	0.901	-0.073	0.736	0.177	0.409	0.413	0.045	0.208	0.328	0.053	0.807	0.103	0.640
20:0	0.481	0.017	0.140	0.514	-0.189	0.377	-0.095	0.660	-0.419	0.042	-0.357	0.087	-0.409	0.047	-0.286	0.187
22:0	0.037	0.864	0.080	0.709	-0.117	0.585	-0.351	0.093	-0.279	0.186	-0.216	0.311	-0.267	0.207	-0.074	0.736
24:1	0.081	0.705	0.127	0.555	0.051	0.813	0.041	0.850	0.084	0.695	0.151	0.481	0.038	0.860	-0.039	0.861
24:0	0.246	0.246	0.209	0.327	-0.064	0.768	-0.192	0.369	0.151	0.481	0.037	0.864	-0.150	0.484	-0.019	0.933
Liver dhCER	SPT		DEGS		SMPD		ASAH		SPT		DEGS		SMPD		ASAH	
Total	0.246	0.246	0.261	0.218	-0.038	0.860	-0.216	0.312	0.283	0.180	-0.038	0.861	-0.113	0.600	0.086	0.698
16:0	0.789	0.000	-0.030	0.889	-0.615	0.001	-0.338	0.106	0.697	0.000	0.269	0.204	-0.087	0.686	0.397	0.061
18:0	0.698	0.000	-0.226	0.288	-0.571	0.004	-0.254	0.231	0.694	0.000	0.225	0.291	-0.018	0.933	0.279	0.197
24:1	0.315	0.133	0.155	0.469	-0.107	0.618	-0.084	0.697	0.424	0.039	0.361	0.083	0.128	0.551	0.273	0.208
24:0	0.238	0.263	0.262	0.216	-0.031	0.885	-0.213	0.318	0.264	0.212	-0.049	0.819	-0.115	0.594	0.075	0.734

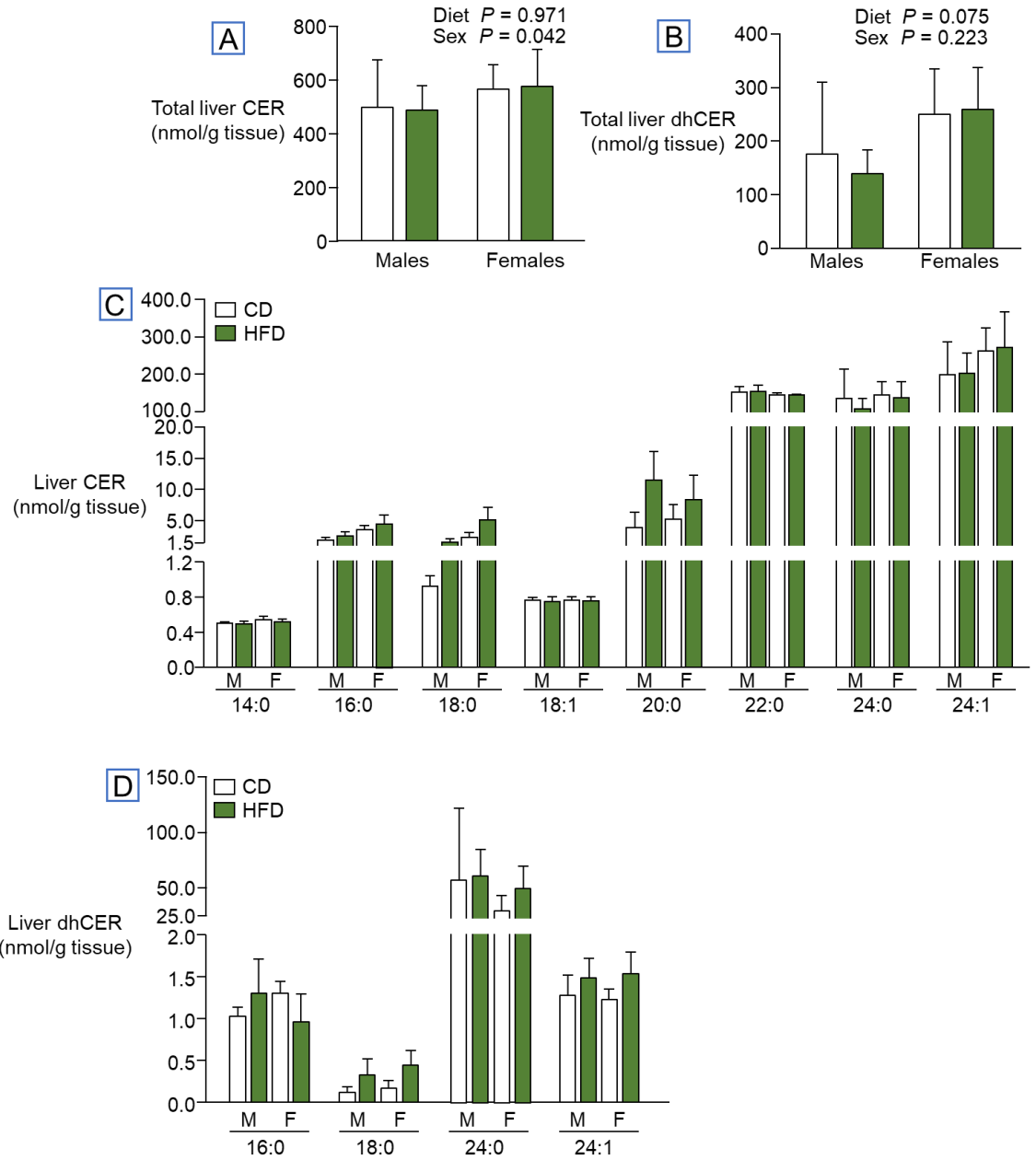
n = 24/diet (*n* = 1 missing for ASAH HFD); Pearson's correlation was used to assess linear relationships between continuous variables. Significant (*P* < 0.05) relationships are highlighted by a dark grey cell and trending significant (*P* < 0.10) relationships are highlighted by a light grey cell.

Supplementary Table S3.8. Correlation matrix for SPT, DEGS, SMPD, and ASAH protein content and mitochondrial CER and dhCER concentrations

Mito CER	Control Diet								High Fat Diet							
	SPT		DEGS		SMPD		ASAH		SPT		DEGS		SMPD		ASAH	
	<i>r</i>	<i>P</i>	<i>r</i>	<i>P</i>	<i>r</i>	<i>P</i>	<i>r</i>	<i>P</i>	<i>r</i>	<i>P</i>	<i>r</i>	<i>P</i>	<i>r</i>	<i>P</i>	<i>r</i>	<i>P</i>
Total	-0.122	0.570	-0.279	0.187	0.052	0.809	0.285	0.177	-0.108	0.616	-0.324	0.123	-0.350	0.094	-0.271	0.211
14:0	0.329	0.116	0.163	0.448	-0.096	0.656	0.350	0.093	0.537	0.007	0.081	0.708	0.008	0.972	0.227	0.297
16:0	0.158	0.460	0.123	0.568	0.132	0.540	0.245	0.249	0.634	0.001	0.221	0.300	0.160	0.455	0.351	0.101
18:1	0.303	0.150	0.058	0.786	-0.122	0.571	0.435	0.034	0.541	0.006	0.116	0.591	0.056	0.794	0.199	0.362
18:0	0.127	0.554	-0.264	0.212	-0.126	0.558	0.301	0.153	0.550	0.005	0.207	0.332	0.085	0.692	0.129	0.557
20:0	0.203	0.342	-0.434	0.034	-0.339	0.105	0.132	0.540	-0.616	0.001	-0.552	0.005	-0.419	0.041	-0.371	0.081
22:0	0.065	0.763	-0.303	0.150	-0.087	0.684	0.405	0.049	-0.649	0.001	-0.516	0.010	-0.344	0.099	-0.353	0.099
24:1	-0.205	0.336	-0.141	0.511	0.179	0.403	0.280	0.186	-0.057	0.791	-0.335	0.109	-0.413	0.045	-0.275	0.204
24:0	-0.010	0.962	-0.452	0.026	-0.143	0.505	0.185	0.387	0.042	0.846	-0.114	0.596	-0.121	0.574	-0.131	0.551
Mito dhCER	SPT		DEGS		SMPD		ASAH		SPT		DEGS		SMPD		ASAH	
Total	0.343	0.101	-0.339	0.105	-0.271	0.201	-0.100	0.643	0.336	0.109	0.179	0.402	0.285	0.178	0.133	0.546
16:0	0.393	0.057	0.224	0.292	-0.093	0.666	0.158	0.462	0.580	0.003	0.241	0.258	0.268	0.205	0.407	0.054
18:0	0.098	0.648	-0.293	0.164	-0.100	0.642	0.314	0.135	0.611	0.002	0.281	0.184	0.319	0.128	0.201	0.359
24:1	0.098	0.648	-0.036	0.867	0.103	0.631	0.321	0.126	0.309	0.142	-0.102	0.635	-0.198	0.354	0.026	0.905
24:0	0.343	0.101	-0.343	0.101	-0.274	0.196	-0.107	0.620	0.331	0.115	0.178	0.405	0.285	0.177	0.130	0.554

n = 24/diet; Pearson's correlation was used to assess linear relationships between continuous variables. Significant (*P* < 0.05) relationships are highlighted by a dark grey cell and trending significant (*P* < 0.10) relationships are highlighted by a light grey cell.

Supplementary Figure S3.1. Sex differences in liver CER and dhCER

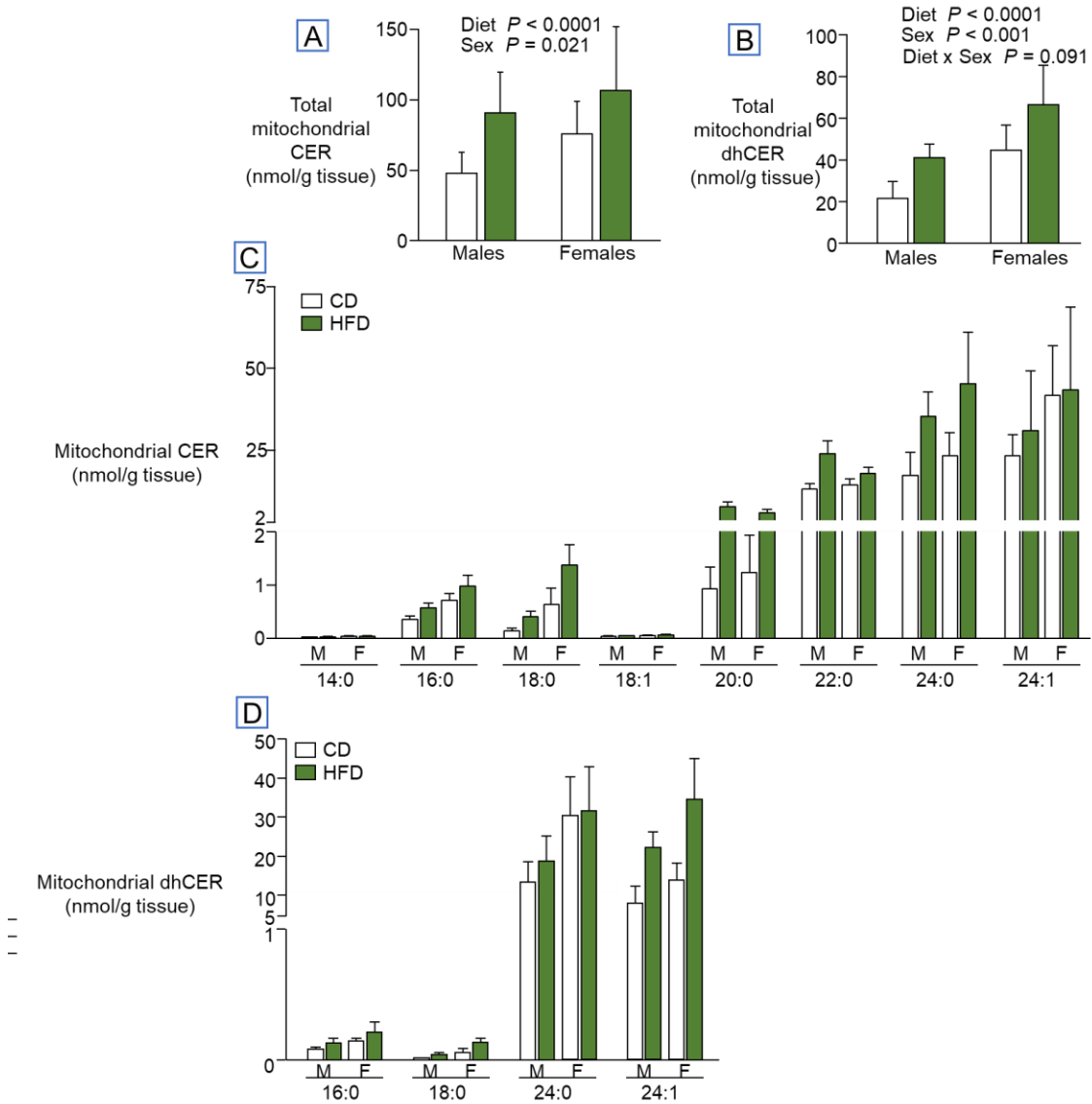


Data are presented as mean \pm SD; $n = 12/\text{diet}/\text{sex}$. Two-way, between-factors ANOVA for total liver CER and dhCER (sex and diet). CD (white bars) versus HFD (green bars) with males (M) and females (F).

A-B: Total liver CER (**A**) or dhCER (**B**).

C-D: Individual liver CER (**C**) and dhCER (**D**) species.

Supplementary Figure S3.2. Sex differences in mitochondrial CER and dhCER

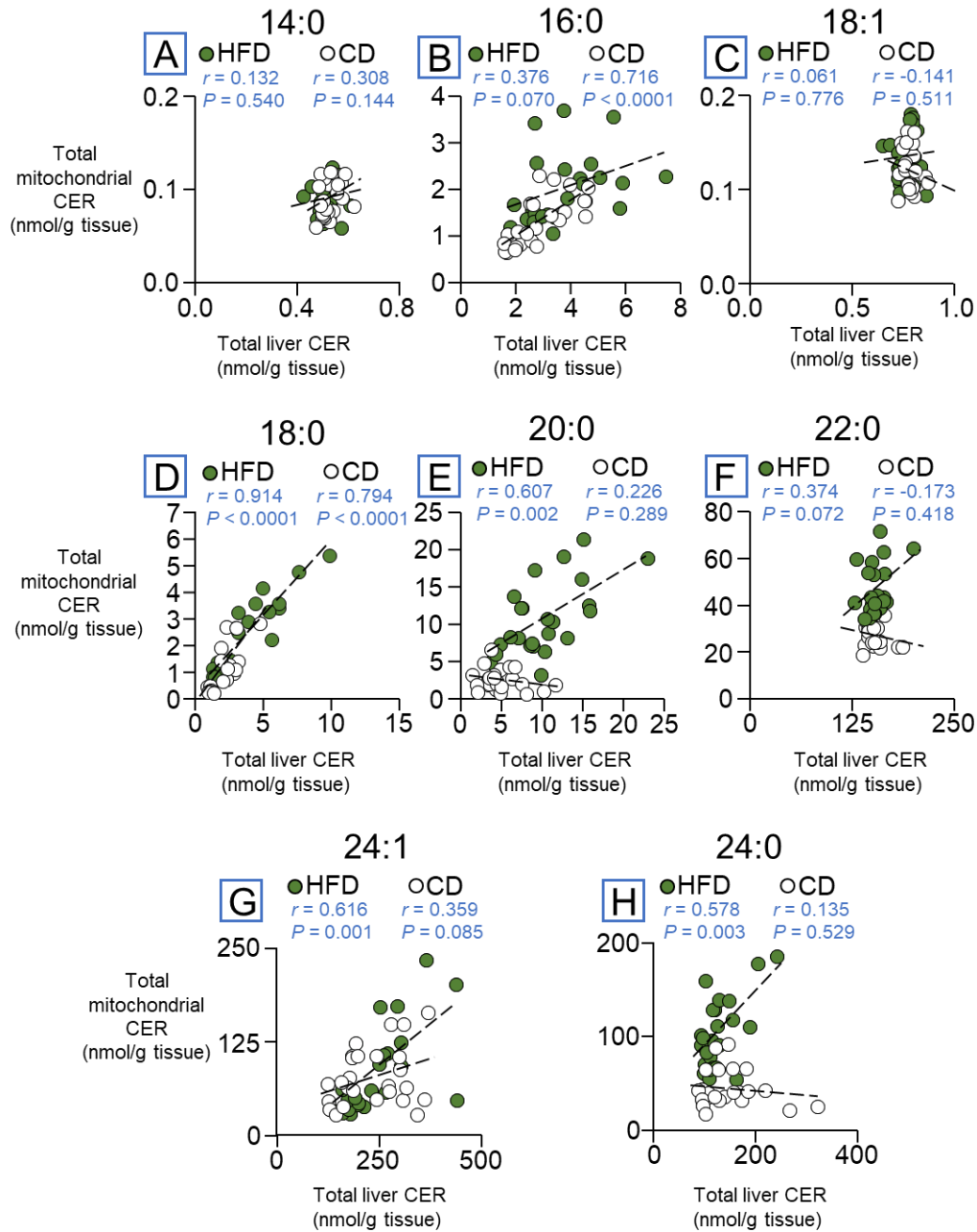


Data are presented as mean \pm SD; $n = 12/\text{diet}/\text{sex}$. Two-way, between-factors ANOVA for total mitochondrial CER and dhCER (sex and diet). CD (white bars) versus HFD (green bars) with males (M) and females (F).

A-B: Total mitochondrial CER (**A**) or dhCER (**B**).

C-D: Individual mitochondrial CER (**C**) and dhCER (**D**) species.

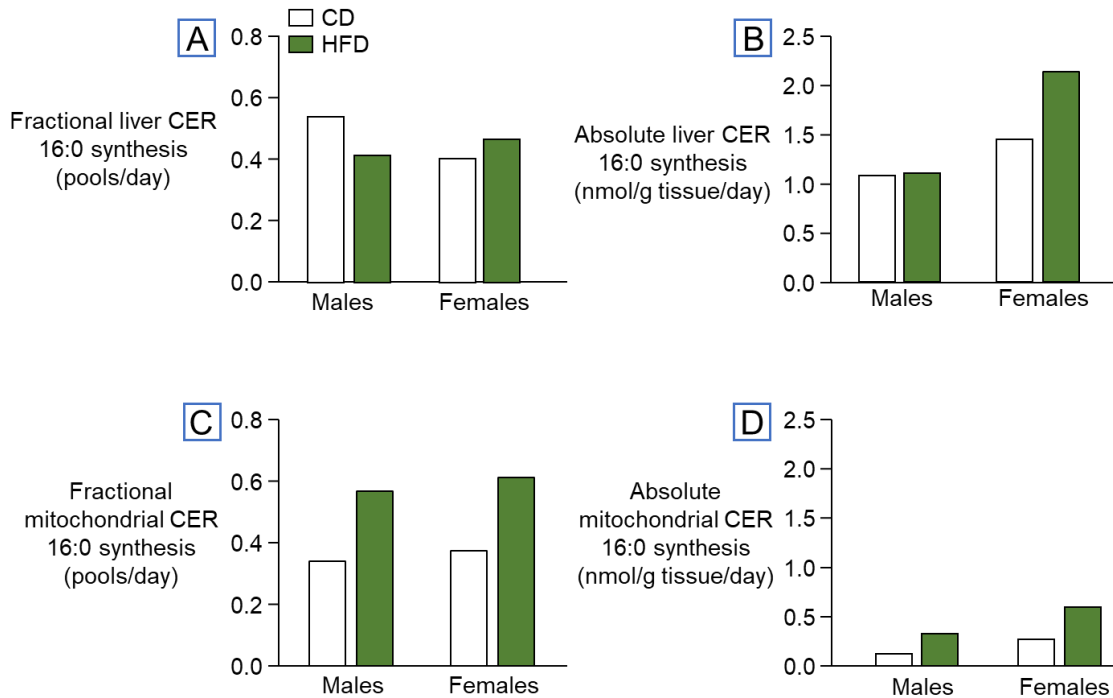
Supplementary Figure S3.3. Relationships between liver and mitochondrial CER



Data accompany **figure 3.8**.

Relationships between individual liver and hepatic mitochondrial CER. Animals fed a HFD ($n = 24$) are shown in green and CD ($n = 24$).

Supplementary Figure S3.4. Fractional and absolute liver and mitochondrial 16:0 CER turnover by sex



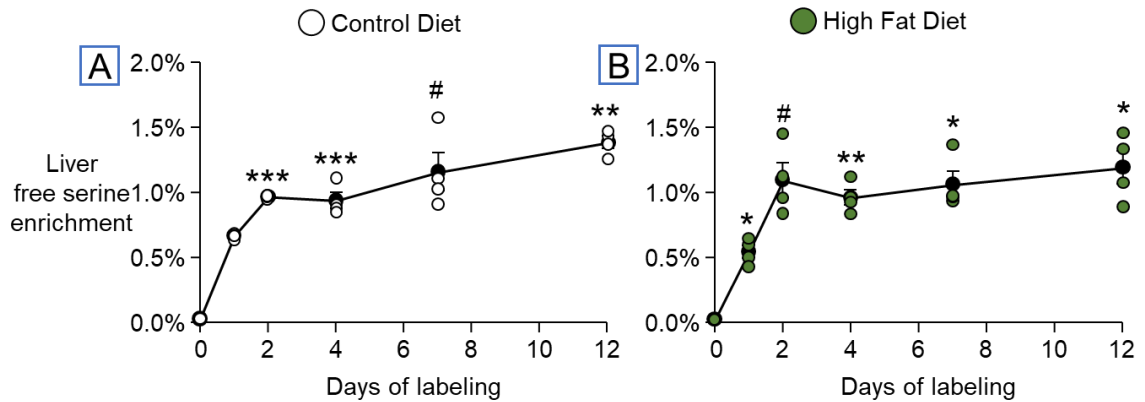
Data accompany figure 3.10.

Data are calculated as fractional (pools/day) and absolute (nmol/g tissue/day) turnover. Enrichment data were fitted to a single exponential curve to produce fractional turnover and plateau %E. Fractional turnover was multiplied by the total pool of 16:0 CER to calculate absolute synthesis. Due to the nature of the experiment and the average of animals within a day and sex used to create a single curve, a single turnover rate was calculated within a diet and sex and thus no statistical analysis was performed.

A-B: Fractional (**A**) and absolute (**B**) synthesis of liver 16:0 CER.

C-D: Fractional (**C**) and absolute (**D**) synthesis of mitochondrial 16:0 CER.

Supplementary Figure S3.5. Percent enrichment of free serine across days

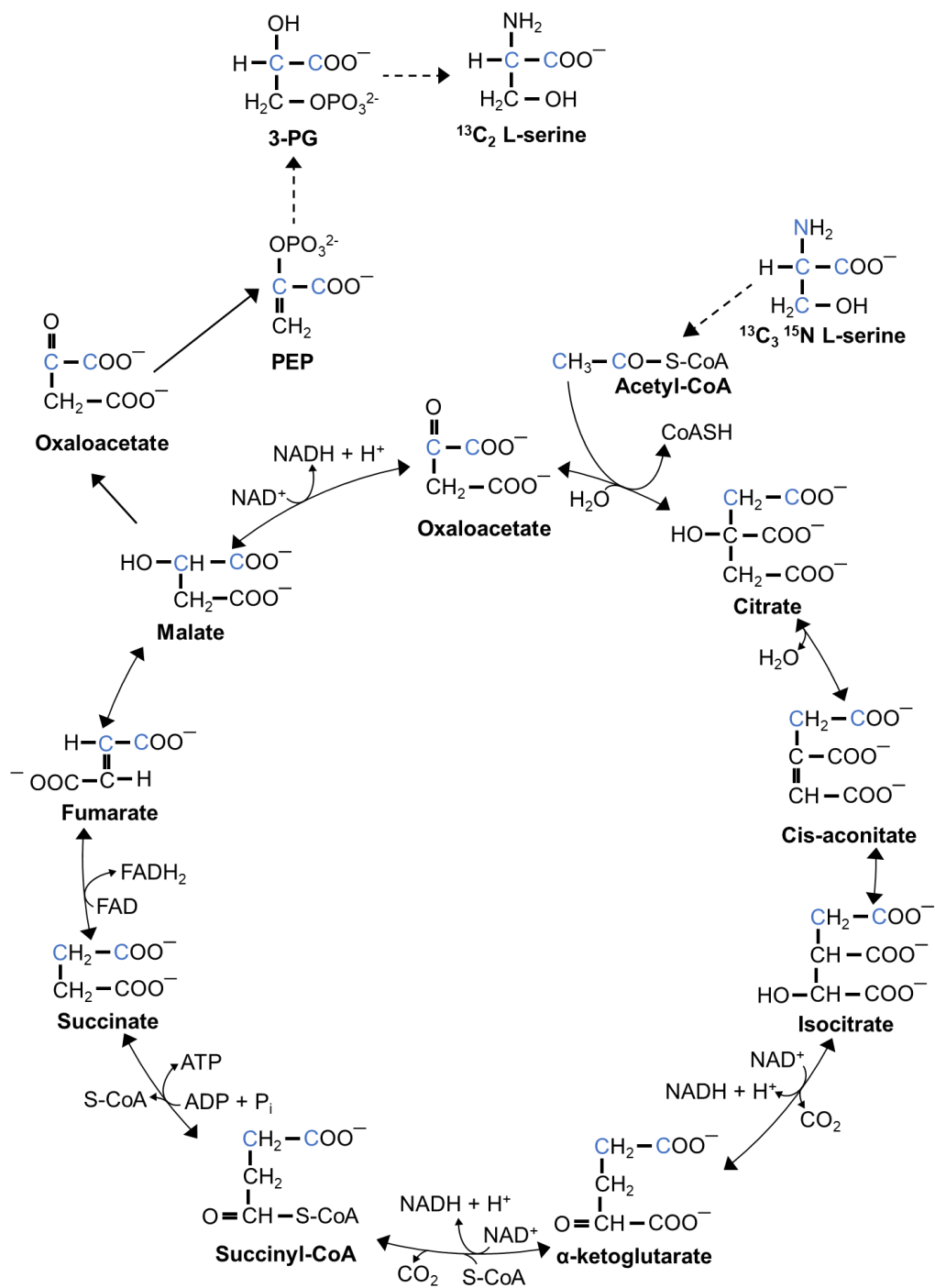


Data accompany **supplementary table S3.3**.

Data are presented as mean \pm SEM in black and individual animals are presented in white for CD and green for HFD ($n = 3-4/\text{timepoint}$). ANOVA for differences across labeling days and post hoc t -test with Bonferroni adjustments # $P < 0.10$, * $P < 0.05$, ** $P < 0.01$, *** $P < 0.001$ versus unlabeled (day 0).

A-B: Liver free serine percent enrichment across labeling days (0, 1, 2, 4, 7, 12) for CD (**A**) and HFD (**B**).

Supplementary Figure S3.6. Metabolic conversion for the generation of a $^{13}\text{C}_2$ labeled serine



Blue indicates a labeled molecule.

SUPPORTING INFORMATION

Hepatic and mitochondrial ceramide kinetics

Justine M. Mucinski¹, Jonas M. McCaffrey¹, R. Scott Rector^{1,2,3}, Takhar Kasumov^{4,5}, Elizabeth J. Parks^{1,2,*}

¹ Department of Nutrition and Exercise Physiology, University of Missouri, Columbia, MO 65212

² Department of Medicine, Division of Gastroenterology and Hepatology, School of Medicine, University of Missouri, Columbia, MO 65212

³ Research Service, Harry S Truman Memorial Veterans Medical Center, Columbia, MO 65201

⁴ Department of Gastroenterology and Hepatology, Cleveland Clinic, Cleveland, OH 44195, USA

⁵ Department of Pharmaceutical Sciences, College of Pharmacy, Northeast Ohio Medical University, Rootstown, OH 44272, USA

***CORRESPONDING AUTHOR:**

Elizabeth J. Parks, PhD

One Hospital Drive School of Medicine NW 406

University of Missouri

Columbia, Missouri 65212

Email: parksej@missouri.edu

RUNNING TITLE: Hepatic and mitochondrial ceramide kinetics

AUTHOR CONTRIBUTION: JMM, EJP, and RSR were involved in study design and methods; JMM and JMM generated the data; TK provided methodology and analysis expertise; JMM analyzed data and wrote the manuscript; All authors contributed to data interpretation and to editing the manuscript.

AUTHOR DISCLOSURES: None.

REFERENCES

1. Hirschberg K, Rodger J, and Futerman AH. The long-chain sphingoid base of sphingolipids is acylated at the cytosolic surface of the endoplasmic reticulum in rat liver. *Biochemical Journal* 290 (Pt 3), 751-757, (1993), PMID:8457204.
2. Mandon EC, Ehses I, Rother J, van Echten G, and Sandhoff K. Subcellular localization and membrane topology of serine palmitoyltransferase, 3-dehydrosphinganine reductase, and sphinganine N-acyltransferase in mouse liver. *Journal of Biological Chemistry* 267, 11144-11148, (1992), PMID:1317856.
3. Han G, Gupta SD, Gable K, Niranjanakumari S, Moitra P, Eichler F, Brown RH, Jr., Harmon JM, and Dunn TM. Identification of small subunits of mammalian serine palmitoyltransferase that confer distinct acyl-CoA substrate specificities. *Proceedings of the National Academy of Sciences of the United States of America* 106, 8186-8191, (2009), PMID:19416851.
4. Venkataraman K, Riebeling C, Bodennec J, Riezman H, Allegood JC, Sullards MC, Merrill AH, Jr., and Futerman AH. Upstream of growth and differentiation factor 1 (uog1), a mammalian homolog of the yeast longevity assurance gene 1 (LAG1), regulates N-stearoyl-sphinganine (C18-(dihydro)ceramide) synthesis in a fumonisin B1-independent manner in mammalian cells. *Journal of Biological Chemistry* 277, 35642-35649, (2002), PMID:12105227.
5. Laviad EL, Albee L, Pankova-Kholmyansky I, Epstein S, Park H, Merrill AH, Jr., and Futerman AH. Characterization of ceramide synthase 2: tissue distribution, substrate specificity, and inhibition by sphingosine 1-phosphate. *Journal of Biological Chemistry* 283, 5677-5684, (2008), PMID:18165233.
6. Mizutani Y, Kihara A, and Igarashi Y. Mammalian Lass6 and its related family members regulate synthesis of specific ceramides. *Biochemical Journal* 390, 263-271, (2005), PMID:15823095.
7. Kitatani K, Idkowiak-Baldys J, and Hannun YA. The sphingolipid salvage pathway in ceramide metabolism and signaling. *Cellular Signalling* 20, 1010-1018, (2008), PMID:18191382.
8. Marchesini N, and Hannun YA. Acid and neutral sphingomyelinases: roles and mechanisms of regulation. *Biochemistry and Cell Biology* 82, 27-44, (2004), PMID:15052326.
9. Bionda C, Portoukalian J, Schmitt D, Rodriguez-Lafrasse C, and Ardail D. Subcellular compartmentalization of ceramide metabolism: MAM (mitochondria-associated membrane) and/or mitochondria? *Biochemical Journal* 382, 527-533, (2004), PMID:15144238.
10. Shimeno H, Soeda S, Sakamoto M, Kouchi T, Kowakame T, and Kihara T. Partial purification and characterization of sphingosine N-acyltransferase (ceramide synthase) from bovine liver mitochondrion-rich fraction. *Lipids* 33, 601-605, (1998), PMID:9655376.

11. Andrieu-Abadie N, Gouaze V, Salvayre R, and Levade T. Ceramide in apoptosis signaling: relationship with oxidative stress. *Free Radical Biology and Medicine* 31, 717-728, (2001), PMID:11557309.
12. Raichur S, Wang S, Chan P, Li Y, Ching J, Chaurasia B, Dogra S, Öhman M, Takeda K, Sugii S, Pewzner-Jung Y, Futerman A, and Summers S. CerS2 haploinsufficiency inhibits β -oxidation and confers susceptibility to diet-induced steatohepatitis and insulin resistance. *Cell Metabolism* 20, 687-695, (2014), PMID:25295789.
13. Turpin SM, Nicholls HT, Willmes DM, Mourier A, Brodesser S, Wunderlich CM, Mauer J, Xu E, Hammerschmidt P, Brönneke HS, Trifunovic A, LoSasso G, Wunderlich FT, Kornfeld J-W, Blüher M, Krönke M, and Brüning JC. Obesity-induced CerS6-dependent C16:0 ceramide production promotes weight gain and glucose intolerance. *Cell Metabolism* 20, 678-686, (2014), PMID:25295788.
14. Hammerschmidt P, Ostkotte D, Nolte H, Gerl MJ, Jais A, Brunner HL, Sprenger HG, Awazawa M, Nicholls HT, Turpin-Nolan SM, Langer T, Kruger M, Brugger B, and Brüning JC. CerS6-derived sphingolipids interact with mff and promote mitochondrial fragmentation in obesity. *Cell* 177, 1536-1552.e1523, (2019), PMID:31150623.
15. Siskind LJ. Mitochondrial ceramide and the induction of apoptosis. *Journal of Bioenergetics and Biomembranes* 37, 143-153, (2005), PMID:16167171.
16. Gudz TI, Tserng KY, and Hoppel CL. Direct inhibition of mitochondrial respiratory chain complex III by cell-permeable ceramide. *Journal of Biological Chemistry* 272, 24154-24158, (1997), PMID:9305864.
17. Di Paola M, Cocco T, and Lorusso M. Ceramide interaction with the respiratory chain of heart mitochondria. *Biochemistry* 39, 6660-6668, (2000), PMID:10828984.
18. Zigdon H, Kogot-Levin A, Park JW, Goldschmidt R, Kelly S, Merrill AH, Jr., Scherz A, Pewzner-Jung Y, Saada A, and Futerman AH. Ablation of ceramide synthase 2 causes chronic oxidative stress due to disruption of the mitochondrial respiratory chain. *Journal of Biological Chemistry* 288, 4947-4956, (2013), PMID:23283968.
19. Chaurasia B, Tippetts TS, Monibas RM, Liu J, Li Y, Wang L, Wilkerson JL, Sweeney CR, Pereira RF, Sumida DH, Maschek JA, Cox JE, Kaddai V, Lancaster GI, Siddique MM, Poss A, Pearson M, Satapati S, Zhou H, McLaren DG, Previs SF, Chen Y, Qian Y, Petrov A, Wu M, Shen X, Yao J, Nunes CN, Howard AD, Wang L, Erion MD, Rutter J, Holland WL, Kelley DE, and Summers SA. Targeting a ceramide double bond improves insulin resistance and hepatic steatosis. *Science* 365, 386-392, (2019), PMID:31273070.
20. Kroesen BJ, Pettus B, Luberto C, Busman M, Sietsma H, de Leij L, and Hannun YA. Induction of apoptosis through B-cell receptor cross-linking occurs via de novo generated C16-ceramide and involves mitochondria. *Journal of Biological Chemistry* 276, 13606-13614, (2001), PMID:11278517.
21. Thomas RL, Jr., Matsko CM, Lotze MT, and Amoscato AA. Mass spectrometric identification of increased C16 ceramide levels during

- apoptosis. *Journal of Biological Chemistry* 274, 30580-30588, (1999), PMID:10521441.
22. Bhatti JS, Bhatti GK, and Reddy PH. Mitochondrial dysfunction and oxidative stress in metabolic disorders - A step towards mitochondria based therapeutic strategies. *Biochimica et Biophysica Acta - Molecular Basis of Disease* 1863, 1066-1077, (2017), PMID:27836629.
 23. Jiang M, Li C, Liu Q, Wang A, and Lei M. Inhibiting ceramide synthesis attenuates hepatic steatosis and fibrosis in rats with non-alcoholic fatty liver disease. *Frontiers in Endocrinology* 10, (2019), PMID:31616384.
 24. Kolak M, Westerbacka J, Velagapudi VR, Wågsäter D, Yetukuri L, Makkonen J, Rissanen A, Häkkinen A-M, Lindell M, Bergholm R, Hamsten A, Eriksson P, Fisher RM, Orešič M, and Yki-Järvinen H. Adipose tissue inflammation and increased ceramide content characterize subjects with high liver fat content independent of obesity. *Diabetes* 56, 1960-1968, (2007), PMID:17620421.
 25. Bergman BC, Brozinick JT, Strauss A, Bacon S, Kerege A, Bui HH, Sanders P, Siddall P, Wei T, Thomas MK, Kuo MS, and Perreault L. Muscle sphingolipids during rest and exercise: a C18:0 signature for insulin resistance in humans. *Diabetologia* 59, 785-798, (2016), PMID:26739815.
 26. Adams JM, Pratipanawatr T, Berria R, Wang E, DeFronzo RA, Sullards MC, and Mandarino LJ. Ceramide content is increased in skeletal muscle from obese insulin-resistant humans. *Diabetes* 53, 25-31, (2004), PMID:14693694.
 27. Haus JM, Kashyap SR, Kasumov T, Zhang R, Kelly KR, DeFronzo RA, and Kirwan JP. Plasma ceramides are elevated in obese subjects with type 2 diabetes and correlate with the severity of insulin resistance. *Diabetes* 58, 337-343, (2009), PMID:19008343.
 28. Apostolopoulou M, Gordillo R, Koliaki C, Gancheva S, Jelenik T, De Filippo E, Herder C, Markgraf D, Jankowiak F, Esposito I, Schlensak M, Scherer PE, and Roden M. Specific hepatic sphingolipids relate to insulin resistance, oxidative stress, and inflammation in nonalcoholic steatohepatitis. *Diabetes Care* 41, 1235-1243, (2018), PMID:29602794.
 29. Luukkonen PK, Sädevirta S, Zhou Y, Kayser B, Ali A, Ahonen L, Lallukka S, Pelloux V, Gaggini M, Jian C, Hakkarainen A, Lundbom N, Gylling H, Salonen A, Orešič M, Hyötyläinen T, Orho-Melander M, Rissanen A, Gastaldelli A, Clément K, Hodson L, and Yki-Järvinen H. Saturated fat is more metabolically harmful for the human liver than unsaturated fat or simple sugars. *Diabetes Care* 41, 1732-1739, (2018), PMID:29844096.
 30. Luukkonen PK, Zhou Y, Sädevirta S, Leivonen M, Arola J, Orešič M, Hyötyläinen T, and Yki-Järvinen H. Hepatic ceramides dissociate steatosis and insulin resistance in patients with non-alcoholic fatty liver disease. *Journal of Hepatology* 64, 1167-1175, (2016), PMID:26780287
 31. Amati F, Dube JJ, Alvarez-Carnero E, Edreira MM, Chomentowski P, Coen PM, Switzer GE, Bickel PE, Stefanovic-Racic M, Toledo FG, and Goodpaster BH. Skeletal muscle triglycerides, diacylglycerols, and ceramides in insulin

- resistance: another paradox in endurance-trained athletes? *Diabetes* 60, 2588-2597, (2011), PMID:21873552.
32. Chathoth S, Ismail MH, Alghamdi HM, Zakaria HM, Hassan KA, Alshomimi S, Vatte C, Cyrus C, Alsaif HS, Mostafa A, Shaaban H, and Al Ali A. Insulin resistance induced by de novo pathway-generated C16-ceramide is associated with type 2 diabetes in an obese population. *Lipids in Health and Disease* 21, 24, (2022), PMID:35184720.
 33. Razak Hady H, Blachnio-Zabielska AU, Szczerbinski L, Zabielski P, Imierska M, Dadan J, and Kretowski AJ. Ceramide content in liver increases along with insulin resistance in obese patients. *Journal of Clinical Medicine* 8, (2019), PMID:31842461.
 34. Kasumov T, Li L, Li M, Gulshan K, Kirwan JP, Liu X, Previs S, Willard B, Smith JD, and McCullough A. Ceramide as a mediator of non-alcoholic fatty liver disease and associated atherosclerosis. *PloS One* 10, e0126910, (2015), PMID:25993337.
 35. Samad F, Hester KD, Yang G, Hannun YA, and Bielawski J. Altered adipose and plasma sphingolipid metabolism in obesity A potential mechanism for cardiovascular and metabolic risk. *Diabetes* 55, 2579-2587, (2006), PMID:16936207.
 36. Tarasov K, Ekroos K, Suoniemi M, Kauhanen D, Sylvanne T, Hurme R, Gouni-Berthold I, Berthold H, Kleber M, Laaksonen R, and Marz W. Molecular lipids identify cardiovascular risk and are efficiently lowered by simvastatin and PCSK9 deficiency. *Journal of Clinical Endocrinology and Metabolism* 99, E45-E52, (2014), PMID:24243630.
 37. Laaksonen R, Ekroos K, Sysi-Aho M, Hilvo M, Vihervaara T, Kauhanen D, Suoniemi M, Hurme R, Marz W, Scharnagl H, Stojakovic T, Vlachopoulou E, Lokki ML, Nieminen MS, Klingenberg R, Matter CM, Hornemann T, Juni P, Rodondi N, Raber L, Windecker S, Gencer B, Pedersen ER, Tell GS, Nygard O, Mach F, Sinisalo J, and Luscher TF. Plasma ceramides predict cardiovascular death in patients with stable coronary artery disease and acute coronary syndromes beyond LDL-cholesterol. *European Heart Journal* 37, 1967-1976, (2016), PMID:27125947.
 38. Hojjati M, Li Z, Zhou H, Tang S, Huan C, Ooi E, Lu S, and Jiang X. Effect of myriocin on plasma sphingolipid metabolism and atherosclerosis in apoE-deficient mice. *Journal of Biological Chemistry* 280, 10284-10289, (2005), PMID:15590644.
 39. Summers SA. Could ceramides become the new cholesterol? *Cell Metabolism* 27, 276-280, (2018), PMID:29307517.
 40. Anroedh S, Hilvo M, Akkerhuis KM, Kauhanen D, Koistinen K, Oemrawsingh R, Serruys P, van Geuns RJ, Boersma E, Laaksonen R, and Kardys I. Plasma concentrations of molecular lipid species predict long-term clinical outcome in coronary artery disease patients. *Journal of Lipid Research* 59, 1729-1737, (2018), PMID:29858423.
 41. Havulinna A, Sysi-Aho M, Hilvo M, Kauhanen D, Hurme R, Ekroos K, Salomaa V, and Laaksonen R. Circulating ceramides predict cardiovascular

- outcomes in the population-based FINRISK 2002 cohort. *Arteriosclerosis, Thrombosis, and Vascular Biology* 36, 2424-2430, (2016), PMID:27765765.
42. Meeusen J, Donato L, Bryant S, Baudhuin L, Berger P, and Jaffe A. Plasma ceramides. *Arteriosclerosis, Thrombosis, and Vascular Biology* 38, 1933-1939, (2018), PMID:29903731.
 43. Petrocelli JJ, McKenzie AI, Mahmassani ZS, Reidy PT, Stoddard GJ, Poss AM, Holland WL, Summers SA, and Drummond MJ. Ceramide biomarkers predictive of cardiovascular disease risk increase in healthy older adults after bed rest. *The Journals of Gerontology: Series A* 75, 1663-1670, (2020), PMID:32215553.
 44. Snider JM, Luberto C, and Hannun YA. Approaches for probing and evaluating mammalian sphingolipid metabolism. *Analytical Biochemistry* 575, 70-86, (2019), PMID:30917945.
 45. Ecker J, and Liebisch G. Application of stable isotopes to investigate the metabolism of fatty acids, glycerophospholipid and sphingolipid species. *Progress in Lipid Research* 54, 14-31, (2014), PMID:24462586.
 46. Chen Y, Berejnaia O, Liu J, Wang S-P, Daurio NA, Yin W, Mayoral R, Petrov A, Kasumov T, Zhang G-F, Previs SF, Kelley DE, and McLaren DG. Quantifying ceramide kinetics in vivo using stable isotope tracers and LC-MS/MS. *American Journal of Physiology-Endocrinology and Metabolism* 315, E416-E424, (2018), PMID:29509438.
 47. Zabielski P, Daniluk J, Hady HR, Markowski AR, Imierska M, Górski J, and Blachnio-Zabielska AU. The effect of high-fat diet and inhibition of ceramide production on insulin action in liver. *Journal of Cellular Physiology*, (2018), PMID:30067865.
 48. Zabielski P, Błachnio-Zabielska AU, Wójcik B, Chabowski A, and Górski J. Effect of plasma free fatty acid supply on the rate of ceramide synthesis in different muscle types in the rat. *PloS One* 12, e0187136, (2017), PMID:29095868.
 49. Noto D, Di Gaudio F, Altieri IG, Cefalu AB, Indelicato S, Fayer F, Spina R, Scrimali C, Giammanco A, Mattina A, Indelicato S, Greco M, Bongiorno D, and Averna M. Automated untargeted stable isotope assisted lipidomics of liver cells on high glucose shows alteration of sphingolipid kinetics. *Biochim Biophys Acta Mol Cell Biol Lipids* 1865, 158656, (2020), PMID:32045699.
 50. Wigger D, Gulbins E, Kleuser B, and Schumacher F. Monitoring the sphingolipid de novo synthesis by stable-isotope labeling and liquid chromatography-mass spectrometry. *Frontiers in Cell and Developmental Biology* 7, 210, (2019), PMID:31632963.
 51. Skotland T, Ekroos K, Kavaliauskiene S, Bergan J, Kauhanen D, Lintonen T, and Sandvig K. Determining the turnover of glycosphingolipid species by stable-isotope tracer lipidomics. *Journal of Molecular Biology* 428, 4856-4866, (2016), PMID:27363608.
 52. Haynes CA, Allegood JC, Wang EW, Kelly SL, Sullards MC, and Merrill AH, Jr. Factors to consider in using [U-¹³C]palmitate for analysis of sphingolipid biosynthesis by tandem mass spectrometry. *Journal of Lipid Research* 52, 1583-1594, (2011), PMID:21586681.

53. Berdyshev EV, Gorshkova I, Skobeleva A, Bittman R, Lu X, Dudek SM, Mirzapioazova T, Garcia JG, and Natarajan V. FTY720 inhibits ceramide synthases and up-regulates dihydrosphingosine 1-phosphate formation in human lung endothelial cells. *Journal of Biological Chemistry* 284, 5467-5477, (2009), PMID:19119142.
54. Berdyshev EV, Gorshkova IA, Usatyuk P, Zhao Y, Saatian B, Hubbard W, and Natarajan V. De novo biosynthesis of dihydrosphingosine-1-phosphate by sphingosine kinase 1 in mammalian cells. *Cellular Signaling* 18, 1779-1792, (2006), PMID:16529909.
55. Tserng KY, and Griffin RL. Ceramide metabolite, not intact ceramide molecule, may be responsible for cellular toxicity. *Biochemical Journal* 380, 715-722, (2004), PMID:14998372.
56. Tserng KY, and Griffin R. Studies of lipid turnover in cells with stable isotope and gas chromatograph-mass spectrometry. *Analytical Biochemistry* 325, 344-353, (2004), PMID:14751270.
57. Snider JM, Snider AJ, Obeid LM, Luberto C, and Hannun YA. Probing de novo sphingolipid metabolism in mammalian cells utilizing mass spectrometry. *Journal of Lipid Research* 59, 1046-1057, (2018), PMID:29610123.
58. Martinez-Montanes F, and Schneiter R. Following the flux of long-chain bases through the sphingolipid pathway in vivo using mass spectrometry. *Journal of Lipid Research* 57, 906-915, (2016), PMID:26977056.
59. Blachnio-Zabielska AU, Persson X-MT, Koutsari C, Zabielski P, and Jensen MD. A liquid chromatography/tandem mass spectrometry method for measuring the in vivo incorporation of plasma free fatty acids into intramyocellular ceramides in humans. *Rapid Communications in Mass Spectrometry* 26, 1134-1140, (2012), PMID:22467464.
60. Chung JO, Koutsari C, Blachnio-Zabielska AU, Hames KC, and Jensen MD. Intramyocellular ceramides: Subcellular concentrations and fractional de novo synthesis in postabsorptive humans. *Diabetes* 66, 2082-2091, (2017), PMID:28483801.
61. Chung JO, Koutsari C, Blachnio-Zabielska AU, Hames KC, and Jensen MD. Effects of meal ingestion on intramyocellular ceramide concentrations and fractional de novo synthesis in humans. *American Journal of Physiology-Endocrinology and Metabolism* 314, E105-E114, (2018), PMID:28970356
62. Ardail D, Popa I, Alcantara K, Pons A, Zanetta JP, Louisot P, Thomas L, and Portoukalian J. Occurrence of ceramides and neutral glycolipids with unusual long-chain base composition in purified rat liver mitochondria. *FEBS Letters* 488, 160-164, (2001), PMID:11163764.
63. Rector RS, Morris EM, Ridenhour S, Meers GM, Hsu F-F, Turk J, and Ibdah JA. Selective hepatic insulin resistance in a murine model heterozygous for a mitochondrial trifunctional protein defect. *Hepatology* 57, 2213-2223, (2013), PMID:23359250.
64. Thyfault JP, Rector RS, Uptergrove GM, Borengasser SJ, Morris EM, Wei Y, Laye MJ, Burant CF, Qi NR, Ridenhour SE, Koch LG, Britton SL, and Ibdah JA. Rats selectively bred for low aerobic capacity have reduced hepatic

- mitochondrial oxidative capacity and susceptibility to hepatic steatosis and injury. *The Journal of Physiology* 587, 1805-1816, (2009), PMID:19237421.
65. Bligh EG, and Dyer WJ. A rapid method of total lipid extraction and purification. *Canadian Journal of Biochemistry and Physiology* 37, 911-917, (1959), PMID:13671378.
 66. Kasumov T, Huang H, Chung Y-M, Zhang R, McCullough AJ, and Kirwan JP. Quantification of ceramide species in biological samples by liquid chromatography electrospray ionization tandem mass spectrometry. *Analytical Biochemistry* 401, 154-161, (2010), PMID:20178771.
 67. Wolfe RR, and Chinkes DL. *Isotope tracers in metabolic research: principles and practice of kinetic analysis*. John Wiley & Sons, 2004.
 68. Li L, Willard B, Rachdaoui N, Kirwan JP, Sadygov RG, Stanley WC, Previs S, McCullough AJ, and Kasumov T. Plasma proteome dynamics: analysis of lipoproteins and acute phase response proteins with $2\text{H}_2\text{O}$ metabolic labeling. *Molecular & Cellular Proteomics* 11, M111 014209, (2012), PMID:22393261.
 69. Rector RS, Thyfault JP, Morris RT, Laye MJ, Borengasser SJ, Booth FW, and Ibdah JA. Daily exercise increases hepatic fatty acid oxidation and prevents steatosis in Otsuka Long-Evans Tokushima Fatty rats. *American Journal of Physiology-Gastrointestinal and Liver Physiology* 294, G619-G626, (2008), PMID:18174272.
 70. Andrikopoulos S, Blair AR, Deluca N, Fam BC, and Proietto J. Evaluating the glucose tolerance test in mice. *American Journal of Physiology-Endocrinology and Metabolism* 295, E1323-1332, (2008), PMID:18812462.
 71. Matthews DR, Hosker JP, Rudenski AS, Naylor BA, Treacher DF, and Turner RC. Homeostasis model assessment: insulin resistance and beta-cell function from fasting plasma glucose and insulin concentrations in man. *Diabetologia* 28, 412-419, (1985), PMID:3899825.
 72. Lemaitre RN, Yu C, Hoofnagle A, Hari N, Jensen PN, Fretts AM, Umans JG, Howard BV, Sitlani CM, Siscovick DS, King IB, Sotoodehnia N, and McKnight B. Circulating Sphingolipids, Insulin, HOMA-IR, and HOMA-B: The Strong Heart Family Study. *Diabetes* 67, 1663-1672, (2018), PMID:29588286.
 73. Neeland IJ, Singh S, McGuire DK, Vega GL, Roddy T, Reilly DF, Castro-Perez J, Kozlitina J, and Scherer PE. Relation of plasma ceramides to visceral adiposity, insulin resistance and the development of type 2 diabetes mellitus: the Dallas Heart Study. *Diabetologia*, (2018).
 74. Xia JY, Holland WL, Kusminski CM, Sun K, Sharma AX, Pearson MJ, Sifuentes AJ, McDonald JG, Gordillo R, and Scherer PE. Targeted induction of ceramide degradation leads to improved systemic metabolism and reduced hepatic steatosis. *Cell Metabolism* 22, 266-278, (2015), PMID:26190650.
 75. Tserng K-Y, and Griffin R. Quantitation and molecular species determination of diacylglycerols, phosphatidylcholines, ceramides, and sphingomyelins with gas chromatography. *Analytical Biochemistry* 323, 84-93, (2003).

76. Zhang Z, Chen L, Liu L, Su X, and Rabinowitz JD. Chemical basis for deuterium labeling of fat and NADPH. *Journal of the American Chemical Society* 139, 14368-14371, (2017), PMID:28911221.
77. Lambert JE, Ramos-Roman MA, Browning JD, and Parks EJ. Increased de novo lipogenesis is a distinct characteristic of individuals with nonalcoholic fatty liver disease. *Gastroenterology* 146, 726-735, (2014), PMID:24316260.
78. Busch R, Kim YK, Neese RA, Schade-Serin V, Collins M, Awada M, Gardner JL, Beysen C, Marino ME, Misell LM, and Hellerstein MK. Measurement of protein turnover rates by heavy water labeling of nonessential amino acids. *Biochimica et Biophysica Acta* 1760, 730-744, (2006), PMID:16567052.
79. Lee WN, Bassilian S, Guo Z, Schoeller D, Edmond J, Bergner EA, and Byerley LO. Measurement of fractional lipid synthesis using deuterated water ($2H_2O$) and mass isotopomer analysis. *American Journal of Physiology* 266, E372-383, (1994), PMID:8166257.
80. Lee WN, Bergner EA, and Guo ZK. Mass isotopomer pattern and precursor-product relationship. *Biological Mass Spectrometry* 21, 114-122, (1992), PMID:1606182.
81. Donnelly KL, Margosian MR, Sheth SS, Lusic AJ, and Parks EJ. Increased lipogenesis and fatty acid reesterification contribute to hepatic triacylglycerol stores in hyperlipidemic Txnip^{-/-} mice. *The Journal of Nutrition* 134, 1475-1480, (2004), PMID:15173414.
82. Gabert L, Vors C, Louche-Pélissier C, Sauvinet V, Lambert-Porcheron S, Draï J, Laville M, Désage M, and Michalski MC. ^{13}C tracer recovery in human stools after digestion of a fat-rich meal labelled with [1,1,1- $^{13}C_3$]tripalmitin and [1,1,1- $^{13}C_3$]triolein. *Rapid Communications in Mass Spectrometry* 25, 2697-2703, (2011), PMID:21913246.
83. Zabielski P, Hady HR, Chacinska M, Roszczyc K, Gorski J, and Blachnio-Zabielska AU. The effect of high fat diet and metformin treatment on liver lipids accumulation and their impact on insulin action. *Scientific Reports* 8, 7249, (2018), PMID:29739997.
84. Gregory JF, 3rd, Cuskelly GJ, Shane B, Toth JP, Baumgartner TG, and Stacpoole PW. Primed, constant infusion with [2H_3]serine allows in vivo kinetic measurement of serine turnover, homocysteine remethylation, and transsulfuration processes in human one-carbon metabolism. *American Journal of Clinical Nutrition* 72, 1535-1541, (2000), PMID:11101483.
85. Birbes H, Luberto C, Hsu YT, El Bawab S, Hannun YA, and Obeid LM. A mitochondrial pool of sphingomyelin is involved in TNF α -induced Bax translocation to mitochondria. *Biochemical Journal* 386, 445-451, (2005), PMID:15516208.
86. Dai Q, Liu J, Chen J, Durrant D, McIntyre TM, and Lee RM. Mitochondrial ceramide increases in UV-irradiated HeLa cells and is mainly derived from hydrolysis of sphingomyelin. *Oncogene* 23, 3650-3658, (2004), PMID:15077187.
87. Abou-Ghali M, and Stiban J. Regulation of ceramide channel formation and disassembly: Insights on the initiation of apoptosis. *Saudi Journal of Biological Sciences* 22, 760-772, (2015), PMID:26587005.

88. Colombini M. Ceramide channels and their role in mitochondria-mediated apoptosis. *Biochimica et Biophysica Acta (BBA) - Bioenergetics* 1797, 1239-1244, (2010), PMID:20100454.
89. Colombini M. Ceramide channels and mitochondrial outer membrane permeability. *Journal of Bioenergetics and Biomembranes* 49, 57-64, (2017), PMID:26801188.
90. Young PA, Senkal CE, Suchanek AL, Grevengoed TJ, Lin DD, Zhao L, Crunk AE, Klett EL, Füllekrug J, Obeid LM, and Coleman RA. Long-chain acyl-CoA synthetase 1 interacts with key proteins that activate and direct fatty acids into niche hepatic pathways. *Journal of Biological Chemistry* 293, 16724-16740, (2018), PMID:30190326.
91. Westerbacka J, Lammi K, Häkkinen A-M, Rissanen A, Salminen I, Aro A, and Yki-Järvinen H. Dietary fat content modifies liver fat in overweight nondiabetic subjects. *The Journal of Clinical Endocrinology & Metabolism* 90, 2804-2809, (2005), PMID:15741262.
92. Tamura Y, Tanaka Y, Sato F, Choi JB, Watada H, Niwa M, Kinoshita J, Ooka A, Kumashiro N, Igarashi Y, Kyogoku S, Maehara T, Kawasumi M, Hirose T, and Kawamori R. Effects of diet and exercise on muscle and liver intracellular lipid contents and insulin sensitivity in type 2 diabetic patients. *The Journal of Clinical Endocrinology & Metabolism* 90, 3191-3196, (2005), PMID:15769987.
93. Cusi K. Role of obesity and lipotoxicity in the development of nonalcoholic steatohepatitis: Pathophysiology and clinical implications. *Gastroenterology* 142, 711-725.e716, (2012), PMID:22326434.
94. Nakamura A, and Terauchi Y. Lessons from mouse models of high-fat diet-induced NAFLD. *International Journal of Molecular Sciences* 14, 21240-21257, (2013), PMID:24284392.
95. Rector RS, Thyfault JP, Uptergrove GM, Morris EM, Naples SP, Borengasser SJ, Mikus CR, Laye MJ, Laughlin MH, Booth FW, and Ibdah JA. Mitochondrial dysfunction precedes insulin resistance and hepatic steatosis and contributes to the natural history of non-alcoholic fatty liver disease in an obese rodent model. *Journal of Hepatology* 52, 727-736, (2010), PMID:20347174.
96. Holland WL, Brozinick JT, Wang LP, Hawkins ED, Sargent KM, Liu Y, Narra K, Hoehn KL, Knotts TA, Siesky A, Nelson DH, Karathanasis SK, Fontenot GK, Birnbaum MJ, and Summers SA. Inhibition of ceramide synthesis ameliorates glucocorticoid-, saturated-fat-, and obesity-induced insulin resistance. *Cell Metabolism* 5, 167-179, (2007), PMID:17339025.
97. Siow DL, and Wattenberg BW. Mammalian ORMDL proteins mediate the feedback response in ceramide biosynthesis. *Journal of Biological Chemistry* 287, 40198-40204, (2012), PMID:23066021.
98. Longato L, Tong M, Wands JR, and de la Monte SM. High fat diet induced hepatic steatosis and insulin resistance: Role of dysregulated ceramide metabolism. *Hepatology Research* 42, 412-427, (2012), PMID:22176347.
99. Montgomery MK, Brown SHJ, Lim XY, Fiveash CE, Osborne B, Bentley NL, Braude JP, Mitchell TW, Coster ACF, Don AS, Cooney GJ, Schmitz-Peiffer

- C, and Turner N. Regulation of glucose homeostasis and insulin action by ceramide acyl-chain length: A beneficial role for very long-chain sphingolipid species. *Biochimica et Biophysica Acta (BBA) - Molecular and Cell Biology of Lipids* 1861, 1828-1839, (2016), PMID:27591968.
100. Kim YR, Lee EJ, Shin KO, Kim MH, Pewzner-Jung Y, Lee YM, Park JW, Futerman AH, and Park WJ. Hepatic triglyceride accumulation via endoplasmic reticulum stress-induced SREBP-1 activation is regulated by ceramide synthases. *Experimental and Molecular Medicine* 51, 1-16, (2019), PMID:31676768.
101. Apostolopoulou M, Gordillo R, Gancheva S, Strassburger K, Herder C, Esposito I, Schlensak M, Scherer PE, and Roden M. Role of ceramide-to-dihydroceramide ratios for insulin resistance and non-alcoholic fatty liver disease in humans. *BMJ Open Diabetes Research & Care* 8, (2020), PMID:33219119.
102. Iqbal J, Walsh MT, Hammad SM, Cuchel M, Tarugi P, Hegele RA, Davidson NO, Rader DJ, Klein RL, and Hussain MM. Microsomal triglyceride transfer protein transfers and determines plasma concentrations of ceramide and sphingomyelin but not glycosylceramide. *Journal of Biological Chemistry* 290, 25863-25875, (2015), PMID:26350457.
103. Lee YS, Li P, Huh JY, Hwang IJ, Lu M, Kim JI, Ham M, Talukdar S, Chen A, Lu WJ, Bandyopadhyay GK, Schwendener R, Olefsky J, and Kim JB. Inflammation is necessary for long-term but not short-term high-fat diet-induced insulin resistance. *Diabetes* 60, 2474-2483, (2011), PMID:21911747.

CHAPTER IV – Histological improvements from increased peripheral substrate disposal: Muscle glucose uptake spares the liver

ABSTRACT

Nonalcoholic fatty liver disease (NAFLD) and nonalcoholic steatohepatitis (NASH) are characterized by multi-tissue insulin resistance and elevations in hepatic lipogenesis. The present study tested the effects of lifestyle intervention (9 months, energy restriction, high intensity interval training) or standard care on histologic regression, glucose utilization (production, EGP and disposal R_d), and lipid metabolism in twenty six patients (mean \pm SD; treatment: $n = 18$, age 47 ± 10 y, BMI 40.2 ± 7.7 kg/m²; standard care: $n = 8$, age 47 ± 10 y, BMI 37.3 ± 7.2 kg/m²) with biopsy-proven NASH (NAFLD activity score, NAS ranging from 1-8; treatment: 5.4 ± 1.1 and standard care: 5.4 ± 1.1). Subjects underwent measurements of insulin sensitivity via two-step, labeled (¹³C₆ glucose) hyperinsulinemic-euglycemic clamps, hepatic DNL using D₂O, and sources of triglycerides (TG) contained within very low-density lipoproteins (VLDL-TG) with palmitate isotopes. Nineteen ($n = 14$ treatment, $n = 5$ standard care) subjects completed follow-up testing and had significant reductions in body weight ($P = 0.001$), liver fat ($P < 0.001$), and plasma glucose ($P = 0.034$). Despite similar reductions in BW, steatosis, and blood biochemistries across all subjects, only treatment subjects reduced total NAS ($P < 0.001$) and the components lobular inflammation ($P = 0.035$) and hepatocellular ballooning ($P < 0.001$). Improved liver histology was negatively related to improvements in VO₂ peak ($r = -0.514$, $P = 0.029$) which tended to increase with treatment ($P = 0.059$). Absolute changes in NAS were associated with EGP ($r = -0.524$, $P = 0.021$) and R_d ($r = -0.654$, $P = 0.002$). Further, absolute change in lobular inflammation and EGP ($r = -0.507$, P

= 0.027) and change in hepatocellular ballooning and R_d ($r = -0.625$, $P = 0.004$) were negatively related. These data demonstrate improvements in liver health may be driven by enhancing peripheral insulin sensitivity through the combined effect of weight loss and exercise. Fasting VLDL-TG DNL was reduced in both groups (treatment: 33% and standard care: 24%) and related to the change in glucose disposal ($r = -0.819$, $P = 0.007$). With specific regard for exercise, the rerouting of substrates away from the liver may reduce nutrient toxicity and contribute to improvements in NASH.

INTRODUCTION

Nonalcoholic fatty liver disease (NAFLD) is the leading cause of liver disease in the U.S. (1-4) and affects nearly 30% of the worldwide population (5-7). NAFLD and the more advanced form, nonalcoholic steatohepatitis (NASH), are closely associated with obesity, type 2 diabetes (T2D), and insulin resistance (8-13) and increase the risk for cardiovascular and all-cause mortality (14). However, the metabolic mechanisms that contribute to the progression and regression of this disease are not well established. Specifically, the interaction of insulin resistance, histological regression, and lipid metabolism in a setting of NASH treatment remains ambiguous.

With no approved pharmacological therapies for the treatment of NAFLD or NASH, the current guidelines recommend weight loss (5-10%) through lifestyle modifications including increased physical activity and reduced energy intake (15-19). Many studies have investigated the impact of exercise (20-37), energy restriction (38-58), or combination lifestyle programs (57-88) on liver health. The greatest metabolic and hepatic improvements are reported in studies with comprehensive lifestyle modifications that meet the current dietary and activity guidelines (15-19) and occur over 6-12 months (78-88). In general, these studies have demonstrated improvements in biochemical (transaminases) and metabolic (glucose, insulin, homeostatic model of insulin resistance [HOMA-IR], oral glucose tolerance test [OGTT], and hyperinsulinemic-euglycemic clamp) parameters, reductions in intrahepatic triglyceride (IHTG) as assessed by

noninvasive imaging techniques (e.g., magnetic resonance spectroscopy or imaging [MRS, MRI], ultrasonography, transient elastography) and, less often, improved histology in paired biopsy analyses (56, 72, 76, 88-92). While non-invasive imaging methods to measure IHTG are often used in the early detection of liver steatosis, they can be problematic in treatment studies as they are poor predictors of histological parameters outside of steatosis (93). Currently, minimal evidence exists on the histologic regression of NASH with treatment and even less is known regarding the in vivo metabolic mechanisms driving histologic improvements.

A key event in the pathogenesis of NAFLD is the loss of adipose tissue insulin sensitivity (94, 95) which results in an overflow of lipid to the liver (96, 97), where ~25% of fatty acids are removed from circulation (98-100). With chronic overnutrition (77, 101-104), the excess flow of fatty acids to the liver from adipose (60%) and dietary (15%) sources and the de novo production of fatty acids from carbohydrates (26%, de novo lipogenesis, DNL) (97) begins to overload the oxidative, storage, and secretory capacity of the organ, resulting in an accumulation of ectopic, hepatic lipid (9, 105-107). At the same time, elevations in circulating fatty acids impact insulin's ability to suppress endogenous glucose production (EGP) (108-114) via gluconeogenesis and glycogenolysis (115). Paradoxically, insulin simultaneously maintains hepatic stimulation of the master transcription factor, sterol regulatory element binding protein 1c (SREBP-1c), to enhance DNL and TG synthesis (116-118). This

process creates more substrate to fuel very low-density lipoprotein (VLDL) assembly and secretion which ultimately contributes to greater systemic insulin resistance (119-121). The transition of steatosis to NASH is characterized by adipose, hepatic, and skeletal muscle insulin resistance (9, 13, 105), however no study has characterized the interaction between histologic regression of liver disease with paired biopsies and changes in insulin sensitivity and lipid metabolism in individuals with NASH.

We tested the effects of weight loss through a nine-month intensive lifestyle program (energy restriction and supervised high intensity interval training, HIIT), on changes in liver histology, insulin sensitivity (EGP and glucose disposal, R_d), and measures of lipid metabolism (circadian NEFA patterns, DNL, TG-rich lipoprotein (TRL)-TG sources, plasma ceramides). For the first time, the present study provides evidence that relieving the liver of excess nutrient burden through routing of substrates towards the periphery, spares the liver and may promote the regression of advanced NASH. The findings provide strong support for therapies aimed at reducing hepatic burden of nutrient overload as a means to prevent and treat NAFLD spectrum of liver disease.

METHODS

Experimental design

The study was approved by the University of Missouri (MU) Health Sciences Institutional Review Board (Protocol # 2008258) and registered under ClinicalTrials.gov # NCT03151798. All subjects provided written informed consent and the study was conducted according to the principles expressed in the Declaration of Helsinki. This study consisted of two phases. In the first phase, we recruited adult patients who were overweight and obese and scheduled for a diagnostic liver biopsy due to suspected liver disease at MU liver health clinic. Following informed consent, a small section of liver tissue collected during the biopsy procedure was graded histologically by a blinded pathologist, according to the Brunt criteria (122). Patients with a NAFLD activity score (NAS) $\geq 4/8$ and who met the inclusion criteria (**table 4.1**) were recruited to participate in the second phase of the study – a diet and exercise lifestyle intervention. Phase two subjects were randomized to a lifestyle intervention or standard of care group and provided informed consent prior to beginning the nine-month treatment phase. All phase two subjects underwent an MRI/MRS liver scan to measure liver fat content, an exercise tolerance test (VO_2 peak), DEXA for body composition, and 24h inpatient metabolic testing including lipid metabolism measurements and a two-step hyperinsulinemic-euglycemic clamp. The same series of tests were repeated after 10.1 ± 1.1 months in addition to a follow-up liver biopsy. **Figure 4.1** shows the overall study design.

Recruitment

Individuals undergoing a diagnostic liver biopsy for suspicion of NAFLD were recruited for phase one. From phase one subjects, those with histological confirmation of advanced NASH (NAS $\geq 4/8$) and who met the other inclusion criteria (**table 4.1**) were recruited for phase two. **Figure 4.2** presents the Consort diagram for both phases. A total of 102 subjects were screened from phase one and 28 were recruited and provided informed consent for phase two. The treatment and standard care arms included 20 and eight subjects, respectively, although four treatment subjects were lost to follow-up.

Phase one - Liver biopsy and blood draw

The liver biopsy procedure was performed at the MU Hospital in an outpatient setting by a trained hepatologist on the research team. A total of six needle passes were made to obtain liver tissue (~50 mg) and a portion of the research sample was transported to pathology where the tissue was stained with hematoxylin and eosin (H&E), Masson's trichrome, reticulum, and iron stains for NASH scoring according to the NASH Clinical Network Scoring System (122). The same pathologist scored each liver biopsy (A.D-A) and was blinded to subject and visit. The pathologist graded the level of steatosis (0-3), lobular inflammation (0-3), and hepatocellular ballooning (0-2) which are components of the NAS (0-8). The biopsy was also graded for level of fibrosis (0-4). Immediately prior to the biopsy, a fasting blood draw was collected to measure plasma glucose, glycosylated hemoglobin (HbA1c), total cholesterol, low density

lipoprotein cholesterol (LDL), high density lipoprotein cholesterol (HDL), and TG, in addition to the liver enzymes alanine aminotransferase (ALT) and aspartate aminotransferase (AST). These assays were processed by a CLIA certified laboratory using standardized procedures and methods (#26D0652092, Quest Diagnostics, St. Louis, MO).

Phase two – Treatment and standard care groups

Following confirmation of NASH and consent to participate in the program, subjects were randomized to active treatment or standard of care (note: the first four subjects were automatically placed into the treatment group). Both groups completed baseline and follow-up testing which included an exercise tolerance test (ETT), anthropometrics, MRI/MRS, and a 24-h inpatient visit including a meal tolerance test (MTT), lipid kinetics measurements, and a two-step hyperinsulinemic-euglycemic clamp. All subjects also returned for an interim visit which was completed in the fifth month of the program to reassess fitness levels, body composition, and blood biochemistries (**figure 4.1**). *Treatment –* Participants randomized to the treatment group participated in both dietary counseling sessions and a supervised HIIT program, described below. *Standard Care –* Subjects were offered a single session with the study dietitian at the start of the program where the dietitian provided weight loss education and encouraged increasing physical activity according to the physical activity guidelines for adults (123). Standard care participants met with study staff again

for interim and follow-up visits and otherwise receive standard medical care as directed by their physician.

Exercise tolerance test, training, and physical activity

All subjects completed a modified Bruce ETT to measure maximal cardiorespiratory capacity at baseline, interim, and follow-up visits. The data were used to determine maximal heart rate and changes in fitness status. The tests were performed on a treadmill or cycle ergometer with simultaneous gas analysis (TrueOne® 2400, Parvo Medics) and a 12-lead electrocardiogram (ECG), as described previously (124). Resting heart rate (Polar USA) and blood pressure (Welch Allyn) were recorded throughout the exercise test. Treatment subjects participated in weekly supervised HIIT sessions which consisted of four, four-minute intervals at 90-95% heart rate max separated by three-minute active pauses at ~50% heart rate max. The heart rate targets were based on the results of individual ETTs at baseline and adjusted at interim. All training sessions were completed on a treadmill, cycle ergometer, or elliptical and intensity was monitored using heart rate monitors (Polar USA). Physical activity was tracked throughout the program using Fitbit® activity trackers.

Dietary counseling and energy intake

Three-day dietary recalls were completed approximately two weeks before baseline, interim, and follow-up visits and the results were used to design three-day prepared food packs provided to each subject before the visits to ensure

weight stability. Dietary recalls were analyzed using Nutrition Data System for Research (NDSR) analysis software. Subjects in the treatment group met with the research dietitian weekly for the first two months, biweekly for months three to five, and monthly for months six to nine (and beyond). Based on current treatment guidelines, the dietitian provided personalized nutrition education with the goal of a 12% weight loss (~500 kcal/day deficit) over the 36-week intervention period (15-17). Emphasis was placed on decreasing sugar intake (<5% of energy, %E) and consuming adequate protein (one g/kg/d) to reduce muscle mass loss. Prior to the final visit, the subjects met with the dietitian to ensure weight stability was achieved for the final metabolic testing and liver biopsy.

Anthropometrics and liver fat by MRI/MRS

Body composition was measured using a Hologic A, S/N 100158 dual x-ray absorptiometry scanner (DEXA, analysis Version 13.5.2, auto whole-body ran beam). Body weight was measured on a digital scale to the nearest 0.1 kg and height was measured using a stadiometer to the nearest 0.1 cm. Subjects underwent an MRI/MRS liver scan to measure liver fat content at baseline and follow-up. Using standardized techniques, localized ¹H-MRS spectra of the liver was acquired with subjects in the supine position using a Phillips 3T Siemens Trio Scanner. IDEAL sequence analysis was used to calculate hepatic proton density fat fraction (125).

Metabolic testing

Baseline and follow-up study visits occurred over two days in the Clinical Research Center (CRC) in the MU Hospital. Upon arrival, subjects were admitted and immediately escorted to radiology for their MRI/MRS liver scan. Following the liver scan, two anterograde intravenous (IV) catheters were placed in contralateral antecubital regions – one for blood drawing and one for isotope infusions. For female subjects, a blood pregnancy test was completed.

Lipid metabolism: As described previously (96, 97, 126), multiple stable isotopes were used to track labeled methyl-palmitate isotopomers (M0, M1, M2, M4/16, M30, and M31) in TRL and free fatty acids (FFA) fractions using gas chromatography mass spectrometry (GC/MS). The FFA sources (dietary, adipose, and DNL) that contribute to hepatic TG synthesis were each labeled with a different isotope (palmitate and D₂O) and expressed as both an absolute concentration (mg/dL) and proportion (%) of the total labeled pool, reflecting intracellular hepatic TG synthesis (96). Despite an extended labeling period, a portion of the VLDL pool will remain unlabeled due to use of intrahepatic stores. Absolute concentration of plasma FFA sources were also calculated, as described previously (96). These sources include adipose tissue, the key contributor to fasting FFA concentrations, and dietary fatty acids, which arise from chylomicrons undergoing peripheral lipolysis via lipoprotein lipase (i.e., spillover pathway) (96, 126, 127). Lipoprotein isolation and enrichment analysis: Within 24h of the study, TRL were isolated via fixed-angle ultracentrifugation at 40,000 rpm for 20h at 15°C in a 50.3Ti rotor (Beckman Instruments). The TRL

and FFA fractions were extracted, underwent thin layer chromatography for TG and FFA separation, and were re-esterified into fatty acid methyl esters (FAME) for GC/MS analysis, as described previously (126). FAME enrichments (d_{31} and $^{13}C_4/^{13}C_{16}$) were quantified using six-point standard curves (96, 97, 126).

Dietary: Subjects consumed a high fat dinner (46% energy, E from fat, 35%E carbohydrates, 19%E protein) containing d_{31} -tripalmitin (dietary fat label added to provide a ~10% enrichment of the unlabeled palmitic acid contained in the dinner). Blood was drawn throughout the evening/night as shown in **figure 4.3** and d_{30} and d_{31} enrichment was analyzed as described above and in extended methodology. Adipose: An infusion of labeled palmitic acid ($^{13}C_4$ or $^{13}C_{16}$; 10 μ g/kg/min), complexed with human albumin was used to calculate the absolute and relative adipose fatty acid contributions to the TRL-TG and plasma NEFA pools from midnight to 8AM. DNL: For two weeks prior to the inpatient testing, subjects consumed labeled water, D_2O (150 mL for the first three days, 100 mL for the remaining 10-12 days). Body water enrichment levels were measured before (unlabeled), during, and at the end of the labeling period (~day 15, inpatient visit) in urine or plasma by Metabolic Solutions (Nashua, NH). Deuterium can be incorporated into newly-made fatty acids (96, 128) which allows for the calculation of DNL by mass isotopomer distribution analysis (MIDA) (129, 130) based on the isotopomer pattern (M0, M1, M2) of the product (16:0 FAME).

Hyperinsulinemic-euglycemic clamp – Following the overnight fast, a third retrograde catheter was placed in a hand vein which was kept in a heated hand box at 45°C to “arterialize” venous blood (131). A primed, continuous infusion of $^{13}\text{C}_6$ glucose began at 6AM for fasting measurements of EGP and R_d (4.1 mg/kg/min over one min, followed by 40 $\mu\text{g}/\text{kg}/\text{min}$). Following a two hour basal period, a four-hour, two-step hyperinsulinemic-euglycemic clamp was initiated to measure EGP, NEFA suppression, and stimulation of peripheral glucose disposal (R_d). Insulin (Humulin-R, Eli Lilly, Indianapolis, IN) was infused at seven mU/m²/min for the first two hours and 50 mU/m²/minute for the final two hours. Plasma glucose concentrations were held constant at the subject’s fasting level (analyzed by YSI Model 2300-D Stat Plus; Yellow Springs, OH) by a variable rate infusion of a $^{13}\text{C}_6$ -glucose labeled, 20% dextrose (wt/vol.) solution adjusted every five minutes using the negative feedback principle described by DeFronzo et al (132). Plasma glucose enrichments were measured by GC/MS using a nine-point standard curve – see extended methodology section for greater detail (133). Fasted and insulin-stimulated measurements of resting metabolic rates were collected during the clamp to quantify substrate oxidation and energy expenditure. Following conclusion of the clamp procedure, subjects consumed a full meal and walked for ~15 minutes to promote contraction-stimulated glucose disposal. Once normoglycemia was confirmed, IV lines were removed, and the subject was discharged. To promote a successful transition into the program, all subjects were provided two weeks of a prepared healthy diet and treatment

participants began their exercise training and dietary counseling. The same series of tests were repeated at follow-up.

CER concentrations

Baseline and follow-up plasma CERs were quantified as previously described (134, 135). Briefly, 100 μ L of plasma was spiked with 50 μ L of C18:1/17:0 (50 ng – non-naturally occurring CER internal standard) and then extracted according to the protocol of Bligh and Dyer (136). The organic phase was removed and dried under nitrogen gas. An azeotropic agent (methylene chloride) was used to remove any additional water and samples were stored in -80°C until analysis. CERs were quantified using high performance liquid chromatography tandem mass spectrometry (HPLC-MS/MS) electrospray ionization (ESI) in positive ion mode. Standards and samples were dissolved in 100 μ L of 0.1% formic acid solution in methanol-water (85:15) and then injected into a Waters HPLC device (2690 Separation Module, Milford, MA) and separated through a Vydac[®] 200MS[™] C8 column (2.1 x 100 mm, 5 μ m, P.J.Cobert Associates, St. Louis, MO). CERs were analyzed using multiple reaction monitoring (MRM) that scans each molecular ion with the combination of mass to charge ratio (m/z) 264 daughter ion across all species on a Thermo Scientific TSQ (Triple-Stage Quadrupole) Quantiva mass spectrometer. Chromatograms were analyzed using Xcalibur[™] (Thermo Scientific[™] 3.0.63). Methodology details, individual CER species, and MRM transitions are listed in the extended methodology section.

Statistical analysis and calculations

Calculations were performed using Microsoft Excel (2016, Redmond, WA) and statistical analysis using R (version 4.1.3), and R studio (Boston, MA). Area under the curve (AUC) for plasma metabolites were calculated according to the trapezoidal rule (137). Glucose appearance and disposal were calculated using standard dilution equations according to Steele's non-steady state equation (133, 138). Suppression of EGP and NEFA were calculated as the difference between basal and step one or two over the basal value for EGP or NEFA concentrations, respectively. Mean differences between treatment and standard care groups were compared across time by mixed model analysis of variance (ANOVA, ez and rstatix packages in R studio) with group (treatment or standard care) as a between-subjects factor and visit (baseline [BL], interim [INT], follow-up [FU]) as a within-subjects factor. When 18-hour concentration data was compared, the same mixed model ANOVA was used with time as an additional within-subjects factor. For any significant interactions, post-hoc analysis with Bonferroni corrections were complete with orthogonal contrast set to compare baseline with interim and baseline with follow-up values. Spearman's rho correlation was used to assess linear relationships between ranked (i.e., NAS, NAS components, and fibrosis scoring) and continuous variables while Pearson's R was used to quantify linear relationships between continuous variables. Unpaired *t*-tests were used when comparing changes in insulin sensitivity within a step (basal, step one, step two) between treatment and control subjects. Data varying across time

were reported as mean \pm standard error (SEM) while static variables (i.e., phase one subject characteristics) were reported as a mean \pm standard deviation (SD). Significance was set at $P < 0.05$, and $P < 0.10$ reported as a trend.

RESULTS

Subject characteristics

Phase one subjects were recruited based on suspicion of NAFLD and accordingly, these subjects on average had elevated liver enzymes (ALT and AST) and histological evidence of NASH (**table 4.2**). Approximately half had clinical diagnoses of T2D, hypertension, and more than half were hyperlipidemic. Phase two participants were recruited from the phase one subjects with NAS $\geq 4/8$, and baseline subject characteristics for the treatment and standard care groups are shown in **table 4.3**. The groups had similar age, weight, and body composition. All subjects had metabolic syndrome and elevated liver enzymes, liver fat, and histological diagnosis of NASH. Standard care participants had higher baseline liver steatosis as determined by both MRS ($P = 0.029$) and histology ($P = 0.047$) than treatment subjects. Approximately 70% of the phase two subjects were clinically diagnosed as having T2D, which was pharmacologically controlled with various glucose lowering medications (**table 4.3**). A total of 14 subjects completed the exercise and dietary intervention (treatment) and five subjects continued with standard care for the same length of time (10.1 ± 1.1 months). All 19 subjects underwent follow-up metabolic testing and a second liver biopsy.

Histologic resolution of NASH

Treatment subjects had a significant reduction in NAS (**figure 4.4A**, $P < 0.001$) with an average decrease of 2.4 ± 0.5 points at follow-up ($-43 \pm 9\%$). The

components of NAS, lobular inflammation (**figure 4.4C**, $-32 \pm 19\%$, $P = 0.035$) and hepatocellular ballooning (**figure 4.4D**, $-75 \pm 10\%$, $P < 0.001$), were also significantly reduced in the treatment group. Steatosis, graded histologically and measured via MRS, decreased in both treatment (**figure 4.4B**, histology: $-26 \pm 11\%$; **figure 4.4F**, MRS: $-39 \pm 2\%$) and standard care (histology: $13 \pm 8\%$; MRS: $28 \pm 7\%$) subjects (histology: $P = 0.031$ and MRS: $P < 0.001$ for main effect of visit). Despite the average 0.4 ± 0.2 point reduction in steatosis, the standard care subjects demonstrated no change in the overall NAS ($+0.2 \pm 0.5$ points) or the components, lobular inflammation ($+0.4 \pm 0.2$ points) and hepatocellular ballooning ($+0.2 \pm 0.4$ points) at follow-up testing. Fibrosis was significantly reduced in the treatment subjects with an average reduction of $45 \pm 15\%$ (**figure 4.4E**, $P = 0.044$). Alternatively, standard care subjects increased average fibrosis scores by 0.8 ± 0.6 points, but this change was not significant (**figure 4.4E**, $13 \pm 13\%$, $P = 0.242$). The almost one-point increase in fibrosis was surprising as previous studies tracking the natural progression of fibrosis demonstrated individuals with NASH progress one stage of fibrosis approximately every seven years (139, 140). Representative histology slides from a single treatment and standard care subject are shown in **figure 4.4G-H**. The NAS was graded using the H&E stained slides and the fibrosis was graded using the trichrome.

Anthropometrics

The treatment group lost an average of $8 \pm 2\%$ of their body weight (**figure 4.5A**, 10.0 ± 2.2 kg) and BMI was reduced by $7 \pm 2\%$ (data not shown, -3.1 ± 0.8 kg/m²). Fat free mass was reduced 2.4 ± 1.3 kg (**figure 4.5B**, $-3 \pm 2\%$) and fat mass 5.6 ± 1.8 kg (**figure 4.5C**, $-9 \pm 3\%$). Losses in fat free mass accounted for 20% of the total weight loss in the treatment subjects. The standard care group also demonstrated reductions in total body weight (-5.9 ± 3.7 kg, $-4 \pm 3\%$) and BMI (data not shown, -1.6 ± 1.4 kg/m², $-3 \pm 4\%$), however, 63% of this weight loss was accounted for by losses in fat free mass (**figure 4.5B**, -3.7 ± 2.1 kg, $-5 \pm 2\%$) while average fat loss was 1.4 ± 2.0 kg ($-2 \pm 4\%$). **Supplementary figure S4.1** presents the body weight losses over time for both groups.

Groups were analyzed together to determine if changes in body composition were related to changes in liver histology. For all correlation analyses, treatment subjects are presented with a filled green circle and standard care subjects with a white circle. Standard care subjects did not drive any correlations. Weight loss and NAS reduction were positively related (**figure 4.6A**, $P = 0.023$) with this relationship being primarily driven by improvements in hepatocellular ballooning (**figure 4.6G**, $P = 0.038$) and lobular inflammation (**figure 4.6E**, $P = 0.097$). Changes in fat mass were positively related to improvements in NAS (**figure 4.6B**, $P = 0.007$) and lobular inflammation (**figure 4.6F**, $P = 0.005$), but not hepatocellular ballooning (**figure 4.6H**, $P = 0.250$). Unlike total weight loss (**figure 4.6C**, $P = 0.231$), changes in fat mass tended to correlate positively with

steatosis (**figure 4.6D**, $P = 0.089$). Improved hepatic fibrosis was not related to changes in body weight or fat mass (data not shown).

Biochemical data

Both groups demonstrated improvements in fasting blood biochemistries at follow-up (**figure 4.7**). Fasting glucose and insulin concentrations were $19 \pm 7\%$ (**figure 4.7A**, -35 ± 13 mg/dL) and $17 \pm 12\%$ (**figure 4.7B**, -7 ± 4 μ U/mL) lower than baseline in the treatment subjects. Standard care subjects also reduced both glucose and insulin concentrations by $31 \pm 7\%$ (-50 ± 15 mg/dL) and $4 \pm 25\%$ (-5 ± 5 μ U/mL), respectively. Accordingly, HbA1c tended to decrease in both groups (**figure 4.7C**; treatment: $-11 \pm 4\%$ and standard care: $-6 \pm 9\%$; $P = 0.058$ main effect of visit). Liver enzymes, ALT and AST, fell by $41 \pm 6\%$ (**figure 4.7D**, -30 ± 8 U/L) and $96 \pm 26\%$ (**figure 4.7E**, -33 ± 10 U/L) in the treatment group and by $32 \pm 24\%$ (-41 ± 25 U/L) and $4 \pm 43\%$ (-21 ± 16 U/L) in standard care. Both ALT and AST were significantly reduced at follow-up in both groups ($P = 0.003$ and $P = 0.019$ - main effect of visit). Baseline NAS was positively related to ALT (data not shown, $r = 0.624$, $P = 0.003$) and AST (data not shown, $r = 0.682$, $P < 0.001$; spearman's rho correlations). Analysis of blood lipids revealed overall reductions in fasting TG, TRL-TG, and total cholesterol, although these changes were not significant. Minimal changes are evident in HDL, LDL, and VLDL cholesterol (**table 4.4**). Fasting NEFA concentrations were reduced by $13 \pm 6\%$ on average in treatment subjects and $13 \pm 8\%$ on average in standard care subjects (**table 4.5**, $P = 0.005$ – main effect of visit).

In addition to fasting concentrations, 18-hour glucose (**figure 4.8**), insulin (**figure 4.9**), NEFA (**figure 4.10**), and TG (**figure 4.11**) were measured during the overnight visits. When comparing groups, each metabolite showed similar patterns across time and, in general, concentrations were reduced at follow-up. For analysis, the 18-hour concentration data were separated into three time periods – postprandial (6PM to midnight), night (midnight to 6AM), and the clamp (6AM to noon). Analysis of individual time segment AUC is presented in **supplementary table S4.1 and figure S4.2**.

Postprandial: In treatment subjects, glucose and insulin concentrations (**figures 4.8-4.9**) increased in tandem, while NEFA dropped (**figure 4.10**). Standard care subjects had higher (treatment 104 ± 8 mg/dL versus standard care 165 ± 32 mg/dL) and more variable baseline glucose concentrations than the treatment subjects (partially due to a lower n in standard care). Similar observations are noted for insulin. Treatment subjects had greater reductions in postprandial insulin concentrations at follow-up, while maintaining glycemia <150 mg/dL (**figure 4.8A** versus **figure 4.9A**). With regard to NEFA, standard care subjects had minimal postprandial decline in concentrations during both study visits despite the elevation in insulin, suggesting adipose tissue insulin resistance was maintained throughout the program (**figure 4.8B** versus **figure 4.10B**). Finally, plasma TG (**figure 4.11**) concentrations were highly variable at baseline for treatment and standard care subjects and this variability decreased for both groups at follow-up. No significant interactions (group x visit x time) were

observed for the postprandial period for any metabolite (P – value on **figures 4.8-4.11**), however a significant main effect of visit was evident for glucose (**supplementary table S4.1**, reduced concentrations baseline to follow-up). Additionally, a significant main effect of time was found for glucose and TG (increased concentrations across time following the meal) and TG had a significant interaction between time and visit indicating the rise in TG concentrations from 6PM to midnight was significantly lower at follow-up (**figure 4.11** and **table S4.1**, $P = 0.019$).

Night: As subjects transition to the postabsorptive phase, reductions in glucose, insulin, and TG concentrations were accompanied by a steady increase in NEFA which continued until the clamp began. Nighttime insulin was significantly reduced in treatment subjects at follow-up across time ($P = 0.020$). A significant main effect of visit was found for glucose ($P = 0.011$), insulin ($P = 0.012$), and NEFA ($P = 0.030$) concentrations (**table S4.1**) while a main effect for time was found for nighttime glucose ($P = 0.030$), insulin ($P < 0.0001$), NEFA ($P < 0.0001$), and TG ($P = 0.036$). In other words, nighttime glucose, insulin, and NEFA were lower at follow-up and all metabolites varied significantly across the nighttime hours (reduced glucose, insulin, and TG; increased NEFA).

In addition to total plasma NEFA concentrations, the sources of plasma NEFA were quantified using a dietary and FFA label and the results are shown in **supplementary figure S4.3**. Total plasma NEFA concentrations from midnight to 8AM were made up of primarily rising adipose derived NEFA in both treatment

and standard care groups. No apparent changes in dietary contributions to NEFA concentrations after treatment were evident in either group, however the total number of subjects precluded adequately-powered statistical comparisons.

Absolute TRL-TG concentrations are shown in **supplementary figure S4.4**.

Similar to total TG concentrations (**figure 4.11**), variability within the treatment subjects dropped at follow-up as did the total TRL-TG content. Interestingly, at baseline, treatment subjects seemed to have delayed clearance of lipoprotein particles (either chylomicron remnants or VLDL) whereas at follow-up they had minimal changes across time. Alternatively, standard care subjects demonstrated little difference in TRL-TG concentrations throughout the program.

Clamp: Upon onset of the insulin infusion for the clamp procedure (8AM), glucose concentrations were held constant with a variable infusion of dextrose, insulin rose, and NEFA concentrations dropped. Clamped glucose concentrations were 18% lower at follow-up in treatment subjects and 26% lower in standard care ($P = 0.008$). At follow-up, subjects had significant reductions in NEFA concentrations during the basal period (6AM – 8AM, $P < 0.01$) and the steady state portion of the high-dose step 2 (11:40AM-12PM, $P < 0.01$). These data suggest greater insulin-stimulated suppression of lipolysis, indicative of improved adipose tissue insulin sensitivity.

Energy intake, physical activity, and fitness levels

Subjects completed three-day food records prior to baseline, interim, and follow-up study visits. Both groups demonstrated reductions in total energy intake (**figure 4.12 A-B**, $P = 0.005$ – main effect of visit) and carbohydrate intake ($P = 0.0001$ – main effect of visit). At follow-up, treatment subjects reduced energy intake by 395 ± 158 kcals/day ($-12 \pm 6\%$) and standard care by 385 ± 153 kcals/day ($-16 \pm 9\%$). Carbohydrate intake was reduced by 297 ± 91 kcal/day ($-24 \pm 7\%$) and 270 ± 362 ($-16 \pm 20\%$) kcal/day in treatment and standard care subjects, respectively. Although absolute protein (treatment: $+27 \pm 30$ kcal/day; standard care: $+17 \pm 43$ kcal/day) and fat (treatment: -130 ± 123 kcal/day; standard care: -131 ± 114 kcal/day) intake did not change throughout the program for either group, the percentage of energy (%E) from protein increased marginally (treatment: $+4.2 \pm 1.6\%E$; standard care: $+3.9 \pm 2.7\%E$) which was accompanied by an increased in total g/kg of protein intake only in treatment subjects (treatment: $+0.25 \pm 0.09$ g protein/kg body weight/day, $P = 0.007$; standard care: $+0.06 \pm 0.12$ g protein/kg body weight/day, $P = 0.307$). Changes in macronutrient and total energy intake did not correlate with changes in NAS or NAS components.

Maximal cardiorespiratory capacity was measured at baseline, interim, and follow-up and treatment subjects demonstrated a significant increase in VO_2 peak from baseline to interim (**figure 4.13A**, $P = 0.029$). A small decline in absolute cardiorespiratory fitness was observed in treatment subjects from interim to follow-up visits (-0.9 ± 0.07 L/min) despite increased time to exhaustion

(**figure 4.13B**, $+2:23 \pm 1:18$ minutes:seconds). Minimal changes to VO_2 peak were observed in standard care subjects (BL to FU: -0.1 ± 0.1 L/min) despite a slight increase in time to exhaustion from baseline ($+1:03 \pm 0:43$ minute:seconds). Improvements in VO_2 peak were negatively related to weight loss (**figure 4.14A**, $P = 0.026$), NAS (**figure 4.14B**, $P = 0.029$), and hepatocellular ballooning (**figure 4.14C**, $P = 0.004$), tended to correlate with reduced fibrosis (**figure 4.14D**, $P = 0.054$) but were not related to hepatic inflammation (data not shown, $r = -0.290$ $P = 0.243$) or steatosis (data not shown, $r = -0.171$, $P = 0.481$). Exercise adherence was monitored throughout the intervention (treatment only) and on average remained above 85% although slight reductions were observed at follow-up (**figure 4.13C**, $-6.9 \pm 3.4\%$, $P = 0.087$). Importantly, 57% subjects were in the active treatment phase during COVID-19 shutdowns which did impact the ability to complete in-house, supervised sessions. Finally, each subject received a FitBit® activity tracker to monitor daily activity and **figure 4.13D** presents average daily steps during the first, second, and third portion of the program. Neither treatment or control subjects had significant changes in daily steps or distance walked (data not shown) throughout the program, but treatment subjects did have two-fold higher average daily physical activity (treatment: $6,083 \pm 525$ steps/day; standard care: $2,903 \pm 671$ steps/day, $P = 0.001$ – main effect of group).

Glucose metabolism

Glucose metabolism was quantified with a two-step, hyperinsulinemic euglycemic clamp at baseline and follow-up. **Table 4.5** presents the results from the clamp including absolute EGP and R_d in $\mu\text{mol}/\text{min}$, NEFA concentrations (mmol/L), and substrate oxidation (mg/kg/min) measurements. When the groups were compared with a mixed model ANOVA (within: visit and between: group), no significant interactions between the groups existed.

Basal and low-insulin: Changes in absolute basal and step one (low insulin) EGP are shown in **figure 4.15A** and the percent change in EGP in **figure 4.15B**. Mirroring the change in fasting glucose (**figure 4.7A**), both groups had reductions in basal EGP at follow-up. Surprisingly, compared to treatment, standard care subjects had greater reductions in basal (treatment: $-5.8 \pm 4.8\%$, standard care: $-10.5 \pm 4.2\%$; $P = 0.237$) and step one (treatment: -7.1 ± 4.8 , standard care: $-14.1 \pm 8.2\%$; $P = 0.244$) EGP at follow-up testing, although the variability across subjects was large and these differences were not significant (**figure 4.15B**). Minimal differences were observed in absolute change from basal to step one EGP suppression (**figure 4.16B**) between groups (treatment: $+1.1 \pm 2.3\%$; standard care: $+2.8 \pm 2.7\%$; $P = 0.416$).

Basal and high-insulin: Unexpectedly, treatment subjects had a reduction in basal to step two (high insulin) EGP suppression at follow-up while control subjects tended to suppress EGP to a greater extent (treatment: $-3.0 \pm 4.1\%$, standard care: $+1.7 \pm 3.2\%$), although the groups were not significantly different ($P = 0.446$). With regard to glucose disposal (**figure 4.17** and **table 4.5**), treatment subjects had similar basal but higher baseline step two R_d than

standard care subjects although this difference was not significant ($P = 0.183$). While both groups demonstrated similar reductions in basal R_d , the groups diverged in step two where treatment subjects had an average increase of $563.9 \pm 277.3 \mu\text{mol}/\text{min}$ (equivalent to 3.0 ± 1.5 more grams of glucose leaving circulation in a 30 minute window) while standard care glucose disposal was reduced by $92.2 \pm 95.7 \mu\text{mol}/\text{min}$ (equivalent to 0.5 ± 0.5 fewer grams of glucose leaving circulation in a 30 minute window). As shown in **figure 4.17B**, treatment subjects had greater percent change in glucose disposal than standard care ($P = 0.009$), demonstrating the impact of combined energy restriction and exercise in increasing peripheral glucose disposal.

Improved insulin sensitivity and liver health: Taken together, the exercise component of the treatment may have resulted in greater peripheral glucose disposal to an extent that glucose production increased to supply necessary energy to skeletal muscle. Furthermore, routing glucose away from the liver may work to relieve the organ of excess nutrients and ultimately support histological improvements. This hypothesis is supported by multiple strong correlations (continued into the next section). 1) Baseline EGP (relative to body weight) was negatively related to lobular inflammation (**figure 4.18A**), indicating an increase in glucose production per kg body weight was associated with lower hepatic inflammation. A similar, but weaker correlation was observed with baseline relative glucose disposal (**figure 4.18B**), supporting a potential therapeutic effect on the liver through routing substrates to the periphery for oxidation. 2) When the changes in glucose production were compared to changes in NAS (**figure**

4.19A) and lobular inflammation (**figure 4.19C**), surprising negative correlations were revealed, providing further support for increased glucose disposal as beneficial for liver health improvement. A similar negative relationship was found between EGP and hepatocellular ballooning but was not significant (**figure 4.19E**). 3) **Figures 4.19 B, D, F** present strong negative relationships between changes in peripheral glucose disposal and changes in NAS, lobular inflammation, and hepatocellular ballooning. Changes in steatosis, either by histology or MRS, were not related to changes in insulin sensitivity (EGP or R_d). 4) While mathematically related, EGP and R_d were positively related during both step one and step two (**supplementary figure S4.6A-B**). Together, these results support a benefit of increased hepatic glucose production and peripheral disposal to spare the liver of excess carbons.

Improved insulin sensitivity, fitness, and energy intake: Regarding improvements in fitness and dietary changes, 5) increased relative glucose disposal was positively related to increased peak respiratory capacity (**figure 4.20B**) and the two-day average distanced walked (**figure 4.20D**) immediately prior to follow-up testing. Increased EGP was positively correlated with activity levels (**figure 4.20C**) but not with VO_2 peak (**figure 4.20A**). 6) Changes in glucose production and disposal correlated negatively with the three-day average carbohydrate intake prior to the follow-up study visit (**figure 4.21A-B**), but only R_d was significant. These data support a potential skeletal muscle crosstalk event in response to increased activity and reduced carbohydrate intake that promoted the unexpected observation of increased glucose production. Although acute

lifestyle changes can have a marked impact on steatosis, with significant reductions in IHTG reported in as little as 48 hours (53), these results indicate a chronic benefit of diverting substrate away from the liver to reduce advanced characteristics of NASH. In other words, IHTG is strongly dependent on recent energy balance (141) while the other components of NAS likely require longer interventions for significant regression.

NEFA suppression and diurnal variations: Finally, insulin-induced NEFA suppression was also quantified during the clamp (**table 4.5 & figure 4.22**) and both groups had significantly greater NEFA suppression during step two (high-insulin) when compared to step one at baseline ($P < 0.0001$, same for follow-up). At follow-up, treatment subjects were able to attain $87 \pm 2\%$ suppression (step two) and standard care subjects reached an average suppression of $79 \pm 6\%$ (step two, **figure 4.22A**). While treatment subjects had minimal absolute increases in NEFA suppression during step one ($0.5 \pm 5.6\%$), standard care subjects demonstrated reduced suppression of adipose tissue lipolysis after the program ($-5.3 \pm 13\%$), though the groups did not differ statistically ($P = 0.164$, **figure 4.22B**). During step two, minimal differences in NEFA suppression were observed between the groups ($P = 0.237$). Surprisingly, when AUC of 18-hour NEFA concentrations (**figure 4.10C**) were compared to changes in histology and insulin sensitivity, a trending negative correlation was found with NAS (**supplementary figure S4.5A**). Upon analysis of individual NAS components, inflammation was identified as being significantly correlated with diurnal changes in NEFA concentrations (**figure S4.5B**). In other words, as subjects' liver health

(particularly inflammation) improved, 18-h NEFA concentrations tended to increase. These results were unexpected but ultimately may support our findings of increased substrate disposal at the periphery in benefiting liver health. Indeed, a trending positive relationship between 18-hour NEFA AUC and the change in step one EGP ($P = 0.059$) suggests these events may work synergistically to improve liver health (**figure S4.5C**).

Substrate metabolism - glucose: Indirect calorimetry was completed before and during the second step of the clamp (data shown in **table 4.5**). Stimulation of glucose oxidation and non-oxidative glucose metabolism was calculated as the change from basal to clamped states. Glucose oxidation increased during the clamp in both treatment and standard care subjects although the stimulation (i.e., the change from basal to clamped states) tended to decrease between study visits but was not statistically different (treatment: $-21 \pm 34\%$, $P = 0.272$; standard care: $-10 \pm 26\%$, $P = 0.367$, data not shown). Non-oxidative glucose metabolism (i.e., glycogen synthesis within skeletal muscle (142)) was calculated as the difference between glucose disposal (basal and step two clamp) and glucose oxidation (measured via indirect calorimetry). Treatment subjects had greater changes in stimulation of non-oxidative glucose disposal ($+87 \pm 49\%$, $P = 0.049$) than standard care subjects ($-10 \pm 37\%$, $P = 0.401$). Stated simply, these data suggest treatment subjects had greater stimulation of glycogen synthesis after the program than standard care subjects. Increased nonoxidative glucose metabolism during the clamp was positively related to the change in EGP (**supplementary figure S4.6C**).

Lipid metabolism

Fatty acid sources used for TG synthesis: Using a multiple stable isotope protocol, the sources of fatty acids contributing to the TRL-TG pool were calculated and the results from seven treatment and two standard care subjects are shown in **figure 4.23**. The proportion of total TRL-TG fatty acids accounted for by the labeling paradigm are shown in **figure 4.23A** and are made up of the sum of dietary (**figure 4.23B**), DNL (**figure 4.23C**), and plasma FFA (**figure 4.23D**) sources. The sum of all isotopically-labeled fatty acid sources were similar at both visits in treatment subjects but tended to be reduced in the two standard care subjects included in this analysis. A proportionally greater quantity of total fatty acids were labeled at baseline in standard care when compared to treatment subjects (e.g., midnight timepoint: $46 \pm 3\%$ versus $69 \pm 19\%$) although this may be an artifact of the small sample size ($n = 2$). The fatty acids that remained unlabeled may have arisen from 1) intestinally-stored unlabeled dietary fatty acids, 2) stored hepatic lipid used for TG assembly, or 3) visceral depots. The proportion of fatty acids from the evening meal contributing to the total TRL-TG pool at midnight increased in the treatment subjects (**figure 4.23B**, $+6 \pm 3\%$, $P = 0.027$) and was unchanged in two standard care subjects ($-21 \pm 13\%$, $P = 0.182$) at follow-up testing. Meal-derived fatty acids originate from TG carried in chylomicrons remnants or from chylomicron-TG recycling within the liver and secretion in VLDL (126, 143, 144). Midnight lipogenesis was 5% higher in standard care subjects at baseline (**figure 4.23C**, treatment $28 \pm 3\%$ versus

standard care $33 \pm 1\%$) and values across at follow-up were reduced similarly in both groups, although the small number of subjects within standard care contributed to the lack of significance across the timepoints. Despite 12+ hours of fasting, neither group demonstrated circadian suppression of lipogenesis before or after the program, unlike other studies (96). Finally, the fraction of labeled plasma fatty acids contributing to the TRL-TG pool was approximately 50-60% lower in standard care subjects at both study visits (**figure 4.23D**). Within a group, the total proportion of TRL-TG from plasma fatty acids was similar at each study visit.

Absolute concentration of the dietary, lipogenic, plasma FFA, and unlabeled sources during the three fasting values (7:30-8:00AM) were averaged and are presented in **figure 4.24A**. The proportional source contribution described above and presented in **figure 4.23** represents intracellular lipid synthesis while absolute concentration of the sources (**figure 4.24A**) better reflects the balance of VLDL turnover within the plasma (96, 97). As only two standard care subjects were included in this analysis, groups were not compared statistically however a compulsory mention is needed noting the differences in total baseline VLDL-TG concentrations between the groups (treatment: 88 ± 27 mg/dL versus standard care: 184 ± 115 mg/dL) and the increased contribution of DNL to total concentration within the standard care subjects. When baseline and follow-up values for each source were compared within the treatment subjects, no differences were found. At baseline, fractional VLDL-TG DNL was positively but

not significantly related to IHTG measured via MRS (data not shown, $r = 0.509$, $P = 0.162$) and tended to correlate with steatosis from histology (data not shown, $r = 0.579$, $P = 0.101$). No significant relationships were observed between baseline fractional or absolute VLDL-TG DNL and NAS, the components, or fibrosis. The small sample size included in this report likely contributed to small effect sizes. With regard to effects of the treatment/standard care, the change in VLDL-TG DNL tended to correlate positively with change in NAS and was significantly related to reduced hepatocellular ballooning and fibrosis (**figure 4.24B-D**). The change in DNL was strongly related to glucose disposal and fitness level (**figure 4.24E-F**), inducing a reduction in lipogenesis was related to improved peripheral insulin sensitivity and cardiorespiratory fitness. However, DNL changes did not correlate with steatosis (MRS or histology), lobular inflammation, or EGP (**supplementary figure S4.7**).

Plasma ceramides

Plasma CERs and dhCERs were quantified using HPLC-MS/MS at baseline and follow-up. Overall, total CER concentrations decreased in both groups (**figure 4.25**, treatment: $-9.4 \pm 7.5\%$; standard care: $-12.6 \pm 11.5\%$), although the change among groups was not different ($P = 0.931$, interaction). When individual species were analyzed separately, only CER 14:0 differed significantly between the groups across time (group x visit interaction; $P = 0.037$, no significant post hoc findings). Both CER 20:0 ($P = 0.011$) and 24:1 ($P = 0.019$) were significantly decreased at follow-up (main effect of visit). dhCERs (**figure 4.26**) were 70-fold

lower in concentration than CER but the two species correlated strongly at baseline (data not shown, $r = 0.688$, $P < 0.001$) as well as the change from baseline to follow-up (data not shown, $r = 0.803$, $P < 0.001$). Total CER and dhCER concentrations (the sum of all individual species) tended to correlate negatively with baseline BW (**supplementary figure 4.8A-B**). Similarly, both CER and dhCER were negatively related to fasting plasma glucose concentrations, but only the association with CER was significant (**supplementary figure 4.8C-D**). Baseline total cholesterol, CER and dhCER were positively related (**supplementary figure 4.8E-F**). A correlation matrix was created for baseline concentrations of individual CER and dhCER species with anthropometrics, fasting blood glucose and cholesterol, and insulin sensitivity (**supplementary table S4.2**). The relationship observed between fasting glucose and total CER seem to be driven by an increase in longer chain plasma CERs (22:0, 24:1, and 24:0). In addition to baseline correlations, the change in BW and fat mass tended to correlate with changes in total CER and dhCER (**figure 4.27** and **supplementary table S4.3**). With regard to liver health, the change in 16:0 CER correlated with changes in steatosis as measured by both histology and MRI (**figure 4.28**). As liver fat was reduced, plasma 16:0 CER increased.

DISCUSSION

Although energy restriction and exercise are well-established therapeutic strategies to treat T2D and cardiovascular diseases (145) and the same modifications make up the current guidelines for the treatment of NASH (15-19), little evidence exists identifying the metabolic changes that occur to promote liver health improvements. The present study represents the first in-depth characterization of the changes in liver histology, insulin sensitivity, and lipid metabolism following an intensive lifestyle program in subjects with advanced NASH. Compared to standard care, subjects who underwent ~10 months of energy restriction and HIIT demonstrated robust improvements in total NAS, the components – lobular inflammation and hepatocellular ballooning, and fibrosis. These changes occurred only in treatment subjects despite similar reductions in total body weight, fasting and 18-h blood biochemistries (i.e., glucose, insulin), plasma aminotransferases, and energy intake in both groups. As already established in previous intervention studies with paired biopsies (56, 72, 88-92), weight loss was related to NAS improvements in all subjects, however with deep metabolic phenotyping, greater insight was gained into the mechanisms driving chronic improvements in liver health. In particular, the greatest improvements may not have been due solely to weight loss, but the combination of energy restriction and physical activity promoting an environment primed for peripheral substrate disposal-driven rerouting of hepatic metabolites.

Lifestyle treatment-induced histologic improvements in NASH

To date, eight studies have investigated the effects of a lifestyle treatment on histology from paired liver biopsies in NAFLD or NASH (56, 72, 76, 88-92). Of these, two were weight loss induced solely via energy restriction (56, 91) while the remaining six studies included unsupervised exercise recommendations (72, 76, 88-90, 92). The current study included both individualized dietary counseling with an emphasis on reducing overall energy intake, simple sugars, and increasing fiber in addition to supervised HIIT. Previous publications reported average reductions in total NAS (average change from refs 56, 72, 76, 88-92: -40%; range: -19 to -55%), steatosis (-40%; -19 to -58%), inflammation (-48%; -32 to -65%), ballooning (-47%; -28 to -75%), and fibrosis (-24%; +5 to -64%). In line with these findings, we observed similar improvements in liver histology (**figure 4.4**) following treatment. While significantly reduced at follow-up, the changes across subjects spanned a wide range (0%-100% NAS reduction), potentially due to 1- lack of adherence to the treatment, 2- minimal total weight loss, or 3- weight regain throughout the program.

With regard to adherence, previous groups have addressed significant concern with long-term intensive lifestyle treatments (88, 89). Surprisingly, longer interventions in NASH resulted in less weight loss (~4.9 kg) (56, 72, 89, 92), than we observed (10.0 ± 2.2 kg, treatment alone) or was reported in six-month studies (~8.4 kg) (89, 90, 92). While all studies demonstrated similar levels of NAS reductions, the results diverged with regard to fibrosis regression. The longer interventions (12+ months) reported an average 10% change in fibrosis

(+5 to -47%, $n = 4$ studies) while the six-month interventions reported an average 60% reduction in fibrosis (-55 to -64%, $n = 3$ studies). Our ten-month study elicited a 45% reduction in fibrosis (0 to -100%) within treatment subjects. Overall, these findings may suggest poor adherence over a longer intervention may contribute to lesser fibrotic improvements. Alternatively, total weight loss may be a determinant of fibrotic regression as the six-month studies had both greater weight loss and reduced fibrosis. However, we did not observe a significant relationship between the changes in body weight and fibrosis. It remains unknown whether the differences in histological changes between studies and among participants are due to variations in program intensity/dietary interventions, lack of adherence, or weight recidivism. However, it was clear, our ~10-month treatment was highly effective at improving total NAS, inflammation, ballooning, and hepatic fibrosis when compared to subjects receiving no structured intervention.

Regardless of the type or duration of intervention, weight loss has been touted as an independent therapy for histologic improvement in NASH and the intervention studies available have investigated this proposed relationship. While most have demonstrated improvements in overall NAS with weight loss (56, 72, 89-92), not all have (88). The present study found a positive relationship between change in weight and NAS (**figure 4.6A**) as has been reported previously (89, 92). However, the subjects receiving standard care also demonstrated an average weight loss of 5.9 ± 1.8 kg ($-4 \pm 3\%$), with minimal changes in liver histology.

Indeed, the degree of weight loss was not different between treatment and standard care subjects ($P = 0.239$; interaction term) although the composition of the body weight loss did differ with standard care subjects losing a greater proportion of their lean mass than treatment subjects. The relative quantity of weight loss in standard care was similar to previous reports demonstrating improved liver histology (72, 89). In particular, one study demonstrated 32% of participants who had $\leq 5\%$ weight loss had NAS improvements (89). Despite the average reduction in weight, only steatosis was significantly lower in standard care subjects while total NAS and fibrosis remained unchanged. In addition to weight loss, standard care subjects also reduced plasma glucose and insulin concentrations (fasting and 18-h), HbA1c, and aminotransferases (ALT and AST). It is of note, the standard care subjects did not receive counseling for energy restriction or exercise training beyond a single education session with a dietician at the start of the program. Thus, the weight loss observed was a result of individual efforts and may have been influenced by the diagnosis of a chronic liver condition. Upon examination of the changes in energy intake (**figure 4.12**), fitness levels (**figure 4.13A**), and daily activity (**figure 4.13D**), these data suggest the reduction in weight observed in standard care subjects was due primarily to reduced energy intake ($P = 0.005$ main effect of visit). In comparison, two previous reports have examined independent effects of dietary interventions on histology in NAFLD/NASH (56, 91) and one reported a smaller degree of weight loss (-2.9 kg) which was accompanied by an average one-point reduction in steatosis (56). Despite a greater weight loss (-5.9 kg), the standard care

subjects from the current study only reduced steatosis by 0.4 points on average. In line with others (89), our results suggest weight loss of <5% via energy restriction may be beneficial for improvements in liver fat, but not the other potentially more deleterious components of NAS or fibrosis. As weight loss was similar between groups, it alone likely did not account for the significant histologic improvements in treatment subjects. Thus, one must question what alternative mechanisms may be interacting to promote an improved liver phenotype. The large fat free mass loss observed in standard care but not treatment subjects may be one potential explanation for these findings. Alternatively, a major difference between the groups was the level of daily activity and supervised HIIT (**figure 4.13**) which likely played a role in maintaining muscle mass within treatment subjects. In support of this, improved peak VO₂ was strongly related to reductions in body weight, NAS, and fibrosis. Overall, our results support the addition of exercise to weight loss as critically important for the histologic resolution of NASH. The results presented here expand upon the previous reports in implicating an alternative mechanism beyond weight loss alone in improving liver health in NASH.

Reroute hypothesis for histologic liver improvements: Examination of changes in glucose metabolism

Of the studies discussed above, only indirect measures of insulin sensitivity (e.g., HOMA-IR, the quantitative insulin sensitivity check index [QUICKI], or insulin sensitivity index [ISI] from an oral glucose tolerance test [OGTT]) were collected.

Thus, this is the first study to characterize the relationships between changes in insulin sensitivity using a hyperinsulinemic-euglycemic clamp and histology in NASH. Unexpectedly, minimal reductions in EGP were observed regardless of group. Our findings differed from previous combined lifestyle intervention studies in T2D or individuals with impaired glucose tolerance which reported significant reductions in EGP (avg 48% decrease) (69, 146). Upon closer inspection of our data, while the overall average step one (low insulin) EGP was reduced across subjects, five treatment participants had elevated relative EGP at follow-up. These five subjects also had an average 4.0 ± 1.0 point reduction in NAS whereas the other nine treatment subjects with reduced EGP had a 1.4 ± 0.3 point reduction in total NAS. Thus, when the change in EGP was compared to the change in NAS, a significant negative relationship was discovered – indicating the subjects with the greatest improvements in liver health via histology were also those with increased EGP (**figure 4.19A**). As no other study has directly compared changes in liver histology and hepatic insulin sensitivity in humans, these findings are the first time this relationship has been reported. Our results challenge the current dogma that 1- implicates elevated EGP with worsening liver disease (8, 113, 147, 148) and 2- associates greater improvements in liver fat, measured noninvasively, with reduced EGP, with (40, 53, 54, 57, 69, 146, 149) and without (27) weight loss. Multiple explanations for our findings are possible and explained in detail below.

1- *Effects of NEFA on EGP*: A study in subjects with obesity (53) demonstrated an acute (48 hour) and chronic (~11 weeks, 7% weight loss) energy restrictive low carbohydrate diet resulted in robust reductions in EGP. In the same subjects described above (53), plasma NEFA concentrations were elevated during the clamp 48 hours following the onset of carbohydrate restriction but returned to pre-study levels following a 7% weight loss. Other studies completed in metabolically-compromised subjects, have shown conflicting results in which increased plasma NEFA, via infusion of intralipid during a clamp or natural elevations in lipoprotein-TG concentrations (non-clamped status), have deleterious impacts on hepatic insulin sensitivity (69, 119, 150, 151). In our study, we observed reduced plasma NEFA concentrations in all subjects at follow-up (**figure 4.18** and **table 4.5**) in addition to increased NEFA suppression (**figure 4.22**). Furthermore, no relationship was observed between step one NEFA and EGP at baseline or follow-up nor did the changes correlate (data not shown) which indicate the circulating NEFA concentrations likely did not acutely affect EGP during the clamp. That being said, an unexpected positive correlation between 18-hour AUC of NEFA concentrations and the change in EGP existed while the same change in AUC NEFA tended to correlate negatively with improvements in NAS (**figure S4.5**). In other words, subjects who increased circadian NEFA concentrations at follow-up had increased EGP and decreased liver disease (NAS). These relationships suggest the potential for elevated 18-hour NEFA concentrations in increasing EGP but, paradoxically, improve liver health. However, subsequent analysis of NEFA AUC during the clamp, showed

no relationship with changes in EGP or NAS. Thus, we believe it unlikely that the observed increases in EGP were a result of increased adipose tissue lipolysis and subsequent NEFA-induced hepatic insulin resistance.

2- The reroute hypothesis: A second explanation is that EGP was increased in response to elevations in glucose storage – either through increased peripheral oxidation or non-oxidative disposal. During the second step of the clamp, treatment subjects significantly increased absolute glucose disposal ($P = 0.032$, within group t -test – baseline to follow-up) primarily through increased non-oxidative glucose metabolism ($P = 0.014$, within group t -test – baseline to follow-up). In line with some (79, 146), but not all (27, 57) previous publications, glucose oxidation measured via indirect calorimetry did increase under insulin-stimulated conditions (**table 4.5**). However, the change in stimulation of glucose oxidation (i.e., the magnitude of increased oxidation from fasting to insulinized states at baseline versus follow-up) was not significantly different for either treatment or standard care subjects. This suggests the relative level of glucose oxidation did not change across time, ultimately supporting the livers' role in routing substrates towards the periphery for glycogen synthesis rather than oxidation. Importantly, the final supervised exercise training session occurred more than 48 hours prior to the clamp to avoid any potential acute effects of training, however upon analysis of the physical activity data using FitBit® trackers, a strong correlation was revealed between the distance walked the two days prior to the study visit and R_d (**figure 4.20**). Enhanced insulin sensitivity

and glycogen synthase activity can persist for 48 hours post exercise (152, 153). Thus, we cannot rule out a potential effect of activity levels impacting both glucose production and disposal.

Finally, the subjects who had the lowest average carbohydrate intake the three days prior to follow-up testing also had the greatest increases in glucose production and disposal. Taken together, enhanced insulin sensitivity at skeletal muscle with the potential for simultaneous depletion of glycogen content from dietary changes (154) may have driven EGP increases in the five treatment subjects through a muscle-centric need to replenish glycogen stores. Ultimately, an increase in glucose production to feed primed skeletal muscle may be mechanistically implicated in improving liver histology through reduced hepatic substrate burden.

Remarkably, one standard care subject also increased EGP at follow-up but demonstrated a two-point increase in total NAS – coming from one point increases in lobular inflammation and hepatocellular ballooning. This subject represents a case in which elevations in glucose production (+118.2 $\mu\text{mol}/\text{min}$) when not accompanied by a substantial rise in glucose disposal (156.3 $\mu\text{mol}/\text{min}$; versus the 1,173.3 $\mu\text{mol}/\text{min}$ increase in the five treatment subjects) elicits significant worsening of liver disease (50% increase). The subject in question had the highest pre-follow-up study carbohydrate intake of all subjects (336.2 g/day) and average to low physical activity level (1.7 miles/day). Taken together,

these findings suggest a reverse “J-shaped” curve may exist with changes in liver histology and increased in EGP responding to increased R_d (hypothetical relationship presented in **figure 4.29A**). This subject provides further evidence of how exercise in addition to energy restriction, irrespective of weight loss, may promote histologic improvements in even the most advanced cases of NASH.

It is well established that excess hepatic nutrient burden is implicated in promoting hepatic insulin resistance, NAFLD development, and progression to more advanced forms (77, 96, 97, 101-104, 144, 155). Here we propose an inter-organ crosstalk model (**figure 4.29B**) in which the liver responds to unknown signals (potentially mediated by chronic release of myokines (156)) from skeletal muscle by increasing the production and routing of substrates away from the liver, thereby relieving oversaturated hepatic metabolic pathways to ultimately reduce oxidative stress and inflammation within the liver. Incidentally, this hypothesis is the reciprocal of one proposed by Petersen et al (157), in which they found insulin resistant skeletal muscle promoted the diversion of ingested carbohydrates away from peripheral glycogen synthesis and into hepatic DNL. The results presented here may extend the widely accepted selective hepatic insulin sensitivity paradox, first identified in mice (158-160) and later described elegantly by Brown and Goldstein (118), into a setting of lifestyle modifications. The interaction between hepatic glucose and lipid metabolism remains at the cornerstone of this paradox, particularly in a setting of elevated IHTG, as observed in NASH.

3- Independent, unknown mechanism: A final potential explanation for our findings is that the liver is improving independently of changes in EGP, although the two processes are occurring simultaneously. Improved histology could be a result of increased peripheral insulin sensitivity alone or due to an independent, unknown mechanism. We think this is highly unlikely due to 1- evidence from previous studies implicating hepatic and peripheral glucose metabolic disturbances in the development of NAFLD (9, 13, 105) and 2- our correlative analyses suggest these outcomes are strongly related. Nevertheless, our interpretations are based on correlations alone and therefore caution is needed when generalizing results for larger populations. To confirm our model, mechanistic basic studies and analysis of skeletal muscle tissue from humans with NASH is needed.

Interactions between hepatic glucose and lipid metabolism in a setting of improved liver histology

As described above, sensitivity of hepatic tissues to insulin is reflected in both glucose production and lipogenesis. However, a bifurcation of insulin sensitivity is revealed in settings of metabolic perturbations like T2D and NAFLD; insulin fails to suppress gluconeogenesis but maintains stimulation of DNL through activation of key lipogenic transcription factors. Our group was the first to report a unique elevation of DNL in subjects with NAFLD (96, 97) and the current data

demonstrate similar results. We expand upon our previous findings in multiple ways.

1- Effects of treatment or standard care on DNL: Weight loss, regardless of group, induced significant reductions in nocturnal and fasting fractional DNL. Smith et al (42) showed similar results following diet-induced moderate (10%) weight loss in subjects with NAFLD. We observed a $33 \pm 14\%$ reduction in fasting fractional DNL in seven treatment subjects while the former study (42) showed a $35 \pm 10\%$ reduction in six subjects. Unlike this report, we did not observe significant relationships between fractional DNL and 18-h glucose or insulin AUCs at baseline or after the program.

2- Peripheral but not hepatic insulin sensitivity correlated negatively to DNL:

While our results were consistent for systemic insulin sensitivity, in opposition to Smith et al (42) we found no relationship between changes in DNL and EGP. We were highly surprised by this observation as our model (**figure 4.29B**) would suggest removing substrate to circulation via gluconeogenesis would reduce the lipogenic potential within the liver. Indeed, a recent report demonstrated mice with phosphoenolpyruvate carboxykinase (PEPCK) knockout resulted in TCA metabolite accumulation and rapid fat accrual within the liver, which was in part attributed to increased DNL (161). Within our proposed model, lower lipogenic flux may be a result of 1- reduced SREBP-1c activation via reductions in insulin concentrations, 2- lower NEFA insult secondary to improved adipose tissue

insulin sensitivity, 3- reduced dietary or circulating substrate. With regard to the final mechanism, subjects reduced carbohydrate intake and added sugars throughout the study and demonstrated enhanced peripheral insulin sensitivity. Together, both reduced substrate coming into the system and greater disposal of excess circulating carbohydrates through oxidation or storage likely lowered the flux of carbons down glycolysis and into lipogenesis. The strong negative correlations between the fractional contribution of DNL to plasma VLDL-TG palmitate and peripheral glucose disposal and VO_2 peak support this theory (**figure 4.24E-F**).

3- DNL and histology: For the first time, relationships between changes in histology and DNL were characterized. While the small sample size limited our effect sizes, our results are supported by previous work from our lab (96, 162) and others (42, 163, 164) demonstrating greater VLDL-TG DNL (or hepatic lipogenic gene/protein expression) occurring in subjects with the greatest liver fat and recent work from our lab demonstrated the same with increasing liver disease by histologic assessment (165). Interestingly, we found no relationship between changes in steatosis (histology or MRS) and fractional DNL, in opposition to a previous report (42). This may suggest changes in DNL were not the key factor in reducing IHTG in these subjects – for example, reductions in steatosis may also be induced through increased hepatic oxidation or secretion of lipid. With dietary and exercise interventions, enhanced fatty acid oxidation has been reported directly in liver tissue (166) and indirectly via calorimetry (167,

168). One mechanism behind these changes is reduction in DNL which would serve to reduce malonyl-CoA levels, a potent inhibitor of CPT, and relieve inhibition on fatty acid oxidation (169). Secretion of hepatic lipid may also serve to reduce liver fat. Improved insulin sensitivity with simultaneous reductions in insulin concentrations may increase secretion of lipotoxic lipids that are implicated in contributing to inflammation and oxidative stress (134, 170). Beyond steatosis alone, the changes in DNL were positively related to hepatocellular ballooning and fibrosis suggesting chronic relief of lipogenic flux may be beneficial for improving hepatic intracellular fat infiltration and subsequent cellular ballooning as well as tissue scarring.

4- Plasma CER in a setting of improved liver disease: Lipotoxic lipid species are implicated in the development and progression of NAFLD and NASH (171-179). In line with previous reports examining the effects of dietary (177, 180-182) and exercise (135, 183) interventions on plasma CER, we observed reduced concentrations across all subjects. However, to our surprise, baseline concentrations were negatively related to weight and fasting glucose concentrations while the change in CER demonstrated similar negative relationships with weight and fat mass loss. Even in the context of reduced CER concentrations, a greater amount within the plasma was indicative of reduced weight. Ceramide 16:0, one species that has garnered attention for its lipotoxic properties (184-187), was negatively related to changes in IHTG as measured both by liver biopsy and MRI. These relationships suggest the greater the

plasma CER 16:0 after treatment the greater the reduction in liver fat, demonstrating that even in a background of reduced total plasma CER concentrations, exporting CER from the liver, particularly lipotoxic species, may confer histologic benefits within the liver. If short term studies were to examine acute weight loss or dietary challenges, one may hypothesize an increased hepatic secretion rate of CER on VLDL particles and acute increases in plasma CER concentrations, similar to the acute effects of weight loss on adipose tissue lipolysis (188). However, we have measured CER within the whole plasma fraction rather than TRL particles, thus, we cannot exclude the possibility of differing results in plasma lipoprotein pools due to other sources of plasma CER. For example, cell culture studies demonstrate primary adipocytes secrete CER and the secretion is induced with proinflammatory marker, tumor necrosis factor alpha (TNF α) (189) which is elevated in NAFLD and NASH (190). Thus, it is likely that a portion of the plasma CER are coming from extrahepatic sources. However, strong data from humans (191) and animals (191, 192) support the liver as the primary source of plasma CER (60-80%). If that assumption is held true for the current participants, our data would suggest hepatic secretion of CER 16:0 may aid in reducing liver fat. A limitation to this hypothesis is the unknown concentration of hepatic CER before and after treatment, thus future studies should quantify changes in hepatic CER content to better identify mechanisms of CER in liver disease regression. In addition to CER quantification, dhCERs, a precursor sphingolipid to CER (**figure 1.6**), were measured in the plasma. Similar relationships were found as reported above for CER with the exception of

changes in liver steatosis. Unlike previous reports (135, 183, 193), baseline CER or dhCER (total or any acyl-chain length) did not correlate with peripheral insulin sensitivity.

Strengths, limitations, and future directions

Multiple strengths to the present study deserve mention. 1- For the first time, both repeated liver biopsies for histologic grading of disease with deep metabolic phenotyping using a multi-tracer isotope protocol to probe hepatic, adipose, and peripheral substrate metabolism were completed in subjects with advanced NASH. This remains the only study to comprehensively address the relationships between histology, EGP, R_d , and lipid metabolism within advanced NASH patients in a setting of intensive lifestyle treatment. 2- While previous studies have performed similar combined interventions, very few included *both* regular dietary counseling (i.e., weekly-monthly sessions with a registered research dietician) and supervised exercise training. Our protocol likely increased the impact of our treatment on metabolic changes and demonstrated the potential for intensive lifestyle modifications to radically improve and eradicate NASH. 3- The long-term nature of our program promoted a wide range of individual responses which allowed for greater probing of the mechanisms responsible for improved histology and insulin sensitivity.

This study also had limitations; 1- While most variables were similar at baseline across both treatment and standard care subjects, the latter group had higher

steatosis at baseline. While similar relative reductions were observed in both groups, the difference in starting liver fat, as measured histologically and by MRI/MRS imaging, may have impacted the results we observed. However, total NAS score was not statistically different between groups at baseline which suggests the other components, lobular inflammation and hepatocellular ballooning were slightly lower in the standard care subjects, even though they were not statistically different from treatment subjects (**figure 4.4** – note *P*-values for main effect of group). It is impossible for us to identify how this may have impacted the changes we observed in both groups.

2- To begin the study, the first five subjects were automatically placed into the treatment group. As such, these non-randomized subjects may have impacted our results in manners unknown to the authors. However, when the changes in histology observed in these subjects versus the remaining treatment group were compared, no differences were observed.

3- The small sample size may have contributed to increased risk of type two errors. Metabolic studies in humans are both costly and time intensive which limit the total number of potential subjects. Recruitment was also limited by both the COVID-19 shutdown of the MU liver clinic elective liver biopsies and the small number of subjects eligible for the study based on disease severity, geographical location, and willingness to participate in a long-term study with high subject burden. Nevertheless, we had excellent subject retention with only two subject discontinuations (one declined to continue and the other was removed by study personal for lack of adherence, **figure 4.2**).

4- The original goal of the lifestyle treatment was a 12% body weight loss to induce the

greatest impact on liver health. Most of the treatment subjects did not achieve this level of weight loss (3/14 subjects, 21%). Despite this, we still observed significant improvements in liver health, suggesting weight loss alone may not be the key factor in improving histology and insulin sensitivity in NASH.

Nonetheless, we cannot be certain the results would be different, had all subjects reached a weight loss of at least 12%. 5- Finally, while not a limitation, it is important to note that weight loss was evident in standard care subjects. While none achieved the 12% weight loss goal of the treatment, it is likely the standard care subjects were motivated to independently initiate lifestyle changes because they were involved in a liver health study and were recently diagnosed with an advanced, chronic liver condition.

To address novel findings reported above, future studies should include direct analysis of skeletal muscle glycogen content and synthesis along with gene and protein expression of key glycolytic and oxidative intermediates. If completed within a similar study design, measurement of local skeletal muscle changes may provide insight to the observed increases in glucose production (i.e., did depleted glycogen content signal an increase in hepatic glucose production and how?). Alternatively, observational studies are needed to profile circulating factors (i.e., exerkines, microRNA, extracellular vesicles) implicated in liver-muscle cross talk and follow-up mechanistic studies should then investigate the systems responsible for modulating hepatic glucose production. Indeed, larger studies are needed to understand differences in responders and non-responders to

lifestyle treatments in the regression of NASH and how elevated glucose production may be related to reduced histologic severity of liver disease in some but not all individuals (e.g., the reverse J shaped curve in **figure 4.29A**).

Relatedly, pharmacologics aimed at rerouting substrates away from the liver may be a promising therapeutic target. When tested with and without exercise, a better understanding of whether increased hepatic substrate secretion in the absence of increased disposal (i.e., exercise) would indeed elicit hepatic and systemic benefits. Caution should be taken as these drug targets may also increase T2D risk (increased plasma glucose) and insulin resistance.

Conclusion

Despite being the cornerstone of NASH treatment, few studies have characterized the mechanisms involved in histologic liver improvements with lifestyle modifications. Here, we demonstrated significant histologic improvements following energy restriction and exercise with particular importance placed upon the physical activity component of the program. While our results were similar to previous publications for treatment subjects, weight loss alone was not sufficient to induce histologic improvements in standard care subjects despite similar reductions in blood biochemistries and plasma liver enzymes. Finally, strong correlations suggest increased glucose production and disposal secondary to improvements in fitness and carbohydrate restriction are implicated in the observed improvements in liver histology. The results from this study support the addition of specific exercise prescriptions to the treatment and prevention of NAFLD and NASH.

EXTENDED METHODOLOGY

Modified Bruce – Exercise tolerance test

The ETT protocol is shown in extended methodology **table EM4.1**.

HIIT protocol

Subjects completed exercise sessions three times per week according to the heart rate targets shown in **extended methodology figure EM4.1** (50% HR max warm up three minutes followed by four repeated bouts of 90-95% HR max – four minutes then 50% HR max -three minutes). All exercise sessions were completed on a motorized treadmill, cycle ergometer, or elliptical. Polar heart rate monitors were used to confirm targets were achieved.

Palmitate – Extraction and GC/MS

Plasma samples were processed to isolate TRL using ultracentrifugation at 40,000 rpm at 15°C in a 50.3Ti rotor (Beckman Instruments, Palo Alto, CA) for 20h (126). The TRL fraction (two ml from the upper layer) and bottom four milliliters (FFA) was collected by tube slicing. Total lipids were extracted using the Folch method (194). The TRL-TG were separated via thin-layer chromatography and fatty acid methyl esters (FAME) were measured using a 6890N gas chromatography coupled to a 5975 mass spectrophotometry detector (Agilent Technologies, Palo Alto, CA) using a DB-225 column (20 m length, inner diameter 0.18 mm, and 0.20 µm film, Part# 121-2223, Agilent J&W GC Columns, ChromTech, Inc., Apple Valley, MN) and helium as a carrier gas. The electron impact was used to selectively monitor ions with mass/charge (m/z) ratios of M_0 ,

M1, M2, M4/16, M30, and M31. Targeted m/z ratios were 270, 271, and 272 for 16:0 labeled with deuterated water, 274 or 286 for 16:0 labeled with a $^{13}\text{C}_4$ or $^{13}\text{C}_{16}$ labeled fatty acid (adipose), and 300 and 301 for 16:0 labeled with dietary d_{31} labeled tripalmitin (all isotopes purchased from Cambridge Isotope Laboratories, Andover, MA). Comparable ion peak areas between standards (Supelco 37 Component FAME Mix, FAME37, EC# 200-838-9, Sigma, St. Louis, MO) and biological samples for the M0 (270 m/z) ion were achieved by dilution or concentration of the sample or adjustment of the volume injected. The percent DNL for 16:0 were calculated by mass isotopomer distribution analysis (129, 130). Details of GC/MS methods are shown in **extended methodology table EM4.2**.

Glucose – Extraction and GC/MS

Plasma samples (100 μL) were deproteinized with ice-cold ethanol, centrifuged and the supernatant was dried under nitrogen gas. Acetic anhydride: pyridine (1:1 vol/vol, 100 μL) was added and the samples incubated at 80°C for 30 minutes. The air vapor was recaptured, and the samples transferred to GC vials with 400 μL of ethyl acetate (final volume 500 μL). Samples were injected (one μL) into a 6890N gas chromatography coupled to a 5975 mass spectrophotometry detector (Agilent Technologies, Palo Alto, CA) using a 19091M column (30m length, inner diameter 0.250m, and 0.25 μm film, Part# 19091M-433, Agilent J&W GC Columns, ChromTech, Inc., Apple Valley, MN) and helium as a carrier gas. The oven was heated to 110°C for one minute and then ramped 15°C per minute until 240°C and held for five minutes with a final

run time of 14.667 minutes. Samples were transferred to the MS at 240°C. Selected ions (m/z : 242-247) were monitored using ChemStation. A nine-point standard curve was used to calculate percent enrichment. Details of GC/MS methods are shown in **extended methodology table EM4.3**.

Ceramide – Extraction and LC/MS

Plasma (100 μ L) samples and internal standard (CER 18:1/17:0, 50ng) were extracted with chloroform and methanol according to Bligh and Dyer (136). The bottom (organic) layer was removed and dried and the remaining water layer re-extracted, and the organic layers collapsed then dried under nitrogen gas. An azeotropic agent (methylene chloride) was used to remove any remaining water. Samples were dissolved in 100 μ L of 0.1% formic acid solution in methanol-water (85:15) and then injected (5 μ L) into a Waters HPLC device (2690 Separation Module, Milford, MA) and separated through an Vydac® 200MS™ C8 column (2.1 x 100 mm, 5 μ m, P.J.Cobert Associates, St. Louis, MO). A Thermo Scientific TSQ (Triple-Stage Quadrupole) Quantiva mass spectrometer was used for ceramide identification and the **extended methodology figure EM4.2** demonstrates the collision induced ionization of CER 18:1/16:0 (CER containing a palmitate on the fatty acyl chain) using this method. Details of GC/MS methods are shown in **extended methodology table EM4.4** and the transitions and retention times for each CER and dhCER analyzed are shown in **extended methodology table EM4.5**.

Power calculation

A power analysis (**extended methodology table EM4.6**) demonstrated 5-18 subjects would be required to detect differences in R_d , EGP, DNL, and plasma CER 16:0. With a current sample size of 19 subjects completed, we have 90% power to detect differences in these outcomes at follow-up.

Extended Methodology Tables and Figures

Table EM4.1. Modified Bruce ETT protocol

Stage	MPH	% grade	Minutes
1	1.7	0%	3
2	1.7	10%	3
3	2.5	12%	3
4	3.4	14%	3
5	4.2	16%	3
6	5.0	18%	3
7	5.5	20%	3

Table EM4.2. Detail of GC/MS methodology (palmitate)

Injection volume	1-2 μ L
Injector temperature ($^{\circ}$ C)	230 $^{\circ}$ C
Transfer line temperature ($^{\circ}$ C)	230 $^{\circ}$ C
Oven	0-1 minutes: 70 $^{\circ}$ C 2-9.67 minutes: 110 $^{\circ}$ C to 240 $^{\circ}$ C (15 $^{\circ}$ C/min) 9.67-4.67 minutes: 240 $^{\circ}$ C

Table EM4.3. Detail of GC/MS methodology (glucose)

Injection volume	1 μ L
Injector temperature ($^{\circ}$ C)	240 $^{\circ}$ C
Transfer line temperature ($^{\circ}$ C)	240 $^{\circ}$ C
Oven	0-3.75 minutes: 70 $^{\circ}$ C to 220 $^{\circ}$ C (40 $^{\circ}$ C/min) 3.75-8.75 minutes: 220 $^{\circ}$ C 8.75-10.75 minutes: 220 $^{\circ}$ C to 230 $^{\circ}$ C (5 $^{\circ}$ C/min) 10.75-14.75 minutes: 230 $^{\circ}$ C

Table EM4.4. Detail of LC/MS methodology (ceramide)

Mobile phases	C) Water + 0.2% formic acid D) Acetonitrile/2-propanol (50/50)+ 0.2% formic acid
Flow	0.3 mL/min
Gradient	0-3 minutes: 65% B 1-4 minutes: 65%B to 100%B 4-16 minutes: 100%B 16-16.1 minutes: 100%B to 65%B 16.1-22 minutes: 65%B

Table EM4.5. Transitions and retention time for all CER and dhCER species analyzed

Ceramide	Transition (m/z)	Retention time (minutes)
18:1/17:0	552.6 → 264	4.42
18:1/14:0	510.5 → 264	4.10
18:1/16:0	538.5 → 264	4.32
18:1/18:1	564.4 → 264	4.35
18:1/18:0	566.4 → 264	4.50
18:1/20:0	594.4 → 264	4.69
18:1/22:0	622.6 → 264	4.84
18:1/24:1	648.6 → 264	4.81
18:1/24:0	650.6 → 264	4.98
Dihydroceramide	Transition (m/z)	Retention time (minutes)
18:0/16:0	540.6 → 266	4.40
18:0/18:0	568.4 → 266	4.57
18:0/24:1	650.6 → 266	4.88
18:0/24:0	652.6 → 266	4.98

Table EM4.6. Power calculation based on previous studies

Repeated measures	Pre-	Post-	Pooled SD	Power	Alpha	n
Increased in R_d^1	4.5	5.7	1.1	90%	0.05	18
Increased in R_d^2	45.1	52.7	5.0	90%	0.05	9
Reduction in EGP ²	3.4	2.3	0.5	90%	0.05	5
Reduction in EGP ³	190	155	20.0	90%	0.05	7
Reduction in DNL ⁴	20.1%	7.2%	9.0%	90%	0.05	14
Reduction in CER 16:0 ⁵	2.6	1.8	0.5	90%	0.05	10

¹ Data from ref. (29), Ex treatment; clamp units: mmol/kg FFM/min/ (pmol/L)

² Data from ref. (36), EX treatment; clamp units are $\mu\text{mol/kg/min}$

³ Data from ref. (57), CR in T2D (9% weight loss); clamp units: mg/min

⁴ Data from ref. (96); CR in NAFLD (10% weight loss); units: % VLDL-TG palmitate

⁵ Data from ref. (171); Plasma CER - EX treatment in T2D (5% weight loss); units: nmol/mL

Figure EM4.1. Heart rate target for HIIT sessions

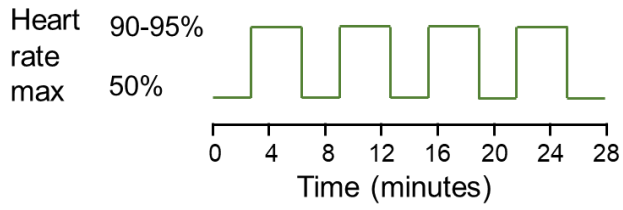
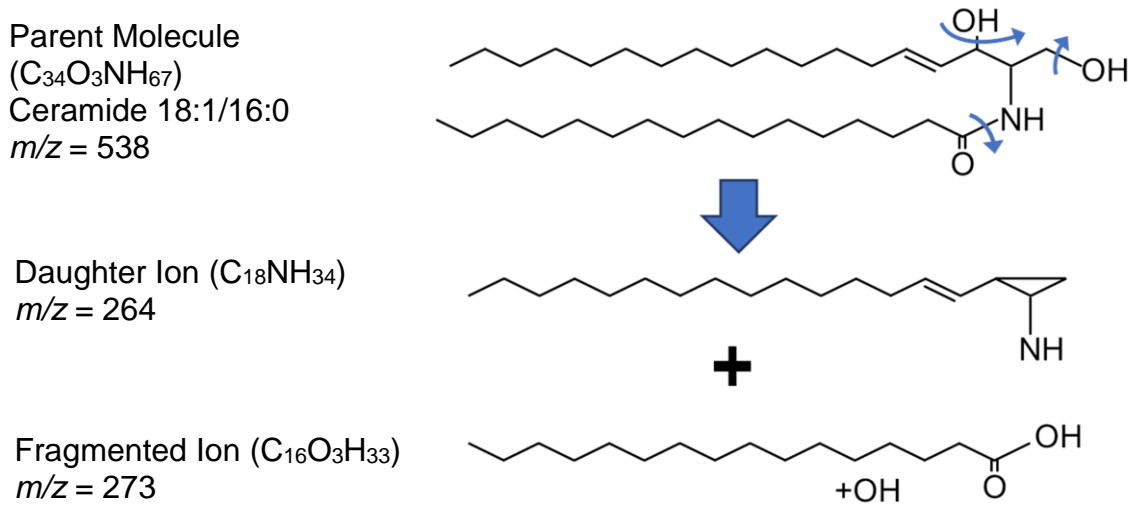


Figure EM4.2. Collision induced ionization of CER 18:1/16:0



TABLES

Table 4.1. Criteria for inclusion and exclusion in Phase II

Criteria for Inclusion

1. Men and women (pre- and post-menopausal)
2. Overweight/obese with BMI ≥ 25.9 or ≤ 50.0 kg/m²
3. Characteristics of the metabolic syndrome, pre-diabetes (fasting glucose 100-125 mg/dL or 2h glucose 140-200 mg/dL) or type 2 diabetes
4. 22-65 years of age
5. Sedentary, ≤ 60 minutes per week of structured physical activity
6. Alcohol intake < 20 g/d

Criteria for Exclusion

1. Acute disease or advanced cardiac or renal disease, anticoagulation therapy, or any severe co-morbid condition limiting life expectancy < 1 year
2. Other causes of hepatitis including hepatitis B & C, autoimmune hepatitis, hemochromatosis, celiac disease, Wilson's disease, alpha-1-antitrypsin deficiency, medication-induced hepatitis, any clinical or biochemical evidence of decompensated liver disease
3. Use of medications that interfere with lipid, protein, or carbohydrate metabolism (steroids, niacin, etc)
4. Pregnant or trying to become pregnant
5. Alcohol intake > 20 g/d
6. Inability to exercise on a bike or treadmill
7. Contraindications of MRS/MRI

Table 4.2. Phase one subject characteristics

Characteristic	Mean \pm SD (n = 98 ¹)
Sex (m/f)	31/67
Age (y)	47 \pm 11
Body weight (kg)	112 \pm 24
BMI (kg/m ²)	39.4 \pm 7.8
AST (U/L) ²	44 \pm 29
ALT (U/L)	58 \pm 37
Cholesterol (mg/dL)	171 \pm 41
LDL (mg/dL) ³	98 \pm 33
HDL (mg/dL)	43 \pm 14
Triglycerides (mg/dL)	185 \pm 133
Glucose (mg/dL)	97 \pm 50
HbA1c (%)	6.8 \pm 1.7%
Type 2 diabetes	48 (49%)
Hyperlipidemia	67 (68%)
Hypertension	49 (50%)
Former smoker	19 (19%)
NAS (0-8) ⁴	4.9 \pm 1.5
Steatosis (0-3)	2.2 \pm 0.6
Lobular Inflammation (0-3)	1.5 \pm 0.7
Hepatocellular ballooning (0-2)	1.2 \pm 0.7
Fibrosis (0-4)	1.2 \pm 1.4

Data expressed as a mean \pm SD or n (%).

¹ Unless otherwise noted.

² n = 97, one sample not analyzed d/t hemolysis

³ Calculated; n = 91, 7 samples had too high [TG] to accurately calculate

⁴ NAS, NAS components, and fibrosis are presented with a decimal (despite whole number scores) to demonstrate subtle differences between groups; n = 97 – two subjects did not have tissues available.

Table 4.3. Baseline phase two subject characteristics

	Treatment (n = 18)	Standard Care (n = 8)	P-value
Sex (m/f)	7/11	2/6	
Age (y)	47 ± 10	47 ± 10	0.937
Body weight (kg) ¹	116 ± 23	108 ± 24	0.383
BMI (kg/m ²)	40.2 ± 7.7	37.3 ± 7.2	0.379
Body fat (%)	45 ± 9%	45 ± 8%	0.914
AST (U/L)	51 ± 39	47 ± 32	0.768
ALT (U/L)	57 ± 34	69 ± 51	0.463
Cholesterol (mg/dL)	161 ± 34	185 ± 37	0.118
LDL (mg/dL) ²	89 ± 28	103 ± 25	0.298
HDL (mg/dL)	40 ± 9	37 ± 13	0.437
Triglycerides (mg/dL)	214 ± 140	343 ± 265	0.114
NEFA (mmol/L)	0.69 ± 0.16	0.78 ± 0.17	0.199
Glucose (mg/dL)	152 ± 58	139 ± 41	0.582
Insulin (uIU/mL)	17 ± 13	20 ± 10	0.466
HbA1c (%)	7.3 ± 1.5%	7.0 ± 1.6%	0.632
Type 2 diabetes ³	12 (67%)	6 (75%)	0.343
Metformin	11 (61%)	7 (88%)	0.193
Insulin	3 (17%)	1 (14%)	0.445
Sulfonyurea	3 (17%)	0 (0%)	0.134
Statin	10 (56%)	3 (38%)	0.208
DPP4 inhibitor	1 (6%)	1 (14%)	0.245
GLP-1 agonist	3 (17%)	3 (38%)	0.279
SGLT-2 inhibitor	6 (50%)	1 (13%)	0.343
Liver fat by MRS (%)	15.7 ± 7.6%	24.4 ± 10.8%	0.029
NAS (0-8) ⁴	5.4 ± 1.1	5.4 ± 1.1	0.886
Steatosis (0-3)	2.2 ± 0.5	2.6 ± 0.5	0.047
Lobular Inflammation (0-3)	1.7 ± 0.6	1.5 ± 0.5	0.503
Hepatocellular ballooning (0-2)	1.6 ± 0.5	1.3 ± 0.7	0.149
Fibrosis (0-4)	1.9 ± 1.4	1.5 ± 1.7	0.488

Data expressed as a mean ± SD or n (%); unpaired, two-tailed students *t*-tests.

¹ From baseline (phase one) biopsy.

² Calculated (excluding one treatment and two control subjects due to too high [TG] to accurately calculate).

³ Concomitant medications at baseline.

⁴ NAS, NAS components, and fibrosis are presented with a decimal (despite whole number scores) to demonstrate subtle differences between groups.

Table 4.4. Blood lipids

Concentration (mg/dL)	Treatment (n = 14)			Standard Care (n = 5)			<i>P</i> -value
	Baseline	Interim	Follow-up	Baseline	Interim	Follow-up	Interaction
TG	219 ± 25	166 ± 32	169 ± 27	343 ± 94	239 ± 31	224 ± 51	0.809
TRL-TG	157 ± 49	84 ± 15	91 ± 16	177 ± 54	160 ± 30	145 ± 33	0.615
Total cholesterol	168 ± 9	172 ± 9	156 ± 9	185 ± 15	179 ± 32	162 ± 18	0.813
HDL cholesterol	40 ± 3	42 ± 2	39 ± 2	33 ± 2	35 ± 3	34 ± 1	0.809
LDL cholesterol ¹	95 ± 8	103 ± 8	90 ± 7	115 ± 5	107 ± 25	98 ± 13	0.723
VLDL cholesterol ¹	31 ± 3	25 ± 2	28 ± 3	30 ± 8	37 ± 7	31 ± 6	0.466

Data expressed as a mean ± SEM.

P-value from interaction term of mixed model ANOVA (group x time).

¹ Calculated: Excluding one subject from treatment and two subjects from standard care due to too high [TG] to accurately calculate.

Table 4.5. Hepatic and peripheral insulin sensitivity and insulin-stimulated substrate metabolism

	Treatment (n = 14)		Standard Care (n = 5)		P-value ¹
	Baseline	Follow-up	Baseline	Follow-up	
<i>EGP (μmol/min)</i>					
Fasting [#]	1,339 ± 92	1,222 ± 49	1,352 ± 130	1,205 ± 113	0.817
Clamp - low insulin ^{2,*}	757 ± 57	675 ± 24	785 ± 72	663 ± 62	0.634
% suppression	43 ± 2%	44 ± 1%	42 ± 3%	44 ± 4%	0.681
Clamp - high insulin ³	503 ± 58	499 ± 40	527 ± 44	454 ± 52	0.480
% suppression	62 ± 4%	59 ± 3%	61 ± 3%	62 ± 2%	0.521
<i>R_d (μmol/min)</i>					
Fasting [#]	1,364 ± 93	1,246 ± 50	1,378 ± 134	1,228 ± 116	0.811
Clamp - low insulin [#]	1,423 ± 119	1,180 ± 78	1,368 ± 178	1,042 ± 435	0.712
Clamp - high insulin [§]	2,323 ± 179	2,887 ± 271	1,692 ± 158	1,600 ± 147	0.186
<i>NEFA (mmol/L)</i>					
Fasting [*]	0.73 ± 0.04	0.64 ± 0.06	0.79 ± 0.09	0.67 ± 0.07	0.628
Clamp - low insulin [§]	0.43 ± 0.03	0.37 ± 0.04	0.50 ± 0.03	0.51 ± 0.10	0.391
% suppression	40 ± 4%	40 ± 4%	34 ± 6%	27 ± 8%	0.495
Clamp - high insulin	0.17 ± 0.04	0.07 ± 0.01	0.20 ± 0.05	0.14 ± 0.03	0.506
% suppression [*]	76 ± 4%	87 ± 2%	72 ± 8%	79 ± 6%	0.576
<i>Substrate Oxidation</i>					
Fasting RQ ⁴	0.78 ± 0.01	0.77 ± 0.01	0.78 ± 0.02	0.74 ± 0.03	0.194
Clamp RQ [*]	0.80 ± 0.01	0.79 ± 0.01	0.81 ± 0.02	0.75 ± 0.02	0.313
Fasting GluOx ⁵	0.71 ± 0.09	0.68 ± 0.12	0.83 ± 0.25	0.55 ± 0.09	0.233
Clamp GluOx ⁶	0.91 ± 0.13	0.79 ± 0.09	1.04 ± 0.18	0.59 ± 0.13	0.529
Fasting Glu NonOx ^{7*}	1.33 ± 0.11	1.51 ± 0.14	1.37 ± 0.17	1.70 ± 0.14	0.377
Clamp Glu NonOx ^{§,‡}	2.61 ± 0.30	3.97 ± 0.56	1.69 ± 0.16	2.18 ± 0.16	0.405
Fasting FatOx ^{8, ‡}	0.86 ± 0.05	0.94 ± 0.08	0.97 ± 0.03	1.21 ± 0.16	0.284
Clamp FatOx [*]	0.75 ± 0.07	0.82 ± 0.08	0.79 ± 0.10	1.08 ± 0.17	0.207

Data expressed as a mean ± SEM or n (%);

Treatment: n = 14, standard care: n = 5, unless otherwise noted below.

¹ Mixed model ANOVA (P-value from interaction term group x time).

* P < 0.05 - Main effect of visit

P < 0.1 - Main effect of visit

§ P < 0.05 - Main effect of group

‡ P < 0.1 - Main effect of group

² Step one: Seven mU/m²/minute.

³ Step two: 50 mU/m²/minute.

⁴ Respiratory Quotient (CO₂/O₂); Missing data from one standard care subject.

- ⁵ Glucose oxidation (mg/kg/min); Missing data from one treatment and two standard care subjects.
- ⁶ Missing data from one standard care subject.
- ⁷ Nonoxidative glucose metabolism (mg/kg/min; glucose disposal – glucose oxidation); Missing data for one treatment subject.
- ⁸ Lipid oxidation (mg/kg/min); Missing data from one standard care subject.

FIGURES

Figure 4.1. Overall study design

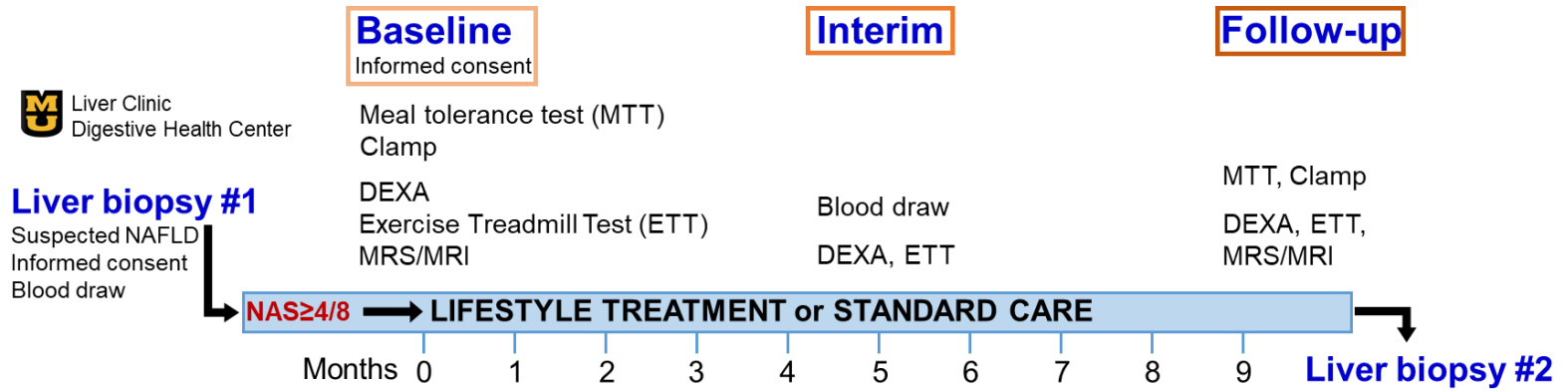
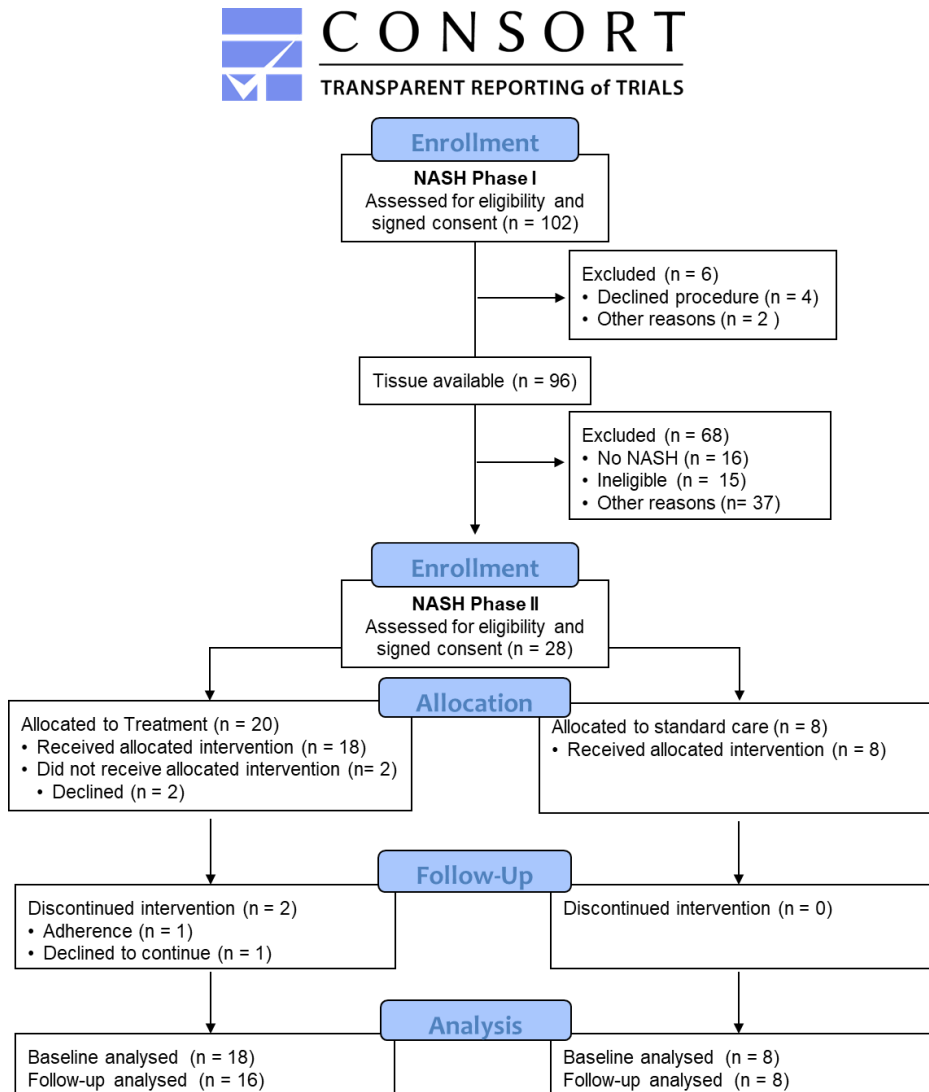


Figure 4.2. Participant recruitment



Note: The follow-up and analysis sections are the anticipated samples sizes once all subjects complete follow-up testing. For the present analysis, a total of 14 treatment and five standard care subjects have completed follow-up testing and are included in all subsequent analyses.

Figure 4.3. Metabolic testing day study design (repeated at baseline and follow-up in all subjects)

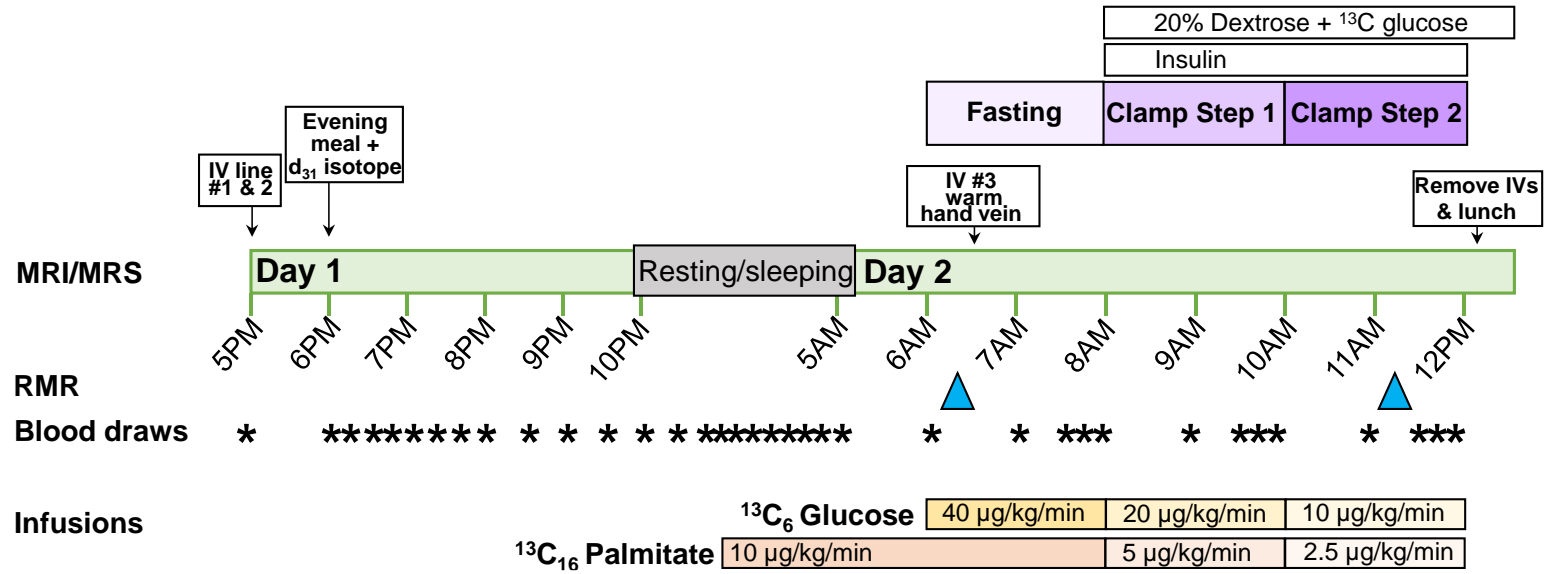
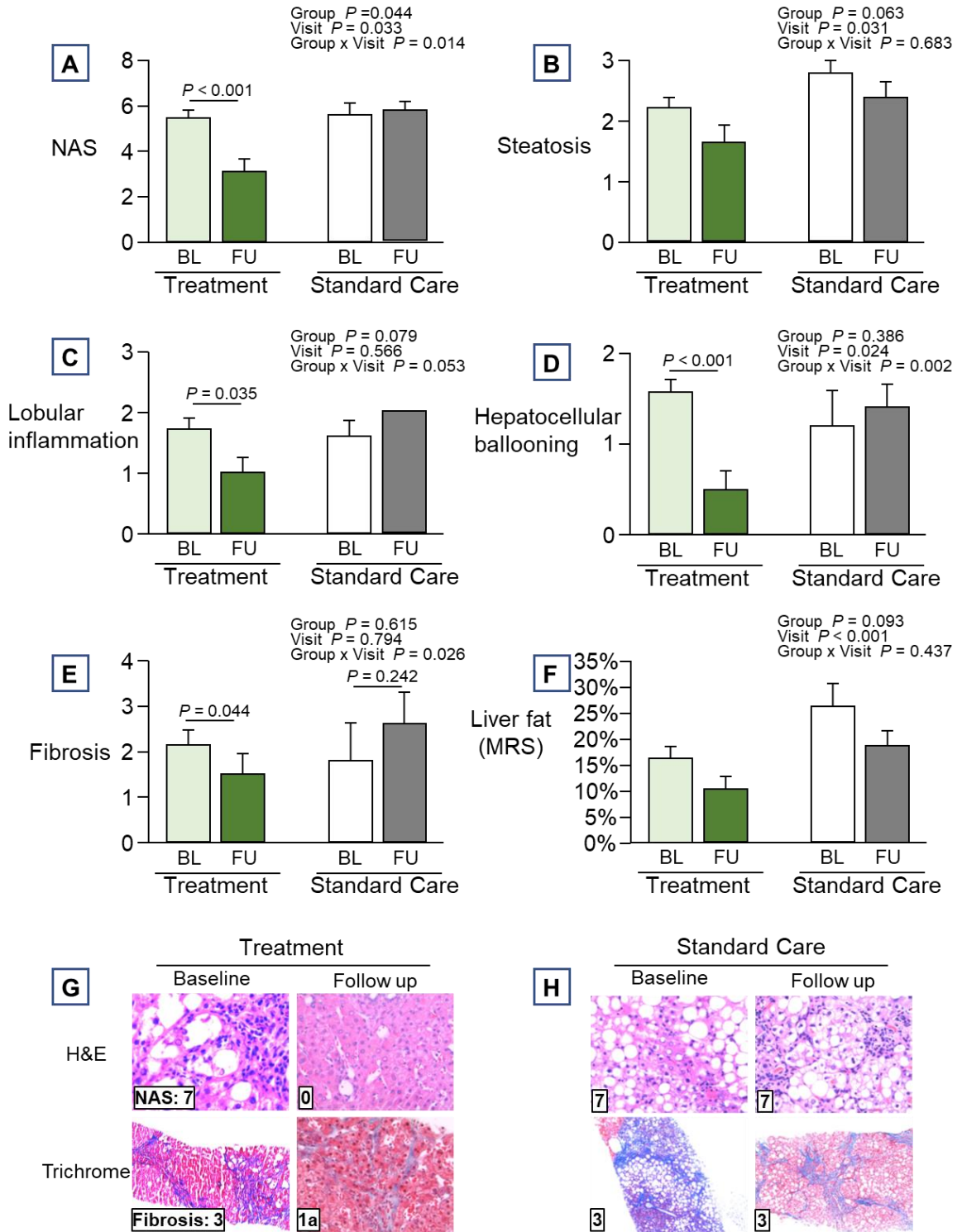


Figure 4.4. Changes in liver histology



Data are presented as mean ± SEM; A-F: Treatment: *n* = 14, Standard care: *n* = 5; H: Treatment: *n* = 12, Standard care: *n* = 5.

Mixed model ANOVA with post-hoc pairwise comparisons for significant interactions with Bonferroni adjustment.

A: Changes in NAS.

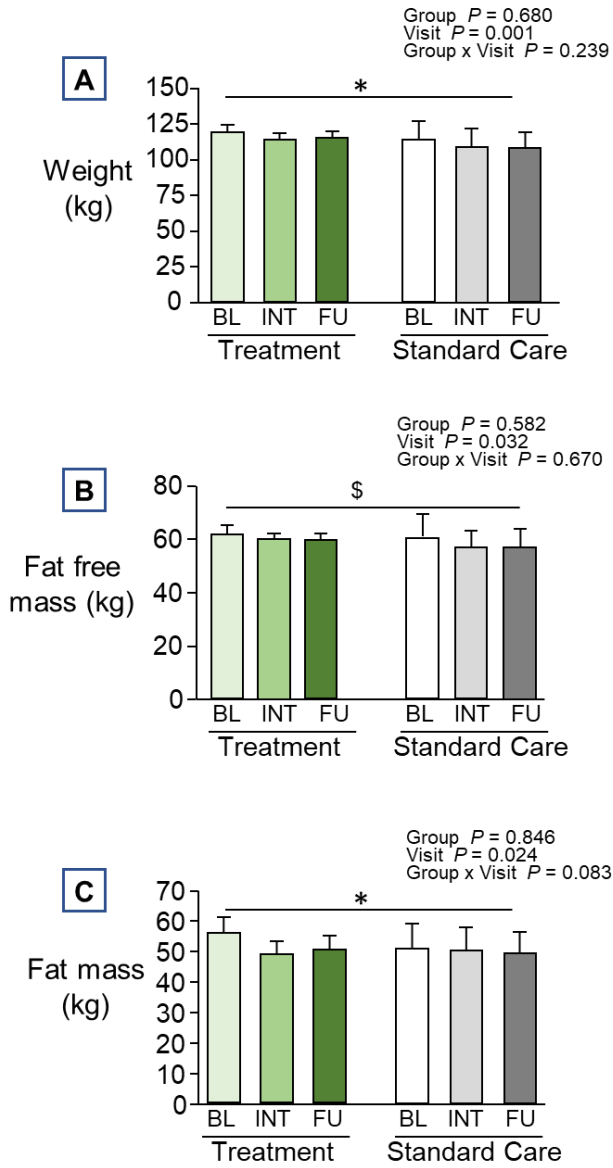
B-D: Changes in the NAS components – (**B**) steatosis, (**C**) lobular inflammation, (**D**) hepatocellular ballooning.

E: Changes in fibrosis.

F: Changes in liver fat by MRS.

G-H: Representative liver H&E and trichrome staining for (**G**) treatment and (**H**) standard care groups.

Figure 4.5. Changes in anthropometrics

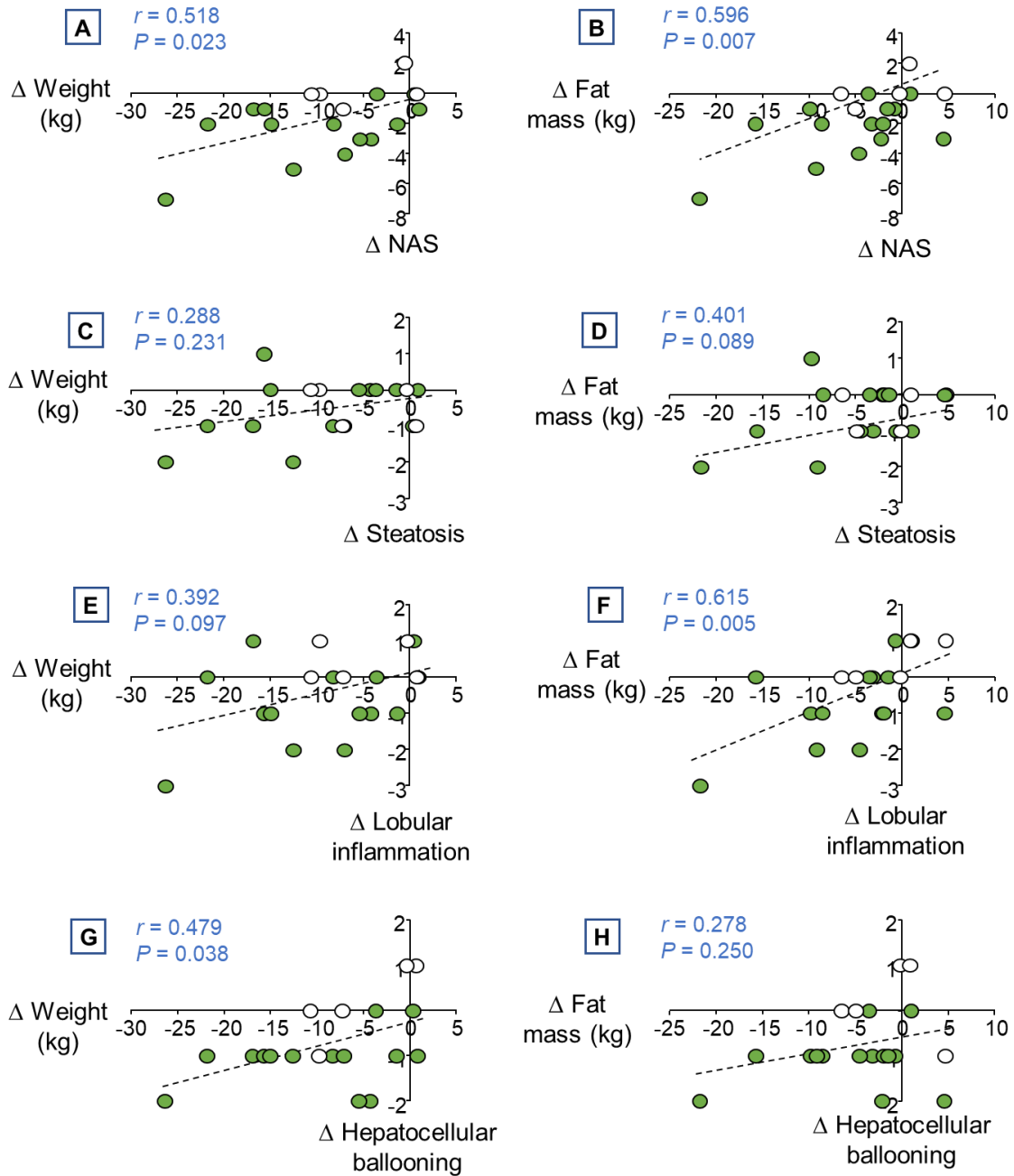


Data are presented as mean \pm SEM; Treatment: $n = 14$, Standard care: $n = 5$. Mixed model ANOVA (group x time) with post-hoc pairwise comparisons for significant interactions with Bonferroni adjustment.

A: Changes in total body weight.

B-C: Changes in body composition - **(B)** fat free mass and **(C)** fat mass.

Figure 4.6. Relationships between changes in liver histology, weight, and fat mass



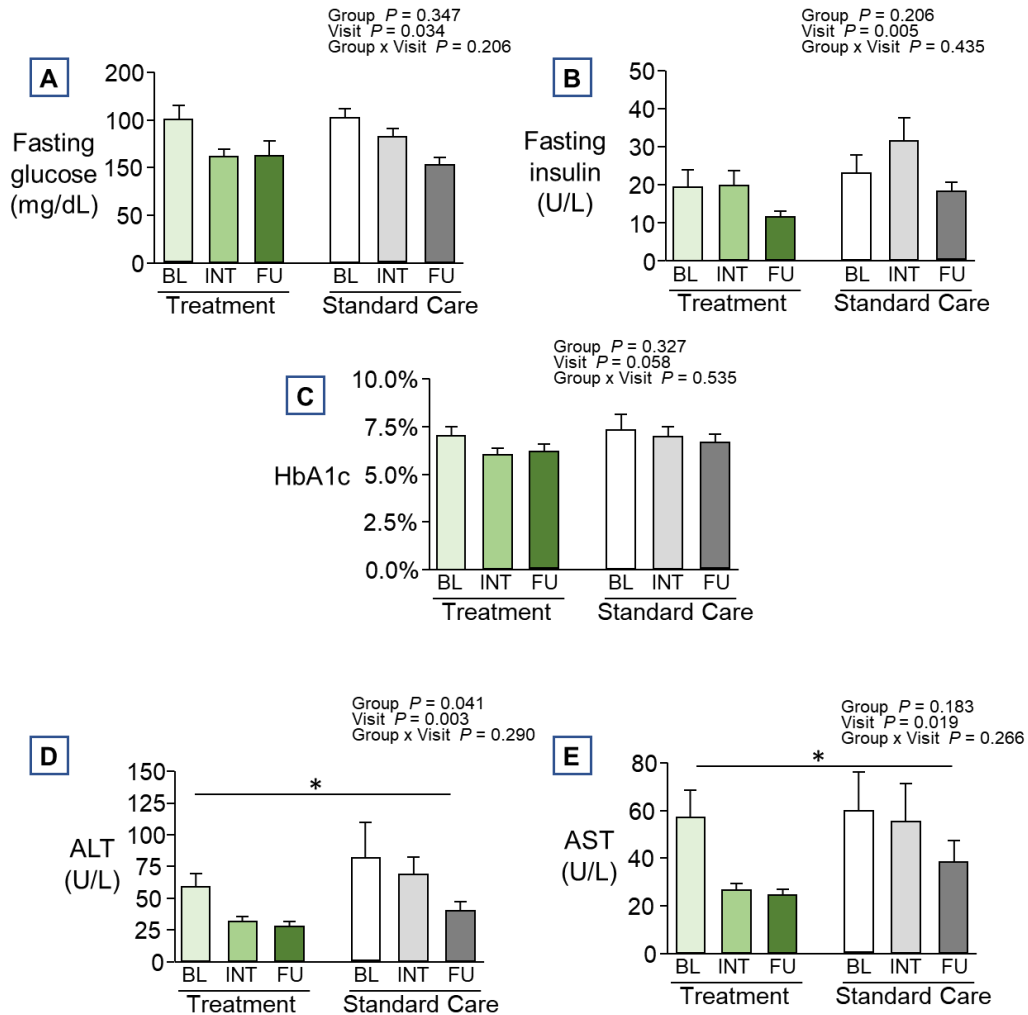
Spearman's correlation was used to assess linear relationships between ranked and continuous variables. Treatment subjects are shown in green circles and standard care in open circles. Treatment: $n = 14$, Standard care: $n = 5$.

A-B: Relationships between changes in NAS and (A) total body weight and (B) fat mass.

C-D: Relationships between changes in steatosis and (C) total body weight and (D) fat mass.

- E-F:** Relationships between changes in lobular inflammation and (**E**) total body weight and (**F**) fat mass.
- G-H:** Relationships between changes in hepatocellular ballooning and (**G**) total body weight and (**H**) fat mass.

Figure 4.7. Changes in fasting blood biochemistries



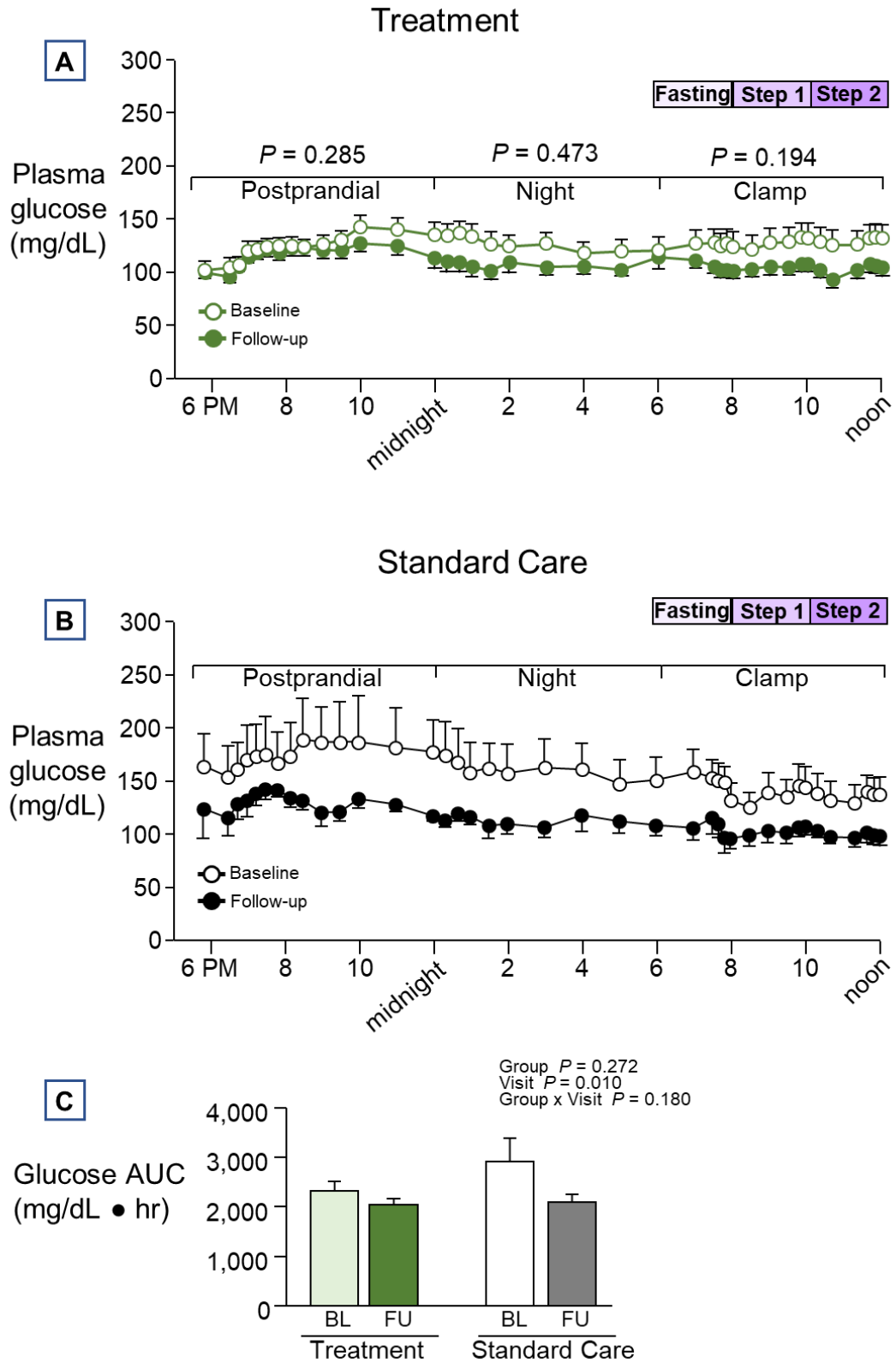
Data are presented as mean \pm SEM; Treatment: $n = 14$, Standard care: $n = 5$. Mixed model ANOVA with post-hoc pairwise comparisons for significant main effect of visit with Bonferroni adjustment.

* $P < 0.05$ BL vs INT and FU (main effect of visit)

A-C: Changes in fasting (A) glucose, (B) insulin, and (C) HbA1c.

D-E: Changes in plasma liver enzymes - (D) ALT and (E) AST.

Figure 4.8. 18-hour dynamics of plasma glucose

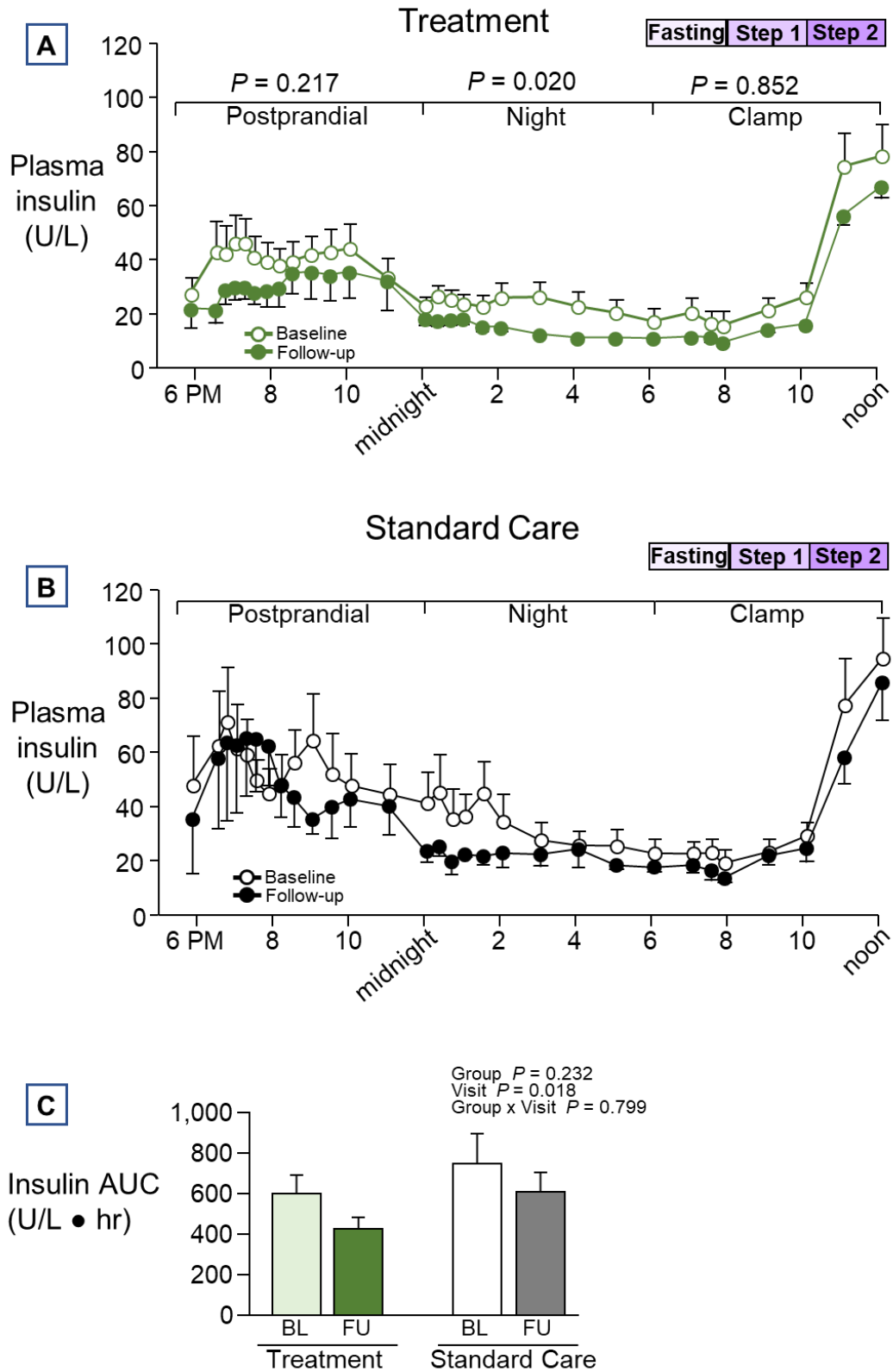


Data are presented as mean \pm SEM; Treatment: $n = 14$, Standard care: $n = 5$ – individual data points missed were filled by averaging the values before and after. The 18-hour overnight study was divided in three time periods for analysis: 6PM to midnight (postprandial), midnight to 6AM (nighttime), and 6AM to noon (clamp).

A-B: Glucose concentrations in treatment (**A**, green) and standard care (**B**, black) groups at baseline (open circles) and follow-up (closed circles). *P*-values represent the interaction term (group x visit x time, mixed model ANOVA) and **supplementary table S4.1A** demonstrates individual comparisons.

C: Total area under the curve (AUC, see related **supplementary figure S4.2A** for individual time segments). Mixed model ANOVA with post-hoc pairwise comparisons for significant main effect of visit with Bonferroni adjustment.

Figure 4.9. 18-hour dynamics of plasma insulin

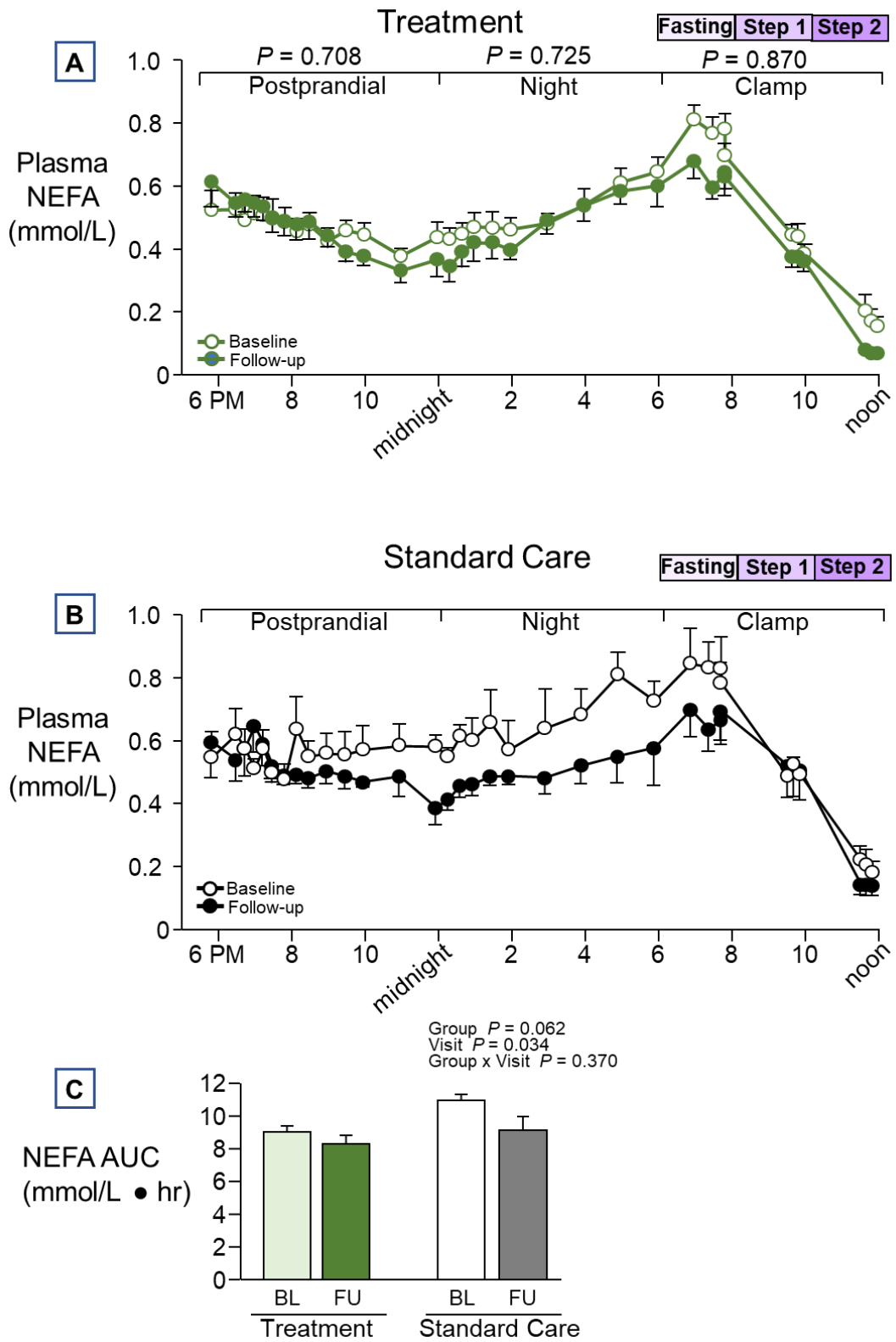


Data are presented as mean \pm SEM; Treatment: $n = 14$, Standard care: $n = 5$ – individual data points missed were filled by averaging the values before and after. The 18-hour overnight study was divided in three time periods for analysis: 6PM to midnight (postprandial), midnight to 6AM (nighttime), and 6AM to noon (clamp).

A-B: Insulin concentrations in treatment (**A**, green) and standard care (**B**, black) groups at baseline (open circles) and follow-up (closed circles). *P*-values represent the interaction term (group x visit x time, mixed model ANOVA) and **supplementary table S4.1B** demonstrates individual comparisons.

C: Total area under the curve (AUC, see related **supplementary figure S4.2B** for individual time segments). Mixed model ANOVA with post-hoc pairwise comparisons for significant main effect of visit with Bonferroni adjustment.

Figure 4.10. 18-hour dynamics of plasma NEFA

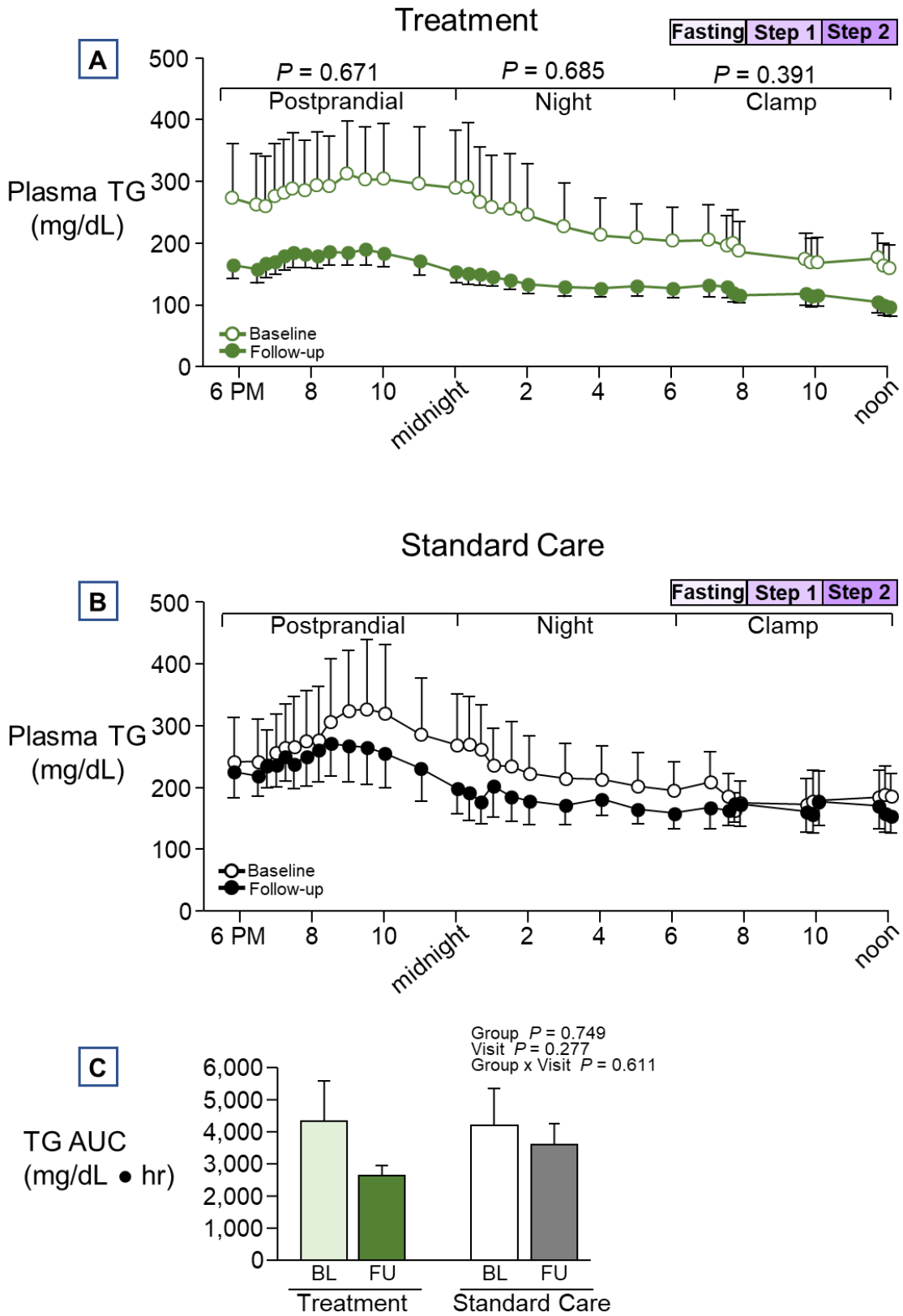


Data are presented as mean \pm SEM; Treatment: $n = 14$, Standard care: $n = 5$ – individual data points missed were filled by averaging the values before and after. The 18-hour overnight study was divided in three time periods for analysis: 6PM to midnight (postprandial), midnight to 6AM (nighttime), and 6AM to noon (clamp).

A-B: NEFA concentrations in treatment (**A**, green) and standard care (**B**, black) groups at baseline (open circles) and follow-up (closed circles). P -values represent the interaction term (group x visit x time, mixed model ANOVA) and **supplementary table S4.1C** demonstrates individual comparisons.

C: Total area under the curve (AUC, see related **supplementary figure S4.2C** for individual time segments). Mixed model ANOVA with post-hoc pairwise comparisons for significant main effect of visit with Bonferroni adjustment.

Figure 4.11. 18-hour dynamics of plasma TG

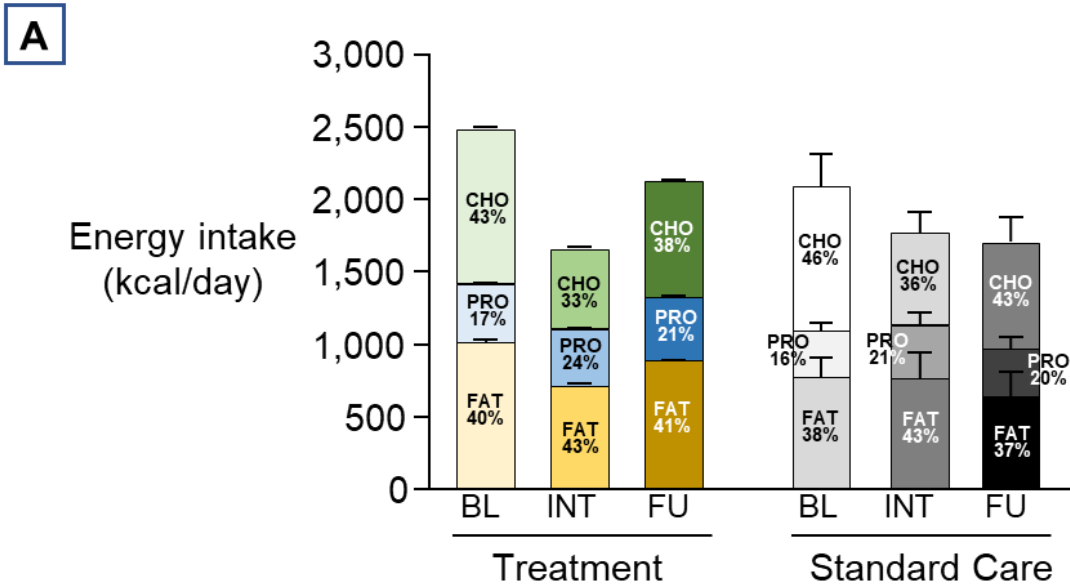


Data are presented as mean \pm SEM; Treatment: $n = 14$, Standard care: $n = 5$ – individual data points missed were filled by averaging the values before and after. The 18-hour overnight study was divided in three time periods for analysis: 6PM to midnight (postprandial), midnight to 6AM (nighttime), and 6AM to noon (clamp).

A-B: TG concentrations in treatment (**A**, green) and standard care (**B**, black) groups at baseline (open circles) and follow-up (closed circles). P -values represent the interaction term (group x visit x time, mixed model ANOVA) and **supplementary table S4.1D** demonstrates individual comparisons.

C: Total area under the curve (AUC, see related **supplementary figure S4.2D** for individual time segments). Mixed model ANOVA with post-hoc pairwise comparisons for significant main effect of visit with Bonferroni adjustment. * $P < 0.05$ BL vs INT and FU (main effect of visit).

Figure 4.12. Changes in energy intake and macronutrients



B

	Group	Visit	Group x Visit
Total Kcal	0.403	0.005*	0.174
CHO	0.995	0.0001**	0.552
PRO	0.183	0.704	0.348
FAT	0.299	0.313	0.266

Data are presented as mean \pm SEM. Treatment: $n = 13$, Standard care: $n = 5$; BL, baseline; INT, interim; FU, follow-up.

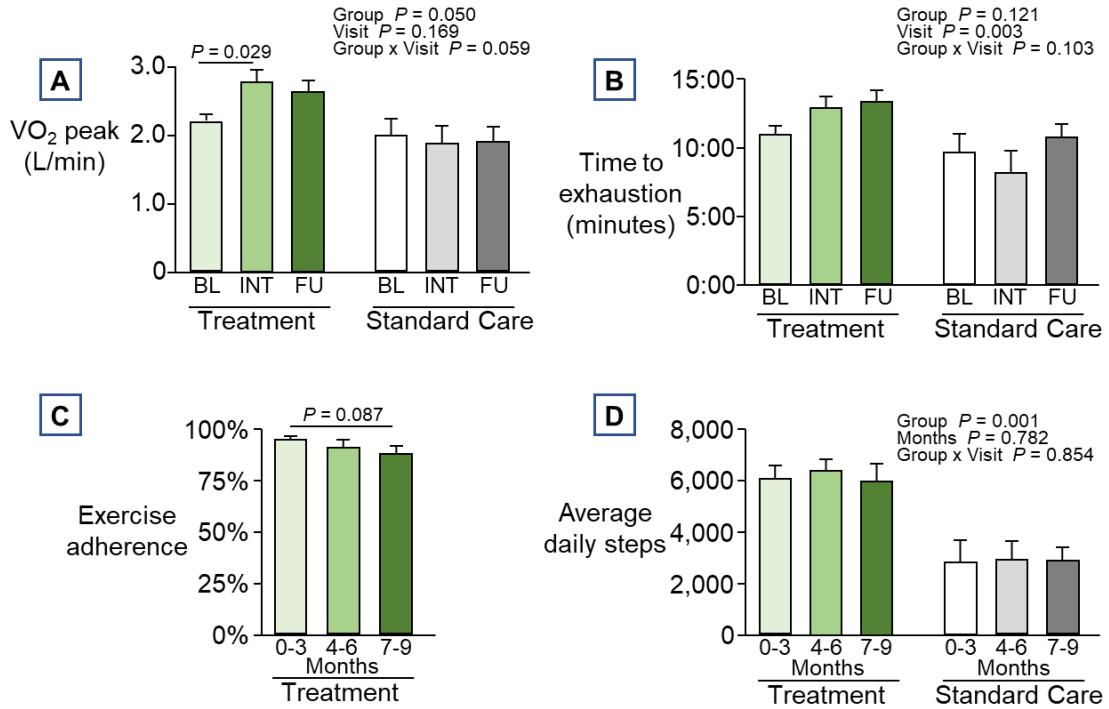
A: Changes in total energy intake and the proportion of carbohydrates (CHO), protein (PRO), and fat (FAT).

B: Results from the mixed model ANOVA with post-hoc pairwise comparisons for significant main effect of visit with Bonferroni adjustment.

* $P < 0.05$ BL vs INT and FU (main effect of visit)

** $P < 0.01$ BL vs INT and FU (main effect of visit)

Figure 4.13. Fitness and physical activity



Data are presented as mean \pm SEM; Treatment: $n = 12$, Standard care: $n = 5$.

A, B, D: Mixed model ANOVA with post-hoc pairwise comparisons for significant interactions with Bonferroni adjustment.

C: One-way repeated measures ANOVA; ($n = 14$).

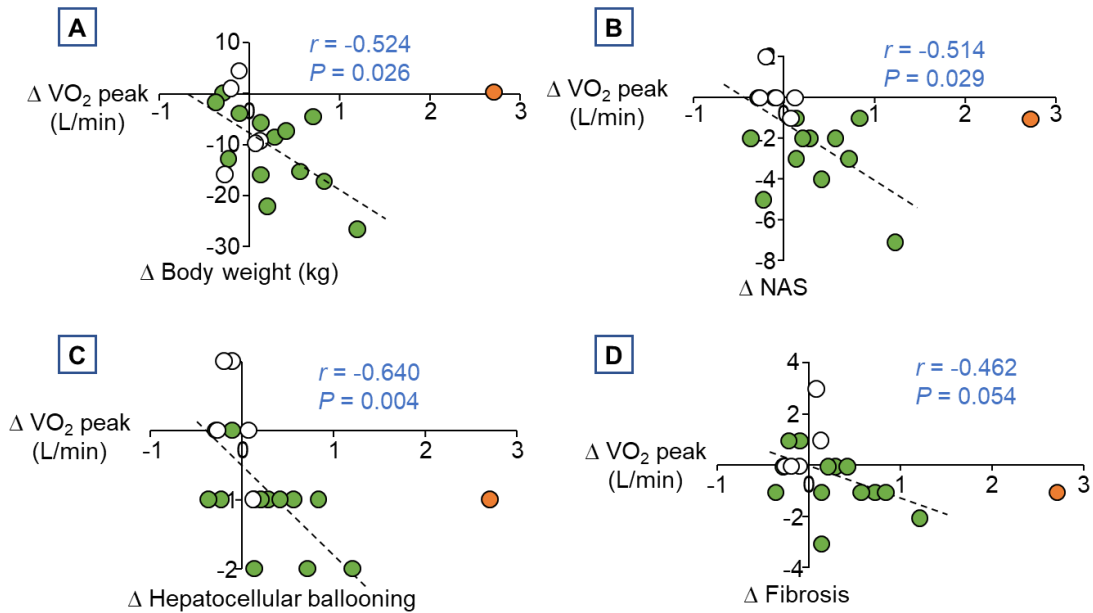
A: Changes in maximal respiratory capacity.

B: Changes in time to exhaustion during the maximal exercise test.

C: Exercise adherence throughout the program for treatment subjects.

D: Changes in average daily steps.

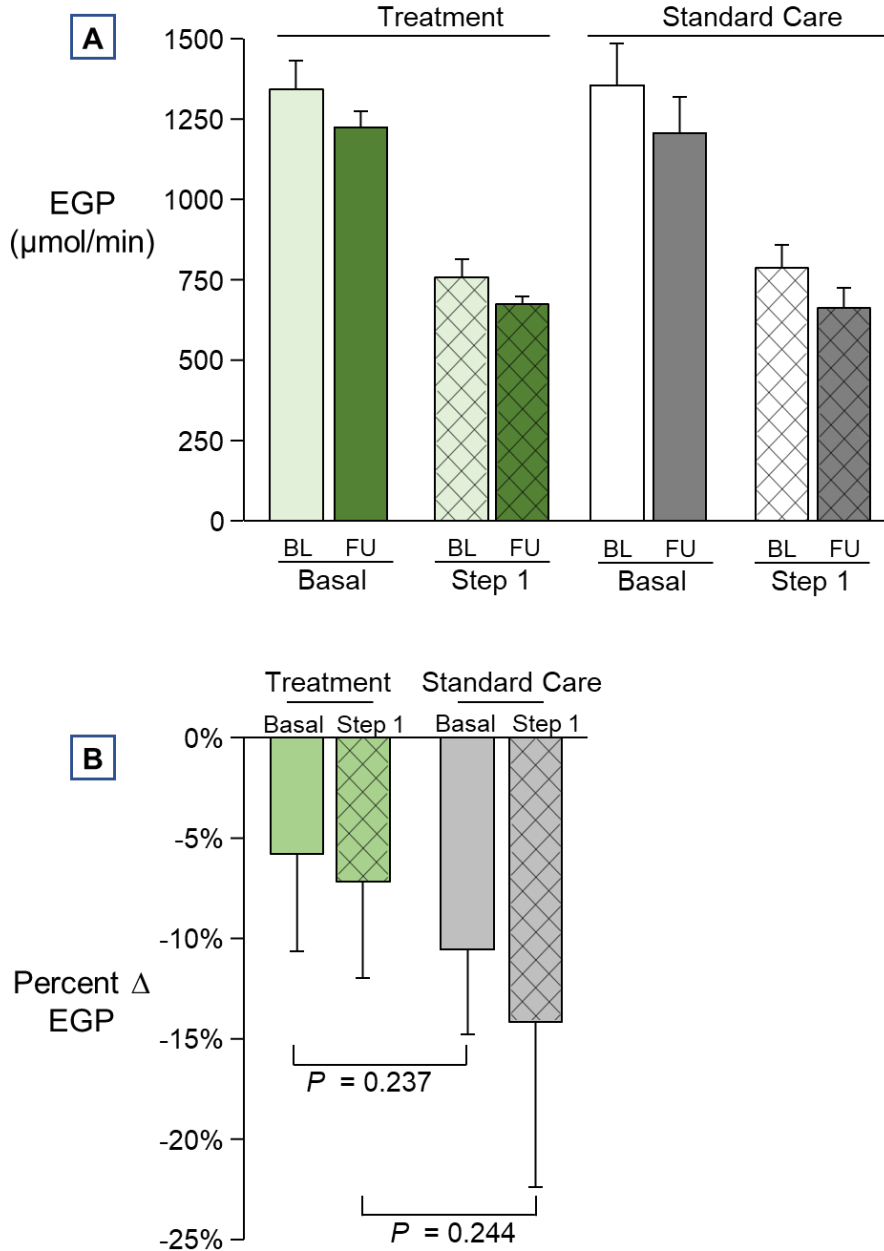
Figure 4.14. Changes in VO₂ peak with changes in body weight and NAS



Spearman's correlation was used to assess linear relationships between ranked and continuous variables. Treatment subjects are shown in green circles and standard care in open circles. One outlying treatment subject was excluded from the correlation analysis but included in the figures (orange circle). Treatment: $n = 13$, Standard care: $n = 5$.

A-D: Relationships between changes in VO₂ peak and (A) body weight, (B) NAS, (C) hepatocellular ballooning, and (D) fibrosis.

Figure 4.15. Absolute glucose production and percent change

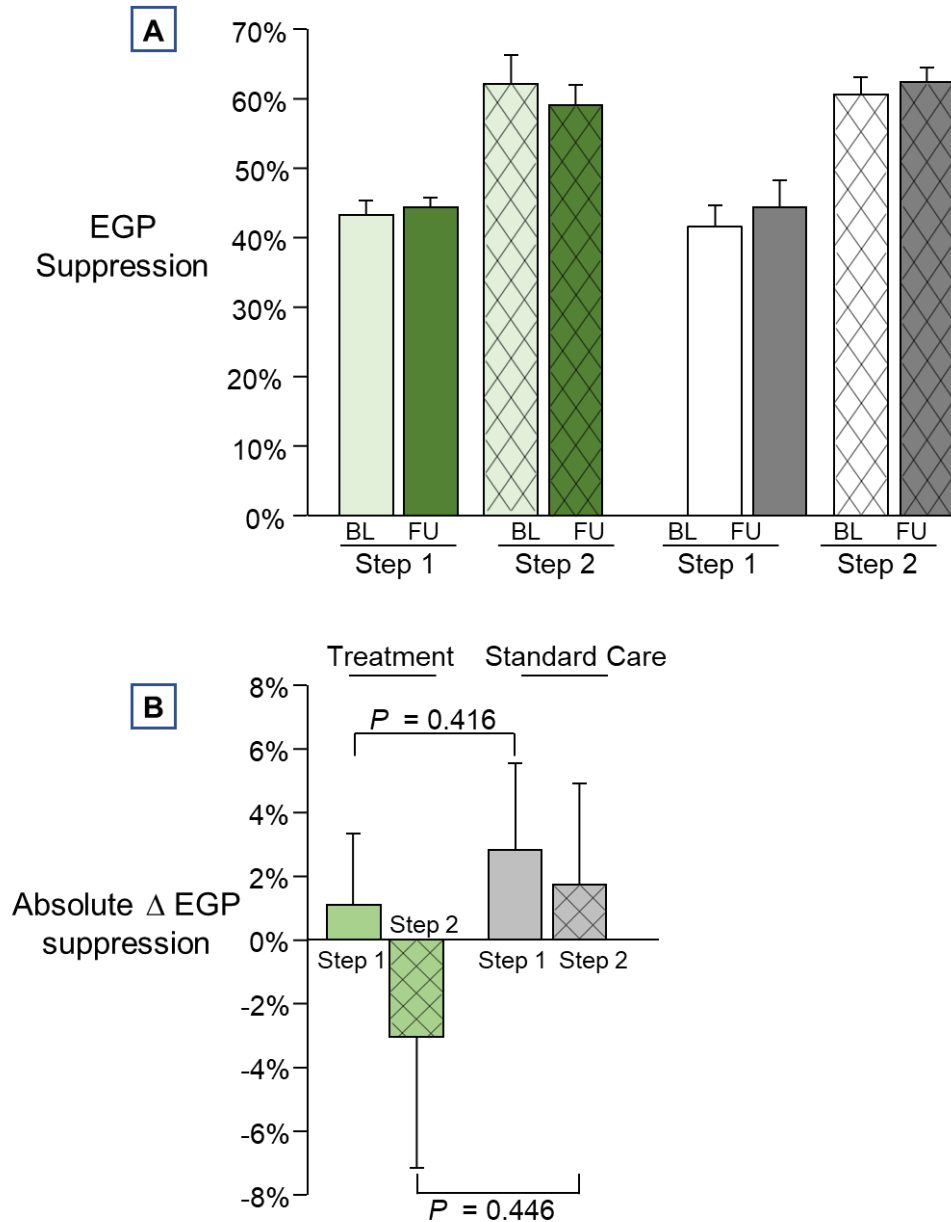


Data are presented as mean \pm SEM; Treatment: $n = 14$, Standard care: $n = 5$.

A: Absolute basal (no insulin, open bars) and step one (low insulin, hatched bars) glucose production ($\mu\text{mol}/\text{min}$) at baseline (light bars) and follow-up (dark bars) in treatment (green) and standard care (grey) subjects. Statistical analysis is presented in **table 4.5**.

B: Percent change from baseline to follow-up in basal and step one (low insulin, hatched bars) glucose production for treatment (green) and standard care subjects (grey). One tailed, unpaired t -test between treatment and standard care subjects within a step (basal or step one).

Figure 4.16. EGP suppression and absolute change in EGP suppression from basal to step one and basal to step two

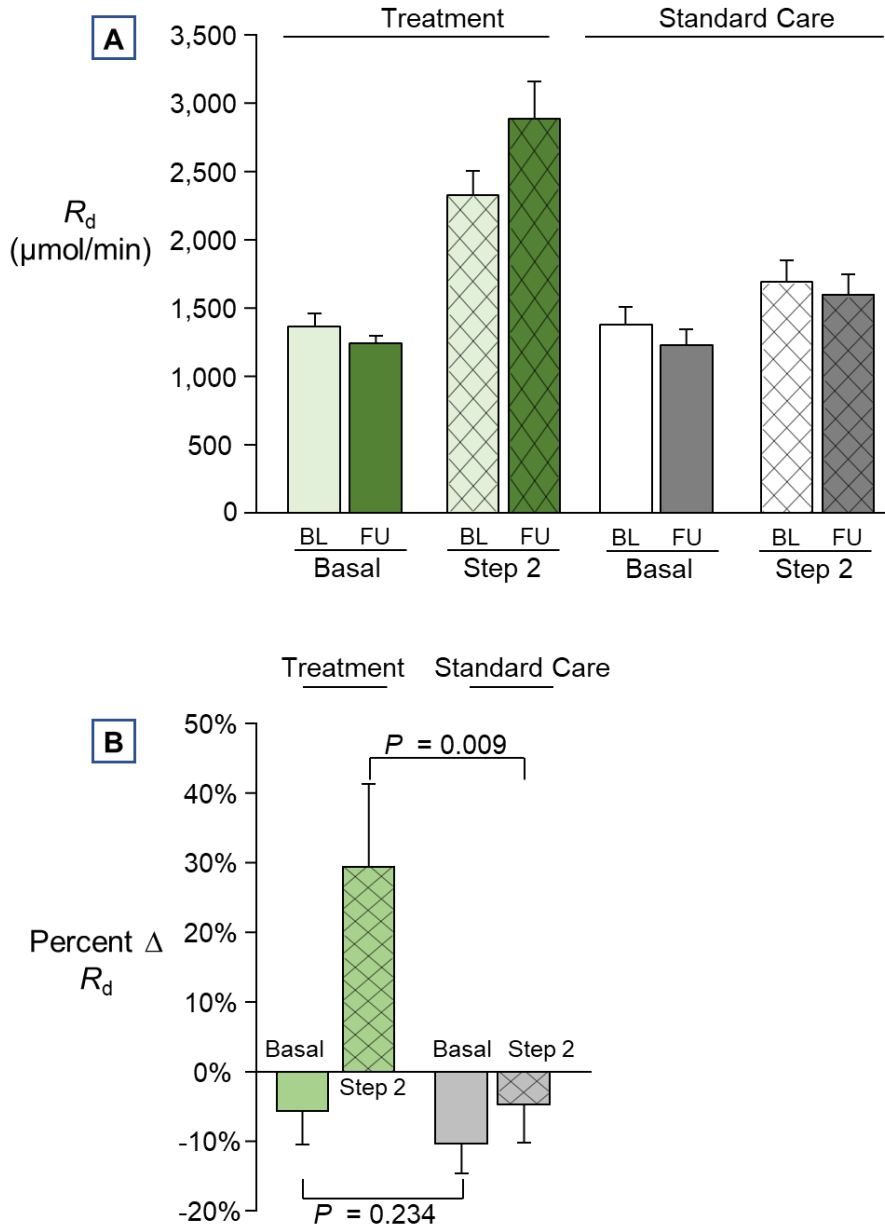


Data are presented as mean \pm SEM; Treatment: $n = 14$, Standard care: $n = 5$.

A: Percent EGP suppression from basal to step one (open bars) and basal to step two (hatched bars) at baseline (light bars) and follow-up (dark bars) for treatment (green) and control (grey). Statistical analysis is presented in **table 4.5**.

B: Absolute change in glucose production from baseline to follow-up in basal to step one (open) and basal to step two (hatched) for treatment (green) and standard care subjects (grey). One-tailed, unpaired t -test between treatment and standard care subjects within a step (step one or step two).

Figure 4.17. Absolute glucose disposal and percent change

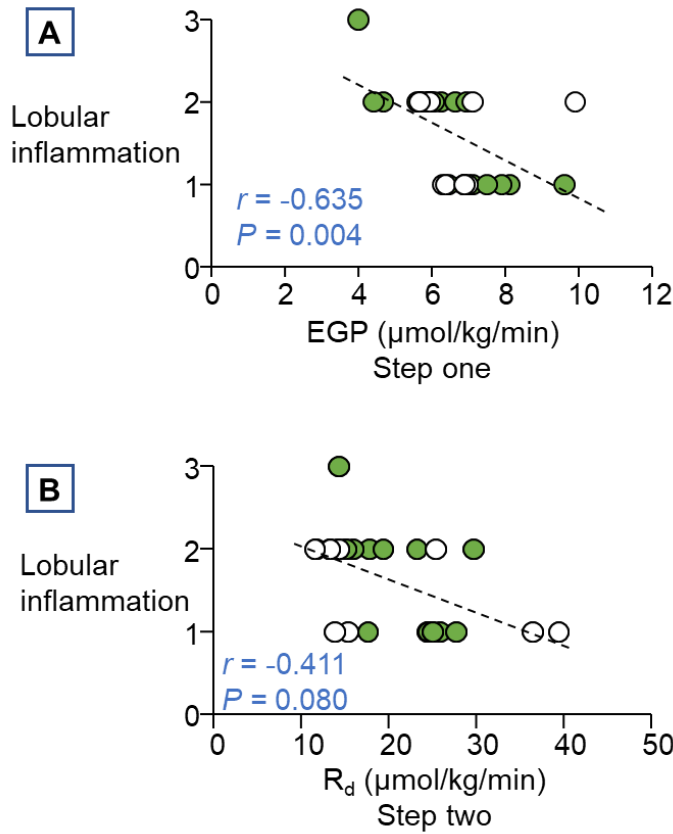


Data are presented as mean \pm SEM; Treatment: $n = 14$, Standard care: $n = 5$.

A: Absolute basal (no insulin, open bars) and step two (high insulin, hatched bars) glucose disposal ($\mu\text{mol}/\text{min}$) at baseline (light bars) and follow-up (dark bars) in treatment (green) and standard care (grey) subjects. Statistical analysis is presented in **table 4.5**.

B: Percent change from baseline to follow-up in basal and step two (high insulin, hatched bars) glucose disposal for treatment (green) and standard care subjects (grey). One-tailed, unpaired t -test between treatment and standard care subjects within a step (basal or step two).

Figure 4.18. Baseline relationships between EGP and R_d with NAS component, lobular inflammation

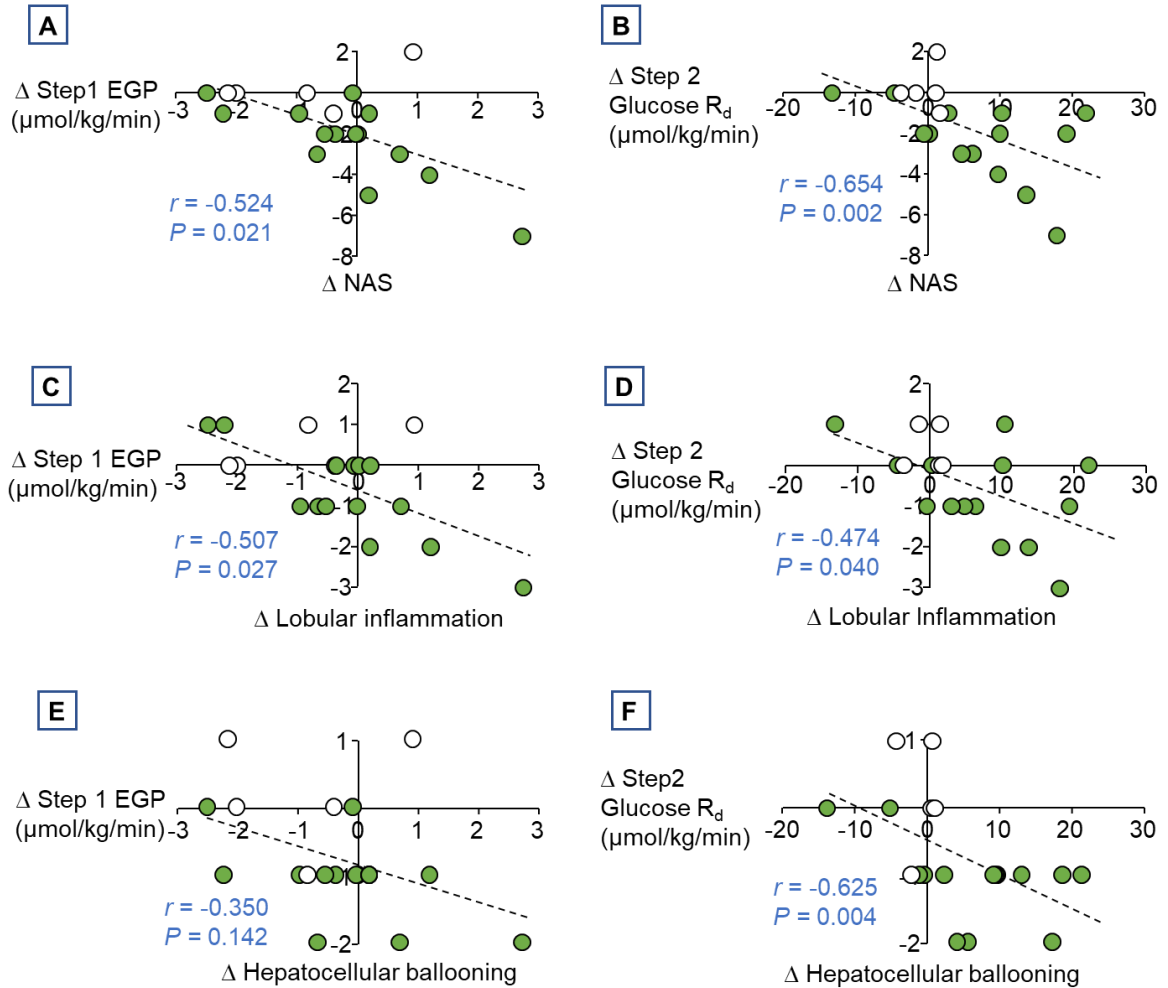


Spearman's correlation was used to assess linear relationships between ranked and continuous variables. Treatment subjects are shown in green circles and standard care in white. All subjects who completed baseline studies are included in these correlations ($n = 26$).

A: Baseline EGP ($\mu\text{mol/kg/min}$, step one – low insulin) and lobular inflammation (graded histologically).

B: Baseline R_d ($\mu\text{mol/kg/min}$, step two – high insulin) and lobular inflammation (graded histologically).

Figure 4.19. Change in EGP and R_d with change in NAS and the components, lobular inflammation, and hepatocellular ballooning

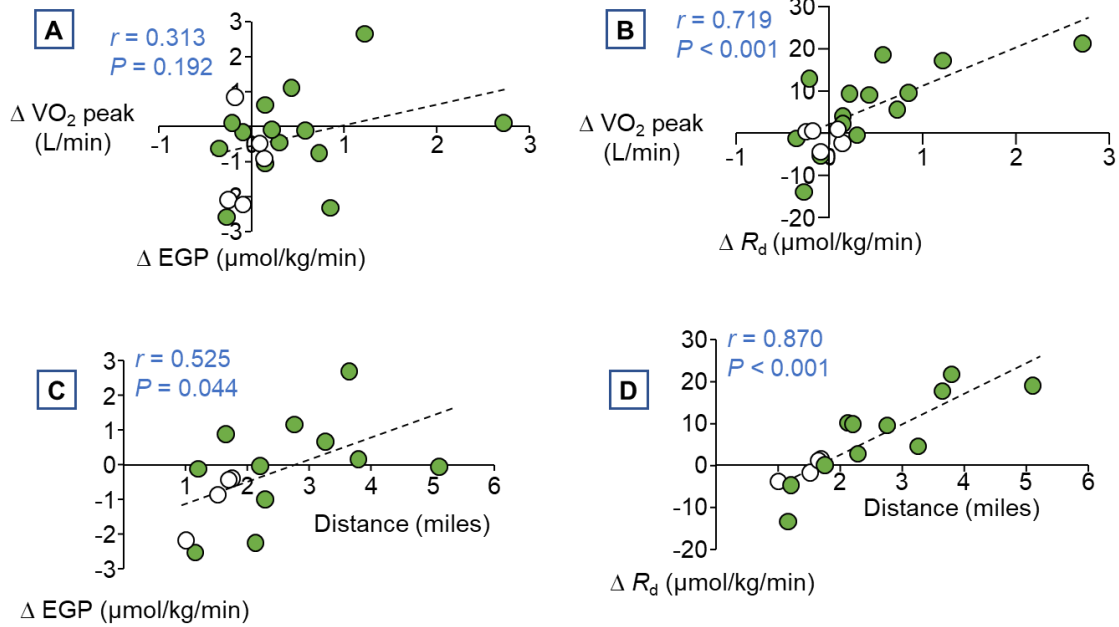


Spearman's correlation was used to assess linear relationships between ranked and continuous variables. Treatment subjects are shown in green circles and standard care in white. Treatment: $n = 14$, Standard care: $n = 5$.

A, C, E: Absolute change in EGP ($\mu\text{mol/kg/min}$, step one – low insulin) and (**A**) NAS, (**C**) lobular inflammation, and (**E**) hepatocellular ballooning.

B, D, F: Absolute change in R_d ($\mu\text{mol/kg/min}$, step two – high insulin) and (**B**) NAS, (**D**) lobular inflammation, and (**F**) hepatocellular ballooning.

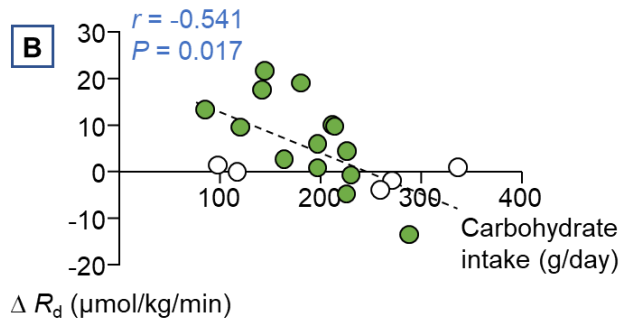
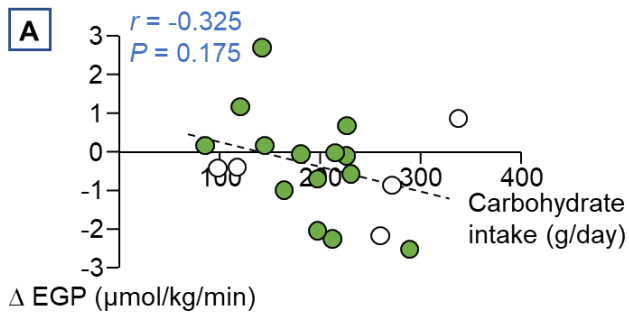
Figure 4.20. Change in EGP and R_d with change in VO_2 peak and activity



Pearson's correlation was used to assess linear relationships between continuous variables. Treatment subjects are shown in green circles and standard care in white.

- A:** Absolute change in EGP ($\mu\text{mol/kg/min}$, step one – low insulin) and peak VO_2 . Treatment: $n = 14$, Standard care: $n = 5$.
- B:** Absolute change in R_d ($\mu\text{mol/kg/min}$, step two – high insulin) and peak VO_2 . Treatment: $n = 14$, Standard care: $n = 5$.
- C:** Absolute change in EGP ($\mu\text{mol/kg/min}$, step one – low insulin) and average distance walked (miles) the two days before follow-up testing. Treatment: $n = 11$, Standard care: $n = 4$ – subjects excluded d/t improper Fitbit usage
- D:** Absolute change in R_d ($\mu\text{mol/kg/min}$, step two – high insulin) and average distance walked (miles) the two days before follow-up testing. Treatment: $n = 11$, Standard care: $n = 4$ – subjects excluded d/t improper Fitbit usage.

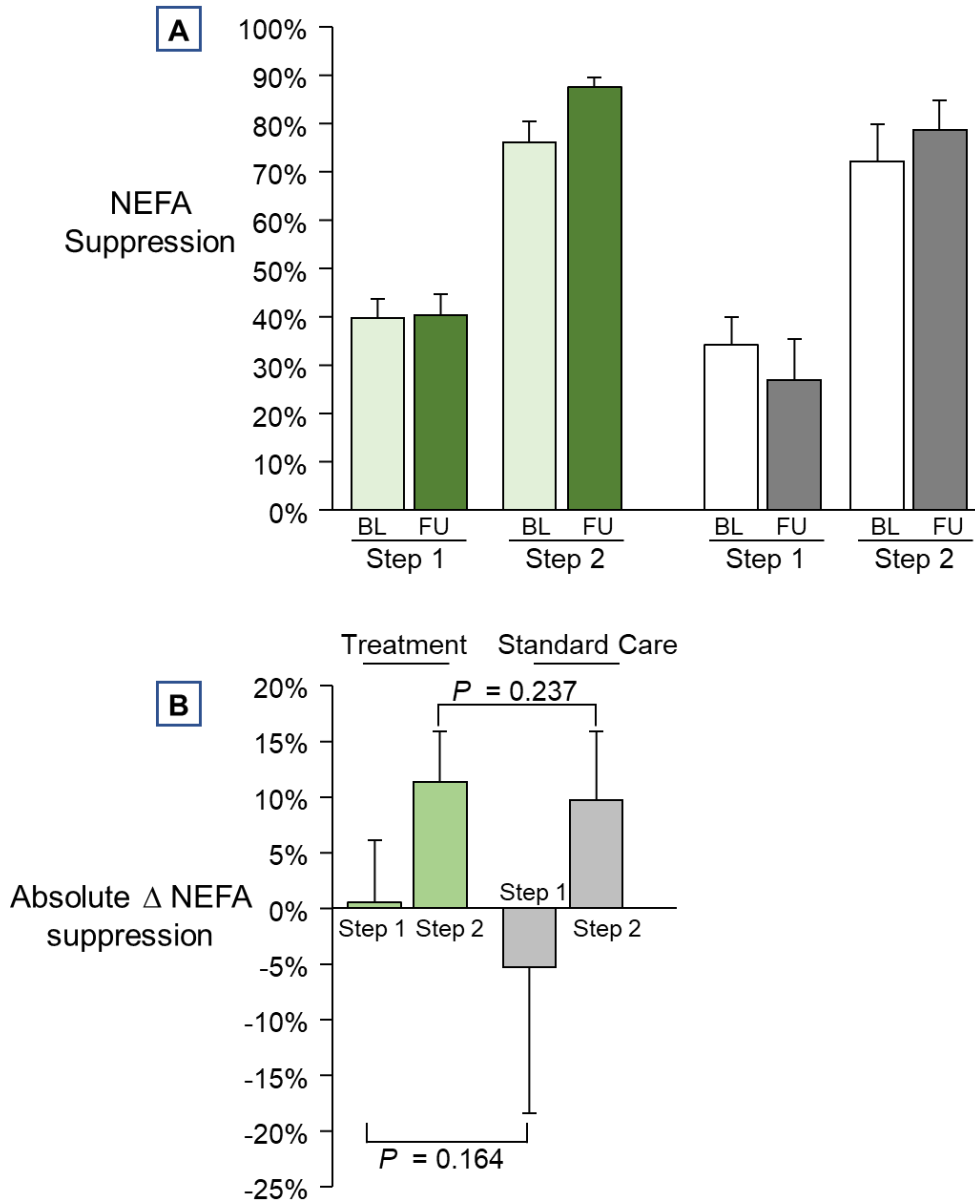
Figure 4.21. Change in EGP and R_d with follow-up carbohydrate consumption



Pearson's correlation was used to assess linear relationships between continuous variables. Treatment subjects are shown in green circles and standard care in white. Treatment: $n = 14$, Standard care: $n = 5$.

- A:** Absolute change in EGP ($\mu\text{mol/kg/min}$, step one – low insulin) and average daily carbohydrate consumption three days before the follow-up testing.
- B:** Absolute change in R_d ($\mu\text{mol/kg/min}$, step two – high insulin) and average daily carbohydrate consumption three days before the follow-up testing.

Figure 4.22. NEFA suppression during step one and step two of the clamp and change from baseline to follow-up

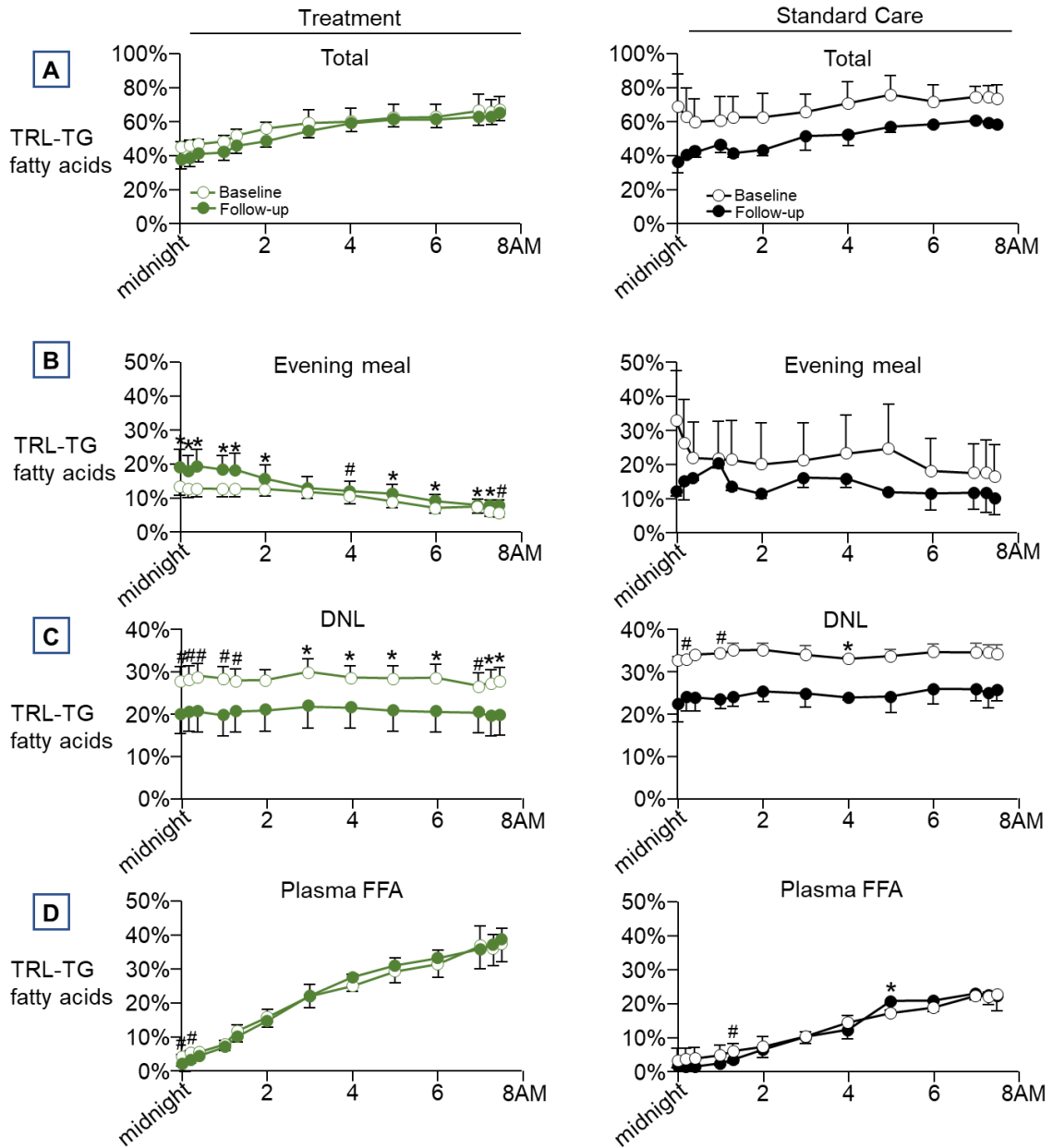


Data are presented as mean \pm SEM; Treatment: $n = 14$, Standard care: $n = 5$.

A: Percent EGP suppression from basal to step one (open bars) and basal to step two (hatched bars) at baseline (light bars) and follow-up (dark bars) for treatment (green) and control (grey). Statistical analysis is presented in **table 4.5**.

B: Absolute change in glucose production from baseline to follow-up in basal to step one (open) and basal to step two (hatched) for treatment (green) and standard care subjects (grey). Unpaired t -test between treatment and standard care subjects within a step (step one or step two).

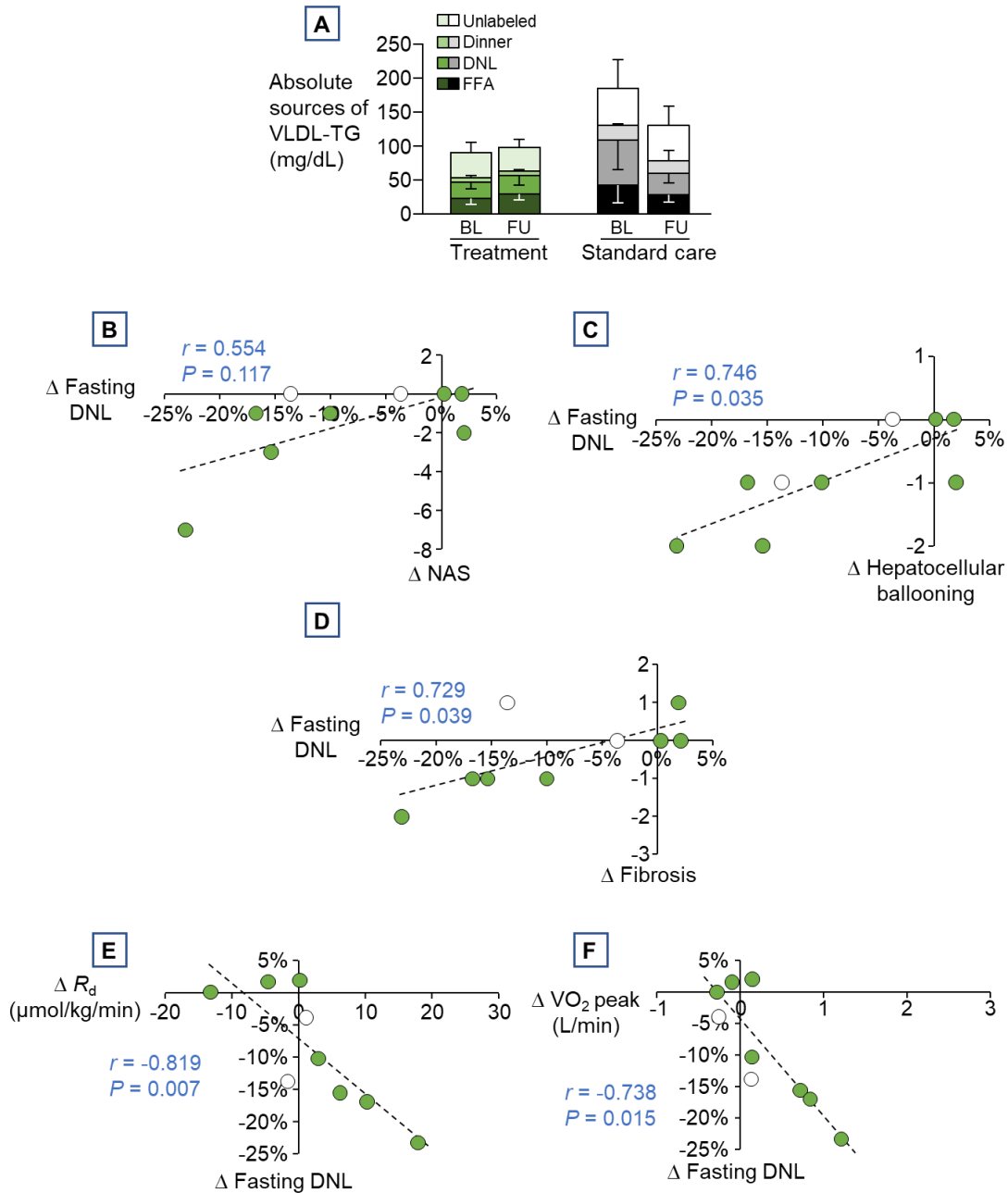
Figure 4.23. Proportion of fatty acid sources becoming labeled in TRL-TG over time



Data are presented as mean \pm SEM; Treatment: $n = 7$ (green), Standard care: $n = 2$ (black). * asterisks and # pound signs denote significant differences between groups at individual time points ($P < 0.05$ or $P < 0.10$, respectively). Open circles: baseline; filled circles: follow-up.

A: Proportion of total fatty acids accounted for in the TRL particles.
B-D: Proportion of fatty acids in TRL particles arising from (B) evening meal, (C) DNL, and (D) plasma FFA pool.

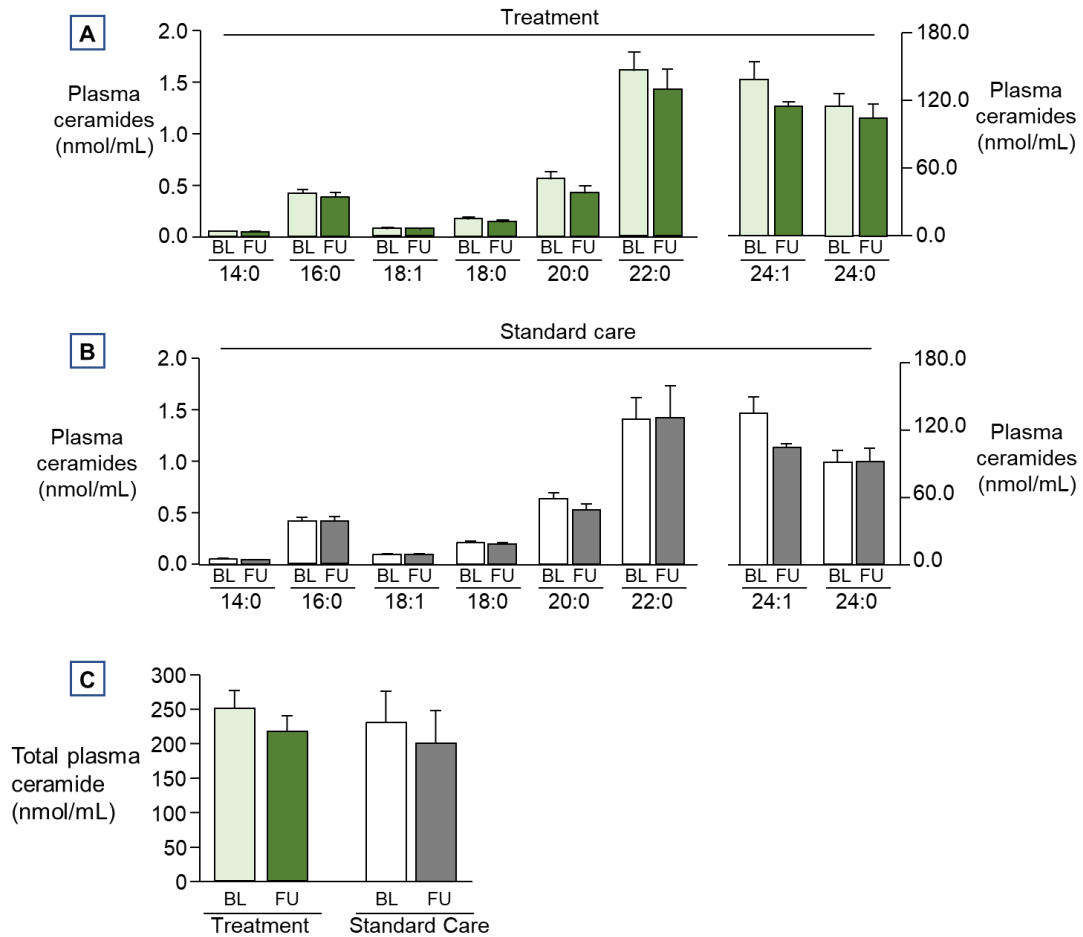
Figure 4.24. Absolute fatty acid sources used for VLDL-TG synthesis and correlations with fasting fractional DNL



A: Data are presented as mean \pm SEM; Treatment: $n = 7$, Standard care: $n = 2$. Due to the small sample size for standard care subjects, paired t -tests were completed to compare treatment across time – no significant differences were found for the various sources contributing to VLDL-TG.

B-F: Relationships between absolute changes in fractional VLDL-TG from DNL and **(B)** NAS, **(C)** hepatocellular ballooning, **(D)** fibrosis, **(E)** glucose disposal (R_d), **(F)** VO₂ peak. Spearman's correlation; Treatment: $n = 7$, Standard care: $n = 2$.

Figure 4.25. Plasma ceramide (CER) concentrations



D

Ceramide	Group	Visit	Group x Visit
14:0	0.595	0.024	0.037
16:0	0.726	0.627	0.675
18:1	0.046	0.703	0.421
18:0	0.107	0.185	0.759
20:0	0.296	0.011	0.819
22:0	0.884	0.669	0.598
24:1	0.921	0.019	0.7123
24:0	0.421	0.701	0.643
Total	0.692	0.149	0.931

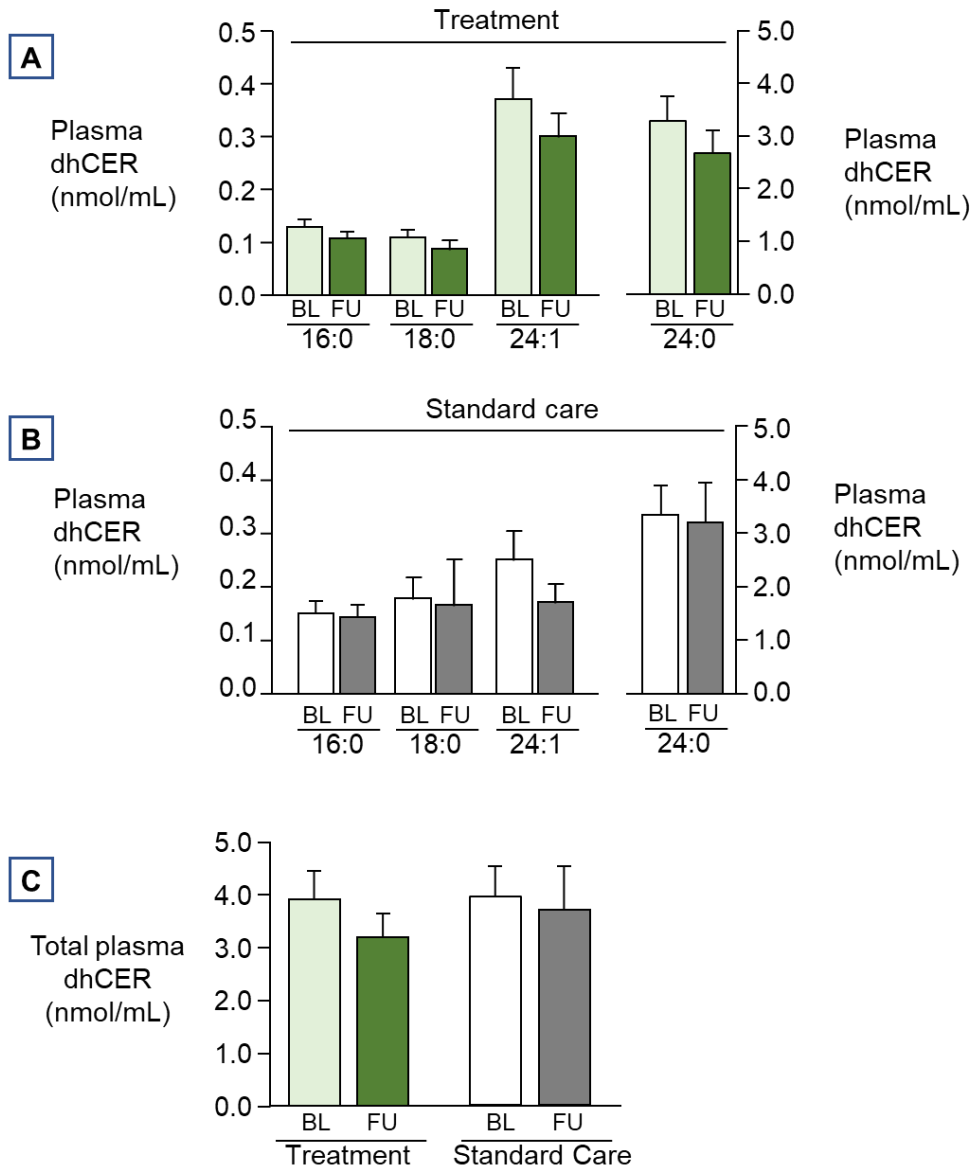
Data are presented as mean \pm SEM; Treatment: $n = 14$, Standard care: $n = 5$.

A-B: Plasma ceramide concentrations for treatment (**A**) and standard care (**B**) groups. Note the secondary axis on the right for 22:0, 24:1, and 24:0 ceramides. All ceramides presented here have an 18:1 backbone as formed by de novo ceramide synthesis.

C: Total ceramide concentrations in plasma (sum of all species presented in A-B).

D: Results from the mixed model ANOVA with post-hoc pairwise comparisons for significant main effect of visit with Bonferroni adjustment.

Figure 4.26. Plasma dihydroceramide (dhCER) concentrations

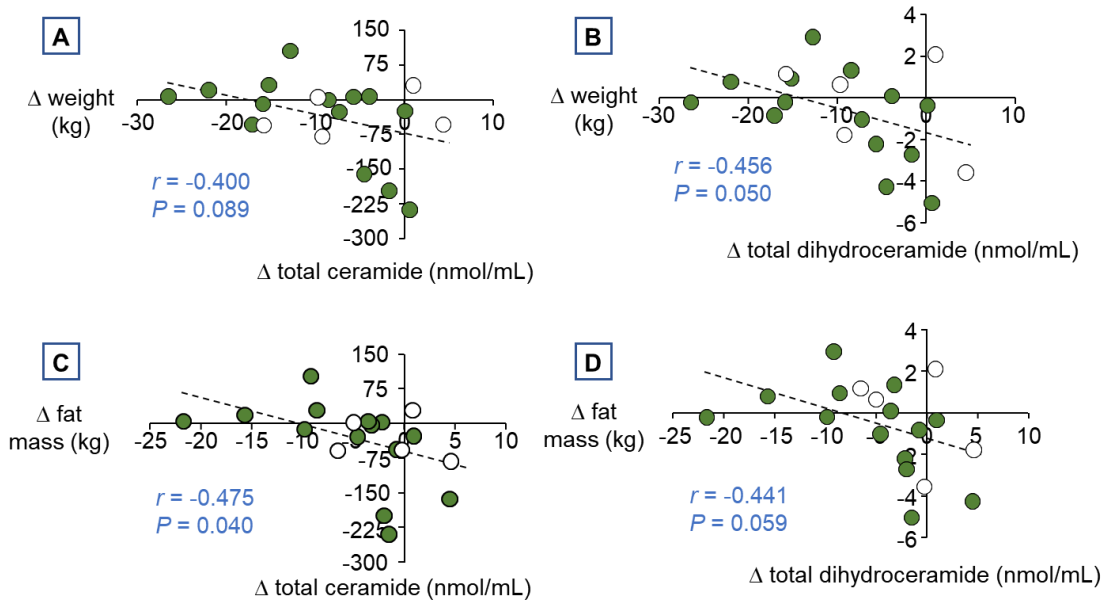


D

dhCER	Group	Visit	Group x Visit
16:0	0.304	0.150	0.862
18:0	0.077	0.507	0.860
24:1	0.162	0.060	0.891
24:0	0.942	0.210	0.968
Total	0.657	0.484	0.664

Data are presented as mean \pm SEM; Treatment: $n = 14$, Standard care: $n = 5$.
A-B: Plasma dihydroceramide concentrations for treatment (**A**) and standard care (**B**) groups. Note the secondary axis on the right for 24:0 dhCER. All dihydroceramides presented here have an 18:0 backbone as formed by de novo ceramide synthesis.
C: Total dhCER concentrations in plasma (sum of the individual species presented in A-B).
D: Results from the mixed model ANOVA.

Figure 4.27. Relationships between change in total ceramides and dihydroceramides with anthropometrics

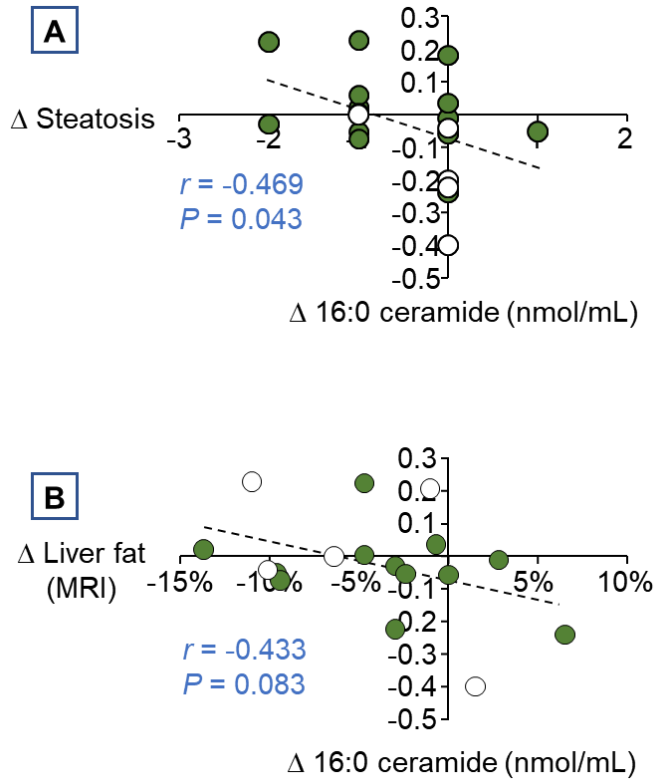


Pearson's correlation was used to assess linear relationships between continuous variables. Treatment subjects ($n = 14$) are shown in green circles and standard care ($n = 5$) in white.

A, C: Relationships between weight and fat mass loss and total plasma ceramide.

B, D: Relationships between weight and fat mass loss and total plasma dihydroceramide.

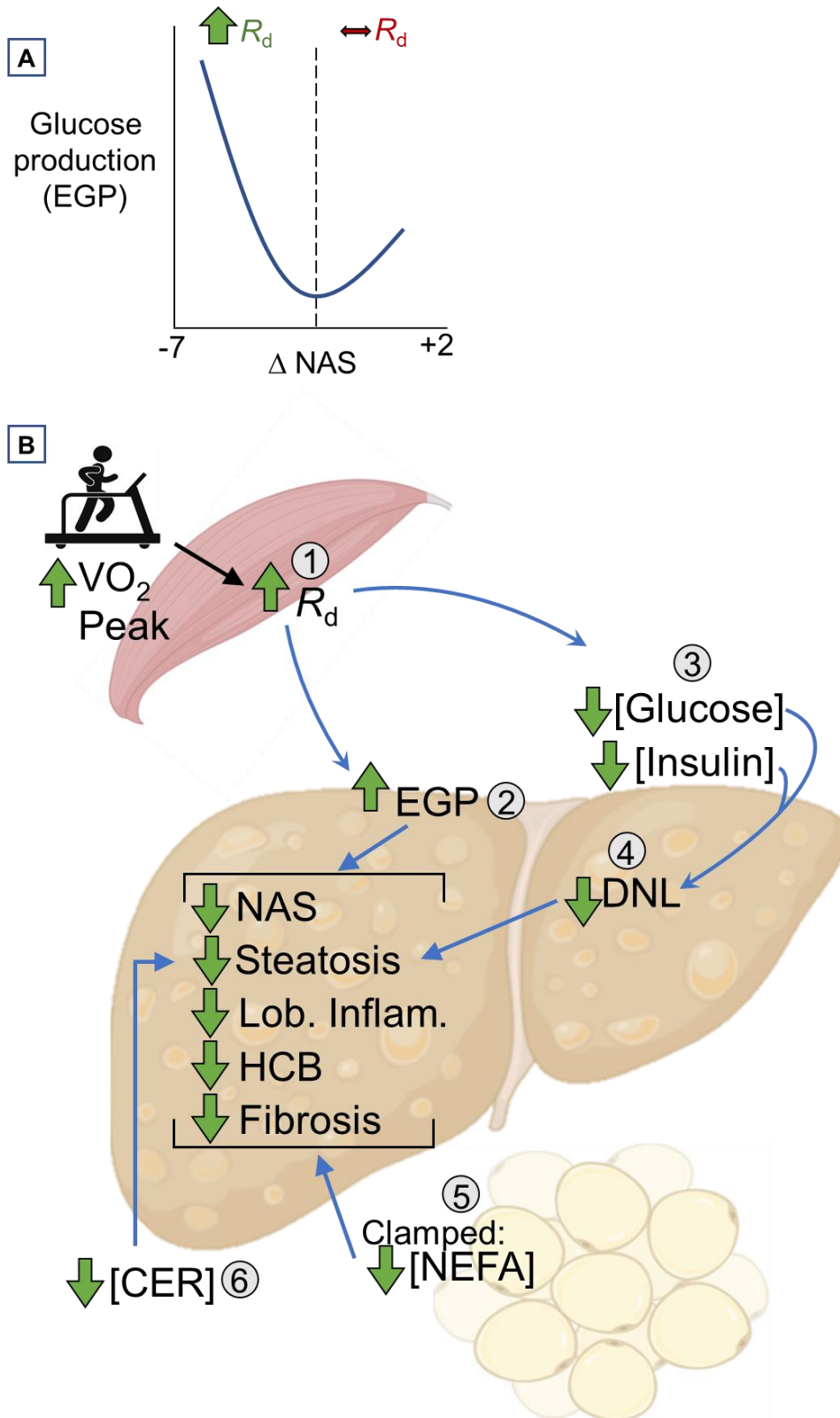
Figure 4.28. Ceramide 18:1/16:0 and liver fat



Spearman's correlation was used to assess linear relationships between ranked and continuous variables. Pearson's correlation was used to assess linear relationships between continuous variables. Treatment subjects are shown in green circles and standard care in white.

- A:** Relationship between steatosis by liver histology and plasma 16:0 ceramide.
Treatment: $n = 14$, Standard care: $n = 5$.
- B:** Relationship between steatosis by MRI and plasma 16:0 ceramide.
Treatment: $n = 12$, Standard care: $n = 5$.

Figure 4.29. Reverse J shaped curve of EGP and NAS and hypothesized model



A: Reverse 'J' -shaped curve hypothesized for the relationship between changes in EGP and NAS.

B: Green arrows represent findings and blue lined arrows represent hypothesized effects of combined diet and exercise program to improve liver histology.

Relief of overburdened liver to improve histology via:

- 1 – Increased disposal of glucose at SM with increased physical activity and VO_2 peak.
- 2 – Increased glucose production and rerouting substrates away from the liver.
- 3 – Reduced plasma insulin and glucose with simultaneous improvements in skeletal muscle insulin sensitivity.
- 4 – Reductions in insulin and glucose leading to reduced transcriptional activation and substrates driving DNL.
- 5 – Improved adipose insulin sensitivity during insulin stimulated conditions.
- 6 – Increased plasma CER (and hypothesized hepatic release) reduces CER-toxicity within the liver.

SUPPLEMENTARY DATA

Supplementary Table S4.1. Results of mixed model ANOVA for 18-h metabolite concentration data separated into three time periods (postprandial, night, and clamp)

A: Glucose	Postprandial	Night	Clamp
Group	0.064	0.259	0.804
Visit	0.028	0.011	0.008
Time	<0.0001	0.030	<0.001
Group x visit	0.075	0.235	0.469
Group x time	0.404	0.620	0.002
Time x visit	0.080	0.148	0.370
Group x time x visit	0.285	0.473	0.194
B: Insulin	Postprandial	Night	Clamp
Group	0.193	0.085	0.392
Visit	0.158	0.012	0.105
Time	0.100	<0.0001	<0.001
Group x visit	0.498	0.641	0.800
Group x time	0.219	0.174	0.350
Time x visit	0.464	0.200	0.228
Group x time x visit	0.217	0.020	0.852
C: NEFA	Postprandial	Night	Clamp
Group	0.209	0.120	0.187
Visit	0.768	0.030	0.014
Time	0.100	<0.00001	<0.00001
Group x visit	0.620	0.193	0.740
Group x time	0.465	0.888	0.644
Time x visit	0.150	0.897	0.061
Group x time x visit	0.708	0.725	0.870
D: TG	Postprandial	Night	Clamp
Group	0.737	0.870	0.606
Visit	0.339	0.235	0.286
Time	0.001	0.036	0.097
Group x visit	0.598	0.671	0.522
Group x time	0.440	0.837	0.321
Time x visit	0.019	0.210	0.494
Group x time x visit	0.671	0.685	0.391

Data accompany **figures 4.8-4.11**; Treatment: $n = 14$; Standard care: $n = 5$. Mixed model ANOVA (within: time and visit; between: group) with post-hoc pairwise comparisons for significant interactions with Bonferroni adjustment. Bolded P values indicate both significant and trending findings.

Supplementary Table S4.2. Baseline correlation analysis of ceramide and dihydroceramides with weight, fasting glucose, total cholesterol, LDL cholesterol, EGP, and R_d

CER	Weight (kg)		Glucose (mg/dL)		TC (mg/dL)		LDL (mg/dL)		EGP ($\mu\text{mol}/\text{min}$)		R_d ($\mu\text{mol}/\text{min}$)	
	<i>r</i>	<i>P</i>	<i>r</i>	<i>P</i>	<i>r</i>	<i>P</i>	<i>r</i>	<i>P</i>	<i>r</i>	<i>P</i>	<i>r</i>	<i>P</i>
Total	-0.322	0.117	-0.480	0.015	0.489	0.013	0.265	0.234	-0.359	0.078	-0.004	0.986
14:0	0.109	0.604	-0.152	0.468	0.314	0.127	0.235	0.292	-0.077	0.716	-0.210	0.314
16:0	-0.152	0.469	-0.301	0.144	0.422	0.035	0.128	0.572	-0.251	0.225	-0.077	0.714
18:1	-0.492	0.012	-0.105	0.619	0.264	0.203	0.106	0.638	-0.509	0.009	-0.169	0.421
18:0	-0.201	0.334	-0.195	0.349	0.618	0.001	0.472	0.027	-0.188	0.367	-0.143	0.496
20:0	-0.320	0.119	-0.346	0.090	0.647	<0.001	0.514	0.014	-0.348	0.088	-0.169	0.418
22:0	-0.338	0.098	-0.477	0.016	0.443	0.026	0.204	0.362	-0.340	0.096	0.056	0.790
24:1	-0.292	0.157	-0.410	0.042	0.503	0.010	0.311	0.159	-0.360	0.077	-0.036	0.865
24:0	-0.304	0.139	-0.488	0.013	0.377	0.063	0.145	0.520	-0.292	0.157	0.041	0.844

dhCER	Weight (kg)		Glucose (mg/dL)		TC (mg/dL)		LDL (mg/dL)		EGP ($\mu\text{mol}/\text{min}$)		R_d ($\mu\text{mol}/\text{min}$)	
	<i>r</i>	<i>P</i>	<i>r</i>	<i>P</i>	<i>r</i>	<i>P</i>	<i>r</i>	<i>P</i>	<i>r</i>	<i>P</i>	<i>r</i>	<i>P</i>
Total	-0.375	0.065	-0.320	0.119	0.394	0.052	0.447	0.037	-0.285	0.168	0.042	0.842
16:0	-0.431	0.031	-0.242	0.243	0.276	0.181	0.373	0.087	-0.296	0.151	-0.060	0.776
18:0	-0.190	0.363	-0.005	0.980	0.411	0.041	0.655	<0.001	-0.094	0.654	-0.242	0.244
24:1	-0.143	0.495	-0.365	0.073	0.464	0.019	0.428	0.047	-0.187	0.372	0.133	0.526
24:0	-0.383	0.059	-0.308	0.134	0.360	0.077	0.411	0.058	-0.285	0.168	0.044	0.836

Data accompany **supplementary figure 4.8**; Treatment: $n = 17$; Standard care: $n = 8$.

Pearson's correlation was used to assess linear relationships between continuous variables. Significant ($P < 0.05$) relationships are highlighted by a dark grey cell and trending significant ($P < 0.10$) relationships are highlighted by a light grey cell.

Supplementary Table S4.3. Change correlation analysis of ceramide and dihydroceramides with weight, BMI, fat mass, AST, and ALT

Δ CER	Weight		BMI		Fat mass		AST		ALT	
	<i>r</i>	<i>P</i>	<i>r</i>	<i>P</i>	<i>r</i>	<i>P</i>	<i>r</i>	<i>P</i>	<i>r</i>	<i>P</i>
Total	-0.400	0.089	-0.423	0.071	-0.475	0.040	0.053	0.832	0.015	0.953
14:0	0.328	0.170	0.301	0.211	0.042	0.865	0.064	0.796	-0.209	0.396
16:0	-0.201	0.410	-0.336	0.160	-0.413	0.079	0.422	0.072	-0.141	0.570
18:1	-0.286	0.235	-0.446	0.056	-0.308	0.200	0.219	0.373	-0.237	0.334
18:0	-0.299	0.214	-0.407	0.084	-0.562	0.012	-0.101	0.684	0.009	0.970
20:0	-0.451	0.053	-0.533	0.019	-0.502	0.028	0.352	0.142	-0.042	0.868
22:0	-0.460	0.047	-0.424	0.070	-0.459	0.048	-0.004	0.987	0.059	0.814
24:1	-0.320	0.181	-0.313	0.192	-0.467	0.044	0.165	0.505	0.117	0.640
24:0	-0.418	0.075	-0.465	0.045	-0.421	0.073	-0.054	0.828	-0.077	0.757

Δ dhCER	Weight		BMI		Fat mass		AST		ALT	
	<i>r</i>	<i>P</i>	<i>r</i>	<i>P</i>	<i>r</i>	<i>P</i>	<i>r</i>	<i>P</i>	<i>r</i>	<i>P</i>
Total	-0.456	0.050	-0.489	0.034	-0.441	0.059	0.224	0.362	0.136	0.584
16:0	-0.570	0.011	-0.644	0.003	-0.446	0.055	0.038	0.878	-0.134	0.590
18:0	-0.251	0.299	-0.295	0.220	-0.303	0.208	0.479	0.037	0.291	0.230
24:1	-0.219	0.367	-0.158	0.518	-0.348	0.144	0.044	0.860	0.250	0.306
24:0	-0.459	0.048	-0.495	0.031	-0.435	0.063	0.219	0.373	0.120	0.629

Data accompany **figure 4.27**; Treatment: $n = 14$; Standard care: $n = 5$.

Pearson's correlation was used to assess linear relationships between continuous variables. Significant ($P < 0.05$) relationships are highlighted by a dark grey cell and trending significant ($P < 0.10$) relationships are highlighted by a light grey cell.

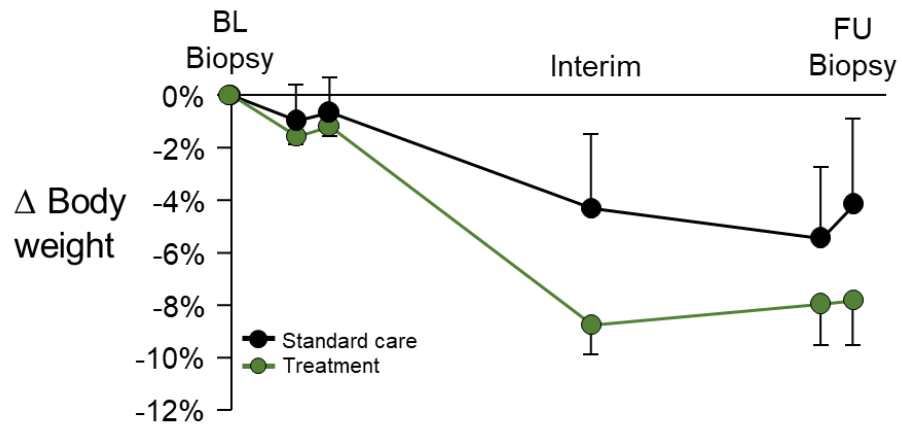
Supplementary Table S4.4. Change correlation analysis of ceramide and dihydroceramides with NAS, NAS components, fibrosis, and total liver fat by MRI

Δ CER	NAS		Steatosis		Lob. Inflamm.		Ballooning		Fibrosis		Liver fat (MRI)	
	<i>r</i>	<i>P</i>	<i>r</i>	<i>P</i>	<i>r</i>	<i>P</i>	<i>r</i>	<i>P</i>	<i>r</i>	<i>P</i>	<i>r</i>	<i>P</i>
Total	-0.192	0.431	-0.295	0.220	-0.188	0.441	0.071	0.774	0.191	0.432	-0.172	0.509
14:0	-0.043	0.860	-0.173	0.479	-0.028	0.909	0.099	0.686	-0.155	0.525	-0.022	0.934
16:0	-0.069	0.778	-0.469	0.043	-0.065	0.790	0.356	0.134	0.354	0.138	-0.433	0.083
18:1	0.149	0.543	-0.218	0.370	0.154	0.528	0.402	0.088	0.410	0.081	-0.520	0.032
18:0	-0.077	0.754	-0.328	0.170	-0.127	0.604	0.257	0.288	0.306	0.203	-0.369	0.145
20:0	0.168	0.492	-0.209	0.391	0.101	0.679	0.375	0.114	0.299	0.214	-0.466	0.059
22:0	0.165	0.499	-0.086	0.727	0.050	0.838	0.266	0.271	-0.005	0.982	-0.258	0.318
24:1	-0.159	0.516	-0.356	0.135	-0.179	0.464	0.137	0.577	0.206	0.397	-0.076	0.772
24:0	-0.297	0.218	-0.266	0.270	-0.286	0.236	-0.059	0.810	0.151	0.537	-0.226	0.384

Δ dhCER	NAS		Steatosis		Lob. Inflamm.		Ballooning		Fibrosis		Liver fat (MRI)	
	<i>r</i>	<i>P</i>	<i>r</i>	<i>P</i>	<i>r</i>	<i>P</i>	<i>r</i>	<i>P</i>	<i>r</i>	<i>P</i>	<i>r</i>	<i>P</i>
Total	0.059	0.811	-0.220	0.364	0.048	0.844	0.314	0.190	0.430	0.066	-0.276	0.284
16:0	-0.050	0.838	-0.147	0.548	-0.097	0.694	0.148	0.545	0.341	0.153	-0.383	0.129
18:0	-0.033	0.894	-0.155	0.526	-0.107	0.663	0.250	0.302	0.301	0.210	-0.060	0.819
24:1	-0.194	0.427	-0.174	0.475	-0.210	0.388	-0.031	0.901	0.119	0.628	-0.133	0.610
24:0	0.063	0.799	-0.221	0.364	0.048	0.844	0.321	0.180	0.436	0.062	-0.281	0.275

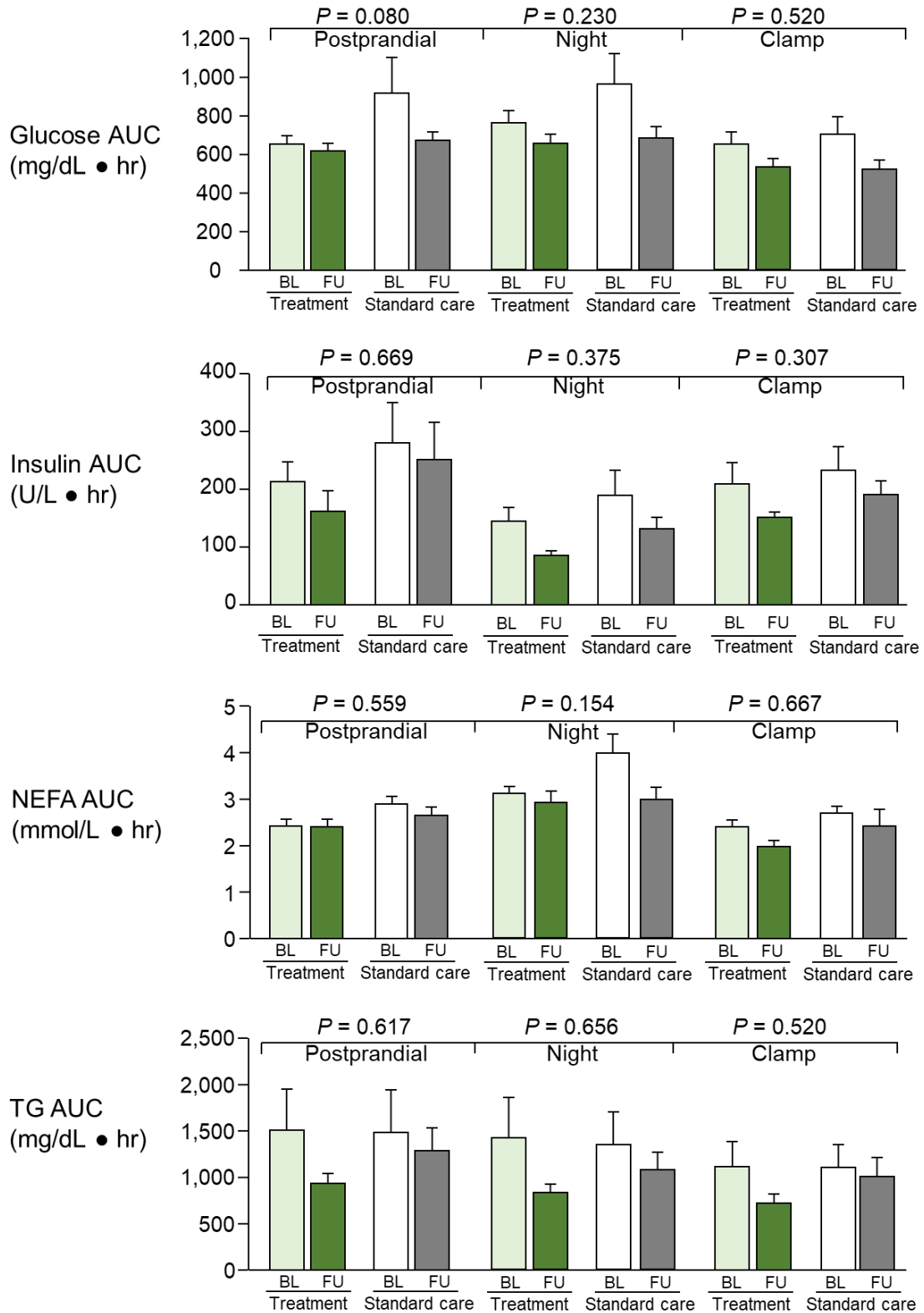
Data accompany **figure 4.28**; Treatment: $n = 14$; Standard care: $n = 5$. Spearman's correlation was used to assess linear relationships between continuous and ranked variables. Significant ($P < 0.05$) relationships are highlighted by a dark grey cell and trending significant ($P < 0.10$) relationships are highlighted by a light grey cell.

Supplementary Figure S4.1. Body weight changes over time



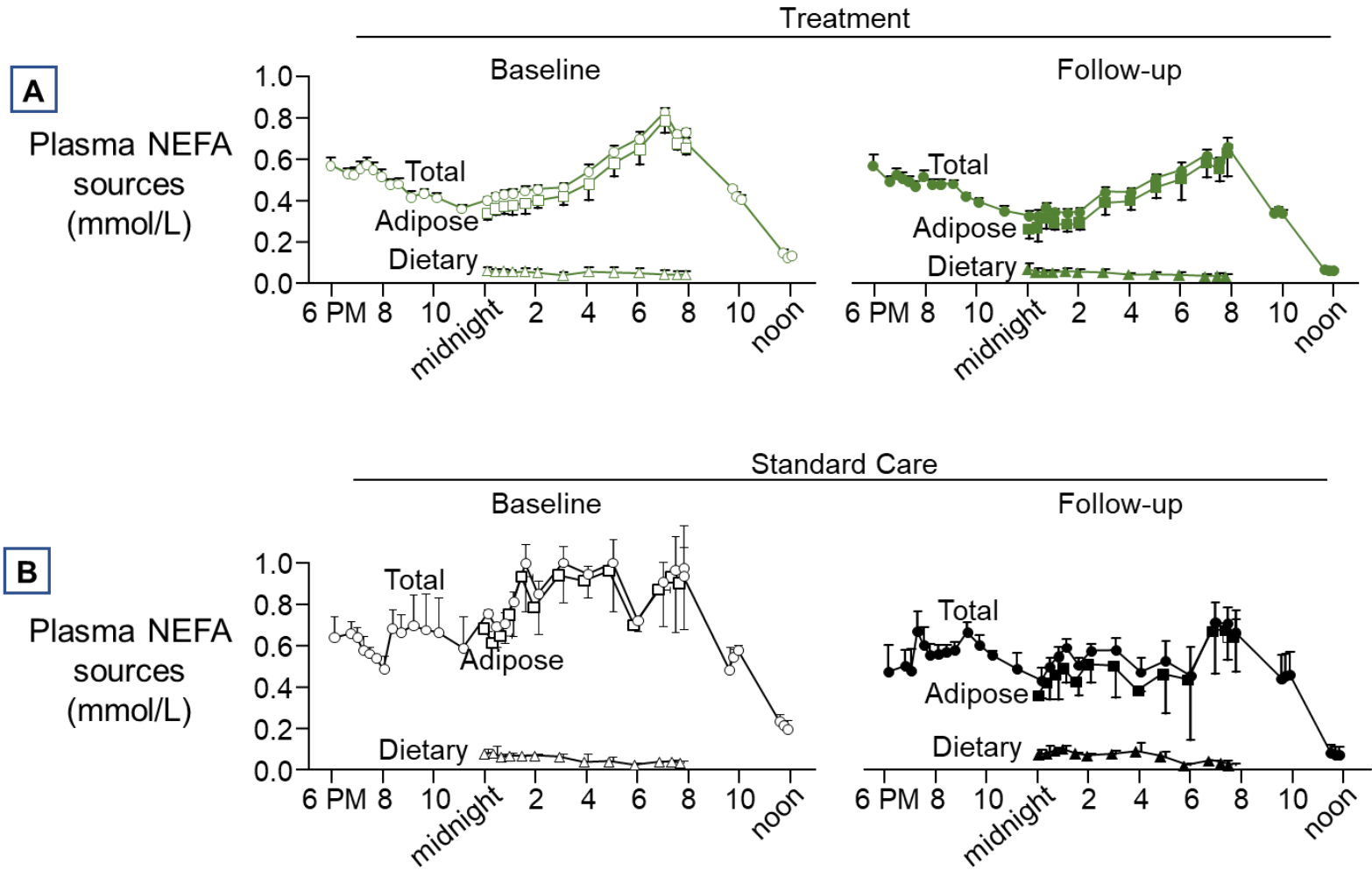
Data accompany **figure 4.5**. Data are presented as mean \pm SEM; Treatment: $n = 14$; Standard care: $n = 5$.

Supplementary Figure S4.2. Time period AUC for plasma (A) Glucose, (B) Insulin, (C) NEFA, and (D) TG.



Data accompany **figures 4.8-4.11**. Data are presented as mean \pm SEM;
Treatment: $n = 14$; Standard care: $n = 5$.
Mixed model ANOVA with post-hoc pairwise comparisons for significant
interactions with Bonferroni adjustment.

Supplementary Figure S4.3. Plasma NEFA sources from midnight to 8AM

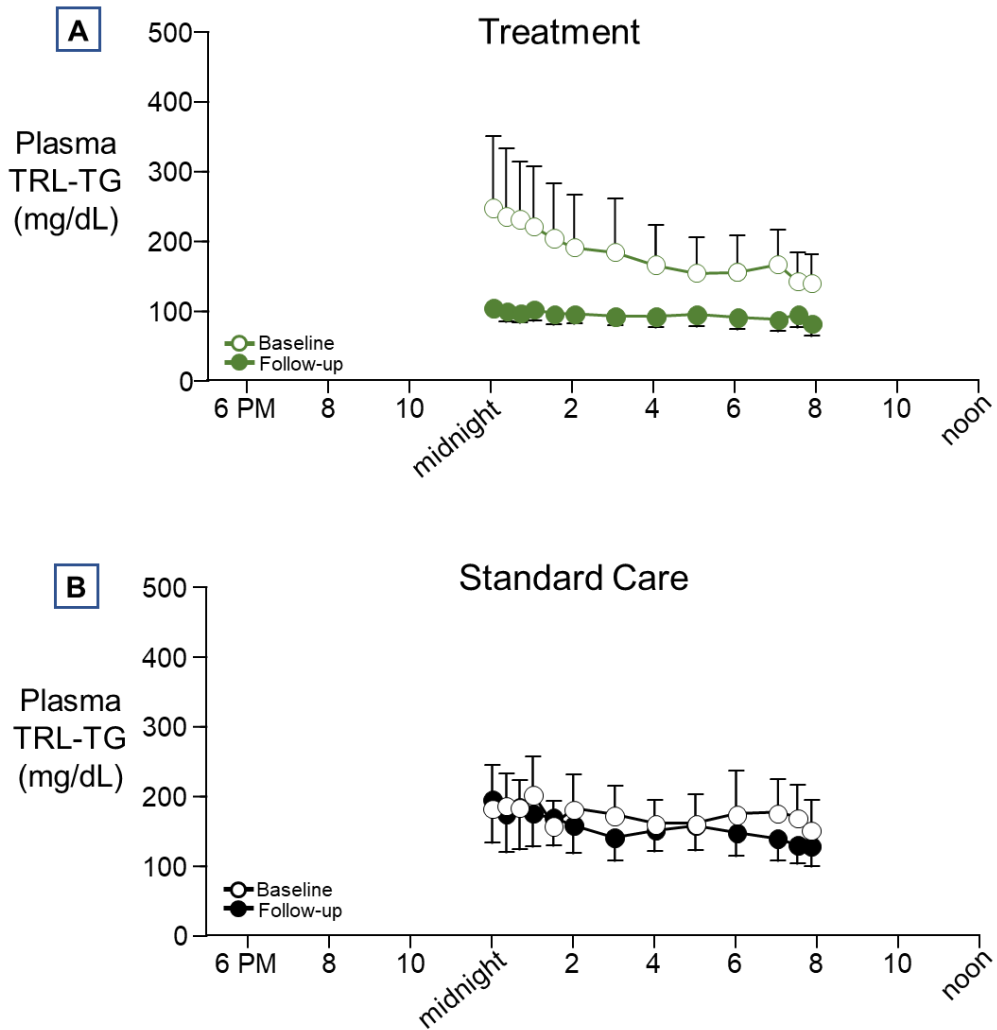


Data accompany **figure 4.10**. Data are presented as mean \pm SEM; Treatment: $n = 7$, Standard care: $n = 2$. Total plasma NEFA is shown in circles (\circ , open=baseline, closed=follow-up), NEFA from adipose is represented by a square (\square), and dietary NEFA from spillover is shown in triangles (\triangle) with treatment subjects shown in green and standard care in black.

A: Total plasma, adipose, and dietary NEFA concentrations in treatment (green) subjects at baseline (open symbols) and follow-up (closed symbols).

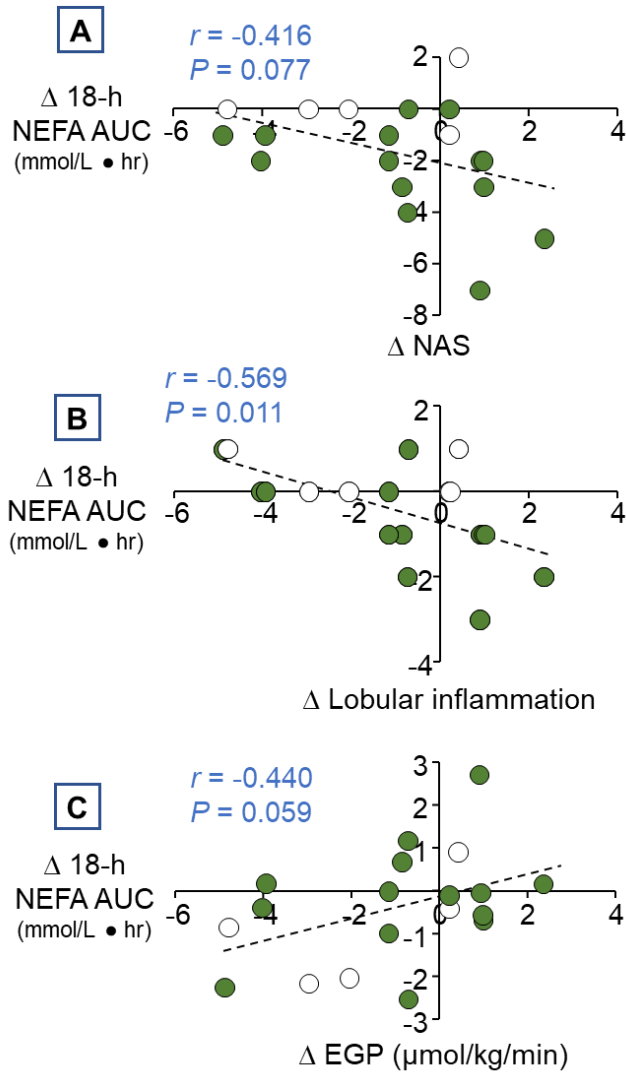
B: Total plasma, adipose, and dietary NEFA concentrations in control (black) subjects at baseline (open symbols) and follow-up (closed symbols).

Supplementary Figure S4.4. Absolute TRL-TG concentrations across time



Data accompany **figures 4.11, 4.24, and 4.25**. Data are presented as mean \pm SEM; Treatment: $n = 14$, Standard care: $n = 5$.

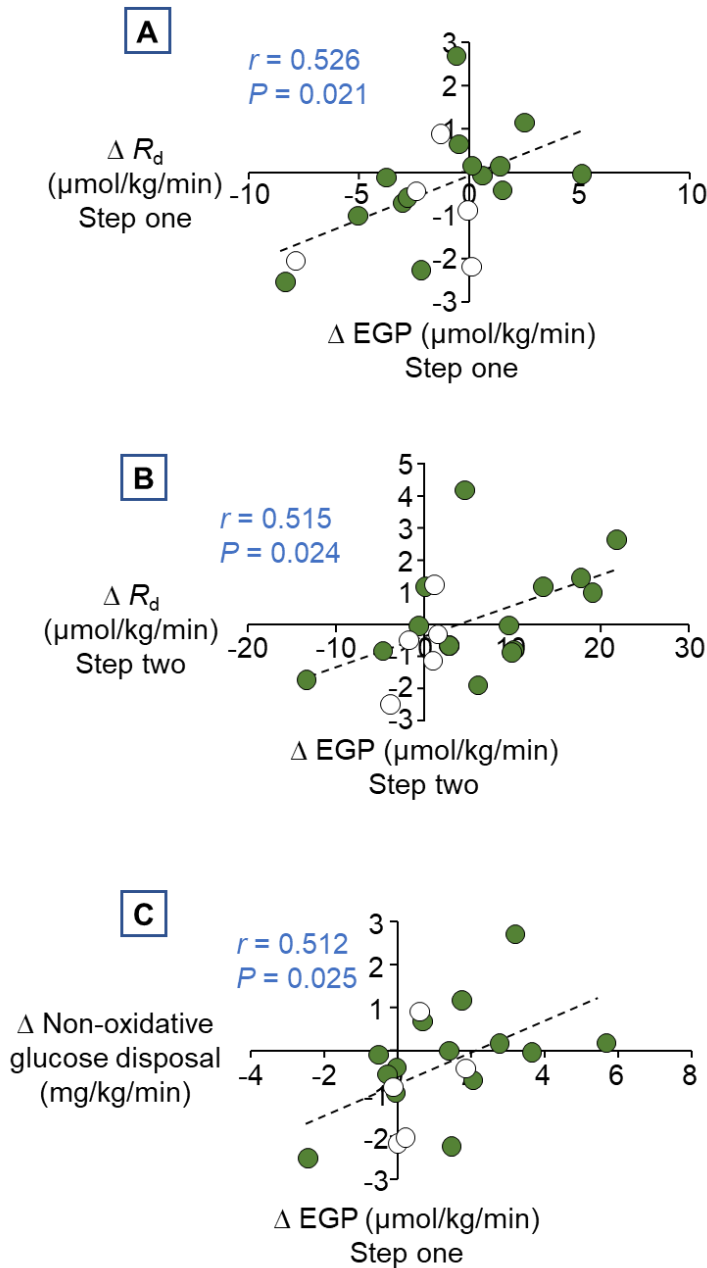
Supplementary Figure S4.5. Relationships between change in 18-hour NEFA AUC and NAS, lobular inflammation, and EGP



Spearman's correlation was used to assess linear relationships between ranked and continuous variables and Pearson's correlation was used for comparisons between two continuous variables. Treatment subjects are shown in green circles and standard care in white. Treatment: $n = 14$, Standard care: $n = 5$.

A-C: Relationships between 18-hour NEFA AUC and change in (A) NAS, (B) inflammation, and (C) EGP.

Supplementary Figure S4.6. Relationships between change in EGP and R_d during different steps of the clamp and EGP with non-oxidative glucose disposal



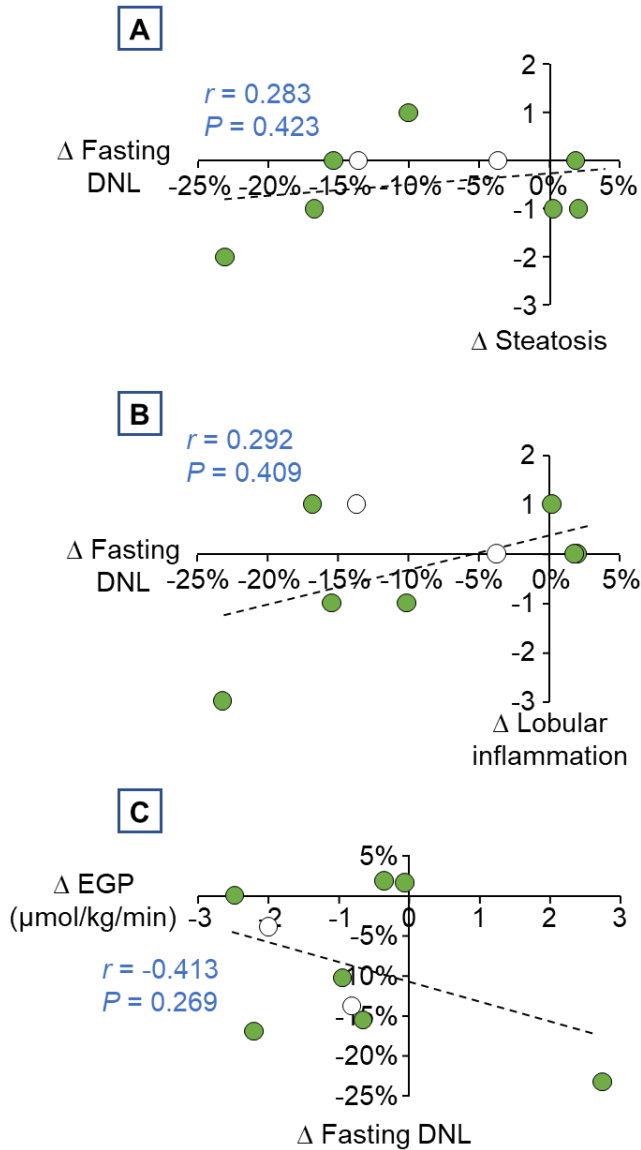
Pearson's correlation was used for comparisons between two continuous variables. Treatment subjects are shown in green circles and standard care in white. Treatment: $n = 14$, Standard care: $n = 5$.

A: Relationship between step one glucose production and disposal.

B: Relationship between step two glucose production and disposal.

C: Relationship between step one EGP and non-oxidative glucose disposal.

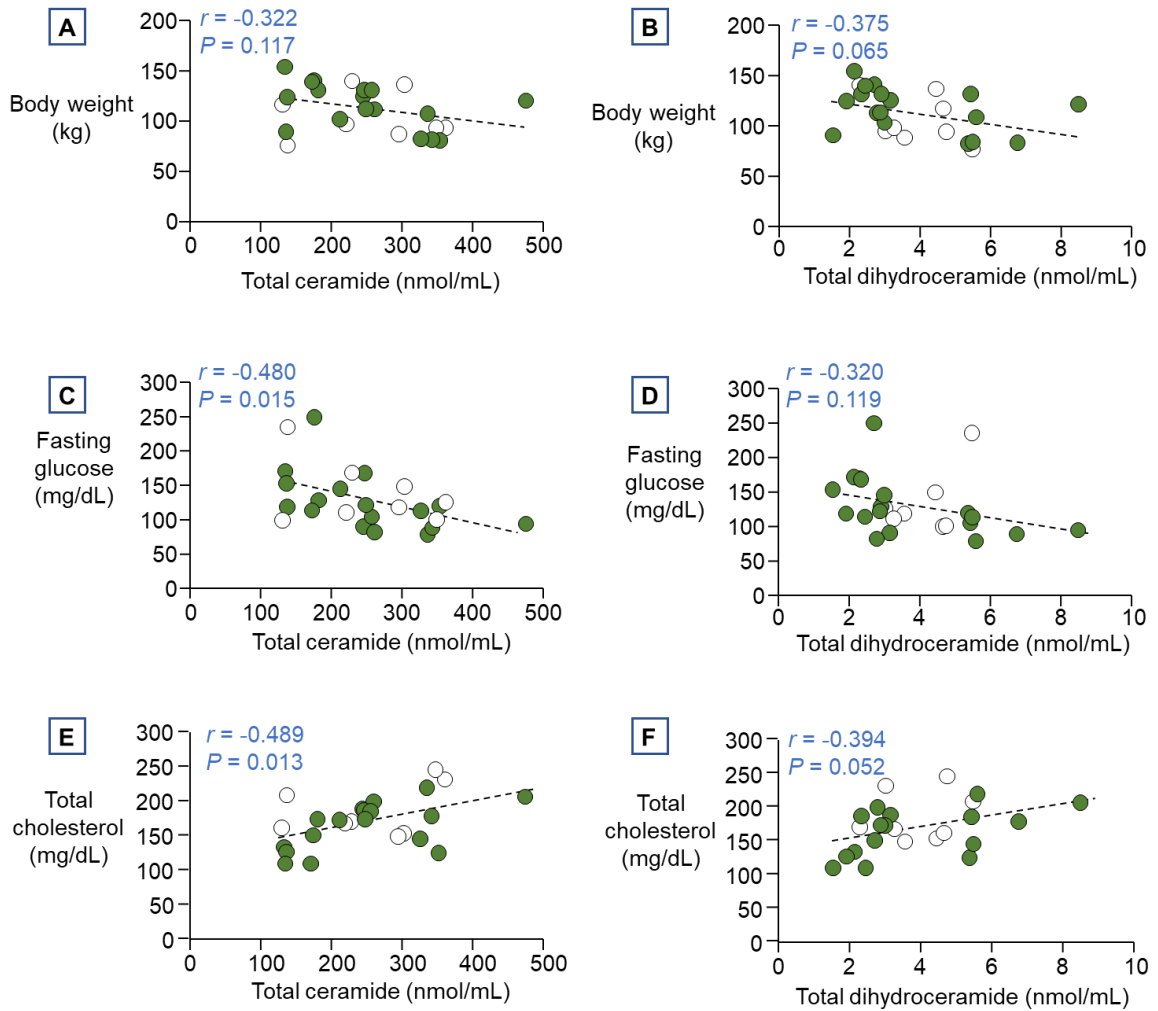
Supplementary Figure S4.7. Relationships between change in fasting fractional DNL and steatosis, lobular inflammation, and glucose production



Data accompany **figure 4.24**.

A-C: Relationships between fractional VLDL-TG from DNL and (A) steatosis, (B) lobular inflammation, and (C) EGP. Spearman's correlation; Treatment: $n = 7$, Standard care: $n = 2$.

Supplementary Figure S4.8. Baseline relationships between total ceramides and dihydroceramides with weight, fasting glucose, and total cholesterol



Pearson's correlation was used to assess linear relationships between continuous variables. Treatment subjects are shown in green circles and standard care in white. Treatment: $n = 17$, Standard care: $n = 8$.

A, C, E: Baseline total ceramides and (A) body weight, (C) fasting glucose, and (E) total cholesterol.

B, D, F: Baseline total dihydroceramides and (B) body weight, (D) fasting glucose, and (F) total cholesterol.

SUPPORTING INFORMATION

Histological improvements from increased peripheral substrate disposal: Muscle glucose uptake spares the liver

Justine M. Mucinski¹, Amadeo F. Salvador^{1,2,3}, Mary P. Moore^{1,4,5}, Talyia M. Fordham¹, Jen M. Anderson¹, Grace Meers^{1,4}, Guido Lastra⁶, Ghassan M. Hammoud², Alberto Diaz-Arias⁷, Jamal A. Ibdah^{1,2,4}, R. Scott Rector^{1,2,4}, Elizabeth J. Parks^{1,2,*}

¹ Department of Nutrition and Exercise Physiology, University of Missouri, Columbia, MO 65212

² Department of Medicine, Division of Gastroenterology and Hepatology, School of Medicine, University of Missouri, Columbia, MO 65212

³ Department of Electrical Engineering and Computer Science, Institute for Data Science and Informatics, University of Missouri, Columbia, MO 65212

⁴ Research Service, Harry S Truman Memorial Veterans Medical Center, Columbia, MO 65201

⁵ Department of Medicine, Columbia University Irving Medical Center, New York, NY, USA.

⁶ Endocrinology and Metabolism, School of Medicine, University of Missouri, Columbia, MO 65212

⁷ Boyce & Bynum Pathology Laboratories, Columbia, MO, 65201

***CORRESPONDING AUTHOR:**

Elizabeth J. Parks, PhD

One Hospital Drive School of Medicine NW 406

University of Missouri

Columbia, Missouri 65212

Email: parksej@missouri.edu

RUNNING TITLE: Histologic improvements in NASH

AUTHOR CONTRIBUTION: EJP, RSR, and JAI were involved in study design and methods; JMM, AFS, MPM, TMF, JMA, GM, GMH, AD-A, RSR, and EJP generated the data; GL provided medical oversight to the project; JMM analyzed data and wrote the paper; All authors contributed to data interpretation and to editing the manuscript.

AUTHOR DISCLOSURES: None.

REFERENCES

1. Goyal NP, and Schwimmer JB. The progression and natural history of pediatric nonalcoholic fatty liver disease. *Clinics in Liver Disease* 20, 325-338, (2016), PMID:27063272.
2. Vernon G, Baranova A, and Younossi ZM. Systematic review: the epidemiology and natural history of non-alcoholic fatty liver disease and non-alcoholic steatohepatitis in adults. *Alimentary Pharmacology and Therapeutics* 34, 274-285, (2011), PMID:21623852.
3. Browning JD, Szczepaniak LS, Dobbins R, Nuremberg P, Horton JD, Cohen JC, Grundy SM, and Hobbs HH. Prevalence of hepatic steatosis in an urban population in the United States: Impact of ethnicity. *Hepatology* 40, 1387-1395, (2004), PMID:15565570.
4. Feldstein AE, Charatcharoenwitthaya P, Treeprasertsuk S, Benson JT, Enders FB, and Angulo P. The natural history of non-alcoholic fatty liver disease in children: a follow-up study for up to 20 years. *Gut* 58, 1538-1544, (2009), PMID:19625277.
5. Younossi ZM, Golabi P, de Avila L, Paik JM, Srishord M, Fukui N, Qiu Y, Burns L, Afendy A, and Nader F. The global epidemiology of NAFLD and NASH in patients with type 2 diabetes: A systematic review and meta-analysis. *Journal of Hepatology* 71, 793-801, (2019), PMID:31279902.
6. Chalasani N, Younossi Z, Lavine JE, Charlton M, Cusi K, Rinella M, Harrison SA, Brunt EM, and Sanyal AJ. The diagnosis and management of nonalcoholic fatty liver disease: Practice guidance from the American Association for the Study of Liver Diseases. *Hepatology* 67, 328-357, (2018), PMID:28714183.
7. Argo CK, and Caldwell SH. Epidemiology and natural history of non-alcoholic steatohepatitis. *Clinics in Liver Disease* 13, 511-531, (2009), PMID:19818302.
8. Korenblat KM, Fabbrini E, Mohammed BS, and Klein S. Liver, muscle, and adipose tissue insulin action is directly related to intrahepatic triglyceride content in obese subjects. *Gastroenterology* 134, 1369-1375, (2008), PMID:18355813.
9. Sanyal AJ, Campbell-Sargent C, Mirshahi F, Rizzo WB, Contos MJ, Sterling RK, Luketic VA, Shiffman ML, and Clore JN. Nonalcoholic steatohepatitis: association of insulin resistance and mitochondrial abnormalities. *Gastroenterology* 120, 1183-1192, (2001), PMID:11266382.
10. Cree MG, Newcomer BR, Katsanos CS, Sheffield-Moore M, Chinkes D, Aarsland A, Urban R, and Wolfe RR. Intramuscular and liver triglycerides are increased in the elderly. *The Journal of Clinical Endocrinology and Metabolism* 89, 3864-3871, (2004), PMID:15292319.
11. Koska J, Stefan N, Permana PA, Weyer C, Sonoda M, Bogardus C, Smith SR, Joannisse DR, Funahashi T, Krakoff J, and Bunt JC. Increased fat accumulation in liver may link insulin resistance with subcutaneous abdominal adipocyte enlargement, visceral adiposity, and hypoadiponectinemia in obese individuals. *American Journal of Clinical Nutrition* 87, 295-302, (2008), PMID:18258617.

12. Kelley DE, McKolanis TM, Hegazi RA, Kuller LH, and Kalhan SC. Fatty liver in type 2 diabetes mellitus: relation to regional adiposity, fatty acids, and insulin resistance. *American Journal of Physiology Endocrinology and Metabolism* 285, E906-916, (2003), PMID:12959938.
13. Lomonaco R, Ortiz-Lopez C, Orsak B, Webb A, Hardies J, Darland C, Finch J, Gastaldelli A, Harrison S, Tio F, and Cusi K. Effect of adipose tissue insulin resistance on metabolic parameters and liver histology in obese patients with nonalcoholic fatty liver disease. *Hepatology* 55, 1389-1397, (2012), PMID:22183689.
14. Stepanova M, Rafiq N, Makhlof H, Agrawal R, Kaur I, Younoszai Z, McCullough A, Goodman Z, and Younossi ZM. Predictors of all-cause mortality and liver-related mortality in patients with non-alcoholic fatty liver disease (NAFLD). *Digestive Diseases and Sciences* 58, 3017-3023, (2013), PMID:23775317.
15. Chalasani N, Younossi Z, Lavine JE, Diehl AM, Brunt EM, Cusi K, Charlton M, and Sanyal AJ. The diagnosis and management of non-alcoholic fatty liver disease: practice Guideline by the American Association for the Study of Liver Diseases, American College of Gastroenterology, and the American Gastroenterological Association. *Hepatology* 55, 2005-2023, (2012), PMID:22488764.
16. European Association for the Study of the L, European Association for the Study of D, and European Association for the Study of O. EASL-EASD-EASO Clinical Practice Guidelines for the management of non-alcoholic fatty liver disease. *Journal of Hepatology* 64, 1388-1402, (2016), PMID:27062661.
17. Glen J, Floros L, Day C, Pryke R, and Guideline Development G. Non-alcoholic fatty liver disease (NAFLD): summary of NICE guidance. *British Medical Journal* 354, i4428, (2016), PMID:27605111.
18. Petroni ML, Brodosi L, Bugianesi E, and Marchesini G. Management of non-alcoholic fatty liver disease. *British Medical Journal* 372, m4747, (2021), PMID:33461969.
19. Romero-Gomez M, Zelber-Sagi S, and Trenell M. Treatment of NAFLD with diet, physical activity and exercise. *Journal of Hepatology* 67, 829-846, (2017), PMID:28545937.
20. St. George A, Bauman A, Johnston A, Farrell G, Chey T, and George J. Independent effects of physical activity in patients with nonalcoholic fatty liver disease. *Hepatology* 50, 68-76, (2009), PMID:19444870.
21. Bacchi E, Negri C, Targher G, Faccioli N, Lanza M, Zoppini G, Zanolin E, Schena F, Bonora E, and Moghetti P. Both resistance training and aerobic training reduce hepatic fat content in type 2 diabetic subjects with nonalcoholic fatty liver disease (the RAED2 randomized trial). *Hepatology* 58, 1287-1295, (2013), PMID:23504926.
22. Hallsworth K, Fattakhova G, Hollingsworth KG, Thoma C, Moore S, Taylor R, Day CP, and Trenell MI. Resistance exercise reduces liver fat and its mediators in non-alcoholic fatty liver disease independent of weight loss. *Gut* 60, 1278-1283, (2011), PMID:21708823.

23. Iwanaga S, Hashida R, Takano Y, Bekki M, Nakano D, Omoto M, Nago T, Kawaguchi T, Matsuse H, Torimura T, and Shiba N. Hybrid training system improves insulin resistance in patients with nonalcoholic fatty liver disease: A randomized controlled pilot study. *The Tohoku Journal of Experimental Medicine* 252, 23-32, (2020), PMID:32863329.
24. Cevik Saldiran T, Mutluay FK, Yagci I, and Yilmaz Y. Impact of aerobic training with and without whole-body vibration training on metabolic features and quality of life in non-alcoholic fatty liver disease patients. *Annales d'Endocrinologie* 81, 493-499, (2020), PMID:32768394.
25. Lee S, Libman I, Hughtan K, Kuk JL, Jeong JH, Zhang D, and Arslanian S. Effects of exercise modality on insulin resistance and ectopic fat in adolescents with overweight and obesity: A randomized clinical trial. *The Journal of Pediatrics* 206, 91-98 e91, (2019), PMID:30554789.
26. Kang DW, Park JH, Lee MK, Kim Y, Kong ID, Chung CH, Lee YH, and Jeon JY. Effect of a short-term physical activity intervention on liver fat content in obese children. *Applied Physiology, Nutrition, and Metabolism* 43, 553-557, (2018), PMID:29262266.
27. Brouwers B, Schrauwen-Hinderling VB, Jelenik T, Gemmink A, Sparks LM, Havekes B, Bruls Y, Dahlmans D, Roden M, Hesselink MKC, and Schrauwen P. Exercise training reduces intrahepatic lipid content in people with and people without nonalcoholic fatty liver. *American Journal of Physiology-Endocrinology and Metabolism* 314, E165-E173, (2018), PMID:29118014.
28. Rezende RE, Duarte SM, Stefano JT, Roschel H, Gualano B, de Sa Pinto AL, Vezozzo DC, Carrilho FJ, and Oliveira CP. Randomized clinical trial: benefits of aerobic physical activity for 24 weeks in postmenopausal women with nonalcoholic fatty liver disease. *Menopause* 23, 876-883, (2016), PMID:27458060.
29. Cuthbertson DJ, Shojaee-Moradie F, Sprung VS, Jones H, Pugh CJ, Richardson P, Kemp GJ, Barrett M, Jackson NC, Thomas EL, Bell JD, and Umpleby AM. Dissociation between exercise-induced reduction in liver fat and changes in hepatic and peripheral glucose homeostasis in obese patients with non-alcoholic fatty liver disease. *Clinical Science (London, England: 1979)* 130, 93-104, (2016), PMID:26424731.
30. de Piano A, de Mello MT, Sanches Pde L, da Silva PL, Campos RM, Carnier J, Corgosinho F, Foschini D, Masquio DL, Tock L, Oyama LM, do Nascimento CM, Tufik S, and Damaso AR. Long-term effects of aerobic plus resistance training on the adipokines and neuropeptides in nonalcoholic fatty liver disease obese adolescents. *European Journal of Gastroenterology and Hepatology* 24, 1313-1324, (2012), PMID:22932160.
31. Lee S, Bacha F, Hannon T, Kuk JL, Boesch C, and Arslanian S. Effects of aerobic versus resistance exercise without caloric restriction on abdominal fat, intrahepatic lipid, and insulin sensitivity in obese adolescent boys: a randomized, controlled trial. *Diabetes* 61, 2787-2795, (2012), PMID:22751691.
32. Fealy CE, Haus JM, Solomon TP, Pagadala M, Flask CA, McCullough AJ, and Kirwan JP. Short-term exercise reduces markers of hepatocyte apoptosis

- in nonalcoholic fatty liver disease. *Journal of Applied Physiology* 113, 1-6, (2012), PMID:22582214.
33. Slentz CA, Bateman LA, Willis LH, Shields AT, Tanner CJ, Piner LW, Hawk VH, Muehlbauer MJ, Samsa GP, Nelson RC, Huffman KM, Bales CW, Houmard JA, and Kraus WE. Effects of aerobic vs. resistance training on visceral and liver fat stores, liver enzymes, and insulin resistance by HOMA in overweight adults from STRRIDE AT/RT. *American Journal of Physiology-Endocrinology and Metabolism* 301, E1033-1039, (2011), PMID:21846904.
 34. van der Heijden GJ, Wang ZJ, Chu ZD, Sauer PJ, Haymond MW, Rodriguez LM, and Sunehag AL. A 12-week aerobic exercise program reduces hepatic fat accumulation and insulin resistance in obese, Hispanic adolescents. *Obesity (Silver Spring)* 18, 384-390, (2010), PMID:19696755.
 35. Johnson NA, Sachinwalla T, Walton DW, Smith K, Armstrong A, Thompson MW, and George J. Aerobic exercise training reduces hepatic and visceral lipids in obese individuals without weight loss. *Hepatology* 50, 1105-1112, (2009), PMID:19637289.
 36. Shojaee-Moradie F, Baynes KC, Pentecost C, Bell JD, Thomas EL, Jackson NC, Stolinski M, Whyte M, Lovell D, Bowes SB, Gibney J, Jones RH, and Umpleby AM. Exercise training reduces fatty acid availability and improves the insulin sensitivity of glucose metabolism. *Diabetologia* 50, 404-413, (2007), PMID:17149589.
 37. Sargeant JA, Bawden S, Aithal GP, Simpson EJ, Macdonald IA, Turner MC, Cegielski J, Smith K, Dorling JL, Gowland PA, Nimmo MA, and King JA. Effects of sprint interval training on ectopic lipids and tissue-specific insulin sensitivity in men with non-alcoholic fatty liver disease. *European Journal of Applied Physiology* 118, 817-828, (2018), PMID:29411128.
 38. Yurtdas G, Akbulut G, Baran M, and Yilmaz C. The effects of Mediterranean diet on hepatic steatosis, oxidative stress, and inflammation in adolescents with non-alcoholic fatty liver disease: A randomized controlled trial. *Pediatric Obesity* 17, e12872, (2022), PMID:34881510.
 39. Chen J, Huang Y, Xie H, Bai H, Lin G, Dong Y, Shi D, Wang J, Zhang Q, Zhang Y, and Sun J. Impact of a low-carbohydrate and high-fiber diet on nonalcoholic fatty liver disease. *Asia Pacific Journal of Clinical Nutrition* 29, 483-490, (2020), PMID:32990607.
 40. Yoshino M, Kayser BD, Yoshino J, Stein RI, Reeds D, Eagon JC, Eckhouse SR, Watrous JD, Jain M, Knight R, Schechtman K, Patterson BW, and Klein S. Effects of diet versus gastric bypass on metabolic function in diabetes. *The New England Journal of Medicine* 383, 721-732, (2020), PMID:32813948.
 41. Goss AM, Dowla S, Pendergrass M, Ashraf A, Bolding M, Morrison S, Amerson A, Soleymani T, and Gower B. Effects of a carbohydrate-restricted diet on hepatic lipid content in adolescents with non-alcoholic fatty liver disease: A pilot, randomized trial. *Pediatric Obesity* 15, e12630, (2020), PMID:32128995.
 42. Smith GI, Shankaran M, Yoshino M, Schweitzer GG, Chondronikola M, Beals JW, Okunade AL, Patterson BW, Nyangau E, Field T, Sirlin CB, Talukdar S, Hellerstein MK, and Klein S. Insulin resistance drives hepatic de novo

- lipogenesis in nonalcoholic fatty liver disease. *Journal of Clinical Investigation* 130, 1453-1460, (2020), PMID:31805015.
43. Otten J, Mellberg C, Ryberg M, Sandberg S, Kullberg J, Lindahl B, Larsson C, Hauksson J, and Olsson T. Strong and persistent effect on liver fat with a Paleolithic diet during a two-year intervention. *International Journal of Obesity (2005)* 40, 747-753, (2016), PMID:26786351.
 44. Razavi Zade M, Telkabadi MH, Bahmani F, Salehi B, Farshbaf S, and Asemi Z. The effects of DASH diet on weight loss and metabolic status in adults with non-alcoholic fatty liver disease: a randomized clinical trial. *Liver International* 36, 563-571, (2016), PMID:26503843.
 45. Lee S, Deldin AR, White D, Kim Y, Libman I, Rivera-Vega M, Kuk JL, Sandoval S, Boesch C, and Arslanian S. Aerobic exercise but not resistance exercise reduces intrahepatic lipid content and visceral fat and improves insulin sensitivity in obese adolescent girls: a randomized controlled trial. *American Journal of Physiology-Endocrinology and Metabolism* 305, E1222-1229, (2013), PMID:24045865.
 46. Haufe S, Haas V, Utz W, Birkenfeld AL, Jeran S, Bohnke J, Mahler A, Luft FC, Schulz-Menger J, Boschmann M, Jordan J, and Engeli S. Long-lasting improvements in liver fat and metabolism despite body weight regain after dietary weight loss. *Diabetes Care* 36, 3786-3792, (2013), PMID:23963894.
 47. Ryan MC, Itsiopoulos C, Thodis T, Ward G, Trost N, Hofferberth S, O'Dea K, Desmond PV, Johnson NA, and Wilson AM. The Mediterranean diet improves hepatic steatosis and insulin sensitivity in individuals with non-alcoholic fatty liver disease. *Journal of Hepatology* 59, 138-143, (2013), PMID:23485520.
 48. Haufe S, Engeli S, Kast P, Bohnke J, Utz W, Haas V, Hermsdorf M, Mahler A, Wiesner S, Birkenfeld AL, Sell H, Otto C, Mehling H, Luft FC, Eckel J, Schulz-Menger J, Boschmann M, and Jordan J. Randomized comparison of reduced fat and reduced carbohydrate hypocaloric diets on intrahepatic fat in overweight and obese human subjects. *Hepatology* 53, 1504-1514, (2011), PMID:21400557.
 49. de Luis DA, Aller R, Izaola O, Gonzalez Sagrado M, and Conde R. Effect of two different hypocaloric diets in transaminases and insulin resistance in nonalcoholic fatty liver disease and obese patients. *Nutricion Hospitalaria* 25, 730-735, (2010), PMID:21336428.
 50. Garinis GA, Fruci B, Mazza A, De Siena M, Abenavoli S, Gulletta E, Ventura V, Greco M, Abenavoli L, and Belfiore A. Metformin versus dietary treatment in nonalcoholic hepatic steatosis: a randomized study. *International Journal of Obesity (2005)* 34, 1255-1264, (2010), PMID:20179669.
 51. Elias MC, Parise ER, de Carvalho L, Szejnfeld D, and Netto JP. Effect of 6-month nutritional intervention on non-alcoholic fatty liver disease. *Nutrition* 26, 1094-1099, (2010), PMID:20022466.
 52. Vitola BE, Deivanayagam S, Stein RI, Mohammed BS, Magkos F, Kirk EP, and Klein S. Weight loss reduces liver fat and improves hepatic and skeletal muscle insulin sensitivity in obese adolescents. *Obesity (Silver Spring)* 17, 1744-1748, (2009), PMID:19498349.

53. Kirk E, Reeds DN, Finck BN, Mayurranjan SM, Patterson BW, and Klein S. Dietary fat and carbohydrates differentially alter insulin sensitivity during caloric restriction. *Gastroenterology* 136, 1552-1560, (2009), PMID:19208352.
54. Viljanen AP, Iozzo P, Borra R, Kankaanpaa M, Karmi A, Lautamaki R, Jarvisalo M, Parkkola R, Ronnema T, Guiducci L, Lehtimaki T, Raitakari OT, Mari A, and Nuutila P. Effect of weight loss on liver free fatty acid uptake and hepatic insulin resistance. *The Journal of Clinical Endocrinology and Metabolism* 94, 50-55, (2009), PMID:18957499.
55. Sato F, Tamura Y, Watada H, Kumashiro N, Igarashi Y, Uchino H, Maehara T, Kyogoku S, Sunayama S, Sato H, Hirose T, Tanaka Y, and Kawamori R. Effects of diet-induced moderate weight reduction on intrahepatic and intramyocellular triglycerides and glucose metabolism in obese subjects. *The Journal of Clinical Endocrinology and Metabolism* 92, 3326-3329, (2007), PMID:17519317.
56. Huang MA, Greenon JK, Chao C, Anderson L, Peterman D, Jacobson J, Emick D, Lok AS, and Conjeevaram HS. One-year intense nutritional counseling results in histological improvement in patients with non-alcoholic steatohepatitis: a pilot study. *The American Journal of Gastroenterology* 100, 1072-1081, (2005), PMID:15842581.
57. Petersen KF, Dufour S, Befroy D, Lehrke M, Hendler RE, and Shulman GI. Reversal of nonalcoholic hepatic steatosis, hepatic insulin resistance, and hyperglycemia by moderate weight reduction in patients with type 2 diabetes. *Diabetes* 54, 603-608, (2005), PMID:15734833.
58. Straznicki NE, Lambert EA, Grima MT, Eikelis N, Nestel PJ, Dawood T, Schlaich MP, Masuo K, Chopra R, Sari CI, Dixon JB, Tilbrook AJ, and Lambert GW. The effects of dietary weight loss with or without exercise training on liver enzymes in obese metabolic syndrome subjects. *Diabetes, Obesity and Metabolism* 14, 139-148, (2012), PMID:21923735.
59. Cai L, Yin J, Ma X, Mo Y, Li C, Lu W, Bao Y, Zhou J, and Jia W. Low-carbohydrate diets lead to greater weight loss and better glucose homeostasis than exercise: a randomized clinical trial. *Frontiers in Medicine* 15, 460-471, (2021), PMID:34185279.
60. Charatchoenwitthaya P, Kuljiratitikal K, Aksornchanya O, Chaiyasoot K, Bandidniyamanon W, and Charatchoenwitthaya N. Moderate-intensity aerobic vs resistance exercise and dietary modification in patients with nonalcoholic fatty liver disease: A randomized clinical trial. *Clinical and Translational Gastroenterology* 12, e00316, (2021), PMID:33939383.
61. Labayen I, Medrano M, Arenaza L, Maiz E, Oses M, Martinez-Vizcaino V, Ruiz JR, and Ortega FB. Effects of exercise in addition to a family-based lifestyle intervention program on hepatic fat in children with overweight. *Diabetes Care* 43, 306-313, (2020), PMID:31227585.
62. Dong F, Zhang Y, Huang Y, Wang Y, Zhang G, Hu X, Wang J, Chen J, and Bao Z. Long-term lifestyle interventions in middle-aged and elderly men with nonalcoholic fatty liver disease: a randomized controlled trial. *Scientific Reports* 6, 36783, (2016), PMID:27830836.

63. Abd El-Kader SM, Al-Shreef FM, and Al-Jiffri OH. Biochemical parameters response to weight loss in patients with non-alcoholic steatohepatitis. *African Health Sciences* 16, 242-249, (2016), PMID:27358638.
64. Al-Jiffri O, Al-Sharif FM, Abd El-Kader SM, and Ashmawy EM. Weight reduction improves markers of hepatic function and insulin resistance in type-2 diabetic patients with non-alcoholic fatty liver. *African Health Sciences* 13, 667-672, (2013), PMID:24250305.
65. Savoye M, Caprio S, Dziura J, Camp A, Germain G, Summers C, Li F, Shaw M, Nowicka P, Kursawe R, Depourcq F, Kim G, and Tamborlane WV. Reversal of early abnormalities in glucose metabolism in obese youth: results of an intensive lifestyle randomized controlled trial. *Diabetes Care* 37, 317-324, (2014), PMID:24062325.
66. Scaglioni F, Marino M, Ciccia S, Procaccini A, Busacchi M, Loria P, Lonardo A, Malavolti M, Battistini NC, Pellegrini M, Carubbi F, and Bellentani S. Short-term multidisciplinary non-pharmacological intervention is effective in reducing liver fat content assessed non-invasively in patients with nonalcoholic fatty liver disease (NAFLD). *Clinics and Research in Hepatology and Gastroenterology* 37, 353-358, (2013), PMID:23273500.
67. Santomauro M, Paoli-Valeri M, Fernandez M, Camacho N, Molina Z, Cicchetti R, Valeri L, Davila de Campagnaro E, and Arata-Bellabarba G. Non-alcoholic fatty liver disease and its association with clinical and biochemical variables in obese children and adolescents: effect of a one-year intervention on lifestyle. *Endocrinología y Nutrición* 59, 346-353, (2012), PMID:22717644.
68. Gronbaek H, Lange A, Birkebaek NH, Holland-Fischer P, Solvig J, Horlyck A, Kristensen K, Rittig S, and Vilstrup H. Effect of a 10-week weight loss camp on fatty liver disease and insulin sensitivity in obese Danish children. *Journal of Pediatric Gastroenterology and Nutrition* 54, 223-228, (2012), PMID:21760546.
69. Haus JM, Solomon TP, Marchetti CM, Edmison JM, Gonzalez F, and Kirwan JP. Free fatty acid-induced hepatic insulin resistance is attenuated following lifestyle intervention in obese individuals with impaired glucose tolerance. *The Journal of Clinical Endocrinology and Metabolism* 95, 323-327, (2010), PMID:19906790.
70. St George A, Bauman A, Johnston A, Farrell G, Chey T, and George J. Effect of a lifestyle intervention in patients with abnormal liver enzymes and metabolic risk factors. *Journal of Gastroenterology and Hepatology* 24, 399-407, (2009), PMID:19067776.
71. Chen SM, Liu CY, Li SR, Huang HT, Tsai CY, and Jou HJ. Effects of therapeutic lifestyle program on ultrasound-diagnosed nonalcoholic fatty liver disease. *Journal of the Chinese Medical Association* 71, 551-558, (2008), PMID:19015052.
72. Nobili V, Manco M, Devito R, Di Ciommo V, Comparcola D, Sartorelli MR, Piemonte F, Marcellini M, and Angulo P. Lifestyle intervention and antioxidant therapy in children with nonalcoholic fatty liver disease: a randomized, controlled trial. *Hepatology* 48, 119-128, (2008), PMID:18537181.

73. Wang CL, Liang L, Fu JF, Zou CC, Hong F, Xue JZ, Lu JR, and Wu XM. Effect of lifestyle intervention on non-alcoholic fatty liver disease in Chinese obese children. *World Journal of Gastroenterology* 14, 1598-1602, (2008), PMID:18330955.
74. Nobili V, Manco M, Devito R, Ciampalini P, Piemonte F, and Marcellini M. Effect of vitamin E on aminotransferase levels and insulin resistance in children with non-alcoholic fatty liver disease. *Alimentary Pharmacology and Therapeutics* 24, 1553-1561, (2006), PMID:17206944.
75. Sreenivasa Baba C, Alexander G, Kalyani B, Pandey R, Rastogi S, Pandey A, and Choudhuri G. Effect of exercise and dietary modification on serum aminotransferase levels in patients with nonalcoholic steatohepatitis. *Journal of Gastroenterology and Hepatology* 21, 191-198, (2006), PMID:16706832.
76. Ueno T, Sugawara H, Sujaku K, Hashimoto O, Tsuji R, Tamaki S, Torimura T, Inuzuka S, Sata M, and Tanikawa K. Therapeutic effects of restricted diet and exercise in obese patients with fatty liver. *Journal of Hepatology* 27, 103-107, (1997), PMID:9252081.
77. Tamura Y, Tanaka Y, Sato F, Choi JB, Watada H, Niwa M, Kinoshita J, Ooka A, Kumashiro N, Igarashi Y, Kyogoku S, Maehara T, Kawasumi M, Hirose T, and Kawamori R. Effects of diet and exercise on muscle and liver intracellular lipid contents and insulin sensitivity in type 2 diabetic patients. *The Journal of Clinical Endocrinology & Metabolism* 90, 3191-3196, (2005), PMID:15769987.
78. Sun WH, Song MQ, Jiang CQ, Xin YN, Ma JL, Liu YX, Ma L, Lin ZH, Li CY, Liu L, Zhang M, Chu LL, Jiang XJ, Wan Q, Zhou L, Ren R, and Meng LF. Lifestyle intervention in non-alcoholic fatty liver disease in Chengyang District, Qingdao, China. *World Journal of Hepatology* 4, 224-230, (2012), PMID:22855698.
79. Albu JB, Heilbronn LK, Kelley DE, Smith SR, Azuma K, Berk ES, Pi-Sunyer FX, Ravussin E, and Look AARG. Metabolic changes following a 1-year diet and exercise intervention in patients with type 2 diabetes. *Diabetes* 59, 627-633, (2010), PMID:20028945.
80. Cheng S, Ge J, Zhao C, Le S, Yang Y, Ke D, Wu N, Tan X, Zhang X, Du X, Sun J, Wang R, Shi Y, Borra RJH, Parkkola R, Wiklund P, and Lu D. Effect of aerobic exercise and diet on liver fat in pre-diabetic patients with non-alcoholic-fatty-liver-disease: A randomized controlled trial. *Scientific Reports* 7, 15952, (2017), PMID:29162875.
81. Oshakbayev K, Bimbetov B, Manekenova K, Bedelbayeva G, Mustafin K, and Dukenbayeva B. Severe nonalcoholic steatohepatitis and type 2 diabetes: liver histology after weight loss therapy in a randomized clinical trial. *Current Medical Research and Opinion* 35, 157-165, (2019), PMID:30431378.
82. Catalano D, Trovato GM, Martines GF, Randazzo M, and Tonzuso A. Bright liver, body composition and insulin resistance changes with nutritional intervention: a follow-up study. *Liver International* 28, 1280-1287, (2008), PMID:18435716.
83. Larson-Meyer DE, Heilbronn LK, Redman LM, Newcomer BR, Frisard MI, Anton S, Smith SR, Alfonso A, and Ravussin E. Effect of calorie restriction with or without exercise on insulin sensitivity, beta-cell function, fat cell size,

- and ectopic lipid in overweight subjects. *Diabetes Care* 29, 1337-1344, (2006), PMID:16732018.
84. Larson-Meyer DE, Newcomer BR, Heilbronn LK, Volaufova J, Smith SR, Alfonso AJ, Lefevre M, Rood JC, Williamson DA, Ravussin E, and Pennington CT. Effect of 6-month calorie restriction and exercise on serum and liver lipids and markers of liver function. *Obesity (Silver Spring)* 16, 1355-1362, (2008), PMID:18421281.
 85. Shah K, Stufflebam A, Hilton TN, Sinacore DR, Klein S, and Villareal DT. Diet and exercise interventions reduce intrahepatic fat content and improve insulin sensitivity in obese older adults. *Obesity (Silver Spring)* 17, 2162-2168, (2009), PMID:19390517.
 86. Kantartzis K, Thamer C, Peter A, Machann J, Schick F, Schraml C, Konigsrainer A, Konigsrainer I, Krober S, Niess A, Fritsche A, Haring HU, and Stefan N. High cardiorespiratory fitness is an independent predictor of the reduction in liver fat during a lifestyle intervention in non-alcoholic fatty liver disease. *Gut* 58, 1281-1288, (2009), PMID:19074179.
 87. Thamer C, Machann J, Stefan N, Haap M, Schafer S, Brenner S, Kantartzis K, Claussen C, Schick F, Haring H, and Fritsche A. High visceral fat mass and high liver fat are associated with resistance to lifestyle intervention. *Obesity (Silver Spring)* 15, 531-538, (2007), PMID:17299127.
 88. Eckard C, Cole R, Lockwood J, Torres DM, Williams CD, Shaw JC, and Harrison SA. Prospective histopathologic evaluation of lifestyle modification in nonalcoholic fatty liver disease: a randomized trial. *Therapeutic Advances in Gastroenterology* 6, 249-259, (2013), PMID:23814606.
 89. Vilar-Gomez E, Martinez-Perez Y, Calzadilla-Bertot L, Torres-Gonzalez A, Gra-Oramas B, Gonzalez-Fabian L, Friedman SL, Diago M, and Romero-Gomez M. Weight loss through lifestyle modification significantly reduces features of nonalcoholic steatohepatitis. *Gastroenterology* 149, 367-378.e365, (2015), PMID:25865049.
 90. Vilar Gomez E, Rodriguez De Miranda A, Gra Oramas B, Arus Soler E, Llanio Navarro R, Calzadilla Bertot L, Yasells Garcia A, and Del Rosario Abreu Vazquez M. Clinical trial: a nutritional supplement Viusid, in combination with diet and exercise, in patients with nonalcoholic fatty liver disease. *Alimentary Pharmacology and Therapeutics* 30, 999-1009, (2009), PMID:19691668.
 91. Tendler D, Lin S, Yancy WS, Jr., Mavropoulos J, Sylvestre P, Rockey DC, and Westman EC. The effect of a low-carbohydrate, ketogenic diet on nonalcoholic fatty liver disease: a pilot study. *Digestive Diseases and Sciences* 52, 589-593, (2007), PMID:17219068.
 92. Promrat K, Kleiner DE, Niemeier HM, Jackvony E, Kearns M, Wands JR, Fava JL, and Wing RR. Randomized controlled trial testing the effects of weight loss on nonalcoholic steatohepatitis. *Hepatology* 51, 121-129, (2010), PMID:19827166.
 93. Bril F, Barb D, Lomonaco R, Lai J, and Cusi K. Change in hepatic fat content measured by MRI does not predict treatment-induced histological improvement of steatohepatitis. *Journal of Hepatology* 72, 401-410, (2020), PMID:31589891.

94. Utzschneider KM, and Kahn SE. The role of insulin resistance in nonalcoholic fatty liver disease. *The Journal of Clinical Endocrinology & Metabolism* 91, 4753-4761, (2006), PMID:16968800.
95. Lomonaco R, Ortiz-Lopez C, Orsak B, Webb A, Hardies J, Darland C, Finch J, Gastaldelli A, Harrison S, Tio F, and Cusi K. Effect of adipose tissue insulin resistance on metabolic parameters and liver histology in obese patients with nonalcoholic fatty liver disease. *Hepatology* 55, 1389-1397, (2012), PMID:22183689.
96. Lambert JE, Ramos-Roman MA, Browning JD, and Parks EJ. Increased de novo lipogenesis is a distinct characteristic of individuals with nonalcoholic fatty liver disease. *Gastroenterology* 146, 726-735, (2014), PMID:24316260.
97. Donnelly KL, Smith CI, Schwarzenberg SJ, Jessurun J, Boldt MD, and Parks EJ. Sources of fatty acids stored in liver and secreted via lipoproteins in patients with nonalcoholic fatty liver disease. *Journal of Clinical Investigation* 115, 1343-1351, (2005), PMID:15864352.
98. Iozzo P, Turpeinen AK, Takala T, Oikonen V, Bergman J, Gronroos T, Ferrannini E, Nuutila P, and Knuuti J. Defective liver disposal of free fatty acids in patients with impaired glucose tolerance. *The Journal of Clinical Endocrinology and Metabolism* 89, 3496-3502, (2004), PMID:15240637.
99. Iozzo P, Bucci M, Roivainen A, Nägren K, Järvisalo MJ, Kiss J, Guiducci L, Fielding B, Naum AG, Borra R, Virtanen K, Savunen T, Salvadori PA, Ferrannini E, Knuuti J, and Nuutila P. Fatty acid metabolism in the liver, measured by positron emission tomography, is increased in obese individuals. *Gastroenterology* 139, 846-856, 856.e841-846, (2010), PMID:20685204.
100. Rigazio S, Lehto HR, Tuunanen H, Nagren K, Kankaanpää M, Simi C, Borra R, Naum AG, Parkkola R, Knuuti J, Nuutila P, and Iozzo P. The lowering of hepatic fatty acid uptake improves liver function and insulin sensitivity without affecting hepatic fat content in humans. *American Journal of Physiology: Endocrinology and Metabolism* 295, E413-419, (2008), PMID:18505832.
101. Heath RB, Karpe F, Milne RW, Burdge GC, Wootton SA, and Frayn KN. Selective partitioning of dietary fatty acids into the VLDL TG pool in the early postprandial period. *Journal of Lipid Research* 44, 2065-2072, (2003), PMID:12923230.
102. Westerbacka J, Lammi K, Häkkinen A-M, Rissanen A, Salminen I, Aro A, and Yki-Järvinen H. Dietary fat content modifies liver fat in overweight nondiabetic subjects. *The Journal of Clinical Endocrinology & Metabolism* 90, 2804-2809, (2005), PMID:15741262.
103. Tamura S, and Shimomura I. Contribution of adipose tissue and de novo lipogenesis to nonalcoholic fatty liver disease. *The Journal of Clinical Investigation* 115, 1139-1142, (2005), PMID:15864343.
104. Cusi K. Role of obesity and lipotoxicity in the development of nonalcoholic steatohepatitis: Pathophysiology and clinical implications. *Gastroenterology* 142, 711-725.e716, (2012), PMID:22326434.

105. Fabbrini E, Mohammed BS, Magkos F, Korenblat KM, Patterson BW, and Klein S. Alterations in adipose tissue and hepatic lipid kinetics in obese men and women with nonalcoholic fatty liver disease. *Gastroenterology* 134, 424-431, (2008), PMID:18242210.
106. Iozzo P, Turpeinen AK, Takala T, Oikonen V, Bergman Jr, Grönroos T, Ferrannini E, Nuutila P, and Knuuti J. Defective liver disposal of free fatty acids in patients with impaired glucose tolerance. *The Journal of Clinical Endocrinology & Metabolism* 89, 3496-3502, (2004), PMID:15240637.
107. Malhi H, and Gores G. Molecular mechanisms of lipotoxicity in nonalcoholic fatty liver disease. *Seminars in Liver Disease* 28, 360-369, (2008), PMID:18956292.
108. Staehr P, Hother-Nielsen O, Landau BR, Chandramouli V, Holst JJ, and Beck-Nielsen H. Effects of free fatty acids per se on glucose production, gluconeogenesis, and glycogenolysis. *Diabetes* 52, 260-267, (2003), PMID:12540595.
109. Bajaj M, Berria R, Pratipanawatr T, Kashyap S, Pratipanawatr W, Belfort R, Cusi K, Mandarin L, and DeFronzo RA. Free fatty acid-induced peripheral insulin resistance augments splanchnic glucose uptake in healthy humans. *American Journal of Physiology: Endocrinology and Metabolism* 283, E346-352, (2002), PMID:12110541.
110. Boden G. Free fatty acids-the link between obesity and insulin resistance. *Endocrine Practice* 7, 44-51, (2001), PMID:11250769.
111. Ferrannini E, Barrett EJ, Bevilacqua S, and DeFronzo RA. Effect of fatty acids on glucose production and utilization in man. *Journal of Clinical Investigation* 72, 1737-1747, (1983), PMID:6138367.
112. Bugianesi E, Gastaldelli A, Vanni E, Gambino R, Cassader M, Baldi S, Ponti V, Pagano G, Ferrannini E, and Rizzetto M. Insulin resistance in non-diabetic patients with non-alcoholic fatty liver disease: sites and mechanisms. *Diabetologia* 48, 634-642, (2005), PMID:15747110.
113. Seppala-Lindroos A, Vehkavaara S, Hakkinen AM, Goto T, Westerbacka J, Sovijarvi A, Halavaara J, and Yki-Jarvinen H. Fat accumulation in the liver is associated with defects in insulin suppression of glucose production and serum free fatty acids independent of obesity in normal men. *Journal of Clinical Endocrinology and Metabolism* 87, 3023-3028, (2002), PMID:12107194.
114. Marchesini G, Brizi M, Bianchi G, Tomassetti S, Bugianesi E, Lenzi M, McCullough AJ, Natale S, Forlani G, and Melchionda N. Nonalcoholic fatty liver disease: a feature of the metabolic syndrome. *Diabetes* 50, 1844-1850, (2001), PMID:11473047.
115. Boden G, Cheung P, Stein TP, Kresge K, and Mozzoli M. FFA cause hepatic insulin resistance by inhibiting insulin suppression of glycogenolysis. *American Journal of Physiology: Endocrinology and Metabolism* 283, E12-19, (2002), PMID:12067837.
116. Horton JD, Goldstein JL, and Brown MS. SREBPs: activators of the complete program of cholesterol and fatty acid synthesis in the liver. *Journal of Clinical Investigation* 109, 1125-1131, (2002), PMID:11994399.

117. Brown MS, and Goldstein JL. The SREBP pathway: regulation of cholesterol metabolism by proteolysis of a membrane-bound transcription factor. *Cell* 89, 331-340, (1997), PMID:9150132.
118. Brown MS, and Goldstein JL. Selective versus total insulin resistance: A pathogenic paradox. *Cell Metabolism* 7, 95-96, (2008), PMID:18249166.
119. McGarry JD. What if Minkowski had been ageusic? An alternative angle on diabetes. *Science* 258, 766-770, (1992), PMID:1439783.
120. Musso G, Gambino R, De Michieli F, Cassader M, Rizzetto M, Durazzo M, Faga E, Silli B, and Pagano G. Dietary habits and their relations to insulin resistance and postprandial lipemia in nonalcoholic steatohepatitis. *Hepatology* 37, 909-916, (2003), PMID:12668986.
121. Cassader M, Gambino R, Musso G, Depetris N, Mecca F, Cavallo-Perin P, Pacini G, Rizzetto M, and Pagano G. Postprandial triglyceride-rich lipoprotein metabolism and insulin sensitivity in nonalcoholic steatohepatitis patients. *Lipids* 36, 1117-1124, (2001), PMID:11768156.
122. Brunt EM, Janney CG, Bisceglie AM, Neuschwander-Tetri BA, and Bacon BR. Nonalcoholic steatohepatitis: a proposal for grading and staging the histological lesions. *The American Journal of Gastroenterology* 94, 2467-2474, (1999), PMID:10484010.
123. Liguori G, and Medicine ACoS. *ACSM's guidelines for exercise testing and prescription*. Lippincott Williams & Wilkins, 2020.
124. Winn NC, Liu Y, Rector RS, Parks EJ, Ibdah JA, and Kanaley JA. Energy-matched moderate and high intensity exercise training improves nonalcoholic fatty liver disease risk independent of changes in body mass or abdominal adiposity — A randomized trial. *Metabolism: Clinical and Experimental* 78, 128-140, (2018), PMID:28941598.
125. Idilman IS, Tuzun A, Savas B, Elhan AH, Celik A, Idilman R, and Karcaaltincaba M. Quantification of liver, pancreas, kidney, and vertebral body MRI-PDFF in non-alcoholic fatty liver disease. *Abdominal Imaging* 40, 1512-1519, (2015), PMID:25715922.
126. Barrows BR, and Parks EJ. Contributions of different fatty acid sources to very low-density lipoprotein-triacylglycerol in the fasted and fed states. *Journal of Clinical Endocrinology and Metabolism* 91, 1446-1452, (2006), PMID:16449340.
127. Muthusamy K, Nelson RH, Singh E, Vlazny D, Smailovic A, and Miles JM. Effect of insulin infusion on spillover of meal-derived fatty acids. *The Journal of Clinical Endocrinology and Metabolism* 97, 4201-4205, (2012), PMID:22977275.
128. Murphy EJ. Stable isotope methods for the in vivo measurement of lipogenesis and triglyceride metabolism. *Journal of Animal Science* 84 Suppl, E94-104, (2006), PMID:16582096.
129. Hellerstein MK, and Neese RA. Mass isotopomer distribution analysis at eight years: theoretical, analytic, and experimental considerations. *American Journal of Physiology* 276, E1146-1170, (1999), PMID:10362629.

130. Hellerstein MK, and Neese RA. Mass isotopomer distribution analysis: a technique for measuring biosynthesis and turnover of polymers. *American Journal of Physiology* 263, E988-1001, (1992), PMID:1443132.
131. McGuire EA, Helderman JH, Tobin JD, Andres R, and Berman M. Effects of arterial versus venous sampling on analysis of glucose kinetics in man. *Journal of Applied Physiology* 41, 565-573, (1976), PMID:985402.
132. DeFronzo RA, Tobin JD, and Andres R. Glucose clamp technique: a method for quantifying insulin secretion and resistance. *American Journal of Physiology-Endocrinology and Metabolism* 237, E214, (1979), PMID:382871.
133. Wolfe RR, and Chinkes D. *Isotope Tracers in Metabolic Research*. Hoboken, NJ: John Wiley & Sons, Inc., 2005.
134. Mucinski JM, Manrique-Acevedo C, Kasumov T, Garrett TJ, Gaballah A, and Parks EJ. Relationships between very low-density lipoproteins-ceramides, -diacylglycerols, and -triacylglycerols in insulin-resistant men. *Lipids* 55, 387-393, (2020), PMID:32415687.
135. Kasumov T, Huang H, Chung Y-M, Zhang R, McCullough AJ, and Kirwan JP. Quantification of ceramide species in biological samples by liquid chromatography electrospray ionization tandem mass spectrometry. *Analytical Biochemistry* 401, 154-161, (2010), PMID:20178771.
136. Bligh EG, and Dyer WJ. A rapid method of total lipid extraction and purification. *Canadian Journal of Biochemistry and Physiology* 37, 911-917, (1959), PMID:13671378.
137. Le Floch JP, Escuyer P, Baudin E, Baudon D, and Perlemuter L. Blood glucose area under the curve. Methodological aspects. *Diabetes Care* 13, 172-175, (1990), PMID:2351014.
138. Steele R. Influences of glucose loading and of injected insulin on hepatic glucose output. *Annals of the New York Academy of Sciences* 82, 420-430, (1959), PMID:13833973.
139. Younossi ZM, Marchesini G, Pinto-Cortez H, and Petta S. Epidemiology of nonalcoholic fatty liver disease and nonalcoholic steatohepatitis: Implications for liver transplantation. *Transplantation* 103, 22-27, (2019), PMID:30335697.
140. Singh S, Allen AM, Wang Z, Prokop LJ, Murad MH, and Loomba R. Fibrosis progression in nonalcoholic fatty liver vs nonalcoholic steatohepatitis: a systematic review and meta-analysis of paired-biopsy studies. *Clinical Gastroenterology and Hepatology* 13, 643-654 e641-649; quiz e639-640, (2015), PMID:24768810.
141. Jacome-Sosa MM, and Parks EJ. Fatty acid sources and their fluxes as they contribute to plasma triglyceride concentrations and fatty liver in humans. *Current Opinion in Lipidology* 25, 213-220, (2014), PMID:24785962.
142. Beck-Nielsen H. Mechanisms of insulin resistance in non-oxidative glucose metabolism: the role of glycogen synthase. *Journal of Basic and Clinical Physiology and Pharmacology* 9, 255-279, (1998), PMID:10212838.
143. Mucinski J, Vena J, Ramos-Roman MA, Szuszkiewicz-Garcia M, McLaren DG, Previs S, Shankar S, Lassman M, and Parks E. High throughput LC-MS method to investigate postprandial lipemia: Considerations for future precision

- nutrition research. *American Journal of Physiology: Endocrinology and Metabolism*, (2020).
144. Timlin MT, Barrows BR, and Parks EJ. Increased dietary substrate delivery alters hepatic fatty acid recycling in healthy men. *Diabetes* 54, 2694-2701, (2005), PMID:16123359.
 145. Look ARG, Wing RR, Bolin P, Brancati FL, Bray GA, Clark JM, Coday M, Crow RS, Curtis JM, Egan CM, Espeland MA, Evans M, Foreyt JP, Ghazarian S, Gregg EW, Harrison B, Hazuda HP, Hill JO, Horton ES, Hubbard VS, Jakicic JM, Jeffery RW, Johnson KC, Kahn SE, Kitabchi AE, Knowler WC, Lewis CE, Maschak-Carey BJ, Montez MG, Murillo A, Nathan DM, Patricio J, Peters A, Pi-Sunyer X, Pownall H, Reboussin D, Regensteiner JG, Rickman AD, Ryan DH, Safford M, Wadden TA, Wagenknecht LE, West DS, Williamson DF, and Yanovski SZ. Cardiovascular effects of intensive lifestyle intervention in type 2 diabetes. *New England Journal of Medicine* 369, 145-154, (2013), PMID:23796131.
 146. Kelley DE, Kuller LH, McKolanis TM, Harper P, Mancino J, and Kalhan S. Effects of moderate weight loss and orlistat on insulin resistance, regional adiposity, and fatty acids in type 2 diabetes. *Diabetes Care* 27, 33-40, (2004), PMID:14693963.
 147. Lomonaco R, Bril F, Portillo-Sanchez P, Ortiz-Lopez C, Orsak B, Biernacki D, Lo M, Suman A, Weber MH, and Cusi K. Metabolic impact of nonalcoholic steatohepatitis in obese patients with type 2 diabetes. *Diabetes Care* 39, 632-638, (2016), PMID:26861926.
 148. Armstrong MJ, Hazlehurst JM, Hull D, Guo K, Borrows S, Yu J, Gough SC, Newsome PN, and Tomlinson JW. Abdominal subcutaneous adipose tissue insulin resistance and lipolysis in patients with non-alcoholic steatohepatitis. *Diabetes, Obesity & Metabolism* 16, 651-660, (2014), PMID:24962805.
 149. Lim EL, Hollingsworth KG, Aribisala BS, Chen MJ, Mathers JC, and Taylor R. Reversal of type 2 diabetes: normalisation of beta cell function in association with decreased pancreas and liver triacylglycerol. *Diabetologia* 54, 2506-2514, (2011), PMID:21656330.
 150. Schenk S, Harber MP, Shrivastava CR, Burant CF, and Horowitz JF. Improved insulin sensitivity after weight loss and exercise training is mediated by a reduction in plasma fatty acid mobilization, not enhanced oxidative capacity. *Journal of Physiology* 587, 4949-4961, (2009), PMID:19723783.
 151. Unger RH. Lipotoxicity in the pathogenesis of obesity-dependent NIDDM. Genetic and clinical implications. *Diabetes* 44, 863-870, (1995), PMID:7621989.
 152. Burke LM, van Loon LJC, and Hawley JA. Postexercise muscle glycogen resynthesis in humans. *Journal of Applied Physiology (1985)* 122, 1055-1067, (2017), PMID:27789774.
 153. Mikines KJ, Farrell PA, Sonne B, Tronier B, and Galbo H. Postexercise dose-response relationship between plasma glucose and insulin secretion. *Journal of Applied Physiology (1985)* 64, 988-999, (1988), PMID:3284873.

154. Burke LM. Re-examining high-fat diets for sports performance: Did we call the 'nail in the coffin' too soon? *Sports Medicine* 45 Suppl 1, S33-49, (2015), PMID:26553488.
155. Sunny NE, Parks EJ, Browning JD, and Burgess SC. Excessive hepatic mitochondrial TCA cycle and gluconeogenesis in humans with nonalcoholic fatty liver disease. *Cell Metabolism* 14, 804-810, (2011), PMID:22152305.
156. Pedersen BK, and Febbraio M. Muscle-derived interleukin-6--a possible link between skeletal muscle, adipose tissue, liver, and brain. *Brain, Behavior, and Immunity* 19, 371-376, (2005), PMID:15935612.
157. Petersen KF, Dufour S, Savage DB, Bilz S, Solomon G, Yonemitsu S, Cline GW, Befroy D, Zeman L, Kahn BB, Papademetris X, Rothman DL, and Shulman GI. The role of skeletal muscle insulin resistance in the pathogenesis of the metabolic syndrome. *Proceedings of the National Academy of Sciences of the United States of America* 104, 12587-12594, (2007), PMID:17640906.
158. Cook JR, Langlet F, Kido Y, and Accili D. Pathogenesis of selective insulin resistance in isolated hepatocytes. *Journal of Biological Chemistry* 290, 13972-13980, (2015), PMID:25873396.
159. Li S, Brown MS, and Goldstein JL. Bifurcation of insulin signaling pathway in rat liver: mTORC1 required for stimulation of lipogenesis, but not inhibition of gluconeogenesis. *Proceedings of the National Academy of Sciences of the United States of America* 107, 3441-3446, (2010), PMID:20133650.
160. Biddinger SB, Hernandez-Ono A, Rask-Madsen C, Haas JT, Aleman JO, Suzuki R, Scapa EF, Agarwal C, Carey MC, Stephanopoulos G, Cohen DE, King GL, Ginsberg HN, and Kahn CR. Hepatic insulin resistance is sufficient to produce dyslipidemia and susceptibility to atherosclerosis. *Cell Metabolism* 7, 125-134, (2008), PMID:18249172.
161. Deja S, Duarte J, Fletcher JA, Kucejova B, Fu X, Vale G, Young J, Browning J, and Burgess SC. 368-OR: Activation of hepatic gluconeogenesis is required to suppress DNL and stimulate ketogenesis during fasting. *Diabetes* 69, (2020).
162. Donnelly KL, Smith CI, Schwarzenberg SJ, Jessurun J, Boldt MD, and Parks EJ. Sources of fatty acids stored in liver and secreted via lipoproteins in patients with nonalcoholic fatty liver disease. *Journal of Clinical Investigation* 115, 1343-1351, (2005), PMID:15864352.
163. Eissing L, Scherer T, Todter K, Knippschild U, Greve JW, Buurman WA, Pinnschmidt HO, Rensen SS, Wolf AM, Bartelt A, Heeren J, Buettner C, and Scheja L. De novo lipogenesis in human fat and liver is linked to ChREBP-beta and metabolic health. *Nature Communications* 4, 1528, (2013), PMID:23443556.
164. Diraison F, Moulin P, and Beylot M. Contribution of hepatic de novo lipogenesis and reesterification of plasma non esterified fatty acids to plasma triglyceride synthesis during non-alcoholic fatty liver disease. *Diabetes and Metabolism* 29, 478-485, (2003), PMID:14631324.
165. Syed-Abdul MA, Moore MP, Wheeler A, Ganga RR, Diaz-Arias A, Rector RS, Ibdah JA, and EJ P. De novo lipogenesis and the progression of NAFLD.

- In: *Nutrition and Exercise Physiology*. MoSpace: University of Missouri-Columbia, 2022.
166. Rector RS, Thyfault JP, Morris RT, Laye MJ, Borengasser SJ, Booth FW, and Ibdah JA. Daily exercise increases hepatic fatty acid oxidation and prevents steatosis in Otsuka Long-Evans Tokushima Fatty rats. *American Journal of Physiology-Gastrointestinal and Liver Physiology* 294, G619-G626, (2008), PMID:18174272.
 167. Jong-Yeon K, Hickner RC, Dohm GL, and Houmard JA. Long- and medium-chain fatty acid oxidation is increased in exercise-trained human skeletal muscle. *Metabolism: Clinical and Experimental* 51, 460-464, (2002), PMID:11912554.
 168. van Loon LJ, Jeukendrup AE, Saris WH, and Wagenmakers AJ. Effect of training status on fuel selection during submaximal exercise with glucose ingestion. *Journal of Applied Physiology (1985)* 87, 1413-1420, (1999), PMID:10517772.
 169. Ter Horst KW, Vatner DF, Zhang D, Cline GW, Ackermans MT, Nederveen AJ, Verheij J, Demirkiran A, van Wagenveld BA, Dallinga-Thie GM, Nieuwdorp M, Romijn JA, Shulman GI, and Serlie MJ. Hepatic insulin resistance is not pathway selective in humans with nonalcoholic fatty liver disease. *Diabetes Care* 44, 489-498, (2021), PMID:33293347.
 170. Lewis GF, and Steiner G. Acute effects of insulin in the control of VLDL production in humans. *Diabetes Care* 19, 390-393, (1996), PMID:8729170.
 171. Kasumov T, Li L, Li M, Gulshan K, Kirwan JP, Liu X, Previs S, Willard B, Smith JD, and McCullough A. Ceramide as a mediator of non-alcoholic fatty liver disease and associated atherosclerosis. *PloS One* 10, e0126910, (2015), PMID:25993337.
 172. Alkhouri N, Dixon LJ, and Feldstein AE. Lipotoxicity in nonalcoholic fatty liver disease: not all lipids are created equal. *Expert Review of Gastroenterology & Hepatology* 3, 445-451, (2009), PMID:19673631.
 173. Luukkonen PK, Zhou Y, Sädevirta S, Leivonen M, Arola J, Orešič M, Hyötyläinen T, and Yki-Järvinen H. Hepatic ceramides dissociate steatosis and insulin resistance in patients with non-alcoholic fatty liver disease. *Journal of Hepatology* 64, 1167-1175, (2016), PMID:26780287
 174. Promrat K, Longato L, Wands JR, and de la Monte SM. Weight loss amelioration of non-alcoholic steatohepatitis linked to shifts in hepatic ceramide expression and serum ceramide levels. *Hepatology Research* 41, 754-762, (2011), PMID:21794038.
 175. Wasilewska N, Bobrus-Chociej A, Harasim-Symbor E, Tarasów E, Wojtkowska M, Chabowski A, and Lebensztejn DM. Increased serum concentration of ceramides in obese children with nonalcoholic fatty liver disease. *Lipids in Health and Disease* 17, 216, (2018), PMID:30208901.
 176. Simon J, Ouro A, Ala-Ibanibo L, Presa N, Delgado TC, and Martínez-Chantar ML. Sphingolipids in non-alcoholic fatty liver disease and hepatocellular carcinoma: Ceramide turnover. *International Journal of Molecular Sciences* 21, (2019), PMID:31861664.

177. Luukkonen PK, Sädevirta S, Zhou Y, Kayser B, Ali A, Ahonen L, Lallukka S, Pelloux V, Gaggini M, Jian C, Hakkarainen A, Lundbom N, Gylling H, Salonen A, Orešič M, Hyötyläinen T, Orho-Melander M, Rissanen A, Gastaldelli A, Clément K, Hodson L, and Yki-Järvinen H. Saturated fat is more metabolically harmful for the human liver than unsaturated fat or simple sugars. *Diabetes Care* 41, 1732-1739, (2018), PMID:29844096.
178. Kurek K, Piotrowska DM, Wiesiolek-Kurek P, Lukaszuk B, Chabowski A, Gorski J, and Zendzian-Piotrowska M. Inhibition of ceramide de novo synthesis reduces liver lipid accumulation in rats with nonalcoholic fatty liver disease. *Liver International* 34, 1074-1083, (2014), PMID:24106929.
179. Xia JY, Holland WL, Kusminski CM, Sun K, Sharma AX, Pearson MJ, Sifuentes AJ, McDonald JG, Gordillo R, and Scherer PE. Targeted induction of ceramide degradation leads to improved systemic metabolism and reduced hepatic steatosis. *Cell Metabolism* 22, 266-278, (2015), PMID:26190650.
180. Rosqvist F, Kullberg J, Stahlman M, Cedernaes J, Heurling K, Johansson HE, Iggman D, Wilking H, Larsson A, Eriksson O, Johansson L, Straniero S, Rudling M, Antoni G, Lubberink M, Orho-Melander M, Boren J, Ahlstrom H, and Riserus U. Overeating saturated fat promotes fatty liver and ceramides compared with polyunsaturated fat: A randomized trial. *The Journal of Clinical Endocrinology and Metabolism* 104, 6207-6219, (2019), PMID:31369090.
181. Tuccinardi D, Di Mauro A, Lattanzi G, Rossini G, Monte L, Beato I, Spiezia C, Bravo M, Watanabe M, Soare A, Kyanvash S, Armirotti A, Bertozzi SM, Gastaldelli A, Pedone C, Khazrai YM, Pozzilli P, and Manfrini S. An extra virgin olive oil-enriched chocolate spread positively modulates insulin-resistance markers compared with a palm oil-enriched one in healthy young adults: A double-blind, cross-over, randomised controlled trial. *Diabetes/Metabolism Research and Reviews* 38, e3492, (2022), PMID:34435429.
182. Dube JJ, Amati F, Toledo FG, Stefanovic-Racic M, Rossi A, Coen P, and Goodpaster BH. Effects of weight loss and exercise on insulin resistance, and intramyocellular triacylglycerol, diacylglycerol and ceramide. *Diabetologia* 54, 1147-1156, (2011), PMID:21327867.
183. Kasumov T, Solomon TPJ, Hwang C, Huang H, Haus JM, Zhang R, and Kirwan JP. Improved insulin sensitivity after exercise training is linked to reduced plasma C14:0 ceramide in obesity and type 2 diabetes *Obesity* 23, 1414-1421, (2015), PMID:25966363.
184. Gosejacob D, Jäger PS, Vom Dorp K, Frejno M, Carstensen AC, Köhnke M, Degen J, Dörmann P, and Hoch M. Ceramide synthase 5 is essential to maintain C16:0-ceramide pools and contributes to the development of diet-induced obesity. *Journal of Biological Chemistry* 291, 6989-7003, (2016), PMID:26853464.
185. Hammerschmidt P, Ostkotte D, Nolte H, Gerl MJ, Jais A, Brunner HL, Sprenger HG, Awazawa M, Nicholls HT, Turpin-Nolan SM, Langer T, Kruger M, Brugger B, and Bruning JC. CerS6-derived sphingolipids interact with mff and promote mitochondrial fragmentation in obesity. *Cell* 177, 1536-1552.e1523, (2019), PMID:31150623.

186. Hla T, and Kolesnick R. C16:0-ceramide signals insulin resistance. *Cell Metabolism* 20, 703-705, (2014), PMID:25440051.
187. Turpin SM, Nicholls HT, Willmes DM, Mourier A, Brodesser S, Wunderlich CM, Mauer J, Xu E, Hammerschmidt P, Brönneke HS, Trifunovic A, LoSasso G, Wunderlich FT, Kornfeld J-W, Blüher M, Krönke M, and Brüning JC. Obesity-induced CerS6-dependent C16:0 ceramide production promotes weight gain and glucose intolerance. *Cell Metabolism* 20, 678-686, (2014), PMID:25295788.
188. Vernon RG. Effects of diet on lipolysis and its regulation. *Proceedings of the Nutrition Society* 51, 397-408, (1992), PMID:1480634.
189. Chaurasia B, Kaddai VA, Lancaster GI, Henstridge DC, Sriram S, Galam DLA, Gopalan V, Prakash KNB, Velan SS, Bulchand S, Tsong TJ, Wang M, Siddique MM, Yuguang G, Sigmundsson K, Mellet NA, Weir JM, Meikle PJ, Bin M, Yassin MS, Shabbir A, Shayman JA, Hirabayashi Y, Shiow S-ATE, Sugii S, and Summers SA. Adipocyte ceramides regulate subcutaneous adipose browning, inflammation, and metabolism. *Cell Metabolism* 24, 820-834, (2016), PMID:27818258.
190. Hui JM, Hodge A, Farrell GC, Kench JG, Kriketos A, and George J. Beyond insulin resistance in NASH: TNF-alpha or adiponectin? *Hepatology* 40, 46-54, (2004), PMID:15239085.
191. Iqbal J, Walsh MT, Hammad SM, Cuchel M, Tarugi P, Hegele RA, Davidson NO, Rader DJ, Klein RL, and Hussain MM. Microsomal triglyceride transfer protein transfers and determines plasma concentrations of ceramide and sphingomyelin but not glycosylceramide. *Journal of Biological Chemistry* 290, 25863-25875, (2015), PMID:26350457.
192. Chaurasia B, Tippetts TS, Monibas RM, Liu J, Li Y, Wang L, Wilkerson JL, Sweeney CR, Pereira RF, Sumida DH, Maschek JA, Cox JE, Kaddai V, Lancaster GI, Siddique MM, Poss A, Pearson M, Satapati S, Zhou H, McLaren DG, Previs SF, Chen Y, Qian Y, Petrov A, Wu M, Shen X, Yao J, Nunes CN, Howard AD, Wang L, Erion MD, Rutter J, Holland WL, Kelley DE, and Summers SA. Targeting a ceramide double bond improves insulin resistance and hepatic steatosis. *Science* 365, 386-392, (2019), PMID:31273070.
193. Huang H, Kasumov T, Gatmaitan P, Heneghan HM, Kashyap SR, Schauer PR, Brethauer SA, Kirwan JP, and Kirwan JP. Gastric bypass surgery reduces plasma ceramide subspecies and improves insulin sensitivity in severely obese patients. *Obesity* 19, (2011), PMID:21546935.
194. Folch J, Lees M, and Sloane GH. A simple method for the isolation and purification of total lipids from animal tissues. *Journal of Biological Chemistry* 226, 497-509, (1957), PMID:13428781.

CHAPTER V – Noninvasive fatty acid oxidation in NASH: The utility of labeled breath tests to monitor changes in liver health?

ABSTRACT

Reduced hepatic mitochondrial activity is thought to be a major component of the pathogenesis of nonalcoholic steatohepatitis (NASH). Methods to predict liver mitochondrial activity in vivo are lacking and this project's goal was to use a noninvasive breath test to quantify complete mitochondrial fat oxidation and determine how test results changed when liver disease state was altered over time. Subjects (9 men, 16 women, 47 ± 8 years, 112 ± 23 kg; mean \pm SD) underwent a diagnostic liver biopsy and liver tissue histologically-scored by a pathologist using the NAFLD activity score (NAS, 0-8). To assess hepatic mitochondrial activity, a stably-labeled medium chain fatty acid (23.4 mg $^{13}\text{C}_4$ -octanoate) was consumed orally and breath samples collected over 135 min. Total CO_2 production rates were measured by respiratory gas analysis, breath $^{13}\text{CO}_2$ by isotope ratio mass spectrometry, and endogenous glucose production (EGP) using a hyperinsulinemic, euglycemic clamp. At baseline testing, subjects oxidized $23.4 \pm 3.9\%$ (range: 14.9-31.5%) of the octanoate dose and octanoate oxidation (OctOx) was significantly correlated with fasting plasma glucose levels ($r = -0.474$, $P = 0.017$) and EGP ($r = -0.441$, $P = 0.028$). Nineteen of the subjects returned 10.1 ± 1.1 months later for follow-up metabolic tests and repeat liver biopsies. The change in OctOx in units of relative percent dose oxidized per body weight (%/kg BW) was negatively related to reductions in EGP ($r = -0.481$, $P = 0.037$) and tended to correlate with reduced fasting glucose ($r = -0.398$, $P = 0.091$). At follow-up, subjects had significant reductions in total NAS and steatosis and the change in liver steatosis tended to correlate with increased

OctOx (%/kg BW, $r = -0.409$, $P = 0.083$). The use of a ^{13}C -octanoate breath test should be further tested in patients with NASH as a predictor of changes in liver health over time and may be used to investigate physiological processes that improve liver lipid burden.

INTRODUCTION

Nonalcoholic fatty liver disease (NAFLD) is the most prevalent liver disease in the world (1) and is characterized by an excess of liver fat, tissue injury, and insulin resistance (2-4). The diagnosis of NAFLD and the more advanced form, nonalcoholic steatohepatitis (NASH) requires a liver biopsy to histologically grade the extent of steatosis, inflammation, and hepatocellular ballooning (5). While multiple factors likely contribute to the pathogenesis of NASH, mitochondrial dysfunction is currently being investigated as a key factor in contributing to the progression of the disease (6-8). Data from cell culture (9, 10), animal models (11-18), and humans (6, 19-23) have demonstrated impaired hepatic fatty acid oxidation (FAO), increased reactive oxygen species (ROS) production, reduced respiration, and morphological mitochondrial changes in a setting of NAFLD and NASH. However, noninvasive methods to measure mitochondrial function are limited, and of those that exist, the results are inconsistent. Without obtaining additional liver tissue during a liver biopsy, the characterization of mitochondrial function is challenging. Further, due to the invasive nature of the liver biopsy, frequent monitoring of disease progression is difficult. Verified noninvasive methods to measure and track changes in hepatic mitochondrial function are needed.

Our group (7) and others (24) have profiled hepatic lipid metabolism using stable isotope tracers including deuterated water (D_2O) and labeled glucose, palmitate, and acetate (25). Carbon-labeled breath tests using substrates that are fully

oxidized to CO₂ (e.g., ¹³C-methionine, ¹³C- ketoisocaproate, ¹³C-octanoate) have been used to measure hepatic mitochondrial activity (26-28). Labeled octanoate, a medium-chain fatty acid, has been used in rodents (29), and humans (27, 30-33) for this purpose. When consumed, the octanoic acid is absorbed into enterocytes and transported to the liver via the portal vein (34). Once in the liver, octanoate bypasses the carnitine transport system (35), diffusing directly into the mitochondria where acetyl coenzyme A (CoA) is produced during β-oxidation (36-39) and flows through the tricarboxylic acid (TCA) cycle producing CO₂ which is then expelled in the breath (**supplementary figure S5.1**). Conflicting results have been reported in studies testing this labeled fatty acid breath test in subjects with NAFLD or NASH (27, 31-33). For example, patients with NASH had elevated ¹³CO₂ recovery when compared to healthy controls matched for age, gender, and BMI (27), while two similar studies found no difference in octanoate oxidation (OctOx) between NASH and healthy subjects (31, 33). Yet another study found reduced OctOx in NASH compared to NAFLD (33). No investigations have compared OctOx in biopsy-proven NASH patients with measures of liver glucose metabolism, nor have the effects of a lifestyle intervention in NASH patients on OctOx been evaluated.

The purpose of the current study was to determine how hepatic mitochondrial activity, measured via ¹³C-OctOx breath test, was related to indicators of liver health in individuals with biopsy-proven NASH. Additionally, in a subset of subjects, repeat OctOx breath tests were used to understand how oxidation

changed in patients whose liver disease either improved, stayed the same, or worsened over ten months. We hypothesized that participants with greater liver fat would have lower OctOx, indicating reduced mitochondrial activity, and that changes in liver health (either positive or negative) would be reflected in changes in hepatic OctOx over time.

METHODS

Protocol

The study was approved by the University of Missouri (MU) Health Sciences Institutional Review Board (Protocol # 2008258) and registered under ClinicalTrials.gov # NCT03151798. All subjects provided written informed consent and the study was conducted according to the principles expressed in the Declaration of Helsinki. Subjects ($n = 25$) with advanced NASH were recruited following a diagnostic liver biopsy for histologic grading of liver disease. Liver biopsy tissues were reviewed by a single pathologist and graded for NAFLD activity score (NAS) via the Brunt criteria (5), which is made up of three components; steatosis, lobular inflammation, and hepatocellular ballooning. Subject characteristics are shown in **table 5.1**. Sedentary (<60 minutes/week of structured physical activity) male and female subjects between 22-65 years of age who consumed less than two standard alcoholic drinks per day (<20 g/d) and had characteristics of metabolic syndrome (40) were screened for inclusion. Individuals with acute disease, advanced cardiac or renal disease, anticoagulation therapy, severe comorbid conditions limiting life expectancy <1 year, hepatitis-causing illnesses (hepatitis B and/or C viruses, autoimmune hepatitis, hemochromatosis, celiac disease, Wilson's disease, alpha-1-antitrypsin deficiency, medication-induced hepatitis, or any other clinical or biochemical evidence of decompensated liver disease), steroid or drug use known to cause NAFLD, or pregnant women were excluded.

Within 3.1 ± 1.9 months of the baseline liver biopsy, a fatty acid breath test was performed in which $\Delta 1,2,3,4$ ^{13}C ; octanoic acid (**figure 5.1A**; isotopic purity: 99%, Cambridge Isotope Laboratories, Andover, MA) was delivered orally in orange juice. Prior to the test, each subject completed a three-day food record and food preference surveys which were used to prepare a controlled three-day pre-study diet. The prepared diets were similar in composition and energy content to each subjects' habitual food preferences to support maintenance of body weight, as acute changes in energy intake and body weight may influence liver metabolism (41). The breath test was performed on the fourth day, following a 12h fast. Approximately two weeks after the breath test, subjects were admitted to the Clinical Research Center (CRC) at the MU Hospital and underwent a stable-isotope labeled, hyperinsulinemic euglycemic clamp to determine endogenous glucose production (EGP) as previously described (42). EGP was measured in the fasting state and under seven $\text{mU}/\text{m}^2/\text{minute}$ insulin (43).

The present analysis also includes data from nineteen subjects who returned after 10.1 ± 1.1 months for follow-up tests. These subjects had received either standard of care ($n = 5$) or participated in a supervised lifestyle intervention ($n = 14$). Subjects receiving standard care met with a registered dietitian once at the beginning of the study to discuss lifestyle changes that could improve their liver health. Any additional instruction was provided by their physician independently of the study. The subjects in the lifestyle program regularly met with the study dietitian for nutritional counseling (2-4x/month) and an exercise physiologist for

supervised high intensity interval training (HIIT, 3x/week). At the end of the program, each subject completed a follow-up OctOx breath test, hyperinsulinemic euglycemic clamp, and underwent a second liver biopsy.

Octanoate oxidation breath test

The protocol for the OctOx test performed at baseline and follow-up is shown in **figure 5.1B**. At approximately 0700 (-20 minutes), subjects were admitted to the CRC and fasting CO₂ production rate was measured using a metabolic cart (Parvomedics, Salt Lake City, UT) and an unlabeled breath sample was collected into an Exetainer® evacuated breath vial (Labco, Ceredigion, UK) using a disposable plastic straw. Each subject then consumed 23.4 mg of ¹³C₄-octanoate (25 µL, **figure 5.1A**) mixed thoroughly into orange juice (Minute Maid®; Sugar Land, TX). The volume of juice was equivalent to 10% of each subject's daily energy requirement (44) and provided an average bolus of 54.4 ± 2.1 grams of sugar at baseline and 55.1 ± 2.2 grams at follow-up. The juice was consumed within 10 minutes, and an additional 2-4 ounces of water was used to rinse the drinking glass. Fed-state CO₂ production rates were measured four times over 135 minutes, each time for 15 minutes. Breath samples were collected intermittently throughout the test at 15, 30, 45, 65, 85, 105, and 135 minutes (denoted by a four point star in **figure 5.1B**). Following the test, subjects ate ad libitum and were discharged from the CRC. Within two weeks of the breath test, subjects returned to undergo a hyperinsulinemic euglycemic clamp to quantitate EGP. Two anterograde intravenous lines were placed – for isotope

administration in the antecubital region and for blood draws in the hand along with the use of a heated hand box (45). A primed-continuous infusion of [U-¹³C₆]-glucose (22 μmol/kg over one minute, followed by 0.2 μmol/kg/min) was administered to quantitate fasting EGP. Following this, insulin was infused at seven mU/m²/minute and plasma glucose concentrations (analyzed by YSI Model 2300-D Stat Plus; Yellow Springs, OH) held constant at the subject's fasting level by a variable rate infusion of a ¹³C₆-glucose labeled 20% dextrose (wt/vol.) solution adjusted every five minutes using the negative feedback principle described by DeFronzo et al (43). Plasma glucose enrichments were measured by gas chromatography/mass spectrometry (46).

Octanoate calculations & statistical analysis

The amount of ¹³CO₂ in the breath samples was measured by Metabolic Solutions (Nashua, NH) with a Sercon ABCA2 isotope ratio mass spectrometer (IR-MS, Sercon, Ltd., Crewe, United Kingdom). The percent atom excess in delta per million (parts per thousand) ¹³C relative to the international standard Vienna Pee Dee Belemnite (VPDB) was used to calculate OctOx (47). OctOx (**equation 5.1**) was calculated as the product of steady state CO₂ production rates and the percent ¹³CO₂ atom excess in breath. The production rate was corrected using an estimate of the body's bicarbonate pool (48) and divided by

$$\left(\frac{\left(\frac{VCO_2 * \text{Atom excess}}{\text{Bicarbonate factor (0.81)}} \right)}{4} \right) * 148.18 \left(\frac{\text{g}}{\text{mol}} \right) \quad \text{Equation 5.1}$$

the number of labels within the isotope (4). The molecular weight of the labeled octanoate is 148.18 g/mol.

The homeostatic model assessment for insulin resistance (HOMA-IR) was calculated by the product of fasting insulin ($\mu\text{IU/mL}$) and glucose (mg/dL) divided by the constant 405 (49). EGP was calculated according to the equations of Steele (50). Calculations were performed using Microsoft Excel 2013 and correlation analyses (Pearson for parametric, Spearman for nonparametric – continuous versus ranked variables) using StatView®, 5.0.1 software (2008). Paired, one-tailed *t*-tests were used to when compare baseline to follow-up characteristics. An alpha level of ≤ 0.05 was considered significant while ≤ 0.10 was considered trending. Data are presented as mean \pm SD for static variables (i.e., body weight, age) and as mean \pm SEM for values measured over time.

RESULTS

As shown in **table 5.1**, 9 males and 16 females with an average age of 47 ± 8 y and body weight (BW) of 112 ± 23 kg (mean + SD) were included. All subjects were recruited based on a biopsy-confirmed diagnosis of NASH (NAS $\geq 4/8$) which is the composite of scores for steatosis (0-3), inflammation (0-3), and hepatocellular ballooning (0-2). Additionally, subjects demonstrated multiple characteristics of advanced liver disease including fibrosis (measured histologically), elevated serum aspartate transaminase (AST), alanine transaminase (ALT) concentrations, and HOMA-IR (51). 72% of the subjects had type 2 diabetes (T2D, medication used is shown in **supplementary table S5.1**). Wide variability in OctOx was observed across subjects throughout the 135-minute breath test (**figure 5.2A**). Average peak oxidation occurred between 30-60 minutes following ingestion, although individual analysis demonstrated a wide range of peak OctOx (23-104 minutes). Total octanoate oxidized was $23.4 \pm 3.9\%$ of the 23.4 mg dose (**table 5.1**, range: 14.9-31.5%). When divided into baseline BW, 0.22 ± 0.06 %/kg BW was oxidized (range: 0.13-0.33 %/kg). Upon analysis of characteristics that may be related to fractional oxidation we found no association with BW, exercise capacity, liver enzymes, NAS, or fibrosis. However, OctOx was associated with multiple indicators of glucose metabolism. The higher the OctOx (percent dose), the lower the fasting plasma glucose concentration (**figure 5.2B**), glycosylated hemoglobin (HbA1c, **figure 5.2C**), and fasting EGP (**figure 5.2D**).

Based on the study's goal to determine if changes in OctOx were associated with changes in liver health, data from all subjects are presented together.

Importantly, fitness levels improved in the subjects undergoing HIIT (+0.31 L/min, $P = 0.022$) while standard care subjects demonstrated no change in VO_2 peak (-0.09 L/min, $P = 0.154$). Mean changes in NAS, steatosis, fibrosis, and OctOx (% dose) are presented in **table 5.1** and **figure 5.3** (individual changes with treatment subjects represented by yellow line and control by grey lines).

Supplementary figure S5.2 presents the same data separated by subject. On average, subjects lost $7 \pm 1\%$ of their BW, serum AST and ALT were reduced $31 \pm 13\%$ and $38 \pm 7\%$ respectively, and HOMA-IR decreased by $31 \pm 10\%$ at follow-up. Fasting EGP (relative to fat free mass, FFM) trended downward ($-1.3 \mu\text{mol/FFM/min}$, $P = 0.063$) and insulin stimulated EGP was significantly reduced ($-1.0 \mu\text{mol/FFM/min}$, $P = 0.017$). The NAS and steatosis were significantly reduced ($P < 0.01$) while fibrosis did not change significantly ($P = 0.192$, **figure 5.3**). Some subjects demonstrated robust reductions in NAS, steatosis, or fibrosis, while others had minimal change or even increased (**supplementary figure S5.2A-C**).

In terms of the breath test, no significant differences were found in the mean total percent dose of OctOx from baseline to follow-up (**table 5.1**) and **figure 5.3D** and **supplementary figure 5.2D** show the average and individual changes observed across visits. **Figure 5.4** demonstrates that the percent change in relative OctOx tended to correlate with changes in fasting glucose and was significantly related

to the percent change in relative fasting EGP. No relationships were found between changes in OctOx and total NAS, although a trending negative relationship was observed between the change in relative percent octanoate dose oxidized (%/kg) and the change in steatosis (**figure 5.5A**). In other words, as steatosis was reduced, OctOx increased. Neither lobular inflammation and hepatocellular ballooning (the other components of the NAS) nor fibrosis were related to changes in OctOx. Finally, a plasma marker of liver injury, ALT, was also negatively related to absolute change in OctOx quantity (milligrams, **figure 5.5B**).

DISCUSSION

The present study used an in-vivo, isotope-labeled breath test in subjects with biopsy-proven NASH to determine the relationship between medium chain fatty acid (octanoate) oxidation and measures of liver health. A subset of the subjects underwent a second breath test and liver biopsy after approximately ten months to show, for the first time, a significant relationship between the change in OctOx and fasting EGP and a trending relationship with steatosis, a component of the histologic NAS assessment. Those subjects who had the greatest reduction in hepatic glucose production and liver steatosis, exhibited the greatest increases in OctOx. These findings were supported by trending relationships between changes in OctOx and ALT, a plasma marker of liver injury, and fasting glucose concentrations. Overall increased oxidation of octanoate may be a noninvasive indicator of improved liver health and could be further tested as a predictor of glucose production and liver fat in subjects with NASH.

Liver health and mitochondrial function: insight from previous breath tests

Although liver biopsies grade disease severity in only a small, superficial segment of the liver, no noninvasive test to date, whether serum-based or imaging, has been able to characterize disease severity as precisely as the liver biopsy (52). Breath tests measuring hepatic function began nearly 50 years ago when Hepner and Vesell quantified hepatic drug metabolism in patients with portal cirrhosis using radiolabeled aminopyrine (53). Since then, numerous breath tests have been developed to measure liver function (26-28, 30, 54, 55),

as comprehensively reviewed by Di Ciaula et al (56). For a medium-chain fatty acid like octanoate, numerous independent studies suggest that when it is given orally, its oxidation is specific to the liver (34, 38, 57). Octanoate fatty acid is absorbed into the portal vein (34) and clears first pass to the liver. It does not require the presence of the carnitine transport system to enter the mitochondria, making it highly oxidizable (58). Indeed, the carbon from ^{13}C -labeled octanoate appears in human breath CO_2 within 15 minutes and peaks, on average, within 60 minutes (**figure 5.2A**).

We found no association between NAS and OctOx at baseline although multiple characteristics of glucose metabolism were related (**figure 5.2B-D**). These relationships suggest that individuals with greater metabolic dysfunction may exhibit lower OctOx when compared to a healthy counterpart. In line with this hypothesis, Braun et al (33) showed that subjects with more advanced NASH exhibited lower OctOx compared to those with lesser liver disease (i.e., steatosis). Similarly, using a ^{13}C -methionine breath test, Banash et al (26) found reduced oxidation, indicative of mitochondrial dysfunction, with greater liver disease, while a ^{13}C - ketoisocaproate test used by Portincasa et al (28) demonstrated reduced mitochondrial decarboxylation, a reflection of mitochondrial activity of the cytochrome P450 system, in advanced NASH compared to healthy subjects or those with steatosis alone. Although not all studies have agreed with these findings. Schneider et al (31) found no differences in OctOx between patients with NASH vs healthy controls and Miele

et al (27) found *greater* OctOx in subjects with NASH compared to healthy controls. Although the current study did not include a healthy group for comparisons, one goal was to measure changes in OctOx and disease severity following ten months of standard care or treatment (diet and exercise).

Improvements in NASH and hepatic FAO

Previous studies examining the effects of lifestyle treatment on humans with NASH have shown significant reductions in disease severity; one study demonstrated a 55% reduction in NAS and a 58% reduction in steatosis following a 12-month lifestyle intervention (59, 60). We also observed reductions in NAS (-30%) and steatosis (-23%) at follow-up across all subjects. Taken together, increased weight loss and physical activity may have increased mitochondrial oxidative capacity and reduced cellular inflammation thereby improving the ability of the mitochondria to burn fatty acids. The current study represents the first-time repeated breath tests in conjunction with repeat liver biopsies were completed in subjects with NASH. As the amount of liver steatosis was reduced, the relative amount of the octanoate dose oxidized tended to increase (**figure 5.5A**). An important caveat of comparing our results to previous studies, is that physical activity has been shown to increase the expression of carnitine palmitoyl transferase (CPT), a key enzymatic step in long-chain FAO (61) while exercise cessation decreased CPT expression through malonyl-CoA inhibition (62). As described above, octanoic acid does not require CPT for entry into the mitochondria and therefore, even in subjects with elevated malonyl-CoA and

CPT inhibition (i.e., individuals with high de novo lipogenesis) this method can be utilized to assess the β -oxidation machinery of the mitochondria and the oxidation of the acetyl-CoA in the TCA cycle. Furthermore, it suggests the improvements in hepatic FAO following weight-loss may be partially independent of CPT. Finally, as only a subset of the subjects underwent exercise training and they did not drive any of the relationships presented, we do not expect physical activity to be a key driver in increased OctOx. Indeed, improved fitness and OctOx were not related. In sum, this breath test provides greater insight into the post-CPT FAO and TCA cycling and may serve as a marker for changes in liver health with weight loss.

Hepatic mitochondrial activity and glucose production

A key event in the pathogenesis of NAFLD is increased substrate burden (63-67) which overwhelms the liver's capacity to oxidize, store, and secrete metabolites ultimately leading to the accrual of liver fat (22, 68-70) and decline in mitochondrial function (6, 23). Indeed, elegant work has demonstrated a loss of hepatic mitochondrial activity in advanced NASH (6) and a complementary report found significant structural defects in hepatic mitochondria from NASH patients (22). Simultaneously, in states of excess nutrient burden-induced insulin sensitivity (71, 72), the liver's ability to suppress gluconeogenesis is blunted, resulting in excess EGP, which is the primary driver of elevated plasma glucose concentrations in the fasting state (4). An increased ability of the liver to oxidize fatty acids may play a mechanistic role in liver health improvements, potentially in

response to reduced nutrient burden and subsequent improvements in glucose metabolism.

In the present study, lower levels OctOx were related to multiple indicators of hepatic insulin resistance – i.e., those participants with the lowest OctOx were those with the greatest fasting plasma glucose concentrations, the highest HbA1c, and fasting EGP (**figure 5.2**). Our follow-up studies in a subset of the participants demonstrate that increased OctOx after ten months of either standard care or a diet and exercise lifestyle intervention was related to reductions in fasting EGP and glucose concentrations (**figure 5.4**). As established above, reduced energy intake leading to weight loss and subsequent reductions in nutrient flux to the liver may allow metabolic pathways, including FAO, to improve oxidative capacity and reduce liver fat. This hypothesized model is graphically presented in **figure 5.6**. Importantly, the breath test used here is not able to distinguish changes in hepatic mitochondrial function beyond complete FAO but may in turn serve as a marker of enhanced or reduced metabolic flux through β -oxidation and TCA pathways.

Individual differences

Results from baseline testing revealed a wide range of OctOx values between subjects highlighting the importance of examining individual responses. Multiple factors may impact individual response including 1- subject sex, 2- gastric emptying, or 3- physical activity levels. Regarding subject sex, a previous

investigation in individuals with NASH who underwent the same OctOx breath test reported higher $^{13}\text{CO}_2$ recovery in women than men (31). One potential mechanism for increased oxidation in women is hormonal regulation of hepatic fatty acid metabolism (73, 74). However, we found no differences in FAO or disease severity based on sex in our subjects. It is important to note this study was not designed to identify sex differences, thus these comparisons were underpowered. Second, delayed gastric emptying may also have contributed to variability between subjects (75, 76), although in the present study, the use of a liquid vehicle (orange juice) reduced any delay associated with solid food meals. Upon analysis of time to peak oxidation (53 ± 5 minutes), we found no correlation with percent octanoate oxidation, suggesting gastric emptying likely did not influence oxidation in the current subjects. Future studies proposing orally administered compounds to assess metabolism should consider gastric emptying effects. Finally, acute effects of physical activity during the days preceding data collection may have impacted both hepatic FAO (77-79) and insulin sensitivity (79-81). Both acute and chronic exercise may directly (via regulation of gene or protein expression) or indirectly (through decreased malonyl-CoA inhibition) increase hepatic FAO. Minimal evidence is available in humans demonstrating the former, and the latter would likely not impact the results of our study as octanoate enters the mitochondria independent of CPT. Acute bouts of physical activity have been shown to reduce fasting EGP, however our subjects did not exercise within the two days prior to the clamp procedure to minimize the impacts

of acute activity on hepatic insulin sensitivity. Regardless, variability observed in both FAO and insulin sensitivity may have been acutely impacted by exercise.

Limitations

This study had a number of limitations to consider. The primary limitation relates to the nature of metabolic studies in which multiple measurements are collected over time (e.g., biopsies, OctOx, and euglycemic clamp), which limits the sample size. Nonetheless, the relationships observed were strengthened by the wide range of OctOx and other variables. Second, all subjects had advanced NASH (NAS ranging from 4-7). To determine whether OctOx level is lowered consistently at every incremental increase in NAS score (from 0-8), future studies should include individuals with lower levels of liver disease, and even patients who are healthy, if liver tissue is available for histology. Nonetheless, the present data support a connection between liver health and OctOx due to the repeated-measures study design. Lastly, instead of separately measuring the extent of CO₂ trapping in the bicarbonate pool for each subject, we used an established correction factor to estimate this outcome (48). The present subjects' body weights and ages were similar to the original cohort used to establish the correction factor and we chose to use this factor to reduce subject burden.

Conclusions

In summary, the use of a noninvasive, medium-chain fatty acid oxidation breath test demonstrated that the oxidation of octanoate may be a predictor of changes

in liver health in subjects with NASH but requires further validation. This method may be a useful research tool in NASH studies of large samples sizes.

Octanoate breath tests may be a simple method for capturing progression or changes in liver fat content and hepatic mitochondrial function without the need for multiple biopsies.

TABLES

Table 5.1. Subject characteristics

Characteristic	All subjects* (n = 25)	Baseline# (n = 19)	Follow-Up# (n = 19)	<i>P</i> -value
Sex (m/f)	9/16	7/12		
Age (y)	47 ± 8	45 ± 10	46 ± 10	
Body Weight (kg)	112 ± 23	119 ± 22	111 ± 20	<0.001
NAS (0-8) ¹	5.5 ± 1.1	5.5 ± 1.2	3.9 ± 2.1	0.001
Steatosis (0-3) ¹	2.3 ± 0.6	2.4 ± 0.6	1.8 ± 1.0	0.004
Fibrosis Score (0-4) ¹	1.9 ± 1.5	2.1 ± 1.4	1.8 ± 1.7	0.192
AST (U/L)	51.1 ± 36.6	58.2 ± 39.3	28.4 ± 13.1	0.001
ALT (U/L)	56.5 ± 30.0	58.5 ± 32.1	32.0 ± 13.3	<0.001
HOMA-IR	6.3 ± 5.3	6.7 ± 5.9	3.8 ± 1.7	0.006
Fasting EGP (µmol/FFM/min)	22.2 ± 3.5	22.3 ± 3.5	21.0 ± 2.8	0.063
EGP (µmol/FFM/min) ²	23.3 ± 6.7	23.3 ± 6.8	19.6 ± 6.1	0.017
OctOx (% dose)	23.4 ± 3.9	23.8 ± 3.7	24.0 ± 4.6	0.401

All values are mean ± SD. *P* – values from paired, one-tailed *t*-tests.

* All subjects are included in these averages.

Only subjects (treatment: *n* = 14, standard care: *n* = 5) who completed a follow-up breath test and liver biopsies are included in these averages for comparison.

¹ A decimal is included (despite whole number scores) to demonstrate subtle differences between baseline and follow-up.

² Insulin-stimulated (seven mU/m²/minute).

FIGURES

Figure 5.1. Molecular structure of labeled octanoate and study design of noninvasive breath test

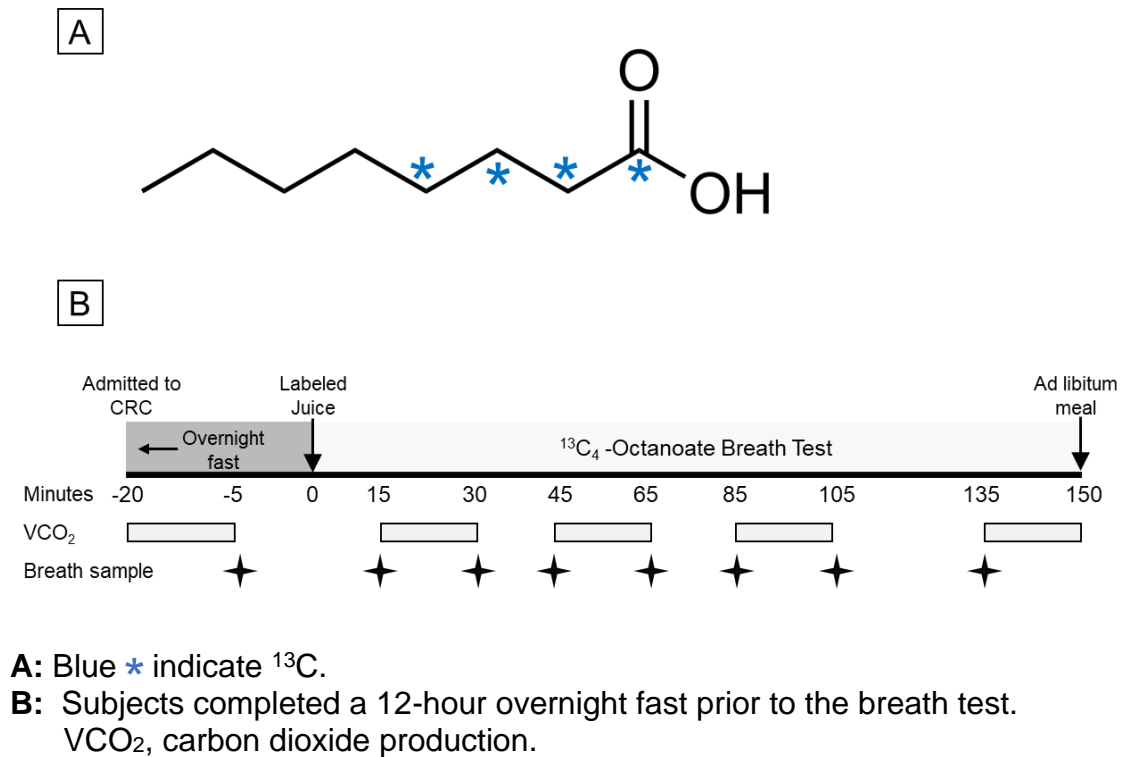
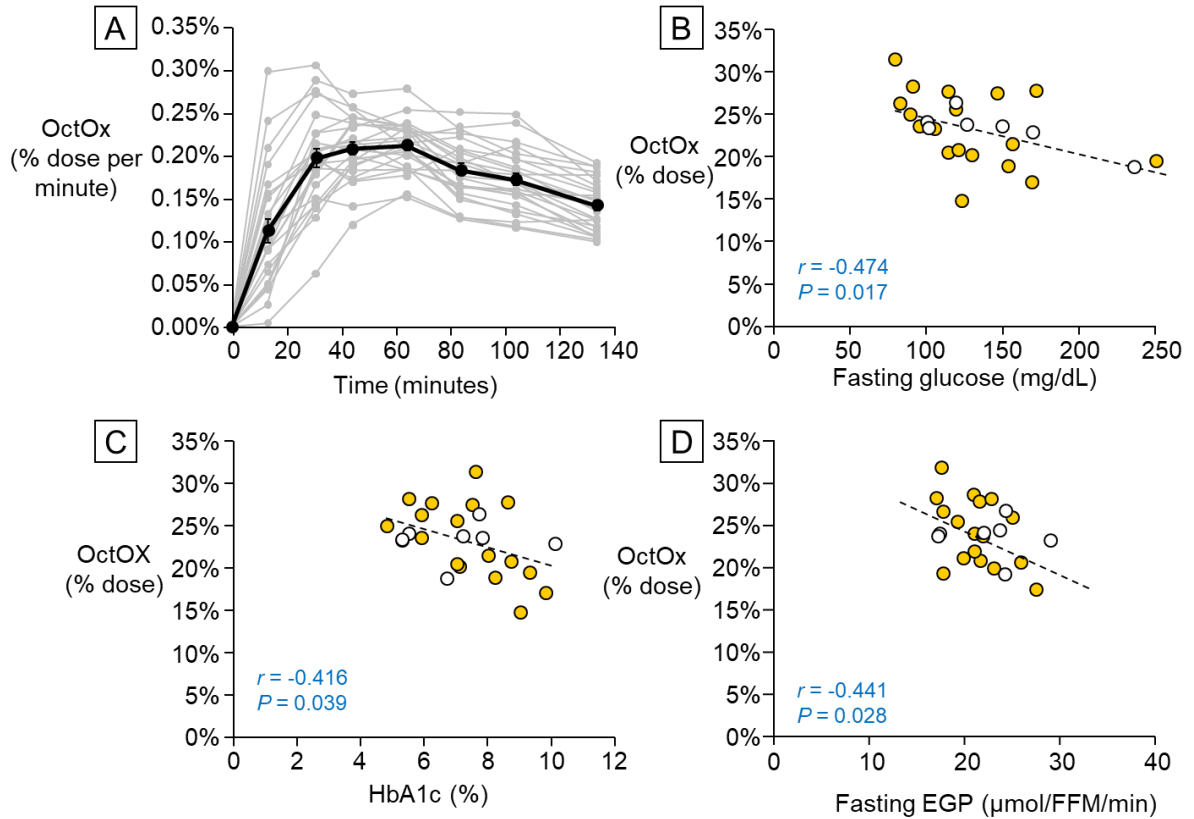


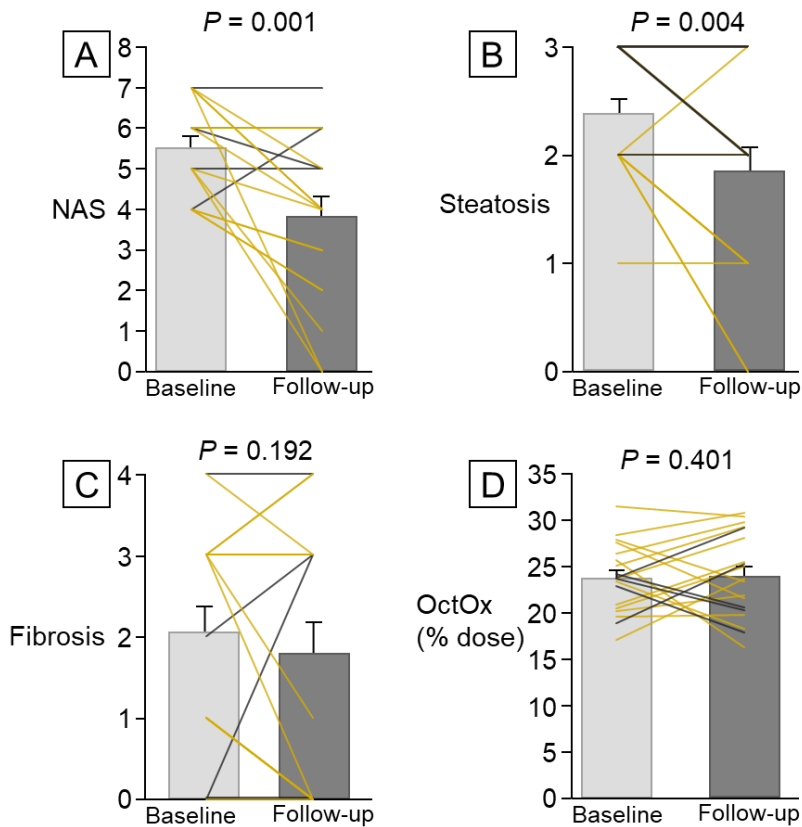
Figure 5.2. Time course of percent octanoate dose oxidized (OctOx) per minute and baseline correlations with markers of glucose metabolism



A: Mean percent (%) dose oxidized per minute \pm SEM is shown in black; individual subjects are shown in grey.

B-D: Pearson's correlations between baseline percent dose OctOx and **(B)** fasting glucose, **(C)** HbA1c, and **(D)** fasting EGP relative to fat free mass, FFM. $n = 25$; Treatment ($n = 18$) shown in yellow and standard care ($n = 7$) shown in white circles.

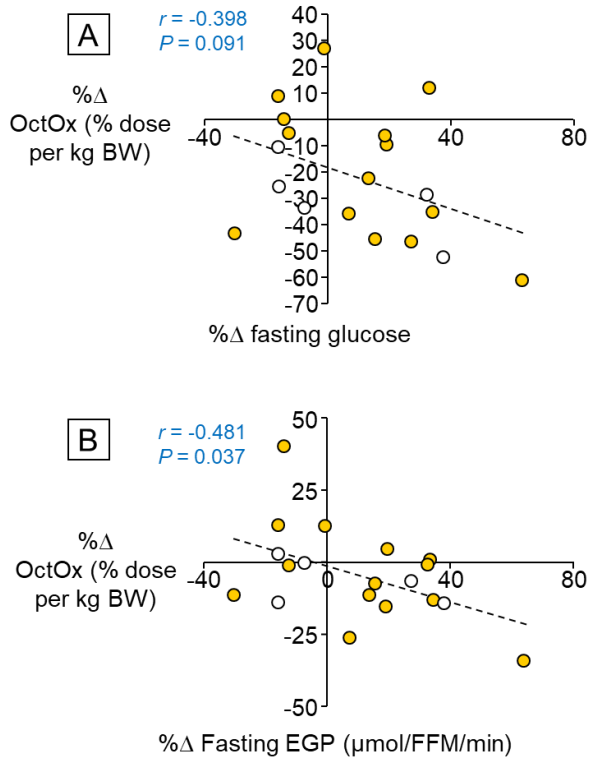
Figure 5.3. Average and individual changes in NAS, steatosis, fibrosis, and percent (%) octanoate dose oxidized (OctOx)



Data are presented as mean \pm SEM; Treatment: $n = 14$, yellow lines; Standard care: $n = 5$, grey lines. Paired, one-tailed t -test for baseline to follow-up comparisons in all subjects. Note: Many individual subject lines overlap and individual data is presented in **supplementary figure S5.2**.

- A:** Changes in total NAS.
- B:** Changes in the NAS component, steatosis.
- C:** Changes in fibrosis.
- D:** Changes in percent dose OctOx.

Figure 5.4. Correlations between changes in octanoate oxidized (OctOx) and fasting glucose and fasting EGP

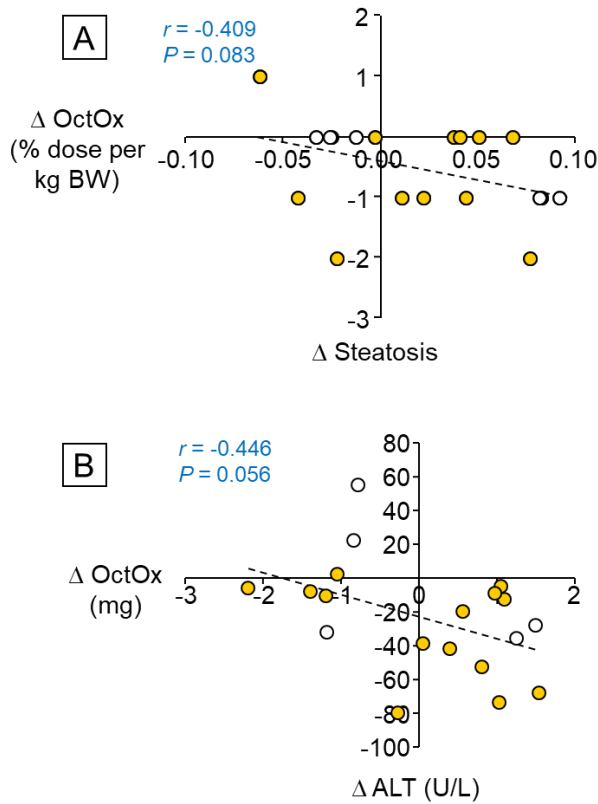


Treatment (yellow): $n = 14$, Standard care (white): $n = 5$.

A: Pearson's correlation between percent (%) changes (Δ) in fasting glucose and percent dose OctOx per kg BW.

B: Pearson's correlation between percent changes in fasting EGP (relative to fat free mass, FFM) and percent dose OctOx per kg BW.

Figure 5.5. Correlations between changes in octanoate oxidized (OctOx) and markers of liver health – steatosis and ALT

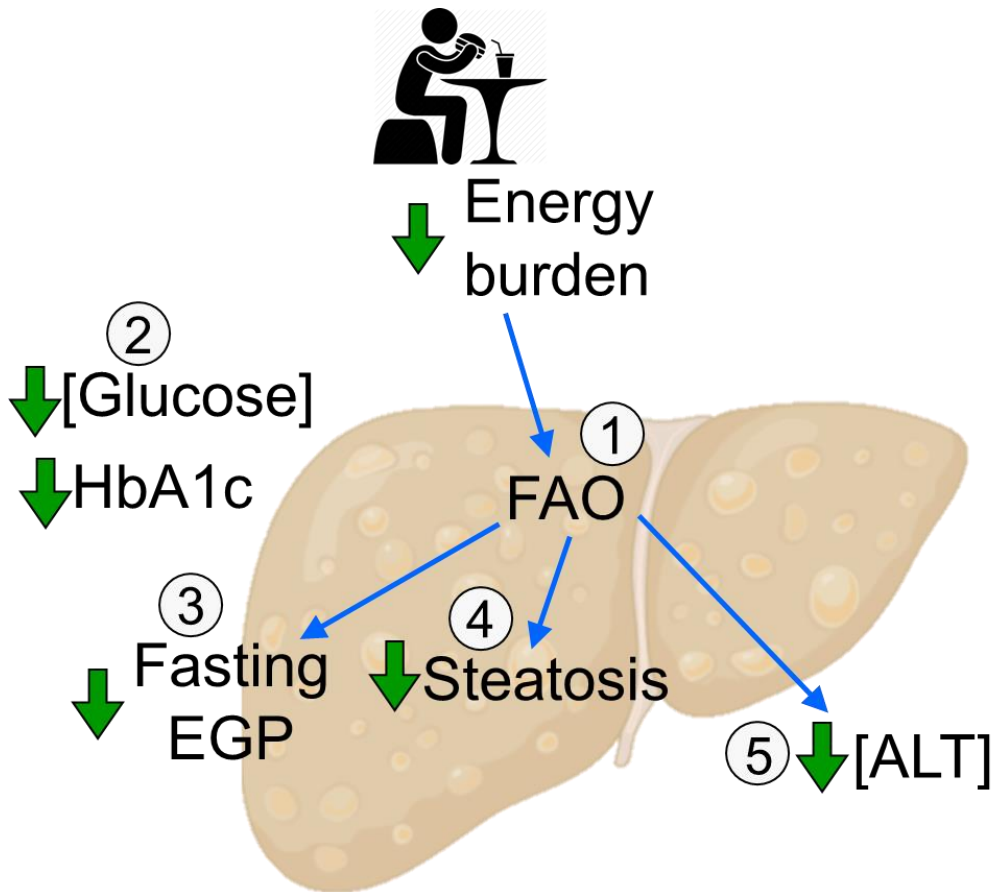


Treatment (yellow): $n = 14$, Standard care (white): $n = 5$.

A: Spearman's nonparametric correlation between absolute changes (Δ) in steatosis and percent (%) dose OctOx per kg BW

B: Pearson's correlation between absolute changes in ALT and total milligrams of OctOx.

Figure 5.6. Model of improved liver health with changes in FAO



Green arrows represent findings, and the blue lines represent hypothesized effects of increased FAO to improve liver histology.

Relief of overburdened liver to improve histology via:

- 1, 2, 3 – Increased FAO was negatively related to markers of glucose metabolism (plasma glucose concentrations, HbA1c, and fasting EGP) at baseline. Reductions in energy burden at follow-up testing may have partially driven the negative associations between FAO, plasma glucose, and fasting EGP.
- 4, 5 – Elevated FAO was associated with greater reductions in liver steatosis and the plasma marker of liver injury, ALT.

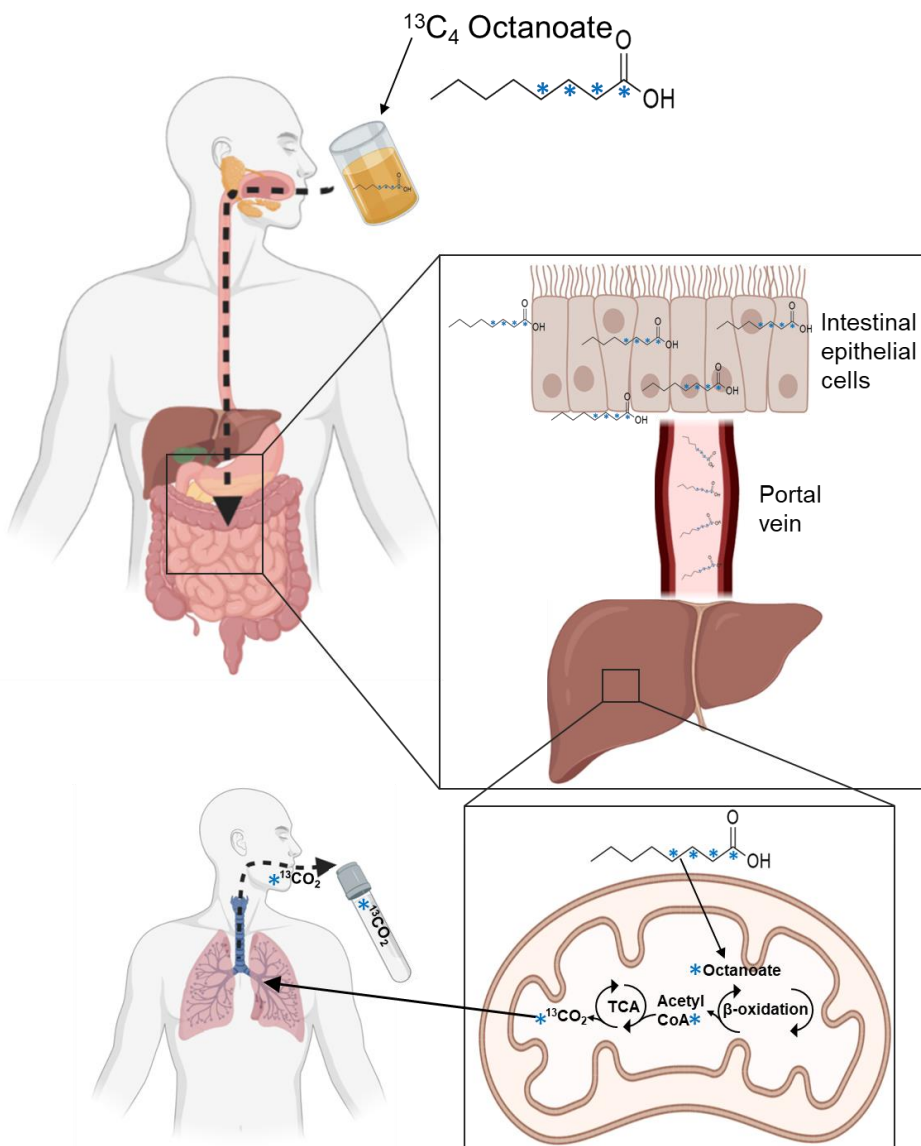
SUPPLEMENTARY DATA

Supplementary Table S5.1. Baseline diabetic status and subject medications

Diabetes status	<i>n</i> (%)
Type 2 Diabetes	18 (72%)
Drug type *	<i>n</i> (%)
Metformin	17 (68%)
Insulin	4 (17%)
Sulfonyurea	3 (13%)
Statins	12 (48%)
DPP4 inhibitor	2 (8%)
GLP-1 agonists	6 (24%)
SGLT-2 inhibitors	2 (8%)

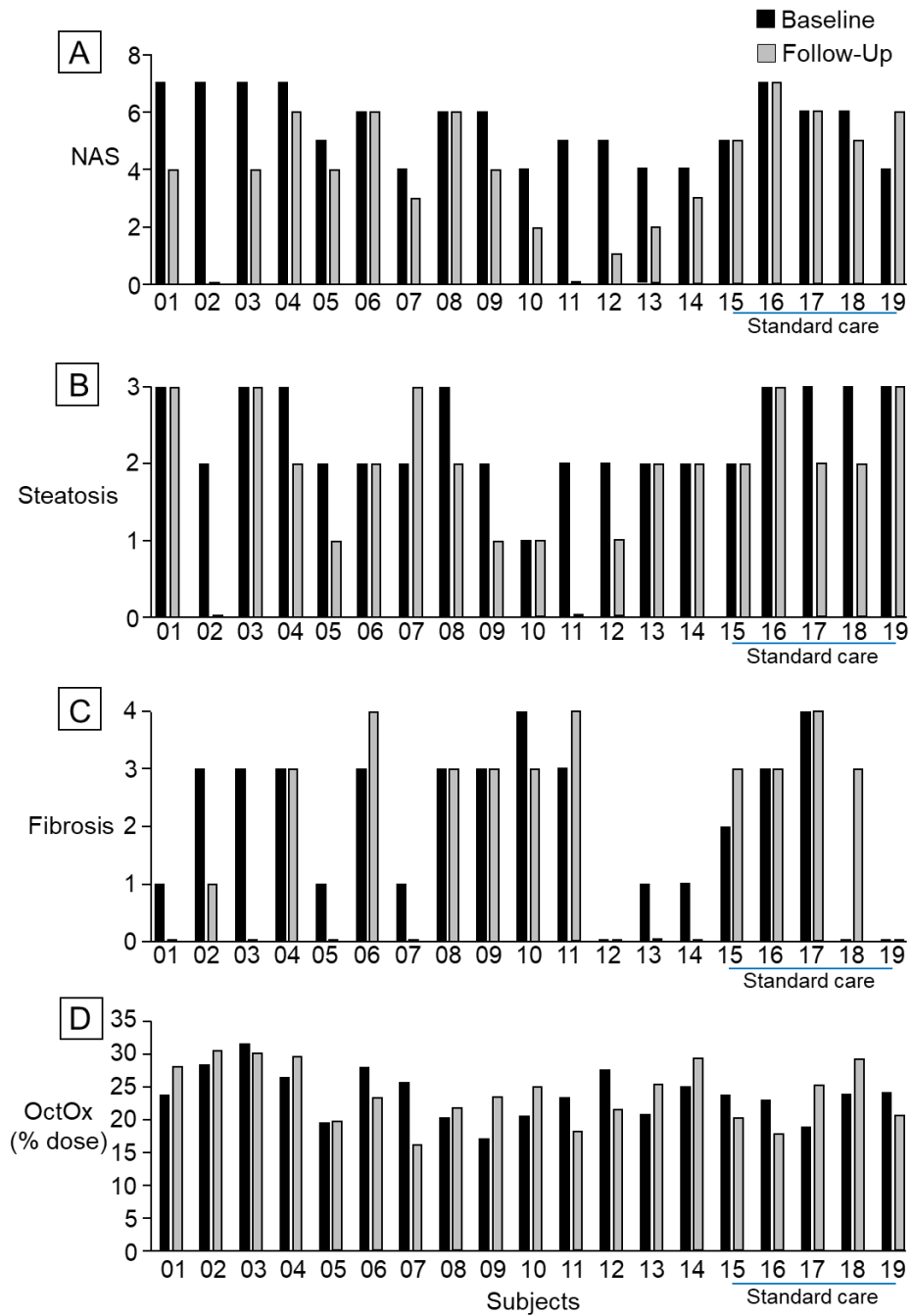
*Active medications at baseline for all subjects $n = 25$ (including controls; $n = 7$).

Supplementary Figure S5.1. Schematic demonstrating delivery of oral $^{13}\text{C}_4$ octanoate to the liver through portal transport and oxidation



Mechanism of oral delivery of octanoate to hepatic tissues.

Supplementary Figure S5.2. Individual changes in NAS, steatosis, fibrosis, and total octanoate oxidized (OctOx)



Data are related to **figure 5.3**.

A-D: Individual subject data from baseline to follow-up for (A) NAS (0-8), (B) Steatosis (0-3), (C) Fibrosis (0-4), and (D) OctOx (% dose).

Notes: 1- Small bars just above the x-axis indicate a score of zero for NAS (subjects 02, 11), steatosis (11), and fibrosis (01, 03, 05, 07, 12, 13, 14, 18, 19);
2- The participants who received standard of care are subject numbers 15-19.

SUPPORTING INFORMATION

Noninvasive fatty acid oxidation in NASH: The utility of labeled breath tests to monitor changes in liver health?

Justine M. Mucinski¹, Alisha M. Perry¹, Alberto Diaz-Arias², Jamal A. Ibdah^{1,3,4}, R. Scott Rector^{1,3,4}, Elizabeth J. Parks^{1,3,*}

¹ Department of Nutrition and Exercise Physiology, University of Missouri, Columbia, MO 65211

² Boyce & Bynum Pathology Professional Services, Columbia MO, 65201, USA

³ Department of Medicine, Division of Gastroenterology and Hepatology, University of Missouri School of Medicine, Columbia, MO 65201

⁴ Research Service, Harry S Truman Memorial Veterans Medical Center, Columbia, MO, 65211

***CORRESPONDING AUTHOR:**

Elizabeth J. Parks, PhD
One Hospital Drive School of Medicine NW 406
University of Missouri
Columbia, Missouri 65212
Email: parksej@missouri.edu

RUNNING TITLE: Hepatic octanoate oxidation in NASH

AUTHOR CONTRIBUTION: EJP, RSR, and JAI were involved in study design and methods; JMM, AMP, AD-A, GMH, RSR, and EJP generated the data; JMM and AMP analyzed data and wrote the paper; All authors contributed to data interpretation and to editing the manuscript.

AUTHOR DISCLOSURES: None.

REFERENCES

1. Younossi Z, Anstee QM, Marietti M, Hardy T, Henry L, Eslam M, George J, and Bugianesi E. Global burden of NAFLD and NASH: trends, predictions, risk factors and prevention. *Nature Reviews Gastroenterology & Hepatology* 15, 11-20, (2017), PMID:28930295.
2. Diehl AM, and Day C. Cause, pathogenesis, and treatment of nonalcoholic steatohepatitis. *New England Journal of Medicine* 377, 2063-2072, (2017), PMID:29166236.
3. Hardy T, Oakley F, Anstee QM, and Day CP. Nonalcoholic fatty liver disease: Pathogenesis and disease spectrum. *Annual Review of Pathology: Mechanisms of Disease* 11, 451-496, (2016), PMID:26980160.
4. Korenblat KM, Fabbrini E, Mohammed BS, and Klein S. Liver, muscle, and adipose tissue insulin action is directly related to intrahepatic triglyceride content in obese subjects. *Gastroenterology* 134, 1369-1375, (2008), PMID:18355813.
5. Brunt EM, Janney CG, Bisceglie AM, Neuschwander-Tetri BA, and Bacon BR. Nonalcoholic steatohepatitis: a proposal for grading and staging the histological lesions. *The American Journal of Gastroenterology* 94, 2467-2474, (1999), PMID:10484010.
6. Koliaki C, Szendroedi J, Kaul K, Jelenik T, Nowotny P, Jankowiak F, Herder C, Carstensen M, Krausch M, Knoefel Wolfram T, Schlensak M, and Roden M. Adaptation of hepatic mitochondrial function in humans with non-alcoholic fatty liver is lost in steatohepatitis. *Cell Metabolism* 21, 739-746, (2015), PMID:25955209.
7. Sunny NE, Parks EJ, Browning JD, and Burgess SC. Excessive hepatic mitochondrial TCA cycle and gluconeogenesis in humans with nonalcoholic fatty liver disease. *Cell Metabolism* 14, 804-810, (2011), PMID:22152305.
8. Satapati S, Kucejova B, Duarte JAG, Fletcher JA, Reynolds L, Sunny NE, He T, Nair LA, Livingston K, Fu X, Merritt ME, Sherry AD, Malloy CR, Shelton JM, Lambert J, Parks EJ, Corbin I, Magnuson MA, Browning JD, Burgess SC, and Burgess SC. Mitochondrial metabolism mediates oxidative stress and inflammation in fatty liver. *Journal of Clinical Investigation* 125, 4447-4462, (2015), PMID:26571396.
9. da Silva RP, Kelly KB, Leonard KA, and Jacobs RL. Creatine reduces hepatic TG accumulation in hepatocytes by stimulating fatty acid oxidation. *Biochimica et Biophysica Acta* 1841, 1639-1646, (2014), PMID:25205520.
10. Stefanovic-Racic M, Perdomo G, Mantell BS, Sipula IJ, Brown NF, and O'Doherty RM. A moderate increase in carnitine palmitoyltransferase 1a activity is sufficient to substantially reduce hepatic triglyceride levels. *American Journal of Physiology-Endocrinology and Metabolism* 294, E969-977, (2008), PMID:18349115.
11. Ibdah JA, Perlegas P, Zhao Y, Angdisen J, Borgerink H, Shadoan MK, Wagner JD, Matern D, Rinaldo P, and Cline JM. Mice heterozygous for a defect in mitochondrial trifunctional protein develop hepatic steatosis and

- insulin resistance. *Gastroenterology* 128, 1381-1390, (2005), PMID:15887119.
12. Seo YS, Kim JH, Jo NY, Choi KM, Baik SH, Park JJ, Kim JS, Byun KS, Bak YT, Lee CH, Kim A, and Yeon JE. PPAR agonists treatment is effective in a nonalcoholic fatty liver disease animal model by modulating fatty-acid metabolic enzymes. *Journal of Gastroenterology and Hepatology* 23, 102-109, (2008), PMID:18171348.
 13. Zhang D, Liu ZX, Choi CS, Tian L, Kibbey R, Dong J, Cline GW, Wood PA, and Shulman GI. Mitochondrial dysfunction due to long-chain Acyl-CoA dehydrogenase deficiency causes hepatic steatosis and hepatic insulin resistance. *Proceedings of the National Academy of Sciences of the United States of America* 104, 17075-17080, (2007), PMID:17940018.
 14. Morris EM, McCoin CS, Allen JA, Gastecki ML, Koch LG, Britton SL, Fletcher JA, Fu X, Ding WX, Burgess SC, Rector RS, and Thyfault JP. Aerobic capacity mediates susceptibility for the transition from steatosis to steatohepatitis. *The Journal of Physiology* 595, 4909-4926, (2017), PMID:28504310.
 15. Rector RS, Morris EM, Ridenhour S, Meers GM, Hsu F-F, Turk J, and Ibdah JA. Selective hepatic insulin resistance in a murine model heterozygous for a mitochondrial trifunctional protein defect. *Hepatology* 57, 2213-2223, (2013), PMID:23359250.
 16. Rector RS, Thyfault JP, Uptergrove GM, Morris EM, Naples SP, Borengasser SJ, Mikus CR, Laye MJ, Laughlin MH, Booth FW, and Ibdah JA. Mitochondrial dysfunction precedes insulin resistance and hepatic steatosis and contributes to the natural history of non-alcoholic fatty liver disease in an obese rodent model. *Journal of Hepatology* 52, 727-736, (2010), PMID:20347174.
 17. Thyfault JP, Rector RS, Uptergrove GM, Borengasser SJ, Morris EM, Wei Y, Laye MJ, Burant CF, Qi NR, Ridenhour SE, Koch LG, Britton SL, and Ibdah JA. Rats selectively bred for low aerobic capacity have reduced hepatic mitochondrial oxidative capacity and susceptibility to hepatic steatosis and injury. *The Journal of Physiology* 587, 1805-1816, (2009), PMID:19237421.
 18. Patterson RE, Kalavalapalli S, Williams CM, Nautiyal M, Mathew JT, Martinez J, Reinhard MK, McDougall DJ, Rocca JR, Yost RA, Cusi K, Garrett TJ, and Sunny NE. Lipotoxicity in steatohepatitis occurs despite an increase in tricarboxylic acid cycle activity. *American Journal of Physiology-Endocrinology and Metabolism* 310, E484-494, (2016), PMID:26814015.
 19. Nakamuta M, Kohjima M, Higuchi N, Kato M, Kotoh K, Yoshimoto T, Yada M, Yada R, Takemoto R, Fukuizumi K, Harada N, Taketomi A, Maehara Y, Nakashima M, and Enjoji M. The significance of differences in fatty acid metabolism between obese and non-obese patients with non-alcoholic fatty liver disease. *International Journal of Molecular Medicine* 22, 663-667, (2008), PMID:18949388.
 20. Kohjima M, Enjoji M, Higuchi N, Kato M, Kotoh K, Yoshimoto T, Fujino T, Yada M, Yada R, Harada N, Takayanagi R, and Nakamuta M. Re-evaluation of fatty acid metabolism-related gene expression in nonalcoholic fatty liver

- disease. *International Journal of Molecular Medicine* 20, 351-358, (2007), PMID:17671740.
21. Pérez-Carreras M, Del Hoyo P, Martín MA, Rubio JC, Martín A, Castellano G, Colina F, Arenas J, and Solis-Herruzo JA. Defective hepatic mitochondrial respiratory chain in patients with nonalcoholic steatohepatitis. *Hepatology* 38, 999-1007, (2003), PMID:14512887.
 22. Sanyal AJ, Campbell-Sargent C, Mirshahi F, Rizzo WB, Contos MJ, Sterling RK, Luketic VA, Shiffman ML, and Clore JN. Nonalcoholic steatohepatitis: association of insulin resistance and mitochondrial abnormalities. *Gastroenterology* 120, 1183-1192, (2001), PMID:11266382.
 23. Moore MP, Cunningham RP, Meers GM, Johnson SA, Wheeler AA, Ganga RR, Spencer NM, Pitt JB, Diaz-Arias A, Swi AI, Ibdah JA, Parks EJ, and R.S. R. Reduced hepatic mitochondrial metabolism and markers of mitochondrial turnover in humans are linked to NAFLD progression. *American Diabetes Association 80th Scientific Session Abstract #2020-A-4368-Diabetes; Presentation #311-OR*, (2020), PMID:Chicago, 2020. Manuscript in Review.
 24. McCullough A, Previs S, and Kasumov T. Stable isotope-based flux studies in nonalcoholic fatty liver disease. *Pharmacology and Therapeutics* 181, 22-33, (2018), PMID:28720429.
 25. Bastarrachea RA, Veron SM, Vaidyanathan V, Garcia-Forey M, Voruganti VS, Higgins PB, and Parks EJ. Protocol for the measurement of fatty acid and glycerol turnover in vivo in baboons. *Journal of Lipid Research* 52, 1272-1280, (2011), PMID:21415122.
 26. Banasch M, Ellrichmann M, Tannapfel A, Schmidt WE, and Goetze O. The non-invasive (13)C-methionine breath test detects hepatic mitochondrial dysfunction as a marker of disease activity in non-alcoholic steatohepatitis. *European Journal of Medical Research* 16, 258-264, (2011), PMID:21810560.
 27. Miele L, Grieco A, Armuzzi A, Candelli M, Forgione A, Gasbarrini A, and Gasbarrini G. Hepatic mitochondrial beta-oxidation in patients with nonalcoholic steatohepatitis assessed by 13C-octanoate breath test. *American Journal of Gastroenterology* 98, 2335-2336, (2003), PMID:14572600.
 28. Portincasa P, Grattagliano I, Lauterburg BH, Palmieri VO, Palasciano G, and Stellaard F. Liver breath tests non-invasively predict higher stages of non-alcoholic steatohepatitis. *Clinical Science (London, England: 1979)* 111, 135-143, (2006), PMID:16603025.
 29. Shalev T, Aeed H, Sorin V, Shahmurov M, Didkovsky E, Ilan Y, Avni Y, and Shirin H. Evaluation of the 13C-octanoate breath test as a surrogate marker of liver damage in animal models. *Digestive Diseases and Sciences* 55, 1589-1598, (2010), PMID:19731033.
 30. Armuzzi A, Zocco MA, Miele L, Gabrielli M, Carloni E, De Lorenzo A, Grieco A, Pola P, Gasbarrini GB, and Gasbarrini A. Hepatic mitochondrial beta-oxidation assessment in healthy subjects by sodium 13C-octanoate breath test. *Gastroenterology* 118, A924-A925, (2000).
 31. Schneider AR, Kraut C, Lindenthal B, Braden B, Caspary WF, and Stein J. Total body metabolism of 13C-octanoic acid is preserved in patients with non-

- alcoholic steatohepatitis, but differs between women and men. *European Journal of Gastroenterology and Hepatology* 17, 1181-1184, (2005), PMID:16215429.
32. Mawatari H, Inamori M, Fujita K, Yoneda M, Iida H, Endo H, Hosono K, Nozaki Y, Yoneda K, Akiyama T, Takahashi H, Goto A, Abe Y, Kirikoshi H, Kobayashi N, Kubota K, Saito S, and Nakajima A. The continuous real-time ¹³C-octanoate breath test for patients with nonalcoholic steatohepatitis using the BreathID system. *Hepato-Gastroenterology* 56, 1436-1438, (2009), PMID:19950806.
 33. Braun M, Pappot O, Zuckerman E, Sulkes J, Kitai Y, Moreno M, Cohen O, Shmilovitz-Weiss H, Rotman Y, Zamirs D, Melnik S, Tur-Kaspa R, and Ben-Ari Z. The innovative real time Breath-ID® test system diagnoses and predicts the extent of hepatic injury in patients with non-alcoholic fatty liver disease. *Journal of Hepatology* 44, S249, (2006).
 34. Bloom B, Chaikoff IL, and Reinhardt WO. Intestinal lymph as pathway for transport of absorbed fatty acids of different chain lengths. *American Journal of Physiology-Legacy Content* 166, 451-455, (1951), PMID:14857202.
 35. Fritz IB. Carnitine and its role in fatty acid metabolism. *Advances in Lipid Research* 1, 285-334, (1963), PMID:14248955.
 36. Bach AC, and Babayan VK. Medium-chain triglycerides: an update. *The American Journal of Clinical Nutrition* 36, 950-962, (1982), PMID:6814231.
 37. Guillot E, Vaugelade P, Lemarchal P, and Rérat A. Intestinal absorption and liver uptake of medium-chain fatty acids in non-anaesthetized pigs. *British Journal of Nutrition* 69, 431-442, (1993), PMID:8489999.
 38. DeLany JP, Windhauser MM, Champagne CM, and Bray GA. Differential oxidation of individual dietary fatty acids in humans. *The American Journal of Clinical Nutrition* 72, 905-911, (2000), PMID:11010930.
 39. Wolfe RR, and Jahoor F. Recovery of labeled CO₂ during the infusion of C-1- vs C-2-labeled acetate: implications for tracer studies of substrate oxidation. *The American Journal of Clinical Nutrition* 51, 248-252, (1990), PMID:2106256.
 40. Grundy SM, Brewer HB, Jr., Cleeman JI, Smith SC, Jr., and Lenfant C. Definition of metabolic syndrome: report of the National Heart, Lung, and Blood Institute/American Heart Association conference on scientific issues related to definition. *Arteriosclerosis, Thrombosis, and Vascular Biology* 24, e13-18, (2004), PMID:14766739.
 41. Schwarz JM, Neese RA, Turner S, Dare D, and Hellerstein MK. Short-term alterations in carbohydrate energy intake in humans. Striking effects on hepatic glucose production, de novo lipogenesis, lipolysis, and whole-body fuel selection. *Journal of Clinical Investigation* 96, 2735-2743, (1995), PMID:8675642.
 42. Ramos-Roman MA, Syed-Abdul MM, Adams-Huet B, Casey BM, and Parks EJ. Lactation versus formula feeding: Insulin, glucose, and fatty acid metabolism during the postpartum period. *Diabetes* 69, 1624-1635, (2020), PMID:32385056.

43. DeFronzo RA, Tobin JD, and Andres R. Glucose clamp technique: a method for quantifying insulin secretion and resistance. *American Journal of Physiology-Endocrinology and Metabolism* 237, E214, (1979), PMID:382871.
44. Harris JA, and Benedict FG. A biometric study of human basal metabolism. *Proceedings of the National Academy of Sciences of the United States of America* 4, 370-373, (1918), PMID:16576330.
45. Abumrad NN, Rabin D, Diamond MP, and Lacy WW. Use of a heated superficial hand vein as an alternative site for the measurement of amino acid concentrations and for the study of glucose and alanine kinetics in man. *Metabolism: Clinical and Experimental* 30, 936-940, (1981), PMID:7022111.
46. Wolfe RR. *Radioactive and stable isotope tracers in biomedicine: Principles and practice of kinetic analysis ohn Wiley & Sons, Inc, Somerset, NJ.* John Wiley & Sons, Inc., 1992, p. 471.
47. Berglund M, and Weiser M. Isotopic composition of the elements 2009 (IUPAC Technical Report). *Pure and Applied Chemistry* 83, 397-410, (2011).
48. van Hall G. Correction factors for ¹³C-labelled substrate oxidation at whole-body and muscle level. *Proceedings of the Nutrition Society* 58, 979-986, (1999), PMID:10817166.
49. Matthews DR, Hosker JP, Rudenski AS, Naylor BA, Treacher DF, and Turner RC. Homeostasis model assessment: insulin resistance and beta-cell function from fasting plasma glucose and insulin concentrations in man. *Diabetologia* 28, 412-419, (1985), PMID:3899825.
50. Steele R, Wall JS, De Bodo RC, and Altszuler N. Measurement of size and turnover rate of body glucose pool by the isotope dilution method. *American Journal of Physiology* 187, 15-24, (1956), PMID:13362583.
51. Motamed N, Miresmail SJ, Rabiee B, Keyvani H, Farahani B, Maadi M, and Zamani F. Optimal cutoff points for HOMA-IR and QUICKI in the diagnosis of metabolic syndrome and non-alcoholic fatty liver disease: A population based study. *Journal of Diabetes Complications* 30, 269-274, (2016), PMID:26718936.
52. Piazzolla VA, and Mangia A. Noninvasive Diagnosis of NAFLD and NASH. *Cells* 9, (2020), PMID:32316690.
53. Hepner GW, and Vesell ES. Assessment of aminopyrine metabolism in man by breath analysis after oral administration of ¹⁴C-aminopyrine. Effects of phenobarbital, disulfiram and portal cirrhosis. *New England Journal of Medicine* 291, 1384-1388, (1974), PMID:4427643.
54. Armuzzi A, Candelli M, Zocco MA, Andreoli A, De Lorenzo A, Nista EC, Miele L, Cremonini F, Cazzato IA, Grieco A, Gasbarrini G, and Gasbarrini A. Review article: breath testing for human liver function assessment. *Alimentary Pharmacology and Therapeutics* 16, 1977-1996, (2002), PMID:12452932.
55. Bonfrate L, Grattagliano I, Palasciano G, and Portincasa P. Dynamic carbon ¹³ breath tests for the study of liver function and gastric emptying. *Gastroenterology Report* 3, 12-21, (2015), PMID:25339354.
56. Di Ciaula A, Calamita G, Shanmugam H, Khalil M, Bonfrate L, Wang DQ, Baffy G, and Portincasa P. Mitochondria matter: Systemic aspects of nonalcoholic fatty liver disease (NAFLD) and diagnostic assessment of liver

- function by stable isotope dynamic breath tests. *International Journal of Molecular Sciences* 22, (2021), PMID:34299321.
57. Papamandjaris AA, MacDougall DE, and Jones PJ. Medium chain fatty acid metabolism and energy expenditure: obesity treatment implications. *Life Sciences* 62, 1203-1215, (1998), PMID:9570335.
 58. Bremer J. Carnitine and its role in fatty acid metabolism. *Trends in Biochemical Sciences* 2, 207-209, (1980).
 59. Promrat K, Kleiner DE, Niemeier HM, Jackvony E, Kearns M, Wands JR, Fava JL, and Wing RR. Randomized controlled trial testing the effects of weight loss on nonalcoholic steatohepatitis. *Hepatology* 51, 121-129, (2010), PMID:19827166.
 60. Vilar-Gomez E, Martinez-Perez Y, Calzadilla-Bertot L, Torres-Gonzalez A, Gra-Oramas B, Gonzalez-Fabian L, Friedman SL, Diago M, and Romero-Gomez M. Weight loss through lifestyle modification significantly reduces features of nonalcoholic steatohepatitis. *Gastroenterology* 149, 367-378.e365, (2015), PMID:25865049.
 61. Lira FS, Carnevali LC, Zanchi NE, Santos RVT, Lavoie JM, and Seelaender M. Exercise intensity modulation of hepatic lipid metabolism. *Journal of Nutrition and Metabolism* 2012, 809576, (2012), PMID:22545209.
 62. Rector RS, Thyfault JP, Laye MJ, Morris RT, Borengasser SJ, Uptergrove GM, Chakravarthy MV, Booth FW, and Ibdah JA. Cessation of daily exercise dramatically alters precursors of hepatic steatosis in Otsuka Long-Evans Tokushima Fatty (OLETF) rats. *Journal of Physiology* 586, 4241-4249, (2008), PMID:18617560.
 63. Heath RB, Karpe F, Milne RW, Burdge GC, Wootton SA, and Frayn KN. Selective partitioning of dietary fatty acids into the VLDL TG pool in the early postprandial period. *Journal of Lipid Research* 44, 2065-2072, (2003), PMID:12923230.
 64. Westerbacka J, Lammi K, Häkkinen A-M, Rissanen A, Salminen I, Aro A, and Yki-Järvinen H. Dietary fat content modifies liver fat in overweight nondiabetic subjects. *The Journal of Clinical Endocrinology & Metabolism* 90, 2804-2809, (2005), PMID:15741262.
 65. Tamura S, and Shimomura I. Contribution of adipose tissue and de novo lipogenesis to nonalcoholic fatty liver disease. *The Journal of Clinical Investigation* 115, 1139-1142, (2005), PMID:15864343.
 66. Tamura Y, Tanaka Y, Sato F, Choi JB, Watada H, Niwa M, Kinoshita J, Ooka A, Kumashiro N, Igarashi Y, Kyogoku S, Maehara T, Kawasumi M, Hirose T, and Kawamori R. Effects of diet and exercise on muscle and liver intracellular lipid contents and insulin sensitivity in type 2 diabetic patients. *The Journal of Clinical Endocrinology & Metabolism* 90, 3191-3196, (2005), PMID:15769987.
 67. Cusi K. Role of obesity and lipotoxicity in the development of nonalcoholic steatohepatitis: Pathophysiology and clinical implications. *Gastroenterology* 142, 711-725.e716, (2012), PMID:22326434.
 68. Fabbrini E, Mohammed BS, Magkos F, Korenblat KM, Patterson BW, and Klein S. Alterations in adipose tissue and hepatic lipid kinetics in obese men

- and women with nonalcoholic fatty liver disease. *Gastroenterology* 134, 424-431, (2008), PMID:18242210.
69. Malhi H, and Gores G. Molecular mechanisms of lipotoxicity in nonalcoholic fatty liver disease. *Seminars in Liver Disease* 28, 360-369, (2008), PMID:18956292.
 70. Iozzo P, Turpeinen AK, Takala T, Oikonen V, Bergman J, Gronroos T, Ferrannini E, Nuutila P, and Knuuti J. Defective liver disposal of free fatty acids in patients with impaired glucose tolerance. *The Journal of Clinical Endocrinology and Metabolism* 89, 3496-3502, (2004), PMID:15240637.
 71. McGarry JD. What if Minkowski had been ageusic? An alternative angle on diabetes. *Science* 258, 766-770, (1992), PMID:1439783.
 72. Unger RH. Lipotoxicity in the pathogenesis of obesity-dependent NIDDM. Genetic and clinical implications. *Diabetes* 44, 863-870, (1995), PMID:7621989.
 73. Ferreira LF. Mitochondrial basis for sex-differences in metabolism and exercise performance. *American Journal of Physiology Regulatory Integrative and Comparative* 314, R848-R849, (2018), PMID:29590556.
 74. Pessayre D, Mansouri A, Haouzi D, and Fromenty B. Hepatotoxicity due to mitochondrial dysfunction. *Cell Biology and Toxicology* 15, 367-373, (1999), PMID:10811531.
 75. Mucinski J, Vena J, Ramos-Roman MA, Szuszkiewicz-Garcia M, McLaren DG, Previs S, Shankar S, Lassman M, and Parks E. High throughput LC-MS method to investigate postprandial lipemia: Considerations for future precision nutrition research. *American Journal of Physiology: Endocrinology and Metabolism*, (2020).
 76. Jacome-Sosa M, Hu Q, Manrique-Acevedo CM, Phair RD, and Parks EJ. Human intestinal lipid storage through sequential meals reveals faster dinner appearance is associated with hyperlipidemia. *JCI Insight* 6, (2021), PMID:34369385.
 77. Fuller SE, Huang TY, Simon J, Batdorf HM, Essajee NM, Scott MC, Waskom CM, Brown JM, Burke SJ, Collier JJ, and Noland RC. Low-intensity exercise induces acute shifts in liver and skeletal muscle substrate metabolism but not chronic adaptations in tissue oxidative capacity. *Journal of Applied Physiology (1985)* 127, 143-156, (2019), PMID:31095457.
 78. Gorski J, Oscai LB, and Palmer WK. Hepatic lipid metabolism in exercise and training. *Medicine and Science in Sports and Exercise* 22, 213-221, (1990), PMID:2192222.
 79. De Souza CT, Frederico MJ, da Luz G, Cintra DE, Ropelle ER, Pauli JR, and Velloso LA. Acute exercise reduces hepatic glucose production through inhibition of the Foxo1/HNF-4alpha pathway in insulin resistant mice. *Journal of Physiology* 588, 2239-2253, (2010), PMID:20421289.
 80. Kirwan JP, Solomon TP, Wojta DM, Staten MA, and Holloszy JO. Effects of 7 days of exercise training on insulin sensitivity and responsiveness in type 2 diabetes mellitus. *American Journal of Physiology-Endocrinology and Metabolism* 297, E151-156, (2009), PMID:19383872.

81. Devlin JT, Hirshman M, Horton ED, and Horton ES. Enhanced peripheral and splanchnic insulin sensitivity in NIDDM men after single bout of exercise. *Diabetes* 36, 434-439, (1987), PMID:3102297.

APPENDIX A – NAFLD activity scoring system

Collection date:
Biopsy Number:



Accession:
Subject Name:

TORS Liver Pathology (NASH Clinical Research Network)

NAFLD Activity Score (NAS)

<p>Steatosis (0-3)</p> <p>(0) <5% <input style="width: 50px; height: 20px;" type="text"/></p> <p>(1) 5%-33%</p> <p>(2) >33%-66%</p> <p>(3) >66%</p> <p>Hepatocellular Ballooning (0-2)</p> <p>(0) None <input style="width: 50px; height: 20px;" type="text"/></p> <p>(1) Few balloon cells</p> <p>(2) Many cells/prominent ballooning</p>	<p>Lobular Inflammation (0-3)</p> <p>(0) No foci <input style="width: 50px; height: 20px;" type="text"/></p> <p>(1) <2 foci per 200X field</p> <p>(2) 2-4 foci per 200X field</p> <p>(3) >4 foci per 200X field</p> <p>Unweighted sum of scores (0-8)</p> <p>≥5 correlates with NASH <input style="width: 50px; height: 20px;" type="text"/></p> <p>≤2 correlates with "not NASH"</p>
---	---

NAFLD Staging

<p>Fibrosis (0-4)</p> <p>(0) None</p> <p>(1) Perisinusoidal or periportal</p> <p style="padding-left: 20px;">(1A) Mild, zone 3, perisinusoidal (delicate fibrosis)</p> <p style="padding-left: 20px;">(1B) Moderate, zone 3, perisinusoidal (dense fibrosis)</p> <p style="padding-left: 20px;">(1C) Portal/periportal fibrosis (without perisinusoidal fibrosis)</p>	<p>(2) Perisinusoidal and portal/periportal <input style="width: 50px; height: 20px;" type="text"/></p> <p>(3) Bridging fibrosis</p> <p>(4) Cirrhosis</p>
--	---

Additional features:

<p>Steatosis location (predominant distribution pattern)</p> <p>(0 = Zone 3, 1 = Zone 1, 2 = azonal, 3 = panacinar) <input style="width: 50px; height: 20px;" type="text"/></p> <p>Microvesicular steatosis (contiguous patches)</p> <p>(0 = not present, 1 = present) <input style="width: 50px; height: 20px;" type="text"/></p> <p>Microgranulomas (0 = absent, 1 = present) <input style="width: 50px; height: 20px;" type="text"/></p> <p>Large lipogranulomas (0 = absent, 1 = present) <input style="width: 50px; height: 20px;" type="text"/></p> <p>Portal inflammation</p> <p>(0 = none to minimal, 1 = greater than minimal) <input style="width: 50px; height: 20px;" type="text"/></p> <p>Hepatocellular Dysplasia (0 = absent, 1 = present) <input style="width: 50px; height: 20px;" type="text"/></p> <p>Iron hepatocyte (0-4) <input style="width: 50px; height: 20px;" type="text"/></p> <p>RE Iron (0 = none, 1 = few (Kupffer cells), 2 = majority) <input style="width: 50px; height: 20px;" type="text"/></p>	<p>Acidophil bodies (0 = none to rare, 1 = many) <input style="width: 50px; height: 20px;" type="text"/></p> <p>Pigmented macrophages</p> <p>(0 = none to rare, 1 = many) <input style="width: 50px; height: 20px;" type="text"/></p> <p>Megamitochondria (0 = none to rare, 1 = many) <input style="width: 50px; height: 20px;" type="text"/></p> <p>Mallory hyaline</p> <p>(0 = none to rare, 1 = many) <input style="width: 50px; height: 20px;" type="text"/></p> <p>Glycogenated hepatocyte nuclei</p> <p>(0 = none to rare, 1 = many) <input style="width: 50px; height: 20px;" type="text"/></p> <p>Endothelial Fe (0 = absent, 1 = present) <input style="width: 50px; height: 20px;" type="text"/></p> <p style="padding-left: 20px;">if present:</p>
---	--

TORS Liver Pathology (Ishak System)

Necroinflammatory Scores

<p>A. Periportal or periseptal interface hepatitis (piecemeal necrosis) (0-4)</p> <p>(0) Absent <input style="width: 50px; height: 20px;" type="text"/></p> <p>(1) Mild (focal, few portal areas)</p> <p>(2) Mild/moderate (focal, most portal areas)</p> <p>(3) Moderate (continuous around <50% of tracts or septa)</p> <p>(4) Severe (continuous around >50% of tracts or septa)</p> <p>B. Confluent necrosis (0-6)</p> <p>(0) Absent <input style="width: 50px; height: 20px;" type="text"/></p> <p>(1) Focal confluent necrosis</p> <p>(2) Zone 3 necrosis in some areas</p> <p>(3) Zone 3 necrosis in most areas</p> <p>(4) Zone 3 necrosis + occasional portal-central (P-C) bridging</p> <p>(5) Zone 3 necrosis + multiple (P-C) bridging</p> <p>(6) Panacinar or multiacinar necrosis</p> <p>C. Focal (spotty) lytic necrosis, apoptosis and focal inflammation (0-4)</p> <p>(0) Absent <input style="width: 50px; height: 20px;" type="text"/></p> <p>(1) One focus or less per 10X objective</p> <p>(2) Two to four foci per 10X objective</p> <p>(3) Five to ten foci per 10X objective</p> <p>(4) More than ten foci per 10X objective</p> <p>D. Portal inflammation (0-4)</p> <p>(0) None <input style="width: 50px; height: 20px;" type="text"/></p> <p>(1) Mild, some or all portal areas</p> <p>(2) Moderate, some or all portal areas</p> <p>(3) Moderate/marked, all portal areas</p> <p>(4) Marked, all portal areas</p>	<p>Total score for grading (0-18) <input style="width: 50px; height: 20px;" type="text"/></p> <p>Ishak Stage (0-6) <input style="width: 50px; height: 20px;" type="text"/></p>
--	--

Additional observations:
Pathologist signature: Diaz-Arias, Alberto A

APPENDIX B – Curriculum vita

JUSTINE M. MUCINSKI

PhD Candidate

PERSONAL INFORMATION

Justine M. Mucinski

Laboratory of Elizabeth Parks, PhD
University of Missouri – Columbia
Department of Nutrition and Exercise Physiology
One Hospital Drive, Room NW405, Columbia, MO, 65212
Phone: (616) 826-2975
Email: jmm6nc@mail.missouri.edu



Departmental profile: <https://nep.missouri.edu/faculty/justine-mucinski/>

PubMed Bibliography: <https://tinyurl.com/4ymwcujh>

ORCHID ID: 0000-0003-4432-6638

CV current as of April 29, 2022

EDUCATION

- | | |
|--------------|---|
| 2017-Present | PhD Candidate, Exercise Physiology
Nutrition and Exercise Physiology
University of Missouri, Columbia, MO
Cumulative GPA: 3.95 (4.0 scale) |
| 2016 | BA, Exercise Science (minor: Biology)
Department of Kinesiology
Hope College, Holland, MI
Cumulative GPA: 3.70 (4.0 scale) |

PHD DISSERTATION

Lifestyle treatment in the regression of NAFLD: Insulin resistance, lipid synthesis, and methodological innovation

Doctoral Committee:

Elizabeth J. Parks, PhD (Chair)
R. Scott Rector, PhD (Co-Mentor)
Kevin Fritsche, PhD
Frank Booth, PhD

PROFESSIONAL SUMMARY AND OBJECTIVES

I am a hard-working and self-motivated doctoral candidate in exercise physiology with a great passion for scientific dissemination. I have studied under a nutritional biochemist with an emphasis on liver health in relation to whole-body metabolism and have extensive experience in clinical setting of metabolic disease. I have excellent communication skills (both written and verbal) with 5+ years of experience working with clinical populations (human clinical trials and lifestyle fitness rehabilitation) and 2 years working with preclinical models (animal models). I am quick to pick up concepts with a keen eye for details and the ability to conceptualize the bigger picture simultaneously. I have great multi-tasking, organizational, and time-management abilities. Overall, my long-term goal is to discover safe, effective, and realistic treatments and preventions for chronic, debilitating conditions and diseases.

RESEARCH AND PROFESSIONAL EXPERIENCE

Scientific Training

- 2017-present Graduate Research Assistant, Department of Nutrition and Exercise Physiology, University of Missouri, Columbia, MO, USA. Supervisor: Elizabeth J. Parks, PhD
- 2017 Research Assistant, Nutrition and Exercise Physiology, University of Missouri, Columbia, MO, USA. Supervisor: Elizabeth J. Parks, PhD
- 2015-2016 Undergraduate Research, Department of Kinesiology, Hope College, Holland, MI, USA. Supervisors: Kevin Cole, PhD and Maureen Dunn, PhD

Research Projects

- 2017-Present **Graduate Research Assistantship** – Parks Laboratory, School of Medicine, Department of Nutrition and Exercise Physiology, University of Missouri, Columbia, MO
- 2017-2022 1. *Nutrient overload, insulin resistance, and hepatic mitochondrial dysfunction*
Project: #2008258
Sponsor: NIH R01 DK113701
Investigators: E Parks, PhD; RS Rector, PhD; JA Ibdah, MD, PhD
Dates: 05/01/17 – 04/30/22
Role: Graduate Researcher
Summary: Determine effects of a lifestyle intervention (diet and exercise) on liver health in nonalcoholic steatohepatitis – mitochondrial function, nutrient handling, and liver histology.

- 2018-2022 2. *Quantifying ceramide flux in vivo*
Project: IACUC protocol # 248
Sponsor: University of Missouri
Investigators: JM Mucinski and EJ Parks, PhD
Dates: 2018-present
Role: Graduate Researcher/ PI
Summary: For the first time, quantify newly-made ceramides in humans and rodents using stable isotope tracers with specific focus on liver ceramide synthesis in relation to mitochondrial ceramide content.
- 2018-2022 3. *Fructose induced hepatic de novo lipogenesis in adolescents with obesity*
Project: #1804019121
Sponsor: Weill-Cornell Medical College / Rogosin Institute, NY
Investigators: L Hudgins, MD and EJ Parks, PhD
Dates: 09/01/18 – 08/31/22
Role: Graduate Researcher
Summary: Compare fructose-induced hepatic de novo lipogenesis in prediabetic versus metabolically healthy obese adolescents.
- 2018-2021 4. *A clinical study to assess postprandial metabolism using an oral stable isotope in healthy male subjects*
Project: #231-00
Sponsor: Merck
Investigators: EJ Parks, PhD; DG McLaren, PhD; SF Previs, PhD
Dates: 2012 – 2021
Role: Graduate Researcher
Summary: Randomized, four-period crossover study to test the characteristic of measuring isotope-enriched triglyceride excursions following ingestion of a liquid fat challenge with stable isotope in 12 healthy men.
- 2017-2019 5. *The tailgate study: A pilot study measuring the impact of acute alcohol intake on intrahepatic lipid*
Project: #1211233
Sponsor: The University of Missouri
Investigators: EJ Parks, PhD
Dates: 2014 – 2019
Role: Graduate Researcher

Summary: Tested whether overconsumption of food and alcohol would increase de novo lipogenesis and liver fat.

2017-2018

6. *Evaluation of TVB-2640, a FASN inhibitor, to reduce de novo lipogenesis in subjects with characteristics of the metabolic syndrome*

Project: #2006432

Clinicaltrials.gov: #NCT02948569

Sponsor: 3-V Biosciences

Investigators: C Manrique, MD and EJ Parks, PhD

Dates: 02/2017 – 01/2018

Role: Graduate Researcher

Summary: Tested the effect of the TVB-2640, a pharmacological inhibitor of fatty acid synthase, in obese men with certain metabolic abnormalities that put them at risk for NAFLD.

2015-2016

Undergraduate Research – Regulation of Human Metabolism Senior Project
Department of Kinesiology, Hope College, Holland, MI

2015

7. *The effects of leg press speed on post-activation potentiation of vertical jump performance*

Project: Regulation of Human Metabolism Senior Research

Sponsor: Department of Kinesiology, Hope College, Holland, MI

Investigators: JM Mucinski, T Hatfield, M Sall, KM Winkler, and K Cole, PhD

Dates: 08/2015-12/2015

Role: Undergraduate Researcher

Summary: Determine if different velocities of leg press at 70% of one repetition maximum (1RM) improved vertical jump performance on the Vertek® and Just Jump Mat®

Previous work experience

2017

Research Assistant

Nutrition and Exercise Physiology, University of Missouri, Columbia, MO, USA. Supervisor: Elizabeth J. Parks, PhD

- Rapidly learned and practiced techniques applied within a wet lab setting focused on hepatic, lipid, and metabolic research;
- Review and stay up to date with literature pertaining to metabolic disease and treatment, pharmacological

treatments, NAFLD and NASH; macronutrient metabolism and homeostasis etc.;

- Assisted with in-patient studies for new investigational drug (3VB-2640) trial through coordination and preparation of clinical research participants and research team;
- Fulfilled any additional duties assigned by my supervisor.

2016 – 2017

Lifestyle Fitness Rehab Aide

Hope Network NeuroRehab, Grand Rapids, MI

- Provided lifestyle fitness programming for individuals and groups of consumers receiving clinical and/or residential programs;
- Obtained a deep knowledge of the physical manifestations and the cognitive and emotional deficits that accompany traumatic brain injuries and spinal cord injuries (specific to each client);
- Designed and implemented exercise programs for each client on my case load;
- Engaged client through effective support and encouragement;
- Provided programming with the field to encourage integration within the community;
- Led multiple team programs and consumer activities;
- Maintained current and accurate records of treatment through data collection and established documentation requirements, including, but not limited to: incident reports, treatment notes, behavioral programming, and data collection.

2016

Metabolism Writing Fellow

Klooster Writing Center, Hope College, Holland, MI

- Engaged students through my hands-on support of their writing development within the scope of the Regulation of Metabolism course;
- Assisted the advising professor with enforcing research writing guidelines through effective communication and feedback to students;
- Thoroughly read and quickly learned the goals of the research project and objectives to provide constructive feedback to students doing research in the Hope College metabolism course on their scientific writing.

2016

Health Dynamics Teaching Assistant

- Kinesiology Department, Hope College, Holland, MI
- Support leading faculty during class activities;
 - Deliver proper instruction in various physical activities and body mechanics;
 - Facilitate exam preparation sessions for students

TEACHING AND MENTORING EXPERIENCE

2021 Lipidomics I and II- LC/MS and application of stable isotopes to measure lipid and metabolic flux
NEP 8310: Biochemistry of Lipids
Major Professor: Elizabeth Parks, PhD
Nutrition and Exercise Physiology, University of Missouri, Columbia, MO

2020 Translational Research: Two examples from my graduate training
V BSCI 9435: Molecular Exercise Biology
Major professor: Frank Booth, PhD
Veterinary Biomedical Sciences, University of Missouri Columbia, MO

2018 – present *Mentoring undergraduate and graduate students*
Jonas McCaffrey, Undergraduate student, University of Missouri
Anticipated Graduation: May 2024
Mentored topics: Mouse study design and handling skills, ceramide metabolism and kinetics, hepatic mitochondrial isolation, ceramide isolation from plasma, liver, and mitochondria

Emma Baer, Undergraduate student, University of Missouri
Anticipated Graduation: May 2022
Mentored topics: Glucose derivatization technique; GC/MS general training and peak integration

Alisha Perry, Undergraduate student, Initiative for Maximizing Student Development (IMSD) Scholar – NIH R25 GM135744, Life Sciences Center, University of Missouri
Graduated: May 2021

Mentored topics: Non-invasive fatty acid oxidation data collection and analysis in humans with NASH; writing technique; poster and manuscript preparations

Manuscripts and Presentations:

AM Perry, **JM Mucinski**, A Diaz-Arias, JA Ibdah, RS Rector, EJ Parks. Noninvasive hepatic fatty acid oxidation in biopsy-proven nonalcoholic steatohepatitis. *Frontiers in Physiology – Lipids and fatty acids*, 2021 (pre-submission).

AM Perry, **JM Mucinski**, A Diaz-Arias, JA Ibdah, RS Rector, EJ Parks. Hepatic short chain fatty acid oxidation in nonalcoholic fatty liver disease. Annual Biomedical Research Conference for Minority Students (ABRCMS) – Virtual (2020, November).

AM Perry, **JM Mucinski**, A Diaz-Arias, JA Ibdah, RS Rector, EJ Parks. Fatty acid oxidation in nonalcoholic steatohepatitis (NASH). University of Missouri Undergraduate Research and Creative Achievement Forum, University of Missouri, Columbia, MO; Virtual (2021, April).

AM Perry, **JM Mucinski**, MM Syed-Abdul, J Snawder, A Gaballah, RS Rector, JA Ibdah, EJ Parks. Hepatic short chain fatty acid (SCFA) oxidation in nonalcoholic fatty liver disease. Abstract # C-338; ABRCMS, Anaheim, CA (2019, November).

** Awarded an Outstanding Poster Presentation Award – ABRCMS Scientific Discipline Category: Physiology & Pharmacology*

AM Perry, **JM Mucinski**, MM Syed-Abdul, J Snawder, A Gaballah, RS Rector, JA Ibdah, EJ Parks: Hepatic short chain fatty acid (SCFA) oxidation in nonalcoholic fatty liver disease. Health Sciences Research Day, University of Missouri, Columbia, MO (2019, November).

** Awarded first place in Category 1 Clinical – University of Missouri Health Sciences Research Day*

JM Mucinski, AM Perry, JA Kanaley, NC Winn, EJ Parks. Effects of exercise on hepatic short chain fatty acid oxidation (SCFAO). Poster #60; Southwest American College of Sports Medicine Chapter Meeting, Newport Beach, CA (2019, October).

2018

Sports Nutrition Graduate Teaching Assistant
Nutrition and Exercise Physiology, University of Missouri,
Columbia, MO

- Grade all course work and examinations
- Provide support for students and faculty as needed
- Guest lecture and proctor exams

- 2015 – 2016 Health Dynamics Teaching Assistant
Kinesiology Department, Hope College, Holland, MI
- Support leading faculty during class activities
 - Deliver proper instruction in various physical activities and body mechanics
 - Facilitate exam preparation sessions for students

AWARDS AND HONORS

- 2022 American Kinesiology Association National Doctoral Scholar Award
- 2022 American Kinesiology Association Regional Doctoral Scholar Award and Regional Writing Award
- 2022 James L McGregor Scholarship, Department of Nutrition and Exercise Physiology, University of Missouri-Columbia, MO (\$250)
- 2022 M. Harold Laughlin Scholarship, University of Missouri-Columbia, MO (\$500)
- 2022 Keystone Symposia: Inter Organ Crosstalk in Non-Alcoholic Steatohepatitis (NASH), Department Travel Award, Laboratory of Dr. Elizabeth Parks, School of Medicine, University of Missouri-Columbia, MO (\$2,200)
- 2021 Gamma Alpha Gamma Dissertation Year Fellowship, Graduate School, University of Missouri-Columbia, MO (\$9,014)
- 2021 Edward J. O'Brien Scholarship, Department of Nutrition and Exercise Physiology, University of Missouri-Columbia, MO (\$500)
- 2021 Research Development Award, Graduate Professional Council, University of Missouri-Columbia, MO (\$600)
- 2021 Conference Presentation Travel Award – American Diabetes Association, Graduate Professional Council, University of Missouri-Columbia, MO (\$150)
- 2021 Professional Development Travel Award – Keystone Symposia: Lipidomics in Health and Disease, Graduate Professional Council, University of Missouri-Columbia, MO (\$159)
- 2020 Campbell Harrison Scholarship, College of Human and Environmental Sciences, University of Missouri-Columbia, MO (\$500)
- 2019 American Diabetes Association, Departmental Travel Award, Laboratory of Dr. Elizabeth Parks, School of Medicine, University of Missouri-Columbia, MO (\$1,000)
- 2019 Travel Award – American Diabetes Association, Graduate Professional Council, University of Missouri-Columbia, MO

	(\$600)
2018	Experimental Biology, Department Travel Award, Laboratory of Dr. Elizabeth Parks, School of Medicine, University of Missouri-Columbia, MO (\$1,300)
2018	KinMet – Kinetics in Metabolism, Departmental Travel Award, Laboratory of Dr. Elizabeth Parks, School of Medicine, University of Missouri-Columbia, MO (\$502)
2018	Isotope Tracer Course, Departmental Travel Award, Laboratory of Dr. Elizabeth Parks, School of Medicine, University of Missouri-Columbia, MO (\$2,000)
2018	Metabolomic Basics – Dr. Takhar Kasumov, Departmental Travel Award, Laboratory of Dr. Elizabeth Parks, School of Medicine, University of Missouri-Columbia, MO (\$1,200)
2017	Adeline M. Hoffman Fellowship, College of Human Environmental Sciences, University of Missouri-Columbia, MO (\$3,500/year, two years)
2016	Spring- Dean's List
2016	Magna Cum Laude, Hope College, Holland, MI
2015	Spring & Fall- Dean's List
2014	Spring & Fall- Dean's List
2013	Fall- Dean's List
2012	Fall- Dean's List
2012	Distinguished Scholar Award, Hope College, Holland, MI (\$5,000/year, Four years)

PUBLICATIONS

Peer-Reviewed Publications

1. **JM Mucinski**, JE Vena, MA Ramos-Roman, ME Lassman, M Szuszkiewicz-Garcia, DG McLaren, SS Shankar, EJ Parks. High throughput LC-MS method to investigate postprandial lipemia: Considerations for future precision nutrition research. *American Journal of Physiology: Endocrinology and Metabolism*, 2021; 320(4): E702-E715. PMID: 33522396.
2. MM Syed-Abdul, M Jacome-Sosa, Q Hu, AH Gaballah, NC Winn, NT Lee, **JM Mucinski**, CM Manrique-Acevedo, G Lastra, JM Anderson, AM Juboori, BD Bartholow, EJ Parks. Tailgate study: Differing metabolic effects of a bout of excessive eating and drinking. *Alcohol*, 2021; 90: 45-55. PMID: 33232792.
3. MP Moore, R Cunningham, R Dashek, **JM Mucinski**, RS Rector. A fad too far? Dietary strategies for the prevention and treatment of NAFLD. *Obesity (Silver Spring)*, 2020; 28(10): 1843-1852. PMID: 32893456.
4. **JM Mucinski**, CM Manrique-Acevedo, T Kasumov, TJ Garrett, AH Gaballah, EJ Parks. Relationship between VLDL-ceramides, -diacylglycerols, and -

triacylglycerols in insulin resistant men. *Lipids*, 2020; 55(4): 387-393. PMID: 32415687

5. MP Moore* and **JM Mucinski***. Impact of nicotinamide riboside supplementation on skeletal muscle mitochondria and whole-body glucose homeostasis: Challenging the current hypothesis. *The Journal of Physiology*, 2020; 598: 3327-3328. PMID: 32463114
*Co-first authors

Manuscripts in preparation

1. **JM Mucinski**, EJ Parks, T Kasumov. Stable isotopes and LC-MS quantify ceramide kinetics in vivo. *Analytical Biochemistry*, (pre-submission).
2. AM Perry, **JM Mucinski**, A Diaz-Arias, JA Ibdah, RS Rector, EJ Parks. Noninvasive hepatic fatty acid oxidation in biopsy-proven nonalcoholic steatohepatitis. *Frontiers in Physiology – Lipids and fatty acids*, (pre-submission).
3. **JM Mucinski**, AF Salvador, MP Moore, GM Meers, S Johnson, G Lastra, JA Ibdah, RS Rector, EJ Parks. Histological improvements from increased peripheral substrate disposal: Muscle glucose uptake spares the liver. *Frontiers in Physiology – Lipids and fatty acids*, (pre-submission).

Selected abstracts

1. **JM Mucinski**, MP Moore, JA Ibdah, RS Rector, EJ Parks. Paradoxical increases in glucose appearance and 24h FFA with NASH treatment. Keystone Symposia: Inter Organ Crosstalk in Non-Alcoholic Steatohepatitis (NASH), Keystone, CO (2022, February).
2. CEP Fenton, TM Fordham, JM Anderson, MP Moore, **JM Mucinski**, JA Ibdah, RS Rector, EJ Parks. Using Fitbit data to predict cardiometabolic health outcomes. Health Sciences Research Day, University of Missouri, Columbia, MO (2021, November).
3. **JM Mucinski**, NS Nallapeta, MP Moore, JA Ibdah, RS Rector, EJ Parks. Lifestyle treatment-induced improvements in nonalcoholic steatohepatitis (NASH). Submission #2021-A-5162-Diabetes; American Diabetes Association 81st Virtual Scientific Sessions (2021, June).
* Accepted as an oral presentation – Monday June 28th 3:45pm (given virtually)
4. AM Perry, **JM Mucinski**, A Diaz-Arias, JA Ibdah, RS Rector, EJ Parks. Fatty acid oxidation in nonalcoholic steatohepatitis (NASH). University of Missouri Undergraduate Research and Creative Achievement Forum, University of Missouri, Columbia, MO; Virtual (2021, April).

5. AM Perry, **JM Mucinski**, A Diaz-Arias, JA Ibdah, RS Rector, EJ Parks. Hepatic short chain fatty acid oxidation in nonalcoholic fatty liver disease. ABRCMS – Virtual (2020, November).
6. **JM Mucinski**, N Sharma, MP Moore, JA Ibdah, RS Rector, EJ Parks. Role of glucose flux to elevate hepatic lipogenesis in biopsy-proven NASH. Submission #2020-A-4368-Diabetes; American Diabetes Association 80th Scientific Sessions (2020, June).
* Accepted as an oral presentation – Monday June 15th 2:15pm (given virtually)
7. AM Perry, **JM Mucinski**, MM Syed-Abdul, JM Snawder, A Gaballah, RS Rector, JA Ibdah, EJ Parks. Hepatic short chain fatty acid (SCFA) oxidation in nonalcoholic fatty liver disease. Health Sciences Research Day, University of Missouri, Columbia, MO (2019, November).
* Awarded first place in Category 1 – Clinical
8. AM Perry, **JM Mucinski**, MM Syed-Abdul, JM Snawder, A Gaballah, RS Rector, JA Ibdah, EJ Parks. Hepatic short chain fatty acid (SCFA) oxidation in nonalcoholic fatty liver disease. Abstract # C-338; ABRCMS, Anaheim, CA (2019, November).
* Awarded an Outstanding Poster Presentation Award – ABRCMS Scientific Discipline Category: Physiology & Pharmacology
9. **JM Mucinski**, AM Perry, JA Kanaley, NC Winn, EJ Parks. Effects of exercise on hepatic short chain fatty acid oxidation (SCFAO). Poster #60; Southwest American College of Sports Medicine Chapter Meeting, Newport Beach, CA (2019, October).
10. **JM Mucinski**, MM Syed-Abdul, TJ Garrett & EJ Parks. Very low-density lipoprotein ceramides and hepatic lipid accumulation. *Diabetes*, 2019; 68. doi:10.2337/db19-1900-P %J Diabetes. Poster #1900-P; American Diabetes Association 79th Scientific Sessions, San Francisco, CA (2019, June).
11. RD Arreola, MM Syed-Abdul, N Le, A Gaballah, **JM Mucinski**, EJ Parks. Fibroblast growth factor-21 and human metabolism. Undergraduate Research & Creative Achievements Forum, University of Missouri, Columbia, MO (2019, April).
12. **JM Mucinski**, MM Syed-Abdul, TJ Garrett & EJ Parks. Inverse relationship between very low-density lipoprotein (VLDL) ceramides, diacylglycerols, and triacylglycerols in human hepatic lipid accumulation. *FASEB*, 2019; 33(S1): lb567-lb567, doi:10.1096/fasebj.2019.33.1_supplement.lb567. Poster #LB567; Experimental Biology, Orlando, FL (2019, April).
13. Z Powell, JM Snawder, **JM Mucinski**, N Le, RD Arreola, MM Syed-Abdul, J Otto, AM Perry, EJ Parks. Analysis of physical activity on the days

- immediately after exercise. Life Sciences Research Day, University of Missouri, Columbia, MO (2019, March).
14. RD Arreola, MM Syed-Abdul, N Le, CM Manrique-Acevedo, A Gaballah, **JM Mucinski**, W McCulloch, EJ Parks. Fibroblast growth factor-21 and its relationship to human liver fat synthesis: Impact of a new therapeutic agent. Poster #T-P-3383; The Obesity Society, Nashville, TN (2018, November).
 15. **JM Mucinski**, T Hatfield, M Sall, K Winkler. The effects of leg press speed on post-activation potentiation of vertical jump performance. Celebration of Undergraduate Research, Hope College, Holland, MI (2016, April).

LECTURES AND PRESENTATIONS

- “Paradoxical increases in glucose appearance and 24h FFA with NASH treatment,” Keystone Symposia: Inter Organ Crosstalk in Non-Alcoholic Steatohepatitis (NASH), Keystone, CO (02/08/2022)
- “Lipidomics: Ceramides in health and disease,” presented to the course entitled, “Nutritional Biochemistry of Lipids” directed by Elizabeth Parks, PhD (11/16 & 18/2021)
- “Lifestyle treatment-induced improvements in nonalcoholic steatohepatitis (NASH),” Nutrition and Exercise Physiology Seminar Series, University of Missouri, Columbia, MO (09/30/2021)
- “Lifestyle treatment-induced improvements in nonalcoholic steatohepatitis (NASH),” 81st Scientific Sessions of the American Diabetes Association, Virtual conference (06/28/2021).
- “Translational Research: Two examples from my graduate training,” presented to the course entitled, “Molecular Exercise Biology” directed by Frank Booth, PhD (12/01/2020)
- “Role of glucose flux to elevate hepatic lipogenesis in biopsy-proven NASH,” 80th Scientific Sessions of the American Diabetes Association, Virtual conference (06/15/2020).
- “High throughput LC-MS method to investigate postprandial lipemia: Considerations for future precision nutrition research,” KinMet, Chicago, IL (05/04/2020)
- “Hepatic short chain fatty acid (SCFA) oxidation in nonalcoholic fatty liver disease,” Southwest American College of Sports Medicine Chapter Meeting, Newport Beach, CA (10/26/2019)

“Very low-density lipoprotein ceramides and hepatic lipid accumulation,” 79th Scientific Sessions of the American Diabetes Association, San Francisco, CA (06/09/2019)

“Inverse relationship between very low-density lipoprotein (VLDL) ceramides, diacylglycerols, and triacylglycerols in human hepatic lipid accumulation,” Experimental Biology, Orlando, FL (04/9/2019)

“The effects of leg press speed on post-activation potentiation of vertical jump performance,” Celebration of Undergraduate Research, Hope College, Holland, MI (04/2016)

ACADEMIC SERVICE

2018 - present	Current – Mentor, undergraduate students, Parks Laboratory
2017 - present	Current – Graduate Student Association Member, Nutrition and Exercise Physiology
2019-20	President, Graduate Student Association, Nutrition and Exercise Physiology
2019-20	Finance Chair, Graduate Student Association, Nutrition and Exercise Physiology <ul style="list-style-type: none">• Applied for travel funding on behalf of the organization• Received ~\$4,000 for graduate student travel over two years
2018-19	Vice President, Graduate Student Association, Nutrition and Exercise Physiology
2018-19	Graduate Professional Council Representative, Nutrition and Exercise Physiology
2018-19	Finance Committee Member, Graduate Professional Council <ul style="list-style-type: none">• Reviewed travel funding applications and graded based on quality and merit
2018-19	Student Allocation Organization Committee Member, Graduate Professional Council <ul style="list-style-type: none">• Reviewed university funding applications for student organizations and graded based on quality and merit
2018	Sports Nutrition Graduate Teaching Assistant, Nutrition and Exercise Physiology, University of Missouri, Columbia, MO
2016	Mentor, Foundations for Fitness, Kinesiology Department, Hope College, Holland, MI
2016	Health Dynamics Teaching Assistant, Kinesiology Department, Hope College, Holland, MI

PROFESSIONAL MEMBERSHIPS

2019 – present	American College of Sports Medicine – Southwest Chapter
2017 – present	American Society of Nutrition

2017 – present American Physiological Society

ADVANCED TECHNICAL TRAININGS

- 2/11/2021 Mouse Handling Workshop
Directed by: Animal Care Quality Assurance, IACUC of MU
Veterinary Medicine, University of Missouri, Columbia, MO
- 01/2020–05/2020 Responsible Conduct of Research Through Enactment, Empowerment, and Engagement
Directed by: Mark Milanick, PhD
University of Missouri, Columbia, MO
- 08/2019–12/2019 Hierarchical/Multilevel Linear Modeling
Directed by: Francis Huang, PhD
University of Missouri, Columbia, MO
- 06/2019 Quantitative Foundations: Statistical Computing and Graphics with R
Directed by: Matthew Easter, PhD
University of Missouri, Columbia, MO
- 12/2018 Metabolomics: Basics
Laboratory of Takhar Kasumov
Northeastern Ohio Medical University, Rootstown, OH
- 10/28 – 11/2/2018 11th annual Isotope tracers in Metabolic Research: Principles and Practice of Kinetic Analysis
Sponsored by: NIH/MMPC
Vanderbilt University, Nashville, TN

CERTIFICATIONS

- 2017 – present Miscellaneous Training: Citizenship@Mizzou (diversity training), Graduate Assistant Teaching Training
- 2017 – present Laboratory Research: blood borne pathogens, chemical management, laboratory safety
- 2017 – present Clinical Research: HIPAA (research subject/patient privacy), good clinical practice, human subjects' protection, working with the IACUC, working with mice in the research setting, biosecurity
- 2016 – present First Aid, CPR, AED- Adult and Child

GRANTS SUBMITTED

08/2018 NASH	<i>Synergy between triacylglycerol and ceramide synthesis in</i> NIH F31 (NIDDK) – Ruth L. Kirschstein Predoctoral Individual NRSA Not discussed – \$150,000
12/2020	Resubmission: Impact score: 39 – \$150,000
08/2019	<i>Mechanisms of ceramide contributions to CVD risk</i> NIH F31 (NHLBI) – Ruth L. Kirschstein Predoctoral Individual NRSA Impact score: 58 Percentile: 52 – \$150,000
04/2020	Resubmission: Not discussed – \$150,000

VITA

Justine Marie Mucinski was born in Grand Rapids, Michigan. She attended Hope College in Holland, MI where she earned her bachelor's degree in exercise science with a minor in biology. Justine then worked for Hope Network, a nonprofit dedicated to helping individuals with disabilities live independently. During this time, she developed exercise prescriptions for individuals with brain and spinal cord injuries and explored options for her graduate training. With her passion for learning about metabolism in varying metabolic states, Justine was drawn to labs that studied metabolic processes. Her search led her to the department of Nutrition and Exercise Physiology at the University of Missouri where she ultimately joined the laboratory of Dr. Elizabeth Parks and was co-mentored by Dr. R. Scott Rector. Justine completed her doctorate degree in 2022 and will pursue postdoctoral training in skeletal muscle and mitochondrial metabolism in Dr. James DeLany's Lab at the AdventHealth Translational Research Institute in Orlando, FL.